

Topics in Stereochemistry, Volume 16

Editors

Ernest L. Eliel

Samuel H. Wilen

Norman L. Allinger

JOHN WILEY & SONS

**TOPICS IN
STEREOCHEMISTRY**

VOLUME 16

ADVISORY BOARD

STEPHEN J. ANGYAL, *University of New South Wales,
Sydney, Australia*

ALAN R. BATTERSBY, *Cambridge University, Cambridge,
England*

GIANCARLO BERTI, *University of Pisa, Pisa, Italy*

F. ALBERT COTTON, *Texas A & M University,
College Station, Texas*

JOHANNES DALE, *University of Oslo, Oslo, Norway*

DAVID GINSBURG, *Technion, Israel Institute of Technology,
Haifa, Israel*

JEAN-MARIE LEHN, *Collège de France, Paris, France*

JAN MICHALSKI, *Centre of Molecular and Macromolecular
Studies, Polish Academy of Sciences, Lodz, Poland*

KURT MISLOW, *Princeton University, Princeton, New Jersey*

MICHINORI ÔKI, *Tokyo University, Tokyo, Japan*

VLADIMIR PRELOG, *Eidgenössische Technische Hochschule,
Zurich, Switzerland*

GÜNTHER SNATZKE, *Ruhruniversität, Bochum, Federal Republic
of Germany*

JOHN B. STOTHERS, *University of Western Ontario, London,
Ontario, Canada*

HANS WYNBERG, *University of Groningen, Groningen,
The Netherlands*

TOPICS IN

STEREOCHEMISTRY

EDITORS

ERNEST L. ELIEL
Professor of Chemistry
University of North Carolina
Chapel Hill, North Carolina

SAMUEL H. WILEN
Professor of Chemistry
City College, City University of New York
New York, New York

NORMAN L. ALLINGER
Professor of Chemistry
University of Georgia
Athens, Georgia

VOLUME 16

AN INTERSCIENCE ® PUBLICATION
JOHN WILEY & SONS
New York • Chichester • Brisbane • Toronto • Singapore

An Interscience® Publication
Copyright © 1986 by John Wiley & Sons, Inc.

All rights reserved. Published simultaneously in Canada.

Reproduction or translation of any part of this work
beyond that permitted by Section 107 or 108 of the
1976 United States Copyright Act without the permission
of the copyright owner is unlawful. Requests for
permission or further information should be addressed to
the Permissions Department, John Wiley & Sons, Inc.

Library of Congress Catalog Card Number: 67-13943
ISBN 0-471-83810-1

Printed in the United States of America

10 9 8 7 6 5 4 3 2 1

INTRODUCTION TO THE SERIES

It is patently impossible for any individual to read enough of the journal literature so as to be aware of all significant developments that may impinge on his or her work, particularly in an area such as stereochemistry, which knows no topical boundaries. Stereochemical investigations may have relevance to an understanding of a wide range of phenomena and findings irrespective of their provenance. Because stereochemistry is important in many areas of chemistry, comprehensive reviews of high quality play a special role in educating and alerting the chemical community to new stereochemical developments.

The above considerations were reason enough for initiating a series such as this. In addition to updating information found in such standard monographs as *Stereochemistry of Carbon Compounds* (Eliel, McGraw-Hill, 1962) and *Conformational Analysis* (Eliel, Allinger, Angyal, and Morrison, Interscience, 1965; reprinted by American Chemical Society, 1981) as well as others published more recently, the series is intended also to deal in greater detail with some of the topics summarized in such texts. It is for this reason that we have selected the title *Topics in Stereochemistry* for this series.

The series is intended for the advanced student, the teacher, and the active researcher. A background of the basic knowledge in the field of stereochemistry is assumed. Each chapter is written by an expert in the field and, hopefully, covers its subject in depth. We have tried to choose topics of fundamental importance aimed primarily at an audience of inorganic and organic chemists but involved frequently with basic principles of physical chemistry and molecular physics, and dealing also with certain stereochemical aspects of biochemistry.

It is our intention to produce future volumes at intervals of one to two years. The editors will welcome suggestions as to suitable topics.

We are fortunate in having been able to secure the help of an international board of editorial advisors who have been of great assistance by suggesting topics and authors for several chapters and by helping us avoid, in so far as possible, duplication of topics appearing in other, related monograph series. We are grateful to the editorial advisors for this assistance, but the editors and authors alone must assume the responsibility for any shortcomings of *Topics in Stereochemistry*.

E. L. ELIEL
S. H. WILEN
N. L. ALLINGER

PREFACE

The opening chapter of this volume, contributed by L. Addadi, Z. Berkovitch-Yellin, I. Weissbuch, M. Lahav, and L. Leiserowitz, starts out with a survey of contemporary investigation of enantiomer separation by direct crystallization. The authors, an Israeli team of crystallographers and organic chemists, then describe their pioneering study—including the logic involved—of what constitutes the first independent experimental determination of absolute configuration since the anomalous X-ray diffraction method developed over 30 years ago by Bijvoet. In this chapter, Addadi et al. explain the solution to a long-standing crystallographic problem, namely, how to extract information about absolute configuration from a study of crystal morphology, the external characteristics of crystals.

In the second chapter, Hans Wynberg describes one facet—namely asymmetric catalysis—of the currently very active field of asymmetric synthesis. Wynberg and his co-workers have devised efficient asymmetric syntheses catalyzed by cinchona alkaloids. Several of these reactions are reviewed and rationalized by means of mechanistic models.

By chance rather than by design, the third chapter in this volume also emanates from Israel. Bernard S. Green, Rina Arad-Yellin, and Mendel D. Cohen have surveyed organic reactions in the solid state from the standpoint of the stereochemist. In the first part of the chapter, the authors discuss the stereochemical consequences of the crystallization of conformationally mobile systems. Conformational, crystal-field, and hydrogen-bonding effects, among others, are responsible for the selective crystallization of stereoisomers that may not be dominant in solution. The second part of the chapter is concerned with the stereochemical consequences of chemical, and especially photochemical, reactions in the solid state.

After this volume was submitted to the publisher, we learned that authors Z. Berkovitch-Yellin and Rina Arad-Yellin are twin sisters. This may be the only case where two twins are involved in two independent chapters in one book!

The fourth chapter in this volume, contributed by Helmut Duddleck, is an exceptionally thorough survey of substituent effects on carbon-13 nuclear magnetic resonance (NMR) chemical shifts. Organic chemists and others who are routinely dependent on ^{13}C NMR for structure elucidation and for information about stereochemistry will welcome the summary presented here. Although

Duddeck's approach is largely empirical, he does assess the various transmission mechanisms believed to be responsible for the observed chemical shifts.

We are pleased to welcome Professor Michinori Ôki (University of Tokyo) as a new member of our Editorial Advisory Board.

This is the last volume of the series that is being published under the joint editorial responsibility of the undersigned, inasmuch as Professor Norman L. Allinger, one of the founders of *Topics in Stereochemistry*, is relinquishing his position as editor. The remaining two editors and the publisher take this opportunity to acknowledge Professor Allinger's vital editorial contributions to the series over a period of nearly 20 years.

ERNEST L. ELIEL
SAMUEL H. WILEN
NORMAN L. ALLINGER

Chapel Hill, North Carolina
New York, New York
Athens, Georgia
February 1986

CONTENTS

A LINK BETWEEN MACROSCOPIC PHENOMENA AND MOLECULAR CHIRALITY: CRYSTALS AS PROBES FOR THE DIRECT ASSIGNMENT OF ABSOLUTE CONFIGURATION OF CHIRAL MOLECULES

1

*by L. Addadi, Z. Berkovitch-Yellin, I. Weissbuch,
M. Lahav, and L. Leiserowitz,
Department of Structural Chemistry,
The Weizmann Institute of Science,
Rehovot, Israel*

ASYMMETRIC CATALYSIS BY ALKALOIDS

87

*by Hans Wynberg,
Department of Chemistry,
University of Groningen,
Groningen, The Netherlands*

STEREOCHEMISTRY AND ORGANIC SOLID-STATE REACTIONS

131

*by Bernard S. Green,
Israel Institute for Biological Research,
Ness-Ziona, Israel;
Rina Arad-Yellin,
Department of Organic Chemistry,
The Weizmann Institute of Science,
Rehovot, Israel;
and Mendel D. Cohen,
Department of Structural Chemistry,
The Weizmann Institute of Science,
Rehovot, Israel*

SUBSTITUENT EFFECTS ON ^{13}C CHEMICAL SHIFTS IN ALIPHATIC MOLECULAR SYSTEMS. DEPENDENCE ON CONSTITUTION AND STEREOCHEMISTRY	219
<i>by Helmut Duddeck, Abteilung für Chemie, Ruhr-Universität Bochum, Federal Republic of Germany</i>	
SUBJECT INDEX	325
CUMULATIVE INDEX, VOLUMES 1–16	337

A Link Between Macroscopic Phenomena and Molecular Chirality: Crystals as Probes for the Direct Assignment of Absolute Configuration of Chiral Molecules

L. ADDADI, Z. BERKOVITCH-YELLIN, I. WEISSBUCH,
M. LAHAV, AND L. LEISEROWITZ

*Department of Structural Chemistry
The Weizmann Institute of Science
Rehovot, Israel*

I.	Introduction	2
II.	Statement of the Problem	4
III.	The Bijvoet Method	7
	A. X-Ray Diffraction	7
	B. Neutron Diffraction	9
	C. Independent Proof of the Bijvoet Method	10
IV.	A Bridge Between Crystal Structure, Crystal Morphology, and Molecular Chirality	11
	A. Introduction	11
	B. Crystal Growth in the Presence of "Tailor-Made" Inhibitors	11
	C. Morphological Crystal Engineering	13
	1. <i>E</i> -Cinnamide	13
	2. Benzamide	15
	D. Resolution of Conglomerates by Stereoselective Habit Modifications	16
	1. Pasteur-Type Resolution	16
	2. Glutamic Acid · HCl and Threonine	18
	3. Asparagine · H ₂ O	19
	4. Relative Assignment of Configuration	24
	E. Crystal Dissolution in the Presence of Additives	24
	F. Assignment of the Absolute Configuration of a Chiral Crystal Containing a Polar Axis	27
	1. Modeling Additive Effects on Polar Crystal Growth	27
	2. <i>N</i> -(<i>E</i> -Cinnamoyl)alanine	30
	3. Lysine · HCl. Anisotropic Distribution of Occluded Additive	31
	4. α-Lactose	33
	5. Sucrose	35

G.	Assignment of Absolute Configuration Using Centrosymmetric Crystals	38
1.	Principles	38
2.	(<i>R,S</i>)-Serine	42
3.	(<i>R,S</i>)- <i>N</i> -Acetylvaline	46
4.	Glycine	48
5.	Glycylglycine	51
6.	Centrosymmetric Orthorhombic Crystals	54
H.	Assignment of Absolute Configuration Using Noncentrosymmetric Achiral Crystals	55
I.	Determination of the Absolute Direction of a Polar Axis in a Chiral or Achiral Crystal	58
J.	Reduction in Crystal Symmetry of Solid Solutions	58
V.	Absolute Configuration from Chemical Reactivity in Polar and Enantiopolar Crystals	61
A.	Gas-Solid Reactions in Polar Crystals: Ammonia- <i>p</i> -Bromobenzoic Anhydride	62
B.	Liquid-Solid Reactions in Centrosymmetric Crystals: Osmium Tetroxide-Tiglic Acid	63
C.	Topochemical Reactions in Enantiopolar Crystals: Cinnamide-Cinnamic Acid	65
VI.	The Solvent Effect	66
A.	Introduction	66
B.	Resorcinol	68
VII.	Pyroelectricity, Piezoelectricity, and Optical Activity in Crystals	71
VIII.	Determination of Absolute Configuration by Electron Microscopy	74
A.	Imaging of Macromolecules	74
B.	High-Resolution Electron Microscopy of Molecular Crystals	77
C.	Monolayers and Multilayers	78
IX.	Conclusions	79
	Acknowledgments	80
	Appendix: Explanation of Crystallographic Symbols	80
A.	Miller Indexes	80
B.	Symmetry Operations	81
C.	Relevant Point Symmetries	81
	References	81

I. INTRODUCTION

The manual separation of the enantiomorphous crystals of sodium ammonium tartrate tetrahydrate (Figure 1) by Pasteur in 1848 (1) is historically significant, because it laid the foundations of modern stereochemistry. This experiment demonstrated for the first time that certain classes of molecules display enantiomorphism even when dissolved in solvent. These observations eventually paved the way for the inspired suggestion, made more than two decades later, by van't Hoff (2) and Le Bel (3), of a tetrahedral arrangement of bonds around the carbon atom.

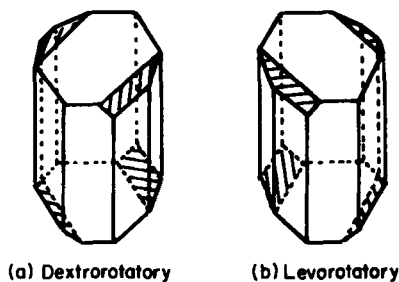


Figure 1. Enantiomorphous crystals of sodium ammonium tartrate $\cdot 4\text{H}_2\text{O}$.

These findings raised the fundamental question of the absolute configuration of a chiral molecule, but no safe method was available for making such an assignment till 100 years after the Pasteur separation. At the turn of the century, Fischer (4) and Rosanoff (5) introduced an arbitrary convention for the absolute configurations of L- and D-glyceraldehyde with which the configurations of other molecules such as sugars and peptides were correlated by chemical degradation. During the first half of the twentieth century, chemists manipulated chiral molecules on a relative scale, making important contributions to mechanistic stereochemistry, especially in the field of nucleophilic and electrophilic substitutions and eliminations, and deriving fundamental rules such as the Walden inversion.

In 1951, Bijvoet (6) assigned the absolute configuration of (+)-tartaric acid by applying the method of anomalous scattering of X-rays to chiral crystals of sodium rubidium tartrate. Over the following 30 years, this method became the standard way of assigning absolute configuration. It is possible to extract the same information by other techniques, such as by calculation of the sign of rotation of linearly polarized light in the dispersed phase (7), but these methods are not widely used and are in general not considered as reliable as that of Bijvoet.

The significance of assigning a three-dimensional structure to a chiral molecule in an absolute way has been questioned by chemists over the years. This was nicely illustrated by Dunitz (8), who stated, in reference to Alice's comment on the taste of looking-glass milk (9), "Which of a pair of enantiomorphous structures corresponds to milk and which to looking-glass milk is a problem which may have no utilitarian significance, but it must have perplexed many chemists and natural philosophers during the last 100 years." This lack of practical significance is true for reactions in dispersed media, but less so for those systems in which a correlation exists between molecular chirality and macroscopic phenomena such as crystal growth and habit, reactivity in two- or three-dimensional crystals, and pyro- and piezoelectricity, or for systems involving interactions between complex biological macromolecular superstructures and small molecules.

Crystal morphology had been widely studied and classified (10) long before crystal structures were solved by X-ray diffraction. Therefore, after Pasteur's discovery, chemical crystallographers had naturally been challenged by the possibility of correlating microscopic molecular chirality with the macroscopic morphological asymmetry of the corresponding crystal. Until a few years ago, attempts in this direction did not bear fruit (11). Recent studies on crystal growth and dissolution in the presence of "tailor-made" additives have provided a straightforward and most reliable way of deducing the absolute configuration of chiral molecules from the change in crystal habit induced by the additive, from the distribution of the occluded additive in the crystal, and from the etch pit formation on the crystal faces induced by the additive on partial dissolution of the crystal.

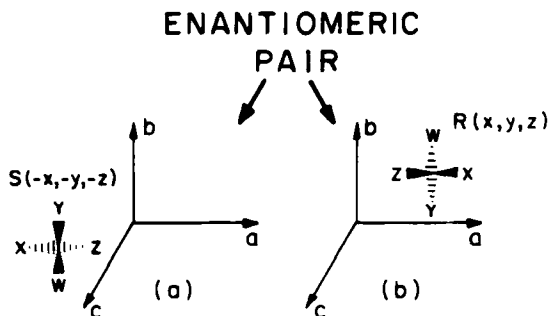
This chapter will be devoted primarily to the assignment of the absolute configuration of a chiral molecule in a crystal by various means. We shall focus mainly on methods that utilize surface structures of crystals, and also examine other avenues that have not yet been experimentally explored but are, in principle, applicable. The review will cover the following topics:

1. Principles of anomalous scattering of X-rays and of neutrons.
2. The use of chiral tailor-made additive molecules through their effect on the morphology of chiral or centrosymmetric crystals during crystal growth.
3. The formation of etch pits by chiral additives present in solution during dissolution of the crystal.
4. The anisotropic distribution of additive molecules that are occluded within the substrate crystal on growth.
5. The formation of hemihedral crystal faces in a chiral crystal as induced by solvent.
6. Chemical reactions in polar and centrosymmetric crystals.
7. Pyroelectricity.
8. Use of diffraction and imaging in electron microscopy.

We shall not cover such other methods as theoretical calculations of the sign of optical rotation, circular dichroism, and so on in solution; these have been recently reviewed in an excellent book by Mason (12).

II. STATEMENT OF THE PROBLEM

The ambiguity involved in assigning the absolute configuration of a chiral molecule in a chiral crystal is presented in Scheme 1. Scheme 1*a* depicts a chiral molecule of, say, configuration *S*, with individual atomic coordinates $-x_i, -y_i, -z_i$ ($i = 1, \dots, n$, for n atoms) in a crystal axial system a, b, c . Scheme 1*b* represents the enantiomeric crystal structure containing a molecule of configuration



Scheme 1

R with a set of atomic coordinates x_i, y_i, z_i , referred to the same axial system. Schemes 1a and b are related by an inversion through the origin.

The X-ray intensity diffraction data of the given crystal do not allow one to specify which of the two sets describes the actual crystal structure and thus the absolute configuration of the molecule when there is no effect of anomalous X-ray dispersion. Under such conditions Friedel's law holds, which states that the X-ray intensity diffraction pattern of a crystal is centrosymmetric whether the crystal structure is centrosymmetric or not. This does not mean that a false crystal structure containing a center of symmetry is obtained as the solution of the structural problem, but rather that the X-ray analysis cannot differentiate between the two enantiomeric structures. A simple mathematical analogy is provided by the two possible square roots of a number: $\sqrt{x^2} = \pm x$.

We first examine some ramifications of Friedel's law in terms of absolute configuration to provide insight into the geometric nature of the problem. Consider a chiral R crystal comprising a set of right hands oriented such that the fingers of the hands are exposed at the (010) face (Figure 2a) (see the Appendix for definitions of crystallographic symbols). The opposite situation occurs in the enantiomorphous S crystal comprising left hands (Figure 2b). This is an example of a crystal containing a polar axis b . A polar direction in a crystal is defined as one whose opposite ends are not related by any symmetry element (except translation). Thus, along a polar direction, the crystal exhibits one-dimensional chirality.

According to Friedel's law, a diffracted X-ray beam from the (010) side of the R crystal will have the same intensity as that from the opposite (0 $\bar{1}$ 0) side. Moreover, the intensity of this beam will be equal in magnitude to those of the diffracted beams from the (010) and (0 $\bar{1}$ 0) planes of the S crystal. On such a basis one cannot distinguish between the R and S structures.

Image projections of a chiral object provide a useful analogy to the above diffraction phenomenon. For example, "medical" X-ray photographs obtained

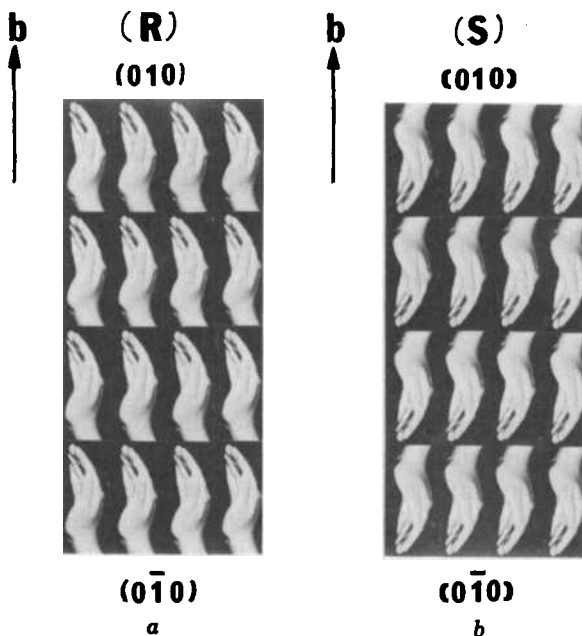


Figure 2. Two enantiomorphous sets of hands arranged in a lattice: (a) right hands forming an *R* crystal; (b) left hands forming an *S* crystal.

by shining X-rays from the $+b$ side of the crystal onto the right and left hands of Figure 2a and b, respectively, would be indistinguishable. But here the analogy with diffraction ends, because if another image projection is taken after a rotation of, say, 90° in a known sense, the combination of the two projections in the respective directions can correspond to only one set of hands, because each projection preserves chirality in two dimensions. This is not true for diffraction, for which even if a set of "pictures" of a crystal is taken at known angles, their combination can still correspond to both of the enantiomers. Indeed, we shall discuss how this difference can be exploited for the assignment of absolute configuration through projection images obtained by electron microscopy (Section VIII).

This discussion brings out an important principle that will reappear time and again in this chapter. If we can assign the absolute direction of the hand *vis-à-vis* the polar axis b (Figure 2), that is, establish whether the wrist or the fingers of the hand point up, then the absolute chirality of the hand is fixed as well. This determination of absolute polarity can be achieved in several ways other than anomalous scattering of X-rays or neutrons, for example, by an external means such as a solvent, a chemical reagent, or a physical measurement (e.g.,

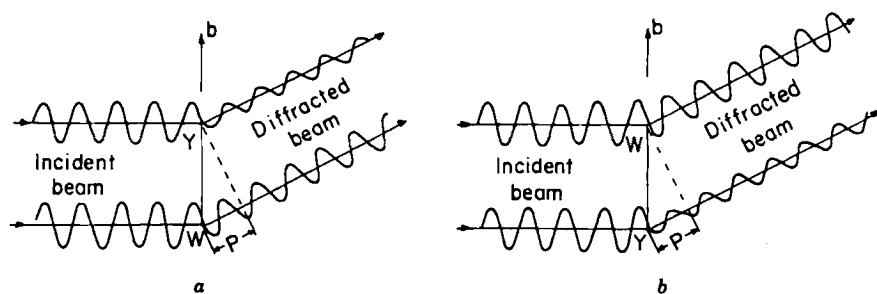
of optical activity or piezo- or pyroelectricity); or by interaction of the crystal surface with a hand that differs slightly from that in Figure 2 at one of the ends.

III. THE BIJVOET METHOD

A. X-Ray Diffraction

The intensity of a diffracted X-ray beam is dependent on, among other factors, the relative phase differences between the individual X-ray waves scattered in the diffracting direction by the atoms in the unit cell (13). Friedel's law is based on the assumption that the phase differences between these waves depend only on the corresponding path differences. This concept is illustrated in Scheme 2 for two atoms W and Y. Scheme 2a shows the diffraction geometry where the vector $W \rightarrow Y$ is along the $+b$ direction, and Scheme 2b shows diffraction in the same direction for the inverted image (i.e., the one in which $W \rightarrow Y$ is along the $-b$ direction). The intensity of the diffracted beam in each arrangement depends on the phase difference Φ between the two wavelets scattered from atoms W and Y. The value of Φ is $2\pi P/\lambda$, where P is the path difference between these two scattered wavelets and λ the wavelength of the scattered radiation. In Scheme 2a the phase of the scattered wave from atom Y is ahead of that from atom W by the angle Φ and in Scheme 2b the phase of the wave scattered from atom W leads that of atom Y by Φ . Under these circumstances the respective amplitudes and intensities of the diffracted beams in arrangements a and b would be equal, because their corresponding phase differences are equal in magnitude.

The above argument assumes that the intrinsic phase change of each wave on being scattered by atoms W and Y is the same and thus can be ignored. This assumption holds in the case of "normal" scattering, that is, if the frequency of the incident radiation is much greater than the critical absorption frequencies of the irradiated atoms. When, however, the incident wavelength is a little shorter



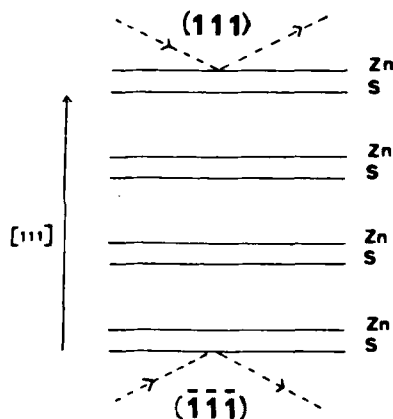
Scheme 2

than that of the absorption edge (i.e., the critical absorption frequencies) of one type of atom, the phase of the wave scattered by this excited atom is intrinsically advanced with respect to those from other atoms that scatter normally. Therefore for such an excited atom the anomalous component of the scattered ray induces a net phase lead, say $\Delta\phi$, of the total scattered wave relative to the phase of the wave that is scattered normally.

Now consider the effect of anomalous scattering on the relative intensities of the diffracted rays in Scheme 2*a* and *b* when atom Y scatters anomalously with an intrinsic phase lead $\Delta\phi(Y)$, and atom W scatters "normally." Under such circumstances, the wave scattered by atom Y in Scheme 2*a* would lead that of atom W by a phase difference of $\Phi + \Delta\phi(Y)$, and the wave scattered by atom Y in Scheme 2*b* would lag behind that of atom W by $-\Phi + \Delta\phi(Y)$. These two phase differences are unequal in magnitude, so the corresponding amplitudes of their resultant waves, and the subsequent intensities, will be different, leading to a breakdown of Friedel's law.

From the relative intensities of the two diffracted waves one can deduce the absolute direction of the vector $W \rightarrow Y$ with respect to the b axis. This type of reasoning was exploited by Nishikawa and Matsukawa (14) in 1928 and independently by Coster, Knol, and Prins (15) in 1930 to determine the absolute polarity of successive layers of zinc and sulfur in a polar crystal of zinc sulfide. In the zinc sulfide crystal, planes of zinc and sulfur alternate parallel to the face (111), as shown in Scheme 3; the distance between the close pairs of zinc and sulfur planes is one-quarter of the whole 111 spacing.

Despite the knowledge that Friedel's law does not hold in anomalous diffraction and that the absolute polarity of the zinc sulfide structure had been determined, the idea that it is fundamentally impossible to determine the absolute



Scheme 3

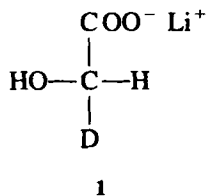
configuration of a chiral molecule by means of an X-ray analysis held until 1949, when Bijvoet showed otherwise (16). Bijvoet realized that establishing the principle of the absolute polarity of vector $W \rightarrow Y$ in Scheme 2 was akin to fixing the polarity of $W \rightarrow Y$ in the chiral structure of Scheme 1, thus allowing one to assign the absolute configuration of the molecule.

Among the first crystal structures studied were those of sodium rubidium tartrate (6) and (L)-isoleucine HBr (17). Following Bijvoet's breakthrough, heavy atoms such as Br and Rb were used for the assignment of absolute configuration, because they are strong anomalous scatterers. This choice was necessitated by the low accuracy of X-ray diffraction intensity measurements obtained by visual recording on photographic films using X-ray cameras. The advent of commercially available diffractometers equipped with scintillation counters, and the subsequent improvement in the accuracy of intensity measurements, made it possible to establish the absolute configuration of crystals containing anomalous X-ray scatterers as light as oxygen. For example, Hope and de la Camp (18) determined the absolute configuration of (+)-tartaric acid and Rabinovich and Hope (19,20) established the absolute configuration of a chiral crystal composed of nonchiral *p,p'*-dimethylchalcone molecules, in which the molar ratio of oxygen to carbon is 1:17.

B. Neutron Diffraction

Scattering of neutrons by nuclei is subject to the same principles as scattering of X-rays by electrons with respect to anomalous dispersion. Several nuclei (e.g., ${}^6\text{Li}$, ${}^{10}\text{B}$, ${}^{113}\text{Cd}$, ${}^{149}\text{Sm}$, ${}^{151}\text{Eu}$, ${}^{157}\text{Gd}$, and ${}^{239}\text{Pu}$) exhibit anomalous scattering of thermal neutrons due to the presence of an absorption resonance at thermal neutron energies (21,22). The Bijvoet technique can therefore also be applied to neutron diffraction. Very little work has been done employing anomalous dispersion of neutrons for assignment of absolute configuration. It is therefore difficult at present to assess the general potential of this technique. Nevertheless, anomalous neutron scattering has been proven to be useful if the absolute configuration of the molecule can be assigned by X-ray diffraction only with difficulty, that is, if the chiral substituents are nuclear isotopes of the same atom. This property was put to elegant use by Johnson and co-workers (23) in the determination of the absolute configuration of the lithium salt of an enzymatically formed α -monodeuterioglycolate (1); they used the large anomalous scattering amplitude of Li combined with the markedly different neutron scattering amplitudes of H and D. It has been shown recently by Dunitz and co-workers (24) that one can distinguish between H and D in a molecule containing two chiral centers using low-temperature X-ray diffraction, because of the different vibrations of H and D atoms. This approach can in principle also be applied to distinguish between H and D in molecules with only one chiral center, for

example 1, provided the chiral crystal structure is not pseudocentrosymmetric and the molecule contains an anomalous X-ray scatterer.



A particularly strong anomalous scatterer is Cd, due to its capacity for absorption (e.g., $^{113}\text{Cd} + n \rightarrow ^{114}\text{Cd}$). The absolute configuration of the (*S*)-glutamate complex of cadmium(II) $[\text{Cd}(\text{S})-\text{glu}](\text{H}_2\text{O})\text{H}_2\text{O}$ has been determined by neutron diffraction employing the natural abundance (12.3%) of ^{113}Cd as the anomalous scattering nuclide (25). It is noteworthy that large anomalous scattering effects are found in electron diffraction, especially low-energy electron diffraction. Applications of such anomalous effects in surface crystallography are expected (26).

C. Independent Proof of the Bijvoet Method

Over the past 30 years the absolute configurations of several hundred optically active compounds have been determined using Bijvoet's method. In almost all cases where comparisons were possible the results were consistent. These absolute configurations were either all correct or all wrong, because till 1972, there was no reliable independent proof that the Bijvoet method gave the correct results. Indeed, Tanaka claimed, on a reexamination of the theory of anomalous scattering in 1972 (27,28), that the anomalous component of the scattered ray should be reversed in sign, and consequently all absolute configurations determined by X-ray diffraction should be changed into their enantiomers.

An independent proof of the Bijvoet method was provided by Brongersma and Mul (29), who determined the absolute polarity of zinc blende from noble gas ion-reflection mass spectroscopy. They reflected a beam of Ne^+ ions with a known energy from the two opposite (111) and $(\bar{1}\bar{1}\bar{1})$ faces of a ZnS crystal (Scheme 3) and measured the energy of the reflected ions in a mass spectrometer. The principle of the method is that the incident ions lose an amount of energy that depends on the mass of the atoms with which they collide. In this way they found the absolute polarity of the crystal (Scheme 3), which proved to be in agreement with that derived by anomalous X-ray scattering. Thus, the final proof of the validity of Bijvoet's analysis came from experiments establishing the absolute polarity of a crystal by interaction of its opposite faces with an external agent.

IV. A BRIDGE BETWEEN CRYSTAL STRUCTURE, CRYSTAL MORPHOLOGY, AND MOLECULAR CHIRALITY

A. Introduction

Pasteur recognized in his experiments on resolution of enantiomers that macroscopic chirality of a crystal implies microscopic chirality of its constituent molecules (the opposite does not necessarily hold). Hence, it would seem possible, as pointed out in Section I, to deduce the absolute configuration of a given chiral molecule directly from the asymmetric morphology of its crystal. Since asymmetry in crystal morphology results from a difference in the relative rates of growth of the crystal in the opposite directions, this requires in principle knowledge of the molecular packing arrangement of the crystal and a sufficient understanding of the mechanisms of its growth.

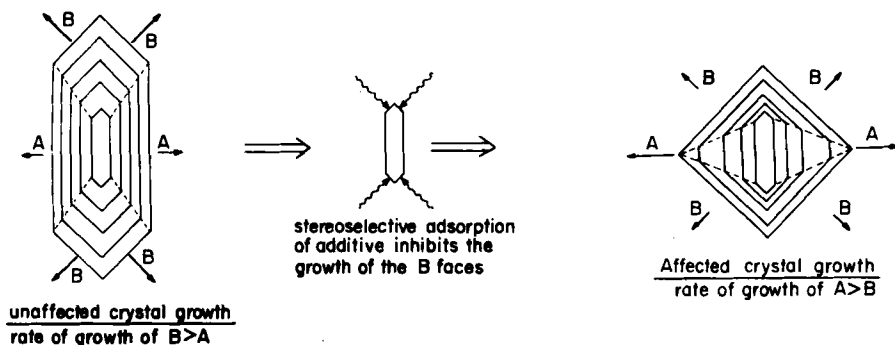
An attempt in this direction was reported first by Waser in 1949 (30); he tried to assign the absolute configuration of resolved tartaric acid by comparing the relative ease of approach of an oncoming molecule to opposite hemihedral crystal faces that were developed to different extents. Waser ignored, however, the determining role played by the solvent in the relative growth of these two opposite faces. Turner and Lonsdale (31) recognized this salient fact. They claimed that the difference in development of these faces must have been due to solvent-surface interactions.

Recent experimental and theoretical studies on crystal growth, especially in the presence of tailor-made inhibitors, provide a link between macroscopic and microscopic chirality. We shall discuss these principles in some detail for chiral molecules. Furthermore, we shall examine whether it is indeed feasible today to establish the absolute configuration of a chiral crystal from an analysis of solvent-surface interactions. Since these analyses are based on understanding the interactions between a growing crystal and inhibitors present in solution, we shall first illustrate the general mechanism of this effect in various chiral and nonchiral systems.

B. Crystal Growth in the Presence of "Tailor-Made" Inhibitors

It has long been recognized that impurities may cause dramatic changes in the morphology of crystals undergoing crystallization (32-35). The interpretation of these morphological changes depends on there being a high degree of specificity in the interactions of the foreign material with the various structured surfaces of the crystal.

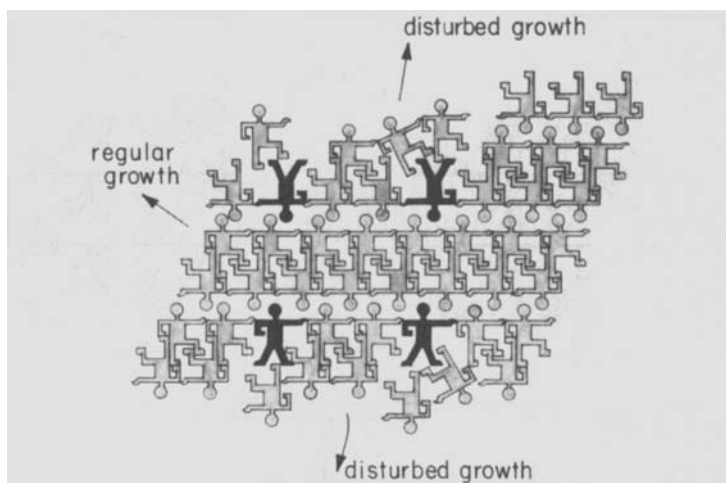
In general, when growth of a given face B is inhibited in the direction perpendicular to the face, its area is expected to increase relative to that of a face A that is unaffected (Scheme 4); that is, the ratio of the area of face B to that of A will be smaller in the pure crystal than in the affected one.



Scheme 4

Thus a comparison of the relative surface areas of crystals grown in pure solvent and in solvents containing additives deliberately introduced into the system allows identification of the faces affected by the additive, and subsequently of the crystallographic directions involved in the inhibition process.

Morphological studies have been carried out over the years on a variety of organic compounds, such as sugars (36–41), alcohols (42), carboxylic acids, amides (43,44), amino acids (45–47), and steroids (43), grown in the presence and absence of additives. Through the observed morphological changes, a stereochemical correlation was established among the molecular structure of the additive, the crystal structure of the substrate, and the affected growth directions, leading to the proposal of a two-step mechanism involving binding of the additive at the growing crystal face, followed by retardation of growth. Slightly modified substrate molecules were found to be particularly effective inhibitors. Such molecules have been used for in-depth investigation of the two-step mechanism. It was found that by virtue of attractive interactions (e.g., ionic and hydrogen bonds), the unmodified (with respect to the substrate) moiety of the additive is bound to suitable sites on growing surfaces of the host crystal in such a way that the modified part of the adsorbed inhibitor emerges from these crystal surfaces. The adsorbing surface can thus bind inhibitor molecules with minimal steric hindrance with respect to the other surfaces (Scheme 5). The modified part, however, perturbs the regular deposition of further layers. Consequently, the rates of growth in these directions are decreased with respect to other unaffected directions, resulting in changes in crystal morphology. Furthermore, the inhibitor may be eventually occluded into the bulk of the crystal via overgrowth. We shall illustrate below this stereochemical rule for a number of systems, including cinnamide, benzamide, and three pairs of enantiomorphs, grown in the presence of chiral inhibitors.



Scheme 5

C. Morphological Crystal Engineering

1. *E*-Cinnamide

E-Cinnamide (43) crystallizes in space group $P2_1/c$. The molecules form hydrogen-bonded cyclic dimers aligned in the direction of the a axis (Figure 3). These dimers are interlinked by $\text{NH} \cdots \text{O}$ hydrogen bonds along b to form a ribbon motif. The ribbons are interleaved along c and a by phenyl-phenyl contacts. Centrosymmetric pairs of cinnamide molecules overlap along c with a plane-to-plane contact of approximately 4 Å (48,49). The pure compound crystallizes as bars elongated in b (Figure 4a). Appropriate inhibitors were designed to modify the morphology of cinnamide crystals along the three principal directions of growth separately (43).

A decrease in the growth rate along a may conceivably be achieved either by disruption of the hydrogen bonds within the cyclic dimer at the site of the additive, or by further weakening of the interactions between the stacked phenyl groups.

N-Methyl-*E*-cinnamide and *p*-chloro-*E*-cinnamide were consequently tested as suitable additives. Both cause cinnamide crystals to grow as thin {100} plates (Figure 4c). In the presence of the former, the *N*-methyl group of the additive molecule, which invariably adopts the synplanar conformation **3a** (50), prevents formation of the dimer, thus inhibiting the attachment of additional cinnamide molecules along a . The additive *p*-chloro-*E*-cinnamide inhibits the deposition of oncoming 100 layers, due to steric hindrance induced by the bulky chlorine atom.

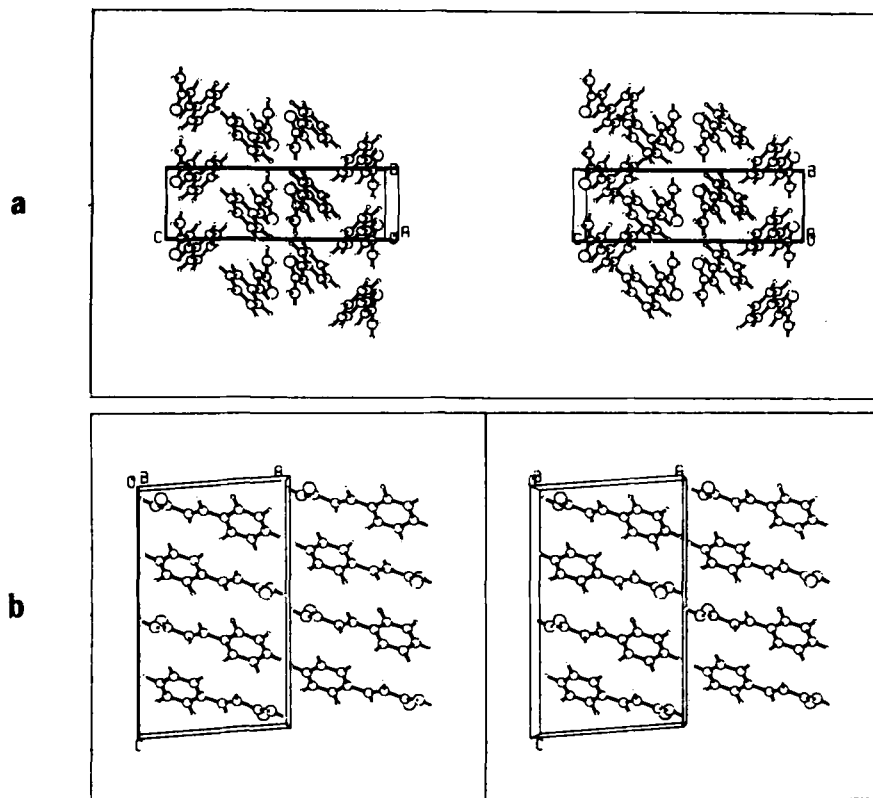
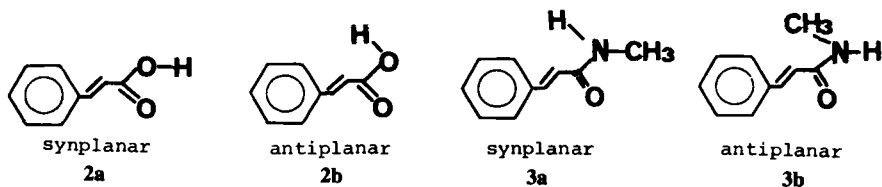
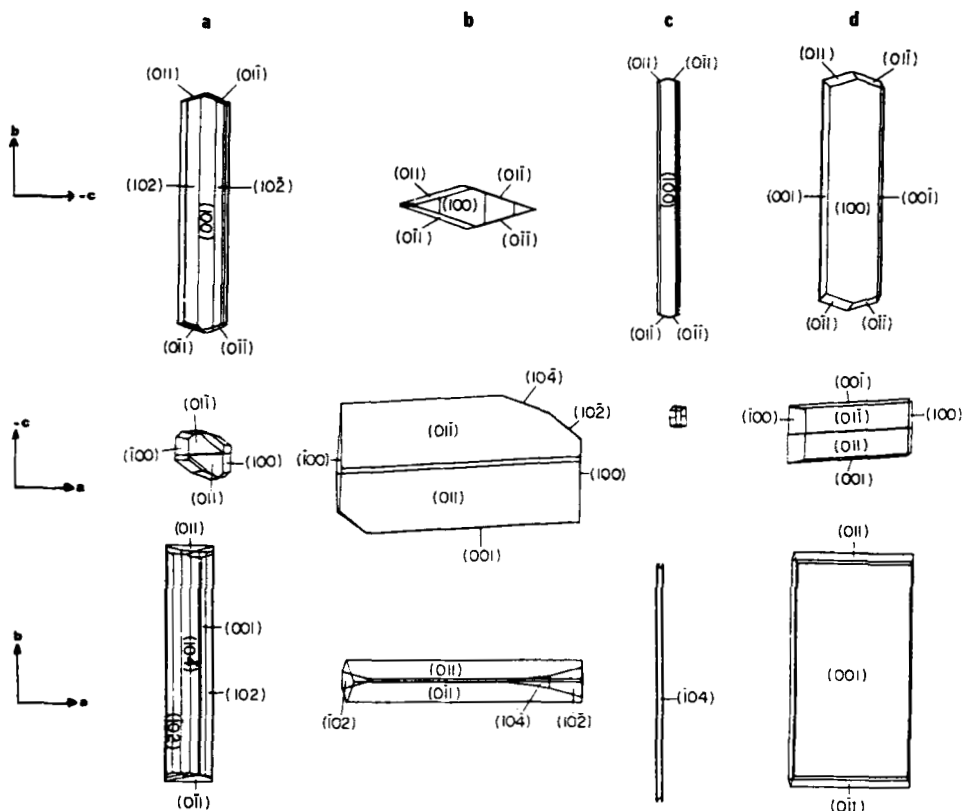


Figure 3. Packing arrangement of *E*-cinnamide: (a) view along the *a* axis; (b) view along the *b* axis.

The driving force for growth of the crystal in the *b* direction is the energy released by formation of the $\text{NH} \cdots \text{O}$ bonds of the ribbon motif. *E*-Cinnamic acid in the stable synplanar conformation **2a** can replace a *E*-cinnamide molecule at the end of the ribbon; however, at the site of the additive, the attractive $\text{NH} \cdots \text{O}$ bond (-6 kcal/mol) is replaced by repulsion between the adjacent oxygen lone-pair electrons of the bound additive molecule and of the oncoming cinnamide molecule ($1-2$ kcal/mol), which leads to an overall loss in energy of $7-8$ kcal/mol at the site of the additive (Scheme 6 on page 16).





As predicted, the presence of cinnamic acid in solution caused cinnamide to crystallize as flat prisms with prominent {011} faces (Figure 4b). The crystal morphology was modified along *c* by the use of amide additives that contain a bulky Cl substituent at the α - or β -carbons of cinnamide. When replacing a substrate molecule, these additive molecules interfere with the deposition of the next 011 layers (Figure 3), yielding {011} platelike crystals (Figure 4d).

2. Benzamide

Benzamide (43,51) crystallizes from ethanol in space group $P2_1/c$. The main features of the crystal structure (52) (Figure 5) are similar to those found in cinnamide. Hydrogen-bonded cyclic dimers are interlinked along the 5.0-Å b axis to form ribbons. The ribbons are stacked along the 5.6-Å a axis, in an

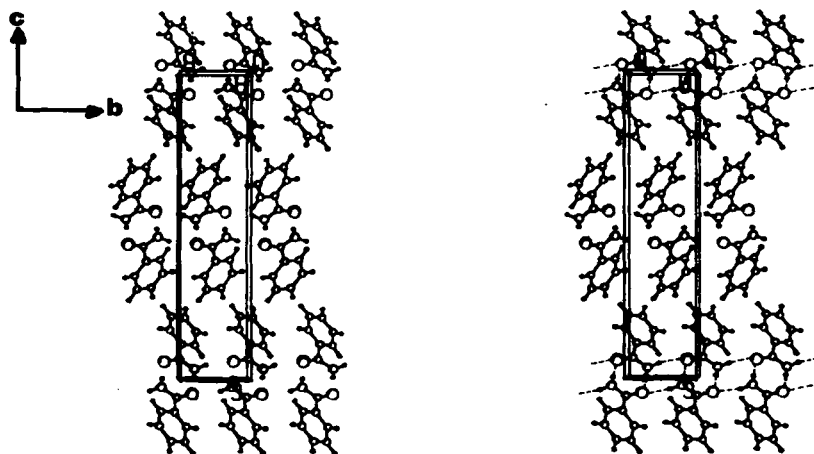
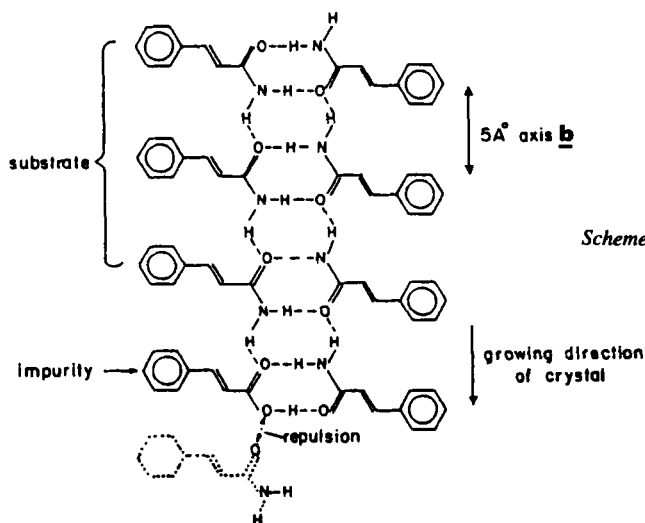


Figure 5. Packing arrangement of benzamide viewed along the a axis.

arrangement determined primarily by Coulomb interactions (53). The ribbon and stack motifs combine to yield stable 001 layers. These tightly packed layers juxtapose along c , interacting via weaker van der Waals forces between phenyl groups. The primary directions of growth are thus along a and b , and growth along c is the slowest, thus explaining the {001} platelike shape of the crystals (Figure 6a). Reasoning as for cinnamide, the additives benzoic acid, *o*-toluamide, and *p*-toluamide were selected to inhibit growth along the b , a , and c axes, respectively. The resulting crystal morphologies are shown in Figure 6b–d.



Scheme 6

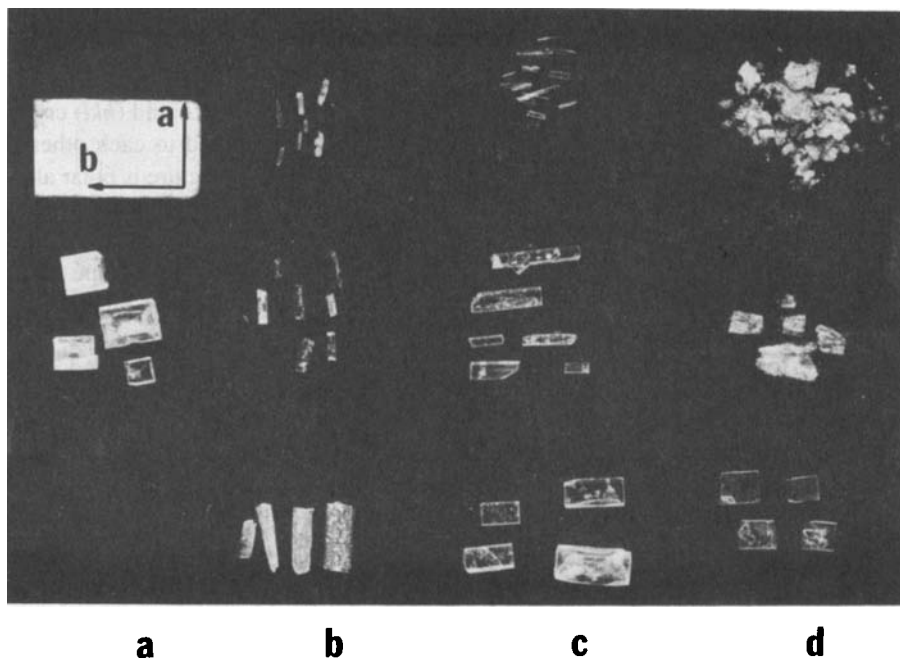
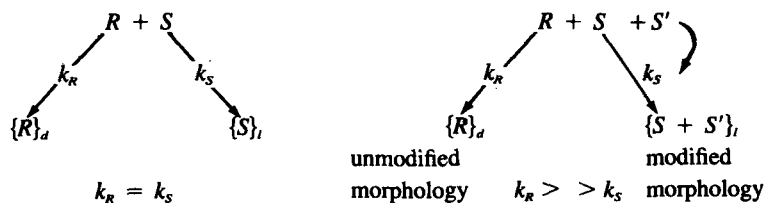


Figure 6. Photographs of crystals of benzamide: (a) pure; (b)–(d) grown in the presence of increasing amounts (from bottom to top) of (b) benzoic acid; (c) *o*-toluid, (d) *p*-toluid. The crystals shown in this photograph (and all those following) varied in size from about 0.1 to 5 mm.

D. Resolution of Conglomerates by Stereoselective Habit Modifications

1. Pasteur-Type Resolution

An extension of the above principles of morphological modification to racemic mixtures, in which each enantiomer (*R* or *S*) crystallizes separately in enantiomorphic crystals (*d* or *l*), naturally suggests the possibility of performing by these means a new manual Pasteur-type resolution (Scheme 7), as well as a kinetic resolution (54).



Scheme 7

Crystals composed of the *R* and *S* enantiomers of the same racemic mixture must be related by mirror symmetry in terms of both their internal structure and external shape. Enantiomorphous crystals may be sorted visually only if the crystals develop recognizable hemihedral faces. [Opposite (*hkl*) and ($\bar{h}\bar{k}\bar{l}$) crystal faces are hemihedral if their surface structures are not related to each other by symmetry other than translation, in which case the crystal structure is polar along a vector joining the two faces. Under such circumstances the hemihedral (*hkl*) and ($\bar{h}\bar{k}\bar{l}$) faces may not be morphologically equivalent.] It is well known that Pasteur's discovery of enantiomorphism through the asymmetric shape of the crystals of racemic sodium ammonium tartrate was due in part to a confluence of favorable circumstances. In the cold climate of Paris, Pasteur obtained crystals in the form of conglomerates. These crystals were large and exhibited easily seen hemihedral faces. In contrast, at temperatures above 27°C sodium ammonium tartrate forms a racemic compound.

Enantiomorphous crystals behave alike in their interactions toward an external achiral molecule. On the other hand, if the inhibitor is a resolved enantiomer, diastereomeric interactions at the surfaces of the growing crystals $\{ \}_d$ or $\{ \}_l$ must be expected and hence affect the *d* and *l* surfaces differently. It follows directly from the mechanism illustrated in Scheme 7 that a chiral tailor-made inhibitor *S'* consisting of a slightly modified *S* molecule will in general be adsorbed only at the crystal surface of the *S* enantiomer and not at the surface of the *R* crystal. This stereoselective adsorption causes the *S* crystals to undergo drastic morphological changes, which allow easy visual identification and separation of the two enantiomorphs (46). We will illustrate this effect for three different conglomerates.

2. Glutamic Acid·HCl and Threonine

The crystal structure and morphology of (*S*)-glutamic acid·HCl are shown in Figure 7. We observe that all side chains are directed along *c* and form hydrogen bonds in this direction (55). Adsorption of any other *S'* amino acid bearing a different side chain will take place at the {001} face at which the side chain emerges. The growth of this face will subsequently be inhibited because of disruption of the hydrogen bonds along *c*. It is evident, on the other hand, that *R'* amino acid molecules cannot be adsorbed at the same surface, because the molecular structures of the substrate and of the additive are of opposite handedness. By symmetry an *R'* amino acid, but not an *S'*, can be adsorbed on the $\{R\}_d$ crystals.

As expected, adsorption of (*S*)-lys, -his, -orn and other amino acids causes the (*S*)-glu·HCl crystals to grow as thinner and thinner plates, and finally as powder at higher and higher inhibitor concentrations, while the (*R*)-glu·HCl

L-GLUTAMIC ACID·HCl

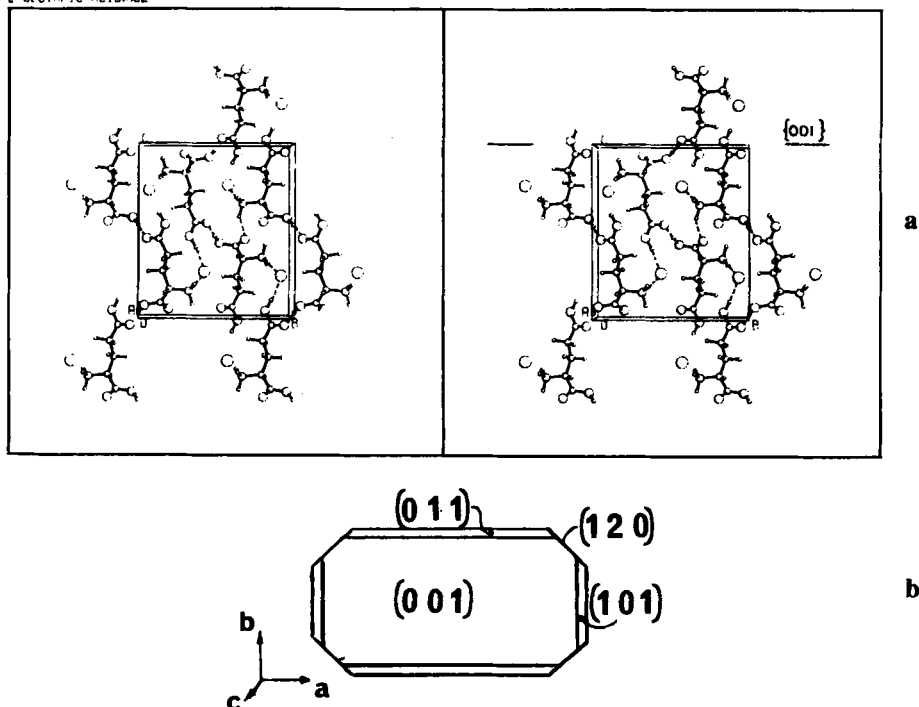


Figure 7. (a) Packing arrangement of (*S*)-glutamic acid·HCl viewed along the *a* axis. (b) Morphology of pure crystals.

crystals preserve their original morphology (Figure 8). An analogous effect of resolved glutamic acid, aspartic acid, asparagine, and other α -amino acids on (*R,S*)-threonine was observed (Figure 9).

3. Asparagine·H₂O

This compound (asn) crystallizes as a conglomerate in space group $P2_12_12_1$ with the structure and prismatic morphology shown in Figure 10 (56). Crystallization of (*R,S*)-asn in the presence of each of various resolved (*S*)- α -amino acids results in the precipitation of crystals of the *R* and *S* enantiomers having different morphologies and that can be easily sorted visually (Figure 11). The crystals of (*R*)-asn preserve their habit, while the *S* crystals assume completely different habits depending on the type of additive.

Of particular interest is the induction of the {010} plates of (*S*)-asn (Figure 11*d*) by additive (*S*)-aspartic acid, for this behavior is analogous to that discussed

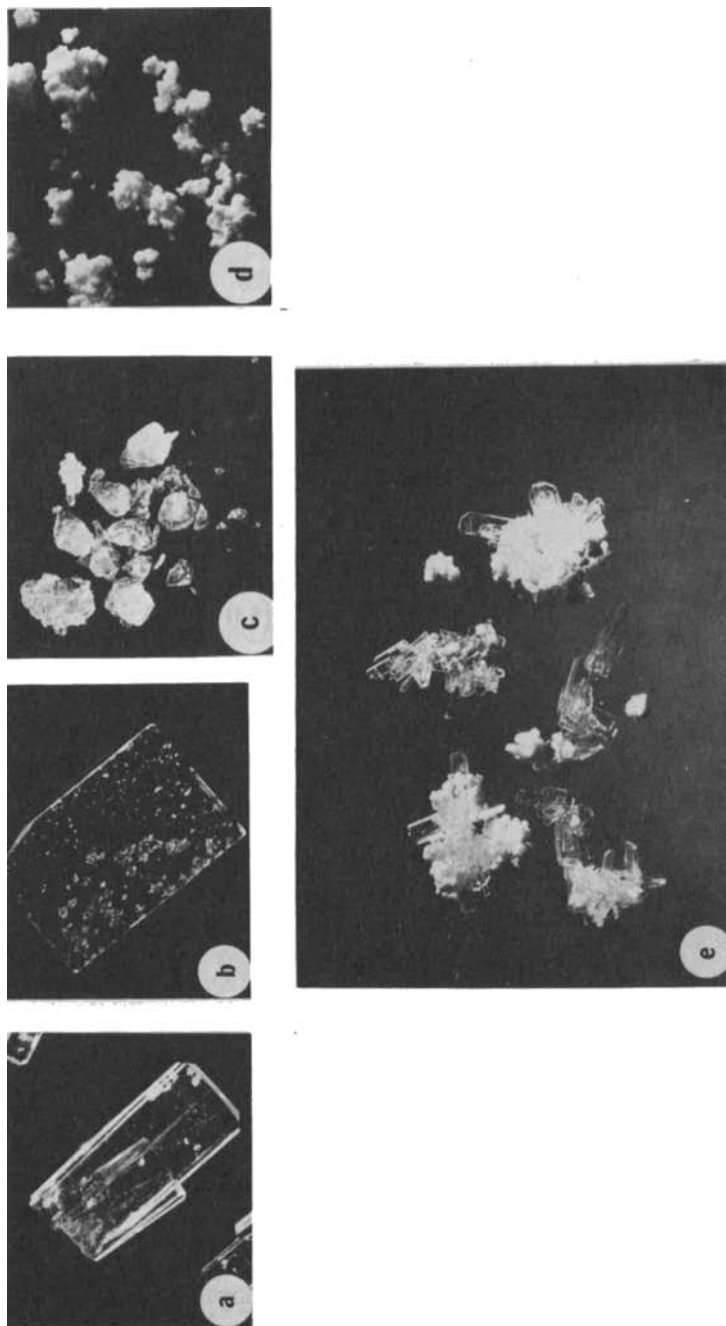


Figure 8. Crystals of (*S*)-glutamic acid·HCl. (a) Pure. (b)–(d) Grown in the presence of increasing amounts of additive (*S*)-lysine: (b) 2 mg/ml; (c) 5 mg/ml; (d) 50 mg/ml. (e) Crystals of racemic glutamic acid·HCl grown in the presence of (*S*)-lysine; the plates are the *R* enantiomer, whereas the powder is the *S*.

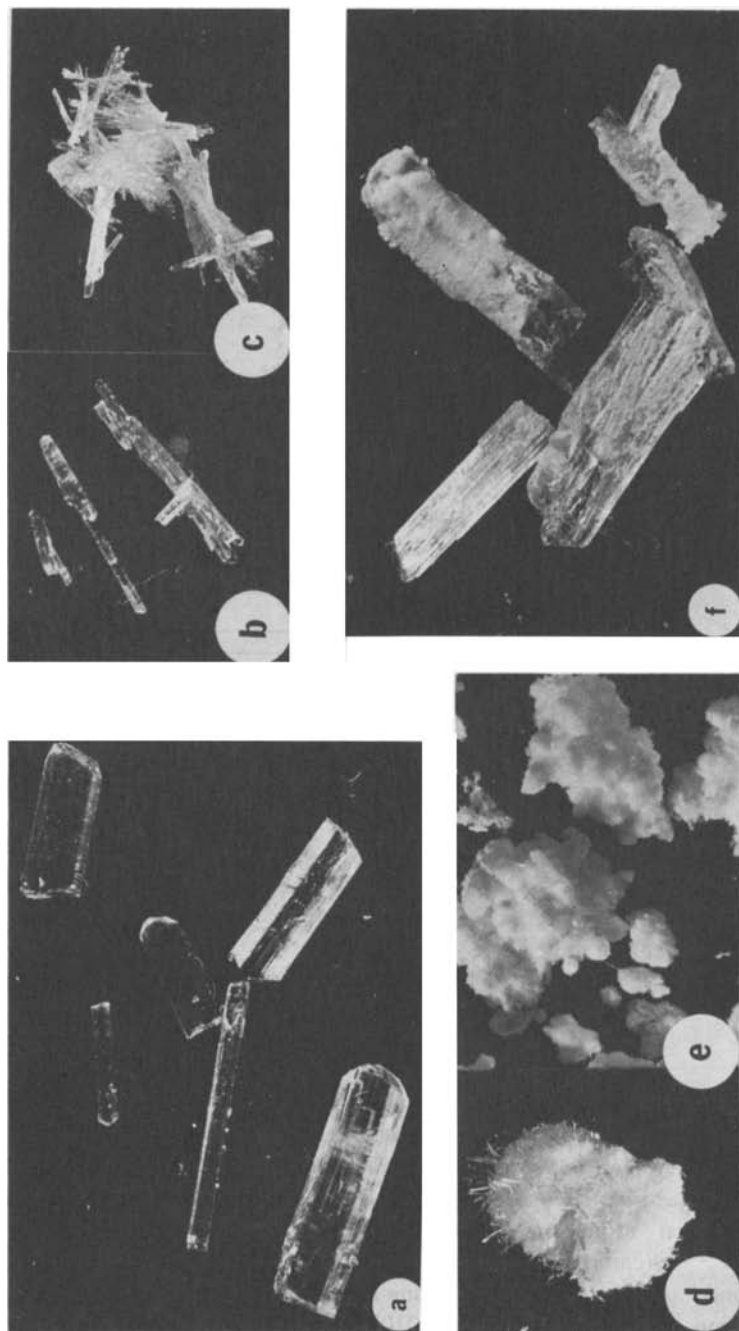


Figure 9. Crystals of (*S*)-threonine. (a) Pure. (b)–(e) Grown in the presence of increasing amounts of (*S*)-glutamic acid: (b) 2.5 mg/ml; (c) 7.5 mg/ml; (d) 15 mg/ml; (e) 30 mg/ml. (f) Crystals of (*R,S*)-threonine grown in the presence of (*S*)-glutamic acid; the bars are the *R* enantiomer and the powder is the *S* enantiomer

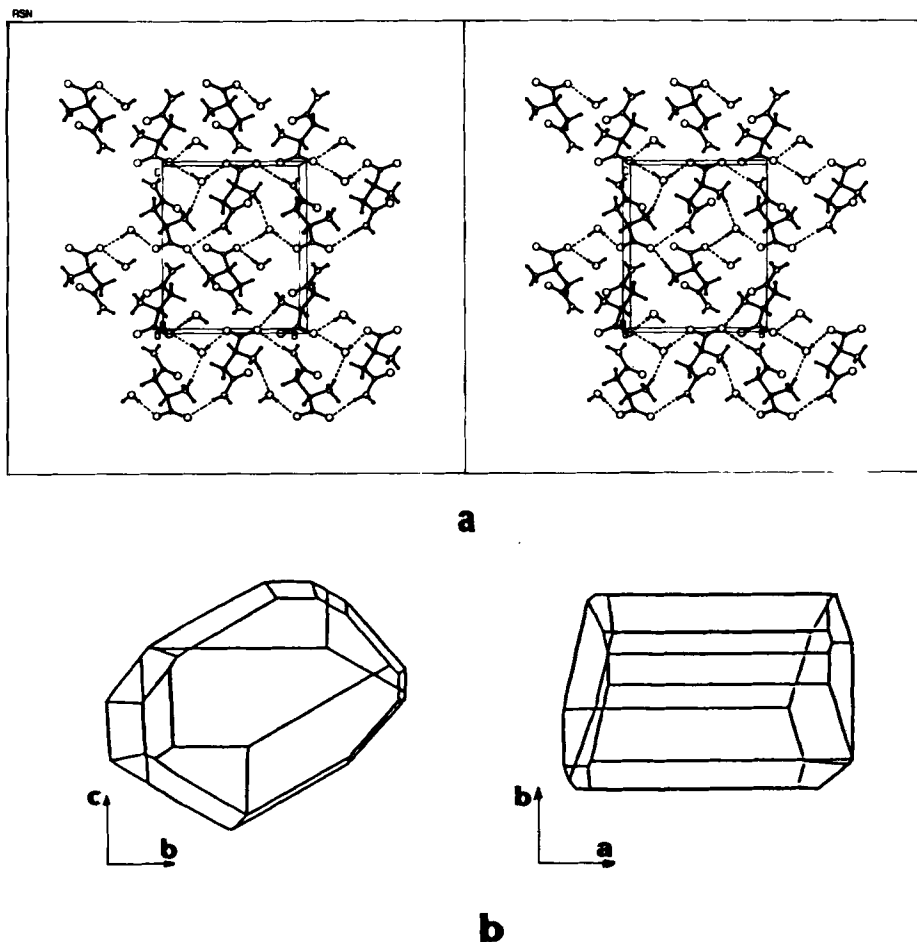


Figure 10. (a) Packing arrangement of (*S*)-asparagine·H₂O viewed along the *a* axis. (b) Morphology of the pure crystal viewed along *a* and *c*.

above involving cinnamide and benzamide grown in the presence of the corresponding carboxylic acids. Here as well, the essential structural change at the site of the additive is the substitution of one amide H atom participating in the $\text{NH} \cdots \text{O}$ (carboxylate) hydrogen bond by a lone-pair electron of the hydroxyl oxygen atom of adsorbed aspartic acid, resulting in an $\text{O}(\text{hydroxyl}) \cdots \text{O}(\text{carboxylate})$ repulsion. Since the substituted $\text{NH} \cdots \text{O}$ hydrogen bond has a main component along *b*, the resulting inhibition develops in this direction, yielding the observed {010} plates. We shall further examine

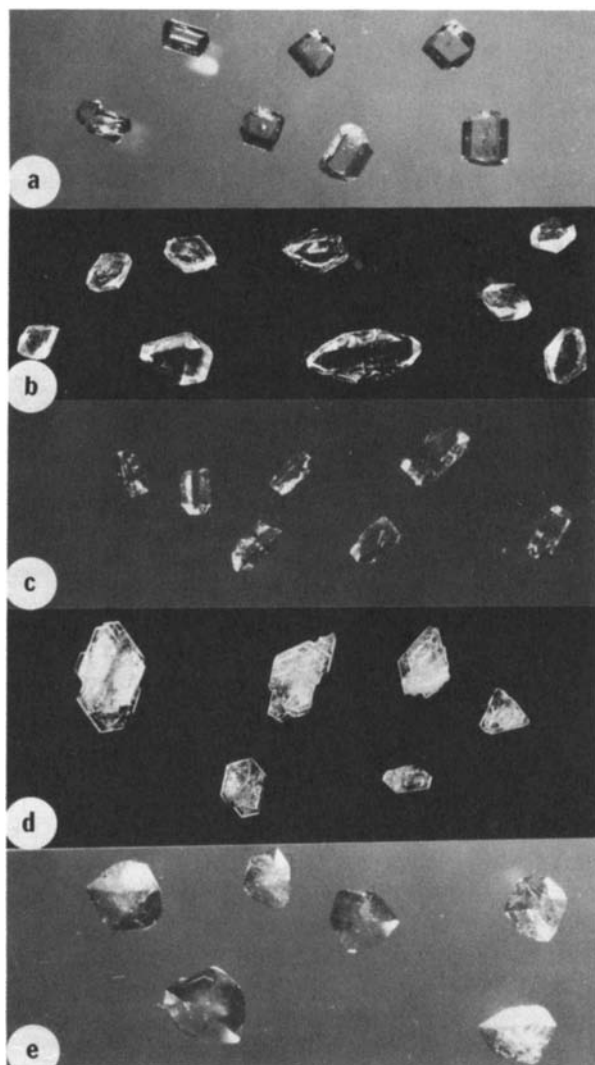


Figure 11. Crystals of (S) -asparagine· H_2O : (a) pure; (b)–(e) grown in the presence of (b) (S) -glutamine, (c) (S) -serine, (d) (S) -aspartic acid; (e) (S) -lysine. In each case the crystals were obtained from (R,S) -asn· H_2O as a mixture of R crystals displaying morphologies as in (a) and S crystals as in (b)–(e), depending on the additive.

this example in Section IV-J, which deals with the reduction in crystal symmetry due to selective adsorption of an inhibitor.

High-pressure liquid chromatographic (HPLC) analysis performed with a chiral mobile phase (57,58) confirmed in all the conglomerate systems that the *S'* inhibitors are selectively occluded only in the bulk of the *S* substrate crystals, typically in amounts of 0.5–1% (and, by symmetry, occlusion of *R'* occurs only in *R* crystals). The selective adsorption causes, furthermore, a drastic decrease in the growth (and possibly nucleation) rate of the affected enantiomer, leading to efficient kinetic resolution; various conglomerate systems have been resolved by this method (54).

4. Relative Assignment of Configuration

The ensemble of these distinct effects (selective morphological modification, selective occlusion, and kinetic resolution) provides a new method for the assignment of relative configuration of chiral molecules. The absolute configuration of the chiral inhibitor can be assigned relative to that of the crystalline enantiomorph with which it selectively interacts, or the absolute configuration of the components of the conglomerate systems can be assigned relative to those of a series of known chiral inhibitors. It is worth noting that the method is not limited to conglomerates, since the two enantiomers can be crystallized separately and in parallel in the presence of the inhibitors.

The technique is related to the quasi-racemate method of Fredga (59). The latter is based on the formation of solid solutions between similar chiral molecules that are homochiral, say *R* and *R'*, as opposed to the formation of quasi-racemates between the corresponding heterochiral molecules, *R* and *S'*. The relative properties of these mixed crystals are analyzed by phase diagrams. Fredga's method is based on intermolecular interactions inside the bulk of the mixed crystals, which are manifested by a change in the thermodynamic properties of the system. Our method is based on interactions at the surface of the growing crystals, which are manifested by kinetic effects; the constraints imposed on the geometry of the guest molecule would appear to be less strict than in the quasi-racemate method. The two techniques have common features, since in both cases one may look on the process as replacement of a "host" by a "guest" molecule at specific lattice sites in the crystal. We shall see, in fact, in Section IV-J, that the principles developed here concerning the occlusion of inhibitors through surface adsorption have a direct bearing on the nature of the solid solutions formed.

E. Crystal Dissolution in the Presence of Additives

Scientists have long recognized that partial dissolution of crystals in the presence of impurities may result in the formation of well-shaped etch pits (60–62). When crystals of calcite, for example, were partially dissolved in the

presence of (D)- or (L)-tartaric, -malic, or -lactic acids, etch pits with enantiomorphous shapes were observed (63,64).

Many attempts have been made over the years to find stereochemical correlations among the structure of a given face undergoing etching, the symmetry and geometry of the etch pit, and the structure of the etchant. Owing to the great complexity of the mechanism of etching, no simple model has evolved with which to predict etch pit formation on a molecular level. Our recent studies on crystal growth in the presence of tailor-made additives set forth a new stereochemical approach to the selection of etchants.

Growth and dissolution of crystals are considered as reciprocal processes that can be interchanged by altering the degree of saturation of the solution. It has been well established that dissolution invariably begins at sites of emerging dislocations (62). At such sites more than one type of facial surface is exposed to the solvent (Scheme 8). In the absence of additives the dissolution fronts propagate from these centers in various directions at the same relative rates as for their growth. Under such circumstances the overall shape of the crystal is almost preserved. On the other hand, when an additive that binds selectively to a given face of the crystal is present in the solution, the crystal dissolves in different directions at rates that differ from those in the pure solvent (in Scheme 8, dots represent adsorbed additive). In particular, the rate of dissolution in a direction perpendicular to the affected face decreases relative to that of the unaffected faces. Subsequently, etch pits are formed at the dislocation centers on the former faces (Scheme 8). The generality of this stereochemical correlation was tested for a number of substrate crystals, including *E*-cinnamide, *asn*·H₂O, and *glu*·HCl. Here we shall illustrate this principle for the enantiomorphous crystals of *asn*·H₂O, as etched by aspartic acid and *N*-methylasparagine (65).

The etching of an enantiomorphous pair of *asn* crystals in the presence of (*R*)-aspartic acid and (*R*)-*N*-methylasparagine is illustrated in Figure 12. Under these conditions, only the *R* crystals are etched (Figure 12a), whereas the *S* crystals dissolve smoothly (Figure 12b). The dramatic differences in the surfaces of the two enantiomorphous crystals after dissolution again make it possible to perform a manual "Pasteur-type" sorting of the *R* and *S* crystals with a quantitative enantiomeric yield.

We mentioned above that aspartic acid binds only to those crystal faces that allow its modified moiety, the hydroxyl oxygen atom, to emerge from the crystal surface, that is, the {010} faces. As expected, partial dissolution of (*R*)-*asn*·H₂O



Scheme 8

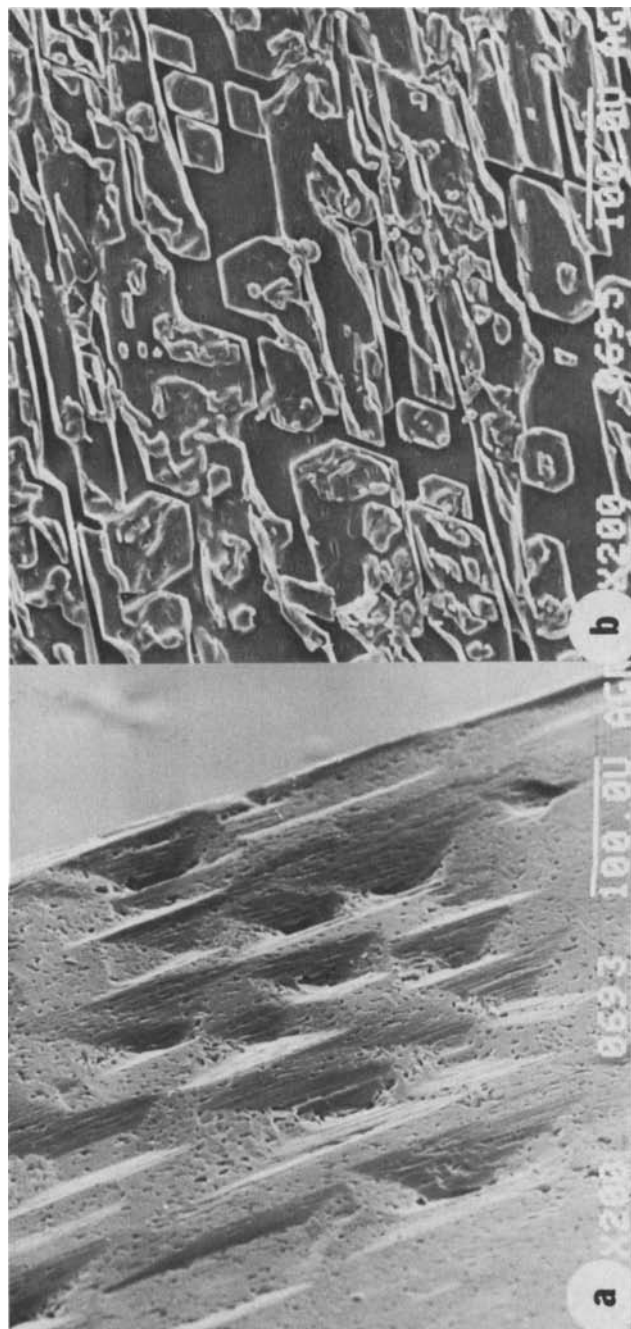


Figure 12. (a), (b) Scanning electron micrographs of the (010) faces of crystals of asparagine- H_2O partially dissolved in the presence of (*S*)-aspartic acid: (a) (*S*)-asparagine crystal; (b) (*R*)-asparagine crystal.

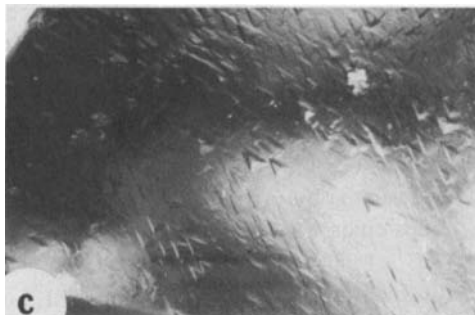


Figure 12 (continued) (c) Optical micrograph of the (101) face of a crystal of (*R*)-asparagine etched by (*R*)-*N*-methylasparagine.

crystals in the presence of (*R*)-aspartic acid yielded etch pits at these faces only.

A similar analysis suggested that *N*-methylasparagine may induce etching on the {101} faces of asn. The *N*-methyl group, in the commonly observed $\text{O}=\text{C}-\text{N}-\text{CH}_3$ synplanar conformation (50) (see 3), would replace that *N*-H group of asn that is aligned almost perpendicular to the {101} face. Indeed, particularly distinct etch pits, shaped as asymmetric scalene triangles, are formed on these faces (Figure 12c). The etch figures on the (101) and (10 $\bar{1}$) faces are related to each other by twofold symmetry about the *a* axis.

F. Assignment of the Absolute Configuration of a Chiral Crystal Containing a Polar Axis

1. Modeling Additive Effects on Polar Crystal Growth

Having established the basic mechanism of interaction between tailor-made additives and crystal surfaces, we return now to the original problem of direct assignment of the absolute configuration of a chiral molecule. We shall first examine how to establish by such means the orientation of a chiral molecule in a chiral crystal.

Broadly speaking, chiral space groups may be divided into two classes: those that contain polar axes, for example, the commonly observed space groups $P2_1$ and $C2$; and those that do not, such as $P2_12_12_1$. Crystal structures belonging to the latter class contain polar directions, but these do not coincide with the crystal axes. We shall focus on chiral crystals containing polar axes, although the method can in principle be applied to all chiral crystals.

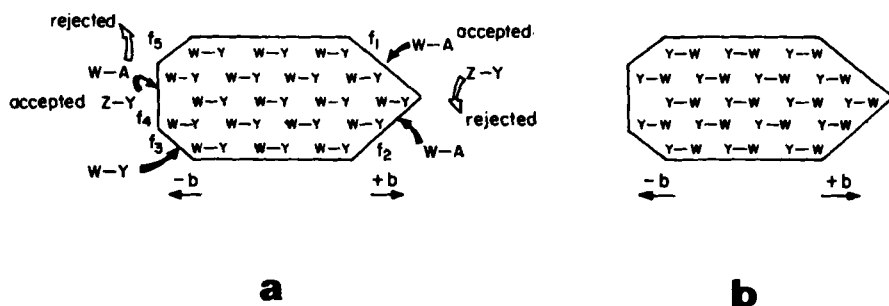
Consider for this purpose a chiral molecule, represented schematically as W-Y, packing in a crystal such that the vector W-Y tends to be parallel to the polar axis (66). (For the chiral space groups that do not contain polar axes, the

vector W-Y would need be parallel to any polar direction in the crystal, e.g., along the body diagonal $a + b + c$ in space group $P2_12_12_1$.) The crystal model is depicted in Scheme 9 for a structure appearing in the space group $P2_1$. By virtue of the crystal (point) symmetry, 2, the faces within each pair (f_1, f_2) and (f_3, f_5) are related by twofold symmetry. The polar nature of the crystal precludes a symmetry relationship between the $+b$ and the $-b$ directions. Thus, the pair of faces (f_1, f_2) cannot be related by symmetry to the pair (f_3, f_5). Notice that in this crystal, only Y groups emerge at faces f_1 and f_2 , whereas W groups emerge at faces f_3, f_4 , and f_5 .

The essence of the problem, as pointed out in Section II, is that conventional X-ray diffraction does not provide information as to whether the molecule W-Y points in the $+b$ or in the $-b$ direction. In other words, it does not allow one to distinguish between the real crystal (Scheme 9a) and the hypothetical enantiomeric structure in which the orientation of W-Y with respect to the b axis is opposite (Scheme 9b).

Applying the two-stage adsorption-inhibition mechanism described above, appropriate additives W-A or Z-Y can be selected to influence asymmetrically the growth rate of the crystal along the polar b axis. An additive W-A will bind to faces f_1 and f_2 , but not to f_3, f_4 , and f_5 , and once bound will hinder growth along $+b$, and possibly in other directions, but not along $-b$ in the real crystal of Scheme 9a (the opposite would happen in the crystal of Scheme 9b). We then expect that on addition of the tailor-made additive, the relative rates of growth in the $+b$ and $-b$ directions will change substantially and that this will be revealed by selective morphological changes.

The morphological differences between crystals grown in the presence and absence of the additive would then indicate the direction of the substrate molecule W-Y with respect to the polar axis. Consequently, the absolute configuration of the crystal and of the chiral molecular constituents can be derived. The additive need not be chiral, and even if it is, the assignment of the absolute configuration



Scheme 9

of the crystal does not require knowledge of the absolute configuration of the additive.

We shall illustrate this approach with four examples. Two of them, lysine·HCl and *N*-(*E*-cinnamoyl)alanine, were originally chosen in order to establish the method (67). The third example, lactose, has been analyzed by Visser and Ben-nema (68) following the same approach. As for the fourth example, sucrose (36–40), we shall demonstrate that its absolute configuration may be assigned by

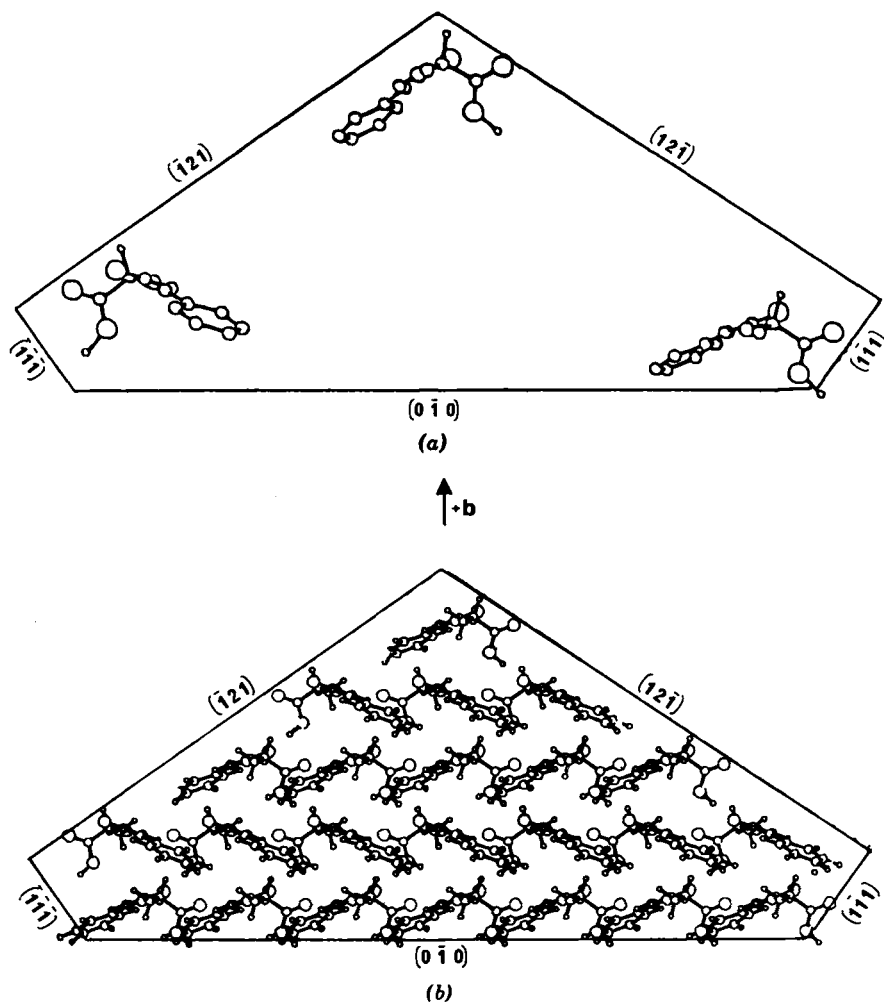


Figure 13. Packing arrangement of *N*-(*E*-cinnamoyl)-(S)-alanine delineated by the faces observed in the pure crystal: (a) for clarity, only three molecules shown; (b) complete arrangement.

analyzing results reported by sugar technologists on the morphological changes in sucrose crystals grown in the presence of di- and trisaccharide additives.

2. *N*-(*E*-Cinnamoyl)alanine

N-(*E*-Cinnamoyl)alanine (67) crystallizes in space group $P2_1$. In the crystal structure of the *S* enantiomer, all the OH groups form hydrogen bonds with a major component along $-b$, while the C(chiral)-H bond is directed along $+b$ (67). The molecular orientations with respect to the crystal faces in the pure crystal are depicted in Figure 13. We found, as expected, that the methyl ester of the substrate of the same absolute configuration induced large $\{1\bar{1}1\}$ faces (Figure 14*b*), thus fixing the absolute direction of the O-H bond with respect to the polar axis and so the absolute configuration of the substrate molecule. On the other hand, *N*-(*E*-cinnamoyl)-(*R*)-alanine of configuration opposite to that of the host, induced,

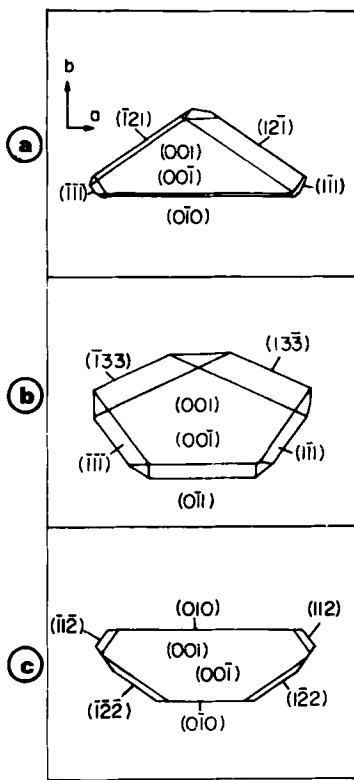


Figure 14. Computer-drawn pictures of measured crystals of *N*-(*E*-cinnamoyl)-(*S*)-alanine: (a) pure; (b) grown in the presence of the methyl ester; (c) grown in the presence of *E*-cinnamoyl-(*R*)-alanine.

as expected, formation of an (010) face (Figure 14c), because adsorption of this molecule can take place only from the $+b$ side of the crystal, since the C-methyl group of the inhibitor points away from the surface along the $+b$ direction.

3. *Lysine·HCl. Anisotropic Distribution of Occluded Additive*

(*S*)- or (*R*)-lysine·HCl crystallizes from water as a dihydrate in a monoclinic structure of space group $P2_1$. The packing arrangement delineated by the crystal faces of the pure form is shown in Figure 15. The lysine molecules are aligned parallel to the b axis, with the $^+H_3N-CH-COO^-$ moiety emerging from the $+b$ end of the crystal. The $\epsilon-NH_3^+$ points toward $-b$ and is hydrogen bonded to a molecule in a direction perpendicular to the $\{1\bar{1}0\}$ faces. Additives with a modified carboxyl or α -amino group, such as lysine methyl ester, indeed inhibited growth in the $+b$ direction, inducing development of the (010) face (Figure 16b). Conversely, additives that bear a modified side chain, such as norleucine or

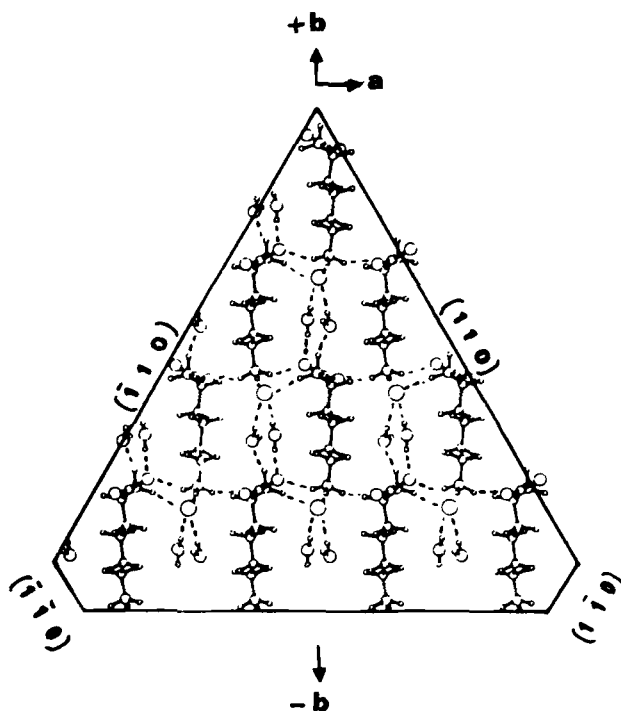


Figure 15. Packing arrangement of (*S*)-lysine·HCl·2H₂O delineated by the observed ($hk0$) crystal faces, viewed along the c axis.

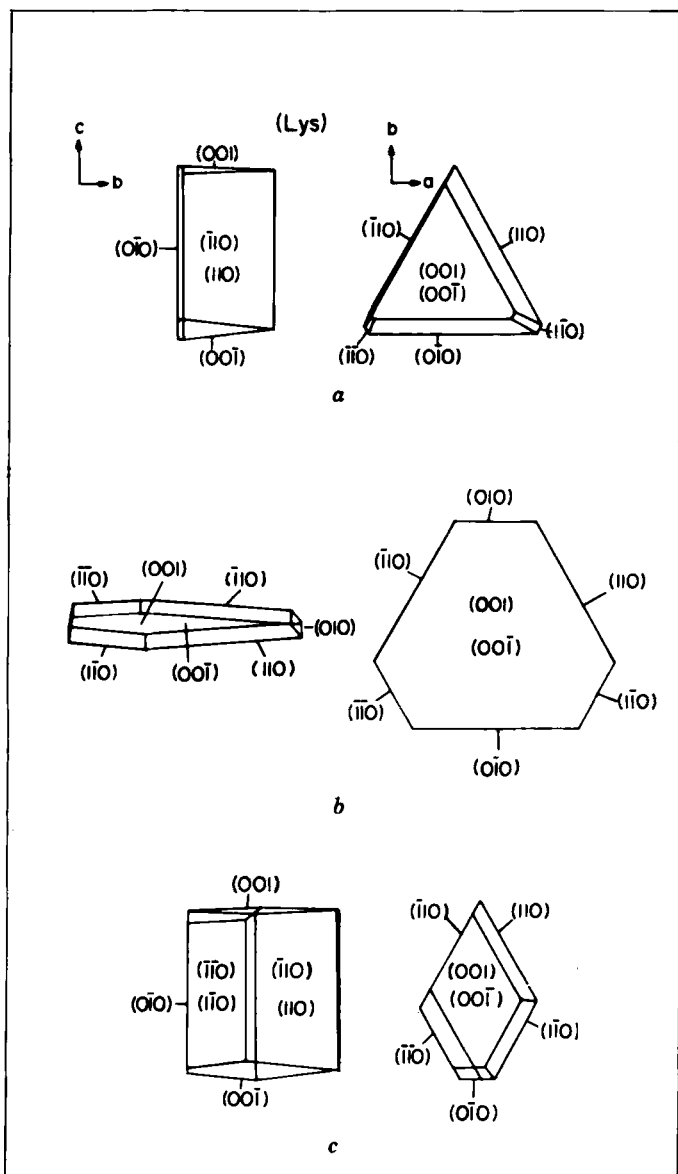


Figure 16. Morphology of measured crystals of (S) -lysine·HCl·2H₂O viewed along the a and c axes: (a) pure; (b), (c) grown in the presence of (b) (S) -lysine methyl ester, (c) (S) -norleucine.

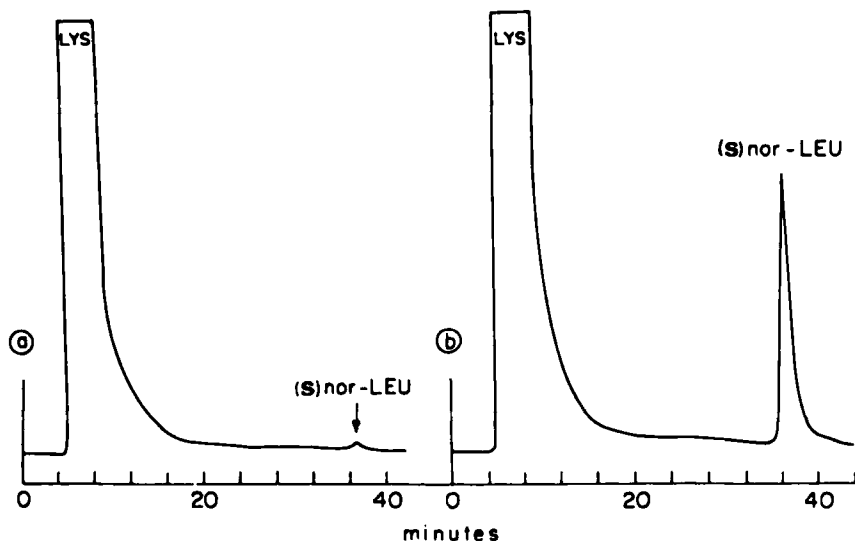


Figure 17. HPLC analysis of (*S*)-norleucine occluded in crystals of (*S*)-lysine. Material taken from (a) the $+b$ side of the crystal, (b) the $-b$ side of the crystal.

norvaline, inhibited growth along the $-b$ direction, with a concomitant pronounced increase in the areas of the $\{1\bar{1}0\}$ faces (Figure 16c), in agreement with the analysis presented above.

Assuming growth of the crystal in both directions from a nucleation center, the selective adsorption of additive molecules at one end of the polar axis implies that the additive must be occluded only in that part of the crystal that had exposed the adsorbing face to solution during growth (because additive may be occluded only through adsorbing faces). Therefore, analysis of the occluded additive at the crystal extremities along the polar b axis must reveal an anisotropic distribution. This expectation was experimentally confirmed for the crystals of (*S*)-lysine·HCl grown in the presence of (*S*)-norleucine. According to the chromatographic analysis of material taken from the $+b$ and $-b$ ends of the crystal, the additive was occluded preferentially at the $-b$ side (Figure 17).

This anisotropic distribution of the occluded additive provides a second independent method of confirming the absolute configuration assigned by means of the morphological changes, once the mechanism of adsorption is known. This principle will be met again in the growth of centrosymmetric crystals.

4. α -Lactose

The influence of β -lactose on the growth of crystals of α -lactose has recently been analyzed by Visser and Bennema (68). The α - and β -lactoses **4a** and **4b** are disaccharides composed of a galactose and an α - or β -glucose moiety linked

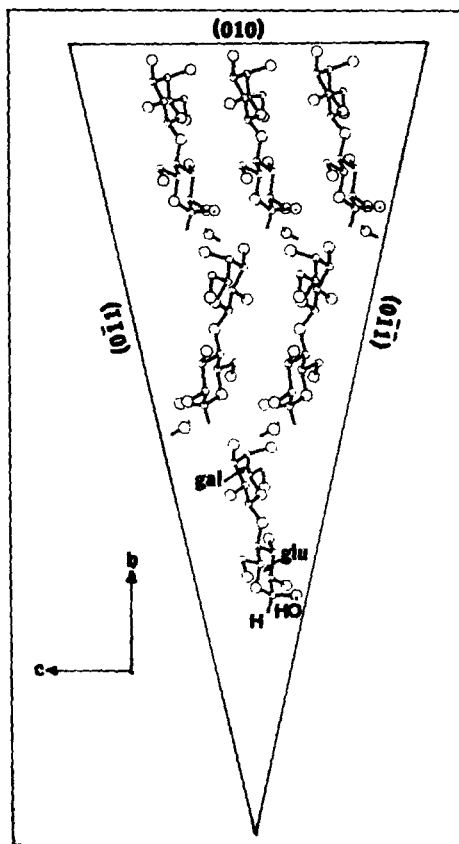
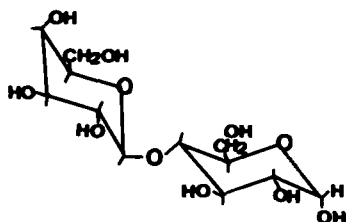
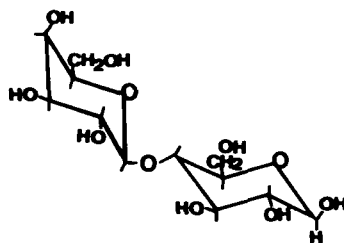


Figure 18. Packing arrangement of α -lactose monohydrate delineated by the observed crystal faces, as viewed along the a axis.

through a glycoside bond. Compounds **4a** and **4b** are anomers that interconvert spontaneously in solution. α -Lactose crystallizes from water as a monohydrate in space group $P2_1$ (Figure 18). The crystals display a characteristic tomahawk- (i.e., wedge-) shaped morphology (69), with the apex at the $-b$ end. The crystals were observed to grow only in the $+b$ direction, which was interpreted by Michaelis and van Krevelde (41) as an inhibition of growth along $-b$ by the β -anomer present in solution. These authors predicted, on this basis, the orientation of the disaccharide with respect to the polar axis, although the crystal structure (70,71) had not been determined at that time. In fact, from the crystal structure it is obvious that β -lactose can be adsorbed only at the $-b$ end of the crystal by virtue of the unmodified galactose moiety. Once adsorbed, the modified β -glucose inhibits growth perpendicular to the $\{011\}$ faces. Therefore, by fixation



4a

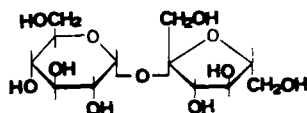


4b

of the absolute polarity of the molecule inside the crystal, its absolute configuration is assigned.

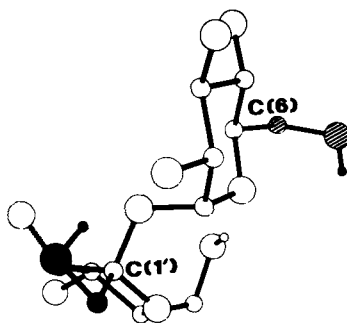
5. Sucrose

The sugar technologists Smythe (37,72), van Hook (39,40), and Mantovani (38) studied the dramatic effect of raffinose (6) on the crystal growth of sucrose (5) during the latter's extraction from molasses. They each carried out careful kinetic studies on these systems, and determined that raffinose inhibits growth at the $+b$ pole of the crystal and also along its $+c$ and $-c$ directions. These observations can be taken advantage of for direct assignment of absolute configuration. Figure 19 depicts the packing arrangement of sucrose. The structure is delineated by the various faces of the crystal; the fructose moiety emerges at the $\{0\bar{1}1\}$ faces, directed toward $-b$, whereas the glucose residue emerges at the $\{110\}$ faces. The raffinose molecule bears a sucrose moiety linked to a galactose unit through a glycoside bond at C-6 of glucose. The O-H vector of the CH_2OH group (hatched circles in 5b) attached to C-6 in sucrose points toward $-b$, the C6-C-O-C adopting a gauche conformation. The faces of the sucrose crystal to which raffinose may adhere depend on the conformation of the trisaccharide 6.



(glucose) (fructose)

5a



5b

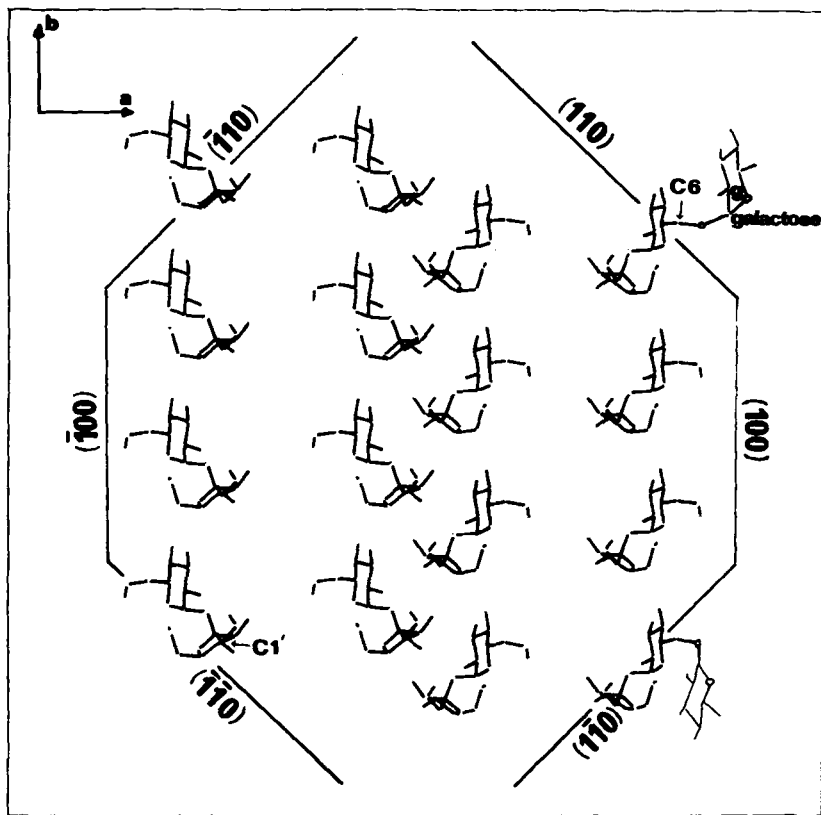
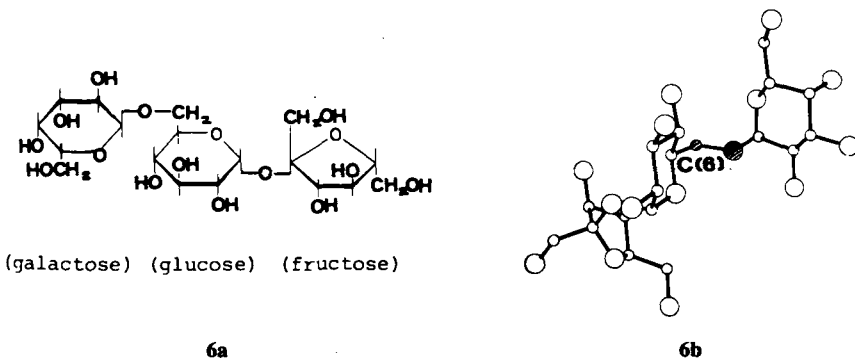


Figure 19. Packing arrangement of sucrose delineated by the observed crystal faces, as viewed along the c axis. The emerging galactose moiety of a raffinose inhibitor molecule has been inserted at the (110) face in the exo conformation. Note that the corresponding hydroxyl of sucrose adopts an endo conformation. The sugar ring inserted at the $(1\bar{1}0)$ face indicates the position that would be taken by the galactose moiety of a raffinose inhibitor molecule in the endo conformation.

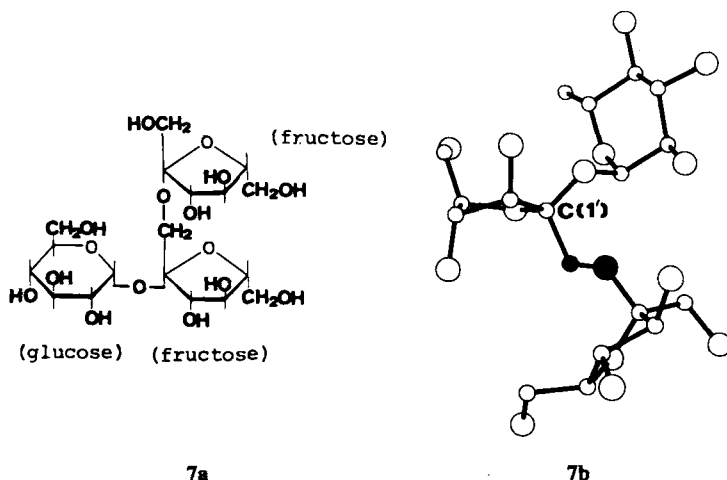
In the fully extended conformation **6b** [i.e., $C6-C-O-C(\text{galactose})$ antiplanar], raffinose may adhere only at the $\{110\}$ faces, whereas in the endo conformation [with $C6-C-O-C(\text{galactose})$ gauche], it may adhere only at the $\{1\bar{1}0\}$ faces and so impede growth along $-b$ (see Figure 19). The latter possibility would be compatible with the observed conformation of the CH_2OH group of sucrose **5b**. Van Hook demonstrated that radiolabeled occluded raffinose is adsorbed through the $\{110\}$ faces of the crystal. Kinetic studies by Smythe demonstrated that raffinose hinders growth along $+b$. From these studies one may infer that raffinose must assume conformation **6b** on the $\{110\}$ surface of the growing crystals of sucrose. Several years after these studies by van Hook



and Smythe, Jeffrey (73) demonstrated that **6b** is indeed the conformation of raffinose in its parent crystal.

Smythe (72) observed that the trisaccharide 1-kestose (**7a**), which bears an additional fructose moiety bound to C1', binds at the $-b$ pole of the crystal of sucrose. This result implies an extended antiplanar conformation (**7b**) of the group C1'-C-O-C(fructose) such that the O-C(fructose) bond (filled circles in **7b**) of the additive would point toward $-b$, away from the crystal interior. Note that, as in the sucrose-raffinose system, the C1'-C-O-H group of sucrose **5b** (filled circles) adopts a gauche conformation with the C-OH bond pointing in the $+b$ direction. It is gratifying that the necessary extended conformation of C1'-C-O-C was later demonstrated in an X-ray crystallographic study of 1-kestose **7b** (74).

Knowledge of the absolute configuration of sucrose may be used to deduce



the general conformational features of the adsorbed trisaccharide molecules **6** and **7** on sucrose crystals. Conversely, the absolute configuration of sucrose (and raffinose and kestose) could have been deduced had the stable conformations of the adsorbed inhibitors been unequivocally known at the time.

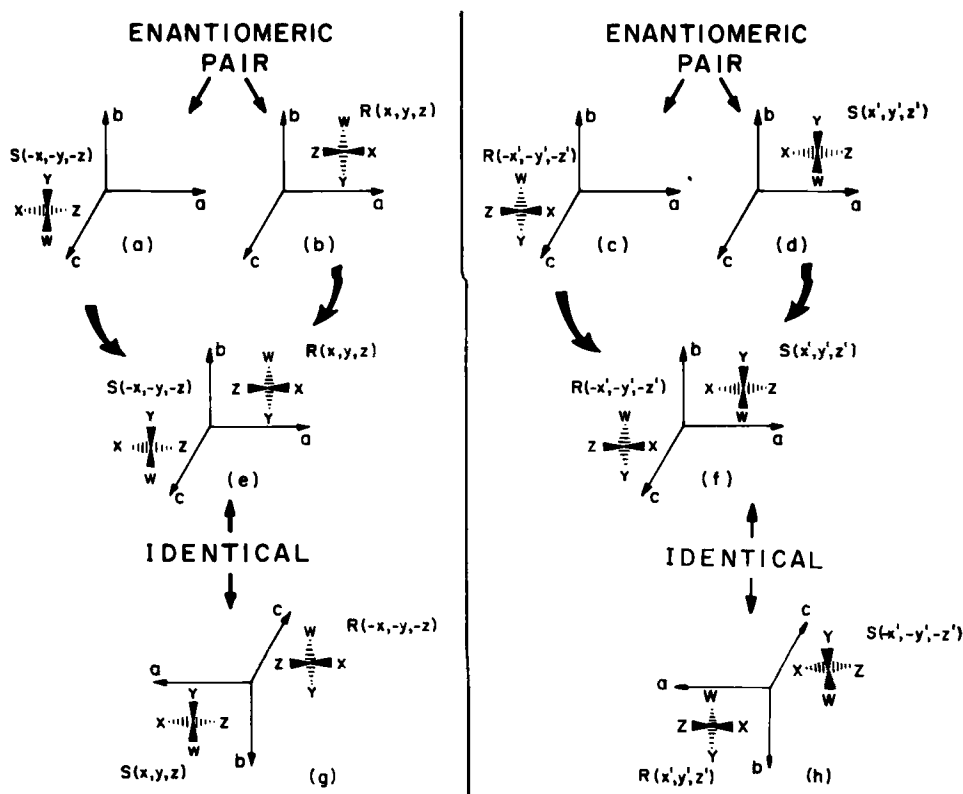
G. Assignment of Absolute Configuration Using Centrosymmetric Crystals

1. Principles

We illustrated in Section II why conventional X-ray diffraction cannot distinguish between enantiomorphous crystal structures. It has not been generally appreciated that, in contrast to the situation for chiral crystals, the orientations of the constituent molecules in centrosymmetric crystals may be unambiguously assigned with respect to the crystal axes. Thus, in principle, absolute configuration can be assigned to chiral molecules in centrosymmetric crystals. The problem, however, is how to use this information which is lost once the crystal is dissolved.

The basic difference between chiral and centrosymmetric crystals is illustrated in Scheme 10. Scheme 10*a* depicts, as in Scheme 1, a chiral molecule of configuration *S* in a chiral crystal that is specified mathematically by a set of atomic coordinates $-x_i, -y_i, -z_i$ ($i = 1, \dots, n$, for n atoms) in an axial system a, b, c chosen to be the right-handed one. The enantiomeric crystal structure (Scheme 10*b*) made up of molecules of configuration *R* is defined by a set of atoms with coordinates x_i, y_i, z_i in the original right-handed axial system. The two structures are related by an inversion through the origin. As pointed out above, conventional X-ray analysis does not allow one to specify which of the two sets of atomic coordinates describes the actual structure. Interchanging the sites of the *R* and *S* molecules, that is, transferring the *R* molecule at x_i, y_i, z_i to the *S* site, yields a set of atomic coordinates $-x'_i, -y'_i, -z'_i$ for *R* (Scheme 10*c*) that cannot be made to coincide with $-x_i, -y_i, -z_i$. The same argument holds for the *S* enantiomer (Scheme 10*d*). This would lead to different (nonisometric) arrangements; that is, the ambiguity exists between Schemes 10*a* and *b*, and *not* between 10*a* and *c*, or 10*b* and *d*.

A centrosymmetric crystal structure contains both sets of atoms with coordinates x_i, y_i, z_i and $-x_i, -y_i, -z_i$, which represent molecules *R* and *S*, respectively (Scheme 10*e*). Again, interchanging the sites of the *R* and *S* molecules results in the nonisometric structure shown in Scheme 10*f*. X-Ray diffraction can therefore not only differentiate between, but identify as well, arrangements 10*e* and 10*f*. In terms of the photographic analogy already used in Section II, the sets of left hands in Figure 20*a* and right hands in Figure 20*b* are equivalent to Schemes 10*a* and 10*b*, respectively. The centrosymmetric arrangement in



Scheme 10

Figure 20c, equivalent to Scheme 10e, is built by interleaving Figures 20a and b such that the backs of the hands are in contact. Figure 20d represents the nonisometric arrangement equivalent to scheme 10. It is obvious that the arrangements of Figure 20c and d are different.

We may describe the centrosymmetric structure in Scheme 10e in terms of the alternative, left-handed axial system by choosing the reverse vectors $-a$, $-b$, $-c$ as the axial set, as shown in Scheme 10g. The whole arrangement remains unchanged, the only difference being that the molecules S and R are now described by coordinate sets x_i, y_i, z_i and $-x_i, -y_i, -z_i$, respectively. By symmetry the same applies to the nonisometric arrangement (Schemes 10f and h).

The use of a reference axial system, whether right- or left-handed, is completely analogous to the Cahn, Ingold, and Prelog convention (75-77) regarding the specification of the absolute configuration of chiral molecules R and S as depicted in Scheme 11 for molecules with large (L), medium (M), and small

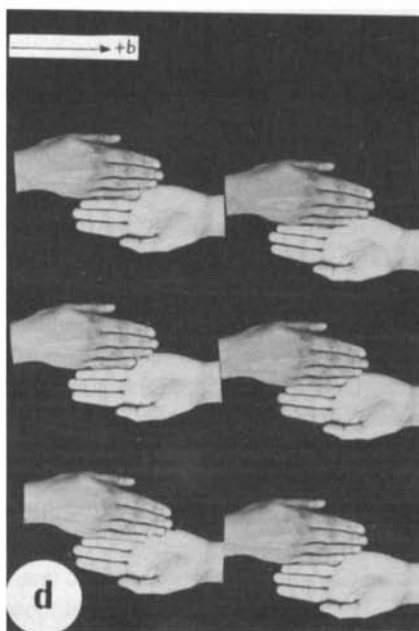
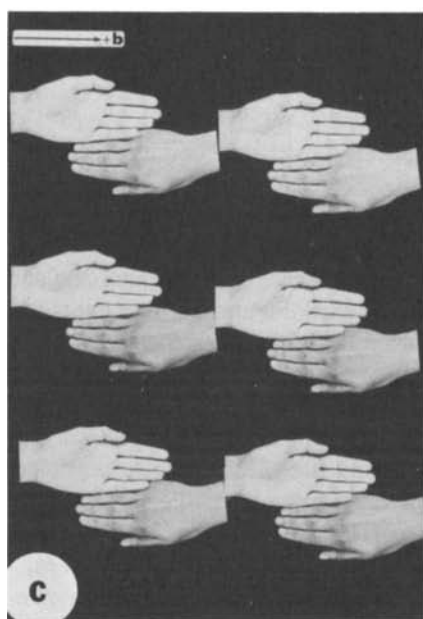
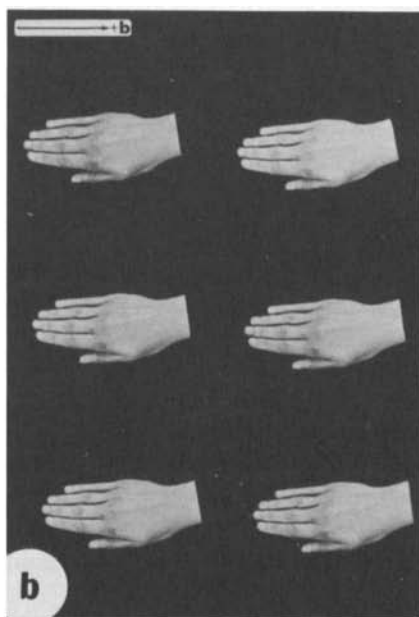
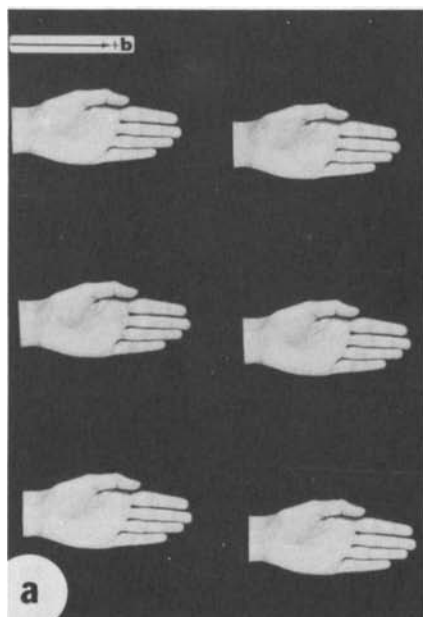
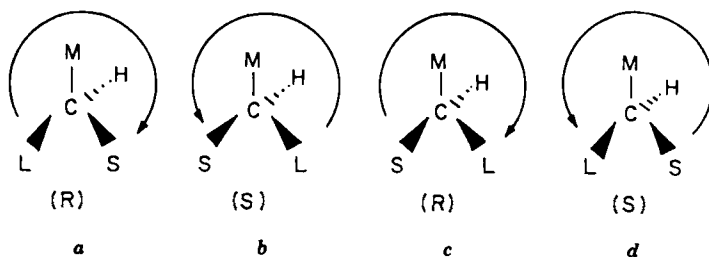


Figure 20. Sets of left and right hands arranged in lattices: (a) a set of left hands arranged in an *S* chiral crystal; (b) a set of right hands arranged in the enantiomorphous *R* chiral crystal; (c) the centrosymmetric arrangement built by interleaving (a) and (b); (d) the centrosymmetric structure nonisometric to (c) built by interchanging the left and right hands of (c) with the best possible overlap.

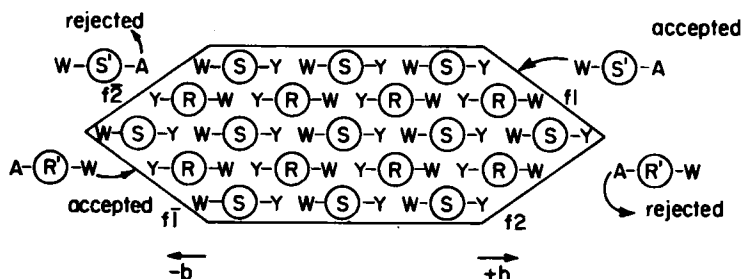


Scheme 11

(S) atoms. In both cases, the reference system does not change the three-dimensional arrangement of the groups around the chiral center. For example, if the sense of rotation had been chosen by convention to go from the small to the large atom (Schemes 11c and d), the corresponding symbols would have been reversed, but the absolute configuration of the molecule would have remained the same.

The known orientation of the two enantiomers in a centrosymmetric crystal can be directly exploited for the assignment of absolute configuration of chiral resolved molecules, provided the structural information embedded in the racemic crystal is transferred to a chiral additive molecule. The direct assignment of the absolute configuration of such resolved additives may thus be determined through the morphological changes they induce selectively in one set of the enantiotopic faces of centrosymmetric crystals with appropriate packing features.

A prerequisite for application of this method is that within the centrosymmetric racemic crystal a specific functional group attached to an *R* molecule points toward the face *f*1 but not toward *f* $\bar{1}$ (Scheme 12). By symmetry, the same functional group attached to an *S* molecule will emerge at the enantiotopic face *f* $\bar{1}$, but not at *f*1. Crystallization of a centrosymmetric crystal in the presence of a chiral additive *R'* designed so that it will fit in the site of an *R* molecule on the growing crystal faces *f* $\bar{1}$ or *f* $\bar{2}$, but not on the enantiotopic faces *f*1 or *f*2,



Scheme 12

will hinder growth in the $-b$ direction but not in the $+b$ direction (Scheme 12). By virtue of symmetry, the enantiomeric additive S' will inhibit growth of faces f_1 and f_2 , while racemic additive R',S' will inhibit growth in both directions, $+b$ and $-b$.

It is useful here to regard a centrosymmetric crystal containing chiral molecules as being enantiopolar. We define an enantiopolar crystal as comprising two enantiomeric sets of intermeshed polar crystal structures related to each other by symmetry elements of the second kind, that is, by a center of inversion or a glide plane (in Figure 20c, which is composed of the two polar arrangements in 20a and b, the fingers of all left hands point toward $+b$ and those of the right hands toward $-b$). By this classification an enantiopolar crystal may also belong to a space group that is noncentrosymmetric yet achiral. In these systems the orientation of the constituent molecules may be unequivocally defined (by conventional diffraction) with respect to some crystallographic directions, but not to all, depending on the space group (see Section IV-H).

We shall illustrate the principle here using four examples of centrosymmetric crystals: (*R,S*)-serine (45,78), *N*-acetylvaline, glycine (47), and glycyglycine (79). All four crystal structures appear in monoclinic symmetry (point symmetry $2/m$).

2. (*R,S*)-Serine

Racemic serine (80) crystallizes in space group $P2_1/a$. Within the structure (Figure 21) the $C_\beta \rightarrow H_{si}$ bond vector of the rigid methylene group of (*R*)-serine has a major component along $+b$ and, by symmetry, the $C_\beta \rightarrow H_{re}$ bond vector of the (*S*)-serine has a major component along $-b$. [We have utilized the Prelog and Helmchen nomenclature (76,77) to specify the diastereotopic C_β -H ligands.] Thus, their replacement by a methyl, as in threonine (thr), will inhibit growth in the b direction. That is, an (*R*)-thr molecule with a side-chain β -carbon of chirality *S* will inhibit growth along $+b$, while the $-CH_3$ group of (*S*)-thr will replace the H_{re} hydrogen of (*S*)-ser and hence inhibit growth along $-b$.

(*R,S*)-Serine forms tabular crystals with point symmetry $2/m$ (Figure 22a); the crystals affected by either (*R*)- or (*S*)-thr exhibit reduced morphological symmetry 2 (the mirror plane is lost) and are enantiomorphous (Figure 22b,c). When (*R,S*)-thr is used as the additive, the morphological symmetry $2/m$ is left unchanged because the effects induced by each additive separately combine. The crystals turn into rhombs, with a clear increase in the areas of the $\{011\}$ side faces relative to those of the pure crystals (Figure 22d) (45, 78).

The changes in morphology seen with the additives in Figure 22b-d with respect to that of the pure crystals (Figure 22a) can be interpreted only in terms of selective adsorption of the *R* enantiomer at faces (011) and

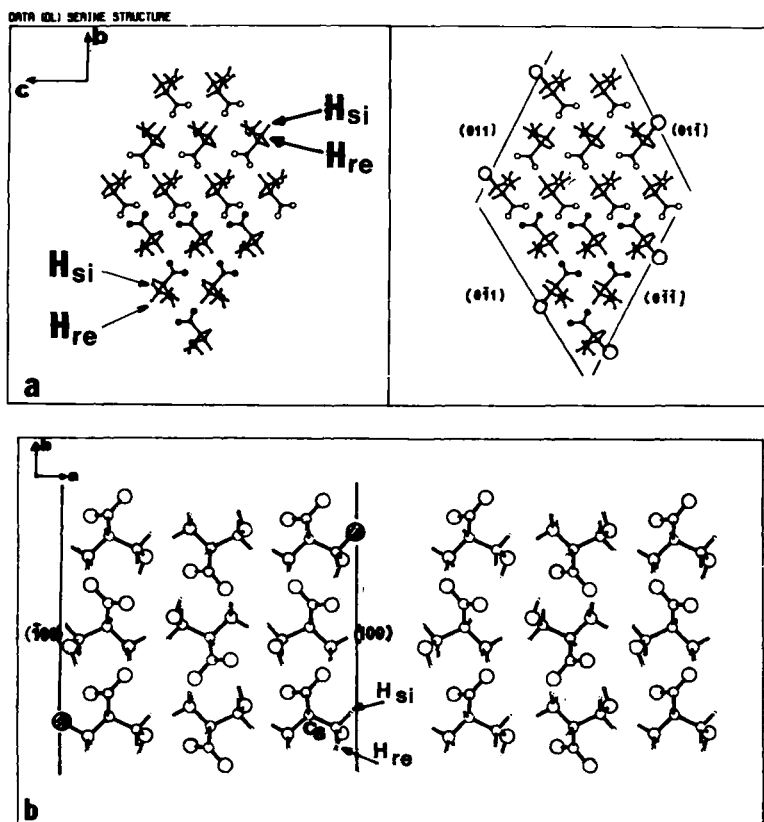


Figure 21. (a) Packing of (*R,S*)-serine viewed along the *a* axis. Each *bc* layer is composed of *R* or *S* molecules only. For clarity only half of each *R* (open circles) and *S* (filled circles) layer is shown. The positions of the four {011} faces are shown with respect to the crystal structure. Threonine additive molecules have been stereospecifically inserted, with the β -methyl groups indicated by large circles. (b) Packing of (*R,S*)-serine viewed along the *c* axis. The positions of the {100} faces are shown with respect to the crystal structure. Allothreonine additive molecules have been inserted, with the methyl groups indicated by large circles.

(01 $\bar{1}$), and of *S* at (0 $\bar{1}$ 1) and (0 $\bar{1}\bar{1}$). According to calculated surface binding energies, (*R*)-thr may easily be adsorbed only on faces (011) and (01 $\bar{1}$) and, by symmetry, (*S*)-thr only on (0 $\bar{1}$ 1) and (0 $\bar{1}\bar{1}$); indeed, threonine is better bound than even the substrate serine by 3 kcal/mol (78). These results fix the absolute chirality of the resolved threonine.

The morphological changes, and our interpretation thereof, imply that in this last experiment (*R,S*)-thr must segregate along the *b* axis during crystal growth; (*R*)-thr, being occluded through the (011) and (01 $\bar{1}$) faces, will predominate at

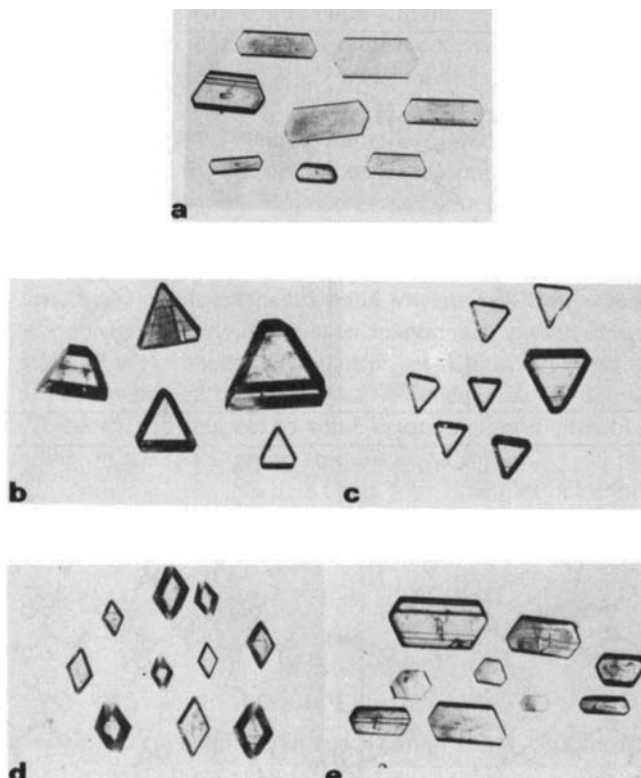


Figure 22. Photographs of (R,S) -serine crystals: (a) Pure; (b)–(d) grown in the presence of (b) (R) -threonine, (c) (S) -threonine, (d) (R,S) -threonine; (e) grown in the presence of resolved or (R,S) -allothreonine.

the $+b$ half of the crystal, whereas (S) -thr will predominate at the $-b$ half. This expectation was confirmed experimentally by HPLC analysis (Figure 23a–c), thus providing an independent means of assigning the absolute configuration of the additive.

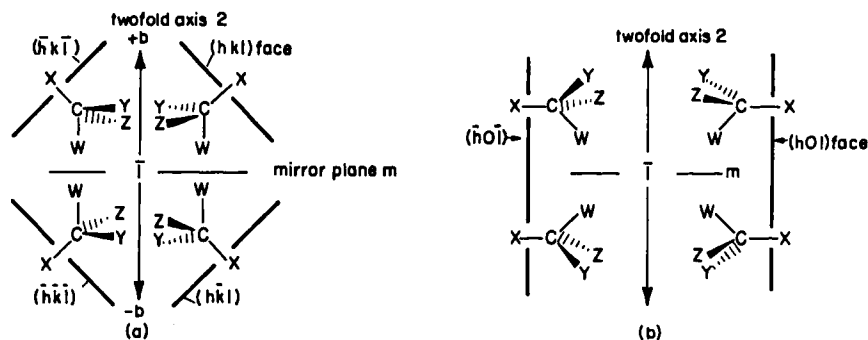
Unlike in polar crystals (Section VI-B), the anisotropic distribution of the two enantiomeric additives along an enantiopolar axis in a centrosymmetric crystal must be symmetrical, since the enantiotopic faces (81) through which they are occluded are equivalent. To assign the absolute configuration of the additive from its distribution, one needs to know only through which faces the additives are adsorbed. For example, if adsorption of racemic additive took place on the well-developed homotopic $\{100\}$ faces of serine, no enantiomeric segregation of occluded racemic additive would occur, because the R and S enantiomers would be embedded through both the (100) and $(\bar{1}00)$ faces. This behavior arises from

the point symmetry $2/m$ of the crystal. In this point group (Scheme 13a), faces related by the twofold axis 2, for example (hkl) and $(\bar{h}\bar{k}\bar{l})$, are homotopic; those related by m symmetry $[(hkl)$ and $(h\bar{k}l)]$ or by a center of symmetry $\bar{1}$ $[(hkl)$ and $(\bar{h}\bar{k}\bar{l})]$ are enantiotopic. On the other hand, the faces for which $k = 0$, that is, $(h0l)$ and $(\bar{h}0\bar{l})$, are related by both a center of inversion $\bar{1}$ and a twofold axis 2 and are thus both enantiotopic and homotopic (Scheme 13b). Therefore, both these faces must be equally affected by R and S additives.

These principles are nicely illustrated by the contrast between the serine-threonine and serine-allothreonine (allothr) systems. The relative orientation of molecular serine *vis-à-vis* its various crystal faces suggests that allothr can be adsorbed on the homotopic $\{100\}$ faces as well as on the enantiotopic $\{011\}$ faces (Figure 21).

According to the surface binding energies, (S)-allothr may be more easily adsorbed than (S)-ser on $\{100\}$ by 2 kcal/mol, and on (011) and $(0\bar{1}\bar{1})$, by 0.7 kcal/mol (78). By symmetry, (R)-allothr is adsorbed with the same relative binding energies on faces $\{100\}$, $(0\bar{1}1)$, and $(01\bar{1})$. This analysis showing that resolved and racemic allothr can each be adsorbed on the principal faces implies that no distinct morphological differences can be expected between (R,S)-ser crystals grown in the presence of resolved or racemic allothr, as was indeed observed (Figure 22e). Furthermore, the fact that (R)- and (S)-allothr are occluded primarily through the large $\{100\}$ faces should mask any enantioselective segregation along the b axis; this was confirmed by HPLC analysis of crystal tips taken from opposite ends of the b axis (Figure 23d,e).

The effect of thr and allothr on the racemic crystals of ser is further manifested independently by dissolution experiments. When rhomblike crystals of ser grown in the presence of (R,S)-thr are dissolved in the presence of (R)-thr, well-formed etch pits develop only at the (011) and $(0\bar{1}\bar{1})$ faces. By virtue of symmetry, similar etch pits form only at the $(0\bar{1}1)$ and $(01\bar{1})$ faces when (S)-thr is present



Scheme 13

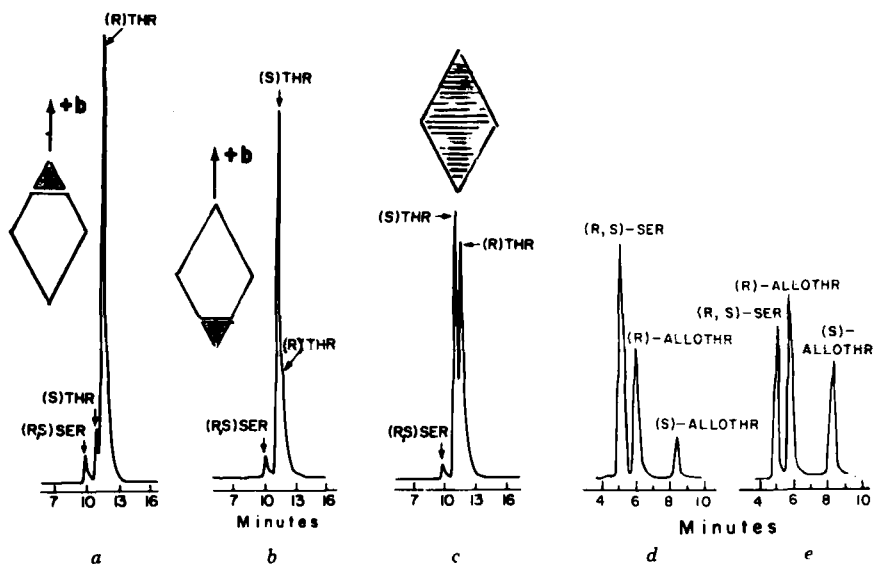


Figure 23. (a)–(c) Enantiomeric analysis of threonine occluded in the rhomblike crystals of (*R,S*)-serine, after preliminary separation of excess serine by ion exchange. Material taken from (a) tip of the crystal at the $+b$ end; (b) tip of the crystal at the $-b$ end; (c) whole crystal. (d), (e) Analysis of occluded allothreonine from the tip of the crystal at the (d) $+b$ end, (e) $-b$ end.

in the solution (Figure 24a,b). On the other hand, both resolved and racemic allothr etch the $\{100\}$ faces primarily, thus demonstrating the sensitivity of the present method (Figure 24c).

3. (*R,S*)-*N*-Acetylvaline

The crystal packing of (*R,S*)-*N*-acetylvaline (Figure 25) is also appropriate for assignment of the absolute configuration of the resolved additives, since the $C_\alpha-C_\beta$ bond is parallel to the enantiopolar b axis. In terms of this packing arrangement (82), it was predicted that the additive *N*-acetyl(phenylglycine) would inhibit crystal growth along the b axis, because once adsorbed it would be oriented so that its emerging phenyl moiety replaced the isopropyl chain of the host molecule. The crystal morphologies of pure substrate and of substrate affected by (*R*)-, (*S*)-, and racemic *N*-acetyl(phenylglycine) are shown in Figure 26. The pure form exhibits prismatic crystals with well-developed $\{100\}$, $\{001\}$, and $\{010\}$ faces. The racemic additive induces the formation of $\{010\}$ plates, which is in obvious accordance with the prediction. The resolved *R* and *S* additives induce pyramids (Figure 26b,c) with well-developed basal faces $(0\bar{1}0)$ and (010) , respectively. This result is in accordance with the fact that the $C_\alpha-C_\beta$ bond of (*R*)- and (*S*)-*N*-acetylvaline points along $-b$ and $+b$, respectively.

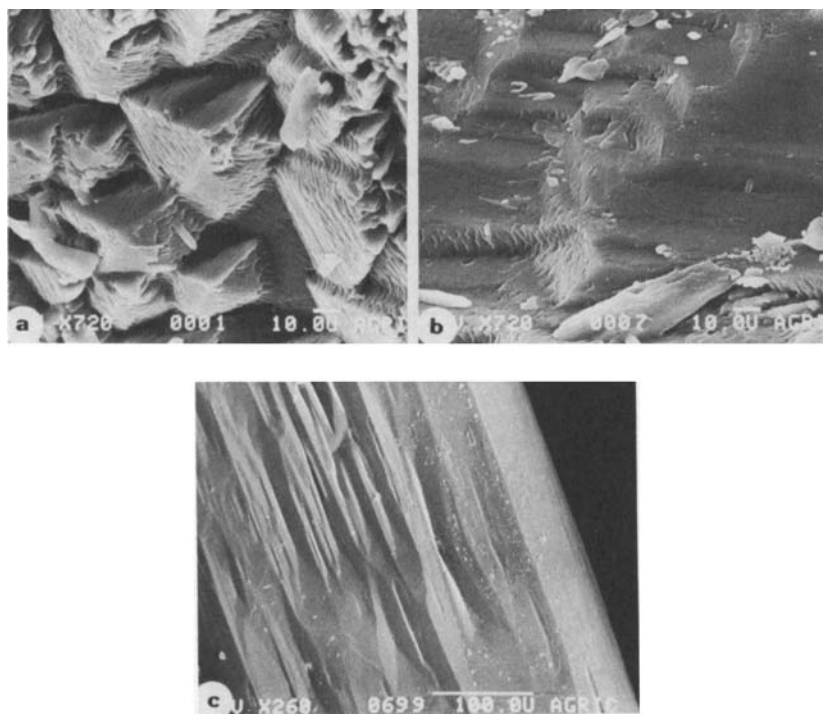


Figure 24. Scanning electron microscope pictures (magnification $\times 720$) of (*R,S*)-ser crystal faces partially dissolved in the presence of (*S*)-thr: (a) (011) face; (b) (011) faces. (c) The (100) face of a crystal of (*R,S*)-ser dissolved in the presence of (*R,S*)-allothr.

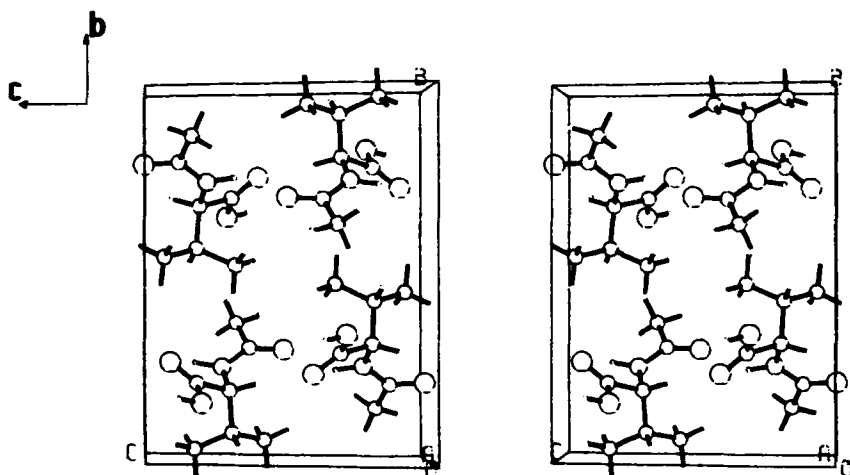


Figure 25. Packing arrangement of (*R,S*)-*N*-acetylvaline viewed along the *a* axis.

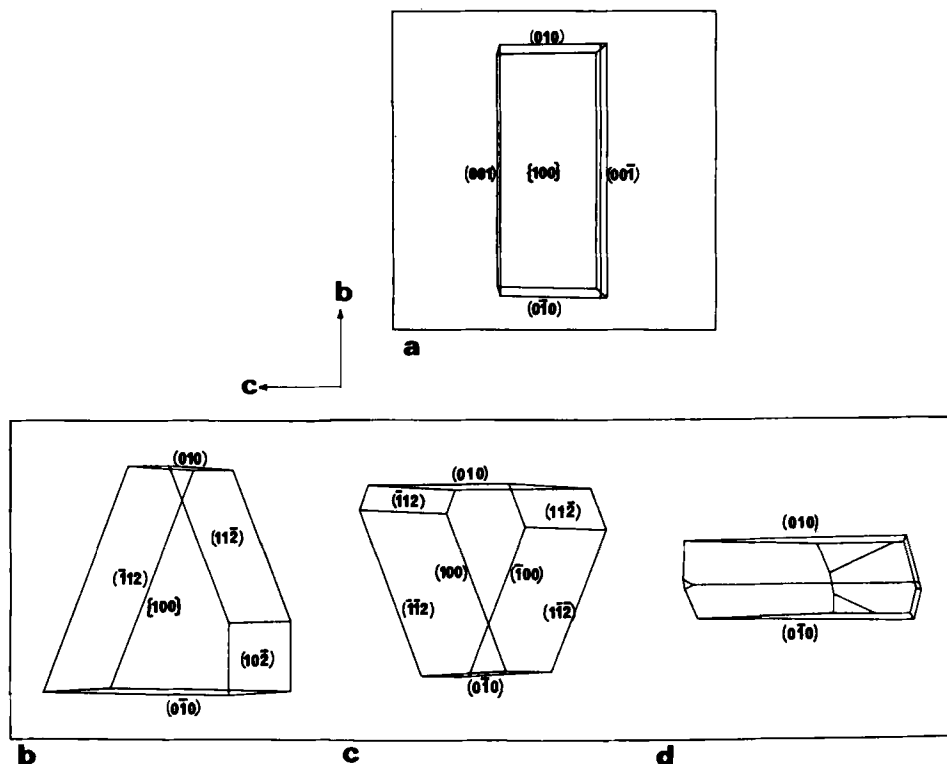


Figure 26. Morphology of measured crystals of (R,S) -*N*-acetylvaline. (a) Pure. (b–d) grown in the presence of *N*-acetylphenylglycine: (b) *R* additive; (c) *S* additive; (d) *R,S* additive.

4. Glycine

The ability of ser crystals to recognize the subtle differences between enantiotopic hydrogens suggested that the crystal of prochiral glycine (gly) may serve as a matrix for the assignment of absolute configuration of all the chiral α -amino acids (47). The glycine molecule, although achiral, has two prochiral hydrogens, H_{re} and H_{si} . In the α -form of the crystal (83), which is of space group $P2_1/n$, the gly molecules form two enantiopolar sets, 1 and 2 (Figure 27). All the molecules in set 1 have the $C-H_{re}$ bond aligned parallel to the b axis and pointing toward $+b$, so that $C-H_{re}$ emerges from the (010) face, while $C-H_{si}$ lies almost perpendicular to it in the ac molecular layer. Only an amino acid additive of chirality *R*, whose side chain will be parallel to the $C-H_{re}$ bond, can be adsorbed at the (010) face and subsequently hinder the crystal growth perpendicular to it. An *S* amino acid cannot be adsorbed on this face, because the side chain would

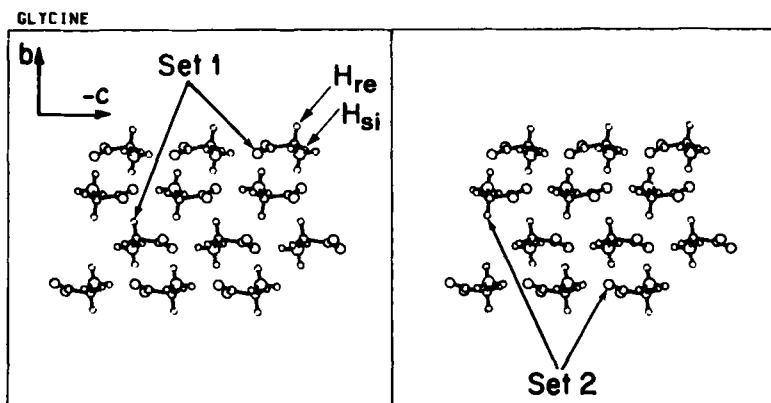


Figure 27. Packing arrangement of the α -form of glycine, viewed along the a axis. The layer of molecules in set 1 has the C-H (*re*) bond directed along $+b$; in set 2 the equivalent C-H (*si*) bond is directed along $-b$.

lie in the ac plane and create severe steric hindrance. By virtue of symmetry, an S amino acid can be adsorbed only at the $(0\bar{1}0)$ face.

Pure gly crystallizes from water in the form of bipyramids, with the b axis perpendicular to the base of the pyramid (Figure 28a). All natural S amino acids other than proline induce a dramatic morphological change at the $-b$ side of the crystals, causing the resultant pyramids to exhibit a predominant $(0\bar{1}0)$ face (Figure 28c). All R amino acids induce the development of a large (010) face (Figure 28b), whereas a racemic additive causes crystallization of $\{010\}$ plates (Figure 28d). The morphological changes can therefore be unambiguously correlated with the absolute configurations of the resolved additives.

α -Amino acid additives ranging in concentration from 0.02 to 0.2% were found in the bulk of the gly crystals. Analysis of these α -amino acids occluded inside single platelike crystals of gly by HPLC demonstrated a total enantioselective segregation along the b axis (Figure 29); as expected, the R amino acids predominated at the $+b$ half of the crystal and the S amino acids at the $-b$ half. As in the case of ser described above, this segregation and dissolution experiments (described below) provide additional independent proof of the validity of the assignments of the absolute configurations of the α -amino acids.

When platelike crystals of gly with well-developed $\{010\}$ faces were partially dissolved in solvents containing variable amounts of resolved R α -amino acids, well-defined etch pits were formed only on the (010) face (Figure 30a). These pits exhibited twofold morphological symmetry with surface edges parallel to the a and c axes of the crystal. The enantiotopic $(0\bar{1}0)$ face dissolved smoothly (Figure 30b), exactly as it does when the crystal is dissolved in a solution of pure gly. As expected, S amino acids induced etch pits on the $(0\bar{1}0)$ face. Racemic

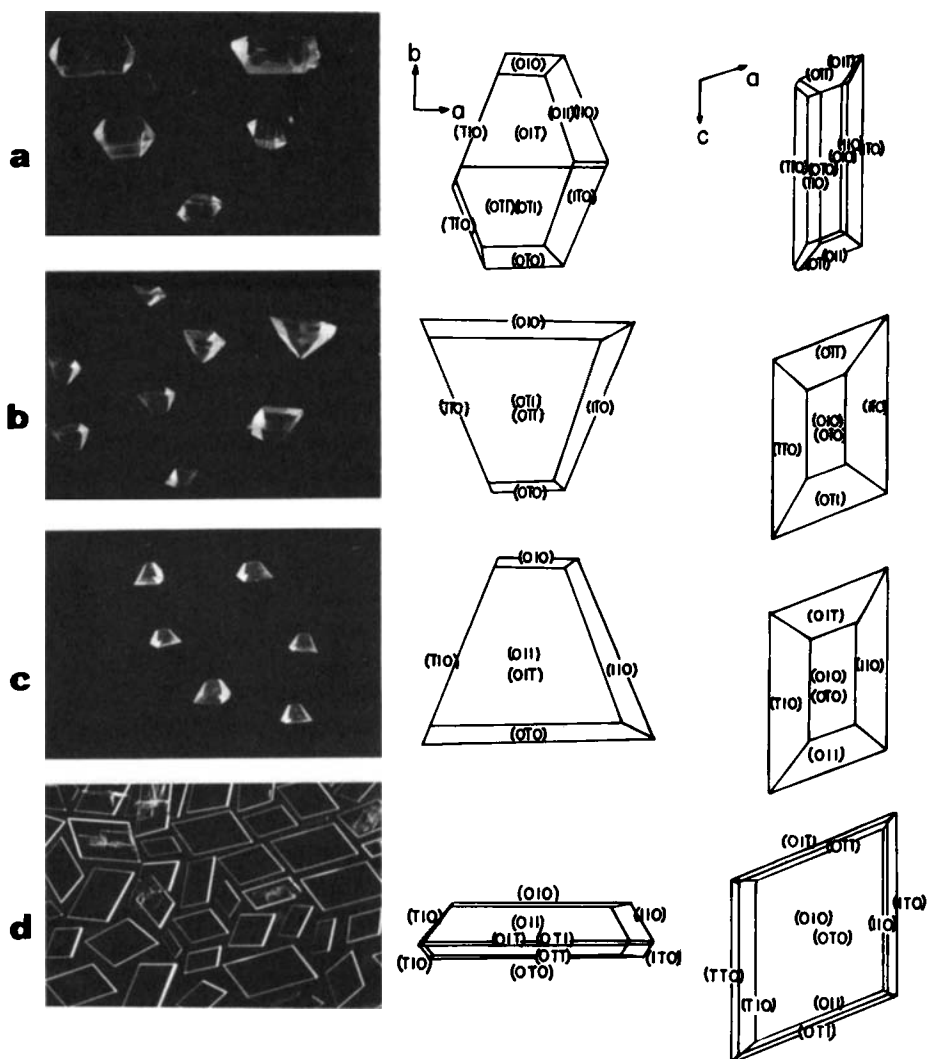


Figure 28. Morphologies of glycine crystals: (a) pure; (b)–(d) grown in the presence of (b) R , (c) S , (d) R, S α -amino acids.

amino acids etched both the (010) and $(0\bar{1}0)$ faces. The special properties of gly, namely its ability to occlude R and S amino acids at the opposite sides of the plate crystals with total enantioselectivity, were further exploited for a new model of generation and amplification of optical activity in closed systems (84).

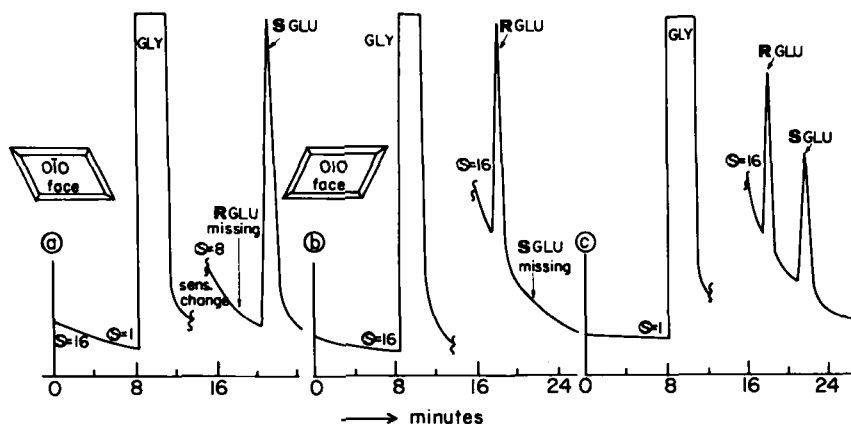


Figure 29. Enantiomeric distribution of (*R,S*)-glutamic acid occluded in {010} platelike crystals of glycine, as measured by HPLC: (a) material shaved from the (0 $\bar{1}$ 0) face of the crystal; (b) material shaved from the (010) face; (c) whole crystal.

5. Glycylglycine

This dipeptide (gly-gly) provides another example in which a prochiral molecule can be used to assign the absolute configurations of resolved additives (79). Glycylglycine appears in the monoclinic space group $P2_1/c$. In the crystal structure (85) (Figure 31), the two methylene hydrogens at the glycine side of the molecule are clearly different; the $C_\alpha-H_{Si}$ bond of the labeled molecule

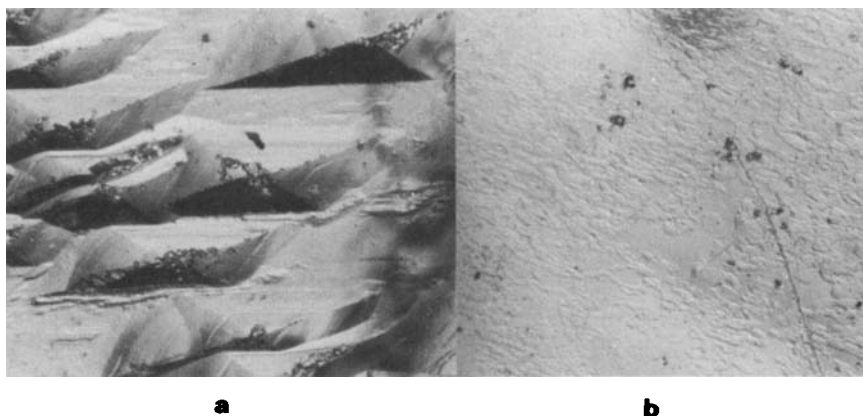


Figure 30. Optical microscope pictures of the {010} faces of a glycine crystal after partial dissolution in the presence of (*R*)-alanine: (a) (010) face; (b) (0 $\bar{1}$ 0) face.

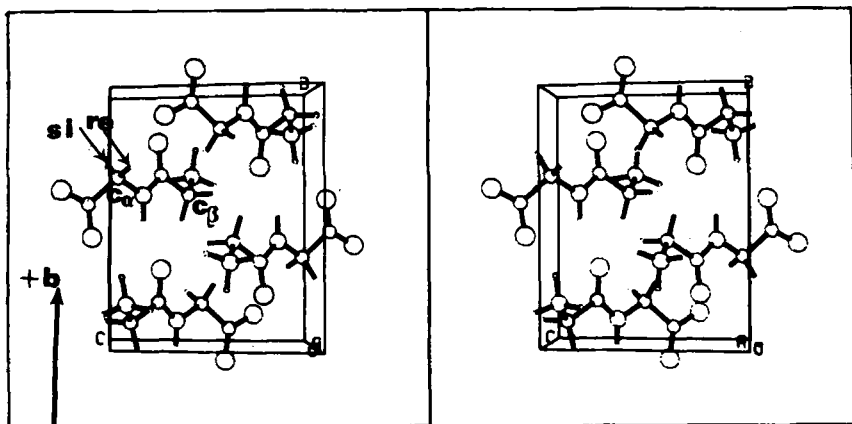


Figure 31. Packing arrangement of gly-gly viewed along the a axis.

is eclipsed with respect to both $\text{C}=\text{O}(\text{amide})$ and $\text{C}=\text{O}(\text{carboxylate})$, while $\text{C}_\alpha\text{--H}_{\text{re}}$ is gauche. Naturally, in a molecule related to this one by a center of inversion, $\text{C}_\alpha\text{--H}_{\text{re}}$ is eclipsed and $\text{C}_\alpha\text{--H}_{\text{si}}$ is gauche. Intramolecular energy calculations (79) were performed for derivatives of gly-gly in which either of the two methylene hydrogens of $\text{C}_\alpha\text{H}_2$ was replaced by a bulky group X. These calculations definitely favor substitution at $\text{C}_\alpha\text{--H}$ gauche, because it involves less steric hindrance. Thus, only H_{re} of the labeled gly-gly molecule can be substituted by the side chain of a glycyl-(*R*)- α -amino acid additive [and by symmetry, only H_{si} of the centrosymmetrically related gly-gly molecule by the side chain of a glycyl-(*S*)- α -amino additive]. The $\text{C}_\alpha\text{--H}_{\text{re}}$ bond has a component, albeit small, along $+b$. The most stable conformation calculated for an adsorbed glycyl-(*R*)-leucine [gly-(*R*)-leu] additive is such that the bulky *sec*-butyl substituent is directed mainly along $+b$, thus allowing assignment of the absolute configuration of the leucine moiety.

Crystals of pure gly-gly are diamond-shaped $\{100\}$ plates (Figure 32a). When grown in the presence of gly-(*R*)-leu, gly-(*S*)-leu, or racemic gly-leu, gly-gly crystals display the habits shown in Figure 32b, c, and d, respectively. Gly-(*R*)-leu induces formation of the $(\bar{1}21)$ and $(12\bar{1})$ faces. By symmetry, gly-(*S*)-leu induces the formation of the enantiotopic faces $(\bar{1}2\bar{1})$ and $(1\bar{2}1)$. The racemic additive yields crystals displaying all four $\{121\}$ faces. Once again, as expected, in such crystals the occluded additives gly-(*R*)-leu and gly-(*S*)-leu are segregated along the b axis, with the former occluded in the $+b$ half of the crystal and the latter in the $-b$ half (Figure 33).

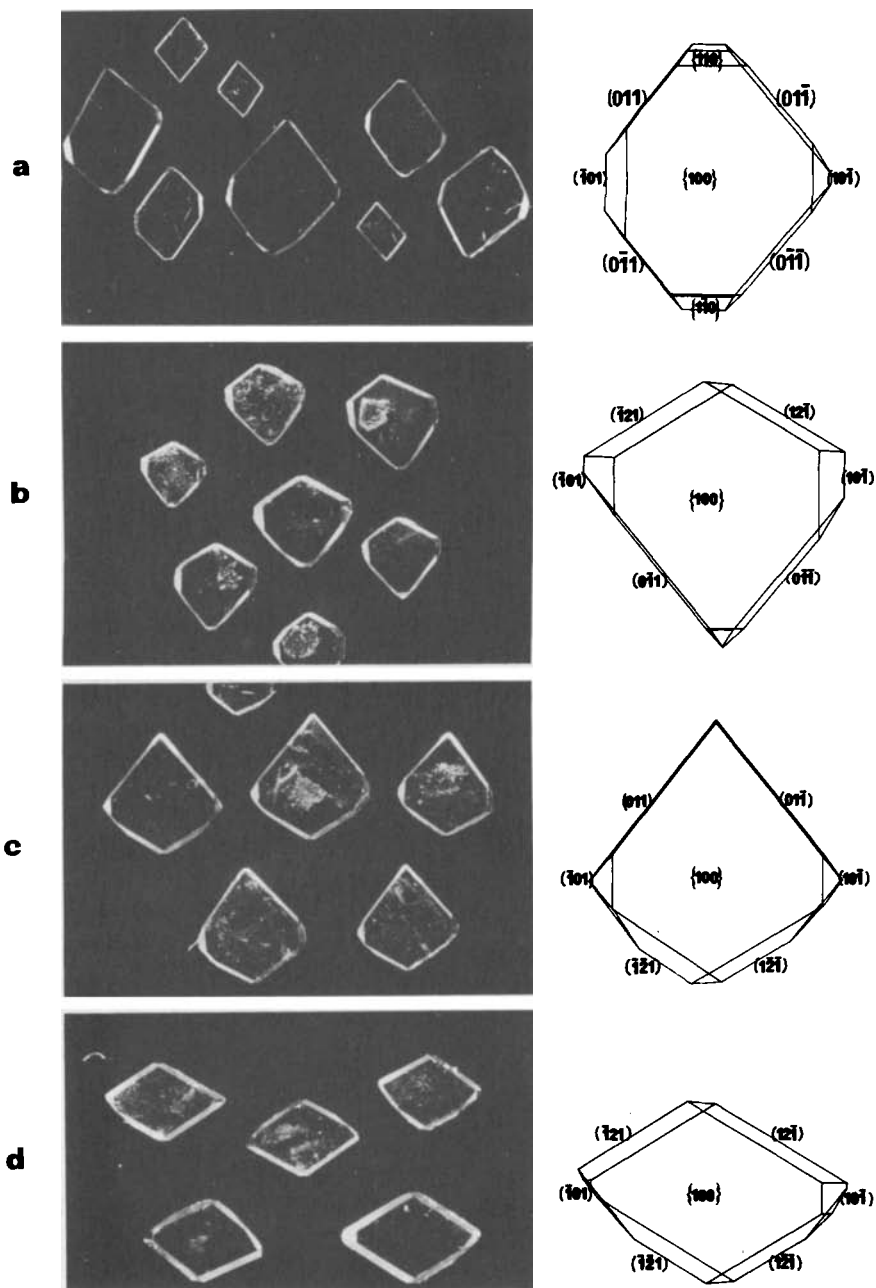


Figure 32. Morphologies of gly-gly crystals: (a) pure; (b)–(d) grown in the presence of (b) gly-(*R*)-leu, (c) gly-(*S*)-leu, (d) gly-(*R,S*)-leu.

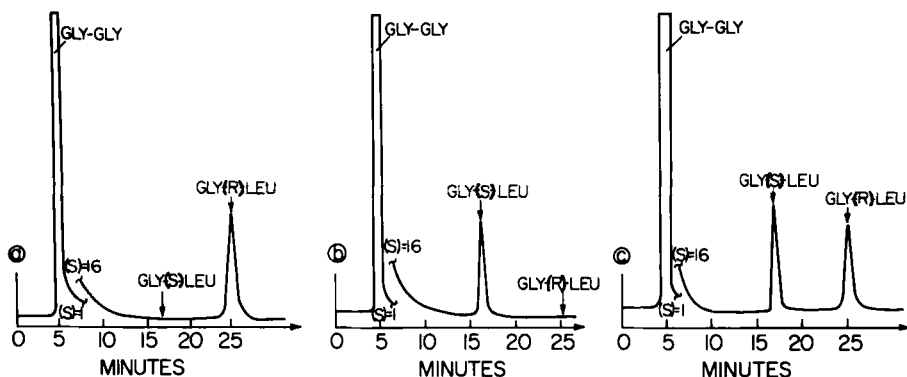
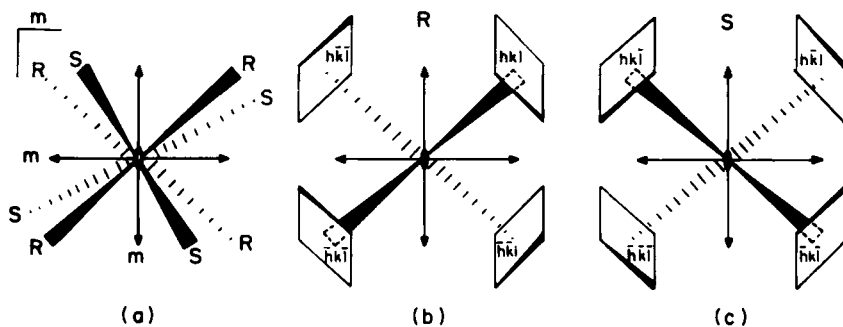


Figure 33. HPLC enantiomeric analysis of gly-leu occluded in crystals of gly-gly. Material taken from (a) tip of the crystal at the $+b$ end, (b) tip of the same crystal at the $-b$ end, (c) whole crystal.

6. Centrosymmetric Orthorhombic Crystals

The above systems, serine, *N*-acetylvaline, glycine, and glycylglycine, all belong to monoclinic space groups of point symmetry $2/m$. In principle, this method of assigning absolute configuration may also be applied to orthorhombic crystals of point symmetry $2/m\ 2/m\ 2/m$, provided that the to-be-modified functional groups tend to be directed toward the body diagonal of the crystal (Scheme 14a). In this case, the two enantiomers form two enantiopolar sets (of point symmetry 222), represented separately in Schemes 14b and c. An R' additive would affect the faces shown in Scheme 14b, and an S' additive the enantiopolar set (Scheme 14c).



Scheme 14

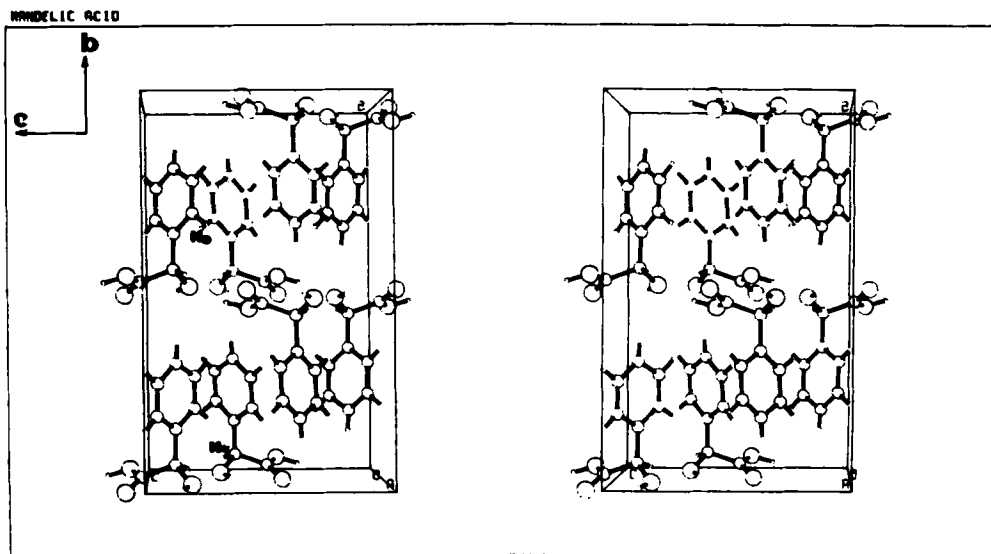
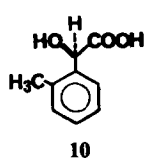
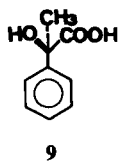
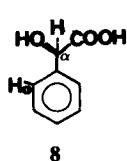


Figure 34. Packing arrangement of (*R,S*)-mandelic acid, viewed along the *a* axis.

(*R,S*)-Mandelic acid (**8**) (**86**) packs in a crystal of the desired symmetry (Figure 34) space group *Pbca*, and the C_{α} -H and C-*ortho*-H bonds are properly oriented toward the body diagonal. Moreover, the crystal develops the eight {111} faces. It was therefore expected that resolved atrolactic acid (**9**) and *o*-methylmandelic acid (**10**) would be adsorbed at only one enantiopolar set of the {111} faces and subsequently be concentrated at the corresponding four corners. However, the experiments did not provide a clear-cut answer. Other systems are presently under consideration.



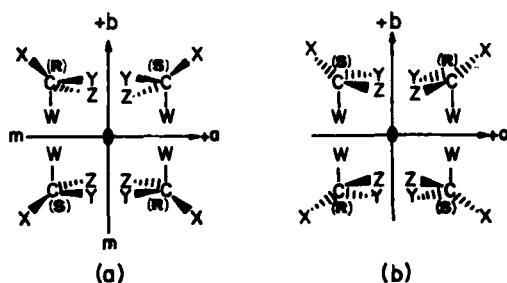
H. Assignment of Absolute Configuration Using Noncentrosymmetric Achiral Crystals

Noncentrosymmetric achiral crystals of monoclinic point symmetry *m* and of orthorhombic point symmetry *mm2* are also appropriate for determination of the absolute configuration of chiral resolved additives. For the point group *m*, only the left or right halves of Schemes 13a are relevant. In such an arrangement,

the directions of *R* and *S* molecules are unambiguously assigned with respect to the unique *b* axis (although not with respect to the *a* and *c* axes; see Section IV-G-1), allowing assignment of the absolute configuration of the chiral resolved additive by means of the affected faces (*hkl*), *k* ≠ 0. The absolute sense of the *a* and *c* axes may also be fixed from the affected faces, provided they are of the type (*hkl*), *h* and/or *l* ≠ 0, *k* = 0.

In the orthorhombic point group *mm*2 there is an ambiguity in the sense of the polar axis *c*. Conventional X-ray diffraction does not allow one to differentiate, with respect to a chosen coordinate system, between the *mm*2 structures of Schemes 15*a* and *b* (these two structures are, in fact, related by a rotation of 180° about the *a* or *c* axis) and therefore to fix the orientation and chirality of the enantiomers with respect to the crystal faces. Nevertheless, by determining which polar end of a given crystal (e.g., face *hkl* or *hkl̄*) is affected by an appropriate additive, it is possible to fix the absolute sense of the polar *c* axis and so the absolute structure with respect to this axis. Subsequently, the absolute configuration of a chiral resolved additive may be assigned depending on which faces of the enantiotopic pair [e.g., (*hkl*) and (*hkl̄*) or (*hkl̄*) and (*hkl*)] are affected.

An example is provided by (*R,S*)-alanine, which crystallizes in space group *Pna*2₁ (i.e., belongs to the above-mentioned point group *mm*2). The packing arrangement (87) is depicted in Figure 35*a*. (*R,S*)-Alanine forms needles when grown in aqueous solution. These crystals are extended in the *c* direction and generally exhibit the four symmetry-related side faces {210} (Figure 35*b*). The crystals grow much faster at one end of the needle than at the opposite end. Both (*R*)- and (*S*)-alanine molecules are oriented with respect to the polar needle axis such that their CO₂⁻ groups are exposed at one end of the needle and their NH₃⁺ groups at the opposite end. The absolute polarity of crystal growth was assigned by growth and dissolution experiments in the presence of methyl alaninate and *N*-methylalanine. The results indicated that the NH₃⁺ groups are exposed at the slow-growing end of the pure crystal and the CO₂⁻ groups at the other



Scheme 15

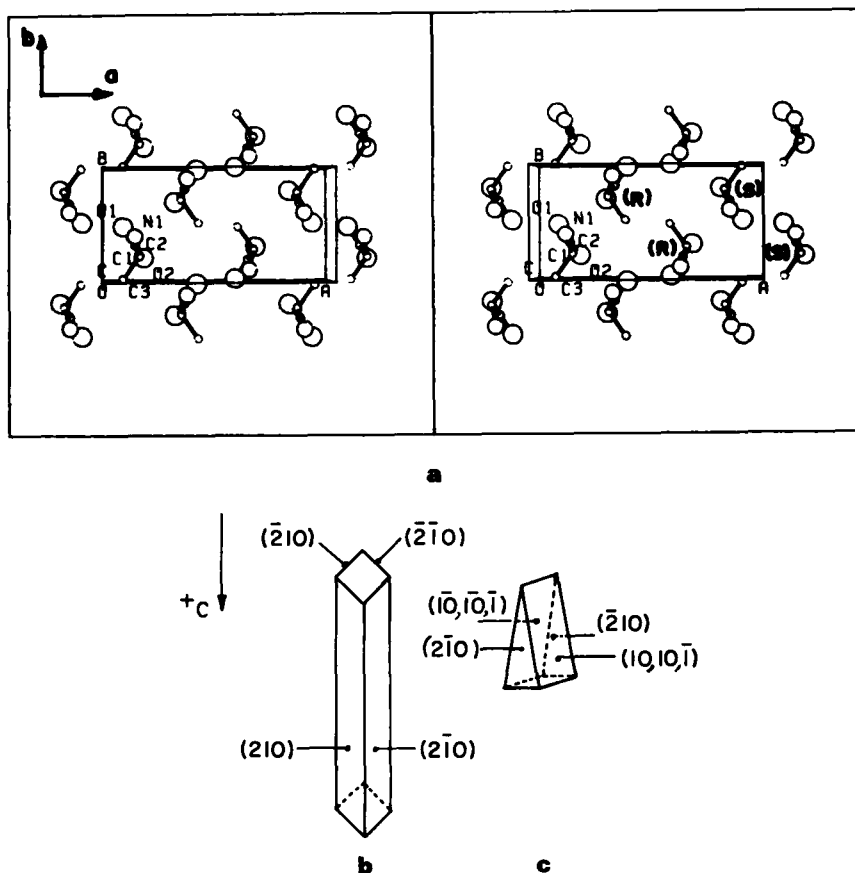


Figure 35. (a) Packing arrangement of (*R,S*)-alanine, viewed along the *c* axis. (b) Morphology of pure (*R,S*)-alanine. (c) Morphology of (*R,S*)-alanine affected by (*S*)-thr.

end, thus fixing the absolute structure of a specimen crystal, in other words, the absolute orientations of the (*R*)- and (*S*)-alanine molecules with respect to the crystal faces (88). The absolute configuration of resolved threonine could now be assigned by its effect, through growth and dissolution, on crystals of (*R,S*)-alanine. Resolved threonine induces pyramid-shaped crystals of (*R,S*)-alanine extended in the *c* direction with morphological symmetry 2 (Figure 35c), as opposed to the *mm*2 symmetry of the pure form. The known absolute polarity of the affected crystal (the fast-growing end of the crystal exposes CO_2^- groups) and the affected side faces of the type $(10, 10, \bar{1})$ and $(\bar{1}0, \bar{1}0, \bar{1})$ are compatible only with an additive of *S* configuration. In general, the crystals

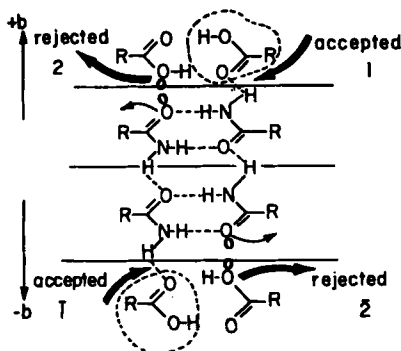
affected by resolved threonine are twinned across the *ab* plane in the center of the crystal, and so are of morphological point symmetry 222.

I. Determination of the Absolute Direction of a Polar Axis in a Chiral or Achiral Crystal

At this stage it should be clear that one may determine the absolute direction of a polar axis via growth or dissolution experiments using tailor-made additives. The noncentrosymmetric crystal may be chiral (e.g., of space group $P2_1$) or achiral (e.g., of space group $Pna2_1$) and the constituent molecules chiral or achiral. In the case of a chiral crystal structure, one is dealing essentially with the assignment of one of the two enantiomeric crystal structures. For an achiral crystal there is only one crystal structure, and the problem resides in the determination of its absolute arrangement with respect to the polar axis. Of particular interest are crystals that do not exhibit hemihedral faces and are composed of achiral molecules. Tailor-made additives may be designed to inhibit growth along the polar axis to assign its absolute direction. These same additives may be used to etch the top or bottom faces at the polar ends of the crystal for independent assignment. Furthermore, one may even etch the side faces of a crystal with an appropriate additive; if the etch figure is asymmetric in shape along the polar axis it provides a relative means of assignment for comparing several specimen crystals. It is noteworthy that if the crystal is achiral and the constituent molecules chiral, as in (*R,S*)-alanine, then one may assign the absolute polarity of the crystal structure by etching the side faces with a resolved additive of known chirality. For example, in Section IV-H we demonstrated how one may assign the absolute configuration of resolved threonine by its effect on the side $\{hk0\}$ faces of (*R,S*)-alanine if one is given the absolute polarity of the specimen crystal. Here we propose a reverse procedure: Given the absolute configuration of the threonine etchant, we assign the absolute polarity of the specimen crystal by observing which homotopic pairs of side faces [e.g., $(hk0)$ and $(\bar{h}\bar{k}0)$ or $(h\bar{k}0)$ and $(\bar{h}k0)$] are etched. An application of the assignment of the absolute structure of specimen crystals of α -resorcinol, which appear in space group $Pna2_1$, is described in Section VI-B.

J. Reduction in Crystal Symmetry of Solid Solutions

In the host/additive systems described above, such as (*R,S*)-ser/(*R,S*)-thr and glycine/(*R,S*)- α -amino acids, the change in crystal habit and the enantiomeric segregation of occluded additive indicates that only a subset of the possible symmetry-related sites may be occupied by an additive depending on through which faces the additives are occluded. Such an effect would lead to a reduction in the overall symmetry of the host/additive crystal.



Scheme 16

This reduction in crystal symmetry is conveniently illustrated in the systems cinnamide, benzamide, or, in general, any amide RCONH_2 packing in a ribbon motif comprising centrosymmetric hydrogen-bonded dimers interlinked by translation (Scheme 16).

In accordance with the structural analysis presented in Section IV-C-1, the corresponding acid additive RCOOH must be preferentially adsorbed at the end of the growing ribbon at those sites where the carbonyl group of the acid can be hydrogen bonded to the NH group of the amide emerging from the crystal surface. These are the surface sites in Scheme 16 labeled 1 and $\bar{1}$ at the $+b$ and $-b$ ends of the ribbon, respectively. Adsorption at sites 2 and $\bar{2}$ should be inhibited because it involves repulsion between the carbonyl oxygen of an amide molecule emerging at the surface and the hydroxyl group of the acid (the pairs of sites 2 and $\bar{1}$ and $\bar{2}$ and 1 are, in fact, crystallographically identical in the bulk, but they are different at the surface). Once an acid molecule is adsorbed at sites 1 or $\bar{1}$, the local center of inversion of the hydrogen-bonded dimer is destroyed. Since the additive is preferentially occluded through surface sites 1 and $\bar{1}$ at the $+b$ and $-b$ ends, respectively, of the growing crystal, the centrosymmetric nature of each half of the crystal along b is also eliminated macroscopically, no matter how little acid is occluded. For cinnamide and benzamide grown in the presence of the corresponding carboxylic acids, this leads to a lowering of symmetry from $P2_1/c$ to $P2_1$. Since the two halves of the crystal are related by inversion, the whole crystal will not macroscopically reveal a reduction in symmetry by techniques such as optical rotation, frequency doubling of monochromatic light, or piezo- or pyroelectricity, but each half may. X-Ray or neutron diffraction, on the other hand, may reveal such a reduction for the whole crystal (because diffraction takes place from microscopic mosaic blocks), provided the scattering power of host and additive are sufficiently different.

Another apt example is provided by the host/additive system glycine/(R,S)-

α -amino acids (Section IV-G-4). The *R* and *S* amino acids are occluded through the glycine (010) and (0 $\bar{1}$ 0) faces, respectively. Thus, the $+b$ half of the {010} glycine plate contains the *R* amino acid, whereas the $-b$ half contains the *S* acid. Consequently, the overall space group symmetry of each half of the plate is reduced from $P2_1/n$ in the pure form to $P2_1$, where the two halves are related by an overall center of inversion. It is interesting that in the system (*R,S*)-ser/(*R,S*)-thr (Section IV-G-2), the symmetry of each quadrant of the crystal will be reduced from $P2_1/a$ to $P1$ because the additives are occluded through the side faces {011} in only one of the four symmetry-related sites.

Were it possible to establish, by diffraction methods, the reduced symmetry of the affected crystal, as well as to map the atomic positions of the occluded additive, then by knowing through which face the additive is adsorbed, one might deduce the absolute configuration of the additive by conventional diffraction. Naturally the amount of occluded additive must be sufficient to be observed by diffraction methods (e.g., as high as 5% if there is no dramatic difference in the scattering powers of the host and additive). The method is particularly apt for polar crystals that do not contain polar axes (e.g., orthorhombic crystals), because in such systems it has not proven possible to deduce absolute configuration from the change in crystal habit in a straightforward way.

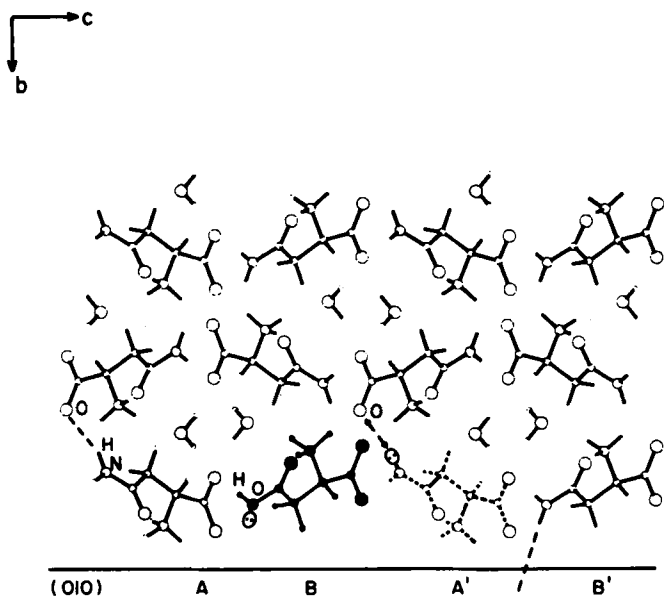


Figure 36. Packing arrangement of (*S*)-asparagine·H₂O, viewed along the *a* axis. The crystallographically related sites at the (010) surface are indicated by A and B. Aspartic acid can be substituted preferentially at site B (or B'), rather than at A (or A') because of O::O repulsion.

A host-additive system that illustrates the above principles and lends itself to this method is asparagine/aspartic acid, in which as much as 16% of the guest can be occluded and which thus may be regarded as a solid solution. The change in crystal habit of asparagine induced by aspartic acid has been explained in terms of adsorption of aspartic acid at the {010} faces (Section IV-D-3). Aspartic acid should be preferentially adsorbed at the B and B' sites on an {010} face, and in such a way that the lone-pair lobes of the hydroxyl oxygen atom emerge from the crystal face (Figure 36). Under such a condition, aspartic acid may occupy only two of the four symmetry-related sites, so the space group of asparagine/aspartic acid would be $P12_11$, in contrast to $P2_12_12_1$ in the pure crystal. This reduction from orthorhombic to monoclinic symmetry may be deduced from the Laue symmetry of the diffraction pattern, provided that aspartic acid is occluded through only one of the two opposite {010} faces. Otherwise the crystal will contain two halves, each of symmetry $P12_11$, related to each other by overall twofold symmetry about the a or c axis passing through the center of the crystal. The reduction in symmetry of each half will thus be masked, in a manner analogous to that for a twinned crystal, so the overall crystal will appear to be orthorhombic. This effect may be circumvented, because the crystals appear as {010} plates and can be grown on a glass bottom, so the additive can be essentially occluded through one side only.

Conventional X-ray diffraction did not allow detection of the drop in symmetry of asparagine/aspartic acid, because the X-ray scattering powers of the guest and host are too similar (89,90). Thus we embarked on a neutron diffraction study with asparagine C-H (protonated) and aspartic acid C-D (deuterated), taking advantage of the radically different neutron scattering amplitudes of H and D (91). This neutron study demonstrated which molecular site is preferentially occupied by aspartic acid and also allowed us to establish the absolute configuration of guest aspartic acid (and naturally also of asparagine) by choosing that enantiomorphous crystal structure which is consistent with adsorption of aspartic acid from that {010} face exposed to solution such that the lone pair of the hydroxyl oxygen atom emerges from the face.

V. ABSOLUTE CONFIGURATION FROM CHEMICAL REACTIVITY IN POLAR AND ENANTIOPOLAR CRYSTALS

In principle, an anisotropic reaction performed on a crystal of polar symmetry may fix the absolute direction of the polar axis. In the case of an asymmetric reaction carried out in a centrosymmetric (enantiopolar) crystal, one may establish the absolute configuration of the chiral product. The degree of reliability of the assignment will depend on knowledge of the various states of the reaction pathway. Here we briefly describe some heterogeneous reactions in polar and enantiopolar crystals that illustrate this approach.

A. Gas-Solid Reactions in Polar Crystals: Ammonia-*p*-Bromobenzoic Anhydride

Curtin and Paul have carried out a series of elegant studies on the reactivity of single crystals of acids and anhydrides with gaseous ammonia (92,93). They demonstrated that these reactions are highly anisotropic, with the ammonia

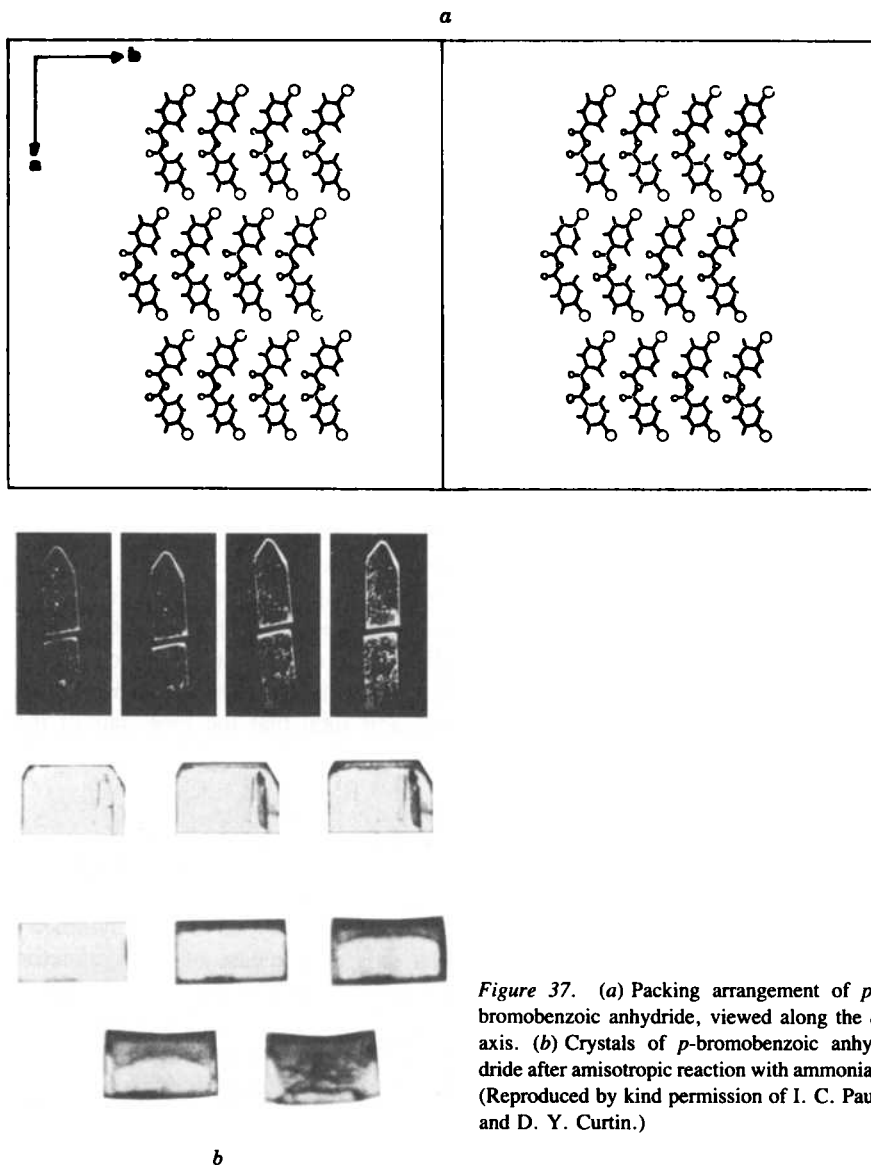


Figure 37. (a) Packing arrangement of *p*-bromobenzoic anhydride, viewed along the *c* axis. (b) Crystals of *p*-bromobenzoic anhydride after anisotropic reaction with ammonia. (Reproduced by kind permission of I. C. Paul and D. Y. Curtin.)

molecules able to attack those faces at which the oxygen atoms of the acid or anhydride groups are exposed. The other faces of the crystals, which are dominated by other functional groups, are less affected by the ammonia.

These observations were extended to polar single crystals of *p*-bromobenzoic anhydride, which appear in the monoclinic space group *C*2. Inspection of the arrangement of the molecules in the crystal (Figure 37*a*) reveals that the $>\text{C}=\text{O}$ vectors of the carbonyl groups are almost parallel to the polar axis. The well-developed {100} platelike faces of the crystal expose the *p*-bromophenyl groups, but the access of ammonia to the carbonyl groups appears to be from the sides and not from the large {100} faces of the crystal. Furthermore, it has been observed that initiation of the reaction is favored at the *+b* side of the crystal along the polar axis. Figure 37*b* shows single crystals of *p*-bromobenzoic anhydride reacted anisotropically with ammonia.

A correlation between the absolute orientation of the carbonyl groups and the side on which the ammonia molecules react with the anhydride was established by an X-ray analysis employing the anomalous-dispersion method. Ammonia was found to attack the crystal preferentially from the side of the carbonyl oxygen atom. The authors proposed a mechanism whereby an ammonia molecule becomes hydrogen bonded to an oxygen atom of one of the carbonyl groups, so that the nitrogen atom is in a favorable position for attack of the sp^2 face of the other carbonyl group.

In this study, an important piece of information was gleaned regarding the mechanism of the reaction from the assignment of the absolute sign of the polar axis. Of course, in transformations of this type, if the reaction mechanisms are well established, one may proceed in a reverse manner and assign the absolute polarity of the crystal (and therefore the absolute configuration of the chiral molecules) by determining the preferential direction of the attack.

B. Liquid-Solid Reactions in Centrosymmetric Crystals: Osmium Tetroxide-Tiglic Acid

Recently, Holland and Richardson (94) reported an elegant study on the addition of OsO_4 to the two enantiotopic faces of tiglic acid, which packs in the centrosymmetric triclinic space group $P\bar{1}$. The cell contains two molecules that form coplanar hydrogen-bonded dimers oriented almost parallel to the $\{2\bar{1}0\}$ crystal faces (Figure 38). These authors selected this crystal structure because the centrosymmetrically related molecules at a $\{2\bar{1}0\}$ surface are effectively related by twofold symmetry about an axis perpendicular to the crystal surface. They performed an asymmetric synthesis exploiting the fact that OsO_4 adds in *cis* fashion to double bonds by an attack perpendicular to the plane of the $\text{C}=\text{C}$ system.

They proposed that at a $\{2\bar{1}0\}$ crystal surface the OsO_4 will add to the molecule

tiglic acid

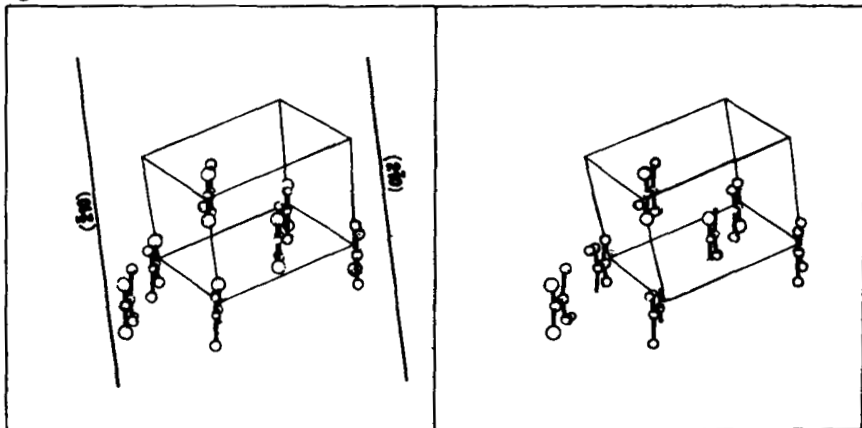
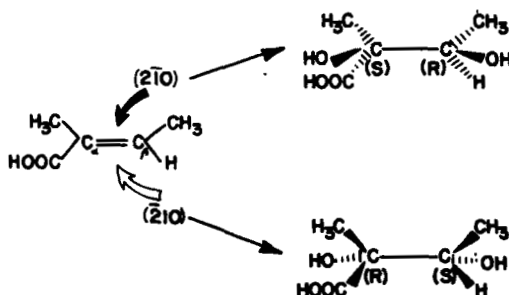


Figure 38. Packing arrangement of tiglic acid, viewed along the $\{210\}$ face. The two opposite enantiotopic faces $(\bar{2}10)$ and $(2\bar{1}0)$ are designated.

prevalently from that side of the double bond which faces outward. Since the crystal structure is centrosymmetric, the absolute orientation of the two molecules is directly assigned with respect to the crystal axes for any given crystal. We may thus deduce that the absolute configuration of the diol formed at face $(2\bar{1}0)$ is $C_\alpha(S)C_\beta(R)$, whereas the one formed at $(\bar{2}10)$ is of absolute configuration $C_\alpha(R)C_\beta(S)$, as shown in Scheme 17.



Scheme 17

C. Topochemical Reactions in Enantiopolar Crystals: Cinnamide-Cinnamic Acid

An asymmetric photosynthesis may be performed inside a crystal of *E*-cinnamide grown in the presence of *E*-cinnamic acid and considered in terms of the analysis presented before on the reduction of crystal symmetry (Section IV-J). We envisage the reaction as follows: The amide molecules are interlinked by $\text{NH} \cdots \text{O}$ hydrogen bonds along the *b* axis to form a ribbon motif. Ribbons that are related to one another across a center of inversion are enantiomeric and are labeled *l* and *d* (or *l'* and *d'*) (Figure 39). Molecules of *E*-cinnamic acid will be occluded into the *d* ribbon preferentially from the $+b$ side of the crystal and into the *l* ribbon from the $-b$ side. It is well documented that *E*-cinnamide photodimerizes in the solid state to yield the centrosymmetric dimer truxillamide. Such a reaction takes place between close-packed amide molecules of two enantiomeric ribbons, *d'* and *l* or *d* and *l'* (95). It has also been established that solid solutions yield the mixed dimers (**11a**) and (**11b**) (Figure 39) (96). Therefore, we expect preferential formation of the chiral dimer **11a** at the $+b$ end of the crystal and of the enantiomeric dimer **11b** at the $-b$ end of the crystal. Preliminary experimental results are in accordance with this model (97).

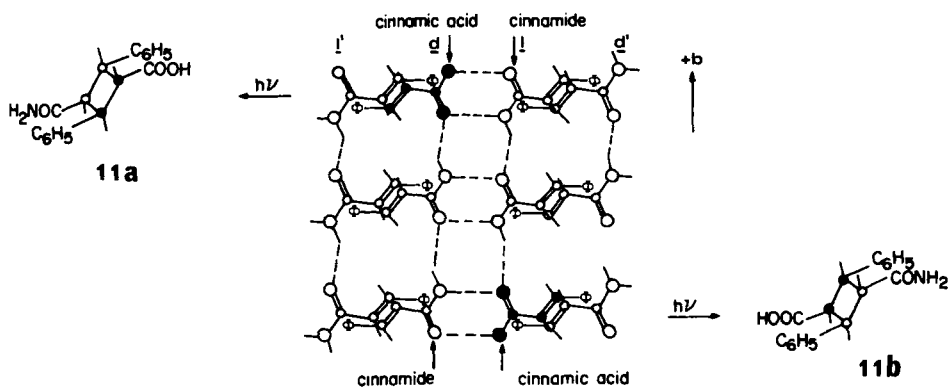


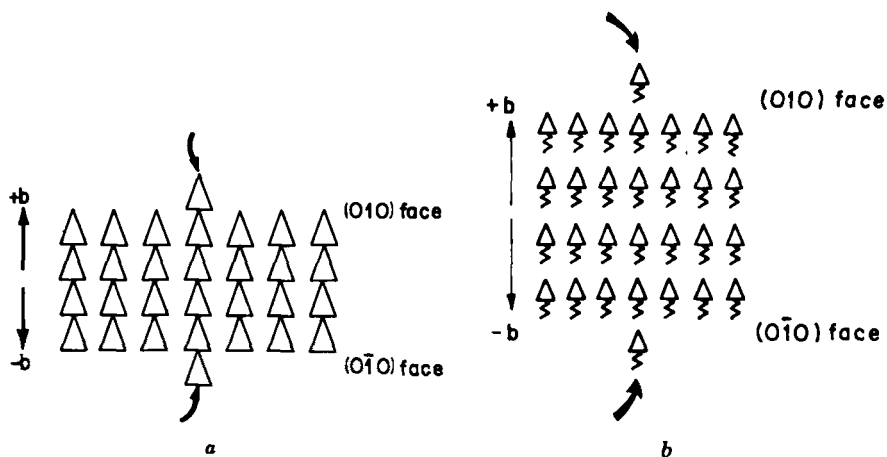
Figure 39. Four ribbons of cinnamide (phenyl = Φ) molecules. Ribbons *l* and *l'*, *d* and *d'* are related by translation. Ribbons *d'* and *l*, *d* and *l'* make plane-to-plane contacts of 4 Å across centers of symmetry. Ribbon *l'* is above *d*, and ribbon *d'* is below *l*. Cinnamic acid molecules (filled circles) have been introduced into the structure in the allowed sites, assuming the crystal grows from the center in the two opposite directions $+b$ and $-b$. The dimers obtained at the two opposite sides are enantiomeric.

VI. THE SOLVENT EFFECT

A. Introduction

We have already pointed out in Section IV-A that it is possible in principle to deduce from the macroscopic asymmetric habit of a chiral polar crystal the absolute configuration of its constituent molecules. Waser (30) tried to establish the absolute configuration of D-tartaric acid by correlating the different rates of growth of the opposite hemihedral faces of the D-tartaric crystal with the relative ease of binding of an oncoming tartaric acid molecule at either face. He took into account only intermolecular distances between the crystal and the to-be-attached molecule. The basic flaw of Waser's argument, as recognized by Turner and Lonsdale (31), is that, in these terms only, the ease of approach is identical at either face.

We shall try, with simple model structures, to outline some of the factors that could lead to a difference in the rates of growth of opposite polar faces. Scheme 18a depicts a polar crystal composed of triangular molecules that exhibits polar faces (010) and (0 $\bar{1}$ 0). It is clear that the distance of a triangle to be attached from the (010) face is the same as that from the (0 $\bar{1}$ 0) face, in accordance with Turner and Lonsdale's argument. If the atoms at the apex or base of the triangle are strongly polarizable, then the electron density distribution of the to-be-attached molecules and of the molecules at the (010) or (0 $\bar{1}$ 0) surfaces may be different from that of molecules in the bulk; under such circumstances the interaction energies between a to-be-attached molecule and the hemihedral (010) and (0 $\bar{1}$ 0) faces may be different. Furthermore, if the molecule comprises rigid and flexible



Scheme 18

moieties arranged as in Scheme 18*b*, then entropy factors surely play a role in the relative ease of molecular docking in the surface sites at either end. The solvent also may interact differently with the (010) and (0 $\bar{1}$ 0) surfaces in Scheme 18. We shall try to show that under favorable circumstances, it may be possible to correlate the absolute polarity of a crystal with the effect of solvent on its hemihedral faces. One of the major obstacles to assessing the role of the solvent is the unscrambling of the relative contributions played by internal structure and the various solvent-surface interactions in determining crystal morphology. To assign the relative roles played by the crystal structure and solvent, one can compare the habits of crystals obtained from various solvents with the theoretical (i.e., calculated) crystal habit, which depends only on crystal structure. The theoretical habit should match the crystal morphology obtained by sublimation.

We briefly describe the derivation of the theoretical habits of crystals. A controlling factor in crystal growth is the energy of the interactions between neighboring molecules in the bulk of the crystal. According to Hartman and Perdok (98), the crucial relationship is between the attachment energy E_{att} , that is, the energy released per molecule when a new layer is attached to the crystal face, and the layer energy E_l , which is defined as the energy released per molecule when a new layer is formed. E_l measures the stability of a layer and E_{att} controls

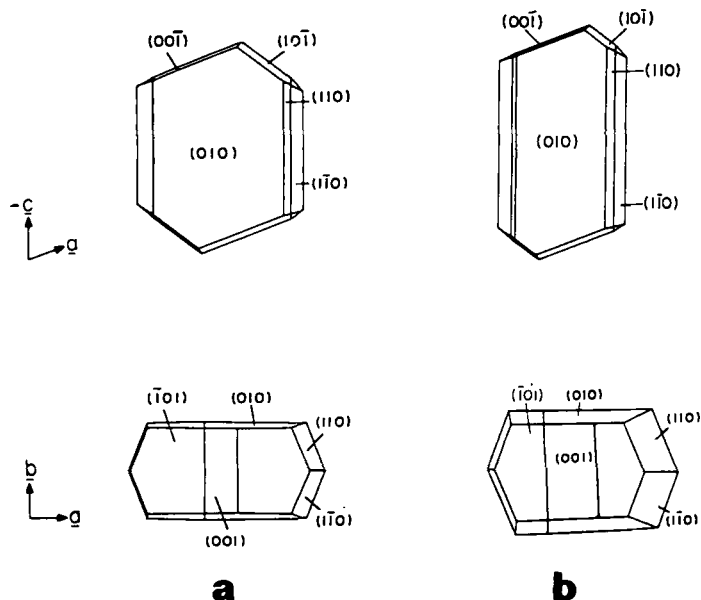


Figure 40. Morphology of glycine crystals: (a) theoretical; (b) observed (glycine obtained by sublimation).

the growth rate perpendicular to this layer. A study of the relationship between the internal structure of the crystal and its morphology led to the working hypothesis (98) that the morphological importance of a crystal face decreases with increasing attachment energy. From the known crystal structure it is possible to calculate the corresponding values of E_{att} for various low-index faces. This information is used to derive the theoretical form (99), that is, the calculated morphology of the crystal which best represents the crystal habit obtained by sublimation (100). To derive the habit of the crystal grown from solution in the presence or absence of additives, one must take into account substrate-solvent and substrate-additive interactions at the crystal-solution interface (100,101).

As a model system, the theoretical morphology of α -glycine was computed and was found to be in good agreement with the morphology of glycine crystals obtained by sublimation (cf. Figures 40*a* and *b*) (47,100). Its habit is distinctly different from that of glycine grown from aqueous solution (Figure 28*a*). The most striking differences between the two forms (Figure 40 vs. Figure 28*a*) are the complete disappearance of the $\{001\}$ and $\{10\bar{1}\}$ faces, the formation of $\{011\}$, and the drastic reduction in the relative area of $\{010\}$ in the latter. We account for these differences in terms of the higher affinity of the water solvent for the crystal faces $\{110\}$ and $\{011\}$ than for $\{010\}$. To establish the relative affinities of these faces for water, the Coulomb potential energy of each of the four faces was calculated at closest-approach distances from the surface. From these maps we concluded that the $\{010\}$ face is the least polar and $\{011\}$ the most polar. Thus, preferential adsorption of water molecules on the polar faces, primarily on $\{011\}$, causes a reduction in the growth rate normal to these faces relative to that of $\{010\}$, with a concomitant increase in their surface area. Several other systems were studied, including benzamide, cinnamide (43,100), and serine (78). These studies yielded theoretical forms consistent with the observed habits.

Some of the difficulties encountered in establishing the effect of solvent on crystal growth may be circumvented by focusing on polar crystals. This is because the difference in the rates of growth of opposite faces (hkl) and ($\bar{h}\bar{k}\bar{l}$) along a polar direction must arise primarily from differences in their solvent-surface interactions. Thus, one generally does not have to be concerned with faces other than the hemihedral ones in question. We illustrate below an approach to understanding solvent-surface interactions in the polar crystals of resorcinol (102).

B. Resorcinol

A benchmark study on the effect of solvent on growth of polar crystals was carried out by Wells (42) in 1949. He found that in aqueous solution at room temperature the α -form of resorcinol (space group $Pna2_1$), **12a**, grows unidirectionally along the polar c axis. The crystal exhibits "benzene-rich" $\{011\}$ faces at one end of the c axis and "O(hydroxyl)-rich" $\{0\bar{1}\bar{1}\}$ faces at the other end

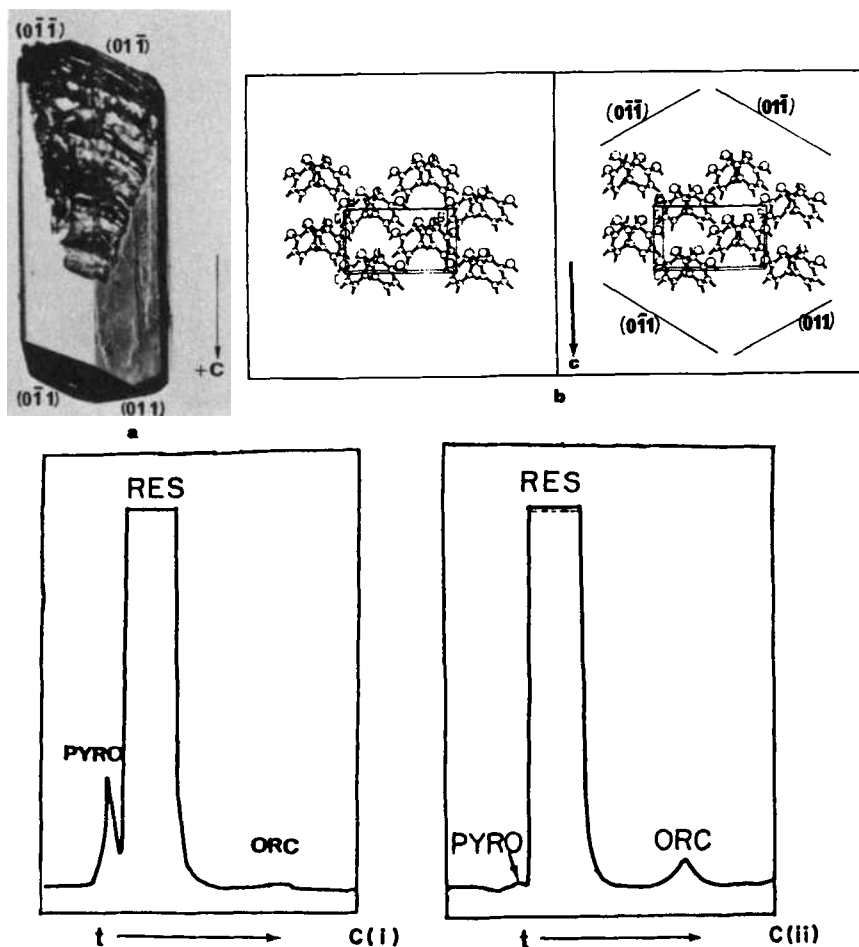
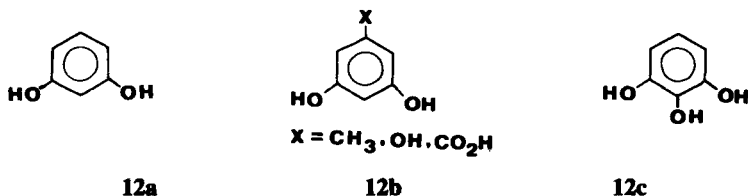


Figure 41. (a) Crystal of α -resorcinol obtained from water. (b) Packing arrangement of α -resorcinol viewed along a . (c) Distribution of occluded additives **12b** (orcinol, $X = CH_3$) and **12c** (pyrogallol) at the opposite ends of a crystal of α -resorcinol as determined by HPLC: i, material taken from one end of crystal (at $-c$ pole); ii, material taken from the opposite end (at $+c$ pole). PYRO, pyrogallol; RES, resorcinol; ORC, orcinol.

(Figure 41a,b). Wells interpreted this growth along c as a result of relatively strong adsorption of water to the O(hydroxyl)-rich faces thus inhibiting their growth. The absolute direction of growth along the polar axis with respect to the crystal structure, however, could not be fixed at that time. Recently, Davey, Bourne, and Milisavljevic (103–106) have proposed that strong surface–water interactions should enhance crystal growth. Indeed, by the use of oriented growth



on silica surfaces (106), they deduced that the O(hydroxyl)-rich $\{0\bar{1}\bar{1}\}$ faces grow faster than the $\{011\}$ faces in aqueous solution. To resolve this contradiction, we have assigned the absolute direction of growth of the resorcinol crystal in aqueous solution by employing the additives **12b** and **12c**, which by the established mechanism must be adsorbed at the benzene-rich [i.e., $\{011\}$] and O(hydroxyl)-rich [i.e., $\{0\bar{1}\bar{1}\}$] faces, respectively. The segregation of these two occluded additives along the polar c axis of crystals of resorcinol grown in their presence is shown in Figure 41c.

The absolute direction of growth of several specimen crystals in aqueous solution was independently assigned by the Bijvoet method. We found that the unidirectional growth in water takes place primarily at the oxygen-rich faces (102). However, we propose a mechanism that is more in line with Wells's thinking than the one proposed by Davey. We tend toward the paradoxical view that there is a higher affinity of water for the benzene-rich faces. This can be understood in terms of the detailed structure of the faces: The benzene-rich face is crisscrossed by grooves forming pockets at their intersections, whereas the oxygen-rich face is relatively flat (Figure 42). Within an 011 molecular layer three of every four OH groups participate in $\text{OH} \cdots \text{O}$ hydrogen bonds; the fourth OH group emerges from a benzene-rich $\{011\}$ face to form a hydrogen bond with the next layer. Furthermore, two of the four C–H bonds per molecule emerge from the $\{011\}$ face; these aromatic C–H bonds are known to participate in $\text{CH} \cdots \text{O}$ interactions (107). Thus, for the solvent water, it is preferable to consider $\{011\}$ and $\{0\bar{1}\bar{1}\}$ as acidic and basic, respectively, rather than as benzene rich and O(hydroxyl) rich. This point was confirmed by electrostatic potential surfaces calculated at these two faces (102). Moreover, the more “hilly” nature of the $\{011\}$ face, as manifested by van der Waals potential surfaces, indicated that solvent can be more strongly adsorbed at this face than at $\{0\bar{1}\bar{1}\}$. Thus we maintain that Wells's interpretation that growth of a crystal face is inhibited by strong adsorption of solvent is essentially correct, although in the case of resorcinol he drew the incorrect conclusion about the growth direction by assuming that water is adsorbed preferentially on the O(hydroxyl)-rich face.

This approach to studying solvent–surface interactions is encouraging. We intend to apply it to the crystals of enantiomers in order to assign their absolute configurations and so close the circle started by Waser.

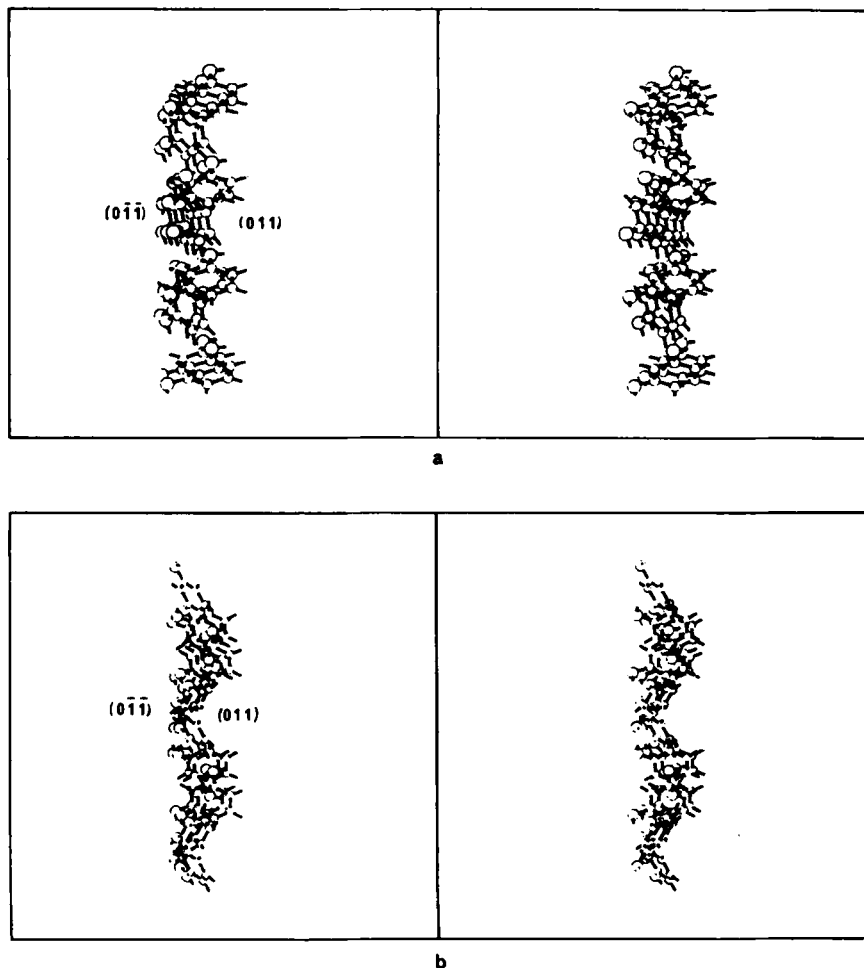


Figure 42. 011 layer of resorcinol viewed along two directions, showing surface structure of the opposite faces (011) and $(0\bar{1}\bar{1})$: (a) viewed along the a axis; (b) viewed along $-b + c$.

VII. PYROELECTRICITY, PIEZOELECTRICITY, AND OPTICAL ACTIVITY IN CRYSTALS

Macroscopic physical phenomena in polar crystals, such as pyroelectricity, piezoelectricity, and optical activity, would appear to be useful for the assignment of absolute polarity of crystals, provided that one can explain such phenomena at the required level in terms of the atomic arrangement. It appears from the

literature (108) that piezoelectricity offers little scope for assignment of absolute configuration, since only the very simplest of structures (e.g., zinc blende-type and wurtzite-type structures) have been amenable to analysis. As to optical activity in crystals, Glazer and co-workers (109) recently concluded from a study of the literature that the causes of optical activity in crystals are still largely unknown. Pyroelectricity (108), on the other hand, does offer possibilities, to which we now address ourselves.

In a pyroelectric crystal a small change in temperature produces a proportional change in the electric polarization vector \mathbf{P} . This vector is nonzero along a polar direction in a noncentrosymmetric space group. The pyroelectric coefficient along a polar axis may be obtained by measuring the charges developed at the opposite ends of the crystal during a known change of temperature. A correct prediction of the sign, and the magnitude if possible, of the pyroelectric coefficient in terms of the crystal structure will yield the absolute polarity of the crystal. Thus, for a pyroelectric crystal containing chiral molecules of known polarization (e.g., a zwitterion) one may deduce the absolute configuration of the molecule from the measured pyroelectric effect.

We illustrate this approach with studies carried out on the ferroelectric crystals of triglycine sulfate (TGS). A ferroelectric material is pyroelectric, but the spontaneous polarization \mathbf{P} may be reversed in sign by application of a reverse electric field. The latter induces a phase transformation of the structure to its mirror image through atomic displacement. This is in keeping with the fact that the atomic arrangement in a ferroelectric exhibits minor deviations from a centrosymmetric one so only minor changes are required to switch the structure to its mirror image.

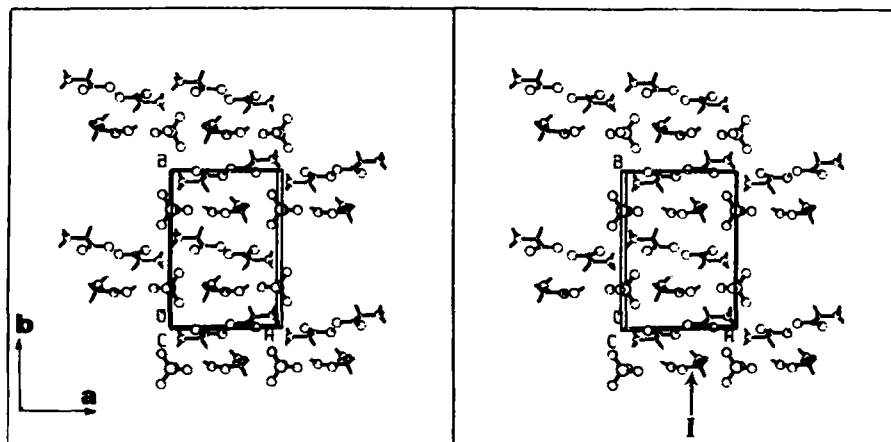


Figure 43. Packing arrangement of TGS, viewed along the c axis. Glycine I is indicated by an arrow.

The crystal structure of TGS in the ferroelectric phase is monoclinic $P2_1$ (Figure 43) (110). (TGS undergoes a phase change at $\sim 50^\circ\text{C}$ to the paraelectric phase, in which a mirror plane perpendicular to the b axis is added to the structure, yielding $P2_1/m$ symmetry.) It is possible to convert one enantiomorphous arrangement to the other by reorienting the molecule through application of a reverse electric field along the unique axis b .

Fletcher, Keve, and Skapski (110) have shown that the reversible electric dipole of TGS that gives rise to the polarization vector \mathbf{P} along the b axis is the one associated with glycine molecule I (see Figure 43). They found that the direction of the measured positive sense of \mathbf{P} in a single crystal of TGS tallied with the direction of an electric dipole based on an absolute arrangement of molecules as determined by the Bijvoet method. This correlation between the absolute arrangement of atoms of glycine I and the measured \mathbf{P} is illustrated in Figure 44 for the two enantiomorphous structures.

Single crystals of ferroelectric TGS grown from solution generally contain domains of the two enantiomorphous phases (110). This juxtaposition of enantiomorphous domains may be explained in terms of the minor deviations of the crystal structure from a centrosymmetric arrangement. The relative concentrations of the two enantiomorphous phases in a single crystal may be determined by means of anomalous dispersion of X-rays (111,112).

Lock (113) found that TGS crystals grown in the presence of resolved alanine are unipoled; that is, they contain only one enantiomorphous phase. Thus it should be possible to assign the absolute configuration of the occluded additive by measuring the electric dipole of the crystal, provided that one can predict which enantiomorph of TGS is induced by the resolved additive.

Recently, Curtin and Paul (114) have used the pyroelectric effect for the direct assignment of the absolute structure of crystals of p -bromobenzoic anhydride.

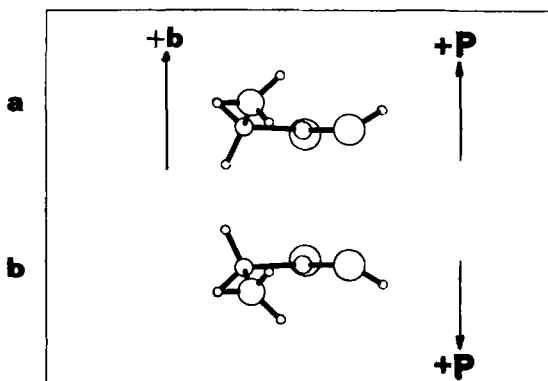


Figure 44. Absolute atomic arrangement of glycine I in TGS (see Figure 43) and the direction of the electric polarization vector \mathbf{p} for the two enantiomorphous states (a) and (b) (ref. 110).

VIII. DETERMINATION OF ABSOLUTE CONFIGURATION BY ELECTRON MICROSCOPY

The simplest way to assign the absolute configuration of a chiral molecule would certainly be by direct inspection of the molecule itself. Were the technical means at hand powerful enough to allow it, no other technique could compete with one providing a direct three-dimensional "photograph" of the molecule in question. Since at present, electron microscopes can achieve resolutions as low as 3 Å, we are indeed not far from this goal.

In contrast to diffraction, electron imaging techniques are subject to the same fundamental laws as light imaging, and can therefore provide an unambiguous answer to the problem of the reconstruction of an object in three dimensions, provided sufficient resolution can be achieved.

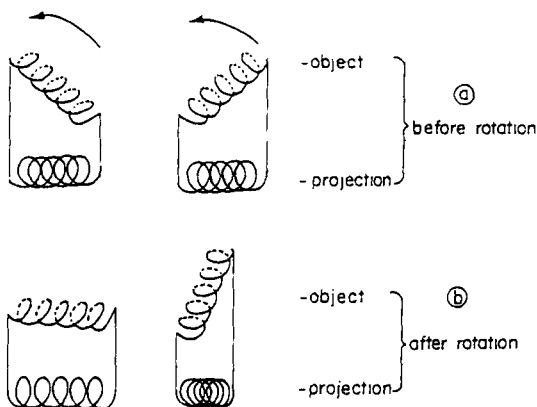
We shall discuss this topic under two main headings: assignment of absolute configuration by imaging of (i) the secondary structure of macromolecules and (ii) the structure of a chiral molecule in a chiral crystal.

A. Imaging of Macromolecules

The idea of assigning the absolute configuration of chiral molecules by electron microscopy was suggested by Arigoni (115). The basic data is derived from the fact that the chiral secondary structure of a macromolecule like DNA or a protein α -helix is unequivocally determined by the absolute configuration of the primary chiral building blocks (in the examples, 2-D-deoxyribose or α -amino acids, respectively). This means that the two helices of opposite handedness built from a sequence of, say, α -amino acids of the same absolute configuration *S* are nonisometric objects of different energy and geometry. One of the two is more stable and is commonly observed in biological systems. The helicity of the macromolecules, and in particular the size of the pitch, can therefore be unequivocally correlated with the absolute configuration of the component α -amino acids (or deoxyribose in the case of DNA).

Suppose that one takes an electron micrograph of such a helical molecule at a resolution sufficient to reveal the helix structure. This micrograph will appear as a projection of the helix in two dimensions (Scheme 19a) and will still not allow one to distinguish between a dextro- and levorotatory helix positioned as mirror images as in Scheme 19a. An unequivocal solution to the problem may be achieved, in analogy to the optical solution illustrated in Section II, if a second micrograph is taken with the plane of the sample tilted in a known direction, yielding a new two-dimensional projection (Scheme 19b).

Direct visualization of unstained and uncoated biological materials by electron microscopy is made difficult by the poor interactions of electrons with the light atoms of organic materials (C, N, O, H, etc.) and by the high susceptibility of



Scheme 19

these materials to electron damage. The latter disadvantage prevents the use of high levels of radiation, while the former causes low contrast and chromatic aberration. The limit of achievable resolution is thus not set by the electron microscope, but rather by the sample.

Dark-field electron microscopy (in which the image is formed from the scattered beam), when combined with improved techniques of sample handling and preparation and minimal radiation exposure, can lead to images of sufficiently undamaged DNA at a resolution of $\sim 10 \text{ \AA}$ (116). Figure 45 shows such an image in which the two-dimensional projection of the helix is clearly visible on the undamaged part of the molecule.

The kind of information we are seeking therefore seems within reach, but is at the very limit of the performance available today from electron microscopy of uncoated and unstained biological macromolecules. Some improvements may be obtained by staining, for example with uranyl acetate. This stain binds specifically to phosphate groups along the DNA chain without modifying the helix

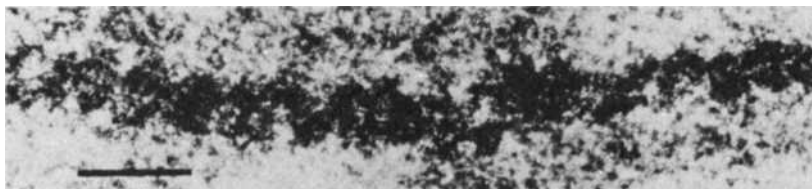


Figure 45. Dark-field micrograph of a small segment of unstained, unshadowed, naked double-stranded DNA from a bacteriophage. A relatively well-preserved image of the two-dimensional projection of the double helix is seen in the left half. The scale bar equals 35 \AA (116). (Reproduced with kind permission from the *Annual Review of Biophysics and Bioengineering*, Vol. 8 © 1979 by Annual Reviews, Inc.)

structure and allows better visualization and resolution in the dark-field image (117).

Increased resolution coupled with smaller radiation damage might be achieved by imaging of macromolecules that tend to associate in two-dimensional lattices. This technique, which has been applied to membrane proteins, consists in taking electron micrographs of the ordered array of hundreds of macromolecules with a weak electron dose and then computing a Fourier transform of the photographic intensities obtained by scanning the picture with a microdensitometer. In the Fourier transform the noise is easily distinguished from genuine features associated with a repetitive structure, and it can be filtered out. The object is then reconstructed from a filtered Fourier transform, yielding an image at much higher resolution (118). By this technique resolutions of 7 Å have been achieved for membrane proteins (119).

To overcome the disadvantages of radiation damage and chromatic aberration inevitably associated with techniques of direct visualization, biological samples are normally stained or shadowed with heavy atoms to outline structural detail before being analyzed by scanning electron microscopy. It is also possible to coat a macromolecule only on its exposed side when the molecule is lying on a microscope grid. Shadowing gives the sample a three-dimensional contrast that *a priori* might allow direct observation of the helicity of the macromolecule. The use of a contrast agent to model the fine details of the structure unfortunately sets a lower limit of ca. 60 Å on the resolving power. This is insufficient, in general, for the purpose of determining the helicity of the structure. A superstructure with a pitch of >60 Å can easily be detected by coating and shadowing.

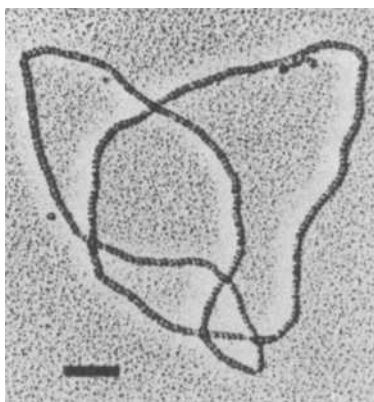


Figure 46. Electron micrograph of a Rec-A-protein-coated catenane produced by Tn3 resolvase, shadowed at an angle of 7° with carbon platinum. The scale bar equals 1000 Å (120). (Reproduced by kind permission from *Nature*, Vol. 304, 559. Copyright © 1983 by Macmillan Journals, Ltd.)

However, there remains the question of whether the chirality of the superstructure is still unequivocally defined by that of the building blocks.

In a recent paper, Krasnow and co-workers (120) applied a Rec A protein coating to DNA knots and catenanes to enhance visualization of the helical DNA segments and, in particular, to determine the absolute handedness of the knots. The Rec A protein is known to bind cooperatively to duplex DNA, forming a stiffened complex about 100 Å in diameter in the presence of ATPase (121).

The complex clearly shows cross-striations (Figure 46) on unidirectionally platinum-shadowed specimens that always correspond to a right-handed helix. It seems logical therefore to assume that these striations correspond to the helicity of the DNA molecule itself. In Krasnow's application, in particular, the easily visualized superstructure can be exploited for determination of the absolute handedness of the knots, once the two helices are known to have the same chirality. In the absence of previous knowledge on the DNA helicity, however, this assumption would be equivocal, and no conclusions about the absolute configuration of the molecules could be drawn. The same can be said about amphipathic chiral molecules, which have recently attracted renewed attention, owing to their ability to form helical fibers or other chiral organizations displaying macroscopic enantiomorphism (122-126).

B. High-Resolution Electron Microscopy of Molecular Crystals

The techniques of high-resolution electron microscopy of molecular crystals have developed within the last 15 years to such an extent that today individual atoms can be discerned, especially in highly conjugated aromatic materials (127) and organometallics (128). The resolution that has been obtained in these cases is as high as 3 Å. This becomes possible in molecular crystals because image averaging over extended areas of the crystal (several thousands of molecules) reinforces the true details associated with the repetitive molecular structure while canceling out noise.

Not every molecular crystal can be resolved at 3 Å resolution, especially not ones built of aliphatic nonconjugated molecules, which have lower electron densities and are more subject to radiation damage. The final aim of obtaining a direct three-dimensional picture of the chiral molecule itself thus cannot yet be pursued. Assignment of absolute configuration by lattice imaging, however, may be achieved even at lower resolutions (129).

In terms of the original discussion of Section II, what one needs to know is the orientation of the chiral molecule in a chiral crystal relative to the crystal axes. The absolute orientation of the molecule or of a sequence of molecules in the crystal can be determined by high-resolution electron microscopy, especially in cases like rubidium tartrate or other organometallics in which the problem is to determine the relative position of the heavy metal ion with respect to the

organic counterion. The only constraint (for crystals with a unique polar axis) is that imaging of the crystal will not be performed along the polar axis. In this situation a two-dimensional projection would reveal only superimposed atoms without it being possible to distinguish those above from those below the plane. After imaging, the orientation of the molecule must still be correlated with the crystallographic axes of the crystal. At least two electron diffraction photographs must be taken at different angles to the incident beam, on the same sample area on which imaging was performed, to establish the absolute direction of the three axes. Assignment of absolute configuration then follows directly from the combination of this information with the knowledge of the crystal structure, as in the case of X-rays.

Although no experiment of this kind has been performed, the problem seems to be solvable and to be limited only in that the system studied must have appropriate packing and be suited to imaging in terms of radiation damage stability and electron density (the latter must be high). In contrast to the assignment of absolute configuration by direct macromolecular imaging, the method is not in principle different from the previously described ones, because the solution is again provided by an additional physical technique, electron microscopy, that solves the ambiguity arising from diffraction phenomena.

C. Monolayers and Multilayers

A monolayer structure at the atomic level has recently been determined using electron diffraction and imaging methods (130). This accomplishment means that one can now assign the absolute configurations of chiral molecules of Langmuir-Blodgett monolayers from their two-dimensional diffraction patterns (say of the layer $hk0$) provided that the relative molecular arrangement of the monolayer can be deduced (from the diffraction pattern or by other means). The absolute configuration of the molecules can be derived simply from the absolute sense of the diffraction axes of the spectrum (i.e., clockwise or anticlockwise in going from a^* to b^* across the angle γ^*) because the orientation of the molecules perpendicular to the monolayer is known.

This approach may also be applied to racemic bilayers built up from homochiral Langmuir-Blodgett monolayers. By measuring the two-dimensional diffraction pattern from such a bilayer it is possible to deduce the molecular chirality of each of the two monolayers in the order they were inserted to construct the bilayer. This approach can be extended to multilayers. Thus, in principle, we close the circle started in Section IV-G-1. It is possible to assign the absolute configuration of chiral molecules in centrosymmetric crystals provided that one can construct the crystal (in this case the multilayer) by adding homochiral layers one by one.

IX. CONCLUSIONS

The purpose of this review is two pronged. We have discussed the far-reaching manifestations of molecular chirality in crystals on the macroscopic scale, and have described the various direct methods for the assignment of absolute configuration of chiral molecules in solids. Our analysis has been confined to the solid state, because of the difficulties associated with the direct assignment of absolute configuration in the dispersed phase (12).

The reduction in molecular freedom arising from creation of a repetitive structure in the solid would seem to provide the necessary means for the assignment of absolute configuration. Even then, although one can determine by conventional diffraction the relative arrangement of the atoms in the solid with the highest accuracy, the elusive piece of information is the absolute configuration of the molecule. Introduction of a chiral molecule into a crystal lattice in fact transforms a microscopic problem into a macroscopic one unless one can establish an interpretable link between the molecular chirality and macroscopic observables of the crystal. What is lacking is an orientational parameter, one that relates the orientation of the molecule to the crystal axes. It is this parameter which is the common thread linking the various methods described in this chapter and which allows us to put all the work into a simple understandable framework.

Bijvoet realized that one may assign the absolute configuration of a chiral crystal by resolving this orientational ambiguity through the anomalous scattering of X-rays. However, the overwhelming success of the Bijvoet method resulted in the comparative neglect of studies linking macroscopic properties of solids and molecular chirality. This deficiency became evident when Tanaka, in 1972, claimed that the absolute configurations of all determined structures should be reversed (27,28). An independent experimental method was subsequently conceived of and performed on zinc blende crystals to verify the conclusions based on the underlying law of anomalous scattering.

We have discussed here the other possible methods of linking macroscopic phenomena to molecular chirality in crystals. These are the morphological effect of crystal-growth inhibitors, surface etchants, selective occlusion of additives, solvent-surface interactions, and pyroelectricity. These methods are, in principle, equivalent to that of Bijvoet, but differ in generality, in ease of application, in the depth of our understanding of the mechanisms involved, and, therefore, in reliability. Properties such as the optical activity of crystals and solvent effects on the growth of crystals cannot at this stage be regarded as sufficiently understood. On the other hand, techniques such as those based on chemical reactivity or pyroelectricity of crystals will never be of wide applicability, although they may be reliable. In fact, the approach to date has been quite the reverse, namely to use the known absolute configuration of the system to understand such macroscopic phenomena.

Until recent times, the Bijvoet method provided the only reliable means for the direct assignment of absolute polarity to noncentrosymmetric crystals and, as a corollary, absolute configuration to chiral molecules. The use of additives is a viable alternative. It has the advantage of combining a number of independent and trustworthy approaches, such as morphological changes, selective occlusion, and selective etching. The method also has the virtue of simplicity, allowing one to appreciate additional changes in properties of the system, such as the lowering of the internal symmetry of the crystal and changes in internal structure, and also to analyze fine intermolecular interactions. Finally, the understanding of these macroscopic phenomena at the molecular level may have important bearing on the systematic design of new materials of interest having predictable properties.

ACKNOWLEDGMENTS

We are deeply indebted to D. Arigoni and J. D. Dunitz (Eidgenössische Technische Hochschule, Zurich) for stimulating and inspiring discussions. We thank Edna Gati, Jan van Mil, Fred Wireko, Linda J. W. Shimon, Felix Frolov, and Marianne Idelson, who performed many of the experiments described in this work. We owe thanks to the U.S./Israel Binational Foundation, Jerusalem; The Israel Academy of Sciences; the Volkswagen Stiftung; and the Petroleum Fund administered by the American Chemical Society for financial support of our work. One of us (L. A.) is incumbent of the Helena Rubinstein Career Development Chair.

APPENDIX: EXPLANATION OF CRYSTALLOGRAPHIC SYMBOLS

A crystal *unit cell* is defined by the three lattice vectors a, b, c and the angles α, β, γ . The systems referred to are defined as follows:

Triclinic:	$\alpha \neq \beta \neq \gamma \neq 90^\circ$.
Monoclinic:	$\alpha = \gamma = 90^\circ, \beta \neq 90^\circ$.
Orthorhombic:	$\alpha = \beta = \gamma = 90^\circ$.

A. Miller Indexes

- hkl : Defines the crystal planes with intercepts $a/h, b/k, c/l$.
- (hkl) : Defines a specific face.
- $\{hkl\}$: Defines all the symmetry-related faces; for example, in a centrosymmetric monoclinic crystal $\{112\}$ comprises (112) , $(\bar{1}\bar{1}\bar{2})$, $(\bar{1}1\bar{2})$, and $(1\bar{1}2)$.

hkl layer: Defines a layer of molecules at the (*hkl*) or ($\bar{h}\bar{k}\bar{l}$) face.

B. Symmetry Operations

m = mirror plane.

$\bar{1}$ = center of inversion.

2 = twofold axis.

2₁ = twofold screw axis.

The glide operations are indicated by *a*, *c*, or *n*, depending on the direction of the translation component.

C. Relevant Point Symmetries

The monoclinic point symmetry 2 comprises a twofold axis and applies to the commonly observed monoclinic chiral space groups *P*2₁ and *C*2.

The monoclinic point symmetry 2/*m* is the combination of a twofold axis and a mirror plane perpendicular to it. This combination automatically generates a center of inversion $\bar{1}$ at their intersection. This point symmetry applies to all centrosymmetric monoclinic crystals of such space groups as *P*2₁/*a*, *P*2/*a*, and *C*2/*c*.

The orthorhombic point symmetry 222 comprises three intersecting twofold axes perpendicular to each other. It applies to the commonly observed orthorhombic space group *P*2₁2₁2₁.

Orthorhombic symmetry *mm*2 comprises two mirror planes perpendicular to each other, which automatically generates a twofold axis along the line of intersection. This point symmetry applies to all noncentrosymmetric orthorhombic crystals that have mirror or glide planes such as those of space groups *Pna*2₁ and *Pca*2₁.

Point symmetry *mmm* (shorthand for 2/*m*, 2/*m*, 2/*m*) comprises three perpendicular mirror planes, which automatically generates three perpendicular twofold axes at their lines of intersection, and a center of symmetry at the origin. This point group applies to all orthorhombic centrosymmetric crystals, such as those of space group *Pbca*.

REFERENCES

1. Pasteur, L. *Ann. Phys.* **1848**, 24, 442.
2. Van't Hoff, J. H. *Arch. Neerl. Sci. Exactes. Nat.* **1874**, 9, 445.
3. Le Bel, J. A. *Bull. Soc. Chim. France* **1874**, 22, 337.
4. Fischer, E. *Chem. Ber.* **1891**, 24, 2683.
5. Rosanoff, M. A. *J. Am. Chem. Soc.* **1906**, 28, 114.

6. Bijvoet, J. M.; Peerdeman, A. F.; Van Bommel, J. A. *Nature* **1951**, *168*, 271.
7. Kirkwood, J. G.; Wood, W. W.; Fickett, W. J. *Chem. Phys.* **1952**, *20*, 561.
8. Dunitz, J. D. "X-Ray Analysis and the Structure of Organic Molecules"; Cornell University Press: Ithaca, New York, 1979, p. 129.
9. "Perhaps looking-glass milk isn't good to drink," wondered Alice in "Through the Looking Glass" by Lewis Carroll.
10. Groth, P. "Chemische Kristallographie," Bd. 1-5; Verlag von Wilhelm Engelmann: Leipzig, 1919.
11. Dunitz, J.D. in G. M. J. Schmidt et al. "Solid State Photochemistry"; D. Ginsburg, Ed.; Verlag Chemie: Weinheim, 1976, p. 261.
12. Mason, S. F. "Molecular Optical Activity and Chiral Discrimination"; Cambridge University Press: Cambridge, England, 1980.
13. In ref. 8, pp. 1-72.
14. Nishikawa, S.; Matsukawa, R. *Proc. Imp. Acad. Japan* **1928**, *4*, 96.
15. Coster, D.; Knol, K. S.; Prins, J. A. Z. *Phys.* **1930**, *63*, 345.
16. Bijvoet, J. M. *Proc. Koninkl. Ned. Akad. Wetenschap.* **1949**, *B52*, 313.
17. Trommel, J.; Bijvoet, J. M. *Acta Crystallogr.* **1954**, *7*, 703.
18. Hope, H.; de la Camp, U. *Acta Crystallogr.* **1972**, *A28*, 201.
19. Rabinovich, D.; Hope, H. *Acta Crystallogr.* **1975**, *A31*, S128.
20. Green, B. S.; Rabinovich, D.; Shakked, Z.; Hope, H.; Swanson, K. *Acta Crystallogr.* **1981**, *B37*, 376.
21. "International Tables for X-Ray Crystallography." Vol. IV; The Kynoch Press: Birmingham, England, 1974.
22. Stehn, J. R.; Goldberg, M. D.; Mayurno, B. A.; Wiener-Chasman, R. "Neutron Cross Section" (BNL 325); Brookhaven National Laboratory: 1964.
23. Johnson, C. K.; Gale, J.; Taylor, M. R. L.; Rose, I. A. J. *Am. Chem. Soc.* **1964**, *87*, 1852.
24. Seiler, P.; Martinoni, B.; Dunitz, J. D. *Nature* **1984**, *309*, 435.
25. Flook, R. J.; Freeman, H. C.; Scudder, L. *Acta Crystallogr.* **1977**, *B33*, 801.
26. Okaya, Y. In "Crystallographic Computing"; Ahmed, F. R., Hall, S. R., Huber, C. P., Eds.; Munksgaard: Copenhagen, 1970, p. 127.
27. Tanaka, J. *Acta Crystallogr.* **1972**, *A28*, 229.
28. Tanaka, J.; Katayama, C.; Ogura, F.; Tatemitsu, H.; Nakagawa, H. *Chem. Comm.* **1973**, 21.
29. Brongersma, H. H.; Mul, P. M. *Chem. Phys. Lett.* **1973**, *19*, 217.
30. Waser, J. J. *Chem. Phys.* **1949**, *17*, 498.
31. Turner, E. E.; Lonsdale, K. J. *Chem. Phys.* **1950**, *18*, 156.
32. Buckley, H. E. "Crystal Growth"; Wiley: New York, 1951.
33. Wells, A. F. *Phil. Mag.* **1946**, *37*, 180, 217, 605.
34. Kern, R. *Bull. Soc. Fr. Miner. Crystallogr.* **1953**, *76*, 391.
35. Hartman, P. In "Physics and Chemistry of the Organic Solid State," Vol. 1; Fox, D.; Labes, M. M.; Weisberger, A., Eds.; Interscience: New York, 1963, p. 369. *Idem. Ibid.*, Vol. 2; p. 873.
36. Dunning, W. J. D.; Albon, N. "Growth and Perfection of Crystals"; Doremus, R. H.; Roberts, B. W.; Turnbull, D., Eds.; Wiley: London, 1958, p. 416.
37. Smythe, B. M. *Aust. J. Chem.* **1967**, *20*, 1115.
38. Mantovani, G.; Gilli, G.; Fagioli, F. *Compt. Rend. XIII Assembly* **1967**, *C115*, 289.
39. Van Hook, A. *Kristal. Acad. Nauk. SSSR Inst. Kristallogr.* **1968**, *8*, 45.
40. Van Hook, A. J. *ASSBT* **1981**, *21*, 130.
41. Michaelis, A. S.; van Kreveld, A. *Neth. Milk Dairy J.* **1966**, *20*, 163.
42. Wells, A. F. *Disc. Faraday Soc.* **1949**, *5*, 197.

43. Berkovitch-Yellin, Z.; van Mil, J.; Addadi, L.; Idelson, M.; Lahav, M.; Leiserowitz, L. *J. Am. Chem. Soc.* **1985**, *107*, 3111.
44. Addadi, L.; Berkovitch-Yellin, Z.; Weissbuch, I.; van Mil, J.; Shimon, L. J. W.; Lahav, M.; Leiserowitz, L. *Angew. Chem. Int. Ed. Engl.*, **1985**, *24*, 466.
45. Addadi, L.; Weissbuch, I.; Berkovitch-Yellin, Z.; Lahav, M.; Leiserowitz, L.; Weinstein, S. *J. Am. Chem. Soc.* **1982**, *104*, 2075.
46. Addadi, L.; Berkovitch-Yellin, Z.; Domb, N.; Gati, E.; Lahav, M.; Leiserowitz, L. *Nature* **1982**, *296*, 21.
47. Weissbuch, I.; Addadi, L.; Berkovitch-Yellin, Z.; Gati, E.; Weinstein, S.; Lahav, M.; Leiserowitz, L. *J. Am. Chem. Soc.* **1983**, *105*, 6615.
48. Leiserowitz, L.; Schmidt, G. M. J. *J. Chem. Soc. A* **1969**, 2372.
49. Wang, J. L. Unpublished results.
50. Leiserowitz, L.; Tuval, M. *Acta Crystallogr.* **1978**, *B34*, 1230.
51. Berkovitch-Yellin, Z.; Addadi, L.; Idelson, M.; Lahav, M.; Leiserowitz, L. *Angew. Chem. Suppl.* **1982**, 1336.
52. Blake, C. C.; Small, R. W. *Acta Crystallogr.* **1972**, *B28*, 201.
53. Berkovitch-Yellin, Z.; Leiserowitz, L. *J. Am. Chem. Soc.* **1980**, *102*, 7677.
54. Addadi, L.; Weinstein, S.; Gati, E.; Weissbuch, I.; Lahav, M. *J. Am. Chem. Soc.* **1982**, *104*, 4610.
55. Sequeira, A.; Rajagopal, H.; Chidambaram, R. *Acta Crystallogr.* **1972**, *B28*, 2514.
56. Verbist, J. J.; Lehman, M. S.; Koetzle, T. F.; Hamilton, W. C. *Acta Crystallogr.* **1972**, *B28*, 3006.
57. Gil-Av, E.; Hare, P. E.; Tishbee, A. *J. Am. Chem. Soc.* **1980**, *102*, 5115.
58. Weinstein, S. *Angew. Chem. Int. Ed. Engl.* **1982**, *21*, 218.
59. Fredga, A. *Tetrahedron* **1960**, *8*, 126.
60. Honess, A. P. "The Nature, Origin and Interpretation of Etch Figures on Crystals"; Wiley: New York, 1927, p. 6.
61. Johnston, W. G. In "Progress in Ceramic Science," Vol. 2; Burke, Z. E., Ed.; Pergamon: Oxford, 1962, p. 175.
62. Franck, F. C. In "Growth and Perfection of Crystals"; Doremus, R. H.; Roberts, B. W. Turnbull, D., Eds.; Wiley: New York, 1958, p. 411.
63. Hari Babu, V.; Subba Rao, V. V. *Progr. Cryst. Growth Charact.* **1984**, *8*, 261.
64. Thomas, J. M.; Evans, E. L.; Clarke, T. A. *J. Chem. Soc. A* **1971**, 2338.
65. Shimon, L. J. W.; Lahav, M.; Leiserowitz, L. *J. Am. Chem. Soc.* **1985**, *107*, 3375.
66. For a recent review on polar crystals, see Paul, I. C.; Curtin, D. Y. *Chem. Rev.* **1981**, *81*, 525.
67. Berkovitch-Yellin, Z.; Addadi, L.; Idelson, M.; Leiserowitz, L.; Lahav, M. *Nature* **1982**, *296*, 27.
68. Visser, R. A.; Bennema, P. *Neth. Milk Dairy J.* **1983**, *37*, 109. Visser, R. A. Ph.D Thesis, Catholic University of Nijmegen, Holland, 1983.
69. Traube, N. *N. Jahrb. F. Min. Geol. USW*, Beilage Bd. 7, 1891, S430.
70. Fries, P. C.; Rao, S. T.; Sundaralingam, M. *Acta Crystallogr.* **1971**, *B27*, 994.
71. Beevers, C. A.; Hansen, H. N. *Acta Crystallogr.* **1971**, *B27*, 1323.
72. Smythe, B. M. *Sugar Technol. Rev.* **1971**, *1*, 191.
73. Jeffrey, G. A.; Park, Y. J. *Acta Crystallogr.* **1972**, *B28*, 257.
74. Berman, H. M. *Acta Crystallogr.* **1970**, *B26*, 290.
75. Cahn, R. S.; Ingold, C.; Prelog, V. *Angew. Chem. Int. Ed. Engl.* **1966**, *5*, 385.
76. Prelog, V.; Helmchen, G. *Angew. Chem. Int. Ed. Engl.* **1982**, *21*, 567.
77. Winter, C. E. *J. Chem. Ed.* **1983**, *60*, 550.
78. Weissbuch, I.; Shimon, L. J. W.; Berkovitch-Yellin, Z.; Addadi, L.; Leiserowitz, L.; Lahav, M. *Isr. J. Chem.* **1985**, *25*, 353.

79. Weissbuch, I.; Berkovitch-Yellin, Z.; Leiserowitz, L.; Lahav, M. *Isr. J. Chem.* **1985**, *25*, 362.
80. Frey, M. N.; Lehman, M. S.; Koetzle, T. F.; Hamilton, W. C. *Acta Crystallogr.* **1973**, *B29*, 876.
81. The terms "enantiotopic" and "homotopic" are used according to the nomenclature introduced by K. Mislow and M. Raban, *Top. Stereochem.* **1967**, *1*, 1.
82. Ariel, S. Ph.D. Thesis, Feinberg Graduate School, Weizmann Institute of Science, Rehovot, Israel, 1981.
83. Legros, S. P.; Kvick, A. *Acta Crystallogr.* **1980**, *B36*, 3052, and references therein.
84. Weissbuch, I.; Addadi, L.; Berkovitch-Yellin, Z.; Gati, E.; Lahav, M.; Leiserowitz, L. *Nature* **1984**, *310*, 161.
85. Freeman, H. C.; Paul, G. L.; Sabine, T. M. *Acta Crystallogr.* **1970**, *B26*, 925.
86. Cameron, T. S.; Duffin, M. *Cryst. Struct. Comm.* **1974**, *3*, 539. Wei, K. T.; Wald, D. L. *Acta Crystallogr.* **1977**, *B33*, 797.
87. Donohue, J. *J. Am. Chem. Soc.* **1950**, *72*, 949.
88. Weissbuch, I.; Shimon, L. J. W.; Wulff, J. Work in progress.
89. Wang, J. L.; Berkovitch-Yellin, Z.; Leiserowitz, L. *Acta Crystallogr.* **1985**, *B41*, 341.
90. Wang, J. L.; M.Sc. Thesis, Feinberg Graduate School, Weizmann Institute of Science, Rehovot, Israel, 1983.
91. Weisinger, Y.; Frolow, F.; McMullan, R.; Leiserowitz, L. Work in progress.
92. Miller, R. S.; Curtin, D. Y.; Paul, I. C. *J. Am. Chem. Soc.* **1974**, *96*, 6340.
93. Duesler, E. N.; Kress, R. B.; Lin, C. T.; Shiau, W. I.; Paul, I. C.; Curtin, D. Y. *J. Am. Chem. Soc.* **1981**, *103*, 875.
94. Chenchalah, P. C.; Holland, H. L.; Richardson, M. F. *J. Chem. Soc. Chem. Comm.* **1982**, 436.
95. Schmidt, G. M. J. *J. Chem. Soc.* **1964**, 2014.
96. Hung, J. D.; Lahav, M.; Luwisch, M.; Schmidt, G. M. J. *Isr. J. Chem.* **1972**, *10*, 585.
97. Van Mil, J.; Vaida, M. Work in progress.
98. Hartman, P.; Perdok, W. G. *Acta Crystallogr.* **1955**, *8*, 49.
99. Hartman, P. *J. Cryst. Growth* **1980**, *49*, 157, 166.
100. Berkovitch-Yellin, Z. *J. Am. Chem. Soc.* in press.
101. Saska, M.; Myerson, A. S. *J. Cryst. Growth* **1983**, *61*, 546.
102. Wireko, F. C.; Berkovitch-Yellin, Z.; Frolow, F.; Lahav, M.; Leiserowitz, L. Submitted for publication.
103. Davey, R. J. *J. Cryst. Growth* **1976**, *34*, 109.
104. Davey, R. J. In "Current Topics in Material Science," Vol. 8; Kaldis E., Ed.; North Holland: Amsterdam, 1982, Chapter 6.
105. Bourne, S. R. *AICHE Symp. Ser.* **1980**, *193*, 76.
106. Milisavljevic, B. C. Ph.D. Thesis, Swiss Federal Institute of Technology, Zurich, 1982 (Dissertation N6898).
107. Berkovitch-Yellin, Z.; Leiserowitz, L. *Acta Crystallogr.* **1984**, *B40*, 159.
108. Abrahams, S. C. In "Anomalous Scattering"; Ramaseshan, S.; Abrahams, S. C., Eds.; Munksgaard: Copenhagen, 1974, p. 199.
109. Glazer, A. M.; Moxon, J. R. L.; Stadnika, K. M.; Thomas, P. A. In "Collected Abstracts of the 13th International Congress of Crystallography"; Bonse, V., Ed.; Hitzegrad: Dortmund, 1984, p. C-150.
110. Fletcher, S. R.; Keve, E. T.; Skapski, A. C. *Ferroelectrics* **1976**, *14*, 775, and references therein.
111. Rogers, D. *Acta Crystallogr.* **1981**, *A37*, 734.
112. Bernardinelli, G.; Flack, H. D. *Acta Crystallogr.* **1985**, *A41*, 500.

113. Lock, P. J. *Appl. Phys. Lett.* **1971**, *19*, 390.
114. Patil, A. A.; Curtin, D. Y.; Paul, I. C. *J. Am. Chem. Soc.* **1985**, *107*, 726.
115. Arigoni, D. Private communication. See also ref. 8, p. 144.
116. Ottensmeyer, F. P. *Ann. Rev. Biophys. Bioeng.* **1979**, *8*, 129.
117. Korn, A. P.; Spitnik-Elson, P.; Elson, D. *J. Biol. Chem.* **1982**, *257*, 7155.
118. Unwin, P. N. T.; Henderson, R. *Sc. Am.* **1984**, *250* (February), 56.
119. Unwin, P. N. T.; Henderson, R. *J. Mol. Biol.* **1975**, *94*, 25.
120. Krasnow, M. A.; Stasiak, A.; Spengler, S. J.; Dean, F.; Koller, T.; Cozzarelli, N. R. *Nature* **1983**, *304*, 559.
121. Di Capua, E.; Engel, A.; Stasiak, A.; Koller, T. *J. Mol. Biol.* **1982**, *157*, 87.
122. Hotten, B. W.; Birdsall, D. H. *J. Colloid Sci.* **1952**, *7*, 284.
123. Tashibana, T.; Kambara, H. *J. Am. Chem. Soc.* **1965**, *87*, 3015.
124. Hidaka, H.; Murata, M.; Onai, T. *J. Chem. Soc. Chem. Comm.* **1984**, 562.
125. Weis, R. M.; McConnel, H. M. *Nature* **1984**, *310*, 47.
126. Nakashima, N.; Asakuma, S.; Kunitake, T. *J. Am. Chem. Soc.* **1985**, *107*, 509.
127. Fryer, J. R.; Smith, J. R. *Proc. Roy. Soc. London* **1982**, *A381*, 225.
128. Uyeda, N.; Kobayashi, T.; Ishizuka, K.; Fuyiyoshi, Y. *Nature* **1980**, *285*, 96.
129. We thank Prof. J. M. Thomas and Dr. W. Jones for useful discussions on this aspect of electron microscopy.
130. Fryer, J. R.; Hann, R. A.; Eyres, B. L. *Nature* **1985**, *313*, 382.

Asymmetric Catalysis by Alkaloids

HANS WYNBERG

*Department of Chemistry
University of Groningen
Groningen, The Netherlands*

I.	Introduction	88
A.	Comparison Between Enzymic and Nonenzymic Asymmetric Catalysis	88
II.	The Chiral Bases—The Cinchona Alkaloids	91
A.	Diastereomeric Nature of Cinchona Alkaloids	91
B.	Conformation and Mechanism	92
C.	The β - Hydroxyamine Portion of the Alkaloid	93
D.	The Quinoline and Quinuclidine Portions of the Alkaloid	95
III.	The Cyanohydrin Reaction	95
IV.	The Michael Reaction	96
A.	Ketoester Donors	96
B.	Other Michael Donors	97
C.	Mechanism of the Reaction	99
V.	The 1,4-Thiol and -Thiolacetate Additions	99
A.	The Absolute Configuration	100
B.	Kinetic Resolution Using the Chiral-Amine-Catalyzed Thiol Addition Reaction	104
C.	Synthetic Utility of Asymmetrically Catalyzed Thiol Addition Reactions	105
D.	Addition of Thiolacetic Acid to Electron-Poor Olefins	107
E.	Miscellaneous Studies	108
F.	The Mechanism of the 1,4-Thiol Addition Reaction	108
VI.	Selenophenol Addition Reaction	110
VII.	Epoxidation of Electron-Poor Olefins	113
A.	Vitamin K ₃ Epoxide	116
B.	The Chalcones	116
C.	Solvent Effects	118
D.	The Cyclohexenones	118
E.	The Catalyst	119
F.	The Mechanism of the Reaction	120
VIII.	Formation of the Phosphorus—Carbon Bond Using Chiral Amine Catalysis	122
IX.	2,2-Cycloaddition Reaction Catalyzed by Quinine Esters	122
X.	1,2-Additions	124
XI.	Conclusions	124
	Acknowledgments	126
	References	127

I. INTRODUCTION

This chapter deals primarily with cinchona-alkaloid-catalyzed asymmetric syntheses.

The use of alkaloids in preparing optically active organic compounds has a venerable past. One hundred and thirty-two years ago Pasteur (1,2) used derivatives of quinine to effect the resolution of racemic acids, and even today the use of alkaloids in resolutions remains widespread (3).

It should come as no surprise that a chapter dealing with asymmetric catalysis should mention resolutions. Resolutions depend primarily on the solubility differences of diastereomers in the ground state. X-Ray analyses of diastereomeric salts (4,5) appear to point to a "best-fit" structure for the least soluble salt. Success in asymmetric catalysis depends on free-energy differences between diastereomeric transition states. When these energy differences approach 2 kcal/mol, resulting in an e.e. of 93% at 25°C, the favored complex, although the result of a termolecular reaction, shows the best-fit characteristics typical of a diastereomeric salt.

A. Comparison Between Enzymic and Non-enzymic Asymmetric Catalysis

Many attempts have been made during the past 50 years to imitate enzymes. Studies in the preparation of "artificial enzymes" (6) and "model enzymes" abound. While it is undoubtedly true that most enzymes can achieve the transformation of an achiral substrate to a chiral one more rapidly and with higher specificity than can be achieved using nonenzymic catalysts, the many limitations to which enzymic catalysis is subject should be properly evaluated. These are as follows:

1. The large to very large molecular weights of most enzymes render them inherently unstable. *In vivo*, most enzymes have half-lives in the range of minutes to hours (7). Obviously, imitating the instability of enzymes is not desirable.
2. Most but not all enzymes are inactivated by solvents other than water. Since many organic reactions proceed best in the absence of water, the design of an asymmetric catalyst must proceed from a premise different from mere enzyme imitation.
3. Many enzymes need cofactors. Here again, a nonenzymic chiral catalyst functioning without a cofactor would offer an advantage.
4. Although in a limited number of cases both enantiomeric forms of a



Figure 1. Enzyme-catalyzed reaction (8).

natural product have been identified as occurring in nature, the corresponding enantiomeric enzymes have never been isolated. In general, it is fair to say that most enzymic reactions proceed to produce a single enantiomer. Since, by contrast, most nonenzymic catalysts are available in enantiomeric or diastereomeric forms, use of these catalysts allows the preparation of either enantiomer of the desired product. Surely this fact alone should encourage the use of nonenzymic chiral catalysts.

5. Except for oxido-reductases, transferases, and hydrolases, most ligases (enzymes that catalyze bond formation) are entirely substrate specific. Thus, fumarate hydratase (or fumarase) reversibly and stereospecifically "adds" water to fumaric acid to produce (S)-(-)-malic acid only (8) (Figure 1), and another enzyme, mesaconase, adds water to mesaconic acid to form (+)-citramalic acid (9) (Figure 2). Although no extensive studies are available, it appears that neither fumarase nor mesaconase will add water stereospecifically to any other α,β -unsaturated acid.

A major advantage that nonenzymic chiral catalysts might have over enzymes, then, is their potential ability to accept substrates of different structures; by contrast, an enzyme will select only "its" substrate from a mixture. Striking examples are the chiral phosphine-rhodium catalysts, which catalyze the hydrogenation of double bonds to produce chiral amino acids (10–12), and the titanium isopropoxide-tartrate complex of Sharpless (11,13,14), which catalyzes the epoxidation of numerous allylic alcohols. Since the enantiomeric purities of the products from these reactions are exceedingly high (>90%), we might conclude



Figure 2. Enzyme-catalyzed reaction (9).

that the generality of nonenzymic catalysts is greater than that of enzymes.

Perhaps the only distinct advantage of enzymic catalysts is their (occasionally) very high turnover rate *in situ*. Thus, the molar activity (formerly called the turnover number) of some enzymes approaches 36,000,000/min/molecule (7). This latter number pertains to carbonic anhydrase C, the enzyme that converts CO_2 to HCO_3^- . However, chemists do not need enzymes to convert CO_2 to HCO_3^- , as long as we are not considering *in vivo* reactions. Since many enzymes have molar activities as low as 1150/min/molecule, we need not consider molar activities of 100 to 500 (for nonenzymic catalysts) as a severe handicap. It is evident that enzymes and nonenzymic chiral catalysts, rather than being competitors, complement one another.

A final word needs to be said about the supposedly unique features of enzymes, namely, their ability to produce enantiomerically pure products. This is not the place to speculate about the stereospecificity of enzymes, a problem that has been discussed elegantly by Cornforth (15). It cannot be denied that the high (>99.9%) enantiomeric purity achieved by enzymes may be uniquely useful in the case of liquid products. However, when crystalline products are obtained in an asymmetric synthesis and the e.e. exceeds 80%, crystallization to enantiomeric purity without excessive loss of material is routinely achieved.

The case in favor of nonenzymic chiral catalysts is summarized in Table 1.

Table 1
Typical Properties of Enzymes and Nonenzymic Catalysts

Property	Enzymes	Nonenzymic Catalysts
Specificity	Substrate specific	Often able to deal with different substrates
Product selectivity	One enantiomer only (per enzyme)	Both enantiomers usually accessible
Molar activity	10^3 to 10^8 /min/molecule	10^2 to 10^3 /min/molecule
Stability	Limited	Virtually unlimited
Cost	High	Moderate
Availability	Limited	Unlimited
Purity	Problematical	High
Solubility	Low	Normal
Functional-group transformations	Difficult	Normal
Modes of action	Sophisticated and complex	Relatively simple

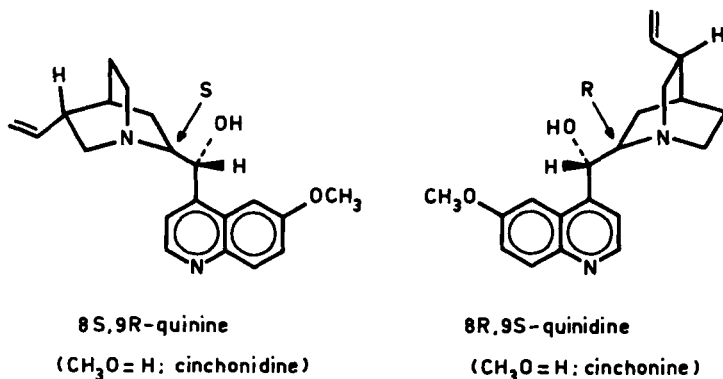


Figure 3. Structures of quinine, cinchonidine, quinidine, and cinchonine.

II. THE CHIRAL BASES—THE CINCHONA ALKALOIDS

The structures of quinine, cinchonidine, quinidine, and cinchonine are shown in Figure 3. Other workers (16,17) have discussed these alkaloids and their use as catalysts in some detail. An excellent discussion of cinchona-alkaloid-catalyzed reactions prior to 1968 was given by Pracejus (18). In this section we discuss only four aspects of these reactions.

A. Diastereomeric Nature of Cinchona Alkaloids

Quinine and quinidine, as well as cinchonidine and cinchonine, are diastereomeric pairs. However, at the critical sites—the β -hydroxyamine portions of the molecules—they are enantiomeric. Thus if quinine is used as the chiral catalyst in an asymmetric transformation (i.e., with one enantiomer being formed in excess), the other enantiomer is formed in excess when quinidine is used. Table 2 gives a representative example, the thiol addition reaction (19).

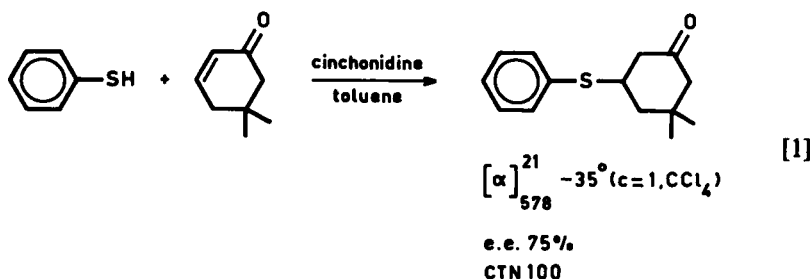
These reactions, performed many times, show, in addition to the reversal of the absolute configuration of the product with the change in the configuration at C-8 and C-9 of the alkaloids, a small but reproducible difference in the e.e. of the product. It is evident that the diastereomeric nature of quinine vs. quinidine and cinchonidine vs. cinchonine expresses itself via small but important energy differences in the "best fits" of the transition states. Noteworthy in this respect is the fine work of Kobayashi (20), who observed larger differences (in the e.e.'s of products) when the diastereomeric cinchona alkaloids were used as catalysts after having been copolymerized with acrylonitrile (presumably via the vinyl side chain of the alkaloids).

Table 2
The Cinchona Alkaloids in the Thiol Addition Reaction

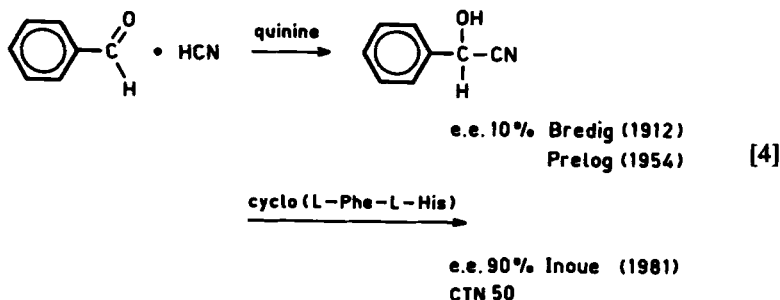
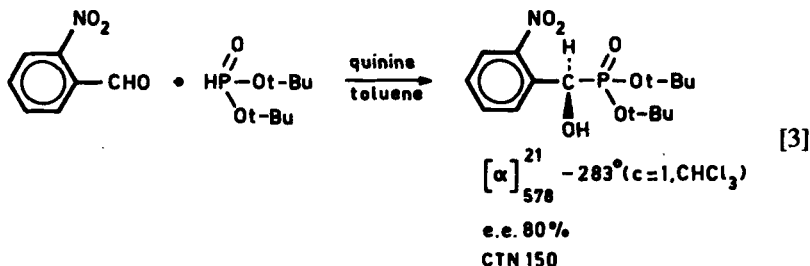
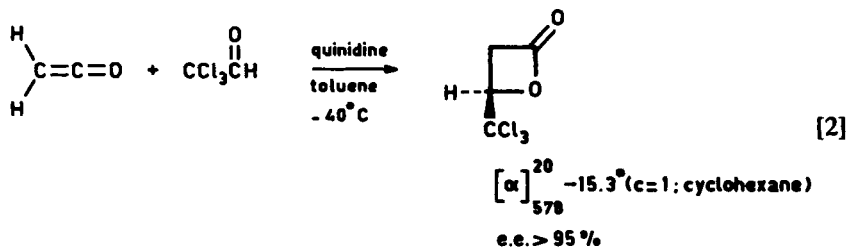
$[\alpha]_{578}^{21} 40^\circ$ ($c = 1, \text{CCl}_4$) e.e. 44% CTN100				
Catalyst	Abs. Conf. at		Product Conf.	e.e. (%)
	C-8	C-9		
Quinine	<i>S</i>	<i>R</i>	<i>R</i>	44
Quinidine	<i>R</i>	<i>S</i>	<i>S</i>	55
Cinchonidine	<i>S</i>	<i>R</i>	<i>R</i>	62
Cinchonine	<i>R</i>	<i>S</i>	<i>S</i>	67

B. Conformation and Mechanism

When quinine (or any of its diastereomers) is used as a catalyst in reactions involving relatively simple substrates such as (i) thiophenol and 5,5-dimethylcyclohexenone (19) (eq. [1]), (ii) ketene and chloral (eq. [2]) (21), (iii) *o*-nitrobenzaldehyde and di-*tert*-butyl phosphite (22,23) (eq. [3]) or (iv) benzaldehyde and hydrogen cyanide (16) (eq. [4]),* the determining factor in establishing a reasonable mechanism to explain the high degree of asymmetric induction



*In the equations, "CTN" stands for "catalytic turnover number."



will be adequate insight into the preferred conformation of the alkaloid in solution. The accurate determination of a ground-state conformation in solution is at present rarely feasible, while the determination of the conformation of a transition state must remain the organic chemist's idle dream for some time to come. Our proposed mechanisms for the reactions cited above and all other reactions discussed in this chapter are therefore based on a conformation of quinine in the transition state that appears reasonable on the basis of our results (Figures 4 and 5).

C. The β -Hydroxyamine Portion of the Alkaloid

With one notable exception, namely the ketene-chloral 2,2-addition reaction (21), all of the base-catalyzed 1,2- and 1,4-addition reactions discussed in this

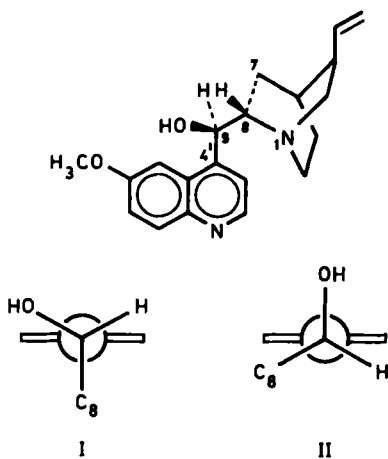


Figure 4. Preferred conformations (I and II) of quinine about the C4'-C9 Bond.

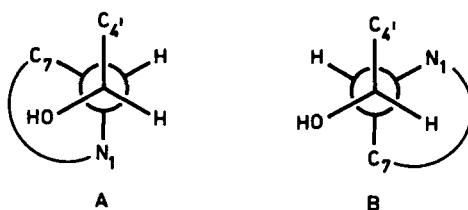


Figure 5. Preferred conformations (A and B) of quinine about the C9-C8 bond.

chapter appear to be subject to bifunctional catalysis. The amine portion of the alkaloid enhances the nucleophilicity of the nucleophile (see Figure 6), whereas the free hydroxyl group enhances the acceptor qualities of the electrophile.

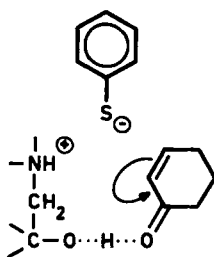


Figure 6. Bifunctional catalysis by β -hydroxyamines.

D. The Quinoline and Quinuclidine Portions of the Alkaloid

Both the aromatic quinoline and the alicyclic quinuclidine portions of the ring fill important functions during the catalytic process. The positioning of their large bulks at crucial angles to one another provides steric hindrance to the active site such that the approach of molecules like chloral (eq. [2]) is limited to one reaction path. In addition, the possibility of π - π (charge-transfer) interactions between the quinoline ring and an aromatic reactant is undoubtedly a factor contributing to quinine's versatility as a chiral catalyst.

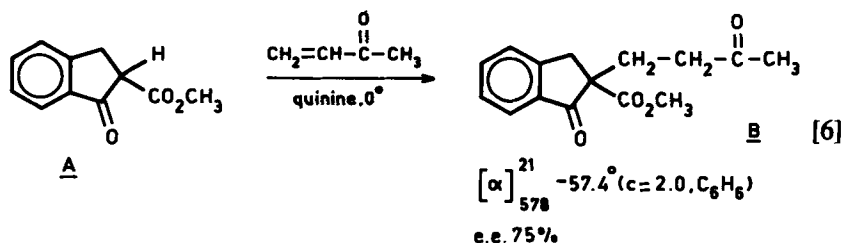
III. THE CYANOHYDRIN REACTION

It is of some historical interest that Kiliani's cyanohydrin synthesis (24) enabled Emil Fischer (25) to carry out the first asymmetric synthesis. Lapworth (26) used this base-catalyzed nucleophilic 1,2-addition reaction in one of the first studies of a reaction mechanism. Bredig (27,28) appears to have been the first to use quinine (29) in this reaction as the chiral basic catalyst. More recently, others (20) have used basic polymers to catalyze the addition of cyanide to aldehydes. The structure of quinine has been known since 1908 (30). Yet it is of critical importance that Prelog's seminal work on the mechanism of this asymmetric transformation (eq. [4]) could not have begun (16) until the configuration of quinine was established in 1944 (31,32).

Since the reaction has been reviewed recently (12) only a few additional facts will be mentioned. Many optically active cyanohydrins can be prepared (33) with e.e.'s of 84 to 100% by the use of the flavoprotein D-oxynitrilase adsorbed on special (34) cellulose ion-exchange resins. Although the enzyme is stable, permitting the use of a continuously operating column, naturally only one enantiomer, usually the *R* isomer, is produced in excess. This (reversible) enzyme-catalyzed reaction is very rapid (34). Nonenzymic catalysts, such as the cinchona alkaloids, permit either enantiomer to be prepared in excess.

An important contribution was recently made by Inoue and co-workers (35) (eq. [4]). Using the chiral cyclic dipeptide cyclo(L-Phe-L-His) these authors obtained a better than 90% e.e. in the reaction of benzaldehyde with cyanide ion. The preparation of the enantiomeric "unnatural" dipeptide obviously poses far fewer problems than the synthesis of an enantiomeric enzyme. It appears that, at least in principle, optically pure cyanohydrins of the desired configuration are accessible via catalysis by chiral amines or amides.

Inoue's work (35), as well as that of others (36) discussed below, points to an important feature in the study of asymmetric catalysis. Once it has been shown that a reaction can be catalyzed by a chiral molecule to produce one enantiomer in excess, practically useful optical yields can usually be achieved given sufficient



This has become something of a standard reaction, since several authors have successfully used different chiral catalysts to effect the conversion in very high chemical and enantiomeric yield. Bergson and Langstrom (41) were the first to show that acrolein and α -isopropylacrolein added to 2-carbomethoxy-1-indanone (A in eq. [6]) in benzene in the presence of the strongly basic tertiary amine (*R*)-(+)-2-(hydroxymethyl)quinuclidine to yield optically active ketoesters. Unfortunately, the quinuclidine catalyst was not enantiomerically pure, and neither the chemical nor the optical yields of the aldehydo ester analogous to B (eq. [6]) were reported.

Concurrently, we had been studying the same reaction using methyl vinyl ketone as the Michael acceptor and quinine as the chiral base (eq. [6]). The ketoesters formed in 87% yield with an e.e. of 76%. The reaction is noteworthy as the first example of a Michael reaction using a chiral amine as catalyst in which the e.e. and the absolute configuration were established. Thus, using (8*S*,9*R*)-quinine (*S*)-(−) ester is produced, while (8*R*,9*S*)-quinidine furnishes the (*R*)-(+) isomer in 69% e.e. Later studies by Cram (36) showed that e.e.'s approaching 99% could be obtained using chiral crown ethers as catalysts. Early attempts (45) to attach quinine to a polymer to facilitate removal of the catalyst from the reaction mixture were disappointing.

Much greater success with chiral polymer catalysts was obtained by Norio Kobayashi (20). The Japanese researcher copolymerized quinine and acrylonitrile, using the vinyl group of the cinchona alkaloid as the connecting site. Enantiomeric yields of nearly 50% were realized with this polymer.

A third variation on this theme was recently reported by Hodge (48), who alkylated the cinchona alkaloids on the quinuclidine nitrogen using the well-known chloromethylated cross-linked polystyrenes. Optical yields were low (10 to 30%) and no significant conclusions were drawn.

B. Other Michael Donors

Using methyl vinyl ketone as Michael acceptor, it was found (42) that a variety of donors gave optically active products when quinine was used as the chiral catalyst. Figure 7 lists the donors. Unfortunately in none of these cases

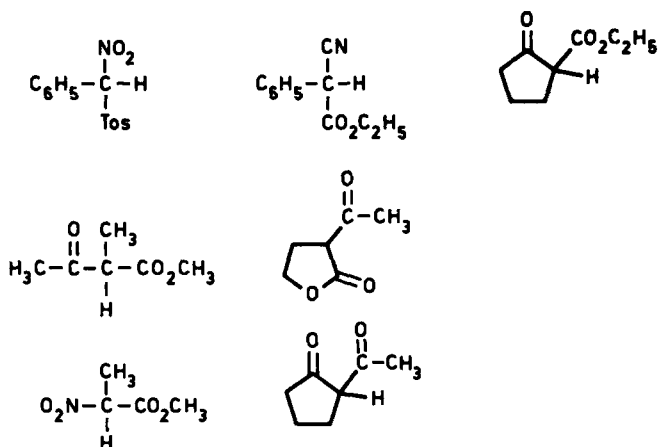
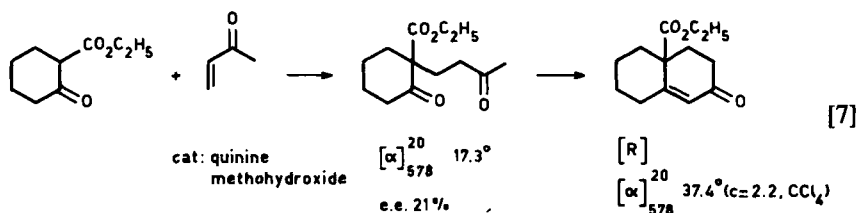


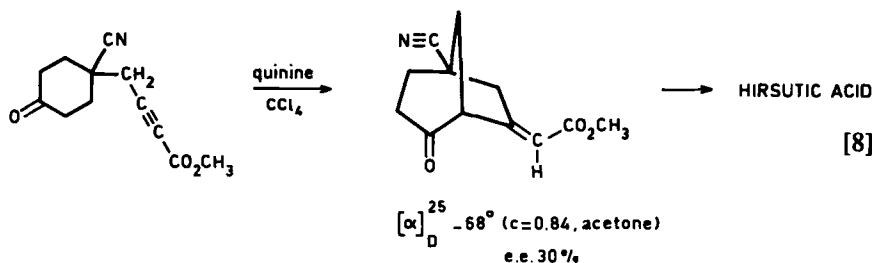
Figure 7. Donors in the quinine-catalyzed Michael Reaction (42).

was the percentage e.e. determined. These reactions are being reinvestigated. More detail is known about the reaction of 2-carboethoxycyclohexanone with methyl vinyl ketone (eq. [7]). Instead of using quinine as the free base, it was found necessary to use the quinine methohydroxide, a much stronger base, as the catalyst. The product was converted to the decalones and the absolute configurations and e.e.'s were determined. The quinine methohydroxide furnished the product having the *R* configuration in 96% chemical and 21% enantiomeric yield (44,92).

The addition of nitromethane to chalcones has been studied using *N*-benzylquininium chloride as the chiral phase-transfer catalyst and fluoride ion as the base (46). The enantiomeric excess was moderate (up to 26%). No conclusions were drawn from this study.

A final example, from the work of Trost (49), represents the only case in which an *intramolecular* Michael reaction has been catalyzed by a chiral amine. When the achiral cyclohexanone is treated with (–)-quinine and heated in toluene solution, the bicyclic ketone is formed in 83% chemical and 30% enantiomeric yield (eq. [8]).





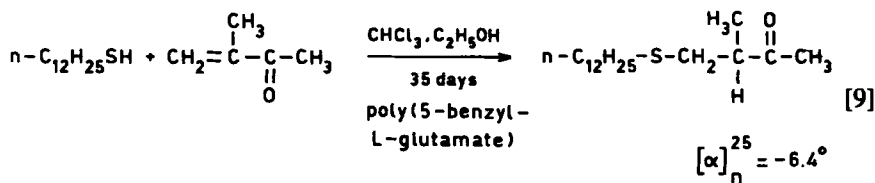
C. Mechanism of the Reaction

Only Cram (36) has published a rationale for the very high (99%) enantiomeric excess achieved in the reaction of methyl vinyl ketone and the hydrindanone in the presence of the chiral crown ether. This mechanism envisions a bimolecular complex comprising the potassium cation and chiral host as one entity and the enolate anion of the hydrindanone as the counterion. Methyl vinyl ketone lies outside this complex. The quinine-catalyzed reaction appears to have a termolecular character, since the hydroxyl of the alkaloid probably hydrogen bonds with the methyl vinyl ketone—enhancing its acceptor properties—while the quinclidine nitrogen functions as the base forming the hydrindanone—alkaloid ion pair.

From the examples cited above, it is evident that a great deal of research remains to be done on the chiral-amine-catalyzed Michael reaction. All mechanistic proposals have been based solely on knowledge of the absolute configuration of the products, while kinetic data as well as steric factors have not been carefully delineated. Since the research thus far has been restricted entirely to products in which just one chiral center is formed, it is clear that there is no lack of problems to be studied.

V. THE 1,4-THIOL AND -THIOLACETATE ADDITIONS

Japanese workers (50,51) were the first to observe optical activity in the addition of thiols to electron-poor olefins (eq. [9]). The e.e. was not determined, but these observations led us to attempt using a cinchona alkaloid as the catalyst in the addition of thiophenol to cyclohexenone. The reaction lends itself admirably to a scope, limitations, and mechanism study, and the results have been published in detail (19). An important mechanistic difference between the addition of the dodecanethiol to isopropenyl methyl ketone and the addition of thiophenol to a cyclohexenone (eq. [1]) lies in the sequence of chirality-producing steps. In the former case, chirality is produced when the proton adds to the α -carbon atom of the ketone—after thiol addition has taken place. In the latter



case, the first, and rate-determining step, bond formation between the sulfur and β -carbon atoms, is also the chirality-producing step. The low e.e.'s in the thiol addition to the isopropenyl ketone are probably a consequence of this difference. Since only a few catalytic asymmetric transformations have been subjected to detailed kinetic analyses, it appears worthwhile to summarize the results of the cyclohexenone study (19):

1. The reaction obeys pseudo-second-order kinetics that are first order in thiol, cycloalkenone, and catalyst.
2. An activation enthalpy of 0 to 4 kJ/mol and an activation entropy of -260 kJ/mol was determined.
3. The strong curvature of the Eyring plots at temperatures below 35°C (see ref. 19a, Table V and Figure 6) points to hydrogen-bonded interactions between catalyst molecules, as already observed in 1969 by Uskokovic (52) in the ^1H nuclear magnetic resonance (NMR) spectrum of dihydroquinine.
4. The solvent effect in this reaction is large. Table 3 lists the effects on the e.e. of a large number of solvents in which the reaction proceeds normally.
5. Acylation of the alcohol hydroxyl of the cinchona alkaloid lowers the reaction rate by a factor of 100 while lowering the e.e. to 10%.

A. The Absolute Configuration (19b)

Since all of the thiol addition products were unknown compounds, except for racemic 3-phenylthiocyclohexanone, it became necessary to devise a method for determining the absolute configuration without resorting to Bijvoet's method (53) for each new compound (see Table 4). This was accomplished by preparing the thioacetal of the adamantanedione, a model 3-thiosubstituted cyclohexanone of known absolute configuration (54) (eq. [10]).

The ultraviolet (UV) and circular dichroism (CD) spectra of the thioacetal are shown in Figure 8. The UV spectrum gives bands for the $n\pi^*$ transition of the carbonyl group at 300 nm and for a sulfur transition at 245 nm. These bands

Table 3
Solvent Effects^a

<p>1.81 mmole 1.56 mmole cinchonidine 0.015 mmole solvent (3 ml) 22°</p>					
Solvent	η (25°C)	Salt	Molar Ratio of Salt to Cinchoni- dine	e.e. ^b (± 2%)	Absolute Configuration
Cyclohexane	2.01			46	<i>R</i>
Carbon tetrachloride				60	<i>R</i>
Benzene	2.27			62	<i>R</i>
Toluene	2.37			62	<i>R</i>
Carbon disulfide	2.63			58	<i>R</i>
Thiophene	2.76			60	<i>R</i>
Chloroform	4.64			55	<i>R</i>
Dichloromethane	8.9			55	<i>R</i>
1,4-Dioxane	2.21			48	<i>R</i>
Ethyl ether	4.2			52	<i>R</i>
Ethyl acetate	6.0			47	<i>R</i>
Tetrahydrofuran	7.4			39	<i>R</i>
Acetone	20.7			23	<i>R</i>
Acetonitrile	36.2			15	<i>R</i>
Pyridine	12.3			3	<i>R</i>
<i>tert</i> -Butyl alcohol	12.2			16	<i>R</i>
Ethanol	24.3			0	
Benzene		(<i>n</i> -Bu) ₄ N ⁺ Cl ⁻	24.0	0	
Benzene		(<i>n</i> -Bu) ₄ N ⁺ Cl ⁻	1.0	2	<i>S</i>
Benzene		(<i>n</i> -Bu) ₄ N ⁺ Cl ⁻	0.24	2	<i>S</i>
Benzene		(<i>n</i> -Bu) ₄ N ⁺ I ⁻	24.0	1	<i>R</i>
Benzene		(<i>n</i> -Bu) ₄ N ⁺ I ⁻	1.0	7	<i>R</i>
Benzene		(<i>n</i> -Bu) ₄ N ⁺ I ⁻	0.24	17	<i>R</i>

^aFrom ref. 19b.

^bData averaged from two or three experiments.

Table 4
Influence of the Structure of Thiol and Enone on the Course of the Asymmetric Thiol
Addition Reaction

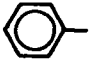
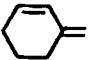
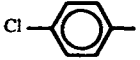
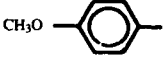
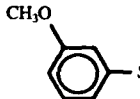
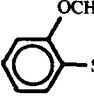


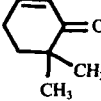
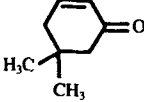
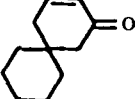
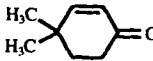

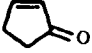
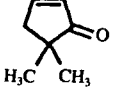

Thiol	Enone	$[\alpha]_{578}^{21}$ (c = 1, CCl ₄)	e.e. ^a (± 2%)	Absolute Con- figura- tion
 SH (1a)	 O (2a)	+ 53	54	R
 SH (1c)	2a	+ 31	35	R
 SH (1d)	2a	+ 43	50	R
 SH (1e)	2a	+ 40	52	R
 SH (1f)	2a	+ 42	50	R
 SH (1g)	2a	+ 32	37	R
 SH (1b)	2a	+ 47	62	R
1b	 O (2b)	+ 67	62	R
1b	 O (2c)	+ 35	75	R
1b	 O (2d)	+ 33	71	R

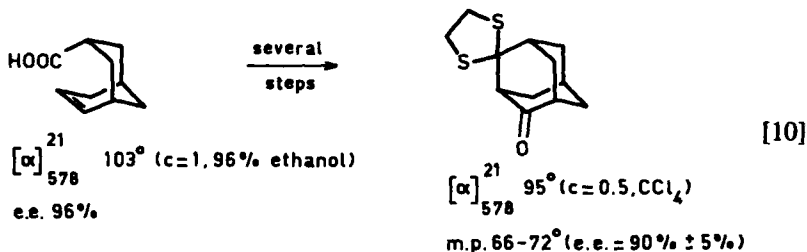
Table 4 (Continued)

Thiol	Enone	$[\alpha]_{578}^{21}$ (c = 1, CCl ₄)	e.e. ^a (± 2%)	Absolute Con-figuration
1b	 (2e)	+ 42 ^b	41 ^b	S
1b	 (2f)	+ 20	65	R
1b	 (2g)	+ 0.4	5	R
1b	 (2h)	+ 35	49	R
1b	 (2i)	+ 68	35	S

^aMost data are averages from two or three experiments.^bReaction carried out in 0.375 ml of benzene.

are also clearly visible in the CD spectrum. The carbonyl $n\pi^*$ Cotton effect is positive ($\Delta\epsilon_{\max} = +5.2$, assuming no overlap with the 245-nm band). Applying the octant rule to this ketone, the thioacetal function is found in a positive octant. Thus a thioacetal at the β -position of a cyclohexanone obeys the octant rule.

Examining the CD spectra of the newly prepared (see Table 4) thiocyclohexanones (for one example, see Figure 8) and making the assumptions that (i) the conformer population is not affected by the nature of the solvent, (ii) the cyclohexanones exist in ideal chair conformations, and (iii) the $\Delta\epsilon_{\max}$ at 300 nm arises exclusively from the $n\pi^*$ transition of the carbonyl group allows one to



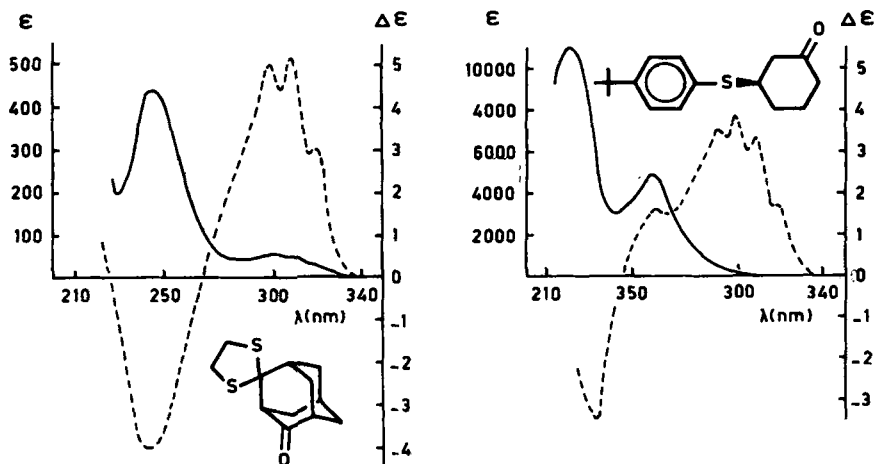


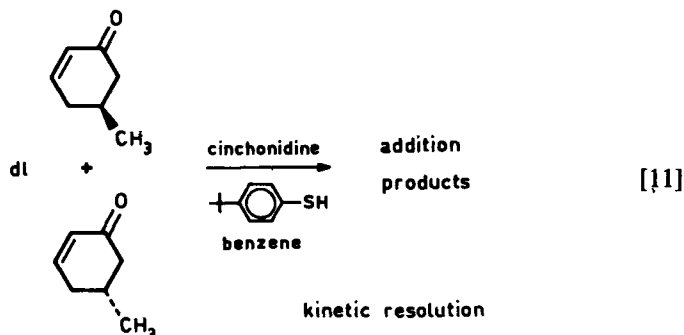
Figure 8. UV (solid lines) and CD (dashed lines) spectra of chiral sulfides (19).

assign the absolute configuration. For *trans*-3-*p*-*t*-butylphenylthio-5-methylcyclohexanone having a positive rotation, a $\delta\Delta\epsilon$ value of +5.5 was found. We conclude that a β -equatorial sulfur substituent in a cyclohexanone obeys the octant rule, with a $\delta\Delta\epsilon$ value of about +5. The absolute configurations of all of the β -substituted thiocyclohexanones listed in Table 4 were assigned similarly. For the cyclopentanones a different approach had to be used, since a fundamental difference exists with respect to the origin of the $n\pi^*$ Cotton effect.

B. Kinetic Resolution Using the Chiral-Amine-Catalyzed Thiol Addition Reaction (55)

In principle, any reaction with a racemate using a chiral reagent can be used to effect a kinetic resolution. Kagan (56) has recently given an analysis of the relationship between the extent of reaction and the enantiomeric excess that can be achieved, while Sharpless (57) has applied kinetic resolution successfully to racemic allyl alcohols using his titanium alkoxide tartrate epoxidation reaction.

We have resolved racemic 5-methyl-2-cyclohexen-1-one by reaction in the presence of catalytic amounts of cinchonidine using a 1.5:1.0 molar ratio of enone to thiophenol (excess enone) in benzene (55). The reaction (eq. [11]) was carried out at room temperature for 18 hr. The purified unreacted cyclohexenone had a rotation $[\alpha]_{578}^{21}$ of +47° ($c = 1.0$, CCl_4), indicating an optical purity of 59% and the *S* configuration. Thus the *R* isomer reacts faster with the thiophenol under these conditions. Sharpless (57) points out that even small differences in relative rate (e.g., 5-10) can provide useful amounts of a substance with high

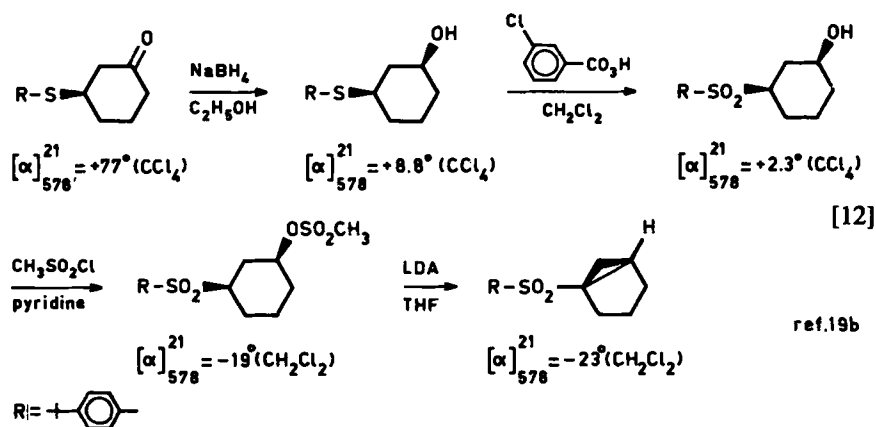


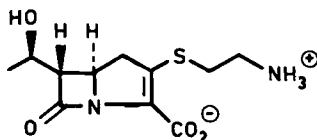
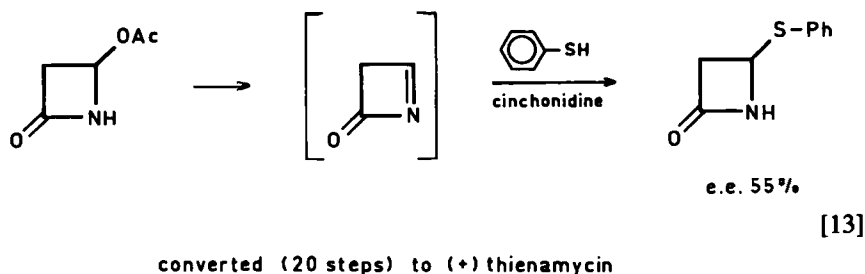
enantiomeric purity. If we further consider that we are dealing with *catalytic amounts* of the “resolving agents” (cinchonidine) it is evident that this approach—catalytic kinetic resolution of electron-poor olefins—justifies further detailed investigation (55).

C. Synthetic Utility of Asymmetrically Catalyzed Thiol Addition Reactions

The relatively high e.e.’s obtained in most of the quinine-catalyzed thiol addition reactions, the wide range of enones and thiols potentially amenable to this reaction, and the versatility of the sulfur (and carbonyl) functionality combine to make this reaction useful in many ways.

One sequence is shown in eq. [12]. Enantiomerically pure (*R*)-3-*t*-butylphenylthiocyclohexanone was reduced to the β -hydroxysulfide in 98% yield [of a mixture of diastereomers; the *cis* isomer is easily separated by crystallization





(19)], oxidized to the β -hydroxysulfone quantitatively, and converted to the crystalline mesylate (m.p. 129 to 132°C) in 67% yield. Treatment of this mesylate with LDA in THF* at -80° furnished the crystalline cyclopropane (m.p. 65.5 to 67°C) in 69% yield. If we assume complete inversion at the carbon of the mesylate leaving group, the absolute configuration of the cyclopropane ($[\alpha]_{578}^{21} = -23^\circ$) is as in eq. [12].

Recently Ikegami used the thiol addition reaction in the preparation of optically pure 4-phenylthioazetidin-2-one, the starting material for an elegant (+)-thienamycin synthesis (58). When 4-phenylsulfonylazetidin-2-one was treated with cinchonidine and thiophenol, the intermediate azetinone underwent a thiol addition reaction and the 4-phenylthioazetidin-2-one was obtained in 54% optical and 96% chemical yield (eq. [13]). Recrystallization of the optically active azetidinone allows isolation of the pure enantiomer from the mother liquor. The phenylthio group is eliminated later in the synthesis of thienamycin.

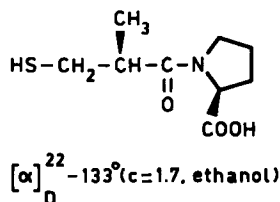


Figure 9. Captopril (Squibb trade name) (59).

*Lithium diisopropylamide (LDA) in tetrahydrofuran (THF).

D. Addition of Thiolacetic Acid to Electron-Poor Olefins

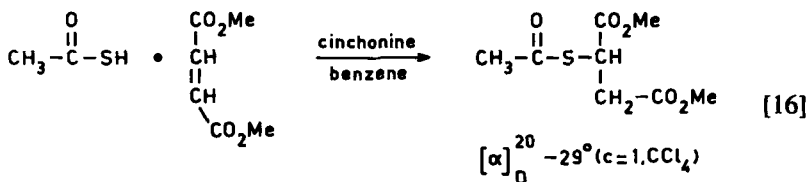
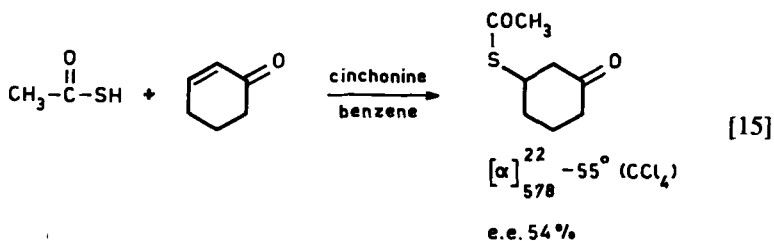
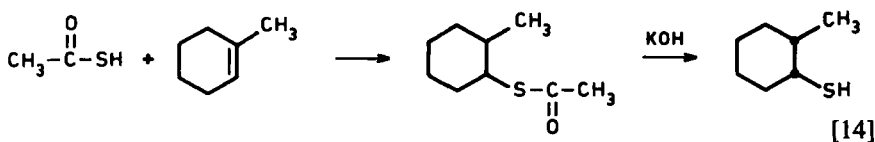
The thiol addition reaction discussed in the previous section does not lend itself readily to the preparation of (chiral) mercaptans.

The latter compounds are of biological importance—cysteine, glutathione, and proteins are examples—and a novel antihypertensive drug, Captopril (Figure 9), also contains this functionality (59). Mercaptans can be prepared by the solvolysis of the thiolacetic acid adducts to olefins.

Although thiolacetic acid additions are free-radical reactions (60), it was found recently that the addition to electron-poor olefins can be base catalyzed (61) (eqs. [14], [15]). Thus the (*S*)-(–) adduct is obtained with an e.e. of 54% when cyclohexenone is treated with thiolacetic acid in benzene in the presence of catalytic amounts of cinchonine. The reaction appears to be quite general, although very high e.e.'s (>80%) have not yet been achieved.

Another example, published by Gawronski (62), shows that α , β -unsaturated esters also will undergo this reaction (eq. [16]). The reaction is slow (25 days for 90% completion) and can be accelerated by a factor of 100 by using the thioester as the acceptor.

The quinine-catalyzed reaction of thiolacetic acid with methyl methacrylate has been studied in several laboratories, but no results have been published, probably because of its potential importance in the commercial synthesis of (–)-Captopril (59). Indications are that optical yields of 20 to 30% can be achieved.



No attempts at optimization have been made. Note that this reaction differs from the one in which cyclohexenone or maleic esters are acceptors in that the chirality-producing step involves proton addition to the α -carbon of the ester. This latter step is probably not rate determining.

E. Miscellaneous Studies

4-Methyl-4-phenylcyclohexa-2,5-dienone, a molecule containing a meso carbon, shows stereoselectivity in its reaction with *p*-*tert*-butylthiophenol catalyzed by cinchonidine (eq. [17]) (63). The *trans*:*cis* ratio was found to be 3:1, with the *cis* adduct showing an e.e. of 77% and the *trans* adduct an e.e. of 50%.

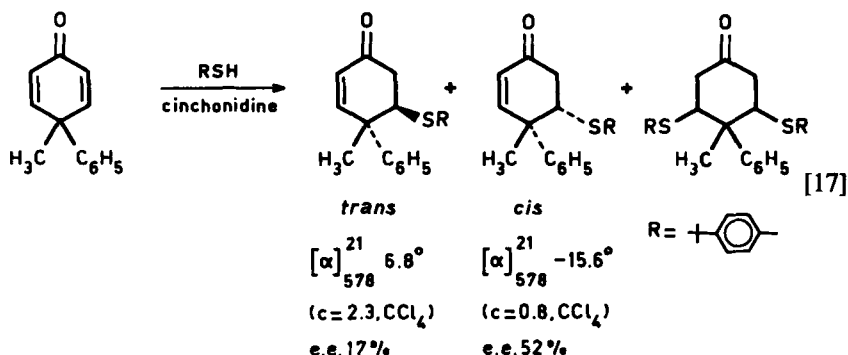
These results may be compared with those of the experiments of Schwartz and Carter (64) and Cohen (65a) with β -phenylglutaric anhydride. [See also the more recent results of Fujita and co-workers with *meso*-2,4-dimethylglutaric acid (65b).] The former group showed that a chiral amine could discriminate between attack at the pro-(*R*) and pro-(*S*) carbonyl groups of the anhydride. The two diastereomers were formed in a ratio of 3:2, with optical purities of about 20%.

The example of the thiol addition reaction to a cyclohexadienone indicates that discrimination of this type can be carried out catalytically; the proximity of the meso carbon to the reaction center increases the stereoselectivity substantially.

F. The Mechanism of the 1,4-Thiol Addition Reaction (19)

The 1,4-thiol addition reaction lends itself well to a mechanistic study, for the following reasons:

1. The reaction is kinetically controlled.
2. No reaction takes place without base catalysis.
3. The reaction is homogeneous and proceeds at a reasonable rate at room temperature.



4. The rate can be measured over a 50° range.
5. The structures of the three transition-state reactants—thiophenol, cycloalkenone, and catalyst—can be varied systematically without extensive synthetic efforts (19).
6. A characteristic solvent effect on the asymmetric induction is observed.

The transition state proposed for the quinine-catalyzed reaction (Figure 10) is based on the following assumptions (19):

1. The favored conformation of quinine is such that the rotamer around the C-9-C-4 bond is chosen that allows the largest substituent—the quinuclidine ring—to lie on one side of the quinoline ring and the hydroxyl and hydrogen to lie on the other side (Figures 4 and 5). This conformation was also considered the most favorable by Prelog (16a) and Meurling (16b). The minimum-energy conformation around the C-9-C-8 bond is probably as shown in Figure 5. Note that in this conformation no hydrogen bond can be formed between the hydroxyl at C-9 and the quinuclidine nitrogen. In epiquinine, [8*S*,9*S*], an intramolecular hydrogen bond to the quinuclidine nitrogen has been shown to exist by infrared (IR) spectroscopy (66). When epiquinine is used as the catalyst, the e.e. drops from 70 to 18% in the standard reaction.

2. The thiophenol forms a (tight) ion pair with the nitrogen of the quinuclidine.

3. The hydrogen of the hydroxyl group of the alkaloid bonds with the carbonyl group of the cycloalkenone.

Transition state *A* is favored over *B*, mainly because in *B* an unfavorable nonbonding interaction occurs between the quinuclidine ring and carbons 5 and 6 of the cyclohexenone ring. Transition state *A* leads, after the thiophenol has added to the cyclohexenone, to the adduct with the correct absolute configuration. The nonbonding interaction between carbons 5 and 6 of the cyclohexenone and the quinuclidine ring allows one to predict that additional steric bulk at these positions should favor transition state *A* even more. This has been shown to be the case, since the highest e.e. (80%) is achieved using 5,5-dimethylcyclohex-

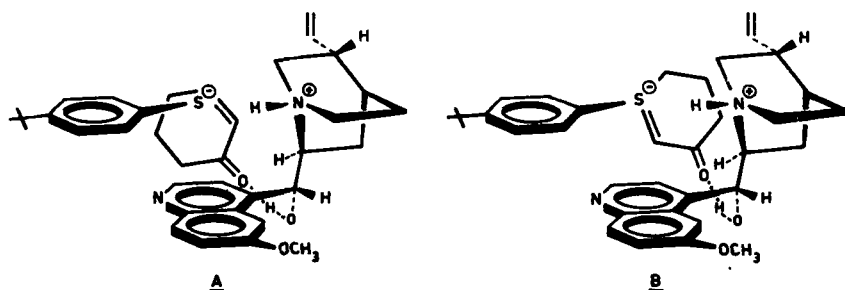


Figure 10. Transition states for 1,4-thiol addition to cycloalkenones.

enone. The important solvent influence (81) can be explained using the transition-state model.

Solvents that interfere or compete with either the ion-pair formation or the hydrogen bonding between the catalyst and the two reactants will lower the extent of asymmetric induction. Experiments corroborate this nicely. Quaternary ammonium salts, when added to the benzene solution in the standard reaction (eq. [1]), reduce the e.e. from 62 to 17% for the iodide and to 0% for the chloride (19b).

Table 3 shows the influence of solvents on the e.e. In all cases the chemical yields were uniformly high.

VI. SELENOPHENOL ADDITION REACTION

The 1,4-addition of selenophenols to cycloalkenones proceeds smoothly under the same conditions used in the thiophenol addition (see Section V) (eq. [18]). Although the e.e. of the products is 40 to 65%, compared with the 60 to 80% achieved in the thiol addition reaction, the solid adducts are readily purified to enantiomeric purity by crystallization (63).

A variety of chiral selenoketones can be prepared (67) in this manner, as Table 5 shows.

Using methods developed by Sharpless (68), Reich (69), and others, the optically active 4,4-dimethyl-2-cyclohexenol is prepared in excellent yield from the corresponding chiral selenide (eq. [19]). The (*S*)-4,4-dimethyl-3-*p*-methylphenylselenocyclohexanone, $[\alpha]_{578}^{RT} 42.1^\circ$ (e.e. 39%), was reduced with sodium borohydride to the (one) diastereomeric alcohol, $[\alpha]_{578}^{RT} 11.0^\circ$, in quantitative yield and converted to the allylic alcohol, $[\alpha]_{578}^{RT} -17.7^\circ$, with an e.e. of 40%.

The careful analysis in this study of the relationship between optical purity, as expressed by the ratio $\alpha_{\text{observed}}/\alpha_{\text{absolute}}$, and the e.e. is instructive. Figure 11 shows exact linearity between these two important measures of purity for the selenoketone in CCl_4 (63).

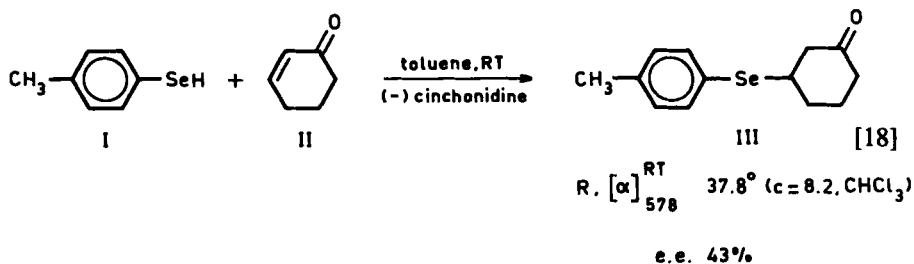


Table 5
Selenophenol Additions Catalyzed by Quinine

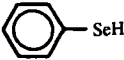
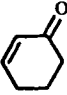
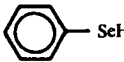
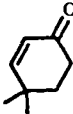
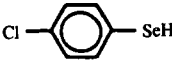
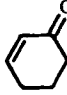

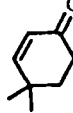

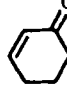

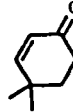



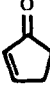

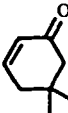

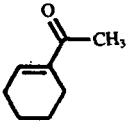

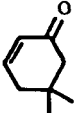
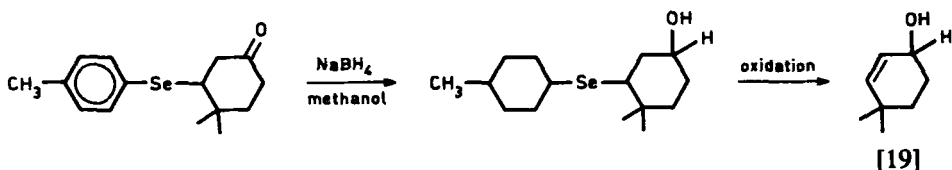
Selenophenol	Cyclo- alkenones ^a	b.p.(°C) (mm Hg)	m.p. ^b (°C)	Rotation ^b		e.e. ^b (%)
				$[\alpha]_{578}^{RT}$	Conc. $\left(\frac{\text{g}}{100 \text{ ml}}\right)$ (solvent)	
		128–130 (0.1)		+ 29.3	6.60 (CHCl ₃)	36
			35–37	+ 23.1	2.12 (CHCl ₃)	20
			68.5–72	+ 17.8	1.18 (CHCl ₃)	21
			81.5–84	+ 11.6	1.58 (CHCl ₃)	13
			23–25.5	+ 46.9	1.00 (CHCl ₃)	53
			72–74	+ 29.4	1.18 (CCl ₄)	26
		148–150 (0.005)		+ 24.8	0.94 (CCl ₄)	65
		140–142 (0.005)	20–21	+ 0.8	1.60 (CCl ₄)	7
			49.5–51	+ 39.4	0.80 (CCl ₄)	60

Table 5 (Continued)

Selenophenol	Cyclo- alkenones ^a	b.p.(°C) (mm Hg)	m.p. ^b (°C)	Rotation ^b		e.e. ^b (%)
				$[\alpha]_{578}^{RT}$	Conc. $\left(\frac{g}{100\text{ ml}}\right)$ (solvent)	
		Oil		~0		0
			38–40	+38.4	1.00 (CCl ₄)	67

^aCinchonidine was used as the chiral catalyst. Chemical yields for all compounds >95%.

^bData are averages from two or more experiments. Values are for product. From ref. 63



$[\alpha]_{578}^{RT}$ 42.1° (c = 0.82, CCl₄)
[R], e.e. 39%

$[\alpha]_{578}^{RT}$ 11.0°
(c = 1.0, CHCl₃)

$[\alpha]_{578}^{RT}$ - 17.7°
(c = 1, CCl₄)
[S], e.e. 40%

Although the mechanism of this reaction has not been studied as thoroughly as that of the thiol addition reaction, there appears to be considerable similarity in the main features of the reaction. Thus, although the transition state may well differ in a number of details, the transition state shown earlier (Figure 10) appears to predict the correct configuration for the products of the selenophenol addition as well as of the thiophenol addition to cyclohexenones.

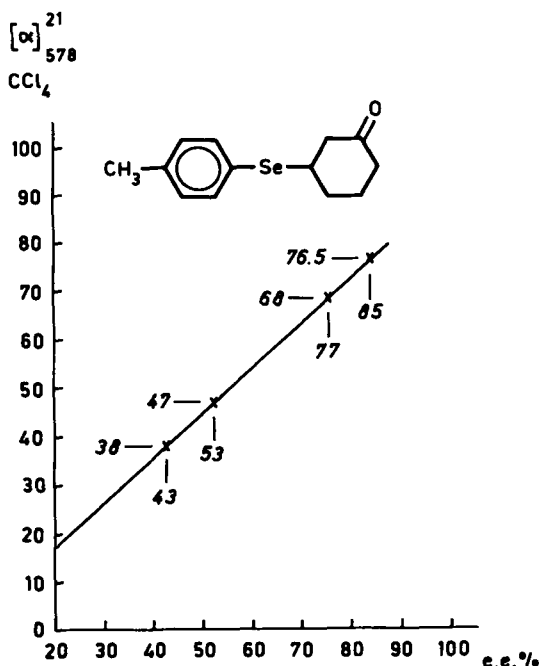


Figure 11. Optical activity (observed) vs. e.e. for 3-*p*-methylphenylselenocyclohexanone.

VII. EPOXIDATION OF ELECTRON-POOR OLEFINS

The publication (70) in 1976 of the preparation of optically active epoxyketones via asymmetric catalysis marked the start of an increasingly popular field of study. When chalcones were treated with 30% hydrogen peroxide under (basic) phase-transfer conditions and the benzylammonium salt of quinine was used as the phase-transfer catalyst, the epoxyketones were produced with e.e.'s up to 55%. Up to that time no optically active chalcone epoxides were known, while the importance of epoxides (arene oxides) in metabolic processes had just been discovered (71). The nonasymmetric reaction itself, known as the Weitz-Scheffer reaction under homogeneous conditions, has been reviewed by Berti (70).

Chiral phase-transfer catalysts, usually prepared from ephedrine, had been employed previously with little success (72).

Although the enantiomeric excesses obtained in the phase-transfer-mediated

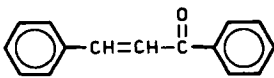
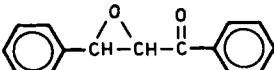
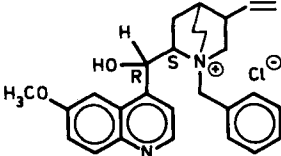
asymmetric epoxidation using chiral ammonium salts have not been exceedingly high, except in a few cases (73), the reaction has a large scope and furnishes optically active epoxides inaccessible by other routes.

Thus chalcones (74,75) quinones (70,73,76), and cyclohexenones (77) are epoxidized successfully to optically active epoxyketones and epoxyquinones, while the Darzens condensation between chloroketones and aromatic aldehydes also furnishes optically active epoxyketones (75). Three reagents have been found useful in these oxidation reactions; 30% hydrogen peroxide, *t*-butyl hydroperoxide, and 28% sodium hypochlorite. Chalcones and naphthoquinones are epoxidized smoothly by hydrogen peroxide, sodium hypochlorite, and *t*-butyl hypochlorite (74). Note that hydrogen peroxide gives one enantiomer, while the latter two reagents give the enantiomer having the opposite configuration (see Table 6).

In eq. [20] the chemical correlation between (*S*)-(-)-phenyllactic acid (known absolute configuration) and (-)-epoxychalcone is shown.

(*S*)-(-)-Phenyllactic acid is converted to the (*S*)-(-)-hydroxyketone via its ester and amide. Reduction of the (-)-epoxychalcone yields the (+)-rotating α -hydroxyketone. Therefore the configuration of the α -carbon of the epoxychalcone must be *R*. Since epoxychalcones are derived from *trans*-chalcones, the configuration of the β -carbon in the epoxychalcone must be *S*, as shown in Figure 12.

TABLE 6
Epoxidation of Chalcones Using Chiral Phase-Transfer Catalysts

	$\xrightarrow[\text{CCl}_4]{\text{quibec, 30\% H}_2\text{O}_2, 10\% \text{ NaOH}}$	 $[\alpha]_{578}^{21} -72.2^\circ (c=0.7, \text{CH}_2\text{Cl}_2)$ e.e. = 34 %
..	$\xrightarrow{t\text{-C}_4\text{H}_9\text{OOH}}$	24°
..	$\xrightarrow{28\% \text{ NaOCl}}$	53°
		
quibec = benzylquininium chloride		

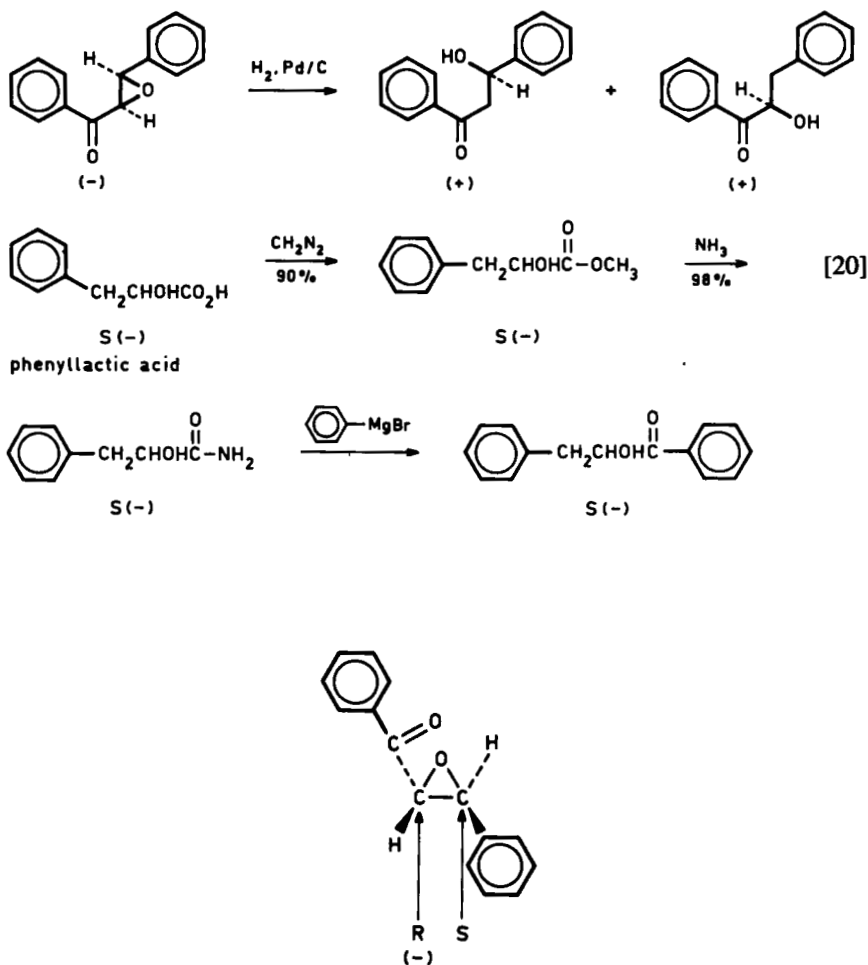
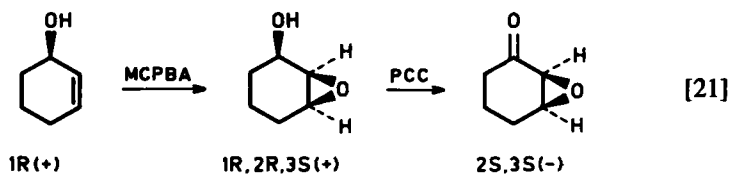


Figure 12. Configuration of (-)-Epoxychalcone (74,80).



The (1R)-(+)-2-cyclohexen-1-ol of known absolute configuration is correlated with the (-)-epoxycyclohexanone as shown in eq. [21] (73,74).

A. Vitamin K₃ Epoxide

Figure 13 shows the structure and absolute configuration of (2R,3S)-(-)-vitamin K₃ epoxide. This epoxide, prepared in optically active form by us (70) in 1976, had been known as a racemate since 1939 (78). It has recently been implicated (79) in prothrombin biosynthesis (80). The absolute configuration as shown in Figure 13 is based on the work of Snatzke (76) and the absolute rotation is $[\alpha]_{436}^{21} = -124^\circ$ (acetone) and $[\alpha]_{578}^{21} = 0^\circ$ (!) (acetone).

B. The Chalcones

Using 30% aqueous hydrogen peroxide, an equal volume of 12% sodium hydroxide solution, an amount of toluene equal to the volume of the aqueous phase, and 50 mg of benzylquininium chloride for every 5 mmol of substrate, chalcones are epoxidized in 24 hr at 22°C. Table 7 lists the results of epoxidation with a dozen chalcones (eq. [22]) (74,77). Although, as mentioned above, the absolute configuration of one chalcone epoxide has been determined, no firm conclusions may be drawn about the absolute configuration of any other chalcone epoxide. It is, of course, tempting to assume that since the epoxides in Table 7 all have the same sign of rotation at the same wavelength and the same temperature and were prepared using the same catalyst, they also have the same absolute configuration. However, the absolute *conformation* of these chalcone

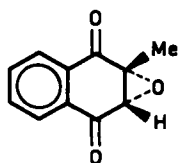
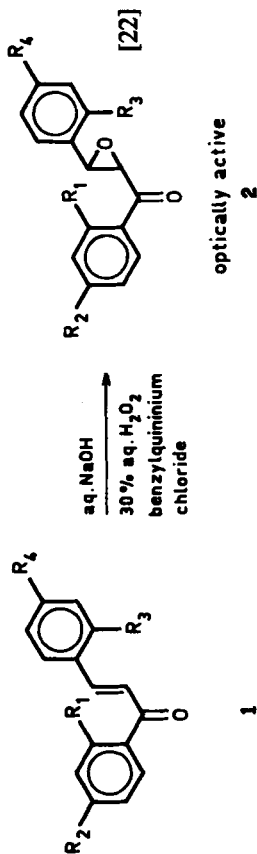


Figure 13. (2R,3S)-(-)-Vitamin K₃ epoxide, $[\alpha]_{436}^{21} = -124^\circ$ (acetone) (78).

TABLE 7
Structural and Solvent Effects in the Asymmetric Induction of Chalcone Epoxides



R_1	R_2	R_3	R_4	Solvent	t (°C)	$[\alpha]_{578}^{RT}$	Concentration (CH_2Cl_2)	e.e.(%)	Method ^a
H	H	H	H	CCl_4	3	-83	($c = 0.69$)	39	Eu(dcm) ₃
H	H	OCH_3	H	Benzene	22	-13.2	($c = 0.33$)	55	Eu(tfc) ₃
OCH_3	H	H	H	Toluene	22	-31.3	($c = 1.0$)	23	Eu(tfc) ₃
H	OCH_3	H	H	Toluene	3	-56	($c = 0.89$)		
H	Br	H	H	Toluene	22	-47.8	($c = 0.69$)	25	Eu(dcm) ₃
H	H	H	Br	Toluene	3	-77	($c = 0.75$)		
H	Br	H	Br	CH_2Cl_2	22	-4.9	($c = 0.29$)		
H	H	H	Cl	Toluene	22	-62	($c = 5.49$)	20	Eu(dcm) ₃
H	H	H	NO_2	Toluene	22	-33	($c = 4.7$)		
CH_3	H	H	H	Toluene	22	-76.6	($c = 0.67$)	48	Eu(dcm) ₃
CH_3	H	CH_3	H	Toluene	22	-32.2	($c = 0.85$)	35	Eu(dcm) ₃
H	H	CH_3	H	Toluene	22	-25.7	($c = 0.90$)		

^aEu(dcm)₃, tris(*d*, *d*-dicamphorylmethanato)europium (III); Eu(tfc)₃, tris(3-trifluoroacetyl-*d*-camphorato)europium (III).

epoxides is unknown and the conformational mobility of these molecules prevents the formulation of easy sector rules. In effect, the absolute configuration must be established for each new chalcone, even though the presumptive evidence for correlation with the one proven case is strong.

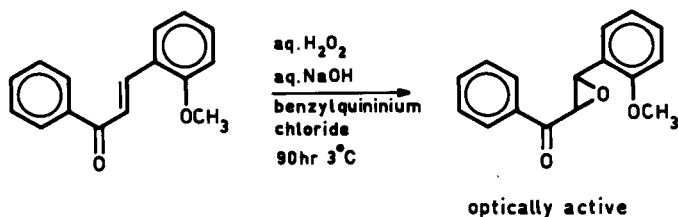
C. Solvent Effects

As is the case in all other quinine-catalyzed reactions, the quininium-salt-catalyzed phase-transfer reactions are subject to strong solvent effects (Table 8) (81). The fact that, *in the presence of water*, polar solvents lower the e.e., whereas apolar solvents raise the e.e., indicates that these are true phase-transfer reactions in which the ion pairs within the organic layer are responsible for the asymmetric induction.

D. The Cyclohexenones

In general, cyclohexenones fail to give optically active products under phase-transfer, hydrogen peroxide, benzylquininium chloride, and basic reaction conditions (77). In fact, it appears that the starting material decomposes, since only water-soluble products are formed. Of several cyclohexenones tried, only one, namely 4,4-diphenylcyclohexenone, furnished an optically active epoxide.

TABLE 8
Solvent Effects in Phase-Transfer Epoxidation (77)



Solvent	Dielectric constant	Chemical yield (%)	e.e. (%)
Benzene	2.28	90	55
Toluene	2.44	90	48
<i>o</i> -Xylene	2.57	86	39
C ₆ H ₅ Cl	5.71	99	34
CH ₂ Cl ₂	9.08	100	27
Nitrobenzene	34.8	95	10

TABLE 9
Inductions Obtained by Varying the Base in the Epoxidation of Cyclohexenone and Chalcone with *t*-Butyl Hydroperoxide (77)

Base	Substrate	$[\alpha]_{578}^{RT}$	e.e. (%)
NaOH	Chalcone	+ 23.9	11
<i>t</i> -BuOK	Chalcone	- 16.0	8
NaOH	Cyclohexenone	- 39	20
LiOH	Cyclohexenone	- 8	4
Ag ₂ O	Cyclohexenone	- 20	10
K ₂ CO ₃	Cyclohexenone	- 37	19

Successful asymmetric epoxidation of 2-cyclohexen-1-one was achieved using *t*-butyl hydroperoxide, toluene, solid sodium hydroxide, and benzylquininium chloride. Cyclohexenone epoxide obtained in this manner has an e.e. of 20% ($[\alpha]_{578}^{20} = -39^\circ$).

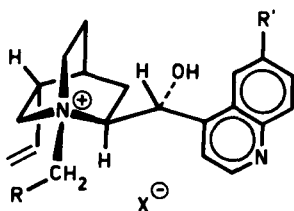
Recently (82), pure 3,5-dimethylcyclohexenone epoxide was obtained by Toda using a complexation method with optically active 1,6-di(*o*-chlorophenyl)-1,6-diphenylhexa-2,4-diyne-1,6-diol. The method was not applicable to unsubstituted 2,3-epoxycyclohexanone (82).

The *t*-BuOOH method of epoxidation is sensitive to the base used. Table 9 shows that the e.e. as well as the absolute configuration of the major enantiomer is affected by the choice of the base.

E. The Catalyst

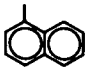
A limited study has been made of the role of the structure of the catalyst in the phase-transfer epoxidation reaction (77). The catalysts tried were mainly salts of quinine (3a-g), cinchonidine (4), ephedrine (5), and a camphor derivative (6) (Figure 14). The conclusions were as follows:

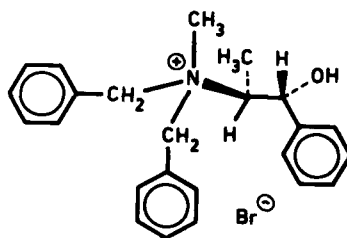
1. The cinchona alkaloids are by far the better all-around catalysts.
2. Modifications in the benzyl portion of the molecule are significant. The nitro group in the benzyl portion of the molecule apparently increases the local polarity of the transition state. The influence on the chemical and enantiomeric yield of variations in the benzyl portion of the quininium salt was dramatically confirmed recently by the work of Dolling and co-workers on the phase-transfer alkylation of a hydrindanone (83).
3. The absolute configurations at C-8-C-9 of the alkaloids govern the absolute configurations of the products; that is, when a quinine or cinchonidine salt (both salts have 8*S*,9*R* configurations) is used, the epoxide produced



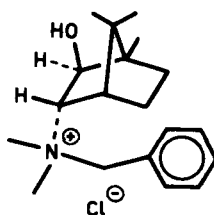
3a-g

4 R' = H

R'	R	X
a -OCH ₃	-C ₆ H ₅	Cl
b "	"	Br
c "	"	I
d "	-C ₆ H ₄ -NO ₂	Cl
e "	-C ₆ H ₄ -CH ₃	"
f "	-C ₆ H ₄ -C(CH ₃) ₃	"
g "		"
H	-C ₆ H ₅	"



5



6

Figure 14. Chiral phase-transfer catalysts.

will have a configuration opposite that of the one obtained using a quinuclidine or cinchonine salt (8*R*,9*S*).

F. The Mechanism of the Reaction

The complexity of phase-transfer asymmetric catalysis and the lack of kinetic data and of precedents make mechanistic proposals of dubious value. Nevertheless, we now present a working hypothesis that explains the results with cyclohexenone and chalcone using hydrogen peroxide or *t*-butyl hydroperoxide. Using a preferred conformation of the benzylquininium salt (Figure 15) and assuming a tight ion pair between the ammonium salt and the peroxide anion and hydrogen bonding between the hydroxyl of the alkaloid and the carbonyl oxygen of the unsaturated ketone allows the drawing of a structure fitting the following description (see Figure 16): The ion pair formed between the *t*-butyl hydroperoxide and the quinuclidine nitrogen of the alkaloid results in a fairly compact structure in which the *t*-butyl group fills a gap within the alkaloid molecule. This is not the

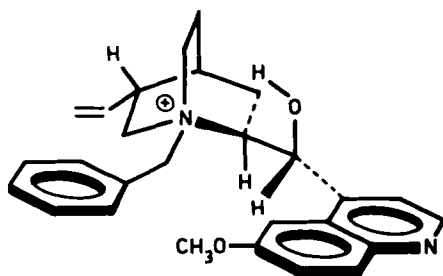


Figure 15. Preferred conformation of benzylquininium chloride (77).

case when the much smaller hydrogen peroxide is used (see drawing on the left in Figure 16). Models show clearly that the *t*-BuOO⁻-quininium complex allows the approach of cyclohexenone or chalcone from one side only, namely from above. In the case of the HOO⁻-quininium complex, the unsaturated ketone can slip sideways into the remaining cavity.

The two transition states for cyclohexenone are shown in an attempt to reproduce the situation that is evident from inspection of the model (Figure 16).

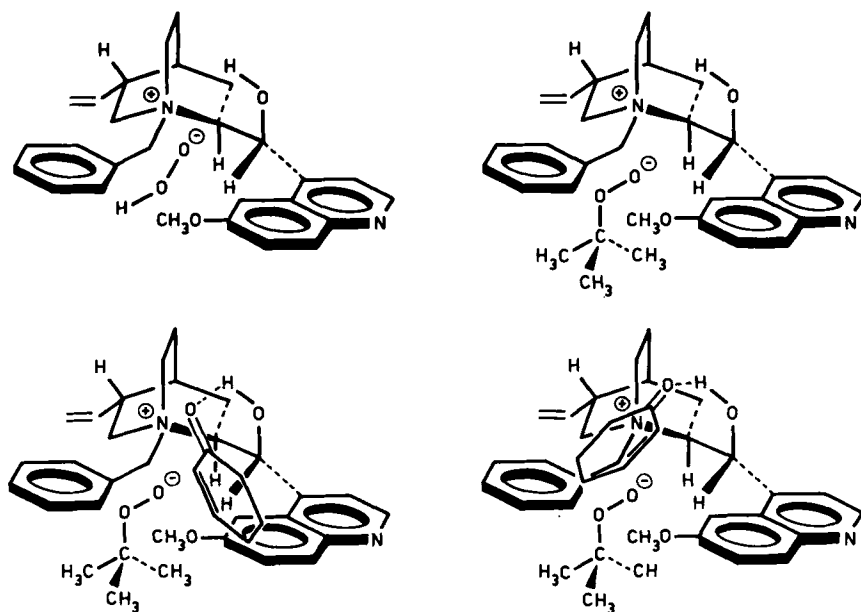
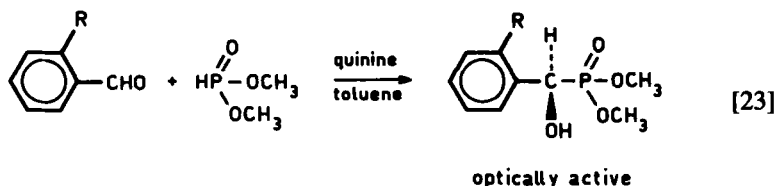


Figure 16. Transition states for asymmetric phase-transfer-catalyzed epoxidation of cyclohexenones (77).

Although not directly within the scope of these alkaloid-catalyzed reactions, it is worthy of note that an Italian group has apparently increased the enantiomeric yields in the epoxidation reactions of chalcones by using chiral polypeptides (84).

VIII. FORMATION OF THE PHOSPHORUS-CARBON BOND USING CHIRAL AMINE CATALYSIS

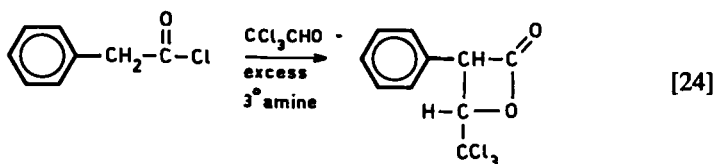
Recently (22,23), we observed that quinine catalyzes the 1,2-addition of phosphite esters to benzaldehydes. When the aldehyde has an ortho substituent, preferably one that aids in restricting the rotation of the aldehyde group, asymmetric induction takes place. In these reactions quinine is 20 times as effective a catalyst as is triethylamine (85) (eq. [23]). Although the e.e. in the reaction shown in eq. [23] is 26% when R = nitro, this percentage rises to 80% when di-*t*-butyl phosphite is used (see also eq. [3]).

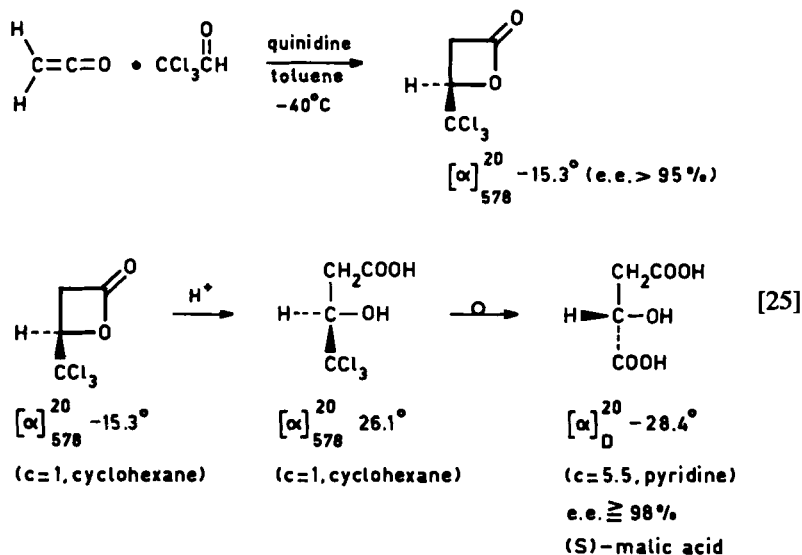


The absolute configurations of the products have now been determined (23) and the reaction promises to be of considerable interest, since Jacques and his colleagues have shown that chiral phosphoric acids are useful resolving agents (86).

IX. 2,2-CYCLOADDITION REACTION CATALYZED BY QUININE ESTERS

In 1966 Borrmann and Wegler (87) reported the base-catalyzed addition of ketenes to chloral to form β -lactones (eq. [24]). Using brucine, these researchers were able to isolate optically active products when ketene itself was used.





The quinine catalyzed reaction of ketene with chloral.

We have studied this reaction in considerable detail (88) and have found that when one uses quinine (eq. [25]) or any one of the chiral bases, a variety of aldehydes react with ketene to form the corresponding β -lactones in excellent chemical and nearly quantitative enantiomeric yields. Equation [25] exemplifies the reaction. Note that mild *basic* hydrolysis of the lactone furnishes a trichlorohydroxy acid that was prepared earlier by McKenzie (89). If one uses quinidine as catalyst, the process furnishes the natural (*S*)-malic acid. Note that ketene first acylates the free hydroxyl group of quinine, so that the actual catalyst is the alkaloid ester.

Recently (88), we showed that the hydrolysis of the trichlorohydroxy acid involves inversion at the chiral center.

The scope of this quinine ester-catalyzed ketene addition reaction is promising. Optically pure α - and β -hydroxycarboxylic acids of either configuration can be prepared with facility.

Based on the known (88,89) absolute configuration of the adduct and earlier work on the interactions of ketene with alkaloids by Pracejus (18), the transition-state picture shown in Figure 17 emerges for the ketene-chloral addition reaction.

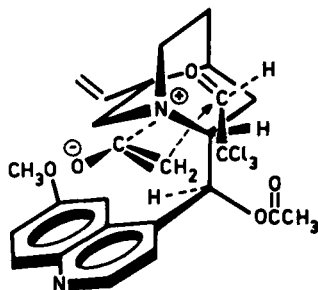


Figure 17. Ketene-chloral-quinidine acetate transition state.

X. 1,2-ADDITIONS

Very recently, we (85) observed that in simple 1,2-additions quinine was again effective. Thus, when diethylzinc is added to a solution of benzaldehyde in toluene in the presence of catalytic amounts of quinine, (–)-phenylethylcarbinol is formed in an e.e. of 72%.

XI. CONCLUSIONS

When penicillin was first introduced as an antibiotic, the term “miracle drug” was coined. In 1944, it was indeed a miracle that such a wide variety of infectious diseases, from pneumonia to tetanus, could be cured by one simple chemical. Only later, when the mode of action of penicillin became partly known, did we realize that many infections were caused by similar microorganisms all of which yield to the antimetabolic action of penicillin.

So, in a way, it is with quinine, known (29) since antiquity as a potent antimalarial. For chemists, the use of quinine in 1854 in the first resolution of a racemate (1,3) marks a milestone: Stereochemistry as we know it today made its debut in that year. In resolutions, quinine and its diastereomers proved to be safe to handle (compare the extreme toxicity of brucine or strychnine with that of quinine), versatile in their applications, and available in reasonably pure form. Little wonder that even today, 131 years after its first use as a resolving agent, quinine (and brucine) continues to be the chemical of choice when one is attempting a new resolution of a racemic acid (90).

There is little doubt in my mind that the versatility that the cinchona alkaloids have exhibited in catalyzing such a diverse range of reactions is due to molecular interactions that to some extent mirror those of importance in resolutions (5).

While a survey of resolving agents lists more than 100 organic bases as having

been used at least once in the resolution of a racemic acid, the cinchona alkaloids account for nearly one-quarter of all resolutions (90).

This same picture unfolds when we examine the use of chiral amines in base-catalyzed reactions. Although in several individual cases (91,92) such as epoxidations (84), one Michael reaction (36), and an intramolecular aldol reaction (93), amino acids (11) or polypeptides (84) are better catalysts than quinine, the range of usefulness of quinine appears to warrant the term "miracle catalyst."

One interesting indication of the unique nature of quinine as a catalyst as well as an antimalarial derives from an observation of ours on quinine analogs (63). While studying the thiol and selenophenol-addition reactions, we prepared cinchona alkaloid analogs through time-consuming syntheses (Figure 18) (63). In none of the many cases studied (especially the standard reaction of thiophenol and cyclohexenone) did the e.e. of the reaction products equal or exceed that of the natural alkaloids themselves. This in itself disappointing result emphasizes once again the unique nature of the quinine molecule.

Making predictions is difficult; however, it seems safe to say that we are at the beginning of a development in organic synthesis with very wide ramifications. It is, for example, not far-fetched to presume that pharmacological and medicinal chemists will glean useful information on the mode of quinine action *in vivo* from its catalytic activity in a test tube. Thus, while catalytic asymmetric syn-

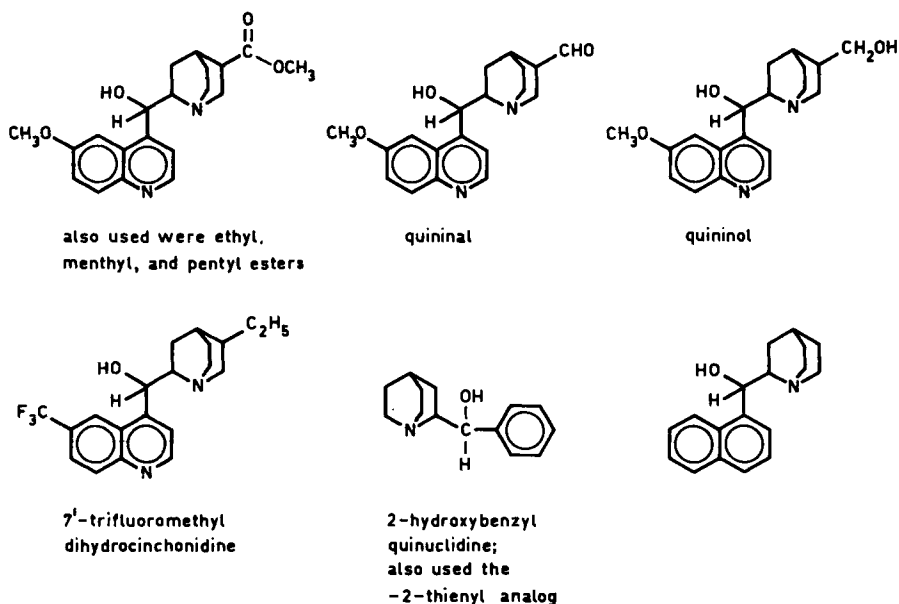


Figure 18. Cinchona alkaloid analogs (63).

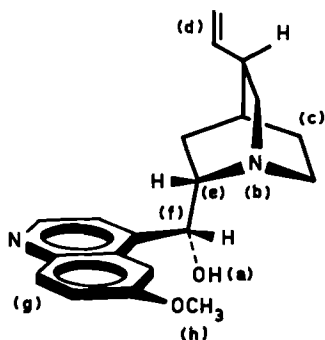


Figure 19. Multifunctional nature of quinine as a catalyst. The various parts of the molecule fill the following roles: (a) hydrogen bond forming; ligand forming with metals; (b) basic amine; (c) aliphatic hydrocarbon—bulk; (d) “handle” to modify; (e,f) epimers available; few conformers; (g) aromatic hydrocarbon—bulk, polarizable; (h) “handle” to modify; steric and polar influence.

thesis promises to become one of the crucial tools for the organic chemist who needs a chiral compound, the study of the mechanism of these catalytic reactions may lead to insight into biological processes.

One aspect of asymmetric catalysis has become clear. Every part of the molecule seems to fulfill a role in the process, just as in enzymic catalysis. Whereas many of us have been used to “simple” acid or base catalysis, in which protonation or proton abstraction is the key step, bifunctional or even multifunctional catalysis is the rule in the processes discussed in this chapter. Thus it is not only the increase in nucleophilicity of the nucleophile by the quinine base (see Figures 6 and 19), nor only the increase in the electrophilicity of the electrophile caused by hydrogen bonding to the secondary alcohol function of the quinine, but also the many steric (i.e., van der Waals) interactions between the quinoline *and* quinuclidine portions of the molecule that exert the overall powerful guidance needed to effect high stereoselection. Important charge-transfer interactions between the quinoline portion of the molecule and aromatic substrates cannot be excluded.

ACKNOWLEDGMENTS

It is clear that this chapter could not have been written were it not for the inspired and enthusiastic work by my many Dutch (and one Swiss) students who are mentioned in the bibliography. To my wife Elly's patience and encouragement I owe the fact that I (barely) made a publisher's deadline. To my secretary Karin, thanks for her diligence and accuracy in transforming a rough manuscript to a readable package.

REFERENCES

1. Pasteur, L. C. *R. Acad. Sci.* **1853**, 37, 162.
2. See Mason, S. F. *Top. Stereochem.* **1976**, 9, 1; and Mason, S. F. "Molecular Optical Activity and the Chiral Discriminations"; Cambridge University Press: Cambridge, 1982, p. 7, for an excellent discussion on Pasteur's and Laurent's early contributions to stereochemistry.
3. Jacques, J.; Collet, A.; Wilen, S. H. "Enantiomers, Racemates and Resolutions"; Wiley: New York, 1981, pp. 254, 257.
4. (a) Yoneda, H. *J. Liq. Chromatogr.* **1979**, 2, 1157. (b) Brianso, M.-C. *Acta Crystallogr.* **1981**, B37, 618; **1976**, B32, 3040.
5. Gould, R. O.; Walkinshaw, M. D. *J. Am. Chem. Soc.* **1984**, 106, 7840.
6. Kellogg, R. M. *Angew. Chem.* **1984**, 96, 769.
7. Lehninger, A. L. "Biochemistry," 2nd ed.; Worth: New York, 1975, p. 208.
8. Chibata, I. *Pure Appl. Chem.* **1978**, 50, 667.
9. Barker, H. A.; Blair, A. H. *Biochem. Prep.* **1962**, 9, 21. See also Hulme, A. C. *Biochim. Biophys. Acta* **1954**, 14, 36, for a suggestion that (–)-citramalic acid occurs in nature.
10. Entry into the extensive literature on this subject can best be obtained through Kagan, H. B.; Fiaud, J. C. *Top. Stereochem.* **1978**, 10, 175 and ref. 11.
11. Kagan, H. B. In "Asymmetric Synthesis," Vol. 5; Morrison, J. D., Ed.; Academic: New York, 1985, pp. 1–39.
12. Morrison, J. D.; Mosher, H. S. "Asymmetric Organic Reactions"; Prentice-Hall: Englewood Cliffs, New Jersey, 1971, remains the best and most accurate survey in this field.
13. Katsuki, T.; Sharpless, B. K. *J. Am. Chem. Soc.* **1980**, 102, 5974. Rossiter, B. E.; Katsuki, T.; Sharpless, B. K. *J. Am. Chem. Soc.* **1981**, 103, 464.
14. Sharpless, B. K.; Woodard, S. S.; Finn, M. G. In "Selectivity—A Goal for Synthetic Efficiency"; Bartmann, W. D.; Trost, B. M., Eds.; Verlag Chemie: Weinheim, 1984, p. 377.
15. Cornforth, J. In "Structures of Complexes Between Biopolymers and Low Molecular Weight Molecules"; Bartmann, W. D.; Snatzke, G., Eds.; Wiley: New York, 1982, pp. 1–16.
16. (a) Prelog, V.; Wilhelm, M. *Helv. Chim. Acta* **1954**, 37, 1634. (b) See also Meurling, L. *Chemica Scripta* **1975**, 7, 90.
17. The mechanism of the cyanohydrin reaction as depicted in ref. 12, p. 141, appears to be in error, but the survey in ref. 12 is excellent.
18. Pracejus, H. *Fortschr. Chem. Forsch.* **1967**, 8, 493.
19. (a) Hiemstra, H.; Wynberg, H. *J. Am. Chem. Soc.* **1981**, 103, 417. (b) Hiemstra, H. Ph.D. Thesis, University of Groningen, Groningen, The Netherlands, 1980.
20. Kobayashi, N.; Iway, K. *J. Am. Chem. Soc.* **1978**, 100, 7071.
21. Wynberg, H.; Staring, E. G. *J. Am. Chem. Soc.* **1982**, 104, 166.
22. Wynberg, H.; Smaardijk, A. A. *Tetrahedron Lett.* **1983**, 24, 5899.
23. See Smaardijk, A. A.; Noorda, S.; Van Bolhuis, F.; Wynberg, H. *Tetrahedron Lett.* **1985**, 26, 493, for the absolute configuration.
24. Kiliani, H. *Ber.* **1886**, 19, 3033.
25. Fischer, E. *Ber.* **1894**, 27, 3231.
26. Lapworth, A. *J. Chem. Soc.* **1903**, 83, 998.
27. Bredig, G.; Fiske, P. S. *Biochem. Z.* **1912**, 46, 7.
28. Bredig, G.; Minaeff, M. *Biochem. Z.* **1932**, 249, 241.
29. Pelletier, J.; Caventou, J. B. *Ann. Chim. Phys.* **1820**, 14, 69, were the first to isolate pure samples of quinine. For historical reviews, see Trier, G., in "Die Alkaloide"; Verlag Borntraeger: Berlin, 1931, pp. 399–437; and Turner, R. B.; Woodward, R. B.; in "The Alkaloids," Vol. III; Manske, R. H. F.; Holmes, H. L., Eds.; Academic: New York, 1953, p. 24.
30. Rabe, P. *Ber.* **1908**, 41, 62.

31. Prelog, V.; Zalan, E. *Helv. Chim. Acta* **1944**, *27*, 535. Prelog, V.; Hafliger, O. *Ibid.* **1950**, *33*, 2021.
32. Woodward, R. B.; Doering, W. E. *J. Am. Chem. Soc.* **1944**, *66*, 849; **1945**, *67*, 860.
33. Becker, W.; Freund, H.; Pfeil, E. *Angew. Chem.* **1965**, *77*, 1139. Becker, W.; Pfeil, E. *J. Am. Chem. Soc.* **1966**, *88*, 4299.
34. Peterson, E. A.; Sober, H. A. *Biochem. Prep.* **1961**, *8*, 43.
35. Oku, J.; Inoue, S. *J. Chem. Soc. Chem. Comm.* **1981**, 229.
36. Cram, D. J.; Sogah, G. D. Y. *J. Chem. Soc. Chem. Comm.* **1981**, 625.
37. Mikolajczyk, M.; Drabowicz, J. *Top. Stereochem.* **1982**, *13*, 333 and ref. 8 therein.
38. Kagan, H. B. *Tetrahedron Lett.* **1984**, *25*, 1049. Pitchen, P.; Dunach, E.; Deshmukh, M. N.; Kagan, H. B. *J. Am. Chem. Soc.* **1984**, *106*, 8188.
39. Bergmann, E. D.; Ginsberg, D.; Pappo, R. In "Organic Reactions," Vol. 10; Adams, R., Ed.; Wiley: New York, 1959, p. 179.
40. See ref. 39, p. 265.
41. Langstrom, B.; Bergson, G. *Acta Chem. Scand.* **1973**, *27*, 3118.
42. Wynberg, H.; Helder, R. *Tetrahedron Lett.* **1975**, 4057.
43. Wynberg, H. *Chimia* **1976**, *30*, 445.
44. Herman, K.; Wynberg, H. *J. Org. Chem.* **1979**, *44*, 2230.
45. Herman, K.; Wynberg, H. *Helv. Chim. Acta* **1977**, *60*, 2208.
46. Colonna, S.; Hiemstra, H.; Wynberg, H. *J. Chem. Soc. Chem. Comm.* **1978**, 238.
47. Colonna, S.; Re, A.; Wynberg, H. *J. Chem. Soc., Perkin I* **1981**, 547.
48. Hodge, P.; Khoshdel, E.; Waterhouse, J. *J. Chem. Soc., Perkin I* **1983**, 2205.
49. Trost, B. M.; Shuey, C. D.; DiNinno, F., Jr.; McElvain, S. S. *J. Am. Chem. Soc.* **1979**, *101*, 1284.
50. Yamaguchi, K.; Minoura, Y. *Chem. Ind.* **1975**, 478.
51. Fukushima, H.; Inoue, S. *Makromol. Chem.* **1976**, *177*, 2807.
52. Uskokovic, M. R.; Gutzwiller, J.; Henderson, T. *J. Am. Chem. Soc.* **1970**, *92*, 203.
53. Bijvoet, J. M.; Peerdeman, A. F.; Van Bommel, A. J. *Nature* **1951**, *168*, 271.
54. Numan, H.; Troostwijk, C. B.; Wieringa, J. H.; Wynberg, H. *Tetrahedron Lett.* **1977**, 1761.
55. Hiemstra, H.; Oudman, D.; Wynberg, H. Unpublished except in ref. 19b. Wynberg, H.; Zordrager, J. Unpublished.
56. Balavoine, G.; Moradpour, A.; Kagan, H. B. *J. Am. Chem. Soc.* **1974**, *96*, 5152.
57. Martin, V. S.; Woodard, S. S.; Katsuki, T.; Yamada, Y.; Ikeda, M.; Sharpless, K. B. *J. Am. Chem. Soc.* **1981**, *103*, 6237.
58. Shibasaki, M.; Nishida, A.; Ikegami, S. *J. Chem. Soc., Chem. Comm.* **1982**, 1324.
59. Squibb trade name for 1-(3-mercapto-2-methyl-1-oxopropyl)-L-proline. Ondetti, M. A.; Cushman, D. W. U.S. Patent 4,046,899, 1977; *ibid.*, *Science* **1977**, *196*, 441.
60. Bordwell, F. G.; Hewett, W. A. *J. Am. Chem. Soc.* **1957**, *79*, 3493.
61. Gawronski, J. K.; Gawronska, K.; Wynberg, H. *J. Chem. Soc., Chem. Comm.* **1981**, 307.
62. Gawronski, J. K.; Gawronska, K.; Kolbon, H.; Wynberg, H. *Recl. Trav. Chim. Pays-Bas* **1983**, *102*, 479.
63. Pluim, H.; Wynberg, H. Unpublished results. Pluim, H., Ph.D. Thesis, University of Groningen, Groningen, The Netherlands, 1982.
64. Schwartz, P.; Carter, H. E. *Proc. Nat. Acad. Sci.* **1954**, *40*, 499.
65. (a) Altschul, R.; Bernstein, P.; Cohen, S. G. *J. Am. Chem. Soc.* **1956**, *78*, 5091. (b) Nagao, Y.; Inoue, T.; Fujita, E.; Tenada, S.; Shiro, M. *J. Org. Chem.* **1983**, *48*, 132.
66. Saszko, J.; Dega-Szafran, Z. *Bull. Acad. Pol. Sci.* **1964**, *12*, 103. Prelog, V.; Haflinger, D. *Helv. Chim. Acta* **1950**, *33*, 2021.
67. Wynberg, H.; Pluim, H. *Tetrahedron Lett.* **1979**, 1251.
68. Sharpless, K. B.; Lauer, R. F. *J. Am. Chem. Soc.* **1973**, *95*, 2697.

69. Reich, H. J.; Chow, F.; Shah, S. K. *J. Am. Chem. Soc.* **1979**, *101*, 6638.
70. Helder, R.; Hummelen, J. C.; Laane, R. W. P. M.; Wiering, J. C.; Wynberg, H. *Tetrahedron Lett.* **1976**, 1831. For reviews, see Berti, G. *Top. Stereochem.* **1973**, *7*, 93, and recent studies by Sharpless (13).
71. Jerina, D. M.; Daly, J. W. *Science* **1974**, *185*, 573.
72. Fiaud, J. C. *Tetrahedron Lett.* **1975**, 3495, reported an e.e. of 6% in ptc. (phase-transfer-catalyzed) alkylation.
73. Wynberg, H.; Marsman, B. G. *J. Org. Chem.* **1980**, *45*, 158. Harigaya, Y.; Yamaguchi, H.; Onda, M. *Heterocycles* **1981**, *15*, 183.
74. Marsman, B. G.; Wynberg, H. *J. Org. Chem.* **1979**, *44*, 2312.
75. Hummelen, J. C.; Wynberg, H. *Tetrahedron Lett.* **1978**, 1089.
76. Snatzke, G.; Wynberg, H.; Feringa, B. L.; Marsman, B. G.; Greydanus, B.; Pluim, H. *J. Org. Chem.* **1980**, *45*, 4094.
77. Marsman, B. G. Ph.D. Thesis, University of Groningen, Groningen, The Netherlands, 1981.
78. Fieser, L. F.; Campbell, W. P.; Fry, E. M.; Gate, M.D. Jr. *J. Am. Chem. Soc.* **1939**, *61*, 3216.
79. Matschiner, J. T.; Bell, R. G.; Amelotti, J. M.; Knauer, T. E. *Biochim. Biophys. Acta* **1970**, *201*, 309.
80. Stenflo, J.; Fernlund, P.; Egan, W.; Roepstorff, P. *Proc. Nat. Acad. Sci.* **1974**, *71*, 2730. Suttie, J. W.; Lawson, A. E.; Canfield, L. M.; Carlisle, T. L. *Fed. Proc. Am. Soc. Exp. Biol.* **1978**, *37*, 2605. See also recent studies by Silverman, R. B. *J. Am. Chem. Soc.* **1981**, *103*, 5939, on the role of thiols in this "cascade."
81. Wynberg, H.; Greydanus, B. *J. Chem. Soc., Chem. Comm.* **1978**, 427.
82. Tanaka, K.; Toda, F. *J. Chem. Soc., Chem. Comm.* **1983**, 1513.
83. Dolling, U. H.; Davis, P.; Gabrowski, E. J. *J. Am. Chem. Soc.* **1984**, *106*, 446.
84. Colonna, S.; Molinari, H.; Banfi, S.; Julia, S.; Masana, J.; Alvarez, A. *Tetrahedron* **1983**, *39*, 1635.
85. Wynberg, H.; Smaardijk, A. A. Unpublished results.
86. Jacques, J.; LeClerq, M.; Brienne, M. *J. Tetrahedron* **1981**, *37*, 1727.
87. Borrmann, D.; Wegler, R. *Chem. Ber.* **1966**, *99*, 1245; **1967**, *100*, 1575.
88. Wynberg, H.; Staring, E. G. *J. J. Chem. Soc., Chem. Comm.* **1984**, 1181.
89. McKenzie, A.; Plenderleith, H. J.; Walker, N. *J. Chem. Soc.* **1923**, *123*, 1090, 2875.
90. Newman, P. "Optical Resolution Procedures for Chemical Compounds," Vol. 2: Acids; Optical Resolution Information Center, Manhattan College: Riverdale, New York, pp. 7-22.
91. Feringa, B. L.; Wynberg, H. *Bioorg. Chem.* **1978**, *7*, 397. Brussee, J.; Jansen, A. C. A. *Tetrahedron Lett.* **1983**, *24*, 3261. The 90% e.e. in the β -naphthol coupling reaction reported by Brussee and Jansen was not due to the chiral catalyst, but was caused by preferential crystallization (personal communication from J. Brussee).
92. For a recent approach using chiral imines as starting material see: Pfau, M.; Revial, G.; Guingont, A.; d'Angelo, J. *J. Am. Chem. Soc.* **1985**, *107*, 273.
93. Hajos, Z. G.; Parrish, D. R. *J. Org. Chem.* **1974**, *39*, 1615.

Stereochemistry and Organic Solid-State Reactions

BERNARD S. GREEN

*Israel Institute for Biological Research
Ness-Ziona, Israel*

RINA ARAD-YELLIN

*Department of Organic Chemistry
The Weizmann Institute of Science
Rehovot, Israel*

MENDEL D. COHEN

*Department of Structural Chemistry
The Weizmann Institute of Science
Rehovot, Israel*

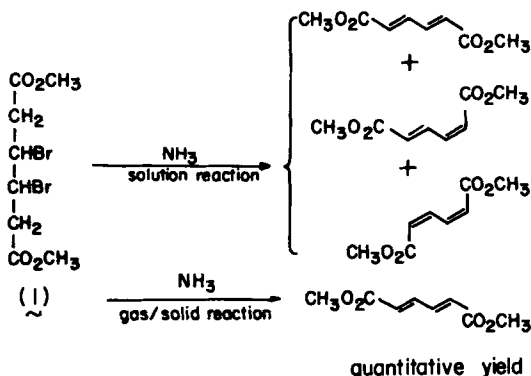
I.	Introduction	132
A.	Geometric Factors in Solid-State Reactions	134
B.	Symmetry Considerations	134
II.	Chemistry Through Crystallization	135
A.	Conformations of Ethanes and Related Compounds	137
B.	Cyclohexanes and Other Alicyclics	138
C.	Conformational Effects in Hydrogen-Bonded Systems	140
D.	The Polyphenyls and Related Compounds	142
E.	Crystallization of Chiral Molecules	146
F.	Crystal-Field Effects on Double Bonds	148
G.	Systems Involving Epimers	150
H.	Structure-Sensitive Molecular Constitution	150
I.	Molecular Structures as Markers for Reaction Pathways	154
J.	Chromoisomerism	157
K.	Proton Transfers	158
III.	Photochemical Solid-State Reactions	166
A.	Solid-State Photodimerization	167
B.	Crystal Engineering: Toward a Systematic Solid-State Chemistry	170
C.	Multiple-Product Solid-State Photodimerizations	173
D.	Photodimerization at Defects	174
E.	Utilization of Solid-State Photodimers	176

F.	Photooligomerization and Photopolymerization	177
G.	Applications of (2 + 2) Photodimerizations in Noncrystalline Phases	179
H.	Solid-State Photorearrangements	180
IV.	Homogeneous Solid-State Reactions	184
V.	Complexes, Clathrates, and Two-Component Solids	193
A.	Clathrates and Inclusion Complexes	194
1.	Polymerization Within Channel Inclusion Complexes	196
2.	Intramolecular Reactions of Guests in Clathrates	196
3.	Gas-Solid Reactions of Clathrates	198
4.	Host-Guest Reactions in Clathrates	199
B.	Solid Solutions-Mixed Crystals	201
VI.	Solid-State Chemistry of Radical Pairs	202
VII.	Asymmetric Synthesis Via Reactions in Chiral Crystals	209
VIII.	Stereochemistry and Crystal Growth	209
	References	209

I. INTRODUCTION

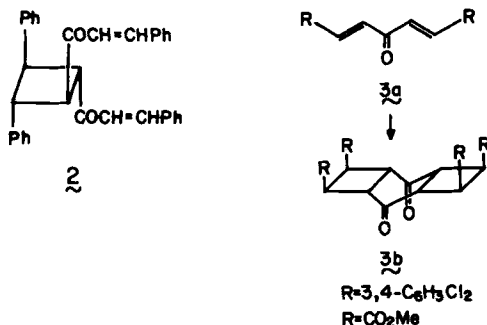
The organic chemist has always aimed at achieving reactions that are highly regio- and stereoselective. With increased success in this direction, and with more and more sophisticated techniques becoming available, it has become an accepted goal to design reaction systems with specificities comparable to those of enzyme-mediated processes. An outstanding feature of enzymatic reactions is the high degree of order in the system and the strict control of the movement along the reaction coordinate from reactant to product. Since crystalline solids are also highly ordered, it would seem attractive to try to exploit them, too, as vehicles for stereospecific reactions.

We ignore here questions as to the techniques one may employ for initiating reactions in crystals. Suffice it to say that there is a long-established (1) and growing (2) area of organic chemistry devoted to the reactions of molecules in crystalline solids. And indeed, in many of these an extraordinary degree of selectivity is found; two examples serve to illustrate this. When the dimethyl ester of *meso*- β,β' -dibromoadipic acid (1) reacts with ammonia (or amines) in solution, dehydrobromination occurs to yield a mixture of *trans*, *trans*-, *cis*, *trans*-, and *cis*,*cis*-dimethyl muconate, as well as varying amounts of amides, which result from attack on the ester function. On the other hand, when the *crystalline* adipate is exposed to gaseous ammonia (or amines), a heterogeneous gas-solid reaction takes place, with the sole product being the *trans*,*trans* muconate (3a). These results are easily explained when the molecules in the reactant crystal have each H-C-C-Br fragment in the antiperiplanar conformation (3b), which is exactly that required for formation of the observed product. Apparently this conformation is favored by crystal forces, at least until the transition state of the reaction is reached.



The second example is an intermolecular crystal-state reaction. Cross-conjugated 1,5-disubstituted 1,4-dien-3-ones in solution undergo both *cis-trans* photoisomerization and photodimerization, yielding complex mixtures of products, including the all-*trans*-substituted cyclobutane **2** in the case of 1,5-diphenyl-1,4-pentadien-3-one. In contrast, dienones such as **3a** in whose crystals adjacent molecules lie parallel and strongly overlapped react in the solid to give **3b** as the sole photoproduct. This isomerically pure tricyclic diketone results, formally, from an eight-center dimerization. It is not formed in the reaction in solution, and could be prepared by other methods only with considerable difficulty (4).

These examples illustrate a number of points. Solid-state reactions can, in many cases, be performed very easily. Their courses are frequently interpretable in terms of straightforward geometrical principles concerning conformation and/or packing of the reactant molecules. It is sometimes possible to design the reactant molecule with suitable substituents to ensure a desired crystal structure



and, thus, to achieve the rational synthesis of a solid-state reaction product ["crystal engineering" (5)].

It is not our aim to provide here a comprehensive review of solid-state organic chemistry. We intend rather to dwell on the interplay between stereochemical factors and solid-state effects, using examples from the literature as illustrations. Before this elaboration, however, we provide a brief discussion of some relevant aspects of organic crystal structures and their roles in determining reaction course.

A. Geometric Factors in Solid-State Reactions

We have referred to the importance of two interrelated factors, the conformation and the relative arrangement of the reactant molecules. A flexible molecule may adopt a variety of conformations in the disperse phase, whereas in the crystal it will rarely adopt more than one. To the extent that the stereochemical course of the reaction is sensitive to conformation, reaction in the solid will be more selective than that in the disperse phase. It is also possible that the conformation found in the crystal is absent in solution, so that the solid-state product is not found at all among the solution products. The packing arrangement of the molecules is particularly significant in polymolecular reactions. In the crystal the relative geometries of the neighbors of any reference molecule will generally be the same for all molecules (although relatively infrequently there are several symmetry-independent reference molecules so that there are two or even three sets of such relative geometries). Thus, in the solid state the number of possible approach geometries for nearest neighbors is very limited, introducing reaction specificity additional to that obtaining in solution. Although both conformation and packing arrangement are determined by the same factor—the drive toward minimum free energy of the crystal—they may lead to chemically distinguishable consequences.

B. Symmetry Considerations

To the extent that a crystal is a perfectly ordered structure, the specificity of a reaction therein is determined by the crystallographic symmetry. A crystal is built up by repeated translations, in three dimensions, of the contents of the unit cell. However, the space group usually contains elements additional to the pure translations, such as a center of inversion, rotation axis, and mirror plane. These elements can interrelate molecules *within* the unit cell. The smallest structural unit that can develop the whole crystal on repeated applications of *all* operations of the space group is called the *asymmetric unit*. This unit can consist of a fraction of a molecule, sometimes fractions of two or more molecules, a single whole molecule, or more than one molecule. If, for example, a molecule lies on a crystallographic center of inversion, the asymmetric unit will contain half

the molecule. If the molecule has no internal symmetry, the asymmetric unit must contain one or more whole molecules. With one molecule in the asymmetric unit all molecules are symmetrically related and therefore have identical conformations and environments. If the asymmetric unit contains more than one molecule, then these molecules are symmetry independent and will have different conformations and environments—although the differences may be small. Similarly, the molecules in different polymorphic forms of a given compound will generally have different conformations and environments. Again, the differences may be so small as to be barely detectable.

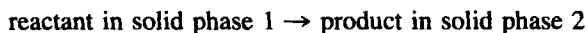
It should be remembered that conclusions based on crystallographic symmetry apply strictly only to the *average* geometry of the molecule at each site. Crystals often suffer various kinds of disorder, in which case individual molecules may depart considerably from the crystallographically determined average geometry.

Finally, reference must be made to the important and interesting chiral crystal structures. There are two classes of symmetry elements: those, such as inversion centers and mirror planes, that can interrelate enantiomeric chiral molecules, and those, like rotation axes, that cannot. If the space group of the crystal is one that has only symmetry elements of the latter type, then the structure is a chiral one and all the constituent molecules are homochiral; the dissymmetry of the molecules may be difficult to detect but, in principle, it is present. In general, if one enantiomer of a chiral compound is crystallized, it must form a chiral structure. A racemic mixture may crystallize as a racemic compound, or it may spontaneously resolve to give separate crystals of each enantiomer. The chemical consequences of an achiral substance crystallizing in a homochiral molecular assembly are perhaps the most intriguing of the stereochemical aspects of solid-state chemistry.

We are now ready to talk about chemistry.

II. CHEMISTRY THROUGH CRYSTALLIZATION

Many solid-state reactions may be pictured as proceeding in two steps. First a "homogeneous" process leads to product molecules dissolved in residual parent matrix. Curtin and Paul, in a review on thermal solid-state reactions (6), divide this step into a number of stages: First, there is a "loosening" of the molecules at the reaction site to be, then molecular change (the true reaction), and finally solid-solution formation. When the concentration of the accumulated product exceeds the solubility limit the second step, the decomposition of this solid solution into separate reactant and product phases, occurs. However, in some cases the solubility limit is very low, so that the overall process appears to become simpler:



In such a case the chemical reaction and the recrystallization step are essentially synchronous and may in the limit be regarded as one and the same process, as has been discussed elegantly by Adler (7). One should distinguish this case from the relatively rare one of a true one-stage process ("homogeneous" or "diffusionless" reaction), in which there is no phase change or interphase boundary. Here the reactant crystal transforms continuously into a product one, with concomitant continuous changes in the crystallographic constants.

In the two-stage process, the product is formed in the first stage in a conformation imposed by the parent lattice. As we have argued above, the environmental change involved in the subsequent phase transformation, solid 1 \rightarrow solid 2, will be associated with some conformational change that indeed may be major.

In this section we treat this last subject: the changes in molecular structure accompanying phase transformation. In many cases, such as geometrical isomerization (8,9), these changes are regarded as chemical reactions:

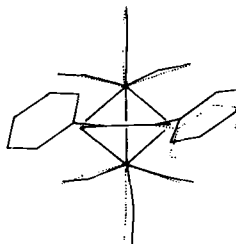
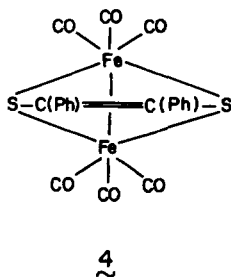
cis in phase 1 \rightarrow trans in phase 2

When the changes in molecular structure are less marked, it becomes a matter of taste whether to continue to use the term "reaction," but we do so in what follows.

We consider here cases in which the crystal interactions play an important role in determining the geometry of the molecules. We must realize, however, that these interactions are generally of appreciably lower energies than those involved in bond-breaking and -forming. On the other hand, torsional distortions frequently require energies similar to or lower than those of the intermolecular interactions in the crystal. We may then expect crystallization to produce appreciable conformational, and sometimes configurational, effects. This is indeed what happens, and most of our examples are of such cases, although we shall see that there are also important cases involving bond-breaking and other processes.

Molecular-geometric changes induced by crystal interactions are most simply seen in systems having symmetry-independent molecules. Thus, in the interesting iron tricarbonyl derivative 4, there are two such molecules in the asymmetric unit, and correspondingly two symmetry-independent environments, leading to molecules of clearly distinguishable geometries. (10) The right-hand figure shows these two conformations superimposed on their common Fe_2S_2 atoms; one of the phenyl groups of the syn conformation (solid line) and one of the anti conformation (dotted line) overlap exactly.

Crystal interactions may lead to a number of readily observable consequences. The molecular geometries may be different in different polymorphic forms of a given compound or, as in the case above, in symmetry-independent sites in a given crystal; a change of molecular substituents remote from the torsionally flexible bonds may change the molecular conformation, as a result of modification

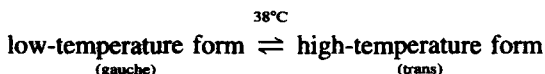


of the crystal structure; or the molecular geometry in the crystal may be different from that dominant in fluid phases. We will give examples of all of these.

A. Conformations of Ethanes and Related Compounds

The 1,2-dihalogenoethanes, $\text{XCH}_2\text{—CH}_2\text{X}$, and a variety of other substituted ethanes are found as mixtures of trans and gauche conformers in the liquid and gas phases, but only as trans in the crystal (11). By contrast, both the pure gauche and trans conformers of 1,1,2,2-tetrachloro- and tetrabromoethane have been isolated in the solid (12). The tetrachloro compound undergoes a reversible, pressure-induced, solid–solid transformation (13). In the high-pressure form the molecules are trans; in the low-pressure form, gauche. In the series $\text{XCH}_2\text{—CH}_2\text{CN}$, with $\text{X} = \text{CH}_3$, Cl , or Br , the trans and gauche conformers coexist in the liquid, but the crystals consist only of molecules of gauche conformation (11).

The molecules $\text{ClCH}_2\text{—COCl}$, $\text{BrCH}_2\text{—COCl}$, $\text{BrCH}_2\text{—COBr}$, and $\text{ClCH}_2\text{—COCH}_3$ all crystallize in only one conformation, that having the substituent on the methylene nearly, or exactly, trans to the carbonyl. Ethylene chlorohydrin, on the other hand, is gauche in the crystal (11). In the liquid or gaseous phases all these molecules are found in two conformations, of which one is essentially identical to that of the molecule in the crystal. The trans and gauche conformers of $\text{ClCH}_2\text{—CONHCH}_3$ coexist in solution. There are two crystal forms, which are thermally interconvertible (14):



The α -diketones XCO—COX , with $\text{X} = \text{CH}_3$, NH_2 , Cl , or CH_3O , all crystallize as planar molecules with the two keto groups trans. Oxalyl chloride displays, in the liquid, two conformations (11).

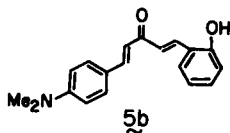
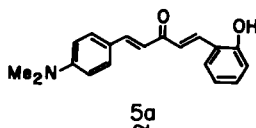
Succinodinitrile is dimorphic, with the high-temperature, “plastic” phase being partially disordered. The molecules of this latter phase are an equilibrium mixture

of trans and gauche conformers (15,16). However, there is no trans form present in the low-temperature phase (17).

In the normal paraffin chains containing four or more carbons many different conformations are conceivable. In the solid, however, the Raman spectra show that all are in the fully extended conformation, so that there is a trans arrangement at all C-C bonds (11,18). In the liquid state a number of conformations coexist, with one of them being the extended-chain one provided the number of carbons is not too large. However, in cetane, with 16 carbons, the Raman lines arising from the extended form are no longer detectable in the liquid.

The complexity that may arise even for a relatively simple molecule is illustrated by iminodiacetic acid, $\text{HO}_2\text{CCH}_2\text{NHCH}_2\text{CO}_2\text{H}$. This acid has three crystal forms. The bond angles and lengths are essentially the same in all the forms, but the torsional angles differ, providing three different molecular conformations (19). In addition, one of the forms has two symmetry-independent molecules, of slightly different conformations, in its asymmetric unit.

Herbstein and co-workers have determined the structures of some "Heilbron complexes" involving various guest molecules included in the host **5**. It is most interesting that the geometry of the host, and with it that of the inclusion site, may vary appreciably with changes in the guest (20). Compare, as examples, the host molecules **5a** and **5b**, for which the corresponding guests are *p*-dimethylaminobenzaldehyde and *m*-dinitrobenzene, respectively. All the C=C double bonds are of *E* configuration. In **5a** these bonds are both syn to the carbonyl (*s*-cis), but in **5b** one is syn, one anti (*s*-trans).



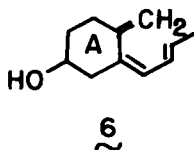
B. Cyclohexanes and Other Alicyclics

It has been reported that pure equatorial chloro- and trideuteriomethoxycyclohexane were obtained by carefully controlled crystallization of the respective liquids (21).

Infrared measurements have been employed (22) to show that for a series of

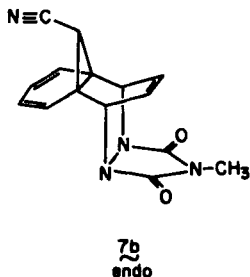
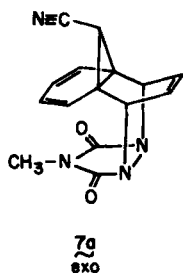
mono- and disubstituted cyclohexanes incorporated into the channels of crystalline thiourea, the conformational equilibria are shifted toward the axial (diaxial) conformer compared with the situation in the liquid (melt or dissolved) state. For example, the equilibrium constant $[(\text{di})\text{axial}]/[(\text{di})\text{equatorial}]$ is greater by a factor of 13 in the clathrate than in the liquid for chlorocyclohexane, and by a factor of 33 for *trans*-1,4-dichlorocyclohexane.

In vitamin D₃ there are two symmetry-independent molecules in the unit cell, with readily distinguishable conformations (23). It is particularly interesting that the A rings, 6, of the two molecules are of different chair conformations, as first suggested by Havinga (24). These two chair forms rapidly interconvert in solution on the nuclear magnetic resonance (NMR) time scale (25). In the so-called α -conformation the hydroxyl is equatorial and the exocyclic $=\text{CH}_2$ is "below" the mean cyclohexane plane; in the β -conformation the hydroxyl is axial and the $=\text{CH}_2$ is above the plane. It is noteworthy that ring A is of α -type in 25-hydroxy-D₃ (26) and in the 4-iodo-5-nitrobenzoate ester of vitamin D₂ (27), whereas it is of β -type in the vitamin D analog studied by Knobler and colleagues (28).



The molecules of *trans*-2,3- and -2,5-dichloro-1,4-dioxanes in the crystal are in the chair conformation with both chlorine atoms occupying axial positions (29). In solution, too, there is a preference for this conformation; however, the dipole moment for the former molecule in solution is higher than expected for the purely diaxial conformation (30).

A case of a thermally induced phase change involving ring inversion was recently described by Kaftory (31). He found that a crystal of the *exo* isomer of the adduct, 7a, of 11-cyano-1,6-methano[10]annulene with 4-methyl-1,2,4-triazoline-3,5-dione is transformed to the *endo* isomer 7b on heating to 175°C. The process involves nucleation and growth of the product phase, but maintains



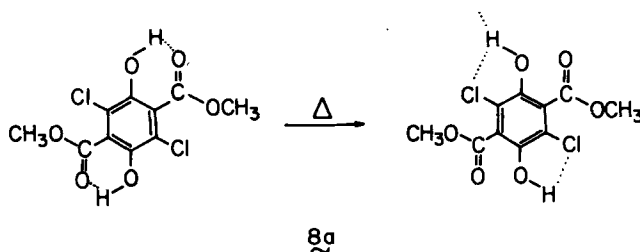
the external shape of the crystal. Kaftory argues that the change of configuration involves simultaneous inversions of the two nitrogens.

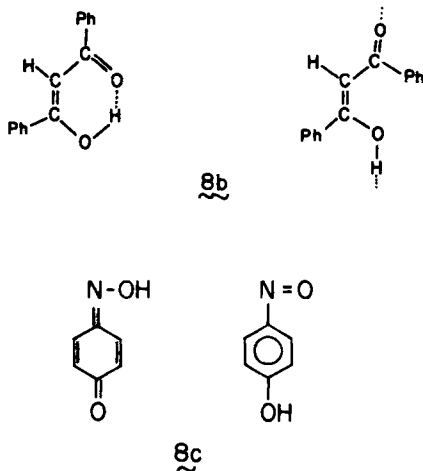
C. Conformational Effects in Hydrogen-Bonded Systems

The polymorphic changes of the iminodiacetic acid referred to above are associated with extensive reorganization of the hydrogen-bond framework. Similarly, conformational and hydrogen-bond changes are found in the change of the white crystal form of dimethyl 3,6-dichloro-2,5-dihydroxyterephthalate (**8a**) into the yellow form (32). The yellow crystal has a single, centrosymmetric molecule in the unit cell, with the hydroxyls intramolecularly hydrogen bonded to the adjacent ester carbonyls. The nonhydrogen atoms are almost coplanar. The white form has an interesting structure: There are two molecules in the unit cell; both are centrosymmetric but they are crystallographically independent of one another. There are intermolecular $\text{O-H} \cdots \text{O}=\text{C}$ hydrogen bonds and, apparently, bifurcated intramolecular bonds. The carbomethoxyl groups of the two molecules are rotated by 80° and 73° from the plane of the benzene ring. It follows from the X-ray results that the phase change is associated with a flipping of alternate aromatic rings through 180° .

Dibenzoylmethane (**8b**) has been the subject of much interest as regards the possibility that its polymorphism is associated with keto-enol tautomerism. Chemical and spectroscopic studies showed that this is not so (33a). This compound had previously been reported to be trimorphic (33b), but one "form" appears, in fact, to be a eutectic mixture of the other two. The molecules in these two polymorphs are both in the same state of tautomerism; they differ in the torsional angle about the $(\text{CH})-(\text{CO})$ bond and in the type of hydrogen bonding in which they participate. It is noteworthy that solutions prepared from these forms at low temperature have differences in chemical and spectroscopic properties that are maintained for some time. For example, such solutions prepared and held at -35° react at different rates with FeCl_3 .

Another system with a tendency to polymorphism and in which one might expect the different crystal forms to be composed of different proton tautomers is benzoquinone oxime-nitrosophenol (**8c**). Here all materials studied proved to





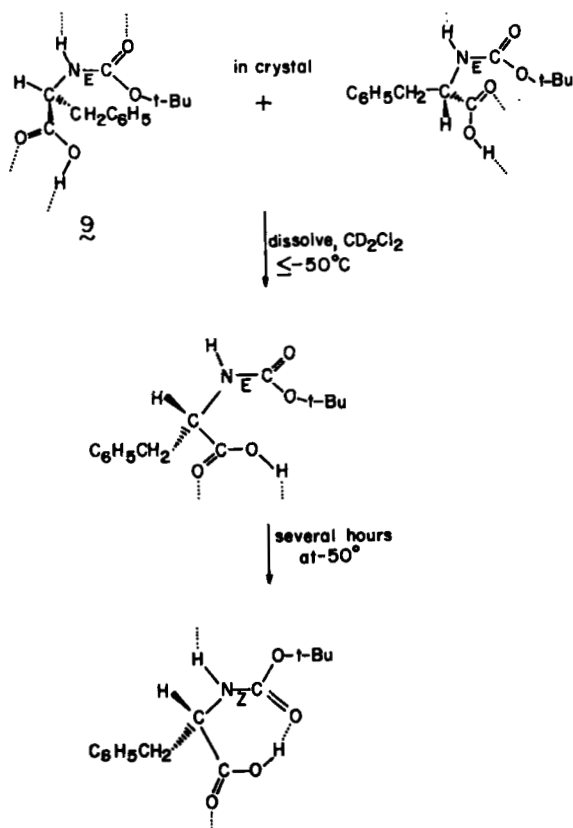
be the quinone oxime tautomers, with an infinite chain of $\text{C}-\text{NOH} \cdots \text{O}=\text{C}$ hydrogen bonds (34a). However, in several unsymmetrically substituted 1,4-benzoquinone oximes the two crystal forms were shown to consist of syn and anti isomers. Thus in (α) 2-chloro-5-methyl-1,4-benzoquinone-4-oxime the oxime group is syn to the chlorine (34b), whereas in the (β) form it appears to be anti (34c).

A system that shows some analogies to dibenzoylmethane is *t*-butoxycarbonyl-phenylalanine (9), studied by Kessler and co-workers (35). X-Ray and NMR studies established that this molecule occurs in the crystal as a mixture of two conformers, both having an *E*-configured urethane bond. On dissolution at low temperatures the urethane configuration remains *E*, but gradually changes to *Z*.

A second example, described by the same authors, is that of the vinylogous amide $\text{RCOCH}=\text{CHNHCH}_3$ (10), where $\text{R} = \text{C}_6\text{H}_{11}$ (cyclohexyl group). In the crystal the molecule is of *E* configuration at the $\text{C}=\text{C}$ double bond, and of *Z* configuration at the partially double bonds $(\text{CO})-(\text{C}=\text{C})$ and $(=\text{C})-(\text{N})$. When this crystal is dissolved at low temperatures two conformers are found, both of *E* configuration at the $\text{C}=\text{C}$. On warming, torsional equilibration occurs, and eventually isomerization about the $\text{C}=\text{C}$ double bond also takes place.

Thus, in these two examples the most stable species in solution is not that found in the crystal. The long lifetimes of the metastable species in solution at low temperatures may indicate that the dissolution process leads initially to polymolecular aggregates in which the intermolecular hydrogen bonds are maintained.

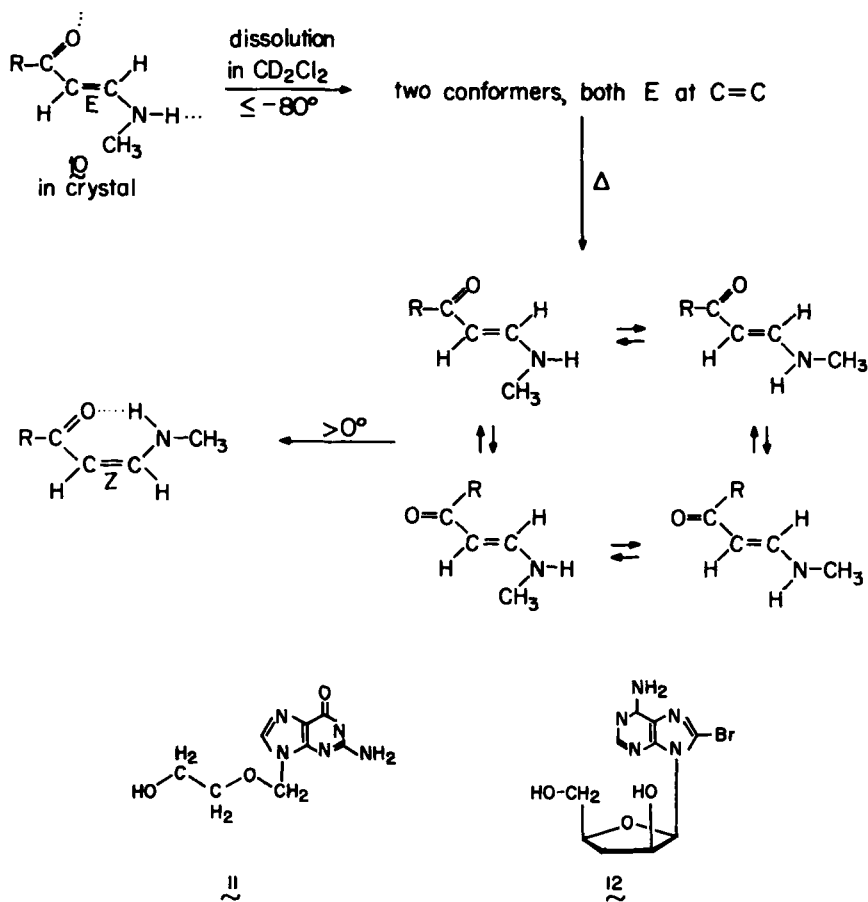
Two examples of conformational effects associated with, and probably even dominated by, changes in the hydrogen-bond network have been reported by Birnbaum and co-workers. Both have three molecules in the asymmetric unit.



One of these is 9-(2-hydroxyethoxymethyl)guanine (11); here the side chain in two molecules is partially folded, while in the third it is of extended conformation (36). The second example is 9-β-D-xylofuranosyladenine (12), where again two molecules have similar conformations while the third is significantly different (37).

D. The Polyphenyls and Related Compounds

A series of compounds that has been studied extensively, both theoretically and experimentally, is the polyphenyls (38–40). In considering these compounds it is very helpful if one has at least a little understanding of the significance of the X-ray crystallographic results. Biphenyl, the first of the series, is known to be nonplanar in the gas phase, with a torsional angle about the central bond of 42°. This is interpreted in terms of relief of steric interference between the



ortho hydrogens, at the cost of some loss of the π -electron conjugation energy. X-Ray analysis of the crystal gives mean positional coordinates of the atoms indicating that the molecule is planar in this phase. It has frequently been stated that this apparent change of conformation on passage from the gas to the crystal is due to crystal forces. However, the X-ray analysis shows also that there is large-amplitude atomic movement, and this complicates the interpretation. Thus, the diffraction data can be taken to indicate that the biphenyl molecule is indeed planar and librates about its long axis as a rigid body. However, these data are also consistent with the occurrence of internal torsion of the two rings, in opposite phase, about the bond between them, with the planar conformation being the most stable one. And there is still another possibility—that there are *two* energy minima, for two, nonplanar, enantiomeric conformations. With respect to the

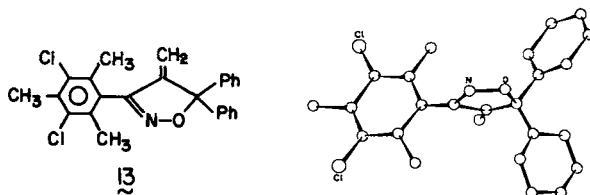
last case, the experimentally observed mean planarity indicates that there is complete conformational disorder (either static or dynamic), in the sense that at any instant there is an equal probability of finding either enantiomer at any given crystal site. The potential-energy surface for torsion about the central bond must be extremely flat, even in the gas phase, and the above ambiguity in our interpretation of the X-ray diffraction data means that we cannot yet decide whether the crystal forces are sufficient to eliminate the barrier in this surface.

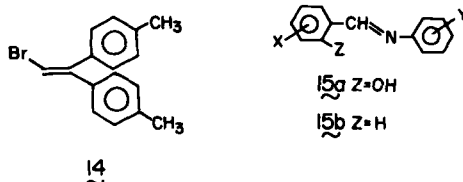
Biphenyl, terphenyl, and quaterphenyl all have room-temperature structures that behave similarly, and also all have low-temperature phases in which only one conformer is present. The torsion angle about the central C–C bond in biphenyl is estimated to be about 10° in the low-temperature form, which is appreciably less than that in the gas phase. In the case of terphenyl, it has been established (41) that the room-temperature structure is disordered; each molecule librates in a double-well potential, with the barrier height being about 0.6 kcal/mol. In the low-temperature form the molecule is stabilized in one of the two minima of the well, and has its terminal rings rotated in the same sense, so that the molecule conserves its center of symmetry. This alternation of rotations between adjacent rings is found (42) also in the low-temperature form of quaterphenyl and results in the molecule being noncentric (even though the crystal structure has a center of symmetry).

It is noteworthy that 4,4'-diamino-3,3'-dimethylbiphenyl is known in only one crystal form (43). The crystal is chiral and the molecules are distinctly nonplanar, with the two phenyl rings being twisted about the linkage between them so as to be mutually inclined at an angle of 41° .

1,3-Cycloaddition of 3,5-dichloro-2,4,6-trimethylbenzonitrile oxide to the double bond of 1,1-diphenylallene gives the isoxazoline **13**. This product was obtained in two crystal forms with marked differences in the torsional angles in the molecule. Thus, for example, the dihedral angle between the unsubstituted phenyl groups is 78° in form I and 88° in form II, and the dihedral angles between the unsubstituted phenyl groups and the substituted phenyl group are 33° and 56° for form I and 71° and 45° for form II (44).

Another molecule for which there seems to be an appreciable conformational difference between the "free" molecule, as determined by calculation, and the molecule in the crystal phase, but where the effect is somewhat masked by the large thermal motion in the latter, is 2-bromo-1,1-di-*p*-tolylethylene (**14**) (45).





In the crystal the atoms of this molecule are found to be distributed in three planes: The two tolyl rings are rotated by 24° (trans to Br) and 68° (cis to Br) with respect to the ethylene plane. Semiempirical Huckel molecular orbital (MO)-type calculations give essentially the same angles in the crystal, but predict 35° and 45° for these angles in the free molecule.

In the cases of the *N*-salicylidene (46) and *N*-benzylidene (47) anilines (**15a** and **15b**), there is less ambiguity arising from thermal motion. For both series of compounds it is believed, on spectroscopic grounds, that the molecules are nonplanar in solution. While there are some crystal phases known in which the molecules retain this conformation (the dihedral angle between the anilino and salicylideneimino planes being of the order of 40°), in others the molecules are definitely planar. In the case of **15a** it has been found that there are marked differences in densities and in photochemical and spectroscopic properties between crystals of the two types.

This brings us to an interesting feature of "crystal engineering." Consider, for example, 4,4'-dichlorobenzylideneaniline. The chloro substituents are remote from the phenyl-C and phenyl-N bonds, which are responsible for the torsional flexibility of the molecule. The chlorines will not, then, directly (sterically) participate in determining the conformation. However, they may play an important role via crystal forces. In particular, it has been argued (48) that there is an attractive interaction between chlorines, and that this results in the observed tendency of dichloroaromatics to crystallize in face-to-face close packing. If this is true of the dichlorobenzylideneaniline it might have the effect of driving the molecule into the planar conformation. This is indeed what is found for one of the two crystal forms of the 4,4'-dichloro derivative (49). It should be added, however, that planar molecules are found also in crystals of some benzylideneanilines not containing chlorines. Further, Hagler and Bernstein (50, 51) have argued, on the basis of a combination of *ab initio* MO and packing calculations, that the effect is a cumulative one, involving all atom-atom interactions, and is not dominated by attractive interchlorine forces.

Another feature that we may refer to here is that of "structural mimicry" (52). It is generally accepted that "a necessary and sufficient condition for formation of solid-solution crystals by two or more organic substances is similarity of shapes and sizes of the component molecules" (53). Consider the two molecules salicylidene-*N*-4-chloroaniline and -4-bromoaniline, which are very similar chemically and, in solution, structurally. Both are dimorphic, with molecules

planar in one crystal form, nonplanar in the other. For the chloro derivative the form having the molecules planar is the stable one; the stable form of the bromo derivative has its molecules nonplanar. In general, the mutual solubility of a chloro compound with the corresponding bromo compound is high. But in the present case, shape restrictions would severely limit the solubility of, for example, the nonplanar bromo molecules in a structure of planar chloro molecules. However, a planar bromo molecule could fit very well into such a structure. This is indeed what is found (54): There exist two series of solid solutions, both spanning the whole composition range, with one composed of planar molecules, one of nonplanar ones. This is an example of a fairly general phenomenon in which a guest molecule in a solid solution adopts a conformation different from the one in its stable crystal and dictated by the host structure. The guest "mimics" the conformation of the host. Many such examples are found in solid-state reactions where the product, as long as it is in solid solution in the reactant crystal, adopts a conformation dictated by this host.

E. Crystallization of Chiral Molecules

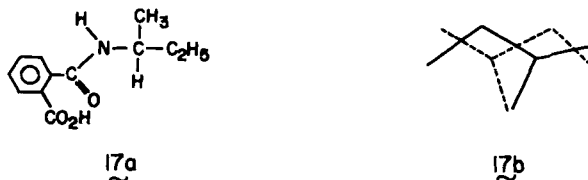
A solution or melt of a racemic mixture of enantiomers may crystallize either as a racemic phase or as a mixture of two resolved enantiomorphic phases. The molecules in these two enantiomorphic phases will be exact mirror images of one another. However, a given enantiomer, say *R*, will have different environments in the racemate and in the resolved crystal and will be conformationally different. Correspondingly, the *R* molecule in the resolved crystal and the *S* molecule in the racemate will not be exact mirror images.

All the crystal forces that we treat in this section can be considered in terms of the "recognition" between a given, reference molecule and the cavity it is to occupy in the crystal. In chiral systems the cavity is clearly of different shape in the *d* and *l* crystals, and this generally results in differential incorporation of *R* and *S* molecules. However, in molecules containing the *sec*-butyl group, discrimination is often ineffective. This is because the two enantiomers can assume different conformations with very similar external shapes, and they can then interchangeably enter the same cavity in the crystal. This effect was recognized some time ago (55), and recently its consequences have been studied in detail (56). In the case where two enantiomers may readily replace one another in the crystal, it follows that there is a tendency to conformational disorder (see biphenyl, above), and in many cases, the resolved enantiomers and the racemates are isostructural.

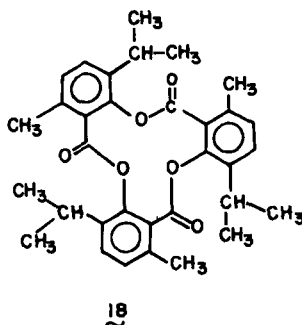
Two types of geometric effects have been found in this context. One of these effects is exemplified by isoleucine (16), in which the *sec*-butyl group adopts a *gauche* conformation and disorder occurs through interchange of ethyl and methyl groups (57). In this situation the *sec*-butyl group has pseudo mirror symmetry.



An example of the second effect is provided by mono-*sec*-butyl phthalamide (**17a**) (56). In the crystal the two enantiomers of this molecule are miscible in all proportions. The racemate crystallizes in space group $P\bar{1}$ (two general positions in the unit cell) with four molecules per unit cell. Thus there are two molecules in the asymmetric unit. The *sec*-butyl moieties adopt the anti conformation (the two geometries are shown schematically in **17b**) and exhibit conformational disorder to different extents at the two symmetry-independent sites.



An example of chiral discrimination is afforded by the clathrates of tri-*o*-thymotide (TOT, **18**). This molecule is known for its ability to form crystalline inclusion complexes with a variety of organic molecules (58). Crystallization of TOT from solutions of appropriate racemic substances affords chiral single clathrate crystals in which the guest enantiomers are incorporated to different degrees (59). The highest enantiomeric purities (measured on extracted guest) were 47% for 2,3-dimethyl-*trans*-oxirane, 38% for 2,4-dimethyl-*trans*-oxetane, and 37% for 2-bromobutane. The authors interpreted the chiral discrimination as due to the difference in the overall fits of the enantiomers in the crystal cage, rather

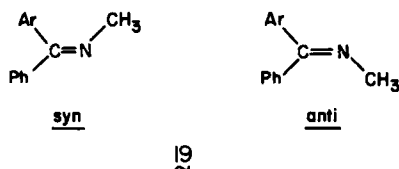


than to a few specific points of contact between the guest and the walls of the cage. An interesting guest is methyl methanesulfinate; in the TOT complex it is found to have an e.e. of 14%, which is maintained on heating to 115°C (under which conditions there is racemization in solution). Thus the complexation provides not only relative stabilization of one enantiomer, but also a kinetic barrier to racemization.

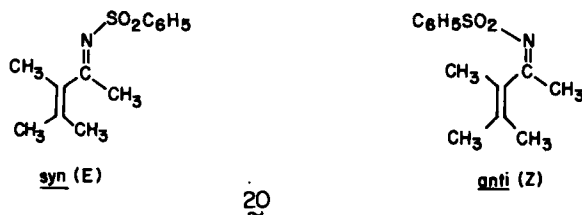
F. Crystal-Field Effects on Double Bonds

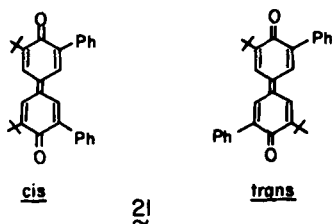
A variety of systems are known in which there are observable crystal-field effects on the configuration about a double bond. Thus, acetaldehyde phenylhydrazone occurs in solution as an equilibrium mixture of syn and anti forms (in benzene the ratio is 3:2), but in the crystal only the anti isomer is found (60).

When *p*-chlorobenzophenone dichloride reacts with methylamine there results an oil consisting of similar amounts of the syn and anti Schiff base **19**. This oil, on standing at room temperature for 2 weeks, transforms to crystals of only the syn isomer. If these crystals are heated above their melting point (125°) for a few minutes, or are dissolved in cyclohexane and allowed to stand at room temperature for 2 weeks, the syn isomer reconverts to a mixture of the two isomers (61a). [This seems to be an example of the so-called second-order or crystallization-induced asymmetric transformations (61b).] A number of systems of this series were known, from previous work, to be dimorphic; however, Curtin and Hausser found no case in which it was established that two crystal forms correspond to different isomers (61a).

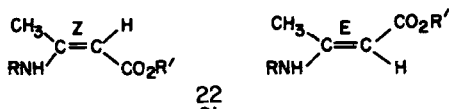


Raban and Carlson (62) found two isomers to be present in solution in the benzenesulfonamide derivative **20**, but only one of these to be present in the crystal. When the solid is dissolved at low temperature, and the solution kept cold, isomerization proceeds only slowly.





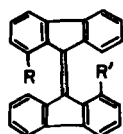
Similar studies have been made on isomerization about $\text{C}=\text{C}$ double bonds. Careful crystallization of the *p*-diphenylquinone **21** gives material containing only one of the two isomers. However, in solution isomerization occurs, albeit with an appreciable activation energy. Rapid quenching of a solution in acetic acid gives almost equal amounts of crystals of the two isomers (63).



3-Alkylamino crotonic esters (**22**) all show in solution the presence of the isomers of both *E* and *Z* configurations, and there is also some evidence for rotamers involving restricted rotation about the $(\text{C}=\text{C})-\text{N}$ and $\text{C}-\text{CO}_2\text{R}$ bonds (64). In all cases studied, when only one crystal form was found the molecular configuration was *Z* about the double bond. For $\text{R} = \text{CH}_2\text{Ph}$, $\text{R}' = \text{C}_2\text{H}_5$, two crystal forms were obtained, one with *E* and one with *Z* molecular configuration.

A number of 1,1'-disubstituted 9,9'-bisfluoronylidenes (**23**) have been studied by variable-temperature (dynamic) NMR of their solutions, either immediately after dissolution of the solids at low temperature or after equilibration (65). It appears that the dominant configuration in equilibrated solutions is a twisted *trans* one (Newman projection along $\text{C}=\text{C}$ shown on the right). In the solid, compounds **23b** and **23c** retain this configuration [as shown for **23b** by X-ray analysis also (66)], whereas **23a** possesses a *cis* configuration.

Nitrosobenzene crystallizes as the *cis* dimer, **24**, whereas in the melt some *cis* dimer, more *trans* dimer, and monomer are present. On the other hand, *o*-

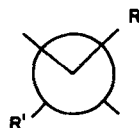


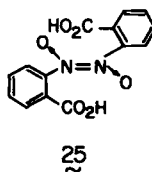
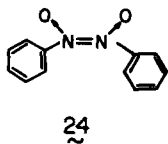
trans-**23**

a: $\text{R}=\text{R}'=\text{CO}_2\text{Me}$

b: $\text{R}=\text{R}'=\text{CO}_2\text{CHMe}_2$

c: $\text{R}=\text{CO}_2\text{Me}$; $\text{R}'=\text{CO}_2\text{CHMe}$

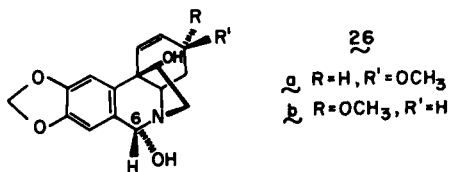




nitrosobenzoic acid crystallizes as the trans-dimer, **25** (67). Some nitroso compounds have been isolated as green, presumably monomer-containing solids (68), and some in both green and colorless crystalline modifications (69). Prout and co-workers found (70) that monomer and cis dimer coexist in the crystal of pentafluoronitrosobenzene. The two species occupy different crystallographic sites, with the monomer being disordered.

G. Systems Involving Epimers

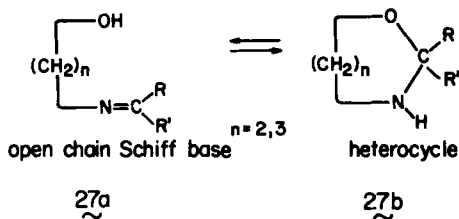
Among the many natural products that may be considered in this category are the alkaloids 6-hydroxycrinamine (**26a**) and haemanthidine (**26b**), which are epimeric in the solid. It is found (71) that in solid **26a** the hydroxyl attached to C-6 is trans to the pyrrolidine ring, whereas for both compounds, there is NMR evidence for epimerization at C-6 in solution (72).



One of the best-known systems involving epimerization is that of *d*-glucose. In aqueous solution the epimeric α - and β -forms are in equilibrium, but each can be obtained by crystallization; ethanol readily affords the pure α -form, whereas pure β may be obtained from pyridine.

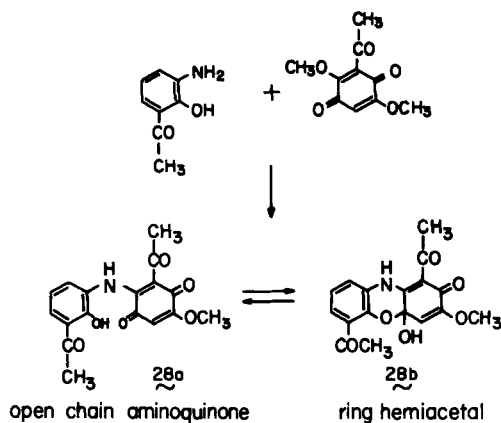
H. Structure-Sensitive Molecular Constitution

We now turn to the question of sensitivity of chemical constitution to crystal-field effects. Here the distribution of the various possible species in a system will be determined by bond-breaking and -forming processes. Except for the case of proton tautomerism, which we will treat at the end of this section, these processes are of high energy. Nevertheless, a variety of systems showing such sensitivity have been encountered.



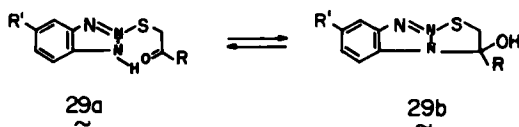
Condensation of β - or γ -amino alcohols with aldehydes or ketones $\text{RR}'\text{CO}$ gives the product **27**. In solution the position of the equilibrium varies with R and R' , and with the solvent (73). When the carbonyl reactant is a substituted benzaldehyde, the solid is found (IR, KBr) to comprise molecules of the open-chain structure **27a**, whereas aliphatic aldehydes and ketones give crystals of dihydro-1,3-benzoxazines, **27b**. An interesting case is that of the condensation product of *o*-hydroxybenzylamine with cyclopentanone, for which McDonagh and Smith (73) suggest that ring and chain tautomers coexist in the solid.

The reaction below leads to a product, 2-(2'-hydroxy-3'-acetoxyphenylamino)-5-methoxy-1,4-benzoquinone (**28**), that, in solution, is an equilibrium mixture of tautomers (74). The two tautomers can be crystallized separately, the open-chain form as black crystals, the ring form as yellow ones; both decompose at 176° .

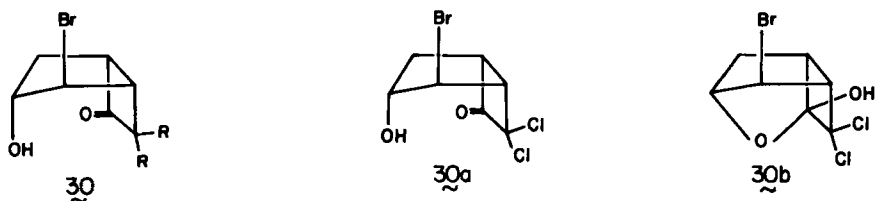


In solution, the aminoketone **29a** is in equilibrium with the heterocyclic carbinolamine **29b**. The equilibrium constant varies with the substituents; the various compounds of the series are, as far as is known, monomorphic, some giving crystals having the molecules in open-chain form, others giving crystals with ring-closed molecules (75).

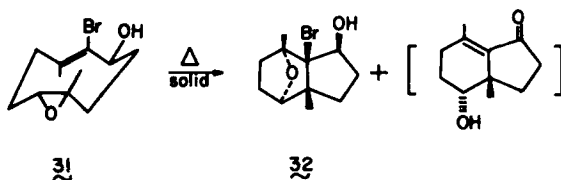
An interesting system has been described by Glen and co-workers (76). It



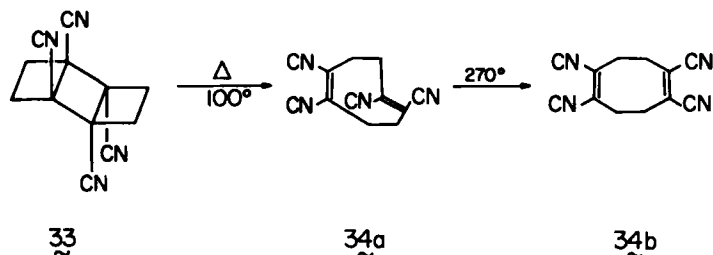
had been shown that in several bicyclo[3.2.0]-6-one derivatives of type **30**, transannular interactions can occur between a 3-endo nucleophilic substituent and the carbonyl group. Glen found that crystals of the material having $R = \text{Cl}$ are of space group $C2/c$ and have 16 molecules in the unit cell. But this space group has only eight general positions in the cell, so there are two, symmetry-independent molecules in the asymmetric unit. These were shown to be the chain and ring tautomers **30a** and **30b**, respectively, which are apparently "frozen out" by packing forces.



Another example of a transannular cyclization that occurs in the solid state is provided by the epoxy alcohol **31**. This compound is stable when dissolved in organic solvents and in 0.25*N* sulfuric acid. However, the crystals transform rapidly to **32**. Although the process is accompanied by partial melting, it appears to be a true solid-state one. Interestingly, the reaction is slowed down appreciably when the dry crystals are covered with ether. Hydrogen bromide is eliminated in the reaction and it may be that an acid-catalyzed process is also occurring; in the presence of solvent this process may be slowed down by the dissolution of the decomposition products in the solvent (77).



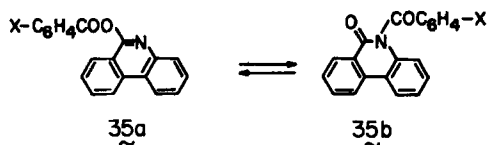
A solid-state transformation that involves an electrocyclic ring opening is described by Bellus and his co-workers (78). They found that when 1,2,5,6-tetracyano-*anti*-tricyclo-[4.2.0.0^{2,5}]octane (**33**) is heated in the crystal, only 1,2,5,6-tetracyano-(*Z,E*)-cycloocta-1,5-diene (**34a**) is formed, as expected on



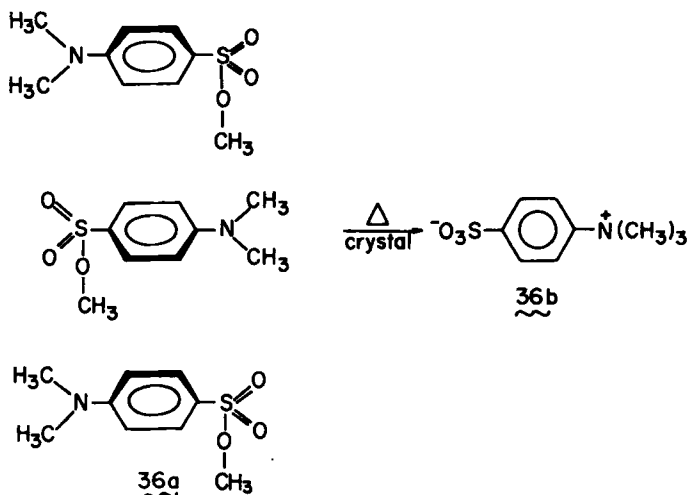
orbital symmetry grounds. This is the first example of a stereospecific cleavage of an *anti*-tricyclo-[4.2.0.0^{2,5}]octane to an isolable (*Z,E*)-cycloocta-1,5-diene, and the stereospecificity is probably a result of the constraint that the crystal imposes on the unimolecular reaction. The process 33 \rightarrow 34a requires only minimal molecular motion in the crystal, and is energetically feasible. On the other hand, a possible second step, 34a \rightarrow 34b, involves extensive displacement in the lattice and is kinetically inhibited.

Crystal-structure-sensitive bond-forming and -breaking processes other than ring-chain tautomerism are also known. For example, acetylation of 4-pyridone in pyridine gives rise to crystalline *N*-acetyl-4-pyridone. When this is dissolved in CH₂Cl₂ it gives a nearly 1:1 equilibrium mixture of this acetyl pyridone and 4-acetoxypyridine. The *N*-acetyl derivative is obtained by crystallization (79).

The system 35a + 35b is in equilibrium in solution; the interconversion formally involves migration of the benzoyl group from an oxygen to a nitrogen atom. Benzoylation of the sodium salt of phenanthridone at -20° gives rise to the *O*-benzoyl derivative 35a, which is stable at low temperatures. When heated alone or in CH₂Cl₂ solution, 35a converts to the *N*-benzoyl derivative 35b, the form that is obtained directly by benzoylation at room temperature. The compounds with X = *p*-MeO or *p*-Cl show similar melting behaviors (80).



As a further example of a solid-solid transformation associated with reorganization of bonds, we take the process described by Bergman and co-workers (81). These investigators have found that solid methyl *p*-dimethylaminobenzenesulfonate (36a) is cleanly converted to the *p*-trimethylammonium benzenesulfonate zwitterion (36b) on standing at room temperature, and more rapidly so at higher temperatures, whereas even the most concentrated solutions of this compound remain unchanged at these temperatures. Crystal structure analysis



indicated that each nitrogen atom in the parent crystal is in alignment with a sulfonate ester methyl group only 3.54 Å away, and therefore the system can readily transfer each ester methyl to its neighboring nitrogen atom. Thus, the relative orientation of neighboring molecules in the crystal is directly implicated in lowering the entropy of activation of the reaction by fixing the relative orientation of the reaction sites and facilitating the chain-reaction sequence.

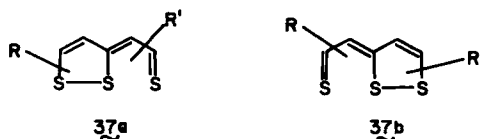
I. Molecular Structures as Markers for Reaction Pathways

The last examples show that crystal forces are, in some cases, sufficient to determine whether the molecule is stable in the crystal or is likely to undergo certain bond-breaking or -forming processes. Note that the crystal forces may alter both the activation parameters of these processes and the free energies of reactant and product. Which of these effects is dominant depends on the crystal and molecular structures and the reaction mechanism (see, for example, ref. 252). Bürgi and Dunitz (82) have considerably extended this approach. The idea is to select some structural fragment or subunit whose geometry varies appreciably during the course of a specific reaction, to determine the structures of as many crystals of different materials containing this subunit as possible, and to try to correlate changes that occur in one structural parameter with changes occurring in other, independent ones. If such a correlation is found, it is possible to arrange the various structures of the subunit in a sequence that can be interpreted as showing the gradual structural deformation that occurs on passage from reactant to product. These authors hypothesize that the observed sequence of structural changes corresponds to the passage of the subunit along a potential-energy valley

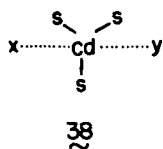
in the relevant parameter space. If this indeed is so, such an analysis provides a unique method for experimentally determining the geometric changes along the whole extent of the reaction coordinate.

Within the context of our chapter, this subject deserves detailed and extensive treatment. However, because of the availability of Dunitz's recent review (82), we limit ourselves to listing the various reactions that have been treated fully in this way, and to describing the principal conclusions.

Structural analyses of the triiodide ion, in crystals of this ion with various counterions, show that the I_3^- unit is always linear, or nearly so, and that there is considerable variety in the $I \cdots I$ distances, which range from 2.67 Å (covalent bond length) to 4.30 Å (nonbonded contact distance). Further, there is strong correlation between the two $I \cdots I$ distances in the $I \cdots I \cdots I$ ion. Very similar correlations were obtained for the $S-S \cdots S$ grouping in the thia-thiophthenes **37**, for the $O-H \cdots O$ groupings in a number of hydrogen-bonded



structures, and for various other linear or near-linear triatomic systems (83). Further, the analytical form of these correlations corresponds closely to that calculated for the $H_2 + H$ system, and to one that can be derived in terms of Pauling's bond-number relationship if one assumes that the sum of the two bond numbers equals unity for all related pairs of distances. This is strongly persuasive evidence that these correlations do indeed represent analogous minimum-energy paths for the reactions in question, namely $I-I + I \rightarrow I + I-I$, $S-S + S \rightarrow S + S-S$, and so on.



Bürgi studied also a series of five coordinated cadmium complexes, **38**, that contain three equatorial sulfur ligands, but in which the fourth and fifth, axial ligands, X and Y, are sometimes iodine, sometimes sulfur, and sometimes oxygen (84). The structural correlations have a clear interpretation in terms of the ligand exchange reaction and are reminiscent of the kind of process that is believed to occur in S_N2 -type nucleophilic substitution reactions:

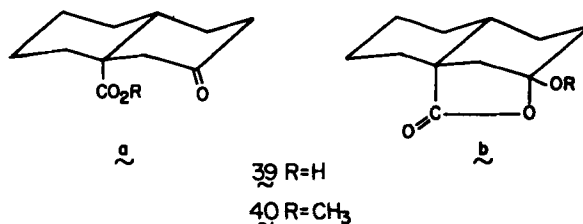


A similar analysis was performed for molecules MX_4 and MX_3Y having tetrahedral symmetry, or which can be regarded as derived from such symmetry as a result of C_{3v} distortions; these have clear implications for S_N1 reactions (85). The curves showing changes in various geometric features of the SO_4 groups in different environments can be regarded as mapping the hypothetical reaction $SO_4^{2-} \rightarrow SO_3 + O^{2-}$. Very similar results were obtained for MSO_3 species (thiosulfates, sulfonates, fluorosulfonates, and amidosulfonates), for PO_4^{3-} and $AlCl_4^-$ tetrahedra, and for MPO_3 and $MSnCl_3$ species. Very interestingly, apart from normalization factors, all the curves appear the same, despite differences in the central atoms (S, P, Al, Sn, etc.) and in the ligand. Unfortunately, the data for deformation of carbon tetrahedra are too sparse to enable us to decide whether these curves describe also the minimum-energy path for S_N1 dissociation of carbon compounds.

Another reaction that has been subjected to this type of analysis is the nucleophilic addition of an amine function to a carbonyl group. Considerable variability in the $N \cdots C(=O)$ distance is found. In an initial study (86), it appeared that in all cases the N, C, and O atoms lie in an approximate local mirror plane (with respect to the groups attached to the carbonyl function, and passing through a carbon atom in all cases), but that the carbonyl carbon is displaced from the plane of its three substituents *toward* the approaching N atom. The observed out-of-plane displacements correlate well with the $N \cdots C$ distance. It seems that as the N approaches the carbonyl C atom, the plane containing this C and its two carbon substituents bends away, and the C–O distance increases. Further, the approach of the nucleophile apparently occurs with its lone pair roughly coincident with the $N \cdots C$ direction, that is, at about 109° to the C–O bond. There is a complication in this treatment of the reaction, in that, with a change in the substituents attached to the N, the geometry about this atom also changes.

An interesting molecule of the type just discussed is 8-dimethylamino-1-naphthoic acid, in whose crystal there are two symmetry-independent molecules in the asymmetric unit. One of these shows distortions in agreement with the above generalizations, whereas there are qualitatively different distortions in the second molecule. The explanation is that the crystal is actually a 1:1 molecular compound of the amino acid, which shows the $N \cdots C=O$ interaction, and the corresponding zwitterion, which does not.

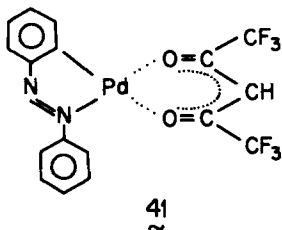
Dunitz, in his review (82), describes also studies on other systems. It should be mentioned that in the $O \cdots C=O$ interaction the correlation is poorer than in $N \cdots C=O$, presumably because the interaction is weaker and more sensitive to perturbation. However, compounds **39** and **40** of this series are worthy of note. The keto acid **39a** and the isomeric lactone alcohol **39b** are in dynamic equilibrium in solution at room temperature, and are present in similar concentrations. This substance has been obtained in only one crystal modification, corresponding to the closed form, **39b**. However, the pattern of bond lengths



and angles indicates that in this molecule there is an appreciable displacement along the reaction path leading from **39b** to **39a**. On the other hand, the interconversion of the two forms of **40** is immeasurably slow in solution, and the species **40a** and **40b** have been crystallized separately. Here the structures on both sides of the transition state for the isomerization process show features that indicate displacement along the corresponding reaction path (87).

J. Chromoisomerism

We have given a variety of examples of polymorphic forms of a given substance having molecules of different conformations, configurations, or constitutions. We can anticipate that in many cases such polymorphs will differ in color, a phenomenon termed "chromoisomerism." This is indeed the case, and is particularly prevalent in donor-acceptor mixtures that form a charge-transfer complex in one of the crystal forms (88). A recent example of another sort is given by Etter and Siedle (89) for the behavior of phenylazophenylpalladium-hexafluoroacetylacetonate (**41**). This compound is obtained from solution in two polymorphic forms, the yellow form from hexane at $<30^{\circ}\text{C}$ and the red form from hot xylene. The red form can be obtained also by heating the yellow form. The two forms are triclinic; the yellow form contains two crystallographically independent molecules in its unit cell, whereas that of the red form has only one molecule per asymmetric unit. The thermal transformation was shown to involve a decrease in the torsion angle of the exocyclic phenyl ring, which decrease provides greater intramolecular overlap between the π -orbitals in this ring and the rest of the diazo molecule and a shift of the long-wavelength band in the optical spectrum.



Another example of a chromoisomeric organometallic compound is described by Simonsen and co-workers (90). The low-temperature modification of bis(*N*-methylphenethylammonium)tetrachlorocuprate, $(\text{C}_6\text{H}_5\text{CH}_2\text{CH}_2\text{NH}_2\text{CH}_3)^+{}_2(\text{CuCl}_4)^{2-}$, is green. At 80°C it is transformed into a yellow crystal form. The two modifications are both monoclinic, but of different space groups. The color difference is presumably caused by changes in the maximum d-d transition of the Cu. While there are differences in cation geometry between the two cases, the spectral shift must be interpreted mainly in terms of the changes in the geometry of the anion. In the green modification the copper atom is situated on a crystallographic center of symmetry with nearly square-planar coordination of the chlorines, with Cl-Cu-Cl angles of nearly 90°. In the yellow form the copper is located on a twofold axis, with the chlorine atoms coordinated to form an irregular, flattened tetrahedron; the Cu-Cl distances are shorter in this form, and the Cl-Cu-Cl angles are appreciably greater than 90°. The anion is hydrogen bonded to the cation in both modifications, with shorter contacts in the green form.

K. Proton Transfers

In general, an hydrogen atom in an hydrogen bond can be considered as having available to it two wells in the potential-energy surface, corresponding to two possible states of the system:



However, in the majority of cases these wells are of very different energies, so that essentially only one of the two states is found. Even in cases where there are measurable concentrations of both tautomers in solution, it may well be that only one occurs in the solid. This is so for the quinone oxime-nitrosophenol system already discussed (34,91), for the monooximes of 1,2- and 1,4-naphthoquinone (91), and for dibenzoylmethane (33) and other 1,3-diketones. Similarly, the furopyridone **42** and the pyranopyridone **43** are in the keto form in the solid, whereas in solution different amounts of enol are also found (92). Compound **44** has recently been shown to exist in the solid only in the 1,4-dihydro form, **a** (93).

An interesting inorganic example is that of nitric acid hydrate. In the liquid



the predominant structure is $(\text{HNO}_3)(\text{H}_2\text{O})$, but, according to both IR (94) and X-ray (95) studies, it is $(\text{NO}_3^-) \cdots (\text{OH}_3^+)$ in the monohydrate crystal.

When the two wells are of similar energies, and the crystal structure allows, the above will no longer be the situation. We may then expect a number of consequences: There may be a measurable displacement of the hydrogen between the two sites induced by such factors as a change in temperature, application of an electric field, and irradiation with light; both tautomers may be present at symmetry-independent sites in the crystal; different tautomers may be present in different crystal modifications; and the presence of molecular substituents that do not directly affect the properties of the hydrogen bond may influence the tautomerism via the crystal structure.

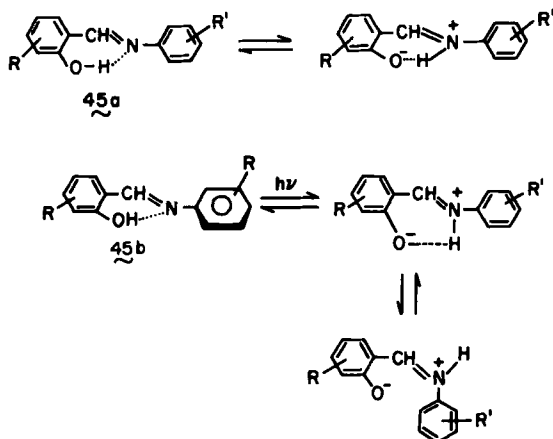
We will give examples of all of these effects. Before doing so we should point out that there is a wealth of literature on this subject, some of which should be accepted only with hesitation. Thus, arguments based only on the color of the crystals are not conclusive (96). The interpretation of IR and Raman data on intramolecular hydrogen bonds is frequently based on very speculative assignments of some of the bands. In early X-ray diffraction studies it was generally not possible to locate the proton, so that arguments about the position of this proton were obtained only indirectly, by consideration of other bond lengths in the molecule. Today one can become much more certain of the situation using combinations of UV and IR spectroscopies, modern X-ray and neutron diffraction techniques, and solid-state NMR. Let us now turn to examples.

In some materials it is known from various physical measurements that it is possible to induce transfer of protons in a homogeneous solid phase. Thus, certain organic solids show electrical conductivity that can be interpreted as being due to intermolecular proton transfer from site to site along a hydrogen-bond chain under the influence of the applied electric field (97). Such proton conduction has been well established for a wide range of inorganic materials, and particularly for ice (98). Further, proton transfers are associated with the appearance of ferroelectric properties in some hydrogen-bonded crystals below certain (the Curie) temperatures. Thus, in potassium dihydrogen phosphate at low temperatures the proton occupies only one of the two possible sites between two oxygens. Above the Curie temperature both sites are equally populated, and the crystal is of higher symmetry (99). Similarly, ice has ferroelectric properties below 100K (100). It is not always clear whether the delocalization of the proton at higher temperatures is a dynamic process or whether there is a static mixture of domains of opposite polarizations.

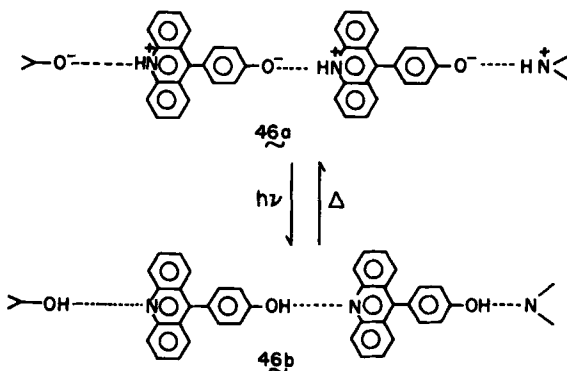
The thermochromic crystalline salicylideneanilines, **45a**, show behavior reminiscent of that described above. (In **45a** and **45b** the Schiff base on the left is as in **15a**.) These materials are light yellow at low temperatures, but become orange-red at elevated temperatures. This change is associated with proton transfer between O and N in the near-planar, close-packed molecules (101). The

process is reversible and apparently involves no disruption of the crystal. The difference in energy between the two species in the crystal is 1.76 kcal/mol for 5-chlorosalicylideneaniline. It has not been established what fraction of the $-OH$ molecules is converted to the $-NH$ form on heating.

Those crystalline salicylideneanilines that are not thermochromic are photochromic; that is, they undergo a reversible color change on exposure to light. In these materials the molecules are markedly nonplanar (**45b**; see discussion on biphenyls in Section II-D) and the crystal structures are very open. It has been suggested that the color change here is due to a two-step process (102):



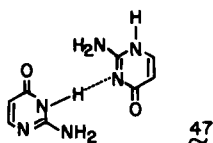
Another photochemically driven proton transfer occurs in the system **46**. This molecule on sublimation at low temperatures crystallizes in form **46a** having infinite chains of intermolecular hydrogen bonds connecting zwitterionic molecules. Its fluorescence at such temperatures is essentially that of the acridinium ion. However, on prolonged UV irradiation, conversion to **46b** occurs and the



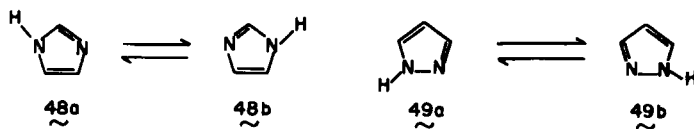
fluorescence gradually changes to that of acridine; this change is reversed only on heating to relatively high temperatures (103).

In none of the above examples of organic crystals is there any evidence on whether or not there is long-range order in the proton-transferred material. It is plausible that the transfers occur initially at random sites in the crystal, which form "defective sites" in the parent structure. Subsequently, the energy required for further transfers may be affected by the initially formed defects, in which case clustering will occur, leading to domains of proton-transferred molecules.

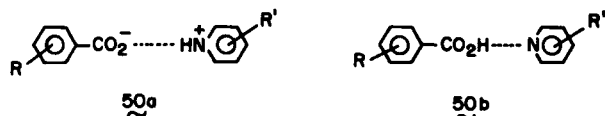
Complete clustering, or segregation, of tautomers may occur during crystal growth. This can lead, for example, to crystals that consist of two tautomers in equal proportions and located at crystallographically independent sites. This is the case for isocytosine, **47** (104). Similarly, in crystalline anthranilic acid the neutral molecule and the zwitterion coexist (105). Another example, **39**, has been mentioned already (82).



In isocytosine and anthranilic acid it seems that any given molecule is always of the same tautomeric form in the crystal; that is, the proton is not moving from site to site in the hydrogen bond. In general, however, the question of whether the proton is localized or not was difficult to answer until the advent of solid-state NMR. Thus, for example, there has been much controversy as regards imidazole, **48**. On the one hand there were the proponents of delocalization; on this basis Zimmerman introduced his controversial theory of "protomerism" (106). Others argued for localization. Recently evidence from high-resolution ¹³C NMR of the solid has provided evidence in support of the latter (107). A similar situation exists for pyrazole, **49** (107).

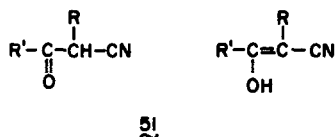


We now turn to substituent-sensitive tautomerism. Johnson and Rumon studied a series of solids derived by cocrystallizing substituted benzoic acids and substituted pyridines (108). Their IR evidence indicated, as expected, that when the benzoic acid is a strong acid and the pyridine a strong base, salts **50a** are formed. For a weak acid and a weak base, hydrogen-bonded pairs of neutral molecules,

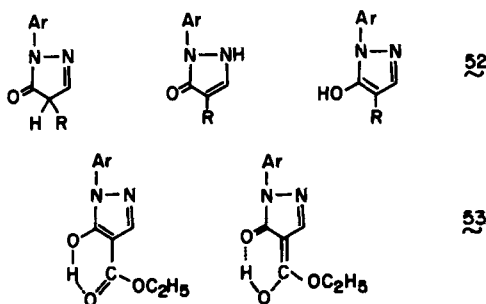


50b, are formed. The determining effect is clearly the relative acid strengths of the two components. A generalization of this aspect, together with structural considerations, has been given by Ubbelohde and Gallagher (109).

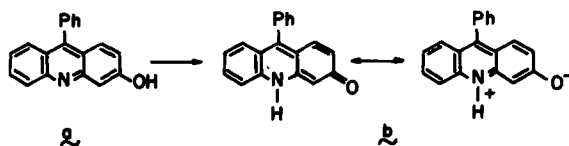
Another example of substituent sensitivity is found in the keto-enol system **51**. According to IR spectra of Nujol mulls, the compounds with R = Ph, R' = H; R = Ph, R' = Me; and R = *p*-ClC₆H₄, R' = Me are in the enol form in the solid. On the other hand, the compounds with R = H, R' = Ph and R = H, R' = *p*-ClC₆H₄ are in the keto form (110).



For the diazine **52** there are three tautomeric forms conceivable. When R = CO₂Et, **53**, the situation is complicated by the possibility of an additional pathway for tautomerism. The IR results for this system are in fact ambiguous, and the investigators mention the possibility of cooperative intermolecular proton transfer being responsible for broad bands in the spectrum (111).



Hadži used IR spectroscopy to study some azophenols and azonaphthols (112). The phenylazophenols were found to be phenolic in the solid state. On the other hand the molecule of 4-phenylazo-1-naphthol is present in the crystal as the hydrazone tautomer. Hadži suggested that in 1-phenylazo-2-naphthol and 2-phenylazo-1-naphthol both tautomers are present. Similar suggestions have been made by others (113,114).

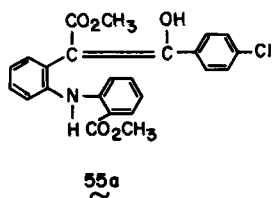


54

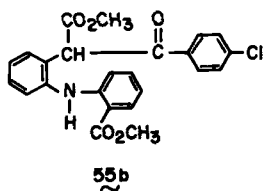
So far we have discussed proton transfers in single-phase systems. We may expect that different tautomers of a given compound will predominate in different crystal forms between which there is extensive reorganization of the hydrogen-bond network. Alternatively, crystals in which one tautomer is partially converted into the other, for example by heat, may become strained and be transformed into a second, more accommodating crystal form.

Campbell and Cairns-Smith (115) found that 3-hydroxy-9-phenylacridine, **54**, as synthesized gave yellow needles melting at 264°C. When these needles are pressed or rubbed they change into a red, amorphous powder. From the colors involved these authors concluded that the transformation involves the change **54a** → **54b**. They suggested that grinding causes local melting with formation of a mixture of tautomers that crystallizes only with difficulty, so that the crystal is converted gradually into a glass. A related system is described by Corbett (116).

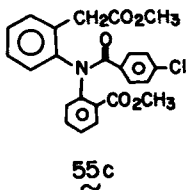
Schulenberg (117) describes the material **55a**, which is obtained from the amide **55c** on reaction with a deficiency of sodium methoxide; the white prisms of the product melt at 110 to 122°C (variable). These crystals give fairly stable solutions, enabling measurement of the NMR spectrum and observation that the material gives a positive FeCl_3 reaction, in accord with the enol structure. After recrystallization a mixture of crystals of **55a** and pale yellow prisms melting at



55a

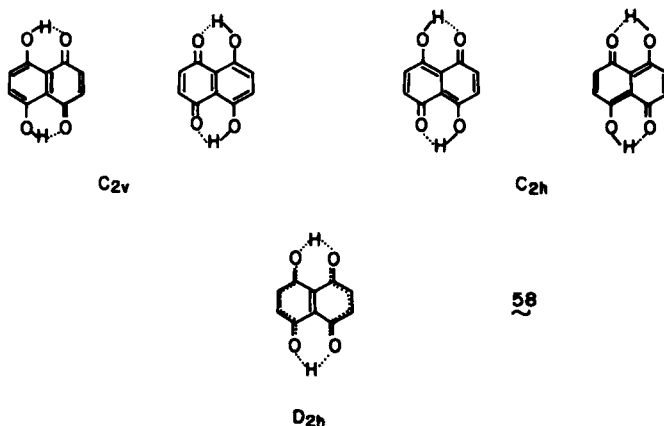


55b



55c

may or may not be close plane-to-plane contacts between the components, associated with charge transfer. The presence or absence of the latter contacts would vary both the acid/base properties of the molecules and the polarizability of the medium in the vicinity of the proton. It is found, for example, that picric acid with 1-bromo-2-naphthylamine gives two crystal forms: One is a yellow hydrogen-bonded salt of constitution $(\text{O}_2\text{N})_3\text{-C}_6\text{H}_2\text{O}^- \cdots \text{H}_3\text{N}^+\text{-C}_{10}\text{H}_6\text{-Br}$, and the other is a red molecular (charge-transfer) complex, $\text{HO}(\text{O}_2\text{N})_3\text{-C}_6\text{H}_2 \cdots \text{C}_{10}\text{H}_6\text{-Br, NH}_2$ (121). The same type of dimorphism is found also among the complexes of polynitrobenzoic acids with aromatic amines (122). Quantitative aspects of the interplay between hydrogen-bonding and charge-transfer interactions have been considered by Dumas and Gomel (123).

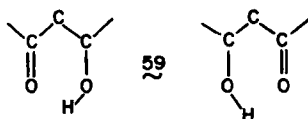


The complexity that may be associated with proton tautomerism in the crystal is illustrated by a recent, elegant, in-depth study of naphthazarin, **58** (124). This substance can in principle exist in a variety of tautomeric forms. Three crystalline modifications, A, B, and C, are known. The investigators find that the C form in fact has different structures at low and high temperatures. At 60K the space group is the noncentric Pc , but at 110K there is an order-disorder transition to a $P2_1/c$ (centric) structure. At low temperatures the hydroxyl hydrogens are ordered, the appropriate molecular formula being 5,8-dihydroxy-1,4-naphthodione (C_{2v}). On the other hand, in the high-temperature form there is disorder, with one-half of a hydrogen atom attached to each oxygen. The point symmetry of the molecule is D_{2h} . This can be interpreted in terms of a rapid exchange of the hydroxylic protons between each pair of oxygen atoms. This interpretation is compatible with the results of solid-state NMR measurements (125). While the localization of hydrogen near one of the oxygen atoms on cooling is primarily an intramolecular process, it is, in fact, conceivable that the order-disorder transformation results from changes in the intermolecular interactions.

In the B form of naphthazarin at 113K all the molecules are also in a C_{2v} configuration. X-Ray diffraction results at room temperature support a model analogous to the high-temperature C form, with crystallographic disorder resulting in a half-hydrogen atom apparently being attached to each oxygen. Solid-state NMR at 143K shows, surprisingly, that rapid, presumably intramolecular proton exchange is occurring in half the molecules (126).

In the A polymorph at room temperature the molecules all lie at crystallographic centers of symmetry, and undoubtedly here too there is hydroxyl hydrogen disorder. The C_{2h} point symmetry, although possible, has not been found in any of the polymorphs.

The authors point out that all 1,3-dicarbonyl compounds exist in the solid as the enol forms, many of which are in the internally hydrogen-bonded syn configuration. All known structures of the latter materials appear to belong to one of two classes: those in which the formal C-O(H) and C=O bonds are significantly different in length, and those in which they are not. The authors term the first group "ordered" and the second "disordered," referring to the possible populations of the two states 59.



III. PHOTOCHEMICAL SOLID-STATE REACTIONS

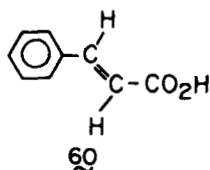
Probably the majority of solid-state reactions that have been studied are photochemical ones, for various good reasons: They are easy to perform; in many cases exposure to sunlight is sufficient. In fact, many such reactions were inadvertently discovered when crystals were observed to bleach or color when lying next to the window. The reactions generally are again two-step ones, the first step being photoreaction in the parent phase (without "thermal loosening") and the second the solid-solid transformation, which can proceed in the dark. This enables isolation of the two steps by appropriate temperature control. Such control is important also from another point of view: The heat added to induce a thermal reaction, together with any heat evolved during the reaction, may well be sufficient to cause local melting or sublimation, and with it loss of stereochemical control. This is readily avoided in photochemical processes.

Since the second of the two steps of the overall process is a phase change, it involves the same features as discussed in the previous section. We therefore concentrate here only on the first step, which is the true "chemical part" of the overall reaction.

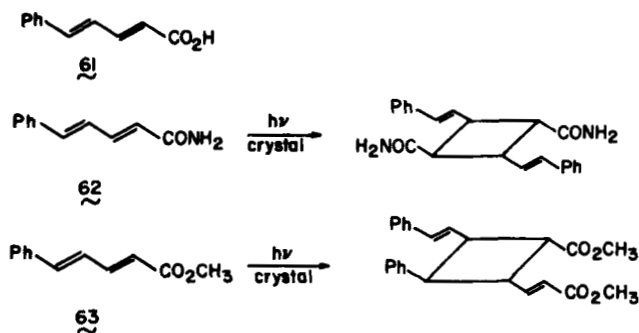
Electronic excitation energy in a crystal is in many cases highly mobile: It may diffuse very rapidly through many thousands of molecules and eventually be trapped at some appropriate "defect" site. If, then, photoreaction occurs at this site, the stereochemistry of the reaction pathway will be determined by the symmetry of this site, and not by the symmetry of the bulk crystal. Nevertheless, the bulk symmetry is found empirically to be the determining factor in most cases studied (topochemical control).

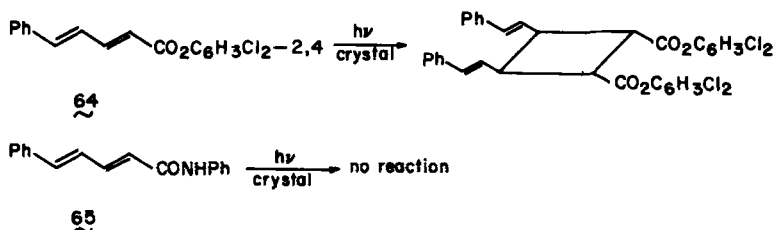
A. Solid-State Photodimerization

This is one of the oldest known solid-state reactions (127) and, in the case of cinnamic acid (60), was the one first used to establish the nature of lattice control of such reactions (128,129). It has been observed in a vast variety of compound types, and has proved to be of great value synthetically.



The (2 + 2) photocyclodimerization of substituted olefins has provided some of the most striking examples of crystal-lattice control of the stereochemistry of a reaction. This may be exemplified by a selection of derivatives of 5-phenylbutadienoic acid (**61**), for which it is observed that the solid-state photobehaviors of the amide **62**, the methyl ester **63**, and the dichlorophenyl ester **64** differ entirely from one another; each affords a single stereo- and regioisomer in high yield, but with different starting materials giving different types of products (130). In solution, irradiation of **63** or other photoactive dienes yields





a complex mixture of many products, including dimers, cis-trans isomers, and cyclization products. The reaction in the crystal typically affords only a single product or none at all, as in the case of the light-stable *N*-phenylamide, **65**.

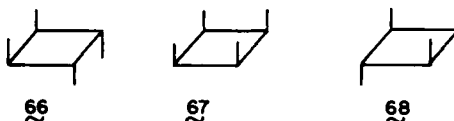
The selectivity that leads to only one (or, rarely, two or three) reaction pathway(s) in the crystal can be rationalized as due to a number of factors: first, the geometric order in the crystal, as a result of which all molecules have identical contacts with their neighbors; second, the structure of the parent crystal, which allows reaction to occur; and third, the reaction's proceeding with minimal atomic movement, so that no high-energy interactions develop between the reacting molecules and their neighbors. (The formation of a more complex mixture of photodimeric products, as obtained from irradiation of **61**, can also be nicely correlated with the monomer packing: **61** crystallizes with two molecules in the asymmetric unit and each of these is apparently oriented for productive photo-reaction with neighboring molecules as well as with the other.)

Most attention has been paid to the second of these factors: In photoactive structures the pair of double bonds that will combine are close (~ 4 Å separation) and nearly parallel, thus having excellent π -electron overlap, which provides strong attractive interaction when one of the molecules is excited (5,128,129). All other double bonds that would lead to stereoisomeric photodimers are too far apart and/or unsuitably oriented to develop such interactions; the corresponding products are therefore not formed. In particular, in light-stable structures, for example that of **65**, no pairs of double bonds having suitable geometry are found (131). Further, comparison of the stereochemistry of the dimer with the structure of a pair of neighboring molecules in the reactant crystal shows that reaction occurs with retention of configuration (the dienes remaining trans-trans on combining) and of local symmetry. Thus, the geometry of the mother crystal determines whether or not reaction occurs and the structure of the photodimer, if any.

An enormous variety of olefinic types have been found to undergo such solid-state (2 + 2) photocyclodimerizations. These include cinnamic acids (128,132); derivatives of cinnamic acids such as esters (133) and amides (134); styrene derivatives (135); stilbenes (136); aliphatic mono- (137), di- (138), and triene (139) dicarboxylic acids and derivatives; 1,4-diarylbutadienes (140) and their vinyls (141), benzylidene acetones (142) and benzylidene acetophenones (143);

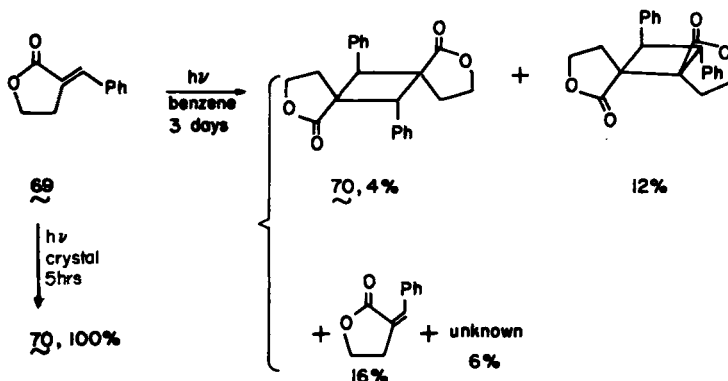
cross-conjugated aromatic (4) and other (144) dienones and their vinylogs (145); benzoquinones (146) and higher quinones (147); pyrones (148); lactones (149); allenes (150); coumarins (151); and others (152).

Most products of solid-state (2 + 2) photodimerization are found to have skeletal configuration **66**, while a few have configuration **67**. This distribution clearly reflects the tendency of the monomers to crystallize in the particular corresponding structures. Reports (153) of solid-state photodimerizations that yield configuration **68** suggest that the range of product stereochemistries available via photodimerization is indeed large.



Some examples from the large number of known solid-state photodimerizations may be used to illustrate the extraordinary selectivity that is routinely observed.

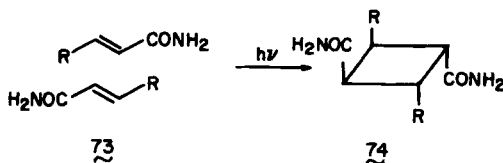
1. Ultraviolet irradiation of the fungicide and plant growth regulator **69** in solution yields four products, with overall conversion of 37% in 3 days. The photodimer **70**, which is the product obtained in lowest yield in solution, is obtained as the sole product (quantitative yield) after only 5 hrs of irradiation of the solid (149).



2. The majority of photodimerization reactions that have been studied in the solid afford products in which chemically equivalent double bonds have combined, as, for example, in **62** and **64** above. This does not have

yet sufficiently understood to allow selection between alternative possible arrangements. If, as one expects, there will be considerable progress in this direction in the future, it will then be possible to decide how to substitute the potential reactant molecule so that it crystallizes in the structure required to yield the product of desired stereochemistry. Today, such "crystal engineering" is possible, to a limited extent, on the basis of a number of empirical packing generalizations that have been uncovered over the years. We discuss some of these in relation to the (2 + 2) photocyclodimerization reaction.

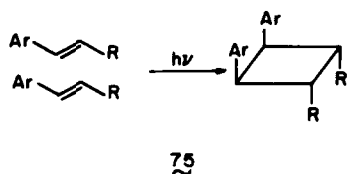
The first of these generalizations treats primary amides. Analysis of the hydrogen-bonding requirements of such amides, in general, and the possible molecular arrangements that can result in the crystal led to rationalization of the empirical observations (155). In the present context, the conclusion is that α,β -unsaturated primary amides will tend to pack closely in the arrangement **73**, so that exposure to light will lead to formation of the centrosymmetric cyclobutanes **74** (α -truxillic acid derivatives for $R = \text{aryl}$). Formation of products of this stereochemistry is indeed found for $R = \text{Ph}$, $4\text{-Cl-C}_6\text{H}_4$, $4\text{-CH}_3\text{-C}_6\text{H}_4$, $4\text{-CH}_3\text{O-C}_6\text{H}_4$, $2\text{-C}_4\text{H}_5\text{S}$ (2-thienyl), Ph-CH=CH- , $\text{NH}_2\text{CO-}$, and $\text{NH}_2\text{CO-CH=CH-C}_6\text{H}_4\text{-}p$, among others.



A second generalization treats dichloro-substituted molecules, and has been referred to briefly above. A large variety of chemically disparate molecules containing two chlorine substituents have been found to crystallize in structures in which the shortest axis of the unit cell is approximately 4 Å long (48,156). Such a short axis is diagnostic of a stacklike molecular arrangement, with all the molecules in the stack lying parallel and well overlapped. Olefinic molecules, such as **75**, that contain a dichlorophenyl group, do indeed pack in this way; they yield on irradiation in the solid the corresponding mirror-symmetric cyclobutane (β -truxinic acid) derivatives. In essentially all the examples, the crystals of the analogous molecules having hydrogen instead of chloro groups are light stable or yield products of different stereochemistry.

Thus, to achieve mirror-symmetric or centrosymmetric cyclobutane derivatives, one would start with monomers that are substituted with dichloro groups or amide functions, respectively. Both the chlorines and the amide groups can subsequently be removed readily, without affecting the stereochemistry of the ring.

A number of other approaches have been employed in attempts to engineer

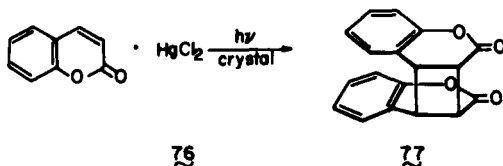


Ar = 3,4-, 2,4- or 2,6- C₆H₃Cl₂

R = CO₂H, CO₂Me, Ph, CO₂Ph, C₆H₅S (2-thienyl)

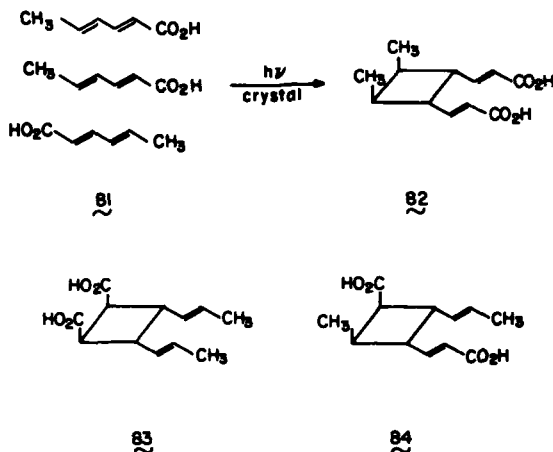
Ph-CH=CH-, (2-C₄H₅S)-CH=CH-, NO₂, CN

structures. Thus, complexation with mercuric chloride has been suggested as a technique for achieving 4 Å structures (5). For example, irradiation of the crystalline complex **76** is the most direct route to the cis,syn photodimer of coumarin, **77** (157).



A recent interesting attempt to engineer cinnamic acids for (2 + 2) photocyclodimerization involves using charge-transfer interactions to bring (different) potential reactants into face-to-face close packing. Crystals of the 1:1 complex 3,4-dimethoxycinnamic acid–2,4-dinitrocinnamic acid were grown and their structure was determined. These components form hydrogen-bonded pairs that lie parallel to one another across a center of symmetry, so that potentially reactive, differently substituted double bonds are close (3.8 Å) and strongly overlapped. However, no photodimer was obtained, possibly because of quenching of the excited state as a result of intermolecular abstraction of hydrogen from a 4-methoxy group by a 4-nitro group. It is noteworthy that the two components, individually and in their own crystals, do yield the topochemical dimers (158).

The formation of a uranyl complex (159), the introduction of a hydrophobic octadecyl group (153) or of specific hydrogen-bonding functions (160), the use of nonbonded interactions involving oxygen (as in 3,4-methylenedioxycinnamic acid) (161), and other approaches (162) have been suggested for directing the molecular packing in crystals. However, too few examples are available to allow evaluation of their generality and utility.

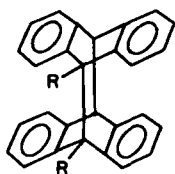
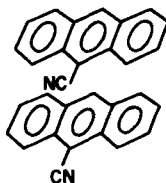


D. Photodimerization at Defects

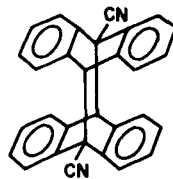
We have mentioned above that if reaction occurs at defects in the structure this may lead to nontopochemical products. Such an effect may be important under certain circumstances; thus, the monomer molecule and its arrangement in the crystal must be such that the excitation energy will be transferred from the ordered crystal to defects at a high rate. *Inter alia* this requires that the long-wavelength absorption band of the monomer be an intense one, so that this effect could be significant in the anthracenes, for example. Further, the defect population of most crystals is extremely small; thus, for a finite amount of the "defect dimer" to be formed, additional defects must be created, for example as a result of strain-induced slip, as the reaction proceeds.

We turn first to the (4 + 4) photodimerization of anthracenes, which has been most extensively studied in this context. In many anthracenes it has been possible to show that in the starting crystals defects are present at which the structure is appropriate for formation of the observed dimer; in others it has been argued that the presence of such defects is very plausible. The weakness of this interpretation, at this stage, is that in no case has it yet proved possible to establish that the reaction indeed occurs at these defect sites.

To give the reader a feel for these effects we refer to two examples. Anthracene itself crystallizes in a structure in which the extent of overlap between molecules in plane-to-plane close packing is negligibly small. We would therefore expect there to be no driving force for the reaction, and the crystal to be light stable. In fact, it undergoes photodimerization to yield **85a**, albeit with low quantum

85: a. $R=H$, b. $R=CN$ 

86

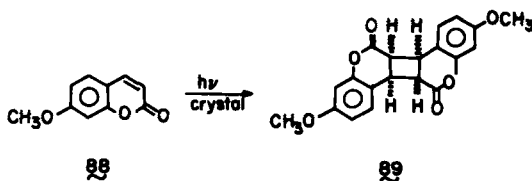


87

yield (164). By contrast, 9-cyanoanthracene, **86**, packs in the crystal in a 4 Å-type structure, so that adjacent molecules are highly overlapped. It undergoes ready photodimerization, but yields the centrosymmetric dimer **87**, rather than the topochemical one **85b** (165).

It should be noted that there are special features of the 9-substituted anthracenes that may introduce complications. The materials dimerize also in solution, yielding exclusively the centrosymmetric dimers, which are analogous to **87**. Further, the few 9,9'-disubstituted dianthracenes that have been prepared are very unstable. Thus the head-to-head approach of two monomers is apparently an energetically unfavorable process. This is not so for the head-to-tail approach, and it is therefore not surprising that structures in which there are overlapped monomers related by centers of symmetry yield topochemical dimers.

Studies of (2 + 2) photocyclodimerizations have suggested that reaction occurs at the site of absorption of light, that is, in the bulk crystal, with reaction there apparently being faster than transfer of the excitation energy to defects (166). It is therefore surprising that crystals of 7-methoxycoumarin, **88**, are reported to dimerize efficiently, since crystal-structure analysis shows no double-bond overlap appropriate for reaction (151). The involvement of a specific defect has been suggested here, too. It is interesting that even in this case the dimerization is highly stereospecific, with only one (**89**) of the four possible photodimers being formed (90% yield). It should be noted that other coumarin derivatives yield the topochemical dimers. An example is 5-chlorocoumarin, which gives the expected mirror-symmetric product analogous to **77** (151).



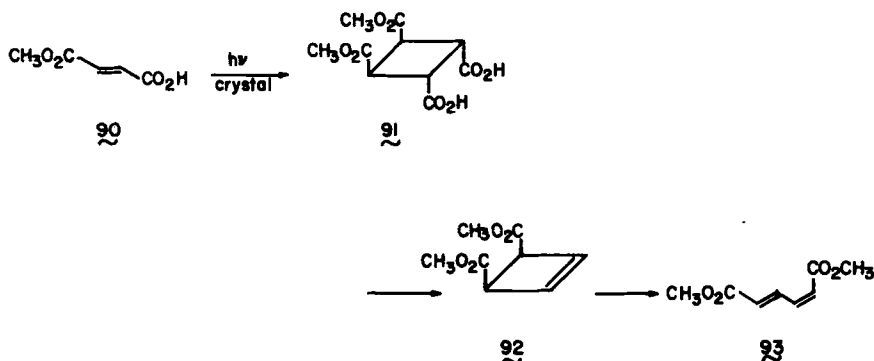
88

89

E. Utilization of Solid-State Photodimers

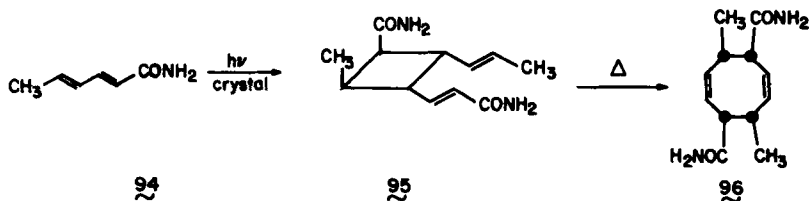
To the organic chemist, the most striking feature of solid-state reactions is the stereochemical purity of the product obtained in most cases. This feature allows conversion by conventional methods of the solid-state product to other materials of desired stereochemistries. We illustrate this by some examples of reactions starting from the cyclobutanes obtained by solid-state (2 + 2) photodimerization.

One such example is a sequence of solution reactions starting from the dimer **91**, which has a *cis*-1,2-dicarboxylic acid arrangement and is obtained by irradiation of monomethyl fumarate, **90**, in the crystal (137). This isomerically pure dimer may be oxidatively decarboxylated, by a variety of methods, to the thermally unstable *cis*-disubstituted cyclobutene **92**, whose smooth disrotatory ring-opening leads to the isomerically pure dimethyl *cis,trans*-muconate, **93** (167).



A large number of substituted acrylic acids, $\text{R}-\text{CH}=\text{CHCO}_2\text{H}$, are known to yield in the solid the *cis*-1,2-dicarboxylic acids of type **91**. This is true, for example, when R = phenyl, substituted phenyl, naphthyl, or styryl. Thus a ring-opening reaction analogous to the above may provide an avenue to isomerically pure *cis,trans*-dienes, *trans,cis,trans*-trienes, and so on.

Another available stereoselective synthetic pathway, starting from *cis*-1,2-divinylcyclobutanes produced in the solid state, is that of ring expansion to 1,5-

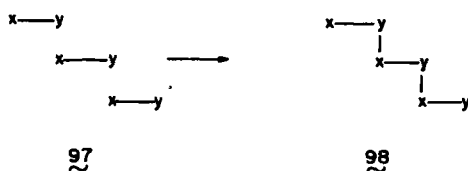


cyclooctadienes via the Cope rearrangement. For example, sorbamide, **94**, affords the pure dimer **95** in the crystal. This, in turn, may be used in the ring-expansion reaction to yield isomerically pure **96** (130). (The dimers **82** and **84**, from sorbic acid, also afford cyclooctadienes; compound **83** does not undergo the Cope rearrangement.)

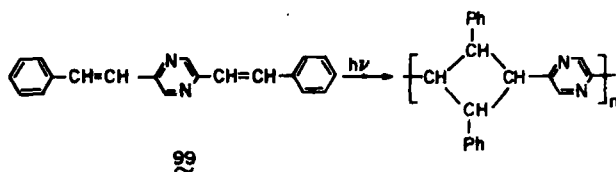
F. Photooligomerization and Photopolymerization

An obvious extension of the studies on photodimerization of crystalline olefins is to solid-state vinyl polymerization (with light, if absorbed, or γ -irradiation), with the aim of achieving stereoregular polymers. In fact, an immense effort has been made in this direction, but with singular lack of success. The explanation is that, for various reasons, the lattice in the vicinity of the chain front becomes progressively more damaged as polymerization proceeds, so that after relatively few steps there is loss of stereochemical control.

Hirshfeld and Schmidt (168) proposed that this problem might not arise in the polymerization of long bifunctional monomers in crystals of suitable structure, as in **97** \rightarrow **98**. They predicted that reaction in such systems would occur via a tilt of each molecule about its center of mass, so that little or no net displacement of the molecules would be involved. In fact, two successful realizations of this approach were subsequently reported, for the diacetylenes, which will be discussed in a later section, and for distyrylpyrazines and related compounds. Here we discuss the latter series.



Hasegawa and co-workers (169) found that one of the two known crystal forms of 2,5-*trans,trans*-distyrylpyrazine (DSP, **99**), undergoes reaction on UV irradiation, yielding a high-molecular-weight, high-melting-point, and highly crystalline polymer. The reaction was described as follows:

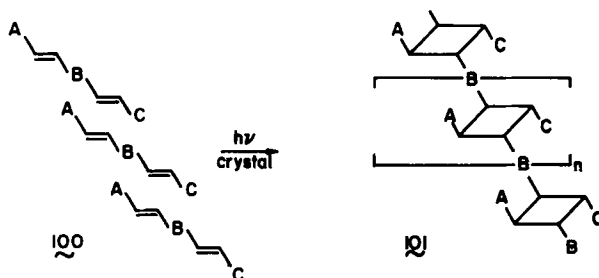


This and related systems have been extensively studied (170).

In the present context the main interest attaches to the stereochemistry of the polymer. From the known crystal structures of various reactive monomers, we would expect the product to be linear and the cyclobutanes all to be centrosymmetric, that is, with chemically identical substituents *trans* at the 1 and 3 positions. The linearity has been established, as has the centrosymmetry of the cyclobutanes in low oligomers. The symmetry of the cyclobutanes in the polymer, however, is less well determined. Nakanishi and colleagues reported (170) that the space group of crystals of the polymer of DSP (**99**) is the same as that of the monomer crystal (*Pbca*). Thus the centers of symmetry relating overlapped double bonds in the monomer transform to centers in the cyclobutanes of the product polymer chain, in keeping with the above stereochemical expectation. Support for this was provided by Jones (171). On the other hand, Wegner and co-workers report (172,173) that the space group of the polymer is in fact *Pca*2₁, which is not centric, and does not require the cyclobutanes to be centrosymmetric. This discrepancy has not been satisfactorily resolved.

This is not a trivial problem, and has important implications for the mechanism of the reaction. However, the bulk of the evidence is for centrosymmetric rings, which would be in keeping with our experience in small-molecule systems. For the present purposes we assume this to be the case. On this basis DSP is one of a class of monomers of crystal structural type **100** that polymerize to polymers **101**. Note that, as is typical of topochemical reactions, there are cases of polymorphism of the monomers, in which only those of structure **100** are reactive. Also small changes in the substitution of this molecule frequently result in changes in crystal structure and reactivity.

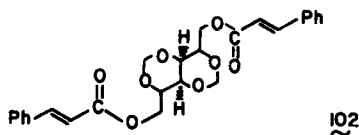
A wide variety of groups B separating the reactive sites have been employed. Apart from the aromatic ring shown for **100**, a polymethylene chain and a bulky sugar alcohol derivative as in **102** have been used (174).



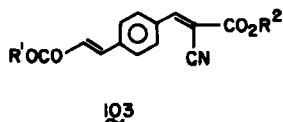
A = C = CO₂H, CO₂ Et, CO₂ Ph, CONH₂ B = *p*-Phenylene

A = C = Ph B =

A = C = 2-Pyridyl B = *p*-Phenylene



A most interesting extension of this type of reaction was performed by Addadi and Lahav (175). Their aim was to obtain chiral polymers by performing the reaction in a crystal of chiral structure. They employed monomers **103**. The initial experiments were with a chiral resolved **103** where R^1 is (*R*)- or (*S*)-*sec*-butyl and R^2 is C_2H_5 . This material indeed crystallizes in the required structure, and yields photodimers and polymers with the expected stereochemistry, and with quantitative diastereomeric yield. It was possible to establish that the asymmetric induction was due essentially only to the chirality of the crystal structure and not to direct influences of the *sec*-butyl. Subsequently they were able, using sophisticated crystal engineering, to obtain chiral crystals from nonchiral **103**, and from them dimers and polymers with high, probably quantitative enantiomeric yields. This may be described as an "absolute" asymmetric polymerization.



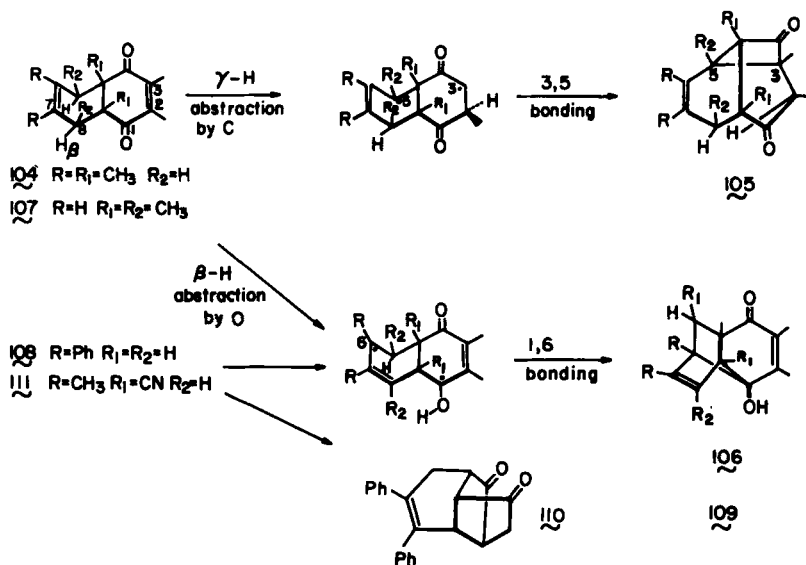
G. Applications of (2 + 2) Photodimerizations in Noncrystalline Phases

Photodimerization of cinnamic acids and its derivatives generally proceeds with high efficiency in the crystal (176), but very inefficiently in fluid phases (177). This low efficiency in the latter phases is apparently due to the rapid deactivation of excited monomers in such phases. However, in systems in which pairs of molecules are constrained so that potentially reactive double bonds are close to one another, the reaction may proceed in reasonable yield even in fluid and disordered states. The major practical application has been for production of photoresists, that is, insoluble photoformed polymers used for image-transfer systems (printed circuits, lithography, etc.) (178). Another application, of more interest here, is the use that has been made of mono- and dicinnamates for asymmetric synthesis (179), in studies of molecular association (180), and in the mapping of the geometry of complex molecules in fluid phases (181). In all of these it is tacitly assumed that there is quasi-topochemical control; in other words, that the stereochemistry of the cyclobutane dimer is related to the pre-reaction geometry of the monomers in the same way as for the solid-state processes.

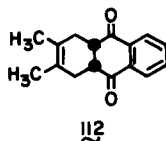
H. Solid-State Photorearrangements

Our knowledge of the influence of conformation on the course of unimolecular photoprocesses has been greatly enriched by the work of Scheffer, Trotter, and co-workers (182). Their initial studies were on a series of adducts obtained by Diels–Alder reactions between 1,3-dienes and *p*-quinones. Consider **104**, which in the crystal has a conformation with the cyclohexene ring in half-chair form and cis-fused to a nearly planar enedione ring. Similar conformations were found in all compounds of the series that were studied. Compound **104** rearranges photochemically to yield the cyclobutanone **105** and the enone alcohol **106**, in the same ratio, 2:1, in solution and in the solid. The proposed mechanisms shown explain the successes in the solid as apparently being due to two factors: The molecular geometry of the parent is favorable for the intramolecular hydrogen abstraction, and the intermediate species formed by the abstraction are ideally arranged to undergo biradical collapse to the products. In particular, we may see that the external shapes of the products are similar to that of the reactant. Results parallel to the above were obtained for reactant molecule **107**, which has $R_1 = R_2 = \text{CH}_3$ and $R = \text{H}$.

A different type of behavior is shown by the reactant **108**. Irradiation of this material in solution gives two products, **109** and **110**, in relative yields of 3:1. The first of these is an enone alcohol, analogous to **106**, and is the sole product of solid-state reaction. The minor product in solution, **110**, is a diketone, of considerably different shape from the reactant. It is believed that in solution the



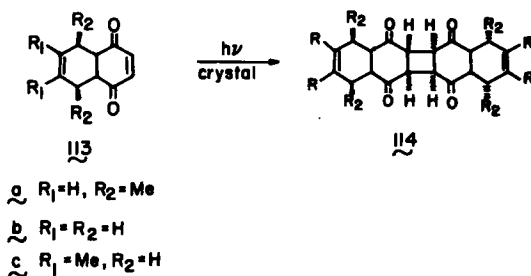
1,6-diradical intermediate, which is the immediate precursor of **109**, can flip into a conformationally very different 3,8-diradical, which leads to **110**. This flipping process cannot occur in the solid. Analogous behaviors are shown by **111**, which has $R = CH_3$, $R_1 = CN$, and $R_2 = H$, and by **112**.



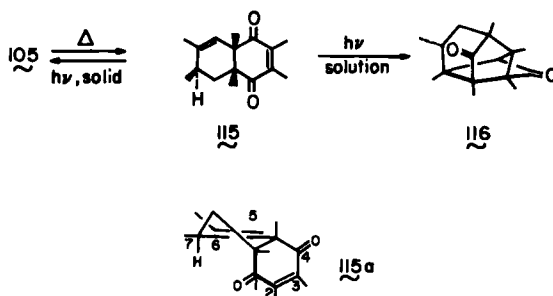
In light of the above conclusions it is argued (182) that the presence of the bridgehead methyls in **104** retards the solution-phase ring-flipping of the radical intermediates, and is thus responsible for the identity of the products from the solid-state and solution processes.

The course of the photoabstraction depends not only on the reactant geometry but also on the particular electronic state of the abstracting moiety. The abstraction by oxygen appears in systems in which $n\pi^*$ states are probably involved. Here one expects that the $n\pi^*$ -derived half-filled oxygen n -orbital must overlap with the to-be-abstracted H atom. In fact, in materials giving enone alcohols, the β -hydrogens all lie suitably placed, almost in the plane of the abstracting carbonyl system. A similar argument relates, in the case of materials that probably have low $\pi\pi^*$ states and that yield cyclobutanones, the C-2 $2p$ atomic orbital and the γ -hydrogens. It is noteworthy that the reactions are effective even when the distances between the abstracting and to-be-abstracted atoms are as large as the sum of the van der Waals radii of these two atoms.

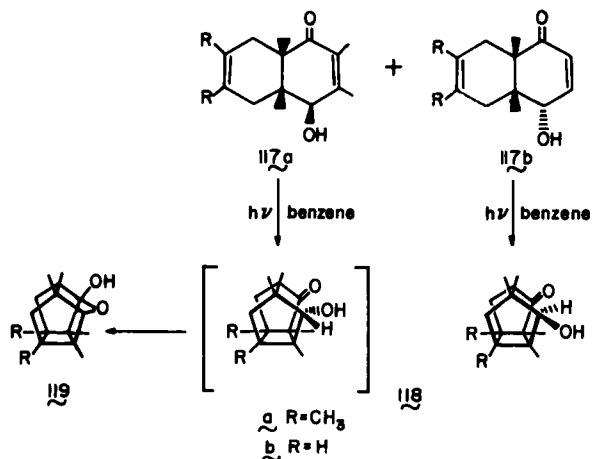
In crystal structures in which there is appreciable intermolecular overlap of the C-2=C-3 double bonds, irradiation of the solid leads only to (2 + 2) cycloaddition. This is true of reactants **113**, which yield in all cases the centrosymmetric dimers **114**, even when the reactant conformation is suited also to intramolecular hydrogen abstraction.



The cyclobutanone **105**, on thermolysis at 190°C, undergoes a retro-ene reaction yielding the crystalline β,γ -unsaturated ketone **115**. This product in the solid regenerates **105** photochemically, in almost quantitative yield, whereas in solution the diketone **116** is the exclusive photoproduct. The ketone **115** is found in the solid to have the conformation **115a**, a conformation that results, presumably, from the requirement for the bulky methyl at C-7 to adopt the pseudo-equatorial rather than the pseudoaxial position. This molecule in fact has a shape

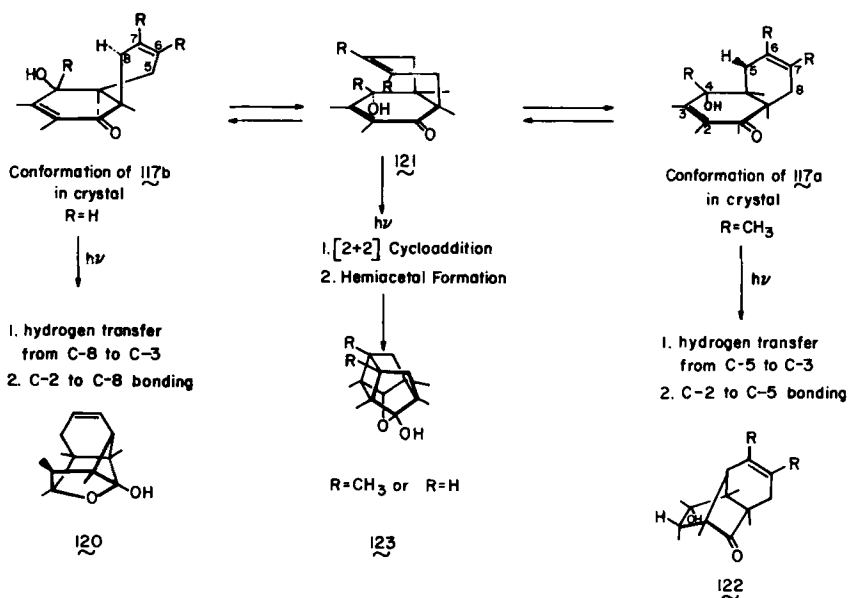


very similar to that of **105**. It is thus reasonable that the **115**-to-**105** conversion occurs in the solid, presumably via initial formation of a bond between C-3 and C-5, followed by intramolecular transfer of the pseudoaxial hydrogen at C-7 to C-2. The dominant conformation of the reactant in solution is probably again **115a**. However, in this phase the reaction is presumed to be initiated by an oxadi- π -methane rearrangement in the $^3(\pi\pi^*)$ state. The subsequent steps that lead to **116** are not clearly defined, but must involve substantial atomic movement and molecular distortion, and would be inhibited in the solid.



The tetrahydroquinones referred to above are readily reduced to tetrahydro-1-naphthoquin-4-ol derivatives, the photochemistry of which is also of interest. In solution these materials, **117**, undergo intramolecular (2 + 2) photocycloaddition to give products, **118**, having the tetracyclo[5.3.0.0^{2,6}.0^{4,2}]decane ring skeleton. If their configuration permits, these products immediately convert into hemiacetals, **119**.

In the solid these materials yield no cage product. Their behaviors depend on the stereochemistry of the hydroxyl-bearing carbon. Representative examples are **117b** (with an α -OH) and **117a** (with a β -OH). Both are found, in the crystal, to have conformations consisting of a half-chair cyclohexene ring cis-fused to a half-chair-like cyclohexenone moiety. In both, the hydroxyl seeks the lower-energy pseudoequatorial position: Since these two compounds have opposite configurations at the C(hydroxyl), their conformations are ring-flipped counterparts. The **a** form gives rise to **122**; the **b** form, to **120** via the keto alcohol. It is suggested that the solution process yielding **123** proceeds via the endo conformation **121**.



In this and the other solid-state processes described in this section, we see that the factors determining the products are as follows:

1. If there are suitable inter- or intramolecular double-bond contacts, (2 + 2) photocycloaddition is the favored process.

2. In the absence of such contacts, intramolecular hydrogen abstraction may occur, the geometric requirements for which are probably determined by the excited electronic state involved.
3. If these requirements are satisfied by the molecular conformation, abstraction will occur.
4. All subsequent processes leading to the product must involve minimal change in the external molecular shape.

IV. HOMOGENEOUS SOLID-STATE REACTIONS

As described above, most solid-state reactions are heterogeneous, in the sense that reactant and product are in different solid phases. In many of these, product crystals first appear as nuclei that grow at the expense of the parent crystal. On the other hand, there are some solid-state reactions that are not accompanied by a phase change and for which, therefore, analogy with a solid-state transformation is not plausible. Such reactions are of particular interest in several respects: They make possible conversion of a single crystal of reactant to a single crystal of product; they enable study, for example by X-ray diffraction, of the structures of the parent and product molecules as functions of the degree of conversion in more or less constant environments; and one can elucidate from them the constraints that the parent crystal imposes both on the reaction pathway and on the conformation of the product. It is in connection with the latter that this subject is of particular interest in the present context. This class of processes has been discussed by Thomas (183).

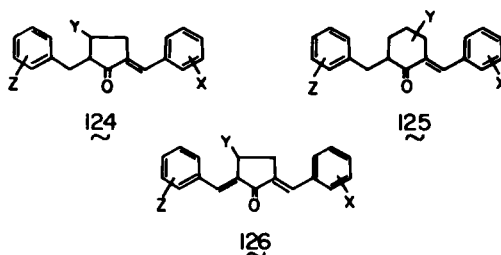
Systems that react in this manner fall into two classes. In the first of these the framework that dominates the crystal structure scarcely participates in the reaction. This is the case, for example, in the reaction of an organic molecule intercalated in graphite or a clay, or of a guest molecule held in a clathrate of urea or thiourea. Some cases of this sort will be treated in the next section.

In the second class of systems the reaction is such that it involves little or no change of the molecular geometry in the vicinity of the reacting sites, nor of the external shape of the crystal. The concept of the "reaction cavity" is useful in this context (184). This cavity is the space in the crystal containing the reactive molecule(s), and its surface defines the area of contact between this molecule and its immediate surroundings. Only if the shape of this cavity is little altered as reaction proceeds will the activation energy for the process be reasonably small and the rate of reaction nonzero.

It must be admitted, however, that while this concept explains many aspects of structural control of reactions in the solid state, we do not yet seem to have real understanding of the factors determining whether a given system will react

by a heterogeneous or homogeneous mechanism, that is, whether or not the reaction will be accompanied by a solid-solid phase transformation. With this limitation in mind we turn to some examples.

We have already described some proton-transfer processes that occur without disruption of the crystal structure. We now treat two other homogeneous reactions. The first of these is the (2 + 2) photocyclodimerization of a number of benzylidene ketones (185,186). These monomers are based on one of the three frameworks **124** to **126**. The three parent molecules and a number of their



derivatives were subjected to X-ray structure analyses and their photochemical behaviors were investigated. Roughly half the compounds were found to dimerize in the crystal on exposure to UV light. The reactions are subject to topochemical control. Thus, for example, the parent molecules **124** (with $X = Y = Z = H$)

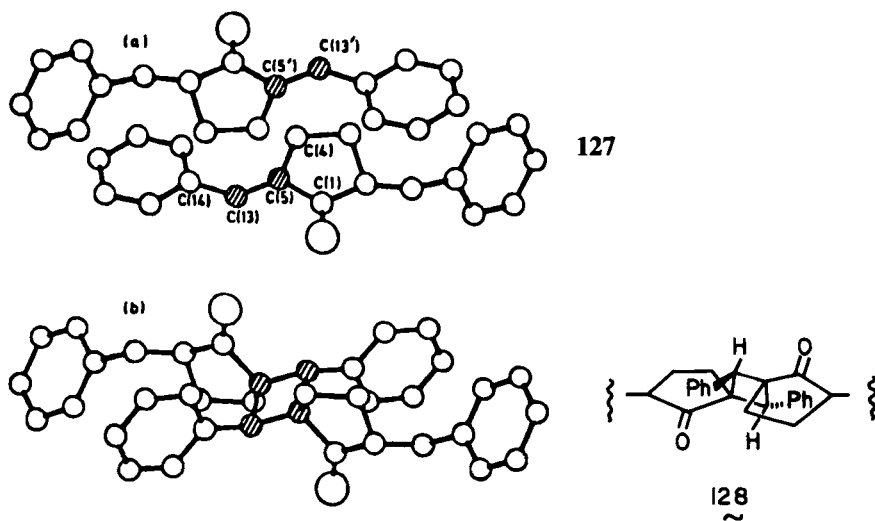


Figure 1. (a) The projection on (001) of the **127** monomer structures, showing two molecules across a center of symmetry. (b) The projection on (001) of the **128** dimer structure. (Reproduced by permission from ref. 186.)

pack with the exocyclic double bonds of neighboring molecules closely packed and strongly overlapped across a crystallographic center of inversion, as in **127**. The molecules combine photochemically to give the centric cyclobutane derivative **128** (Figure 1).

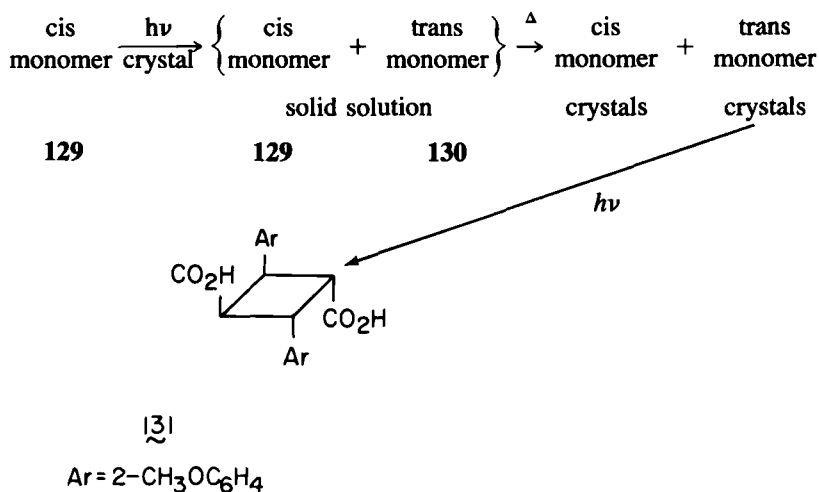
The most interesting aspect of the materials of these systems is their tendency to react in a homogeneous manner. Thus, for example, in the above reaction a single crystal of **127** transforms into a single crystal of **128**. During this process the positions of the X-ray reflections remain unchanged, but there are changes, which are monotonic with the extent of reaction, in the intensity distribution.

This behavior is quite different from that of the cinnamic acids, for example (187). In the latter compounds the intensities of all the X-ray reflections decrease as reaction proceeds, presumably as a result of loss of long-range order. Subsequently there is a stage of nucleation and growth of product crystallites, and with it the appearance of new X-ray reflections.

As shown by comparison of **128** and **127**, the dimer fits very neatly into the cavity in the parent structure; that is, the envelope surrounding two monomers in the parent crystal is hardly changed in shape when these monomers combine to form the dimer. It is not obvious that the fit here is better than in other photodimerizing systems. If it is better, this could be due to a number of factors: First, the reactive double bonds in this series are near the middle of bulky molecules, so that the external shape of a pair of monomers need not be sensitive to dimerization. Further, reaction may proceed with torsional relaxation about the exocyclic single bonds, thus preventing strong intermolecular repulsive interactions. Finally, it is noteworthy that the structure of the dimer **128** obtained from **127** crystal remains almost unchanged on subsequent recrystallization from solution, so that there is no driving force for a solid-solid phase transformation.

Perhaps even more interesting is the behavior of 2-benzyl-5-*p*-bromobenzylidenecyclopentanone (**124**, with X = 4-Br, Y = Z = H). Although, on reaction, the space group of this crystal remains unaltered, there are appreciable changes in the cell dimensions. Thus, *a* changes by -3.77%, *b* by -5.61%, and *c* by 6.52%. The reaction normally involves fracture of the crystal, but can be induced to proceed homogeneously by careful control of such reaction conditions as temperature and rate of conversion.

The sensitivity to temperature is reminiscent of that seen in Ron's study (188) of *o*-methoxy-*cis*-cinnamic acid, **129**. When crystals of this substance are exposed to light at low temperatures (< -80°C), there occurs a gradual isomerization of the molecules to the *trans* form, **130**, with formation of a little of the (2 + 2) photodimer, **131**, of the latter. If this irradiated material is warmed in the dark to +60°C, recooled, and reirradiated for a short while, there is a jump in the amount of dimer. This behavior is interpreted as follows:



In other words, the resolution of the solid solution into separate solid phases of cis and trans molecules is a thermally activated process. It is just this process that is responsible for the distinction between homogeneous and heterogeneous reactions.

These results imply that the type of behavior exhibited by a given system is not necessarily an intrinsic property of the system. It may, in fact, be possible in many cases to switch between two types of behavior by control of the reaction conditions, as it is for **124** and **129**. In the context of this review the interesting aspect is that in such cases one would be able to determine whether the conformation of the product is determined by structural mimicry in the parent phase or by the intermolecular interactions in the crystal of the product.

The second reaction we will treat here that in many cases proceeds by a homogeneous mechanism is the solid-state polymerization of diacetylenes. The photolability of these compounds has long been known (189), but it was not until the appearance of the pioneering works of Hirshfeld and Schmidt (168) and of Wegner (190) that some real understanding of the process was introduced. This led to an explosive interest in the subject, and more than 200 diacetylene derivatives have now been studied, by a wide variety of techniques (191).

Many diacetylenes in the crystal, on exposure to light or high-energy radiation, or on annealing at high temperature below the melting point, undergo polymerization via 1,4-addition. That the reaction is controlled by the structure of the reactant crystal (topochemical control) is shown by its sensitivity to substituents remote from the reaction site, by the marked differences in reactivity between different crystal modifications of a given compound, and by the fact that reaction

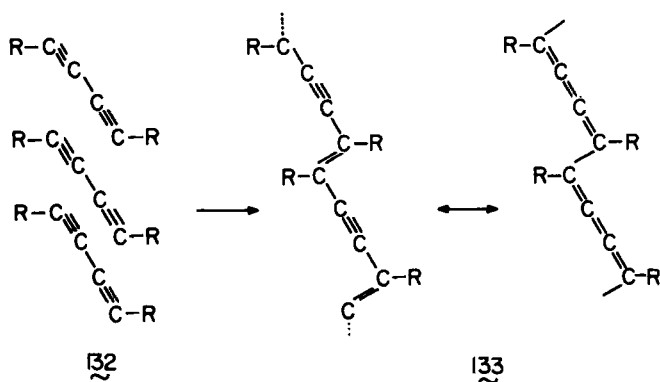
does not occur in the melt and in solution, or even in liquid crystalline solvents. On the other hand the reaction *is* found to occur in mono- and multilayers (192).

As examples, molecules of the form $R-C\equiv C-C\equiv C-R'$ are polymerizable in the crystal when the substituents are as follows: $R = R' = (CH_2)_nCH_3$; $R = R' = (CH_2)_nOH$; $R = R' = (CH_2)_nCO_2H$ and salts of these acids; $R = R' = (CH_2)_nOSO_2-C_6H_4-CH_3$ -*p*; $R = R' = C_6H_4-NHAc$ (*o* and *m*, but not *p*); $R = CH_2OH$, $R' = C\equiv C-CH_2OH$; $R = CH_2OCONHPh$, $R' = C\equiv C-CH_2OCONHPh$; and $R = (CH_2)_nOH$, $R' = (CH_2)_mCH_3$.

In many cases it is possible to convert a single crystal of monomer completely to a single crystal of polymer in a homogeneous process, the perfection of the product crystal being comparable to that of the parent. The synthesis in this way of polymer crystals over 15 cm long and 10 g in weight has been described (193).

The most reliable information on the structure of the polymer has been derived from X-ray diffraction and Raman-spectroscopic studies. In a few cases it has been possible to determine in detail the structures of both the monomer and the corresponding polymer. From such measurements and other optical studies the process is considered to be **132** \rightarrow **133** for a symmetric diacetylene. In polymerizable structures the diacetylene rods are inclined at about 45° to the translation (stack) axis, with the ends of each diacetylene moiety approaching the adjacent triple-bond systems to a distance of ≤ 4 Å. The polymer is a planar system in extended conformation and having alternate R groups trans to one another.

Wegner, in his first publication (190), favored the butatriene-type structure for the backbone. In fact, subsequent work showed that this is a reasonable description of some structures (194,195), but the majority of solved structures are closer to the ene-yne description (196–199). It is customary to consider these two forms as limiting contributors to a mesomeric hybrid. It has been argued, on the basis of Raman studies, that changes in the relative contributions of the



two forms occur as the chain length varies, and may be responsible for the color changes sometimes associated with polymorphic transformations in the polymer (200,201). This interpretation is not, however, firmly established.

A good deal of attention has been paid to the homogeneous vs. heterogeneous behavior in solid-state polymerizations in general, and in that of the diacetylenes in particular. The latter process is considered to proceed via a rotation of the diacetylene rod about its center of mass. However, the reaction involves an $\sim 18\%$ change in the total van der Waals volume of the C atoms associated with the polymer backbone (202), and would thus be expected to involve development of considerable strain, that is, unfavorable intra- and intermolecular contacts. This strain can be minimized if there are features of the monomer structure that can relax geometrically, for example if the monomer molecule has long, flexible side groups or if interstitial molecules are present. In the several cases where it has been possible to compare monomer and polymer structures directly (199,203,204), such relaxation has indeed been found, particularly where the degree of conversion is high. Such a comparison is shown for the diacetylene bis(phenylglutarate) and its polymer in **134** and **135** (note, for example, the changes in the conformations of the peripheral groups) and demonstrates the

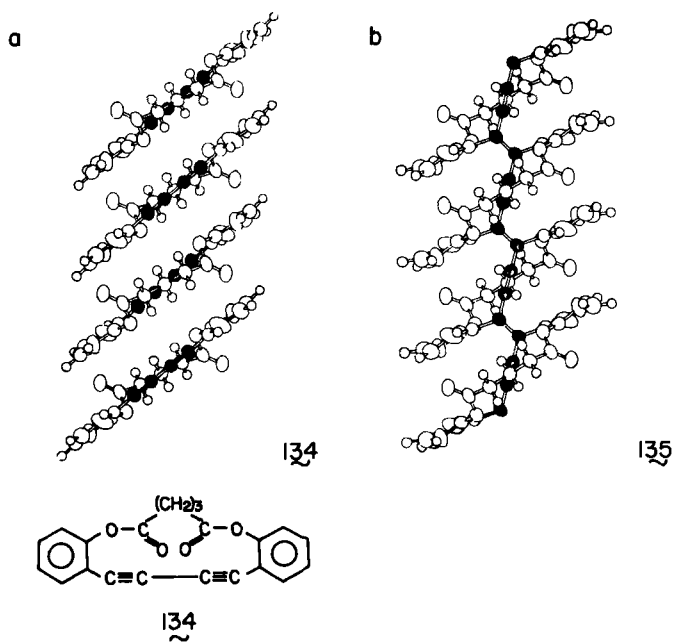
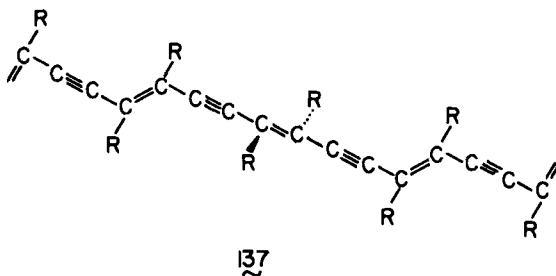
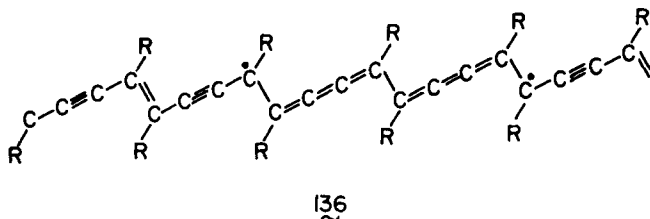


Figure 2. (a) Structure of crystal of monomer **134** (ac projection). (b) Structure of polymer **135** (ac projection). (Reproduced by permission from ref. 194.)

constancy of the reaction cavity (194). It is of interest that the structure of the polymer was determined using a single crystal of a solid solution of polymer (35%) in monomer (Figure 2).

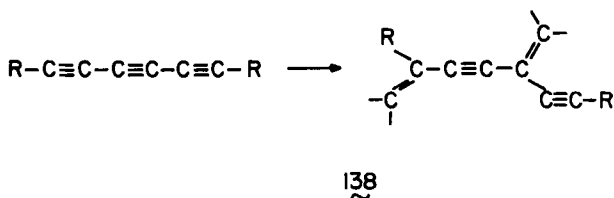
It seems that in these systems that give highly perfect polymer crystals the macromolecular chains initially grow independently of one another. This may be contrasted with the cases in which there is aggregation of polymer chains, although in both the process may proceed homogeneously (205). Schermann and co-workers (206) investigated the role of crystal defects (dislocations) in the polymerization of 2,4-hexadiyne-1,6-diol-bis(*p*-toluenesulfonate). They found that dislocations facilitate nucleation of the thermal polymerization but have no observable influence on the photoinduced reaction, which proceeds homogeneously through the bulk. This distinction is thought to be due to the energies available for overcoming the activation barriers in the two cases, as compared with the energies of the cores of the dislocations (206).

Defects also affect the polymerization by limiting the chain length. Thus, although the dimensions of the polymer crystal may be of the order of centimeters, the chains are thought to be no longer than a few micrometers. Furthermore, the effective conjugation length is considered to be even less. Two types of defects in the chain have been considered to be responsible for this (207). The first is analogous to one proposed previously for polyenes (208). It is suggested that in a polydiacetylene that is overwhelmingly of the ene-yne structure, for example, there may be included limited chain sequences of butatriene structure. Each such sequence will be separated from the rest of the chain by a pair of "bond-alternation" defects, as in **136**. The second possible type of chain defect

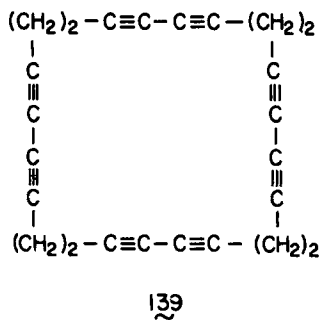


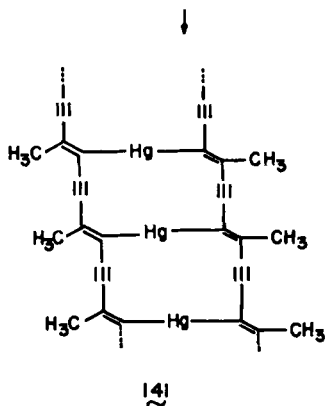
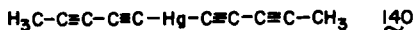
is termed an "orbital flip"; in it one (R)C=C(R) linkage is turned through 90° with respect to the neighboring C-C≡C-C, interrupting the π-orbital overlap, as in 137.

Baughman (209) has stressed that only if there is a unique direction for chain propagation is it possible for large, highly perfect polymer single crystals to form. If there is such uniqueness, all symmetry elements of the monomer lattice are preserved in the product lattice. Nonuniqueness can result in molecular-scale disorder, twinning, or even randomness between parent and product crystal orientations. Baughman (210) and Wegner and co-workers (211) have given much consideration to thermodynamic criteria for single-phase reaction. It has been pointed out (212) that for solid-state polymerizations in general, there can be a transition between homogeneous and heterogeneous mechanisms, with the rate of disintegration of the initially formed solid solution depending on temperature and composition.



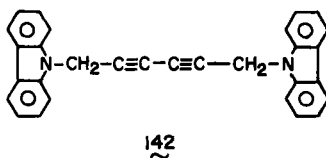
Before leaving the diacetylenes we must note some of the stereochemical varieties available in their polymers. Triynes, 138, also polymerize in the crystal by 1,4-addition (213). Also, cyclic di- and polyenes give polymeric products on irradiation. The exact structure of the polymer, however, has been established only in the polymer 135. Note that alternate side chains in this polymer are on opposite sides of the plane of the main chain; the polymer is thus meso. However, in principle such a reaction could give rise to optically active polymers in suitable structures. The cyclic tetradiyne 139 crystallizes in a polymerizable phase containing interstitial chloroform (209). The polymerization reaction, which involves



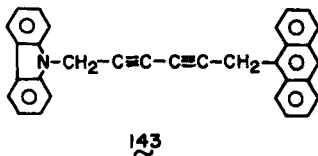


most but not all of the diacetylene functions, probably proceeds by 1,4-addition to give an unusual ladder polymer consisting of four fully conjugated chains joined together via methylene groups to form a cylindrical structure (214).

The mercury-bis(diacetylene) **140** reacts to give a polymer, **141**, that probably consists of two strands of poly(2-butyndiylidene) linked together by mercury atoms (215).



Finally, reference should be made to copolymerization in this series. The diacetylene **142** is (homo)-polymerizable by high-energy radiation, whereas **143**, though structurally very similar, is not. This difference in reactivity is apparently due to the difference between the crystal axial lengths in the direction in which polymerization would be expected to proceed; this length is 4.37 Å for **142** and 4.55 Å for **143** (216). The two monomers are miscible in all proportions in the



solid state. Single crystals of these solid solutions have axial lengths, and reactivities under irradiation, that change smoothly with composition. Their reactions yield single crystals of copolymers having the same compositions as the reactant crystals.

V. COMPLEXES, CLATHRATES, AND TWO-COMPONENT SOLIDS

Almost all the crystalline materials discussed earlier involve only one molecular species. The ramifications for chemical reactions are thereby limited to intramolecular and homomolecular intermolecular reactions. Clearly the scope of solid-state chemistry would be vastly increased if it were possible to incorporate any desired foreign molecule into the crystal of a given substance. Unfortunately, the mutual solubilities of most pairs of molecules in the solid are severely limited (6), and few well-defined solid solutions or mixed crystals have been studied. Such one-phase systems are characterized by a variable composition and by a more or less random occupation of the crystallographic sites by the two components, and are generally based on the crystal structure of one component (or of both, if they are isomorphous).

On the other hand, a very large number of two-component crystals are known in which the components are present in definite proportions, and whose structures are different from those of the separate materials in their crystals. These are the complexes, or "compounds" in the Phase Rule sense.

Finally, there are the "inclusion complexes," which in some senses behave like solid solutions, in others like the above complexes. Thus, for example, many inclusion complexes are of variable composition and their structures are usually determined by the host structure; on the other hand, guest and host must occupy different crystallographic sites (217a).

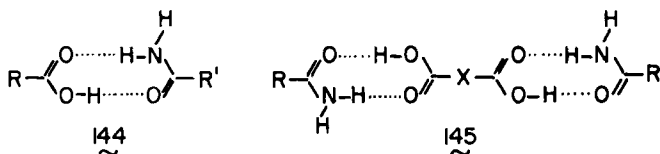
We now consider various examples of two-component crystals, stressing the ways in which the chemical environment of a molecule may be varied from that in its own crystalline phase and, of course, from that in any fluid phase, and the chemical consequences of this variation.

We have referred to salt formation, design of hydrogen-bond frameworks, and use of charge-transfer interactions as possible techniques for crystal engineering. These techniques are certainly as applicable to two-component as to one-component systems.

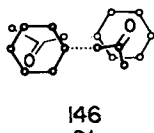
It is perhaps surprising that such a simple expedient as salt formation between, say, a carboxylic acid and an amine has rarely been exploited by the solid-state chemist. Crystallographic studies of such salts (217b) show that the two components can be brought together in various structural patterns, some of which are potentially useful for synthetic purposes.

We have referred to the influence of hydrogen bonding in one-component systems and mentioned the two-component system benzoic acid–pyridine (108). A variety of acid–base systems in addition to the latter are known to give 1:1 complexes. Pfeiffer gives in his book (88) a wealth of information from the older literature on such complexes, as well as on two-component organic–inorganic systems and charge-transfer complexes.

Stable hydrogen-bonded complexes **144** between carboxylic acids and carboxamides have been crystallized and studied. With dicarboxylic acids, 1:2 complexes **145** are formed (218).



Finally, we may mention again briefly charge-transfer complexation. In the one example we gave (Sect. III-B), donor and acceptor molecules were cocrystallized in a successful attempt to achieve close face-to-face packing (158). Charge-transfer effects can, however, also be used in engineering one-component systems. Thus, for example, many molecules that contain both phenyl and keto groups are found to pack in the motif **146**, in which presumably the former group acts as an electron donor and the latter as an acceptor. Such interactions are commonly observed in crystalline quinones (219), and have been used for stabilizing structures suitable for four-center photopolymerization (56).



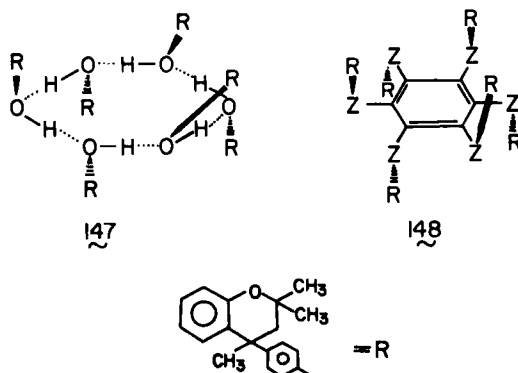
A. Clathrates and Inclusion Complexes

A large number and variety of molecules are known that can crystallize with guests incorporated in cavities in their structures. For some hosts such clathrates are formed only when the guest is of a certain size or shape; other hosts form clathrates with an extraordinary variety of guest types.

In principle all inclusion phenomena that occur in solution may occur also in the solid state. Thus, for example, the well-known crown-type host molecules, whose solution complexes provide a continuing area of active interest, form many stable complexes with guest molecules (220). Several of the crown-type

compounds form also ternary crystalline complexes in arrangements that probably do not exist in solution. For example, dibenzo[18]-crown-6, thiourea, and potassium iodide form a 1:1:1 complex (221) whose crystal structure has been determined (222). Cyclodextrins, whose complexes in solution have been the subject of intensive recent investigations, also form crystalline clathrates. Some of these latter crystals show promise of commercial application as inhibitors of inter- or intramolecular reactions in the pharmaceutical and food-additive industries (223,224).

The majority of clathrate inclusion complexes apparently exist in the crystal state only, and have not been detected in solution. New clathrates are being uncovered regularly, known clathrates are being modified, and even the design of new host molecules is now receiving attention. Although all the clathrates were initially discovered by accident (225), recently the synthesis of a novel series of molecules, termed "hexa hosts," has been achieved, with the aim of clathration. Based on analyses of the crystal structures of the Dianin-type clathrates, **147** (4-*p*-hydroxyphenyl-2,2,4-trimethylchroman), which involve a hexameric unit of ROH molecules held together by hydrogen bonds in such a way that the six R groups alternately point up and down, new molecules were synthesized in which these features were included in covalently bonded units of the same symmetry. Many of these new materials, for example **148** with Z = O, R = Ph or with Z = CH₂, R = OPh, SPh, or SCH₂Ph do indeed form clathrates (226).



Clathrate formation is very attractive for exploitation in solid-state chemistry. It allows one to modify in a simple way the environment of the guest molecule, to place this molecule in a crystalline phase with a structure different from its own (one structure may be chiral, and the other not), and even to achieve a stable crystalline structure at a temperature above the melting point of the pure guest. Some of the variety available for a single compound, acetic acid, is

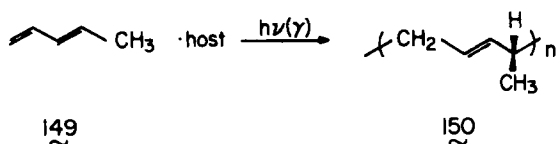
indicated below. The crystalline acid, which melts below room temperature, has a structure in which the molecules are hydrogen bonded in spiral, polymeric chains (227). In the 1:1 complex with deoxycholic acid, the acetic acid molecules are hydrogen bonded in infinite chains that are isolated from one another (228). In a clathrate of the hexa host **148** having $R = (R)\text{-}\alpha\text{-phenylethylsulfonylmethyl}$ and $Z = \text{CH}_2$, a room-temperature stable crystal, the acetic acid is present as hydrogen-bonded dimers (229). In a clathrate of the antibacterial agent furaltadone hydrochloride, acetic acid appears as an isolated monomer hydrogen bonded to the host (230). Finally, in the cage-type clathrate of tri-*o*-thymotide (TOT), **18**, the acid exists in monomeric, non-hydrogen bonded form (231).

As would be expected, clathrates are able to stabilize conformations (22) and intermolecular orientations (232) that are minor or absent in other phases.

More than 200 examples of hosts have been described, and several have been studied as media for chemical reactions. Intramolecular guest reactions, intermolecular guest-guest reactions, reactions of guests with external reagents, and reactions between guest and host have all been demonstrated. Some of these proceed with high stereoselectivity. We give examples below.

1. Polymerization Within Channel Inclusion Complexes

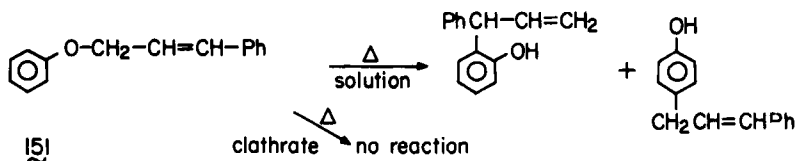
One of the first reactions to be studied systematically in a channel-type clathrate was the polymerization of olefins or diolefins. The ordering of the monomers within the clathrate lattice leads to stereoregular products that are not available by other techniques (232–234). Such radiation-induced stereospecific polymerization has been reported for a number of clathrate hosts (235).



The polymerization of *trans*-1,3-pentadiene, **149**, in a chiral channel inclusion complex with enantiomerically pure perhydrotriphenylene affords an optically active polymer, **150** (236). Asymmetric polymerization of this monomer guest occurs also in deoxycholic acid inclusion complexes (237).

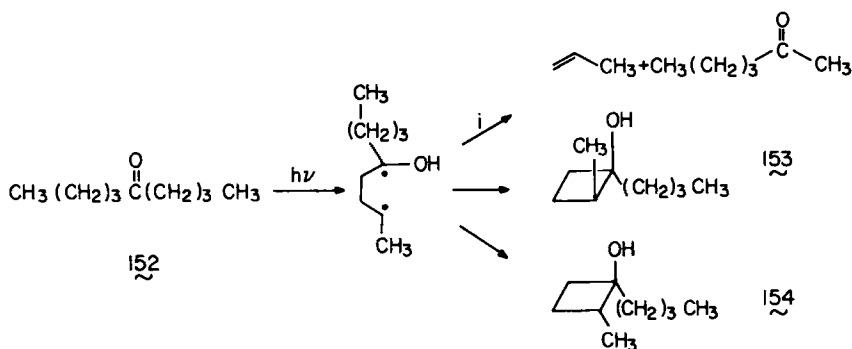
2. Intramolecular Reactions of Guests in Clathrates

We have previously mentioned the kinetic stabilization toward racemization of methyl methanesulfinate included in the cage-type clathrate of TOT (**59**). Such an effect may indeed be expected, since the cage wall is fairly rigid and the heat



of racemization is small compared with the lattice energy of the host. Such inhibition of reaction has been found also for other thermal reactions in clathrates. For example, the Claisen rearrangement of cinnamyl phenyl ether, **151**, proceeds smoothly in fluid phases, but not on heating of the channel-type clathrate of **151** in 4,4'-dinitrobiphenyl (238).

That the situation is different for photochemical reactions is indicated by a particularly interesting recent study of some dialkylketones (239). In solution, 5-nonanone, **152**, reacts photochemically to yield the cyclobutanol **153** and its isomer **154** in comparable amounts. Within the urea clathrate, however, **153** is the dominant product, with only traces of **154** being formed. The cyclobutanols analogous to **153**, that is, having methyl and hydroxyl *cis*, also predominate in the urea-clathrate-mediated photocyclization of 2-hexanone and 2-undecanone. It might be expected that the bulky cyclobutane derivatives, which almost certainly cannot be crystallized in a urea clathrate, would also not be *formed* in such a clathrate. There are decomposition pathways (cleavage reaction *i*) of the diradical intermediate that occur both in the clathrate and in solution. Nevertheless, the ring closure is a major pathway of reaction even in the clathrate.

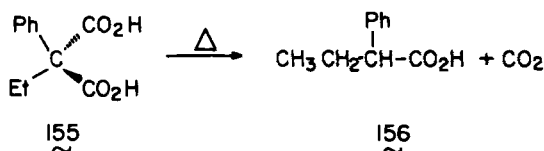


These and other experiments imply that even reactions that proceed via bulky transition states can take place in the clathrate if the initiation is photochemical, perhaps as a result of local deformation of the host lattice, and presumably as a result of the large energy dissipation involved. However, even here there is some lattice control of the reaction pathway.

In keeping with the conclusion that a large degree of molecular motion is

allowable in a photochemical reaction in a clathrate is the observation of the *cis* → *trans*-stilbene photoisomerization in TOT (240). Such large motion, leading to an unexpected product, is found also in the photoaddition of guest to host in the clathrate inclusion complex of acetophenone in deoxycholic acid, discussed below.

While much attention has been paid to the chemistry of cyclodextrin complexes in solution, there have been relatively few studies of their solid-state reactions. One such reaction is the decarboxylation of phenylethylmalonic acid, **155**. In solution this is catalyzed by β-cyclodextrin, and yields racemic 2-phenylbutyric acid, **156** (230). The malonic acid forms a crystalline 1:1 complex with β-cyclodextrin in which decarboxylation occurs at a much lower temperature than in the crystalline diacid. Interestingly, the product formed in the clathrate reaction is nonracemic, the optical yield being 7%.

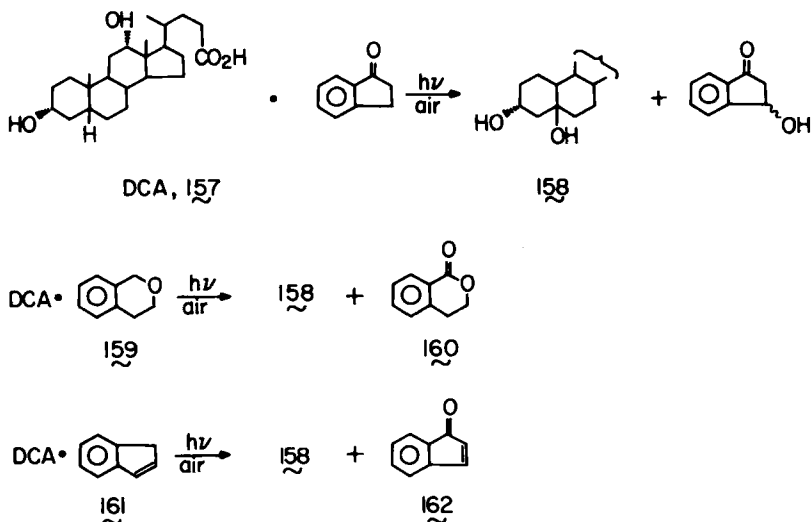


3. Gas-Solid Reactions of Clathrates

In view of the tendency of clathrates to inhibit reactions of the included guests, one might expect that reaction with "outside" species would be effectively precluded, especially if the cavities in the clathrate are inaccessible to the species. However, several intriguing reactions involving gaseous species and guest have been observed, and presumably occur *within* the cavity.

Irradiation in air of the deoxycholic acid (DCA, **157**) complex of indanone leads to oxidation of both the steroid and the guest, yielding 5-β-hydroxy-DCA, **158**, and optically active 3-hydroxyindanone (241). In the presence of air, irradiation of the DCA clathrates of isochromane, **159**, and indene, **161**, leads to reaction with oxidation of the host and of the allylic position of the guest to a keto group (e.g., **159** → **160** and **161** → **162**). The detailed mechanisms of these oxidations remain to be elucidated.

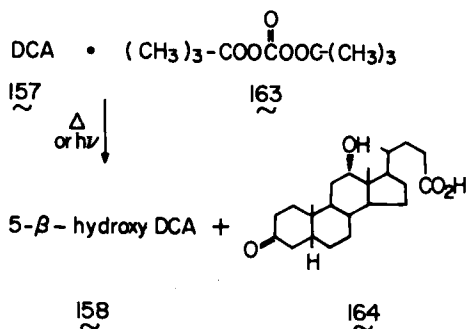
Even less expected, perhaps, are the reactions involving gas-solid addition of HBr, Cl₂, and Br₂ to α,β-unsaturated acid guest species in α- and β-cyclodextrin inclusion complexes (242). Although the chemical yields are not high, the optical yields in some cases are extraordinary. Thus, chlorine addition to methacrylic acid in α-cyclodextrin yields (–)-2,3-dichloro-2-methylpropanoic acid in nearly quantitative optical yield. The β-cyclodextrin-methacrylic acid clathrate undergoes chlorine addition to yield preferentially the *enantiomeric* (+)-product, with an e.e. of 80%.



4. Host-Guest Reactions in Clathrates

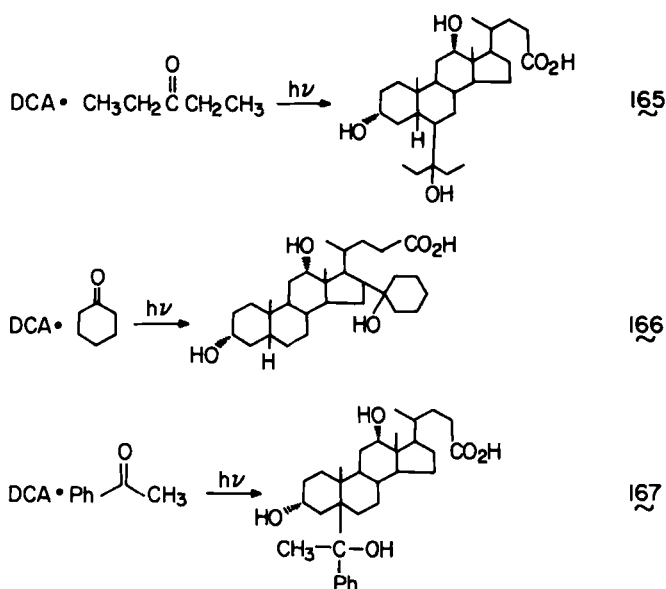
The most extensive study in the field of host-guest reactions in clathrates has been that of Lahav, Leiserowitz, and co-workers (56,241,243) on the choleic acids. The results of these combined chemical and crystallographic investigations are of possible importance for stereoselective steroid functionalization. In these studies potentially reactive guests were activated thermally or photochemically to produce species that attacked the walls of the channel at specific sites determined by the proximity, orientation, and reactivity of the host molecules at the wall relative to the activated guest species.

Deoxycholic acid (DCA), 157, and di-*t*-butyl diperoxycarbonate, 163, react stereospecifically in their clathrate to yield the ketone 164 and 5-β-hydroxy-

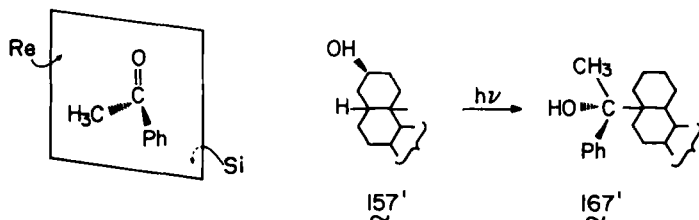


DCA, **158**. Reaction in solution affords numerous products, among which **158** and **164** were not formed in thin-layer chromatography (TLC)-detectable amounts.

The majority of the studies in this series were performed using aliphatic and aromatic ketones as guests. The steroid sites that undergo functionalization vary with the guest used. Thus, irradiation of the DCA·diethyl ketone complex affords the product, **165**, of addition of the ketone to the 6-equatorial position. Exposure of the DCA·cyclohexanone complex to light brings about formation of steroid functionalized in the D-ring, **166**, while irradiation of the acetophenone complex affords the 5- β -DCA adduct, **167**.



In all these reactions, crystallographic studies demonstrated the crystal control responsible for formation of the observed products. Thus, the prereaction ketone oxygen–steroidal hydrogen distance is in all cases $3.4 \pm 0.5 \text{ \AA}$, the ketonic carbon–steroidal (to-be-attacked) carbon distance is of the order of 4 \AA , and the

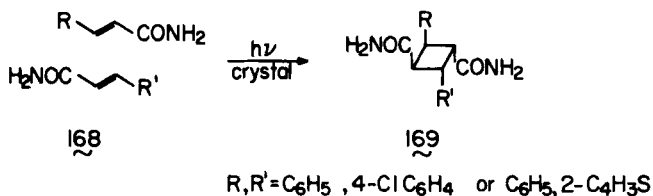


angle between the to-be-attacked C–H bond and the plane of the guest $>\text{C}=\text{O}$ is between 55° and 90° .

The results of the study of the last-mentioned reaction, $\text{DCA} \cdot \text{PhCOCH}_3 \rightarrow \mathbf{167}$, provided a surprise. X-Ray analyses of the structure of the clathrate before and after partial reaction, and of the final product, **167**, showed that the prochiral Re face of the ketone, initially the face more distant from the to-be-attacked host, and not the close-lying Si face, is the one that adds to the steroid. A rationalization of this extraordinary stereochemical effect, which results in formation of a new chiral center with quantitative asymmetric induction, has been proposed (241).

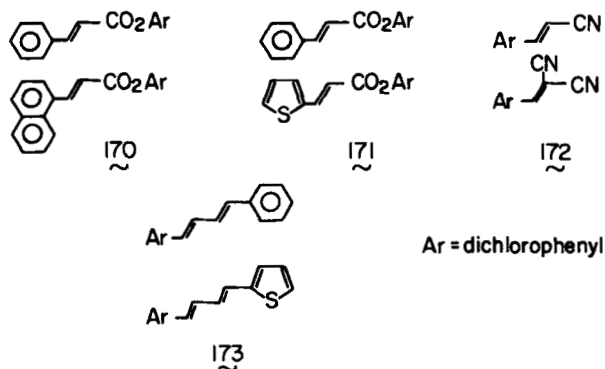
B. Solid Solutions–Mixed Crystals

We have mentioned the limited mutual solubilities of most pairs of organic molecules in the solid state, and the necessary conditions for formation of solid solutions. From a practical point of view the potential for reasonable mutual solubility is good if the two components, separately, crystallize with similar packing motifs, and when there is a strong "anchoring unit" in the structure. The ring-substituted cinnamides, whose hydrogen-bond network ensures a structure in which side-chain double bonds lie antiparallel and strongly overlapped, provided the first example in which reactivity was studied in the mixed crystal (134). The components of **168**, individually, give α -truxillic-acid-type photodimers (**74**); the mixed crystal **168** gives the analogous heterodimer, **169**, in addition to the two homodimers.

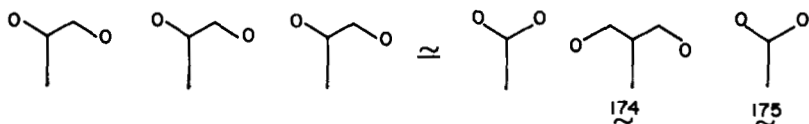


The dichlorophenyl group also functions as a sufficiently strong anchor to allow formation of solid solutions from pairs of structurally similar potentially reactive olefins. A series of such pairs are **170** to **173**. All were found to yield the expected β -truxinic-acid-type photodimers, **75** (135).

An interesting reactive mixed crystal was engineered on the basis of the observed packing of the **103** molecule having $\text{R}^1 = \textit{sec}$ -butyl and $\text{R}^2 = \text{ethyl}$ (175). It was expected that the monomers in which 3-pentyl, **174**, and 2-propyl, **175**, replace the *sec*-butyl would cocrystallize in a chiral, polymerizable arrangement similar to that of **103**. This was indeed what was found, and the resulting



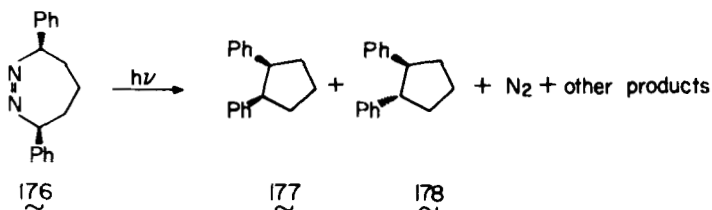
two-component phase was shown to undergo the anticipated topochemical, asymmetric photocycloaddition reaction.

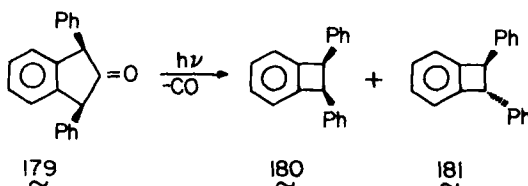


VI. SOLID-STATE CHEMISTRY OF RADICAL PAIRS

Many reactions that proceed with elimination of a gas (N_2 , CO_2 , etc.) and formation of radical-pair intermediates show considerable stereochemical differences in solution and in the crystal. Thus, solid-state photolysis of the diazo compound **176** yields, among other products, *cis*-1,2-diphenylcyclopentane, **177**; no trans isomer, **178**, has been detected. Irradiation of **176** in solution leads to mixtures in which the trans product **178** predominates (244).

Similarly, irradiation of **179** in the solid causes elimination of carbon monoxide and formation, almost exclusively, of *cis*-diphenylbenzocyclobutane, **180**, in which configuration is retained. On the other hand, the major product from photoreaction in solution is the trans isomer, **181** (245).

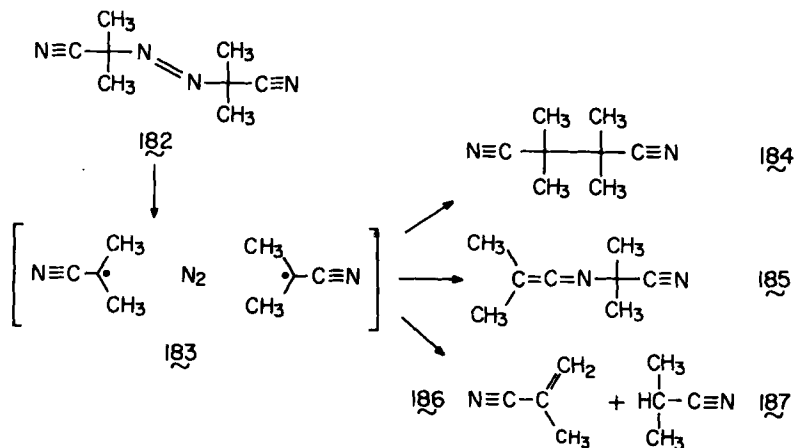




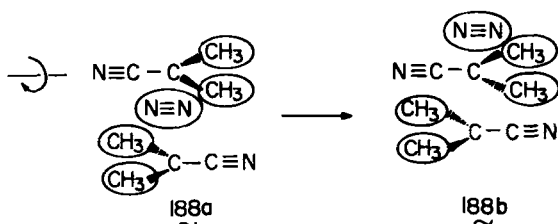
McBride and co-workers have studied extensively the reactions of such free-radical precursors as azoalkanes and diacyl peroxides (246). By employing a variety of techniques, including X-ray structure analysis, electron paramagnetic resonance (EPR), and product studies, and comparing reactions in the crystal and in fluid and rigid solvents, they have been able to obtain extremely detailed pictures of the solid-state processes. We will describe here some of the types of lattice control they have elucidated, and the mechanisms that they suggest limit the efficacy of topochemical control.

Azobisisobutyronitrile, **182**, reacts thermally or photochemically to give the intermediate **183**, which leads, in inert solvents, to combination products **184** and **185**, and disproportionation products **186** and **187**. The parent compound is dimorphic, and both crystal forms behave similarly on photolysis, yielding 95% disproportionation and 5% **184**. In contrast, in both fluid and rigid solution the disproportionation products form only 5% of the total. The cage effect in the solid is almost quantitative.

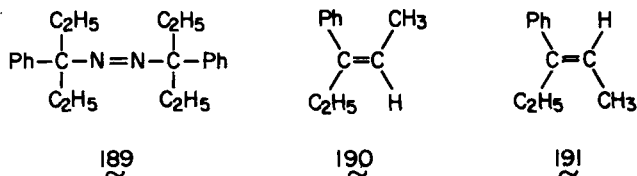
The relative product yields can be rationalized in terms of crystal-structural influences (247). In both crystal forms the packing of the nitrile groups is well-suited for optimizing the dipole-dipole attraction between molecules. For the reaction **183** \rightarrow **185** to occur, one free radical would need to rotate about an axis perpendicular to the plane, thus allowing the nitrile nitrogen to approach



the trivalent carbon of the second radical. Considerable approach of the two radicals of **183** is required for formation of **184**. Both movements would oppose the dipolar forces exerted on the nitrile groups by their neighbors. On the other hand, conversion of **183** to disproportionation products requires only pivoting a radical about the axis of the nitrile group, to bring a methyl group into position for hydrogen transfer to the geminate radical; such pivoting would not be opposed by dipolar forces. McBride has presented evidence showing that this "rotational diffusion" is rate limiting (248); it presumably involves also departure of the nitrogen from the interradsical space (**188a** \rightarrow **188b**).



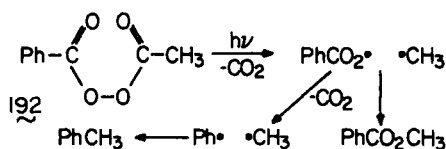
The above example illustrates the influence of the lattice on the *constitution* of the product. The photolysis of azobis-3-phenyl-3-pentane, **189**, provides a case of influence on the product *configuration* (249). In this system, too, the crystal lattice favors disproportionation over combination. Two disproportionation products, the *Z*- and *E*-pentenes **190** and **191**, are formed in the solid, in a ratio of 1:3; the predicted equilibrium ratio is 1:1.6. While the nature of the processes determining this ratio is not clear, it was established that the *Z* isomer is formed under strong lattice control, whereas the *E* isomer is formed in a process with greater, but not complete, molecular freedom.



Examples of the role of the lattice in generating radicals in a given conformation, and in selecting one among many nominally degenerate pathways, have been described (246).

The study of such radical-pair systems by EPR has the considerable advantage

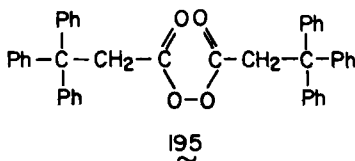
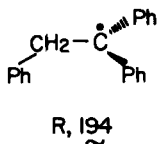
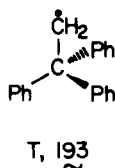
that measurements can be made at very low degrees of conversion, when the parent crystal is essentially undamaged. Let us treat the photolysis of acetyl benzoyl peroxide, **192**, as illustrative. Decomposition of this substance in solution or as a melt gave more than a dozen products, among which no single compound accounted for more than 25% (250). Partial photolysis of the crystalline material, however, gives only the simple cage products, methyl benzoate, from loss of one CO₂, and toluene, from loss of both. Isotope-cross-over experiments show that both products are formed by cage collapse of fragments from single precursor molecules (251).



A more striking specificity appears for **192** containing ¹⁸O in the peroxide positions. Such ester as is formed in fluid solution has complete scrambling of ¹⁸O between carbonyl and ether oxygens, but ester from the solid-state reaction has four times as much label in the ether position as in the carbonyl. The crystalline matrix thus removes a degeneracy of reaction paths that prevails in solution. X-Ray and product studies alone give no convincing explanation for the observed selectivity between the oxygens; however, EPR studies provide valuable additional information. Such studies at different extents of conversion show the consecutive formation of two radical pairs that are structurally very similar, but collapsing at very different rates. McBride and colleagues suggest (251,252) that this effect is due to stress or "pressure" produced during reaction—first as a result of expansion of the reactant molecule during homolysis, and then as a result of liberation of CO₂. Such stress increases the effective rigidity of the lattice and thus retards the reaction in the vicinity of previously reacted molecules, although the induced structural changes are minimal. Careful analysis of the initially formed benzoyloxyl radical shows that it undergoes an irreversible 30° in-plane rotation and that the CO₂ group of this planar radical rotates to exchange oxygen positions. If, as is believed, the first rotation is driven by nonbonded repulsion between the oxygens that were originally linked in the peroxide bond, one must conclude that the reaction's specificity is dictated more by stress among the fragments of the decomposing molecule than by the shape of the cavity that holds them.

This hypothesis of local stress was found to explain conveniently the modes of decomposition also in other systems. The case of 3-methyl-3-phenylbutanoyl peroxide is of interest. The zero-field splitting was measured as a function of

temperature for the pair of neophyl radicals formed by photolysis of this compound at very low temperatures. Surprisingly, even at a temperature at which the lattice allows radical carbons to move to bonding distance, no internal rotation occurs in the surviving radical pairs. The explanation proffered is the following: The radicals are held apart by the pair of CO_2 molecules trapped between them. These molecules are enmeshed with the *t*-butyl rotors of the radical, locking the whole assembly together so that rotation is impossible. Only at 170 K do these CO_2 molecules shift, unlocking the system, in which presumably free rotation then sets in (246).



The rearrangement of 2,2,2-triphenylethyl (T, 193) to 1,1,2-triphenylethyl (R, 194) can be observed readily during the decomposition of 3,3,3-triphenylpropanoyl peroxide (195) (252). Brief photolysis of 195 at low temperatures gives a single radical pair TT. Subsequent warming or further photolysis gives five other well-characterized radical pairs: TT' and four pairs derived from TT or TT' by neophyl rearrangement. Here T' denotes the radical in a strained structure, observed by EPR. Conformational analysis of the precursor molecule shows that one particular phenyl group has a more favorable torsional angle for rearrangement than the others, and it is indeed selected exclusively in three of the four radical pairs produced. In the arrangement of TT, however, a different phenyl migrates. Again, this apparent violation of topochemical principles is readily interpretable in terms of local stress. The location of CO_2 in the precursor molecule is such that after homolysis it should press the radical carbon away from the conformationally favored phenyl and toward the phenyl that does in fact rearrange in TT. Once this stress is released, during preliminary interconversion of pairs, subsequent arrangement can take its topochemical course.

Independent evidence for local stress is provided by measurements of the frequency of the antisymmetric stretching vibration of CO_2 eliminated in crystalline undecanoyl peroxide on photolysis (253). The results indicate that local pressures of tens of kilobars are established. This is very much larger than the lattice strain that has been considered as developing during the polymerization of diacetylenes (254). McBride points out (246) that virtually all reactions cause changes in shape that should create local stress in a solid, so that subsequent

reactions at or near the primary reaction site must occur under influence of the stress.

VII. ASYMMETRIC SYNTHESIS VIA REACTIONS IN CHIRAL CRYSTALS

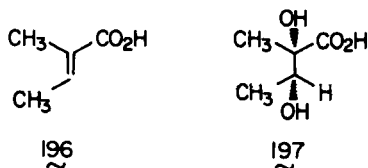
Even starting from achiral molecules it is in some systems possible to achieve crystallization in a chiral structure. Perhaps one of the most striking achievements in organic solid-state chemistry has been the "trapping" of the chirality of such a crystal as the chirality of the stable product of chemical reactions in the crystal. Such asymmetric synthesis has been reviewed (255), and a recent book (256) also provides a thorough discussion of chirality in crystals. The related and fascinating topic of the chemical consequences of the presence of a polar axis in some organic crystals has also been reviewed (257).

The culmination of the studies on asymmetric photodimerization reactions in the solid state was the successful elaboration of chemical systems that are achiral but crystallize in chiral structures, and that yield, on irradiation, dimers, trimers, and higher oligomers in quantitative enantiomeric yield (175,258).

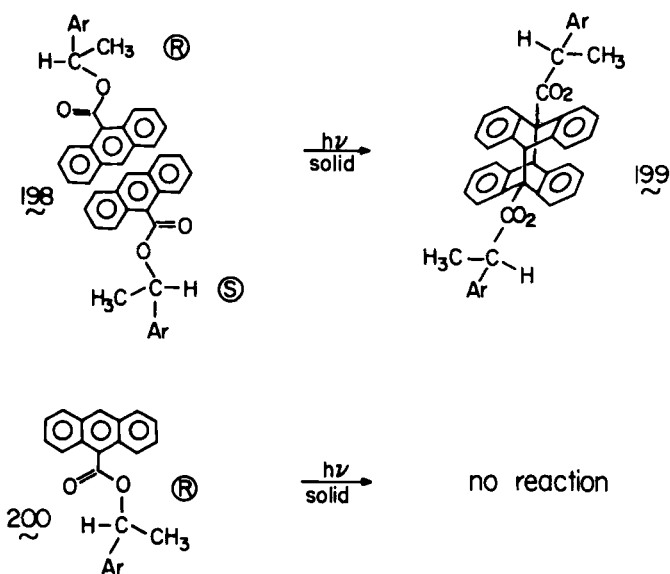
In addition to providing a novel approach to the preparation of chiral compounds, this type of chemistry may allow one to inquire into the subtle stereochemical details of some crystal-state reactions. For example, what are the approach geometry and the preferred side of attack in the addition of bromine to a chiral olefin (259)? What can be learned of the geometry of the labile electronically excited species involved in $(2 + 2)$ photocycloaddition reactions (260)?

In addition, the results of such reactions have suggested plausible models for the mechanism of abiotic generation of optical activity, including an autocatalytic feedback mechanism (261). The latter involves random development of chiral crystals from achiral starting material, and solid-state reaction leading to products in which one enantiomer is in excess and thus can bias subsequent further crystallization (262).

It has been recognized for several years that asymmetric synthesis could probably be achieved also by reaction in appropriate, single, *racemic* crystals (255,263), and this possibility has recently been realized in an elegant study (264) involving comparison of the reactions on "upper" $[(\bar{2}10)]$ and "lower" $[(2\bar{1}0)]$ faces of single crystals of tiglic acid, **196**. Cis dihydroxylation at one face of **196** with aqueous osmium tetroxide solution gave a 60% yield of *threo*-2,3-dihydroxy-2-methylbutanoic acid, **197**, having an optical purity approaching 100%. Reaction on the opposite crystal face produced **197** with the opposite sign of rotation.



As discussed earlier, the packing in the crystal of a resolved chiral species (*R* or *S*) will, in general, differ from that of the racemic substance (*R,S*). One example in which the packing differences have been demonstrated has provided an interesting method for the enhancement of optical purity, based on the differential reactivities of the two types of crystals in a series of 9-anthroic acid esters of 1-aryl ethanols (265). The esters, obtained by the coupling of 9-anthroyl chloride with partially resolved 1-arylethanols, crystallize in two types of structure. Thus, crystals of the *R,S* materials are based on pairs, **198**, of centrosymmetrically related molecules in which the anthracene moieties are closely spaced and strongly overlapped. Such crystals emit characteristic excimer fluorescence, and undergo efficient photodimerization to yield the centric meso dimers, **199**. On the other hand, crystals of the homochiral (*R* or *S*) esters display monomer fluorescence and do not dimerize on exposure to light. In the latter form, **200**, the overlap of the anthracene moieties of the molecules is negligible. For example, 1-arylethyl alcohols containing 25 to 60% excesses of the *R* enantiomer were esterified with a molar excess of 9-anthroyl chloride and then crystallized.



Irradiation of this solid brought about reaction to give the highly insoluble meso dimer formed from **198**. Unreacted monomers, principally of crystal form **200**, were extracted by a suitable solvent, and had enantiomeric purities exceeding 90%.

Finally, one should be cautioned that, occasionally, substances form chiral single crystals of nearly racemic composition. For example, hexahelicene crystals grown from racemic solutions apparently undergo spontaneous resolution, displaying the enantiomorphic space group $P2_12_12_1$; however, the e.e. in the crystal is only ~2%. This material (and probably others as well) has a lamellar, twinned structure in which alternating layers, ~20 μm thick, of optically pure (*P*)-(+) and (*M*)-(–)-hexahelicene are perfectly aligned to build up the observed crystal (266).

VIII. STEREOCHEMISTRY AND CRYSTAL GROWTH

This article would not be complete without reference to the recent studies of Addadi, Berkovitch-Yellin, Lahav, and Leiserowitz on the influence of impurities on crystal growth. However, this topic is the subject of a review elsewhere in this volume, and we therefore limit ourselves to a statement of the nature of the studies.

Crystals grow by addition of molecules from the surroundings to the exposed faces of the crystal. When there are present in the surroundings not only substrate molecules but also impurity molecules that are stereochemically similar to the substrate, these latter molecules may also add to the surfaces. The result will be a retardation of crystal growth (267). Furthermore, since the energy of the attachment of the impurity will differ from face to face, a modification of the crystal morphology may also result (268,269).

These effects have proved important in improving the methods available for resolution of enantiomers by crystallization (267). Furthermore, by studies of the morphological changes induced, one may determine the faces at which the impurities are dominantly attached (270,271). Then, in suitable systems, it is possible to determine the absolute configuration of a polar crystal if one knows that of the impurity (272), or to determine that of the impurity if one knows the structure of the centrosymmetric crystal with which it interacts (270).

REFERENCES

1. For references to some of the early papers, see Cohen, M. D.; Schmidt, G. M. J. *J. Chem. Soc.* **1964**, 1996–2000.
2. (a) See, for example, the proceedings of various international symposia on organic solid state chemistry, some of which have been published in the journal *Molecular Crystals and Liquid*

- Crystals*. (b) Fox, D.; Labes, M. M.; Weissberger, A., Eds.; "Physics and Chemistry of the Organic Solid State"; Vols. I-III; Interscience: New York, 1963-1967.
3. (a) Friedman, G.; Lahav, M.; Schmidt, G. M. J. *J. Chem. Soc., Perkin II* **1974**, 428-432. (b) Kaufman, H. W.; Rabinovich, D.; Schmidt, G. M. J. *J. Chem. Soc., Perkin II* **1974**, 433-435.
 4. Green, B. S.; Schmidt, G. M. J. *Tetrahedron Lett.* **1970**, 4249-4252.
 5. Schmidt, G. M. J. *Pure Appl. Chem.* **1971**, 27, 647-678.
 6. Paul, I. C.; Curtin, D. Y. *Acc. Chem. Res.* **1973**, 6, 217-225.
 7. Adler, G. *Trans. Am. Crystallogr. Assoc.* **1971**, 7, 55-68.
 8. The example of *o,o'*-azodioxytoluene is described by Azoulay, M.; Stymne, B.; Wettermark, G. *Tetrahedron* **1976**, 32, 2961-2966.
 9. The example of azobenzene is described by Cammenga, H. K.; Behrem, E.; Wolf, W.; in "Reactivity of Solids"; Wood, J.; Lindquist, O.; Helgesson, C.; Vannenberg, N. G., Eds.; Plenum: New York, 1977, pp. 481-486.
 10. Bryan, R. F.; Weber, H. P. *J. Chem. Soc., Chem. Comm.* **1966**, 329-330.
 11. For an extensive review of these and other relevant results, see Mizushima, S. J. "Structure of Molecules and Internal Rotation"; Academic: New York, 1954.
 12. Kagarise, R. E. *J. Chem. Phys.* **1956**, 24, 300-305.
 13. Brasch, J. W. *J. Chem. Phys.* **1965**, 43, 3473-3476.
 14. Miyazawa, T. *Bull. Chem. Soc. Japan*, **1969**, 42, 3021-3022.
 15. Fontaine, H.; Bee, M. *Bull. Soc. Fr. Mineral Cristallogr.* **1972**, 95, 441-450; Fontaine, H.; Fouret, R. *Adv. Mol. Relaxation Processes* **1973**, 5, 391-394.
 16. Decamps, M. *Chem. Phys.* **1975**, 10, 199-207.
 17. Fitzgerald, W. E.; Janz, G. E., *J. Mol. Spectrosc.* **1957**, 1, 49-60.
 18. Kitaigorodskii, A. I. "Organic Chemical Crystallography"; Consultants Bureau: New York, 1961.
 19. Bernstein, J. *Acta Crystallogr.* **1979**, 35B, 360-366.
 20. Herbstein, F. H.; Kapon, M.; Reisner, G. M.; Rubin, M. B. *J. Incl. Phenom.*, **1984**, 1, 233-250.
 21. Jensen, F. R.; Bushweller, C. H. *J. Am. Chem. Soc.* **1969**, 91, 3223-3225.
 22. Gustavson, J. E.; Klaeboe, P.; Kvila, H. *Acta Chem. Scand.* **1978**, A32, 25-30.
 23. Trinh-Toan; DeLuca, H. F.; Dahl, L. F. *J. Org. Chem.* **1976**, 41, 3476-3478.
 24. Havinga, E. *Experientia* **1973**, 29, 1181-1193.
 25. Wing, R. M.; Okamura, W. H.; Rego, A.; Pirio, M. R.; Norman, A. W. *J. Am. Chem. Soc.* **1975**, 97, 4980-4985.
 26. Trinh-Toan; Ryan, R. C.; Simon, G. L.; Calabrese, J. C.; Dahl, L. F. *J. Chem. Soc., Perkin II*, **1977**, 393-401.
 27. Hodgkin, D. C.; Rimmer, B. M.; Dunitz, J. D.; Trueblood, K. N. *J. Chem. Soc.* **1963**, 4945-4955.
 28. Knobler, C.; Romers, C.; Braun, P. B.; Hornstra, J. *Acta Crystallogr.* **1972**, 28B, 2097-2103.
 29. (a) Altona, C.; Romers, C. *Rec. Trav. Chim. Pays-Bas* **1963**, 82, 1080-1088. (b) Altona, C.; Knobler, C.; Romers, C. *Acta Crystallogr.* **1963**, 16, 1217-1225.
 30. Altona, C.; Romers, C.; Havinga, E. *Tetrahedron Lett.* **1959**, (10), 16-20.
 31. Kaftory, M. *J. Am. Chem. Soc.* **1983**, 105, 3832-3836.
 32. Byrn, S. R.; Curtin, D. Y.; Paul, I. C. *J. Am. Chem. Soc.* **1972**, 94, 890-898.
 33. (a) Eistert, B.; Weygand, F.; Csendes, E. *Chem. Ber.* **1951**, 84, 745-780. (b) Weygand, C. *Ann.* **1929**, A472, 143-179.
 34. (a) Romers, C.; Shoemaker, C. B.; Fischmann, E. *Rec. Trav. Chim. Pays-Bas* **1957**, 76, 490-

505. (b) Romers, C.; Fischmann, E. *Acta Crystallogr.* **1960**, *13*, 809–813. (c) Fischmann, E.; Romers, C.; Umans, A. J. H. *Acta Crystallogr.* **1960**, *13*, 885–889.
35. Kessler, H.; Zimmermann, G.; Förster, H.; Engel, J.; Oepen, G.; Sheldrick, W. S. *Angew. Chem.* **1981**, *93*, 1085–1086; *Angew. Chem. Int. Ed. Engl.* **1981**, *20*, 1053–1055.
36. Birnbaum, G. I.; Cygler, M.; Kusmierek, J. T.; Shugar, D. *Biochem. Biophys. Res. Comm.* **1981**, *103*, 968–974.
37. Birnbaum, G. I.; Cygler, M.; Ekiel, I.; Shugar, D. *J. Am. Chem. Soc.* **1982**, *104*, 3957–3964.
38. Ramdas, S.; Thomas, J. M. In "Chemical Physics of Solids and Their Surfaces," Vol. 7; Roberts, M. W.; Thomas, J. M., Eds.; Chemical Society: London, 1978, pp. 31–58.
39. Gavezzotti, A.; Simonetta, M. *Chem. Rev.* **1982**, *82*, 1–13.
40. Cailleau, H.; Baudour, J. L.; Zeyen, C. M. E. *Acta Crystallogr.* **1979**, *35B*, 426–432, and papers cited therein.
41. Baudour, J. L.; Cailleau, H.; Yelon, W. B. *Acta Crystallogr.* **1977**, *33B*, 1773–1780.
42. Baudour, J. L.; Delugeard, Y.; Rivet, P. *Acta Crystallogr.* **1978**, *34B*, 625–628.
43. Chawdhury, S. A.; Hargreaves, A.; Sullivan, R. A. L. *Acta Crystallogr.* **1968**, *24B*, 1222–1228.
44. Cannas, M.; Marongiu, G.; Destro, R. *Cryst. Struct. Comm.* **1976**, *5*, 67–70, 71–74.
45. Casalone, G. L.; Mariani, C.; Mugnoli, A.; Simonetta, M. *Acta Crystallogr.* **1967**, *22*, 228–236.
46. Examples include Bregman, J.; Leiserowitz, L.; Schmidt, G. M. J. *J. Chem. Soc.* **1964**, 2068–2085; Bregman, J.; Leiserowitz, L.; Osaki, K. *J. Chem. Soc.* **1964**, 2086–2100.
47. Bernstein, J.; Izak, I. *J. Chem. Soc., Perkin II* **1976**, 429–434.
48. Green, B. S.; Schmidt, G. M. J. Unpublished results, cited in ref. 5.
49. Bernstein, J.; Schmidt, G. M. J. *J. Chem. Soc., Perkin II* **1972**, 951–955.
50. Hagler, A. T.; Bernstein, J. *J. Am. Chem. Soc.* **1978**, *100*, 6349–6354.
51. However, see Mirsky, K.; Cohen, M. D. *Chem. Phys.* **1978**, *28*, 193–204.
52. (a) Sacconi, L.; Ciampolini, M.; Speroni, G. P. *J. Am. Chem. Soc.* **1965**, *87*, 3102–3106. (b) For a recent example of structural mimicry see Jones, W.; Theocharis, C. R.; Thomas, J. M.; Desiraju, G. R. *J. Chem. Soc., Chem. Comm.* **1983**, 1443–1444.
53. Ref. 18, p. 95.
54. Cohen, M. D. *J. Chem. Soc. B* **1968**, 373–376.
55. Petraccone, V.; Ganis, P.; Corradini, P.; Montagnoli, G. *Eur. Polymer J.* **1972**, *8*, 99–105.
56. Addadi, L.; Ariel, S.; Lahav, M.; Leiserowitz, L.; Popovich-Biro, R.; Tang, C. P. In "Chemical Physics of Solids and Their Surfaces," Vol. 8; Roberts, M. W.; Thomas, J. M., Eds.; Chemical Society: London, 1981, pp. 202–245.
57. Benedith, E.; Pedone, C.; Sirigu, A. *Acta Crystallogr.* **1973**, *29B*, 730–733.
58. Arad-Yellin, R.; Green, B. S.; Knossow, M. *J. Am. Chem. Soc.* **1980**, *102*, 1157–1158, and references therein.
59. Arad-Yellin, R.; Green, B. S.; Knossow, M.; Tsoucaris, G. *J. Am. Chem. Soc.* **1983**, *105*, 4561–4571.
60. Bellamy, A. J.; Guthrie, R. D. *J. Chem. Soc. C* **1968**, 2090–2091.
61. (a) Curtin, D. Y.; Hausser, J. W. *J. Am. Chem. Soc.* **1961**, *83*, 3474–3481. (b) See, for example, Havinga, E. *Biochim. Biophys. Acta* **1954**, *13*, 171–174.
62. (a) Raban, M.; Carlson, E. *J. Am. Chem. Soc.* **1971**, *93*, 685–691. (b) Cases 20, 21, and 23 are discussed in the following: Kalinowski, H.-O.; Kessler, H. *Top. Stereochem.* **1973**, *7*, 295–383. Sandstrom, J. *Top. Stereochem.* **1983**, *14*, 83–181.
63. Rieker, A.; Kessler, H. *Chem. Ber.* **1969**, *102*, 2147–2149.
64. Sanchez, A. G.; Valle, A. M.; Bellanato, J. *J. Chem. Soc. B* **1971**, 2330–2335.

65. Gault, I. R.; Ollis, W. D.; Sutherland, I. O. *J. Chem. Soc., Chem. Comm.* **1970**, 269–271.
66. Bailey, N. A.; Hull, S. E. *J. Chem. Soc., Chem. Comm.* **1971**, 960–961.
67. Dietrich, D. A.; Paul, I. C.; Curtin, D. Y. *J. Am. Chem. Soc.* **1974**, *96*, 6372–6380.
68. Bamberger, E.; Ham, W. *Justus Liebigs Ann. Chem.* **1911**, *382*, 82–128.
69. Smith, L. I.; Taylor, F. L. *J. Am. Chem. Soc.* **1935**, *56*, 2460–2463.
70. Prout, C. K.; Coda, A.; Forder, R. A.; Kamenar, B. *Cryst. Struct. Comm.* **1974**, *3*, 30–42.
71. Karle, J.; Estlin, J. A.; Karle, I. L. *J. Am. Chem. Soc.* **1967**, *89*, 6510–6514.
72. King, R. W.; Murphey, C. F.; Wildman, W. C. *J. Am. Chem. Soc.* **1965**, *87*, 4912–4917.
73. McDonagh, A. F.; Smith, H. E. *J. Org. Chem.* **1968**, *33*, 1–8.
74. Schäfer, W.; Schlude, H. *Tetrahedron Lett.* **1968**, 2161–2166.
75. Alper, H.; Keung, E. C. H.; Partis, R. A. *J. Org. Chem.* **1971**, *36*, 1352–1355.
76. Glen, R. C.; Murray-Rust, P.; Riddell, F. G.; Newton, R. F.; Kay, P. B. *J. Chem. Soc., Chem. Comm.* **1982**, 25–26.
77. Heggie, W.; Sutherland, J. K. *J. Chem. Soc., Chem. Comm.* **1972**, 957–958.
78. Bellus, D.; Mez, H.-C.; Rihs, G.; Sauter, H. *J. Am. Chem. Soc.* **1974**, *96*, 5007–5009.
79. Fleming, I.; Philippides, D. *J. Chem. Soc. C* **1970**, 2426–2428.
80. Curtin, D. Y.; Englemann, J. H. *J. Org. Chem.* **1972**, *37*, 3439–3443.
81. (a) Suenik, C. N.; Bonapace, J. A. P.; Mandel, N. A.; Lau, P. Y.; Wood, G.; Bergman, R. G. *J. Am. Chem. Soc.* **1977**, *99*, 851–858. (b) See also Gavezzotti, A. *J. Am. Chem. Soc.* **1983**, *105*, 5220–5225.
82. Dunitz, J. D. "X-Ray Analysis and the Structure of Organic Molecules"; Cornell University Press; Ithaca, 1979, pp. 341–366. Here we essentially summarize this review.
83. Bürgi, H. B. *Angew. Chem.* **1975**, *87*, 461–475; *Angew. Chem. Int. Ed. Engl.* **1975**, *14*, 460–472.
84. Bürgi, H. B. *Inorg. Chem.* **1973**, *12*, 2321–2325.
85. Murray-Rust, P.; Bürgi, H. B.; Dunitz, J. D. *J. Am. Chem. Soc.* **1975**, *97*, 921–922.
86. Bürgi, H. D.; Dunitz, J. D.; Shefter, E. *J. Am. Chem. Soc.* **1973**, *95*, 5065–5067.
87. Chadwick, D. J.; Dunitz, J. D. *J. Chem. Soc., Perkin II* **1979**, 276–284.
88. Pfeiffer, P. "Organische Molekülverbindungen"; Verlag Ferdinand Enke: Stuttgart, 1927.
89. Etter, M. C.; Siedle, A. R. *Mol. Cryst. Liq. Cryst.* **1983**, *96*, 35–38.
90. Harlow, R. L.; Wells, W. J.; Watt, G. W.; Simonsen, S. H. *Inorg. Chem.* **1974**, *13*, 2106–2111.
91. Hadži, D. *J. Chem. Soc.* **1956**, 2725–2731.
92. Spinner, E.; Yeoh, G. B. *J. Chem. Soc. B* **1971**, 279–289.
93. Weis, A.; Frolow, F. *J. Chem. Soc., Chem. Comm.* **1982**, 89–90.
94. Bethel, D. E.; Sheppard, N. *J. Chem. Phys.* **1953**, *21*, 1421.
95. Luzzati, P. V. *Acta Crystallogr.* **1951**, *4*, 239–244.
96. See, for example, the comments of Romers, C. *Acta Crystallogr.* **1964**, *12*, 1287–1294.
97. See, for example, Thomas, J. M.; Evans, J. R.N.; Lewis, T. J. *Disc. Faraday Soc.* **1971**, *51*, 73–84.
98. Engelhardt, H.; Riehl, N. *Phys. Kondens. Mater.* **1966**, *5*, 73–82.
99. Bacon, G. E.; Pease, R. S. *Proc. Roy. Soc. London* **1953**, *A220*, 397–421; **1955**, *A230*, 359–381.
100. Dengel, O.; Eckener, U.; Plitz, H.; Riehl, N. *Phys. Lett.* **1964**, *9*, 291–292.
101. Cohen, M. D.; Schmidt, G. M. J.; Flavian, S. *J. Chem. Soc.* **1964**, 2041–2051.
102. Cohen, M. D.; Schmidt, G. M. J. *J. Phys. Chem.* **1962**, *66*, 2442–2446.
103. Shablya, A. V. In "Elementary Photoprocesses in Molecules"; Neporent, B. S., Ed.; Consultants Bureau: New York, 1968, pp. 145–155.
104. Sharma, B. D.; McConnell, J. F. *Acta Crystallogr.* **1965**, *19*, 797–806.

105. Brown, C. J. *Proc. Roy. Soc. London* **1968**, A302, 185–199.
106. Zimmerman, H. *Angew Chem.* **1964**, 76, 1–9.
107. Elguero, J.; Fruchier, A.; Pellegrin, V. *J. Chem. Soc., Chem. Comm.* **1981**, 1207–1208.
108. Johnson, S. L.; Rumon, K. A. *J. Phys. Chem.* **1965**, 69, 74–86.
109. Ubbelohde, A. R.; Gallagher, K. J. *Acta Crystallogr.* **1955**, 8, 71–83.
110. Chase, B. H.; Walker, J. J. *Chem. Soc.* **1953**, 3518–3525.
111. Newman, G. A.; Pauwels, P. J. S. *Tetrahedron* **1969**, 25, 4605–4615.
112. Hadzi, D. *J. Chem. Soc.* **1956**, 2143–2150.
113. Morgan, K. J. *J. Chem. Soc.* **1961**, 2151–2159.
114. Dehari, C.; Matsunaga, Y.; Tani, K. *Bull. Chem. Soc. Japan* **1970**, 43, 3404–3409.
115. Campbell, N.; Cairns-Smith, A. G. *J. Chem. Soc.* **1961**, 1191–1194.
116. Corbett, J. F. *Spectrochim. Acta* **1964**, 20, 1665–1678.
117. Schulenberg, J. W. *J. Am. Chem. Soc.* **1968**, 90, 1367–1368.
118. Walter, W.; Reubke, K.-J. *Chem. Ber.* **1969**, 102, 2117–2128.
119. Desiraju, G. R. *J. Chem. Soc., Perkin II* **1983**, 1025–1030.
120. Hertel, E.; Mischant, J. *Justus Liebigs Ann. Chem.* **1926**, 451, 179–208.
121. Briegleb, G.; Delle, H. *Z. Elektrochem.* **1960**, 64, 347–355.
122. Matsunaga, Y.; Osawa, R. *Bull. Chem. Soc. Japan* **1974**, 47, 1589–1592.
123. Dumas, J.-M.; Gomel, M. *J. Chim. Phys.* **1975**, 1185–1192.
124. Lehmann, M. S.; Herbstein, F. H.; Kapon, M.; Reisner, G. M.; Kress, R. B.; Wilson, R. B.; Shiau, W.-I.; Duesler, E. N.; Paul, I. C.; Curtin, D. Y. *Proc. Roy. Soc. London* **1985**, A399, 295–319.
125. Fyfe, C. A. Private communication cited in ref. 124.
126. Fyfe, C. A.; Bemis, L.; Childs, R.; Clark, H. C.; Curtin, D. Y.; Davies, J.; Drexler, D.; Dudley, R. L.; Gobbi, G. C.; Hartman, J. S.; Hayes, P.; Klinowski, J.; Lenkinski, R. E.; Lock, C. J. L.; Paul, I. C.; Rudin, A.; Tchir, W.; Thomas, J. M.; Wasylishen, R. E. *Phil. Trans. Roy. Soc. London* **1982**, A305, 591–607.
127. (a) Marckwald, W. *Z. Phys. Chem.* **1899**, 30, 140–145. (b) Ciamician, G.; Silber, P. *Chem. Ber.* **1901**, 34, 2040–2046. (c) For a recent review see Kaupp, G., in "Houben-Weyl Methoden der Organischen Chemie," 4th ed., Vol. IV/5a: Photochemistry, Part I; Muller, E., Ed.; Georg Thieme Verlag: Stuttgart, 1975, pp. 278–412.
128. Cohen, M. D.; Schmidt, G. M. J.; Sonntag, F. I. *J. Chem. Soc.* **1964**, 2000–2013.
129. Schmidt, G. M. J. *J. Chem. Soc.* **1964**, 2014–2021.
130. Green, B. S.; Lahav, M.; Schmidt, G. M. J. *J. Chem. Soc. B* **1971**, 1552–1564.
131. (a) Schmidt, G. M. J. in "Reactivity of the Photoexcited Organic Molecule"; Interscience: New York, 1967, pp. 227–288. (b) Frank, J. K.; Paul, I. C. *J. Am. Chem. Soc.* **1973**, 95, 2324–2332.
132. Ishigami, T.; Murata, T.; Endo, T. *Bull. Chem. Soc. Japan* **1976**, 49, 3578–3583.
133. Arad-Yellin, R.; Green, B. S. Unpublished results.
134. Hung, J. D.; Lahav, M.; Luwisch, M.; Schmidt, G. M. J. *Isr. J. Chem.* **1972**, 10, 585–599.
135. Elgavi, A. Ph.D. Thesis, Weizmann Institute of Science, Rehovot, Israel, 1974.
136. Cohen, M. D.; Green, B. S.; Ludmer, Z.; Schmidt, G. M. J. *Chem. Phys. Lett.* **1970**, 7, 486–490.
137. Sadeh, T.; Schmidt, G. M. J. *J. Am. Chem. Soc.* **1962**, 84, 3970.
138. Lahav, M.; Schmidt, G. M. J. *J. Chem. Soc. B* **1967**, 312–317.
139. Lahav, M.; Schmidt, G. M. J. *Tetrahedron Lett.* **1966**, 2957–2962.
140. Elgavi, A.; Cohen, M. D.; Green, B. S.; Ludmer, Z.; Schmidt, G. M. J. *J. Am. Chem. Soc.* **1972**, 94, 6776–6779.
141. Elgavi, A.; Green, B. S. Unpublished results.

142. Dekker, J.; Dekker, T. G. *J. Org. Chem.* **1968**, *33*, 2604–2605.
143. Jungk, A. E.; Luwisch, M.; Pinchas, S.; Schmidt, G. M. *J. Isr. J. Chem.* **1977**, *16*, 308–310.
144. Cookson, R. C.; Cox, D. A.; Hudec, J. *J. Chem. Soc.* **1961**, 4499–4502.
145. Green, B. S. Unpublished results.
146. Rabinovich, D.; Schmidt, G. M. *J. J. Chem. Soc. B.* **1967**, 144–149.
147. Dekker, J.; van Vuuren, P. J.; Ventner, D. P. *J. Org. Chem.* **1968**, *33*, 464–466.
148. Rieke, R. D.; Copenhafer, R. A. *Tetrahedron Lett.* **1971**, 879–882.
149. Kaupp, G.; Jostkleigrewe, E.; Hermann, H.-J. *Angew. Chem.* **1982**, *94*, 457–458; *Angew. Chem. Int. Ed. Engl.* **1982**, *21*, 435–436.
150. Berkovitch-Yellin, Z.; Lahav, M.; Leiserowitz, L. *J. Am. Chem. Soc.* **1974**, *96*, 918–920.
151. Ramasubbu, N.; Guru Row, T. N.; Venkatesan, K.; Ramamurthy, V.; Ramachandra Rao, C. N. *J. Chem. Soc., Chem. Comm.* **1982**, 178–179.
152. (a) Filler, R.; Piasek, E. *J. Org. Chem.* **1963**, *28*, 221–222. (b) Scheffer, J. R.; Dzakpasu, A. A. *J. Am. Chem. Soc.* **1978**, *100*, 2163–2173. (c) Nakanishi, H.; Jones, W.; Thomas, J. M. *Chem. Phys. Lett.* **1980**, *71*, 44–54.
153. Bolt, J.; Quina, F. H.; Whitten, D. G. *Tetrahedron Lett.* **1976**, 2595–2598.
154. Kutschabsky, L.; Reck, G.; Höhne, E.; Voigt, B.; Adam, G. *Tetrahedron* **1980**, *36*, 3421–3425.
155. Leiserowitz, L.; Schmidt, G. M. *J. J. Chem. Soc. A* **1969**, 2372–2382.
156. Green, B. S.; Leser, J.; Schmidt, G. M. J. To be published.
157. Bregman, J.; Osaki, K.; Schmidt, G. M. J.; Sonntag, F. I. *J. Chem. Soc.* **1964**, 2021–2030.
158. Desiraju, G. R.; Sarma, J. A. R. P. *J. Chem. Soc., Chem. Comm.* **1983**, 45–46.
159. Alcock, N. W.; Herron, N.; Kemp, T. J.; Shoppee, C. W. *J. Chem. Soc., Chem. Comm.* **1975**, 785–786.
160. Adams, J. M.; Pritchard, R. G.; Thomas, J. M. *J. Chem. Soc., Chem. Comm.* **1976**, 358–359.
161. Desiraju, G. R.; Kamala, R.; Kumari, B. H.; Sarma, J. A. R. P. *J. Chem. Soc., Perkin II* **1984**, 181–189.
162. Jones, W.; Ramdas, S.; Theocharis, C. R.; Thomas, J. M.; Thomas, N. W. *J. Phys. Chem.* **1981**, *85*, 2594–2597.
163. Arad-Yellin, R. Ph.D. Thesis, Weizmann Institute of Science, Rehovot, Israel, 1977.
164. (a) Craig, D. P.; Sarti-Fantoni, P. *J. Chem. Soc., Chem. Comm.* **1966**, 742–743. (b) Thomas, J. M.; Williams, J. O. *Mol. Cryst. Liq. Cryst.* **1969**, *9*, 59–79. (c) Cohen, M. D.; Klein, E.; Ludmer, Z. *Chem. Phys. Lett.* **1976**, *37*, 611–613.
165. (a) Heller, E.; Schmidt, G. M. *J. Isr. J. Chem.* **1971**, *9*, 449–462. (b) Cohen, M. D.; Ludmer, Z.; Thomas, J. M.; Williams, J. O. *Proc. Roy. Soc. London* **1971**, *A324*, 459–468.
166. (a) Cohen, M. D.; Cohen, R.; Lahav, M.; Nie, P. L. *J. Chem. Soc., Perkin II* **1973**, 1059–1100. (b) Cohen, M. D.; Cohen, R. *J. Chem. Soc., Perkin II* **1976**, 1731–1735.
167. Leftin, J. H.; Redpath, D.; Pines, A.; Gil-Av, E. *Isr. J. Chem.* **1973**, *11*, 75–77.
168. Hirshfeld, F. L.; Schmidt, G. M. *J. J. Polymer Sci. A* **1964**, *2*, 2181–2190.
169. (a) For a review see Nakanishi, H.; Hasegawa, M.; Sasada, Y. *J. Polymer Sci., Polymer Phys. Ed.* **1977**, *15*, 173–191. (b) Nakanishi, H.; Jones, W.; Thomas, J. M.; Hasegawa, M.; Rees, W. L. *Proc. Roy. Soc. London* **1980**, *A369*, 307–325.
170. Nakanishi, H.; Hasegawa, M.; Sasada, Y. *J. Polymer Sci. A-2* **1972**, *10*, 1537–1553.
171. Jones, W. *J. Chem. Res. [S]* **1978**, 142–143.
172. Meyer, W.; Lieser, G.; Wegner, G. *Makromol. Chem.* **1977**, *178*, 631–634.
173. Meyer, W.; Lieser, G.; Wegner, G. *J. Polymer Sci., Polymer Phys. Ed.* **1978**, *16*, 1365–1379.

174. Bernstein, J.; Green, B. S.; Rejtö, M. *J. Am. Chem. Soc.* **1980**, *102*, 323–328.
175. Addadi, L.; Lahav, M. *J. Am. Chem. Soc.* **1979**, *101*, 2152–2156.
176. Rennert, J.; Ruggiero, E. M.; Rapp, J. *Photochem. Photobiol.* **1967**, *6*, 29–34.
177. Curme, H. G.; Natale, C. C.; Kelley, D. J. *J. Phys. Chem.* **1967**, *71*, 767–770.
178. Williams, J. L. R. *Top. Curr. Chem.* **1969**, *13*, 227–250.
179. Green, B. S.; Rabinsohn, Y.; Rejtö, M. *J. Chem. Soc., Chem. Comm.* **1975**, 313–314.
180. Beak, P.; Zeigler, J. M. *J. Org. Chem.* **1981**, *46*, 619–624.
181. Egerton, P. L.; Hyde, E. M.; Trigg, J.; Payne, A.; Beynon, P.; Mijovic, M. V.; Reiser, A. *J. Am. Chem. Soc.* **1981**, *103*, 3859–3863.
182. For reviews see Scheffer, J. R. *Acc. Chem. Res.* **1980**, *13*, 283–290; Appel, W. K.; Jiang, Z. Q.; Scheffer, J. R.; Walsh, L. *J. Am. Chem. Soc.* **1983**, *105*, 5354–5363.
183. Thomas, J. M. *Nature* **1981**, *289*, 633–634.
184. Cohen, M. D. *Angew. Chem.* **1975**, *87*, 439–447; *Angew. Chem. Int. Ed. Engl.* **1975**, *14*, 386–393.
185. (a) Jones, W.; Nakanishi, H.; Theocharis, C. R.; Thomas, J. M. *J. Chem. Soc., Chem. Comm.* **1980**, 610–611. (b) Nakanishi, H.; Jones, W.; Thomas, J. M.; Hursthouse, M. B.; Motevalli, M. *J. Chem. Soc., Chem. Comm.* **1980**, 611–612.
186. Nakanishi, H.; Jones, W.; Thomas, J. M. *Chem. Phys. Lett.* **1980**, *71*, 44–48.
187. See, for example, Osaki, J.; Schmidt, G. M. *J. Isr. J. Chem.* **1972**, *10*, 189–193.
188. Ron, I. Unpublished results cited in ref. 5.
189. Baeyer, A.; Lansberg, L. *Ber Deutsch. Chem. Ges.* **1882**, *15*, 57–61.
190. Wegner, G. *Z. Naturforsch.* **1969**, *24b*, 824–832.
191. For recent reviews see Baughman, R. H.; Chance, R. R. *Ann. N.Y. Acad. Sci.* **1978**, *313*, 705–724; Baughman, R. H.; Yee, K. C. *J. Polymer Sci. Macromol. Rev.* **1978**, *13*, 219–239; Wegner, G. in “Molecular Metals”; Hatfield, W., Ed.; Plenum: New York, 1979, pp. 209–228; Bloor, D. in “Developments in Crystalline Polymers—I”; Bassett, D. C., Ed.; Applied Science Publishers: Barking, U.K., 1983, pp. 151–193.
192. Day, D. R.; Ringsdorf, H. *Macromol. Chem.* **1979**, *180*, 1059–1063; Tieke, B.; Enkelmann, V.; Kapp, H.; Lieser, G.; Wegner, G. *J. Macromol. Sci.-Chem.* **1981**, *A15*, 1045–1058. Day, D. R.; Lando, J. B. *J. Appl. Polymer Sci.* **1981**, *26*, 1605–1612.
193. Preziosi, A. F.; Morris, R. C.; Baughman, R. H. Unpublished results cited in Baughman, R. H.; Yee, K. C. (191).
194. Day, D. R.; Lando, J. B. *J. Polymer Sci. Polymer Phys. Ed.* **1973**, *11*, 1009–1022.
195. Enkelmann, V.; Lando, J. B. *Acta Crystallogr.* **1978**, *34B*, 2352–2353.
196. (a) Haedicke, E.; Mez, E. C.; Krauch, C. H.; Wegner, G.; Kaiser, G. *Angew. Chem.* **1971**, *83*, 251–252; *Angew. Chem. Int. Ed. Engl.* **1971**, *10*, 266–267. (b) Haedicke, E.; Penzien, K.; Schnell, H. W. *Angew. Chem.* **1971**, *83*, 1024–1025; *Angew. Chem. Int. Ed. Engl.* **1971**, *10*, 940–941.
197. Baughman, R. H. *J. Appl. Phys.* **1972**, *43*, 4362–4370.
198. Kobelt, D.; Paulus, E. F. *Acta Crystallogr.* **1974**, *B30*, 232–234.
199. Enkelmann, V.; Wegner, G. *Angew. Chem.* **1977**, *89*, 432; *Angew. Chem. Int. Ed. Engl.* **1977**, *16*, 416.
200. Chance, R. R.; Baughman, R. H.; Müller, H.; Eckhardt, C. J. *J. Chem. Phys.* **1977**, *67*, 3616–3618.
201. Iqbal, Z.; Chance, R. R.; Baughman, R. H. *J. Chem. Phys.* **1977**, *66*, 5520–5525.
202. Baughman, R. H. and Chance, R. R. (191).
203. Bloor, D.; Kennedy, R. J.; Batchelder, D. N. *J. Polymer Sci., Polymer Phys. Ed.* **1979**, *17*, 1355–1366.
204. Lando, J. B.; Day, D. R.; Enkelmann, V. *J. Polymer Sci., Polymer Symp.* **1978**, *65*, 73–78.

205. Kaiser, J.; Wegner, G.; Fischer, E. W. *Isr. J. Chem.* **1972**, *10*, 157–171.
206. Schermann, W.; Wegner, G.; Williams, J. O.; Thomas, J. M. *J. Polymer Sci., Polymer Phys. Ed.* **1975**, *13*, 753–763.
207. Baughman, R. H.; Chance, R. R. *J. Appl. Phys.* **1976**, *47*, 4295–4300.
208. Pople, J. A.; Walmsley, S. H. *Mol. Phys.* **1962**, *5*, 15–20.
209. Baughman, R. H. In "Contemporary Topics in Polymer Science," Vol. 2; Pearce, E. M.; Schaeffgen, J. R., Eds.; Plenum: New York, 1979, pp. 205–228.
210. Baughman, R. H. *J. Polymer Sci. Polymer Phys. Ed.* **1974**, *12*, 1511–1535.
211. Wegner, G.; Fischer, E. W.; Munoz-Escalona, A. *Makromol. Chem. Suppl.* **1975**, *1*, 521–558.
212. Hardy, G. In "Kinetics and Mechanisms of Polyreactions"; Tüdös, E., Ed.; Akademiai Kiado: Budapest, 1971, p. 571.
213. Kiji, T.; Kaiser, J.; Wegner, G.; Shulz, R. C. *Polymer (London)* **1973**, *14*, 433–439.
214. Banerjee, A.; Lando, J. B.; Yee, K. C.; Baughman, R. H. *J. Polymer Sci., Polymer Phys. Ed.* **1979**, *17*, 655–662.
215. Steinback, M.; Wegner, G. *Makromol. Chem.* **1977**, *178*, 1671–1677.
216. Enkelmann, V.; Schleier, G. Unpublished results. Eichele, H. Thesis, Bayreuth, 1978. Both cited by Wegner, G., in ref. 191.
217. (a) Atwood, J. L.; Davies, J. E. D.; MacNicol, D. D., Eds. "Inclusion Compounds," Vols. 1–3; Academic: London, 1984. (b) Speakman, J. C. In "Structure and Bonding," Vol. 12; Dunitz, J. D., Ed.; Springer Verlag: Berlin, 1972, pp. 141–199.
218. Leiserowitz, L.; Nader, F. *Acta Crystallogr.* **1977**, *B33*, 2719–2733.
219. Bernstein, J.; Cohen, M. D.; Leiserowitz, L. In "The Chemistry of the Quinonoid Compounds"; Patai, S., Ed.; Wiley: New York, 1974, pp. 37–110.
220. Vögtle, F.; Sieger, H.; Müller, W. M. *Top. Curr. Chem.* **1981**, *98*, 107–161.
221. Pederson, C. J. *J. Org. Chem.* **1971**, *36*, 1690–1693.
222. Hilgenfeld, R.; Saenger, W. *Angew. Chem.* **1981**, *93*, 1082–1083; *Angew. Chem. Int. Ed. Engl.* **1981**, *20*, 1045–1046.
223. Saenger, W. *Angew. Chem.* **1980**, *92*, 343–361; *Angew. Chem. Int. Ed. Engl.* **1980**, *19*, 344–362.
224. Szejtli, J., Ed. "Proceedings of the First International Symposium on Cyclodextrins (Budapest)"; Reidel: Dordrecht, The Netherlands, 1982.
225. Hagan, M. "Clathrate Inclusion Compounds"; Reinhold: New York, 1962. Mandelcorn, L., Ed. "Non-Stoichiometric Compounds"; Academic: New York, 1964.
226. (a) MacNicol, D. D.; McKendrick, J. J.; Wilson, D. R. *Chem. Soc. Rev.* **1978**, *7*, 65–87. (b) MacNicol, D. D. In "Inclusion Compounds"; Vol. 2; Atwood, J. L.; Davies, J. E. D.; MacNicol, D. D., Eds.; Academic: London, 1984, pp. 123–168.
227. (a) Jones, R. E.; Templeton, D. H. *Acta Crystallogr.* **1958**, *11*, 484–487. (b) Leiserowitz, L. *Acta Crystallogr.* **1976**, *B32*, 775–802.
228. Craven, B. M.; De Titta, G. T. *J. Chem. Soc., Chem. Comm.* **1972**, 530–531.
229. Freer, A.; Gilmore, C. J.; MacNicol, D. D.; Swanson, S. *Tetrahedron Lett.* **1980**, *21*, 205–208.
230. Goldberg, I. *J. Am. Chem. Soc.* **1982**, *104*, 7077–7084.
231. Arad-Yellin, R.; Green, B. S.; Knossow, M.; Rysanek, N.; Tsoucaris, G. *J. Incl. Phenom.* **1985**, *3*, 317–333.
232. Brown, J. F.; White, D. M. *J. Am. Chem. Soc.* **1960**, *82*, 5671–5678.
233. White, D. M. *J. Am. Chem. Soc.* **1960**, *82*, 5678–5685.
234. Krimm, S.; Shipman, J. J.; Folt, V. L.; Berens, A. R. *J. Polymer Sci. B* **1965**, *3*, 275–278.
235. (a) Miyata, M.; Shinmen, K.; Takemoto, K. *Angew. Makromol. Chem.* **1978**, *72*, 151–160.

- (b) Finter, J.; Wegner, G. *Makromol. Chem.* **1979**, *180*, 1093–1097. (c) Farina, M.; Di Silvestro, G. *J. Chem. Soc., Chem. Comm.* **1976**, 842–843.
236. Farina, M.; Audisio, G.; Natta, G. *J. Am. Chem. Soc.* **1967**, *89*, 5071.
237. Audisio, G.; Silvani, A. *J. Chem. Soc., Chem. Comm.* **1976**, 481–782.
238. Dewar, M. J. S.; Nahlovsky, B. D. *J. Am. Chem. Soc.* **1974**, *96*, 460–465.
239. Casal, H. L.; de Mayo, P.; Miranda, J. F.; Scaiano, J. C. *J. Am. Chem. Soc.* **1983**, *105*, 5155–5156.
240. Arad-Yellin, R.; Brunie, S.; Green, B. S.; Knossow, M.; Tsoucaris, G. *J. Am. Chem. Soc.* **1979**, *101*, 7529–7537.
241. Popovitz-Biro, R.; Chang, H. C.; Tang, C. P.; Shochet, N.; Lahav, M.; Leiserowitz, L. In "Chemical Approaches to Understanding Enzyme Catalysis: Biomimetic Chemistry and Transition-State Analogs"; Green, B. S.; Ashani, Y.; Chipman, D., Eds.; Elsevier: Amsterdam, 1982, pp. 88–105.
242. Tanaka, Y.; Sakuraba, H.; Nakanishi, H. *J. Chem. Soc., Chem. Comm.* **1983**, 974–948.
243. (a) Reference 56, and references cited therein. (b) Popovitz-Biro, R.; Chang, H. C.; Tang, C. P.; Shochet, N.; Lahav, M.; Leiserowitz, L.; *Pure Appl. Chem.* **1980**, *52*, 2693–2704. (c) Popovitz-Biro, R.; Tang, C. P.; Chang, H. C.; Lahav, M.; Leiserowitz, L.; *J. Am. Chem. Soc.* **1985**, *107*, 4053–4058. (d) Tang, C. P.; Chang, H. C.; Popovitz-Biro, R.; Frolov, F.; Lahav, M.; Leiserowitz, L.; McMullen, R. K.; *J. Am. Chem. Soc.* **1985**, *107*, 4058–4070 and references cited therein.
244. Overberger, C. G.; Yaroslowsky, C. *Tetrahedron Lett.* **1965**, 4395–4398.
245. Quinkert, G.; Tabata, T.; Hickmann, E. A. J.; Dobrat, W. *Angew. Chem.* **1970**, *83*, 212–213; *Angew. Chem. Int. Ed. Engl.* **1971**, *10*, 199–200.
246. McBride, J. M. *Acc. Chem. Res.* **1983**, *16*, 304–312.
247. Jaffe, A. B.; Malament, D. S.; Slisz, E. P.; McBride, J. M. *J. Am. Chem. Soc.* **1972**, *94*, 8515–8521.
248. McBride, J. M. *J. Am. Chem. Soc.* **1971**, *93*, 6302–6303.
249. Skinner, K. J.; Blaskiewicz, R. J.; McBride, J. M. *Isr. J. Chem.* **1972**, *10*, 457–570.
250. Walling, C.; Cekovic, Z. *J. Am. Chem. Soc.* **1967**, *89*, 6681–6684.
251. Karch, N. J.; Koh, E. T.; Whitsel, B. L.; McBride, J. M. *J. Am. Chem. Soc.* **1975**, *97*, 6729–6743.
252. Walter, D. W.; McBride, J. M. *J. Am. Chem. Soc.* **1981**, *103*, 7069–7073, 7074–7084.
253. Hollingsworth, M. D. Unpublished results cited in ref. 246.
254. (a) Baughman, R. H. *J. Chem. Phys.* **1978**, *68*, 3110–3121. (b) Kröhnke, C.; Enkelmann, V.; Wegner, G. *Chem. Phys. Lett.* **1980**, *71*, 38–43.
255. Green, B. S.; Lahav, M.; Rabinovich, D. *Acc. Chem. Res.* **1979**, *12*, 191–197.
256. Jacques, J.; Collet, A.; Wilen, S. H. "Enantiomers, Racemates and Resolutions"; Wiley: New York, 1981.
257. Curtin, D. Y.; Paul, I. C. *Chem. Rev.* **1981**, *81*, 525–541.
258. Addadi, L.; van Mil, J.; Lahav, M. *J. Am. Chem. Soc.* **1982**, *104*, 3222–3229.
259. Green, B. S.; Rabinovich, D.; Shakked, Z.; Hope, H.; Swanson, K. *Acta Crystallogr.* **1981**, *B37*, 1376–1380.
260. Elgavi, A.; Green, B. S.; Schmidt, G. M. J. *J. Am. Chem. Soc.* **1973**, *95*, 2058–2059.
261. Green, B. S.; Heller, L. *Science* **1974**, *185*, 525–527.
262. Addadi, L.; van Mil, J.; Gati, E.; Lahav, M. In "Origin of Life"; Wolman, Y., Ed.; Reidel: Dordrecht, The Netherlands, 1981, pp. 355–364.
263. Holland, H. L.; Richardson, M. F. *Mol. Cryst. Liq. Cryst.* **1980**, *58*, 311–314.
264. Chenchiah, P. C.; Holland, H. L.; Richardson, M. F. *J. Chem. Soc., Chem. Comm.* **1982**, 436–437.

- 265. Lahav, M.; Laub, F.; Gati, E.; Leiserowitz, L.; Ludmer, Z. *J. Am. Chem. Soc.* **1976**, *98*, 1620–1622. Ludmer, Z.; Lahav, M.; Leiserowitz, L.; Roitman, L. *J. Chem. Soc., Chem. Comm.* **1982**, 326–328.
- 266. Green, B. S.; Knossow, M. *Science*, **1981**, *214*, 795–797.
- 267. Addadi, L.; Berkovitch-Yellin, Z.; Domb, N.; Gati, E.; Lahav, M.; Leiserowitz, L. *Nature*, **1982**, *296*, 21–26.
- 268. Addadi, L.; Weinstein, S.; Gati, E.; Weissbuch, I.; Lahav, M. *J. Am. Chem. Soc.* **1982**, *104*, 4610–4617.
- 269. Berkovitch-Yellin, Z.; Addadi, L.; Idelson, M.; Lahav, M.; Leiserowitz, L. *Angew. Chem. Suppl.* **1982**, 1336–1345.
- 270. Addadi, L.; Berkovitch-Yellin, Z.; Weissbuch, I.; Lahav, M.; Leiserowitz, L.; Weinstein, S. *J. Am. Chem. Soc.* **1982**, *104*, 2075–2077.
- 271. Weissbuch, I.; Addadi, L.; Berkovitch-Yellin, Z.; Gati, E.; Weinstein, S.; Lahav, M.; Leiserowitz, L. *J. Am. Chem. Soc.* **1983**, *105*, 6615–6621.
- 272. Berkovitch-Yellin, Z.; Addadi, L.; Idelson, M.; Leiserowitz, L.; Lahav, M. *Nature*, **1982**, *296*, 27–34.

Substituent Effects on ^{13}C Chemical Shifts in Aliphatic Molecular Systems. Dependence on Constitution and Stereochemistry

HELMUT DUDDECK

*Ruhr-Universität Bochum
Abteilung für Chemie
Federal Republic of Germany*

Symbols and Abbreviations Used	220
I. Introduction	220
II. Basic Concepts	222
A. Theoretical Considerations	222
B. Transmission Mechanisms	225
1. Inductive Effects	226
2. Neighbor-Anisotropy and Ring-Current Effects	227
3. Electric-Field Effects	228
4. Other Effects	230
III. Substituent Effects and Their Structure Dependence	230
A. α -Effects	233
B. β -Effects	241
C. γ -Gauche Effects	245
D. γ -Anti Effects	254
E. δ -Effects	261
F. Long-Range Effects	265
G. Lone-Electron-Pair Effects	266
IV. Intramolecular Interaction Effects	268
A. Geminal Substituents; Heavy-Atom Effects	270
B. Vicinal Substituents	276
C. Remote Substituents	282
D. Three-Membered Rings	289
V. Survey of Substituent Effects	292
A. ^{13}C Chemical-Shift Calculation Rules	293
B. Specific Substituents and Molecular Systems	300
1. Special Substituents	300
2. Specific Molecular Systems	302
a. Three-Membered Rings	302
b. Four-Membered Rings	302

c. Five-Membered Rings	303
d. Six-Membered Rings	303
e. Polycyclic Systems	305
VI. Conclusion and Prospects	309
Acknowledgments	310
References	311

SYMBOLS AND ABBREVIATIONS USED

δ , δ_{C} , carbon chemical shift, referred to tetramethylsilane ($\delta = 0$) (cf. Sect. I); SCS, substituent-induced chemical shift, or substituent effect: difference between δ 's of a given carbon atom in a monosubstituted and the respective unsubstituted parent molecule (cf. Sect. III); NAE, nonadditivity effect: nonadditivity of individual SCSs in disubstituted molecules (cf. Sect. IV); ICS, intramolecular-interaction chemical shift \equiv NAE (cf. Sect. IV); Δ , polarization effect: difference in δ 's of sp^2 carbon atoms in a double bond (cf. Sect. IV-C); LEF, linear electric field (cf. Sect. II-B-3); SEF, square electric field (cf. Sect. II-B-3).

I. INTRODUCTION

Since the early 1970s nuclear magnetic resonance (NMR) spectroscopy of ^{13}C nuclei has become a powerful tool for elucidation of the structures of organic compounds. A large number of textbooks, monographs, articles, and data collections (1–15) deal with this method, and individual reviews have been devoted to practically all classes of natural products and related organic compounds (16–24).

Nevertheless, ^{13}C NMR spectroscopy has not yet reached the importance and ubiquity of ^1H NMR, and detailed discussions of ^{13}C spectral parameters are still reserved to specialists. One of the reasons is that generally the structure dependence of ^{13}C chemical shifts (δ_{C}) is much more intricate than that for protons. Carbon-13 chemical shifts cover a much larger range (ca. 250 ppm for neutral organic molecules) and are more sensitive to structural changes, reflecting even those at remote sites. Moreover, ^{13}C NMR spectroscopy monitors the very backbone of the molecule and not the periphery. This implies a great advantage over ^1H NMR. Unfortunately, however, it has turned out that the position of a ^{13}C resonance is subject to a variety of structural influences, and often it is very difficult to evaluate their individual contributions. Moreover, it may be unknown if these contributions are additive, cooperative, or counteracting. Finally, the

physical background of many of these structural influences, that is, substituent effects, is not at all fully understood theoretically. An instructive example of this is the famous γ -effect (Sections III-C and III-D).

An inspection of original papers and reviews dealing with the dependence of ^{13}C spectral parameters on structure reveals that aliphatic compounds have been inadequately considered, whereas substituent effects on sp^2 carbon atoms in unsaturated molecules have been widely interpreted in terms of inductive, mesomeric, through-space, or other mechanisms (2-5,8,25-27) and correlated with calculated charge densities or physicochemical parameters such as Hammett constants (27). So, for example, one survey (8) discusses relations of electronic structure and ^{13}C NMR for alkenes, aromatics, and unsaturated functional groups in 62 pages, whereas just 3 are reserved for alkanes, and research in the area of unsaturated compounds is still very active (28) and clearly exceeds corresponding work in the field of substituted aliphatic and alicyclic compounds. The obvious reason is that interpretations correlating δ_{C} with calculations or physicochemical parameters are much easier for π - than for σ -systems.

Even now it is still impossible to present a comprehensive and consistent treatment of the influences of structure on chemical shifts of sp^3 hybridized carbon atoms. In turn, this has led to some frustration concerning the applicability of ^{13}C NMR in confirmation and elucidation of the structures of aliphatic molecules (especially if they are highly substituted) and its ability to monitor electronic states, on which so many hopes had been pinned. Nevertheless, the number of publications using δ_{C} values empirically is still increasing. Thus, it seems that a situation has been reached where physical understanding is becoming buried under an overwhelming mass of uninterpreted or even misinterpreted data.

Thus, this chapter is intended as an inventory and critical summary of what is known, thereby serving as a directory through the complex body of data as well as a warning to the unwary. If beyond that the survey can stimulate NMR specialists and theoreticians to continue and, if possible, intensify their efforts, it will have achieved its objective of being a step toward the ultimate understanding of ^{13}C spectral parameters.

The literature has been covered as far as it was available to the author until the fall of 1983. In the course of the literature search certain difficulties had to be overcome. Many publications contain valuable ^{13}C NMR information without mentioning so explicitly in the title or abstract; thus, the information cannot easily be retrieved, even through *Chemical Abstracts*. Various reviews as well as computer search systems have been utilized as sources. Moreover, due to the enormous wealth of ^{13}C NMR spectral data that has appeared in the last decade it is impossible to include all information available. Omission of certain papers, however, does not at all imply judgment as to their scientific value. In the beginning of this chapter (Sect. II) a brief account is presented of the basic

concepts of ^{13}C chemical shifts. Since these concepts have already been reviewed several times, on various levels of sophistication, the summary is limited to what is needed later in the chapter.

There follows in Sect. III a detailed discussion of substituent effects and their dependence on different geometric relationships of carbon atoms with respect to the perturbing group. This, however, is strictly confined to sp^3 carbon atoms, though allowing for all conceivable kinds of substituents, including unsaturated ones (phenyl, cyano, etc.).

Sect. IV relates to ^{13}C NMR evidence for intramolecular interactions in various types of molecules that have not yet been comprehensively reviewed. In that section, therefore, the restriction to aliphatic molecules has been somewhat relaxed. Excluded, however, are interactions via extended unsaturated systems and conjugation effects.

The last section is a compilation of useful empirical additivity rules for ^{13}C chemical-shift prediction, regardless of underlying transmission mechanisms. Peculiarities of less common substituents are cited, and, finally, substituent-induced ^{13}C signal shifts in various cyclic compounds are discussed, with special emphasis on their use in conformational analysis; I do not, however, claim completeness for this latter discussion.

II. BASIC CONCEPTS

A. Theoretical Considerations

The first theoretical treatment of the nuclear shielding σ^A of a nucleus A was published by Ramsey (29) in 1950. Shortly thereafter, Saika and Slichter proposed a more practical partition of σ^A into three components (30):

$$\sigma^A = \sigma_d^{AA} + \sigma_p^{AA} + \sigma' \quad [1]$$

where σ_d^{AA} is the diamagnetic term due to spherical circulation of electrons (*s*-electrons) and can be represented by the Lamb formula (31):

$$\sigma_d^{AA} = \frac{e^2}{3mc^2} \sum_i \langle r_i^{-1} \rangle \quad [2]$$

with $\langle r_i^{-1} \rangle$ being the mean inverse distance of the *i*th electron. The second component, σ_p^{AA} , is the paramagnetic term resulting from nonspherical electron distribution (*p*-electrons) and taking into account the mixing of ground and excited states by the magnetic field. This term was later formulated for the carbon nucleus by Karplus and Pople (32) as:

$$\sigma_p^{AA} = -\frac{e^2 h^2}{2m^2 c^2} (\Delta E)^{-1} \langle r^{-3} \rangle_{2p} (Q_{AA} + \sum_{B \neq A} Q_{AB}) \quad [3]$$

where ΔE is the mean excitation energy, $\langle r^{-3} \rangle_{2p}$ is the mean value of the $2p$ -electron dimensions and Q_{AA} represents the local charge density and Q_{AB} the bond orders for bonds of the observed carbon atom A to adjacent atoms B. The third term in eq. [1], σ' , includes all neighbor-atom effects on σ^A and has been divided (32) into a contribution: $\sum_{B \neq A} \sigma^{AB}$ from electrons at neighbor atoms B and a ring-current contribution $\sigma^{A, \text{ring}}$ from delocalized electrons.

It has been claimed (32,33) that the dominant factor governing the shielding of carbon nuclei is σ_p^A and that substituent influences on σ^A can be adequately described by this paramagnetic contribution (34). So, for example, the deshielding of a carbon atom by methyl substitution ($C^A-H \rightarrow C^A-CH_3$) has been attributed to a charge-polarization effect contracting the C^A orbitals, that is, decreasing the $2p$ -electron dimensions and thereby enlarging the $\langle r^{-3} \rangle_{2p}$ factor (33). Conversely, an increase of electron density at C^A is associated with an expansion of the $2p$ -electron clouds, that is, a reduction of this factor (35). This, however, requires that ΔE , Q_{AA} , and Q_{AB} be regarded as constant, a condition that at best is met only in a series of very similar compounds such as alkanes. Otherwise, changes in ΔE can no longer be ignored. Unfortunately, ΔE is a difficult factor to estimate, since the nature of the excited states has to be examined carefully to avoid false conclusions (36). In favored cases, ΔE may be equated with the lowest electronic transition, as was done when $C=O$ chemical shifts in ketones were correlated with the $n\pi^*$ transition energies of that chromophore (37). For a variety of substituted alkanes, alkenes, alkynes, and carbonyl compounds, "effective excitation energies" $\overline{\Delta E}$ were defined and calculated using MINDO/1 wave functions (38), and it was claimed that $\overline{\Delta E}$ is the most important factor determining σ_p^A , and is not at all constant even in well-defined compound series.

The idea of a constant diamagnetic term (32,33) has been challenged, and it was concluded from semiempirical calculations that σ_d^A cannot be neglected (39). Mason (40,41) suggested that diamagnetic terms be calculated using Flygare's expression (42):

$$\sigma_d^A = \sigma_d^A (\text{free atom}) + \frac{e^2}{3mc^2} \sum_{B \neq A} \frac{Z_B}{r_B} \quad [4]$$

where Z_B is the atomic number of atom B and r_B its distance from atom A, with the set of B atoms comprising all the atoms in the molecule except the observed carbon atom A. The free-carbon-atom value has been given by Malli and Fraga (43). Additivity was found for "corrected shieldings" ($\sigma^A - \sigma_d^A$) in various linear, cyclic, and branched alkanes, as well as in polysubstituted methane derivatives (40) (cf. Section IV-A), and more recently, Mason reported (44) experimental confirmation of the calculated (42) σ_d^A values from X-ray photoelectron spectroscopy. In conclusion, Mason states (41) that σ_d^A may not

necessarily be more important than σ_p^{AA} in determining σ^{A} , but it can readily be used as a "physical correction" to make σ_p^{AA} a parameter more easily interpretable in terms of structure and bonding variations. Following Mason's approach (40,41), Shabab discussed substituent effects in adamantanes, corresponding heterocycles and bicyclo[2.2.2.]octanes (45).

A compromise between the opposing interpretations of Pople and Mason is offered by Webb and co-workers (46). These authors conclude that it is improper to equate the diamagnetic terms used by the two authors, since in contrast to Pople's σ_d^{AA} , Flygare's contains significant and variable nonlocal contributions and is comparable rather to the gauge-dependent term in the original Ramsey expression (29).

A great many *ab initio* and semiempirical calculations of shielding parameters were carried out and reviewed in the mid-1970s (25,47). Only a few representative studies dealing with substituent effects on the ^{13}C chemical shift will be discussed here. Lazzeretti and Taddei found that for substituted methanes linear correlations between ^{13}C chemical shifts and MOLCAO-calculated σ -electron charge densities exist, but are restricted to substituents of the same row in the periodic system (48). Miyajima and Nishimoto extended these molecular orbital calculations to ethyl, *n*-propyl, isopropyl, and *n*-butyl derivatives (49) and reported deviations from the correlation only for the highly anisotropic substituents $-\text{NO}_2$ and $-\text{CN}$; they thus concluded that substituent effects on α - and β -carbon atoms are mainly inductive in nature. Fluorine effects have attracted particular theoretical interest (47). Thus, Maciel and co-workers (50) succeeded in reproducing ^{13}C chemical shifts of simple fluorine-containing molecules using their INDO perturbation method (51), and so did a Russian group (52). Even in larger and alicyclic compounds like cyclohexanols and D-glucose, charge-density changes due to introduction of hydroxyl groups could be roughly calculated, using extended Hückel theory (EHT) (53); however, configurational variations (equatorial vs. axial hydroxyls) could not be differentiated. The *ab initio* calculations performed by Fliszár and his co-workers (54) for very large saturated compounds like adamantanes and related six-membered polycyclic molecules should be mentioned. Very recently, Schindler and Kutzelnigg (55) presented *ab initio* calculations of ^{13}C chemical shifts in medium-sized organic molecules, mainly hydrocarbons, based on the individual gauge for localized orbitals (IGLO). By this method a system of increments that have direct physical meaning was established. These authors claim that their approach will fill the gap between *ab initio* theory and qualitative understanding (55).

In summary, it may be said that theoretical calculations, both *ab initio* and semiempirical, are not yet feasible, as they are too coarse a tool for the quantitative interpretation of subtle changes in carbon shieldings caused by slight molecular modifications, at least for aliphatic compounds. Nevertheless, they

are of undisputed merit in helping us to understand the electronic basis of the underlying transmission mechanisms.

B. Transmission Mechanisms

As already stated, theoretical calculations are as yet too involved and not accurate enough for routine ^{13}C NMR spectral interpretation, particularly where more complicated molecules are concerned; probably this situation will not change in the near future. Therefore, different approaches have been developed to identify certain influences of structural modifications, for example substituent introduction, on ^{13}C shieldings. The partition of σ^\wedge into two local (σ^\wedge_d and σ^\wedge_p) and several nonlocal contributions (30,32) is reasonable on physical grounds. On that basis, the factors that play a role in organic molecules were divided into two classes (56):

- | | |
|-------------------------|--|
| Local contributions: | local diamagnetic currents
local paramagnetic currents |
| Nonlocal contributions: | neighbor-anisotropy effects
ring-current effects
electric-field effects
steric effects
van der Waals compression
intermolecular (e.g., solvent) effects |

Obviously, it is impossible to differentiate local contributions from effects of remote atoms or groups, so Raynes (56) suggested arranging the various effects according to another criterion, one that is more reasonable in a chemical sense, namely the transmission pathway.

The first group of transmission effects comprises those operating through bonds, that is, inductive, conjugative, and hyperconjugative influences. Neighbor-anisotropy, ring-current, electric-field, van der Waals, and steric effects form the second group, since all of these factors act through space.

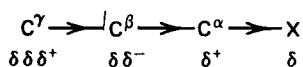
A more sophisticated framework of different interlocking mechanisms was established by Maciel (57), but both Raynes and Maciel stress that dividing the nuclear shielding into independent contributions is unsuccessful on a quantitative basis. Generally, modifications in structure affect the operation not only of one but of several transmission mechanisms, and often these are interdependent. Moreover, the extent to which and direction (shielding or deshielding) in which they are acting may not be calculable. Nevertheless, if one intends to extract detailed structural information from ^{13}C NMR spectra, it is useful—and in many cases indispensable—to be aware of these contributions. To trace their effects on ^{13}C chemical shifts more or less quantitatively, ingenious model compounds

have been designed and their spectra recorded. The discussion of these models comprises the major part of this chapter. The occurrence of such influences and their particular impact with respect to various constitutional and configurational arrangements is the subject of Sect. III, but first a brief summary of the most important factors is presented here.

1. Inductive Effects

Among the earliest research on the transmission of substituent effects was the pioneering work of Lauterbur (58) and of Spiessacke and Schneider (59). For a wide series of substituted methanes and ethanes they found an approximate correlation of ^{13}C chemical shifts with the electronegativity (E) of the substituents (X). So they concluded that inductive effects through σ -bonds play an important role in determining the chemical shifts of α - and β -positioned carbon atoms, and that this effect reflects the substituent's electron-withdrawing or -releasing ability.

Similar trends were observed subsequently for various aliphatic molecular systems (60), and the idea of inductive effects propagated through the σ -skeleton was supported by Pople's CNDO-SCF calculations (61) indicating charge alternation along the chain. (Scheme 1). This latter result is in accordance with the observation that substituents exerting a large paramagnetic shift on the α -carbon signals shift β -carbon signals only to a relatively small extent, and vice versa (Table 1).



Scheme 1

Using a somewhat different approach, Bucci (62) interpreted these substituent influences in terms of a combination of electronegativity and the number m of lone electron pairs at the substituent or at that atom which is directly attached to the α -carbon atom, respectively, and derived the empirical expressions [5] and [6] for ^{13}C chemical shifts referred to tetramethylsilane ($\delta = 0$):

Table 1
Downfield α - and β -Carbon Signal Shifts caused by Halogen Substitution in Cyclohexanes (60), in ppm

	X =			
	F	Cl	Br	I
C^α	62.9	32.2	25.0	4.2
C^β	5.5	9.6	10.3	12.2

$$\text{CH}_3\text{X} : \delta = 55E - 13m - 106 \quad [5]$$

$$\text{CH}_3\text{CH}_2\text{X} : \delta = 45E - 7m - 80 \quad [6]$$

A reasonable physical interpretation, however, was not presented (62).

2. Neighbor-Anisotropy and Ring-Current Effects

In early work, Spiesscke and Schneider (59) pointed out that inductive effects alone cannot account for α - and β -signal shifts. They held diamagnetic neighbor-anisotropy effects (63) arising from anisotropic electron-charge distributions responsible for the deviations in the electronegativity correlations. For bonds with conical symmetry they applied McConnell's magnetic point-dipole approximation (64) for the estimation of this contribution, $\Delta\sigma$:

$$\Delta\sigma = \frac{\Delta\chi}{r^3} (1 - 3 \cos^2 \theta) \quad [7]$$

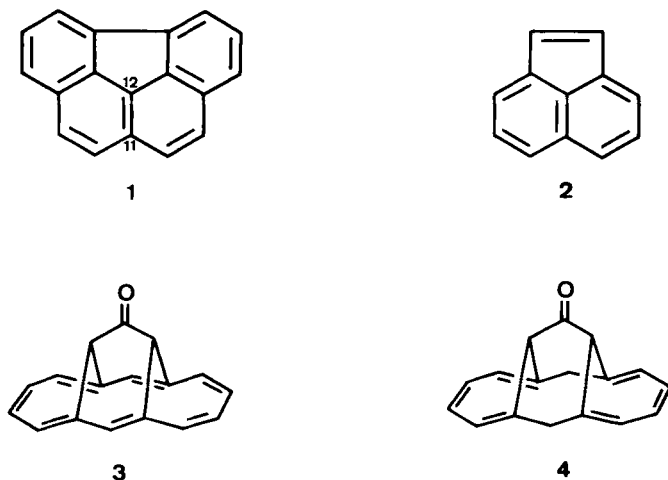
where $\Delta\chi$ is the difference between the magnetic susceptibilities parallel (χ_{\parallel}) and perpendicular (χ_{\perp}) to the bond axis, r is the distance of the carbon atom under consideration from the site of the point dipole, and θ is the angle between the C-X bond direction and the vector r .

Roberts made use of this approach for the rationalization of ^{13}C signal shifts in cyclic alkynes (65) and Jones did so for the shifts in *N*-nitrosopiperidines and -piperazines (66). Both authors, however, emphasized that alternative causes for the signal shifts may be responsible, such as electric-field effects (see Section II-B-3).

The relevance of neighbor-anisotropy effects, especially the magnetic point-dipole approximation, has been questioned (57), since only relatively small signal shifts (in parts per million) can be produced by this mechanism. Therefore, it can be of significance only for ^1H shielding, since the chemical-shift range of that nucleus is unique in being rather narrow, and since the neighbor-anisotropy contribution should influence nuclei of different sorts to the same extent. Thus, it cannot be the cause of major ^{13}C shielding variations.

In fact, it may even be difficult to ascertain its existence as was shown by several authors (cf. Scheme 2). The C(11) and C(12) signals in benzo-[ghi]fluoranthene (1) are 6.6 ppm apart. Since this value is much larger than the 0.3-ppm difference of the corresponding signals in acenaphthylene (2), it was ascribed to ring-current effects (67). The 7-ppm difference of the two carbonyl chemical shifts in 3 ($\delta = 206.1$) and 4 ($\delta = 213.0$) has been attributed the same origin (68).

So it appears that, in general, neighbor-anisotropy effects are small and easily overshadowed by various other effects, and therefore are not of essential importance for ^{13}C shielding interpretations.



Scheme 2

It should be noted that the unusual high-field positions of ^1H and ^{13}C signals in three-membered rings like cyclopropane, oxirane, thiirane, and aziridine have been rationalized in terms of ring currents (69,70).

3. Electric-Field Effects

In recent years another through-space influence has attracted increasing interest as a possible origin of certain NMR signal shifts in the spectra of molecules containing polar groups. According to the original Buckingham formulation (71) such groups can be regarded as fluctuating C–X dipoles. These create electric fields that give rise to electron distortions around a nucleus C(i) under consideration in a conically symmetric C(i)–Y bond and thereby induce C(i) signal shifts ($\Delta\sigma$), which can be expressed as the sum of linear- and square-electric-field effects (71–73):

$$\Delta\sigma = -A E_z - B \langle E^2 \rangle \quad [8]$$

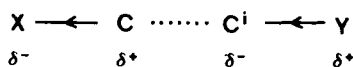
where E is the electric field produced by the point dipole at the site of the nucleus C(i), E_z is its component in the C(i)–Y bond direction, and A and B are constant bond parameters that are independent of the applied electric field, depending only on X.

The first term in eq. [8] is the linear-electric-field (LEF) effect (74–77), which may be interpreted as a charge separation $\Delta Q_{\text{C(i)Y}}$ along the C(i)–Y bond (76):

$$\Delta Q_{\text{C(i)Y}} = P_{\text{C(i)Y}} l_{\text{C(i)Y}}^{-1} q r^{-2} \cos \theta \quad [9]$$

In this equation $P_{C(i)-Y}$ is the polarizability of the C(i)–Y bond, $l_{C(i)-Y}$ its length, r its distance from the point-dipole charge q , and θ the angle to the electric-field vector (76). This expression must be calculated and summed up for all existing bonds between C(i) and adjacent Y atoms.

Due to the LEF the C(i)–Y bond is polarized in such a way that opposite charges are directed at each other as shown in Scheme 3 for an electronegative substituent X. According to commonly agreed-upon views concerning the correlation of charge densities and carbon shieldings, this implies an upfield shift of the signal of C(i) and a downfield shift of that of Y (if Y is a carbon atom). Such findings have in fact been reported for olefinic sp^2 carbons (where C–Y is C=C) even if they are remote from the dipole (78–85).



Scheme 3

This approach has also been applied to saturated C(i) atoms. Due to the much lower polarizabilities of C–H and C–C single bonds, however, the effects are clearly smaller (82), though still detectable. Thus, some effects of substituents X on δ -positioned carbon atoms in cyclohexanes and cholestanes were attributed to LEF effects of the C–X dipoles by Schneider and colleagues (76,77,85). The finding that only minor effects are to be expected in saturated molecules was confirmed by INDO–SCF calculations of electric-field effects on ^{13}C chemical shifts of some model compounds performed by Seidman and Maciel (86). These authors conclude, further, that conformational studies on such systems are not promising (86).

The second contribution in eq. [8] is the square-electric-field (SEF) effect, where $\langle E^2 \rangle$ is the time-averaged square of the electric field E (76):

$$\langle E^2 \rangle = 3I_X P_{CX} r_{C(i)}^{-6} \quad [10]$$

Here I_X is the first ionization potential of X, P_{CX} the polarizability of the C–X bond, and $r_{C(i)}$ the distance between atom C(i) and the center of the C–X bond.

It is clear from the r dependence that the SEF effect will fall off sharply with increasing distance between the perturbing electric dipole C–X and the nucleus C(i) the shielding of which is observed. Thus it is to be expected that this contribution will be effective only at small distances. Some authors have correlated substituent effects on carbon atoms in the β -position with the SEF effect (72,76).

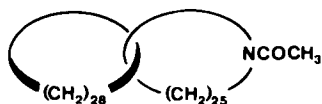
In 1963 Schaefer and co-workers (87) introduced an "intramolecular dispersion effect" in analogy to corresponding intermolecular effects exerted, for example, by halogenated solvents. This concept bears a close resemblance to the SEF contribution as expressed by eq. [10].

4. Other Effects

There are numerous other transmission mechanisms for substituent effects. Those connected with unsaturated frameworks, such as mesomeric effects and correlations with π charge densities and Hammett-type reactivity constants, and intramolecular hydrogen-bonding effects are beyond the scope of this article and are discussed elsewhere (1,8,25,57).

Some other mechanisms will be discussed in later sections: The Grant–Cheney formulation (88) of steric compression effects will appear in the context of γ -gauche substituent effects (Section III-C), and hyperconjugative orbital interactions will be cited in interpretations of γ -anti substituent (Section III-D) and intramolecular interaction effects (Section IV).

Finally, chemical-shift variations originating in van der Waals compression are noteworthy, although very few reports have come to our attention discussing signal shifts of sp^3 carbon atoms in terms of van der Waals interactions. Schill and co-workers (89) found downfield shifts of up to 1 ppm in the [2]-catenane **5** when its ^{13}C resonances are compared with those of the two isolated subunits. From the increase of these chemical-shift differences with increasing distance from the nitrogen atom, these authors concluded that the strongest van der Waals interactions occur in that part of the heterocycle which is opposite to the amide moiety in space (cf. Scheme 4).



Scheme 4

5

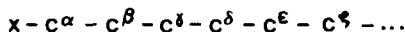
III. SUBSTITUENT EFFECTS AND THEIR STRUCTURE DEPENDENCE

Replacement of a hydrogen atom within an organic molecule, for example an alkane, by a substituent X changes the electronic environments of directly bonded and of more remote carbon nuclei. Thereby ^{13}C NMR signals are shifted either upfield or downfield; the difference between the chemical shifts δ of a certain carbon atom in the substituted and the unsubstituted parent compound is called the substituent effect. For this term the abbreviation SCS (substituent-induced chemical shift) has generally been adopted in the literature and will also be used here. The SCS is given by the equation

$$\text{SCS} = \delta(\text{C} \cdots \text{X}) - \delta(\text{C} \cdots \text{H}) \quad [11]$$

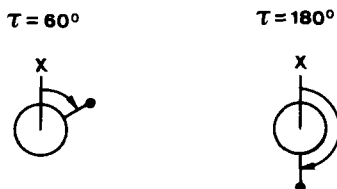
The identity of the substituent X (its chemical notation) is indicated in parentheses. Thus, the substituent effect of a methyl group is designated $\text{SCS}(\text{CH}_3)$.

The observed carbon atom influenced by the substituent is denoted by its position relative to X according to the number of intervening bonds or atoms (Scheme 5).



Scheme 5

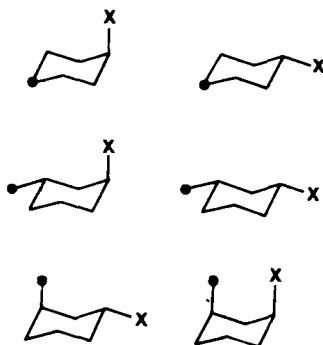
If there are at least three bonds between X and the observed carbon (C^{γ} , C^{δ} , . . .), the geometric relation between the two atoms is no longer defined by bond lengths (l) and bond angles (ϕ) alone. In this situation relevant carbon atoms may be in stereochemically nonequivalent positions merely because of different torsional angles (τ) between the $X-C^{\alpha}$ and the $C^{\beta}-C^{\gamma}$ bonds (e.g., Scheme 6)*.



Scheme 6*

There are two different relative orientations of X and a γ -carbon atom in staggered n -propyl derivatives. Accordingly, we have to make a distinction between γ -gauche (γ_g -SCS) and γ -antiperiplanar (γ_a -SCS) substituent effects.

In cyclohexane derivatives at least six different salient orientations of δ -carbons with respect to a perturbing substituent X are conceivable (Scheme 7). Of these, the one shown last is quite different from all the others, in that the substituent X is very close in space to the syn-axial carbon under observation. The symbol δ_{sa} (sa for syn-axial) is used for the δ -interaction in this conformation.



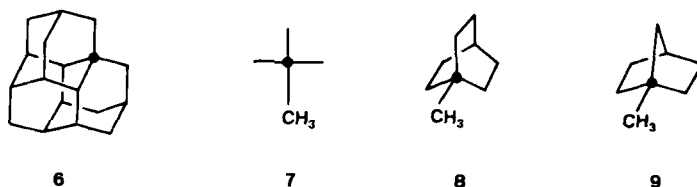
Scheme 7

*Here and elsewhere, the carbon atom observed is marked by a heavy dot (●).

It is a prerequisite for a proper discussion of substituent effects that the molecular framework of the molecule not be altered significantly by the substitution. Otherwise the signal shifts contain a certain contribution from conformational changes of the parent molecule itself. Furthermore, a given SCS may be modified by such conformational changes; that is, it may differ in magnitude in different conformations. Thus, one has to reckon with considerable garbling of the actual SCS if a change of the conformational equilibrium in mobile molecular systems is possible.

The most appropriate way to circumvent these difficulties is by the use of conformationally rigid compounds, such as cyclohexanes, bornanes, other bicyclic molecules, or adamantanes. Even then slight geometric distortions due to X-H-replacements are inevitable; fortunately these can be neglected in most cases. Correspondingly, the vast majority of investigations dealing with structural and especially stereochemical dependence of SCSs have been carried out by measuring the spectra of such rigid cyclic compounds.

The influence of the strain inherent in certain caged compounds on the magnitude of the SCS cannot be ignored either; apparently, a change in the hybridization state of the affected or intervening carbon atoms evoked by bond-angle changes (bonding-orbital distortions) can modulate the transmission of the SCS. Quantitative assessments of these effects, however, are not available, since there are only very few reports, and these are scattered in the literature. Perlin and Koch (90) concluded from extensive investigations of methylated cyclohexanes that an enlarged C-C-C bond angle is associated with a downfield signal shift. A corresponding effect was observed for the quaternary carbon atom in triamantane (6) (91). The α -SCS(CH_3) in 1-methylbicyclo[2.2.2]octane (8) is +3.5, a value very similar to that in molecule 7 (isobutane \rightarrow neopentane), which is +2.7 (92). The corresponding α -SCS(CH_3) in the considerably more strained 1-methylbicyclo[2.2.1]heptane (9), however, is markedly larger (+7.3) (93).



Scheme 8

Finally, changes in SCS magnitudes (94) due to an exceptionally drastic modification of intervening atoms (Table 2) are of interest in this context. The transmission of the β -SCS(X) is greatly attenuated if the quaternary carbon atoms are replaced by silicon; the Si-Si backbone practically acts as an insulator (94).

Table 2
 β -SCS(X) Values^a in Substituted Trimethylbutanes (10) and Corresponding Disilanes (11) on Methyl Carbon Atoms at M¹ (94)

$\begin{array}{c} \text{CH}_3 \quad \text{CH}_3 \\ \quad \\ \text{X}-\text{M}^1-\text{M}^2-\text{CH}_3 \\ \quad \\ \text{CH}_3 \quad \text{CH}_3 \end{array}$	X =	
	Cl	Br
10: M = C	+2.8	+4.7
11: M = Si	+0.3	+0.9

^aIn this particular case the chemical shifts in the halogenated compounds are referred to X = CH₃, rather than X = H.

A. α -Effects

As already stated in Section II-B-1, the α -SCSs of substituents X are determined mainly by the electronegativity $E(X)$; that is, they are governed by inductive effects (Fig. 1). This has also been verified by *ab initio* (54), INDO (52), CNDO/2 (95), and MINDO/3 calculations (96).

The correlation, especially when applied to a variety of parent molecules, is not as good as one might hope, however, indicating that other contributions must be operative. Spiessacke and Schneider (59) were the first to propose the existence of magnetic anisotropy effects (Section II-B-2) whereas Buccì (62) suggested an

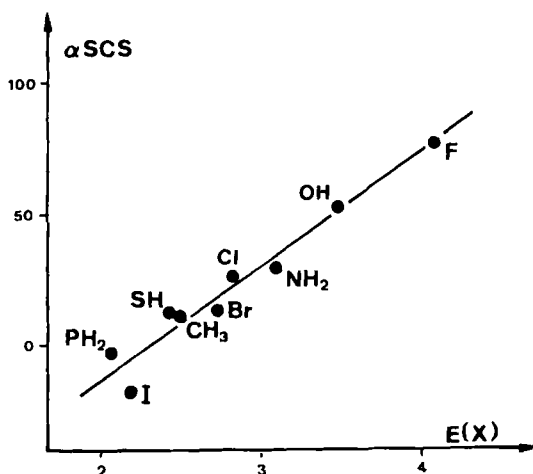


Figure 1. α -SCS values in substituted methanes (CH₃X) plotted against Allred-Rochow electronegativities $E(X)$.

interpretation according to which in addition to $E(X)$, the number of free electron pairs on X plays an important role. This bears some resemblance to Buckingham's electric-field treatment (71) discussed in Section II-B-3.

Inamoto and co-workers (97,98) introduced a new inductive parameter ι (iota) based on atomic properties of X, namely the effective nuclear charge in the valence shell and the effective principal quantum number, as well as $E(X)$ (97). They thereby established a reasonable correlation between the α -SCSs in substituted methanes and ethanes and the ι parameters for a series of substituents not including $X = \text{CN}$ and I (97).

Shabab (45) attributed the α -SCS to a subtle balance of both the paramagnetic and diamagnetic (40–42) shielding contributions in which the latter increases more rapidly than the former with increasing atomic number of X. Thus, the net observed effect becomes less deshielding as the atomic number of X increases (45).

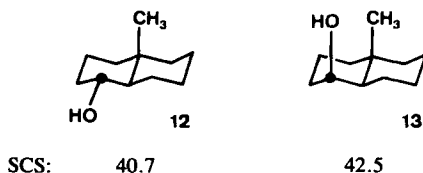
Another interesting approach was proposed by a group of Japanese authors (99) who introduced an entropy term (ΔS°) in addition to Hammett-type constants. The term ΔS° represents entropy differences in the substituted compounds compared with the parent.

The magnitudes of α -SCSs in structurally more complicated organic molecules are much more diverse and cannot be reproduced by theoretical and semitheoretical treatments with sufficient accuracy. Therefore, a wealth of empirical results has been compiled to explore the dependence of the α -SCS on structure, and above all on stereochemistry. Derivatives containing cyclohexane subunits were considered suitable molecular models with which to achieve that end, since they are characterized by conformations with torsional angles near 60° and 180° . Already as early as 1967 Dalling and Grant (100,101) found that $\alpha\text{-SCS}(\text{CH}_3)$ depends strongly on the stereochemical orientation of the methyl group: For an equatorial CH_3 it was 6.0 ± 0.1 , whereas only 1.4 ± 0.3 was measured for an axial one. The same sequence was detected for hydroxy substituents (102) [$\alpha\text{-SCS}(\text{OH}^{\text{eq}}) = 43.2$ and $\text{SCS}(\text{OH}^{\text{ax}}) = 37.8$], and it was postulated that the difference originates in steric interactions between the axial OH and the syn-axial hydrogen atoms at the γ -gauche-oriented carbons. Analogously, Beierbeck and Saunders (103,104) derived contributions for each gauche $X\text{-C}'$ arrangement from a regression analysis of a great variety of cyclohexanes, decalins, and related steroids and triterpenes: -3.0 for $X = \text{CH}_3$ and -2.3 for $X = \text{OH}$. Slightly different values were reported for some diamondoid derivatives (105), probably because of less pronounced deviations from ideal 60° and 180° torsional angles (106–109) in the six-membered rings of these caged compounds. The corresponding parameter for $\alpha\text{-SCS}(\text{OH})$ derived by Djerassi and colleagues (110) from cholestanols and androstanols is similar (-3.5), and was modified later (111), when slight geometric distortions, as determined using Allinger's force field (112), were incorporated.

Substituents from third- or higher-row elements, for example, Cl and Br,

show a different behavior. The α -SCS(Cl^{eq}) and α -SCS(Cl^{ax}) are practically equal in magnitude (7,113–115); that is, they are more or less independent of the number of existing γ -gauche orientations. Moreover, α -SCS(X^{ax}) is even larger than α -SCS(X^{eq}) if X is bromine or iodine (105,113,114,116). It is not easy to understand these findings; maybe a γ -gauche-positioned carbon generates a charge polarization along the C–X bond so that the α -SCS(X^{ax}) increases with increasing polarizability of X (85,114; see also below).

There is a structural influence that can affect the magnitude of α -SCS(OH) and invert the “normal” sequence: $\alpha_{\text{eq}}\text{-SCS} > \alpha_{\text{ax}}\text{-SCS}$.

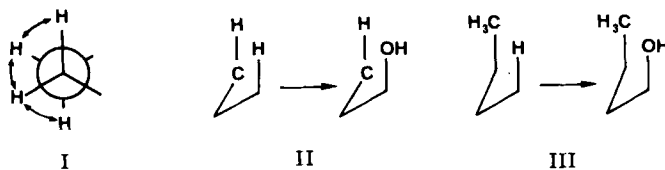


Scheme 9

If there are syn-axial hydroxy and carbon substituents (skew pentane arrangement) as depicted for the methyldecalol **13** (Scheme 9) the α -SCS(OH^{ax}) value may surpass the corresponding α -SCS(OH^{eq}) (117). Downfield shifts of 3.5 (110) and 1.9 ppm (111), respectively, were given as contributing parameters for this kind of molecular moiety. As a result, an empirical equation for predicting α -SCS(OH) in monohydroxy steroids was presented by Schwenzer (111) (Scheme 10). In addition to the base value (36.9), three different parameters for nonbonded interactions are included in the equation: (I) gauche H–H, (II) γ -gauche O–C, and (III) δ -syn-axial O–C. The equation is

$$\alpha\text{-SCS(OH)} = 36.9 + 1.3 n_{\text{I}} - 1.1 n_{\text{II}} + 4.5 n_{\text{III}} \quad [12]$$

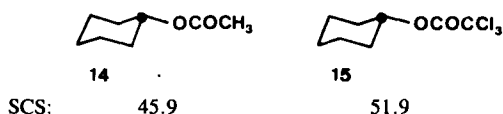
with n_i being the number of occurrences of interaction i (I, II, or III, respectively).



Scheme 10

Considerable variations may occur in the α -SCS of polyatomic substituents $-\text{XY}_n$ ($\text{Y} \neq \text{H}$; $n = 1, 2, \dots$) with identical X (2,113,114). These can often be predicted satisfactorily if one subtracts the individual substituent effects of Y on C^α , which in fact are β -SCS(Y). For example, α -SCS(OH) in methanol is 52.5, whereas α -SCS(OCH_3) in dimethyl ether is 63.2; the difference of ca.



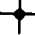
10 is in the typical range for a $\beta\text{-SCS}(\text{CH}_3)$. The atoms Y, however, may alter the $\alpha\text{-SCS}(\text{XY}_n)$ not only by their mere existence, but also by changing the inductive effect of the group XY_n . Kleinpeter and co-workers (118) found an electronegativity dependence of the $\alpha\text{-SCS}$ values of halogenated acetoxy groups ($-\text{OCOCX}_3$) (Scheme 11). Inexplicably, $-\text{OCOCF}_3$ is out of line, its $\alpha\text{-SCS}(\text{OCOCF}_3)$ value being only 43.0 (118).



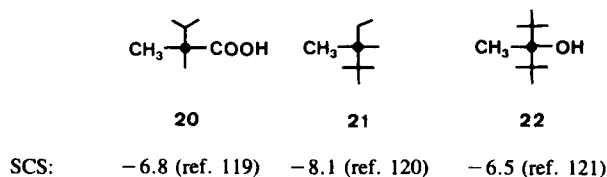
Scheme 11

Branching at the α -carbon atoms is another factor influencing the magnitude of $\alpha\text{-SCS}$ (Table 3). Methyl and hydroxyl effects decrease markedly with progressive substitution of α -hydrogen atoms by methyl groups. The $\alpha\text{-SCS}(\text{CH}_3)$ diminution is reinforced if the hydrogens are replaced by sterically more demanding alkyl groups (**20–22**), which actually lead to sizable upfield $\alpha\text{-SCS}(\text{CH}_3)$

Table 3
 $\alpha\text{-SCS}$ Values in Substituted Methanes (**16**), ethanes (**17**), propanes (**18**), and isobutanes (**19**) (5)

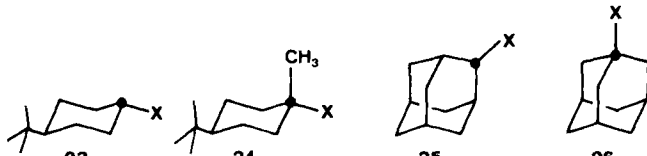
	X =				
	CH_3	OH	Cl	Br	I
CH_3X	8.0	51.3	26.1	11.2	-19.5
 X	10.2	51.3	33.0	21.3	-6.0
 X	9.1	47.5	37.8	28.1	5.0
 X	6.4	43.4	40.1	35.5	16.8

effects (Scheme 12). The trend is inverted for the halogens, and the discrepancies become larger with increasing atomic number of the halogen (122,123) the maximum value being 36.3 when methyl and *tert*-butyl iodide are compared (Table 3). Analogous results have been reported for cyclohexanes **23** and **24** (114) and bridged alicycles like adamantanes **25** and **26** (Table 4).



Scheme 12

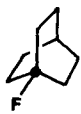
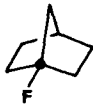
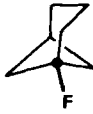



Table 4
 α -SCS Values in Cyclohexanes **23** and **24** (114) and Adamantane Derivatives **25** and **26** (124)

						
$X =$						
	CH ₃	OH	F	Cl	Br	I
23	5.4	44.1	64.5 ^a	32.7	25.0	2.1
24	— ^b	43.8	68.3	43.3	40.4	24.7
25	1.2	36.5	56.4	28.6	23.9	6.7
26	1.6	39.1	62.0	38.5	35.7	19.6

^a α -SCS(F) in 1^{tr}-fluorocyclohexane.

^bNot reported.

Unfortunately, the situation is even more complicated: In bi- and tricyclic compounds the α -SCS may experience further alterations apparently produced by intramolecular strain. The usually large α -SCS(CH₃) in 1-methyl-bicyclo[2.2.1]heptane (**9**) (93) has already been mentioned. The α -effects of other substituents (OH, OCH₃, Cl, I, and COOH) in the same molecular system do not correlate with those in bridgehead-substituted bicyclo[2.2.2]octanes or adamantanes; again this was attributed to internal strain (125). The α -SCS(F)

			
	27	28	29
SCS:	68.5	67.2	59.8
¹ J _{CF} :	185.3	208.1	233.4
			
	30	31	32
SCS:	55.7	46.3	41.4
¹ J _{CF} :	257.6	260.3	332.5

Scheme 13

values in a series of bridgehead-fluorinated bi- and tricycles show an exceptionally wide spread (126) (Scheme 13). The decrease of $\alpha\text{-SCS}(\text{F})$ correlates roughly with increased one-bond carbon-fluorine coupling constants, which are a measure of the s character of the α -carbon atoms (126).

Some research groups have investigated effects of substituents less common in organic chemistry. Quin and co-workers (127,128) determined $\alpha\text{-SCS}$ s of tri- and tetravalent phosphorus substituents in n -alkyl and cyclohexyl derivatives (Tables 5 and 6). The difference between $-\text{PH}_2$ and $-\text{P}(\text{CH}_3)_2$ effects is easily explained by $\beta\text{-SCS}(\text{CH}_3)$ (about 10 ppm for each methyl); this approach, however, is not satisfactory for $\text{P}(\text{OCH}_3)_2$ and PCl_2 , since it would suggest $\alpha\text{-SCS}$ values of ca. 16 (found: 21.4) and ca. 22 (found: 32.5), respectively, for those two substituents. A stereochemical dependence similar to that of $\text{X} = \text{CH}_3$ and OH seems to exist only for the primary phosphine ($\text{X} = \text{PH}_2$) and the compounds with tetravalent phosphorus substituents, whereas the $\alpha\text{-SCS}$ values of the tri-valent functions are quite similar in many cases, regardless of their stereochemical position.

Rather divergent $\alpha\text{-SCS}$ values for di-, tri-, and tetravalent sulfur substituents were reported (Table 7).

As an example of the comparison of Group IVa, substituents, data for pertinent cyclohexane derivatives are presented in Table 8.

Mitchell (135) noted a considerable increase in the $\alpha\text{-SCS}$ values of tin substituents when methyl groups within the substituent were gradually replaced

Table 5
 $\alpha\text{-SCS}$ Values of Alkyl Phosphorus Derivatives (127)

	X =				
	PH_2	$\text{P}(\text{CH}_3)_2$	$\text{P}(\text{OCH}_3)_2$	PCl_2	$\text{PS}(\text{CH}_3)_2$
Methyl	-2.3	19.4	21.4	32.5	— ^a
<i>n</i> -Butyl	— ^a	19.4	20.4	29.5	21.4

^aNot reported.

Table 6
 $\alpha\text{-SCS}$ Values in Isomeric 4-*tert*-Butylcyclohexyl Phosphorus Derivatives

	X =						
	PH_2	$\text{P}(\text{CH}_3)_2$	$\text{P}(\text{OCH}_3)_2$	PCl_2	$\text{PS}(\text{CH}_3)_2$	$^+\text{P}(\text{CH}_3)_3$	$\text{PO}(\text{OCH}_3)_2$
Equatorial X	0.2	12.3	14.0	21.4	14.2	5.1	8.4
Axial X	-3.5	13.0	11.2	22.3	9.7	2.2	4.0
Reference	128	128	128	128	128	128	129

Table 7
 α -SCS Values of Some Sulfur Substituents in Alkyl Derivatives **33** to **35** (130–132)

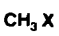

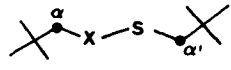
 33		 34		 35	
Subst.	α -SCS	Subst.	α -SCS	Subst.	α -SCS
SH	6.5	SH	11.4	S	28.6
SCH ₃	18.2	S ⁻	11.5	SO	44.2 (α)
SSCH ₃	22.1	SCH ₃	20.9		19.5 (α')
SCOCH ₃	11.8	SOCH ₃	41.2	SO ₂	47.6 (α)
SCSCH ₃	20.6	SO ₂ CH ₃	41.3		22.5 (α')
SO ₂ H	46.4	+S(CH ₃) ₂	29.6		
SO ₃ H	41.2	SO ₂ H	44.3		
		SO ₃ H	38.9		

Table 8
 α -SCS Values in Equatorially Substituted Cyclohexanes (133, 134)

X =					
	C(CH ₃) ₃	Si(CH ₃) ₃	Ge(CH ₃) ₃	Sn(CH ₃) ₃	Pb(CH ₃) ₃
α -SCS	21.9	-0.6	0.9	-2.3	8.0

by chlorine: For Sn(CH₃)₃, α -SCS was -2.4; for Sn(CH₃)₂Cl, 5.1; for Sn(CH₃)Cl₂, 12.7; and for SnCl₃, 20.0. This is clearly an electronegativity effect (135). If the trichlorotin compound is dissolved in water, the α -SCS value increases to 30.1, presumably because of the formation of a six-coordinated complex (135).

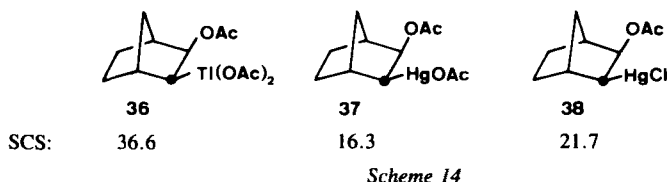
A striking feature of trimethyltin substituents is the linear correlation between the chemical shift of the α -carbon atom in RSn(CH₃)₃ and that of the corresponding atom in the parent hydrocarbon RH (136):

$$\delta^\circ[\text{R-Sn(CH}_3)_3] = 1.13 \times \delta^\circ[\text{R-H}] - 5.0 \quad [13]$$

This correlation is such that α -SCS[Sn(CH₃)₃] is negative (shielding) as long as the chemical shift in the reference compound is smaller than $\delta = 38.5$; when it becomes greater, α -SCS becomes positive (deshielding). This correlation encompasses also some other organostannanes reported subsequently (137). Equation [13] is reminiscent of an analogous relation for aliphatic Grignard derivatives discovered previously (138):

$$\delta^\circ[\text{R-MgX}] = 1.31 \times \delta^\circ[\text{R-H}] - 49.3 \quad [14]$$

The ^{13}C chemical shifts in mercurimethanes $\text{CH}_4-n(\text{HgX})_n$ ($n = 1-4$; $\text{X} = \text{Cl}, \text{Br}, \text{I}, \text{CN}$) were reported comprehensively (139). The α -SCS in cyclohexylmercuric acetate is 20.2 in equatorially and 24.7 in axially substituted $\text{C}_6\text{H}_{11}\text{HgOAc}$ (140).



Thallium(III) substituents (see **36**) exert even larger effects on α -carbon atoms than mercury does (141) (see **37** and **38**); this has been ascribed to displacement of electrons in the carbon-metal σ -bond toward the metal atom, due to its increased nuclear charge.

A comment is appropriate here about α -effects of endocyclic substituents. Such effects are not defined according to eq. [11], since they replace carbon instead of hydrogen atoms in the parent compound. Thus, these SCSs represent differences between the actual shift effects and that of a carbon fragment in the same position.

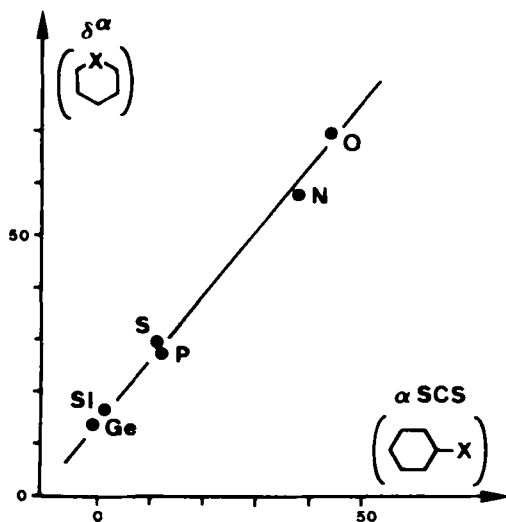


Figure 2. α -Carbon chemical shifts δ^α in pentamethylene heterocycles plotted against α -SCS(X) in cyclohexanes bearing corresponding substituents. Substituents are as follows: O, O vs. OH; N, NCH_3 vs. $\text{N}(\text{CH}_3)_2$; S, S vs. SH; P, PCH_3 vs. $\text{P}(\text{CH}_3)_2$; Si, $\text{Si}(\text{CH}_3)_2$ vs. $\text{Si}(\text{CH}_3)_3$; Ge, $\text{Ge}(\text{CH}_3)_2$ vs. $\text{Ge}(\text{CH}_3)_3$ (114).

Since Eliel and Pietrusiewicz (142) have published a comprehensive review on ^{13}C chemical shifts in saturated heterocycles, the discussion in the present report may be confined to a few basic features for the sake of completeness. It stands to reason that there is an electronegativity dependence of α -carbon chemical shifts. This was demonstrated by Lambert and co-workers (143) for a great variety of pentamethylene heterocycles, and holds also for positively charged species, such as $\text{X} = (\text{CH}_3)_2\text{N}^+$, $(\text{CH}_3)_2\text{P}^+$, CH_3S^+ , Br^+ , and I^+ . The same is suggested by the good correlation of α -carbon chemical shifts in some heterocyclohexanes (143) and the α -SCS values in cyclohexanes with equatorial substituents (Figure 2)(114).

Finally, it should be mentioned that α -SCS(CH_3) values in methylated aliphatic heterocycles are sometimes considerably larger (more paramagnetic) than in corresponding cyclohexanes (142).

B. β -Effects

Even in the early years of ^{13}C NMR spectroscopy it was assumed that substituent effects on β -positioned carbon atoms are dominated by inductive effects (59,144,145). According to Pople's theoretical treatment (61) one expects an electronegativity dependence reversed in sign compared to that for α -carbons (cf. Section II-B-1). This is indeed the case; in Figure 3 a rough electronegativity dependence of β -SCS is depicted. Only monoatomic and hydrogen-bearing atoms were selected for substituents to exclude secondary effects from atoms in γ -

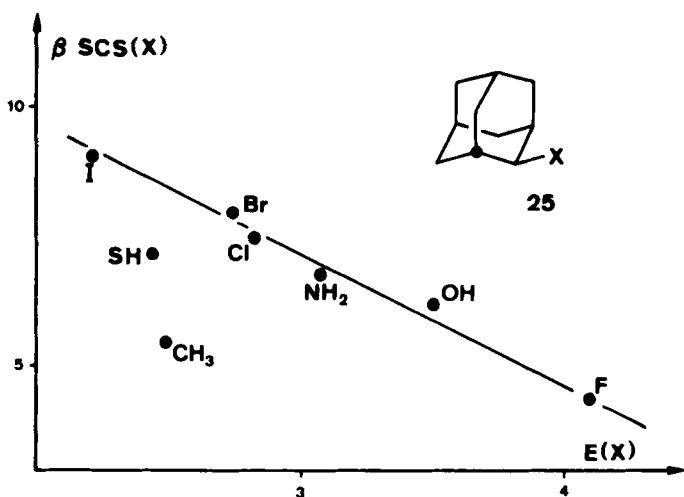
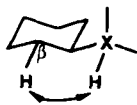


Figure 3. β -SCS(X) in 2-substituted adamantanes 25 plotted against Allred-Rochow electronegativities $E(X)$.

position with respect to C^β . Because the deviations of certain XH_n substituents ($\text{X} = \text{S}, \text{C}$) from the correlation were even worse in 1-substituted adamantanes, they were attributed to shielding contributions due to the existence of 1,3-diaxial hydrogen-hydrogen arrangements at X and C^β as shown in **39** (146):

**39**

Scheme 15

In cyclohexane derivatives the $\beta\text{-SCS}(\text{X})$ values are dependent on the stereochemical orientation of the substituent. Dalling and Grant (100,101) deduced values of 9.0 ± 0.1 for an equatorial and 5.4 ± 0.2 for an axial methyl group from regression analysis of data on 16 methyl cyclohexanes. An analogous sequence was reported for hydroxy substituents in cyclohexanols (102,117): $\beta\text{-SCS}(\text{OH}^{\text{eq}}) > \beta\text{-SCS}(\text{OH}^{\text{ax}})$. Roberts and co-workers (102) rationalized this difference tentatively by assuming that an axial hydroxyl group gives rise to a sterically induced elongation of the $\text{C}^\beta\text{-C}^\gamma$ bond (147), thereby producing a diamagnetic β -carbon signal shift (148). This, however, was questioned (111) when force-field calculations did not indicate such bond lengthening in any of the androstanols investigated. Djerassi and colleagues derived a simple expression for the estimation of $\beta\text{-SCS}(\text{OH})$ in monohydroxy steroids (110):

$$\beta\text{-SCS}(\text{OH}) = 9.3 - 2.4 n \quad [15]$$

where n is the number of gauche orientations of O and γ -carbon atoms connected to the β -carbon atom observed.

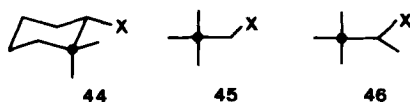
In a more generalized way, Beierbeck and Saunders derived parameter sets

Table 9

$\beta\text{-SCS}(\text{X})$ Values in Bridgehead-Substituted Diamondoid Compounds **41** to **43** (105)

40	41	42	43
No. of $\text{H}^\gamma\text{-X/C}^\gamma\text{-X}$ Orientations			
X	2/0	1/1	0/2
CH_3	6.8	4.5	5.3
OH	7.5	5.7	4.5
Br	11.6	8.5	5.2

for predicting chemical shifts of carbon atoms in the β -position with respect to a substituent in hydrocarbons, alcohols, amines, ketones, and olefins (103,104,146,149) in terms of γ -gauche parameters. This is exemplified by a comparison of β -SCS values in the bridgehead methyl-, hydroxy-, and bromo-substituted diamondoid compounds **41** to **43** (Table 9) (105). Whereas in **41** there are two H^{γ} -X and no C^{γ} -X orientations, these numbers are one and one in **42** and zero and two in **43**, respectively. Correspondingly, the β -SCS values decrease in magnitude (105) to values of about 5. Similar values were reported for heterosubstituent effects on quaternary β -carbons in the molecular systems **44** to **46** (150,151):



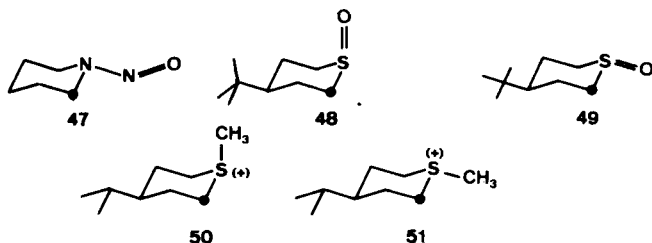
Scheme 16

It has been pointed out that there is a torsional-angle (τ) dependence of β -SCS (cf. **40**) (104). This angular dependence can be adequately described by multiplying the second term in eq. [15] by $\cos \tau$ ($0^\circ \leq \tau \leq 90^\circ$) for the appropriate fragment (104). By that treatment the β -SCS values of methyl, hydroxy, chlorine, and nitro substituents in bornane (93,104,146,152–154) and twistane derivatives (104,155), which cannot be predicted by the simple eq. [15], become understandable. As expected, such an angular dependence does not exist if τ is larger ($90^\circ < \tau < 180^\circ$) (156).

The discussion above has been more or less empirical and descriptive. However, considerable effort has been made to interpret β -SCS on a more physical basis. Electric-field effects (71–75) were invoked to explain signal shifts of β -carbon atoms induced by protonation of amines (157,158) (cf. Section II-B-3). This approach was later extended to other functionalities by Schneider and co-workers, who assumed that the SEF component (E^2) rather than inductive properties of the substituents should be responsible for β -SCS (113). They found fairly linear correlations of β -SCS(X^{ax}) and β -SCS(X^{eq}) in cyclohexyl derivatives (76) and attributed the difference between these for a given X to a widening of the C^{α} - C^{β} - C^{γ} bond angle by 2.2° in the axial conformer (114,159). The decrease of β -SCS in the order primary C^{β} \rightarrow secondary C^{β} \rightarrow tertiary C^{β} \rightarrow quaternary C^{β} was explained by electron-charge polarization in the C^{β} - C^{γ} bond(s) induced by the LEF component of the C^{α} -X dipole, which is already of significance at this distance, though $\langle E^2 \rangle$ still dominates (160). Such an electron flow toward the β -carbon is expected to be much more pronounced in C-C than in C-H bonds because of the polarizability difference ($\alpha_{CH} = 0.79$; $\alpha_{CC} = 1.12$) (150,151,160).

The operation of an electric field has also been invoked to explain β -effects

in some heterocyclic compounds, for example *N*-nitrosopiperidines **47** and -piperazines (66), although magnetic-anisotropy effects were not excluded. In thiane oxides (130,161) the paramagnetic β -SCS of the oxygen atom [$\delta(>\text{SO}) - \delta(>\text{S})$] is 5.5 ppm smaller for the axial than for the equatorial position (**48**: $\delta = 46.9$; **49**: $\delta = 52.4$). This was ascribed to an additional polarization of the equatorial $\text{C}^\beta\text{-H}$ bond by the electric field of the axial $\text{S}=\text{O}$ dipole (161). Analogous chemical-shift differences were observed for β -SCS(CH_3) in *S*-methylthianium salts (130,162,163): $\delta = 35.6$ in **50** and $\delta = 41.2$ in **51** (130).



Scheme 17

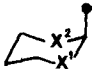

The β -carbon signals in heterocyclohexanes **52** (143) respond to the electronegativity of endocyclic substituents similarly to those of carbon atoms in β -positions with respect to exocyclic substituents. The slopes of chemical shift vs. electronegativity plots for the β -methylene groups in **52** and **53** are negative (Table 10). For the quaternary β -carbon atom in **53**, however, a slight positive slope is observed (164).

Table 10

Chemical Shifts of β -Carbon Atoms in Heterocyclohexanes **52** and **53** Relative to the Respective Carbocycles ($\text{X} = \text{CH}_2$), and Slopes of Plots of β -Carbon Chemical Shifts Against Electronegativities $E(\text{X})$ (143,164)

	$\text{X} =$				Slope [ppm per $E(\text{X})$ unit]
	O	NH	S	Te	
52	-1.1	-0.5	0.5	2.2	-2.5
	0.3	0.7	1.3	2.2	-1.5
53	0.2	-0.3	-3.5	-1.4	+1.1

Table 11
Methyl Chemical Shift Differences ($\delta^{\text{ax}} - \delta^{\text{eq}}$) in Cyclohexane and Thia Analogs (166)

			
	Cyclohex.	54	55
X ¹	CH ₂	S	S
X ²	CH ₂	CH ₂	S
$\delta^{\text{ax}} - \delta^{\text{eq}}$	-5.7	-1.3	+3.3

It is interesting that the difference between axial and equatorial methyl chemical shifts observed in methylcyclohexanes (100,101) is considerably diminished if one β -methylene group is replaced by sulfur (**54**); in 2-methyl-1,3-dithiane (**55**) (two β -methylene groups replaced by S) this difference is even inverted (165,166) (cf. Table 11). This is another example of specific effects in thianes and dithianes (167,168).

C. γ -Gauche Effects

Signals of carbon atoms in γ -gauche (γ_g) positions with respect to a substituent X are generally displaced upfield compared with the reference signals in the parent compounds (X = H). This is the diamagnetic " γ -effect" ¹³C NMR spectroscopy is renowned for. At the same time, this effect stands as a symbol for the general situation concerning the application of chemical-shift parameters to stereochemical problems in organic chemistry: Although the γ -effect is extremely valuable and diagnostically the most useful of all substituent effects, its physical meaning and mechanism are not at all understood.

The upfield shift of signals of carbon atoms in γ -position to a newly introduced substituent was recognized very early. Grant and Paul (169) found a γ -parameter of -2.5 in linear and branched alkanes. Later this group studied various other classes of hydrocarbons (33,88,100,101,170-172) and developed an interpretation of the γ -effects in terms of a polarization of the bond between the carbon concerned and an adjacent, sterically perturbed hydrogen atom (33,88) that has come to be called the "Grant-Cheney approach."



Scheme 18

According to this treatment, repulsive interaction at the hydrogen atoms produces a flux of negative charge toward the carbon atom concerned and thereby

Table 12
 $\gamma_{\text{g}}\text{-SCS(X)}$ Values in 2-Substituted Adamantanes (124)

	X =							
	CH_3	OH	NH_2	COOH	F	Cl	Br	I
$\gamma_{\text{g}}\text{-SCS(X)}$	-6.5	-6.7	-7.0	-4.2	-6.3	-6.9	-6.3	-4.8

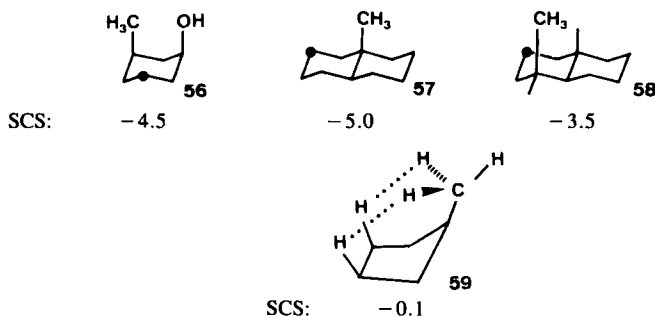
a general electron-orbital expansion. This is associated with a decrease of the $\langle r^{-3} \rangle$ term in the expression for the paramagnetic shielding contribution σ_{p} (32) (eq. [3], p. 222); consequently, the carbon signal is shielded. The authors derived quantitative expressions connecting the observed upfield shifts with repulsive forces $F(r)$ along the C-H bond (see Scheme 18):

$$\gamma_{\text{g}}\text{-SCS} = A F(r) \cos \theta \quad [16]$$

$$= 1680 \times \cos \theta e^{-2.671r} \quad [17]$$

Later, analogous effects were observed for other substituents, (e.g., OH, Cl, Br) even those without hydrogens (2,7). Table 12 shows $\gamma_{\text{g}}\text{-SCS(X)}$ values for various Xs in 2-substituted adamantanes **25** (124).

Many reports have appeared supporting the Grant-Cheney model; for example, $\gamma_{\text{g}}\text{-SCS(OH)}$ values were found in decalols and steroids to vary from -3.3 to -7.3 (110,117). The sizable range was ascribed to different degrees of skeletal distortions such that smaller effects (in absolute values) were associated with enlarged distances of the perturbing groups (7). Thus the relatively small $\gamma_{\text{g}}\text{-SCS(OH)}$ in the molecular substructure **56** (110) is ascribed to outward bending of the clashing CH_3 and OH groups. Similarly, the smaller $\gamma_{\text{g}}\text{-SCS(CH}_3\text{)}$ in the trimethyldecalin **58** as compared with that in **57** was assumed to be brought about by a splaying of the ring associated with an increase of the distance between the methyl group and the axial γ -hydrogen atom (173). The absence of a significant γ -gauche carbon signal shift for the methyl carbon atom in methylcyclopentane (**59**) becomes understandable when one considers that the distance



Scheme 19

between repelling hydrogens is relatively long in every conceivable conformation (174).

Other authors have successfully correlated changes in torsional angles with γ -gauche effects (80,150).

For more examples concerning various molecular systems in staggered conformations, the reader is referred to the compilations of diamagnetic γ -gauche effects in refs. 7 and 9. The disappearance of a noticeable effect when the observed carbon atom is quaternary, that is, when no polarizable C-H bond is present, was also considered to support the above explanation (110,175).

However, it became apparent that the Grant-Cheney treatment was too simple, as an increasing number of papers appeared reporting conspicuous inconsistencies. First, it seemed astonishing that within a series of related compounds γ_g -SCS values are often remarkably constant regardless of the nature and size of X (92,93,115,153,176,177); at other times the relative magnitudes of γ_g -SCS are even opposite to what one might have expected. Thus in a series of 9 α -substituted cortisol derivatives **60** (X = F, Cl, Br) the diamagnetic γ_g -SCS(X) values generally differ in the order Br < Cl < F (178), the largest value being -8.1 for γ_g -SCS(F) on C(1) and the smallest, -2.2 for γ_g -SCS(Br) on C(7) (178). Even larger differences contrary to size are seen in 1-halonaphthalenes **61** (179): The γ_g -SCS(X) values on C(8) are -7.7 (X = F), -3.9 (X = Cl), -1.2 (X = Br), and +3.8 (X = I). The last value is one of the very rare examples of a paramagnetic γ_g -SCS. Clearly, different mechanisms must be acting here; it should be noted that C(8) in **61** is an aromatic carbon atom. Also, there is experimental evidence that steric crowding around the C $^\alpha$ -X moiety leads to a decrease in γ_g -SCS(X) rather than to an increase. This was found, for example, in some conformationally rigid bicyclo[2.2.2]octanes (180,181), dicyclopentadiene derivatives (182), adamantanes (105), and cholestanes (183) (Table 13). Whereas the γ_g -SCS(OH) values are rather constant, those of the

Table 13
 γ_g -SCS(X) Values in Adamantanes **25**, Diamantanes **42**, and Triamantanes **43** (105)


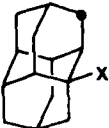
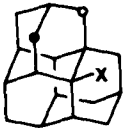
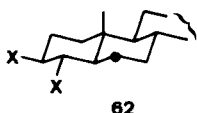
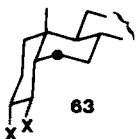
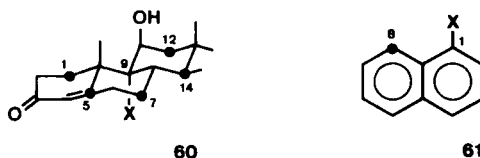
							
	25			42		43	
X						●	○
CH ₃	-6.2			-5.1		-4.6	-5.4
OH	-6.6			-5.8		-5.4	-5.9
Br	-6.1			-5.8		-2.8	-4.1

Table 14
 $\gamma_g\text{-SCS(X)}$ Values in Cholestanes (183); Effects Refer to 5α - and 5β -Cholestane,
 respectively ($\text{X}=\text{H}$)

		
X		
OAc	- 6.2	- 5.9
Br	- 1.2	- 1.8

methyl group are moderately and those of the bromo substituent distinctly reduced in **43**. Even larger differences between OAc and Br were observed for some 3,4-*trans*-disubstituted cholestanes **62** and **63** (183) (Table 14).



Scheme 20

The strongest criticism of the Grant–Cheney concept has been leveled by Beierbeck and Saunders (146). From a number of observations on the spectra of saturated and unsaturated steroids these authors concluded that a diamagnetic signal shift of steric origin does not exist and that the observed upfield-shifting effect is due to the elimination of a 1,3-diaxial hydrogen–hydrogen interaction (Scheme 21).



Scheme 21

Such an arrangement is intrinsically associated with a downfield shift of the signals of the hydrogen-bearing carbon atoms. The physical meaning of this interaction, however, was not specified (146). On the basis of this reinterpretation steric crowding appears to cause downfield rather than upfield shifts (146), a hypothesis that is confirmed by the $\gamma_g\text{-SCS}(\text{Br})$ reductions cited in Tables 13 and 14 and by the appearance of a downfield-shifting $\delta_{\text{sa}}\text{-SCS(X)}$ (cf. Section III-E) (184).

Further doubt about the validity of the original Grant–Cheney model was expressed by Seidman and Maciel (185), whose INDO calculations of proximity effects in hydrocarbons revealed that there is no simple correlation between carbon chemical shifts and calculated electron-density increases caused by steric C–H bond polarization; they report the conformational relation of interacting bonds and groups to be at least equally important, if not more so (185).

Schneider and co-workers (159) attempted to rescue the Grant–Cheney approach, at least for methyl substituents. They refined it by using a modified potential for the repulsive force (186) along with fully relaxed molecular structures as determined by force-field calculations. This indeed led to a satisfactory correlation of γ_g -SCS(CH_3) with repulsive interactions in methylcyclohexane and some methylbicyclo[2.2.1]heptanes (159). Schneider's treatment, however, implies that a signal shift originates not only from steric H–H repulsion but includes effects from secondary carbon-framework distortions (85,159).

Olah and Watkins (187) correlated ^{13}C chemical shifts in crowded phenyl-ethanes with bond-electron polarizations brought about by van der Waals interactions. They found that these effects cannot be confined to one single $\text{C}^\gamma\text{--H}$ bond but operate throughout the whole molecule and produce shielding of ortho and deshielding of α - and meta carbon atoms. The para carbon atoms are unaffected, which is taken as evidence that only the σ -electron systems of the phenyl groups are involved in these steric interactions (187).

Many authors have tried to identify other contributions to γ -gauche substituent effects instead of or in addition to sterically induced bond polarizations. For electronegative substituents, for example F, OR, NR_2 , and Cl, the most obvious interpretation is to assume a through-space electric-field transmission of γ_g -SCS

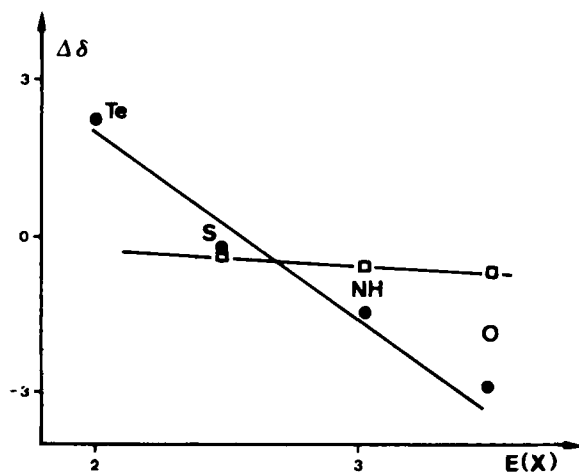


Figure 4. Chemical shifts of C(4) (●) and the axial methyl (□) in 53 [$\Delta\delta$, relative to the respective carbocycle ($X = \text{CH}_2$)] plotted against the electronegativity $E(X)$.

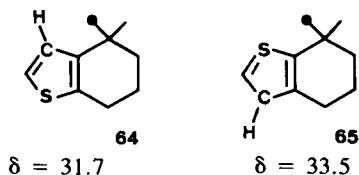
(85,113,114,159,188). Overlap of the substituent's lone-pair n_x with the σ (or σ^*) orbital of the diaxial $\text{C}^\gamma\text{--H}$ bond has also been proposed (114). Wiberg and co-workers (189), however, concluded from their investigation of some halobicyclo[2.2.1]heptanes that neither the magnitude nor even the correct sign of the observed $\gamma_g\text{-SCS}(\text{halogen})$ can be predicted by any variant of electric-field calculations.

In six-membered heterocycles Lambert and co-workers (143,164) noticed a clear electronegativity dependence of $\text{C}(4)$ resonances (Figure 4), the slopes in the plots being -5.3 for **52** and -3.5 ppm/electronegativity unit for **53** (Scheme 22).



In contrast, the chemical shifts of the axial methyl groups in **53** are nearly independent of X (slope = -0.7) (Figure 4). From that finding these authors (164) concluded that electronegativity information is transmitted to a γ -gauche carbon atom only through a rigid pathway of parallel orbitals and that methyl rotation protects this carbon atom from electronic interaction.

It can be seen from Figure 4 that in the thiane **53** ($\text{X} = \text{S}$) the sulfur is shielding the γ -gauche carbon atom more than a methylene group does in the carbocycle **53** ($\text{X} = \text{CH}_2$). This is generally the case in saturated sulfur heterocycles (130). The opposite was found by de Haan and co-workers (190) in thiophene derivatives, for example **64** and **65**. This may be ascribed to the fact that the sulfur electrons contribute to the π -system and hence this atom is different from sulfur atoms in thianes (190). The designation "downfield γ -gauche effect" (190), however, appears to be misleading, since on the basis of the underlying definitions (eq. [11], p. 230) it is, rather, an upfield effect smaller than that of a methine group.

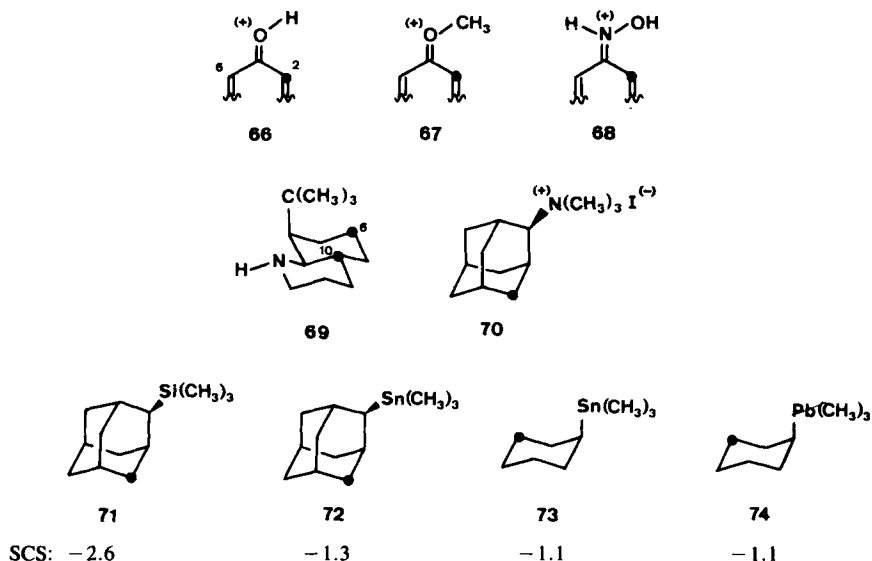


Two more alternative interpretations of γ -gauche effects are worth mentioning in this context. Gorenstein (191) rejected the Grant–Cheney approach and attributed the observed diamagnetic signal shifts to bond-angle and torsional-angle changes, to which "heavy" atoms (^{13}C , ^{19}F , ^{31}P) respond very sensitively (191). On the other hand, Shabab (45) pointed out that a decrease in the distance

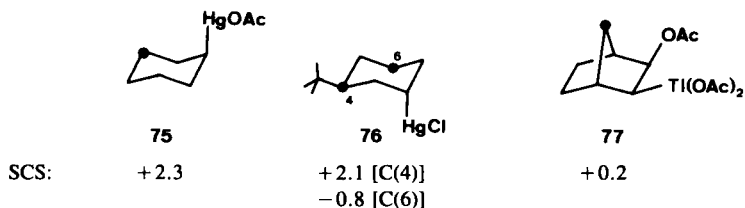
between the observed carbons and nonbonded remote atoms leads to a rapid increase in the diamagnetic shielding contribution σ_d (40–42), and that this alone may be an appropriate explanation for upfield signal shifts.

Up to this point our discussion of γ -gauche effects has demonstrated that the transmission mechanisms are not yet well understood and still open to speculation. The original concept of a steric interaction is highly controversial, and as long as there is no convincing explanation, the use of the deep-rooted term "steric compression shift" must be discouraged.

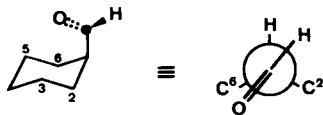
In the following, some γ_g -SCS values of less common substituents are compiled. It is interesting to compare the effects of very small and very large substituents. The shielding effect of the smallest possible, γ_g -SCS(H), in a number of diprotonated benzoquinone derivatives **66** (monitored as differences between C(2) and C(6) signal shifts) was reported to be quite low (-2.3 ± 0.1), whereas corresponding values for CH_3 in **67** (-7.0 ± 1.0) and OH in **68** (-4.6 ± 0.9) appeared to be normal (192). The γ_g -SCS of a *tert*-butyl group was derived from the spectra of some acyclic hydrocarbons; only very small values (-0.2 to -0.5) were found (193), despite the enormous steric demand of this substituent. This is in contrast to the normal upfield-shifting γ_g -SCS[C(CH₃)₃] reported by Eliel and Vierhapper (194) for **69** [-4.3 for C(6) and -7.2 for C(10)] and the γ_g -SCS of -6.4 for N(CH₃)₃⁺ in **70** (183). M(CH₃)₃ groups with M = Si, Sn, or Pb exhibit relatively small γ_g -SCS values (cf. **71** to **74**) (133,134). Even positive γ_g -SCS values of mercury and thallium substituents have been observed (cf. **75** to **77**) (140,141,195).



Scheme 24



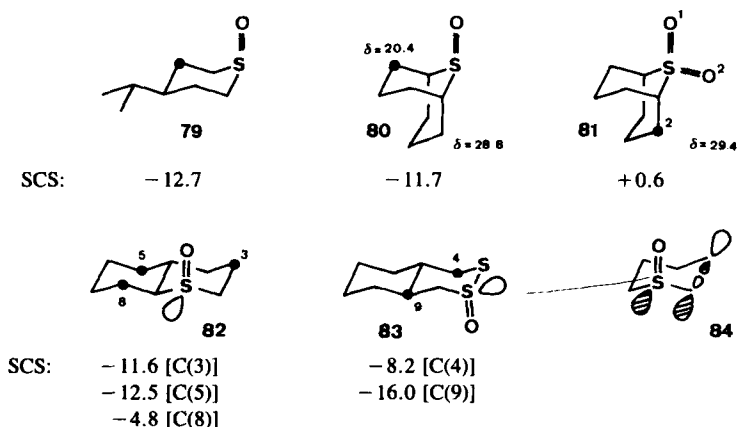
Very recently (196) the first example of a downfield signal shift produced by gauche-oriented CH_2 groups was communicated: The carbonyl resonance in the axial conformer of formylcyclohexane (**78**) is at lower field, by about 1 ppm, than in the equatorial analog. This has been ascribed to the predominance of a conformation in which the formyl hydrogen atom is directed outward and thereby eludes steric interference with the syn-axial H(3) and H(5). Nevertheless, the signals of C(3)/C(5) experience the expected upfield shift of -4.3 (196).



78

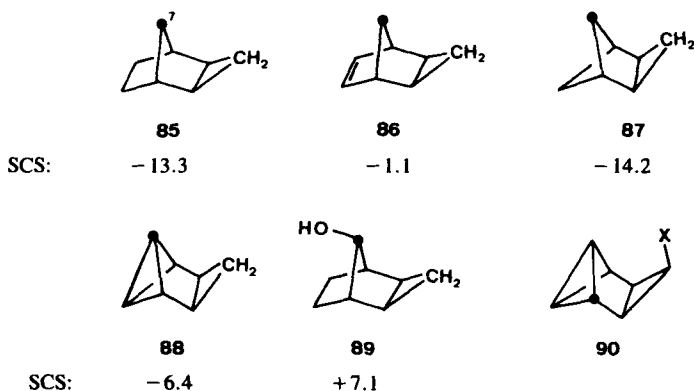
Scheme 25

Oxygen atoms in thiane oxides, such as **79** (130,161) and **80** (197) and related six-membered sulfur heterocycles (142,198) cause extraordinary large γ -gauche effects as compared with the corresponding thianes (cf. **79** and **80** in Scheme 26). The combined effect of both oxygen atoms in sulfones ($>\text{S} \rightarrow >\text{SO}_2$), however, is much less shielding (cf., e.g., **81**) (142,197,199) and similar to that of an equatorial oxygen in thiane oxides. This means that the upfield shift of an axial oxygen atom observed in sulfoxides (**79** and **80**) almost vanishes if there is already an equatorial oxygen atom present. So the $\gamma_g\text{-SCS}$ [O(2)] on C(2) in **81** as compared with **80** is $+0.6$ (197). This fact and recent observations by Evans and co-workers (200,201) suggest that the extraordinarily high upfield shift caused by an axial oxygen in sulfoxides like **79**, **80**, **82**, and **83** originates not so much in its stereochemical position but in the antiperiplanar orientation of the free electron pair at the sulfur atom with respect to the carbon atom concerned (cf. **84** in Scheme 26). This is supported by the observation that the $\gamma_g\text{-SCS(O)}$ is clearly diminished if the γ -carbon is in gauche orientation with respect to the lone pair (C(8) in **82**). These authors conclude that an upfield-shift contribution of approximately 7 ppm results from a hyperconjugative interaction between an equatorial $3p$ -orbital of sulfur (n_s) and the antibonding $\text{C}^\beta\text{-C}^\gamma$ orbital (σ^*) (200,201).



Scheme 26

Introduction of an *exo*-positioned cyclopropane ring into hydrocarbons containing norbornane substructures often leads to large shieldings of C(7) atoms, as in **85** to **88** (202,203). Similar values are found when the cyclopropane methylene group in **88** is replaced by NH (-7.7) or O (-3.5), but if S is attached, the effect is reduced to -0.4 (204). It is dangerous, however, to rationalize these effects in terms of steric interaction. A remarkably large down-field shift is observed if an *exo*-cyclopropane ring is incorporated into a 7-hydroxybicyclo[2.2.1]heptane to form **89** (202). Effects of substituents in such highly strained polycyclic hydrocarbons may show unusual behavior. Whereas in compound **90** the γ -gauche effect of a fluoro substituent is relatively large (-8.4), the corresponding value for chlorine is normal (-5.8) and that of bromine unusually small (-0.6) (205).



Scheme 27

Finally, it should be noted that γ -gauche effects are not confined to carbon atoms. Analogous shifts have been reported for ^{19}F , ^{31}P (191), and ^{15}N nuclei (206). Distinct shieldings of ^{17}O nuclei caused by γ -gauche-oriented methyl or methylene groups were found, too (207).

D. γ -Anti Effects

Of all substituent effects, that caused by γ -anti substituents has been the hardest to understand in terms of transmission mechanisms, notably because the resulting shifts are sometimes upfield and sometimes downfield. So, for example, γ_a -SCS(OH) values range from about +6 (208) to -6 (209). Correspondingly, the discussion about transmission mechanisms is prone to speculation and controversy. At present it is impossible to arrive at a consistent interpretation of this substituent effect; there is no choice but to compile a number of molecular properties that apparently affect the transmission of substituent influences on antiperiplanar carbon atoms.

Direct steric contact and van der Waals compression between the perturbing substituent X and a γ_a -carbon atom under consideration are clearly excluded. It remains to search for through-space and/or through-bond interactions. The first are the classical electric-field effects, whereas the latter consist of inductive effects. Orbital interactions (lone pairs and/or bond orbitals) as possible pathways have been subject to intensive investigations during recent years (210–213), and interactions between atoms via parallel C–C σ -bonds are well known in NMR spectroscopy [cf. the long-range H–H coupling in coplanar W-arrangements; apparently, this is a favorable molecular substructure for σ -electron delocalization (214)]. A rough correlation of γ_a -SCS(X) with electronegativity or inductive σ^*

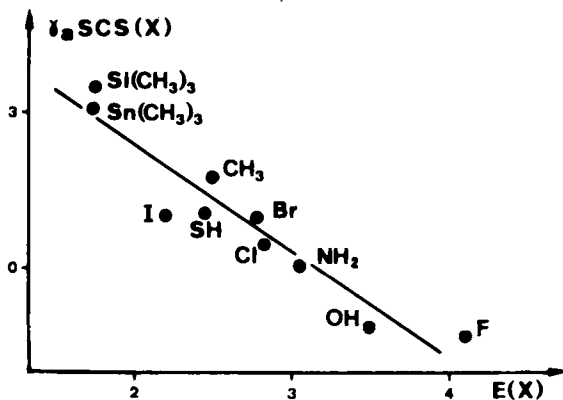


Figure 5. γ_a -SCS(X) values in 2-substituted adamantanes **25** plotted against Allred–Rochow electronegativities $E(X)$.

constants was noticed early when they were compared for series of closely related derivatives of given parent molecules (113,146,164,176,215). This is shown in Figure 5 for 2-substituted adamantanes **25** (105,156,216). The slope of this plot is negative, an observation at variance with the positive slope expected on the basis of Pople's charge-alternation concept (61) (Section II-B-1). A corresponding correlation was reported for ^{19}F nuclei in antiperiplanar γ -position with respect to varying substituents X (217). On the other hand, in compounds with quaternary α -carbons, the slope may indeed be positive, at least if only substituents within the same row of the periodic table are compared (cf. Figure 6) (105,124,215,218); for the halogens, however, a negative slope is again obtained. This discrepancy suggests some fundamental differences in the magnitudes of γ_a -SCS for secondary and tertiary compounds, a subject to which we will return later in this section.

Having considered the inductive effects of substituents X, we will now discuss some experimental findings indicating a contribution of intramolecular electric fields to γ_a -SCS. Schneider and co-workers (76,114,219) have explained the signal shifts on the basis of LEF-induced bond polarizations, although only poor correlations of experimental shifts with calculated charge separations were obtained (76,114). They claimed, however, that there is a significant dependence of electron flow in the bonds to the γ -carbon atoms on the very small electron-density accumulations at β -carbon atoms (76). This is consistent with the observation that pure through-space effects of X on a carbon atom in similar spatial arrangement but without a coplanar σ -framework are much less strong (219):

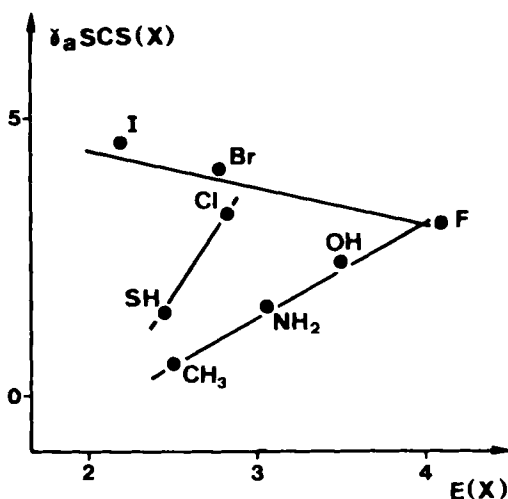
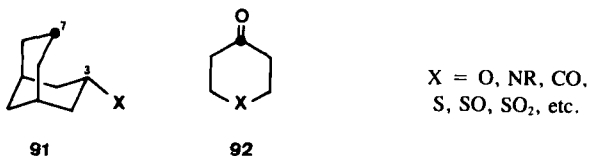


Figure 6. γ_a -SCS(X) values in 1-substituted adamantanes **26** plotted against Allred-Rochow electronegativities $E(X)$.

The effects of 3-exo substituents on C(7) in bicyclononanes **91** are negligible (-0.1 to -0.3 for $\text{X} = \text{Cl}$, Br , or OH). Others (189,220) have considered electric-field effects and rejected them; in particular, Wiberg and co-workers (189) showed that such effects are insufficient to account for the observed shifts.



Scheme 28

In cases where antiperiplanar carbon atoms form highly polarizable bonds to atoms in δ -position, LEF effects can be ascertained more readily. Thus the relatively large sensitivity of carbonyl resonances in **92** to changes in X as compared with corresponding methylene signals (CH_2 in place of CO) was ascribed to this transmission mechanism (199). It has been shown (221–223) that the difference $\Delta\delta$ between the γ_a -SCS(F) of C(4) of **93** and that of C(9) can clearly be linearly related (cf. Figure 7) to the C(4)–Y bond polarizability b_1 (224), leading to charge accumulations at C(4) if this bond is highly polarizable ($\text{Y} = \text{Cl}$ or Br). Consequently, the opposite is observed for γ_a -SCS[Si(CH_3) $_3$] in **94** (223).

There has been intensive discussion in the literature connecting signal shifts

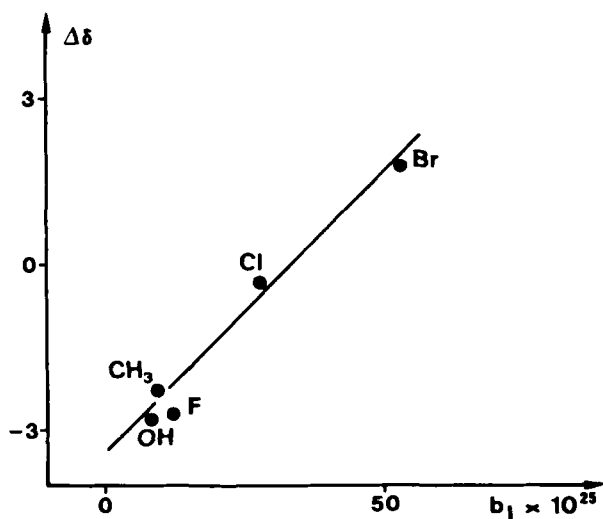
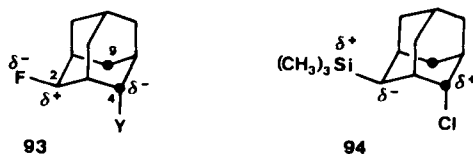
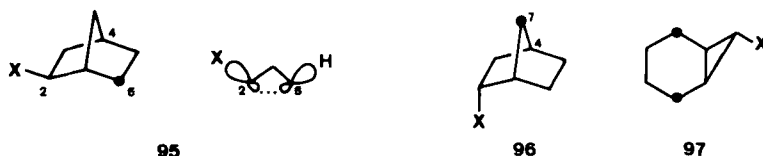


Figure 7. Differences $\Delta\delta$ between γ^a -SCS(F) values at C(9) and C(4) in **93** plotted against C(4)–Y bond polarizabilities b_1 .



Scheme 29

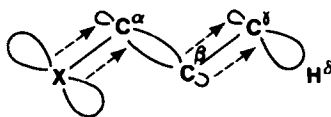
of γ_a -carbon atoms with interactions of bonding and/or lone-pair orbitals. The first such concept, published in 1970, was back-lobe overlap, which was considered to be the origin of unusually large high-field γ_a -SCS(X) values at C(6) in 2-exo-substituted bicyclo[2.2.1]heptanes **95** as compared with effects at C(4) or at C(7) in **96**, which have less favorable orbital orientations (93) (Scheme 30).



Scheme 30

The observed γ_a -SCS(X) values in 7-exo-substituted norcaranes **97** (225) and those of $M(\text{CH}_3)_3$ ($M = \text{Si}, \text{Ge}, \text{Sn}, \text{or Pb}$) in cyclohexyl and bicyclo[2.2.1]heptane derivatives (133) were later interpreted on the same basis. The back-lobe-overlap treatment was further supported by interpretations of ^1H and ^{13}C contact shifts of aliphatic amine signals in the presence of nickel acetylacetonate and by INDO calculations (226,227). Additional support came from extensive investigations of the structure dependence of three-bond coupling constants $^3J_{\text{CX}}$ ($X = \text{H}, \text{C}, \text{or F}$) (228,229), although the interpretation of these data has been subjected to criticism (230).

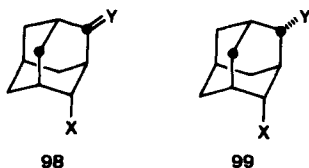
In their pioneering paper about heterosubstituent-induced shifts of antiperiplanar γ -carbon atoms, Eliel and colleagues (220) showed that in secondary substrates, second-row heteroatoms ($X = \text{N}, \text{O}, \text{F}$) give rise to significantly larger upfield-shifting effects than do carbon and heterosubstituents of higher rows ($X = \text{CH}_3, \text{CH}_2, \text{S}, \text{Cl}$). These authors suggest that a hyperconjugative mechanism (Scheme 31) is responsible for the difference. In the following years,



Scheme 31

however, a number of experimental findings appeared that contradicted this hypothesis. For example, phosphorus substituents usually exhibit distinctly negative γ_a -SCS values (128,129,231), even though this element belongs to the

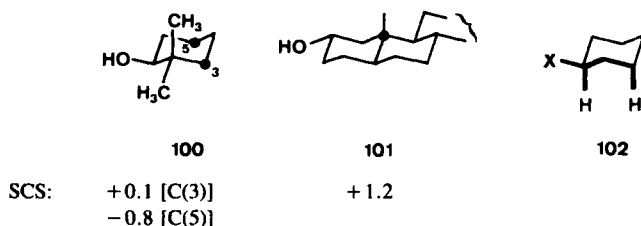
third row. Nevertheless, this approach had great impact on the discussion of γ_{a} -SCS transmission mechanisms. In a somewhat modified version, it was adopted to rationalize γ_{a} -SCS values of heterosubstituents in general, that is, not only of those containing nitrogen, oxygen, and fluorine atoms directly attached to the α -carbon atom (105,216,221,222,232). The main argument for this extension is the fact that γ_{a} -effects of X in substituted adamantanes like **98** and **99** strongly depend on the presence or absence of lone pairs at Y, the intramolecular interactions between X and Y in the two cases being quite different (216,232) (cf. Section IV-C). This interpretation resembled that of Schneider (76), cited above, according to which the γ_{a} -carbon signal shift is caused by an electron-density change at C^{β} induced by an interaction with the lone pair at X (61). Possibly a more rigorous theoretical elaboration will show that the two interpretations—and maybe even the back-lobe-interaction model (Scheme 30)—are more or less equivalent.



Scheme 32

In the mid-1970s NMR spectroscopists became aware of a striking feature of γ_{a} -effects when they studied the dependence of their magnitudes and signs on the substitution pattern at the atoms C^{α} through C^{γ} . Eliel and co-workers (220) had already pointed out that the significant upfield signal shifts of carbon atoms antiperiplanar to N, O, and F do not appear if these substituents are attached to bridgehead carbon atoms; for instance, $\gamma_{\text{a}}\text{-SCS}(\text{F}) = -1.3$ in 2-fluoroadamantane but $+3.1$ in the 1-fluoro isomer (Figures 5 and 6, pp. 254 and 255). Shortly afterward, Stothers and colleagues (208) reported deshielding γ_{a} -SCSs of hydroxyl and methyl groups if the α -carbon atom was quaternary, and Wiseman and Krabbenhoft (233) suggested that the crucial factor is the absence of a hydrogen atom and not the fact that the substituent is angular or fixed at a bridgehead atom in bi- or tricyclic molecules. Indeed, such changes from upfield to downfield were observed in monocyclic tertiary alcohols (234,235) as well. This behavior is not restricted to second-row substituents but is observed also for higher-row heterosubstituents (cf. Figures 5 and 6), although in the latter case an enhancement of downfield shifts is involved, rather than a sign reversal, when a γ_{a} -SCS of a given X in a primary or secondary substrate is compared with that of a tertiary one (151,215). A quaternary α -carbon atom, however, is not a necessary condition for a downfield change in γ_{a} -SCS. It is sufficient that any of the intervening carbon atoms (C^{α} , C^{β} , or C^{γ}) be quaternary (222,236). Examples are **100** (150) and **101** (19,110) (Scheme 33). This led to the conclusion that

the γ_a -SCS(X) is intrinsically downfield and that in primary and secondary substrates there is an additional upfield-shifting contribution from the presence of 1,3-diaxial hydrogen atoms at the α - and γ -carbon atoms (**102**) (146,222), the physical meaning again being mysterious (cf. Beierbeck and Saunders's alternative explanation of γ_g -SCS in Section III-C).



Scheme 33

There are, however, two experimental findings opposing the hypothesis of a more or less independent upfield contribution of that sort: First, the different slopes in Figures 5 and 6 for the series of second-row substituents is inconsistent with this concept. Second, this contribution is not at all constant. This is demonstrated in Figure 8 (223) by the electronegativity dependence of $\Delta\delta$ -values which represent the difference between the γ_a -SCS(X) values at C(9) and C(4)

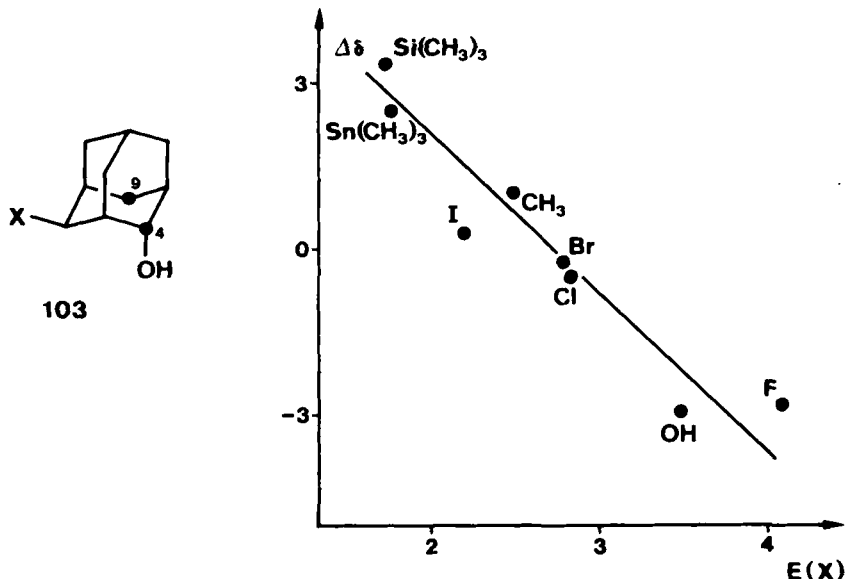

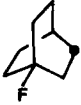





Figure 8. Differences $\Delta\delta$ between γ_a -SCS(X) values at C(9) and C(4) in **103** plotted against Allred-Rochow electronegativities $E(X)$.

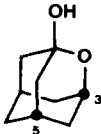
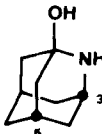
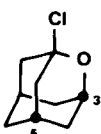
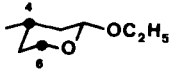
in **103**. The only distinction between the two atoms is the missing 1,3-diaxial hydrogen-hydrogen arrangement in the $\text{X}-\text{C}(4)$ substructure. Thus, $\Delta\delta$ can be regarded as a measure of the contribution of that particular moiety (**102**). The plot indicates a rough but significant electronegativity correlation; that is, the contribution concerned is not an inherent shielding effect associated with a certain structural property. On the contrary, it may vanish or be deshielding, and the magnitude of the electronegativity dependence is even larger than those of the $\gamma_{\text{a}}\text{-SCS}(\text{X})$ values themselves (cf. Figure 5). At present, no satisfactory explanation can be given for this observation.

In 1977 several authors independently reported that the size of $\gamma_{\text{a}}\text{-SCS}(\text{X})$ is a function of the torsional angle τ between the $\text{X}-\text{C}^{\alpha}$ and $\text{C}^{\beta}-\text{C}^{\gamma}$ bonds (155,156,209,219,233), where the optimal, that is, maximally deshielding, effect occurs in a coplanar orientation ($\tau = 180^{\circ}$). A quantitative relation was provided for the $\gamma_{\text{a}}\text{-SCS}$ values of OH, Cl, Br, and I in bridgehead-substituted diamondoid compounds, which fall off to zero in a $\sin \tau$ dependence (156). These changes of $\gamma_{\text{a}}\text{-SCS}$ values with varying geometry of the $\text{X}-\text{C}^{\alpha}-\text{C}^{\beta}-\text{C}^{\gamma}-\text{Y}$ molecular moiety ($\text{Y}^{\delta} = \text{H}$ or C) are consistent with the hyperconjugative transmission mechanisms, since torsional angles other than 180° imply a less favorable orbital overlap. On the other hand, a decrease of bond angles within a coplanar conformation is expected to enhance such an interaction (105,156) due to closer proximity of $\text{X}-\text{C}^{\alpha}$ and $\text{C}^{\beta}-\text{C}^{\gamma}$. An exceptionally impressive verification of this prediction has recently been presented by Della and co-workers (126) (Scheme 34). Clearly, there is a pronounced shielding within the series **104**, **27** to **29**, and **32** correlating with an increase in three-bond carbon-fluorine coupling constants ($^3J_{\text{CF}}$). Apparently, the number of individual pathways leading from F to C^{γ} (one in **104**, **27**, and **28**; two in **29**; and three in **32**) and decreases of the $\text{C}^{\alpha}-\text{C}^{\beta}-\text{C}^{\gamma}$ bond angles are significant influences (126). It should be noted that the number of hydrogen atoms at C^{α} does not play a major role in this case: $\gamma_{\text{a}}\text{-SCS}(\text{F}) = -11.9$ in fluorocyclobutane (237), which is very similar to the value for **29**.

The replacement of the β -carbon atom by oxygen or nitrogen (Scheme 34)

					
	104	27	28	29	32
SCS:	+3.1	+1.3	-3.4	-10.2	-18.7
$^3J_{\text{CF}}$:	10.4	9.4	7.9	17.1	42.5

Scheme 34

			
105	106	107	108
SCS: + 3.9 [C(3)] + 2.7 [C(5)]	+ 3.6 [C(3)] + 2.9 [C(5)]	+ 6.1 [C(3)] + 3.7 [C(5)]	- 3.0 [C(6)] - 0.7 [C(4)]

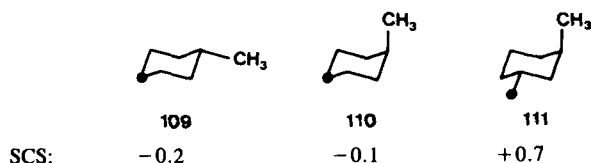
Scheme 34 (continued)

has an effect on γ_a -SCS values of heterosubstituents as well: Downfield γ_a -SCSs are reinforced in tertiary substrates, such as **105** to **107** (156,233,238), whereas an analogous structural modification in **108** leads to an enhanced upfield shift of the γ_a -carbon signal (239). Insertion of sulfur atoms, however, apparently has no significant influence (240), at least on SCSs of group-IVa substituents [$M(CH_3)_3$; $M = C, Si, Ge, Sn, \text{ or } Pb$] at C(4) and C(6) in 2-substituted 1,3-dithianes. This seems to suggest that γ_a -SCS alternations of this sort originate in conformational changes rather than in electronic heteroatom interactions (156). More experimental material, however, is required if we are to gain deeper insight.

In summary, it is the author's conclusion that a universal transmission mechanism governing γ_a -SCS(X) does not exist. Several potential mechanisms are available and which of them dominates depends very much on the rest of the molecule. Clearly, a lot of work needs to be done before chemists will have a comprehensive understanding of γ_a -substituent effects. At the moment it appears to be dangerous to draw stereochemical conclusions from signs and magnitudes of γ_a -SCSs unless a careful investigation of underlying transmission mechanisms in the molecule concerned has been performed. On the other hand, γ_a -SCSs, and especially their structure dependence, have considerable theoretical potential and represent an attractive playground for chemists interested in σ -electron delocalizations.

E. δ -Effects

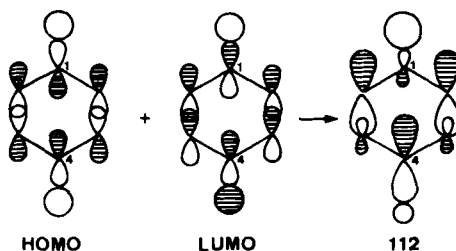
In general, δ -substituent effects are small or even negligible (cf. **109** and **110** in Scheme 35). Lippmaa and Pehk (60) investigated δ -SCS values for a wide range of substituents and reported that they are practically zero in *n*-pentyl and slightly negative in cyclohexyl derivatives. For the latter series a rough correlation with inductive σ^* constants was detected; the largest δ -SCS, however, was only -2.1 ($X = NO_2$). This is in accord with δ -SCS(CH_3) values in cyclohexanes (100,101), although a configuration like **111** (Scheme 35) seems to be somewhat



Scheme 35

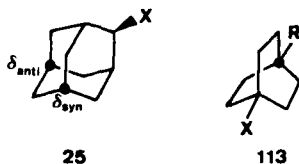
exceptional (241). In the same parent system electronegative substituents X (OH, Cl, Br, etc.) produce larger shielding effects in equatorial than in axial position (76,114). Such δ -SCSs were rationalized on the basis of LEF-induced signal shifts (76,77,81,82,85).

In a completely different interpretation Zefirov (242) proposed a new concept of frontier-orbital mixing (243) to explain how conformational and electronic effects in monosubstituted cyclohexanes are transmitted to remote δ -carbon atoms (Scheme 36). The orbitals at C(1) and C(4) in **112** are considered to be equatorial (242). A perturbation at C(1) (H is replaced by X) produces an electron-density shift from H(4) toward C(4) (242), which is associated with an upfield shift of the latter's signal. Although this approach appears to be quite crude and does not account for axial substituents, it deserves further attention.



Scheme 36

In 2-substituted adamantanes **25** both types of δ -positioned carbon atoms (δ_{syn} and δ_{anti}) exist within one molecule (Scheme 37). Early measurements with limited spectral resolution (176) did not differentiate between their signals. Later (124,244), differences of up to 0.7 ppm were detected, and application of various independent methods, including addition of lanthanide shift reagents (245), determination of longitudinal relaxation times T_1 (246), and evaluation of deuterium

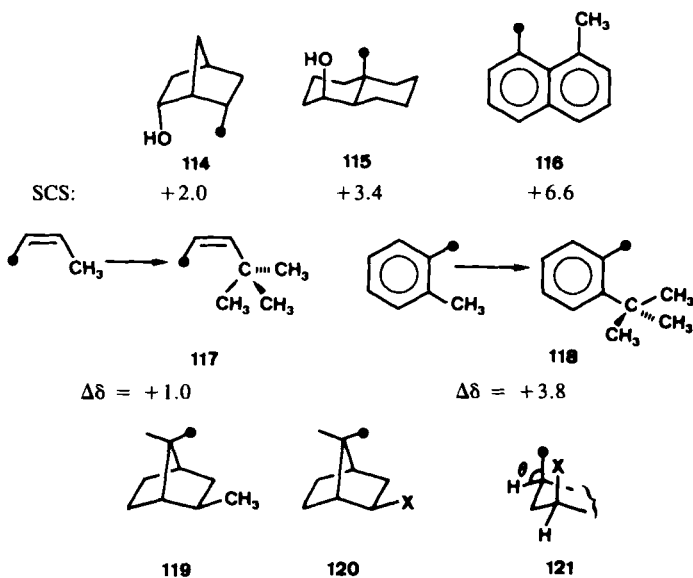


Scheme 37

isotope shifts in selectively deuterated 2-adamantanols (247), unequivocally proved that the signal of the δ_{anti} -carbon atom appears at higher field than that of the δ_{syn} -carbon, in analogy with the situation in axially vs. equatorially monosubstituted cyclohexanes.

In bridgehead-substituted bicyclo[2.2.2]octanes **113** ($R = H, Ph$) the LEF treatment failed to rationalize observed δ -SCS(X) values (189,248). Since the $X-C^{\alpha}$ and $C^{\delta}-R$ bonds are collinear, one expects upfield shifts, with absolute values decreasing in the order $F > Cl > Br > I$. The opposite, however, is found experimentally, so it was concluded that magnetic-field effects are probably responsible for these δ -effects (189).

If the perturbing substituent X and the δ -carbon atom are in syn-axial (sa) position, the magnitudes of the δ -SCSs are in striking contrast to those discussed above. In this configuration distinct deshielding δ_{sa} -SCSs are noticed. Stothers was the first to call attention to this phenomenon (7,117,184,249) in, for example, **114** to **116** (Scheme 38). Deshielding of methyl signals in *cis*-butenes **117** (113), *ortho*-substituted toluenes **118** (250), and various 1,8-dialkynaphthalenes (251) indicates analogous effects.



Scheme 38

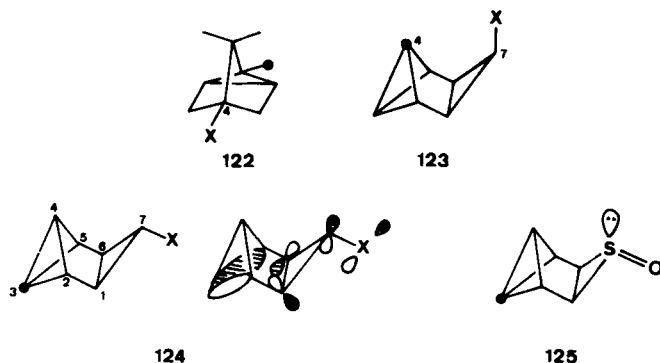
The observation of deshielding δ_{sa} -SCSs was a crushing blow to the Grant-Cheney concept (33,88) correlating shielding γ_g -SCSs with steric compression (cf. Section III-C), since in the δ_{sa} -orientation even more severe spatial interference occurs. An interpretation (252) in which δ_{sa} -SCS is split into loss of γ_{gauche} and introduction of δ -interactions, though quite artificial, may be useful.

Schneider and Weigand (159) calculated -18 for $\delta_{\text{sa}}\text{-SCS}(\text{CH}_3)$ in **119** using the simple Grant–Cheney formulation (eq. [17], p. 246), whereas in fact $+1.3$ is the value found. Similar shift values ($+0.8$ to $+0.9$) are produced by halogen substituents in **120** (189).

Based on their hypothesis that $\gamma_{\text{g}}\text{-SCS}(\text{X})$ is not of steric origin (146), Beierbeck and Saunders conclude that the deshielding of syn-axial δ -carbon atoms is a manifestation of a genuine steric compression effect (146). Accordingly, one would expect that the magnitude of $\delta_{\text{sa}}\text{-SCS}$ should decrease in molecules where the diaxial groups are able to alleviate severe steric interference by splaying (184). A careful analysis of monohydroxy steroids (110), especially when combined with consideration of molecular geometry determined by force-field calculations (111), seems to suggest, on the contrary, that enhanced nonbonded interactions resulting from smaller internuclear distances cause less deshielding of δ_{sa} -carbon atoms.

An alternative explanation of the δ_{sa} -effect based on bond-angle (θ) distortions in **121** has been given by Gorenstein (191). It should be noted that recently, analogous δ_{sa} -effects were observed at ^{17}O nuclei (207).

Clear downfield δ -SCSs ($+1.3$ to $+2.9$) were also observed in 4-substituted tricyclenes **122**, although they have no syn-axial orientation of X and the δ -carbon atom (154). Possibly, the transmission of the δ -SCS is modulated by the intervening cyclopropane moiety (154).



Scheme 39

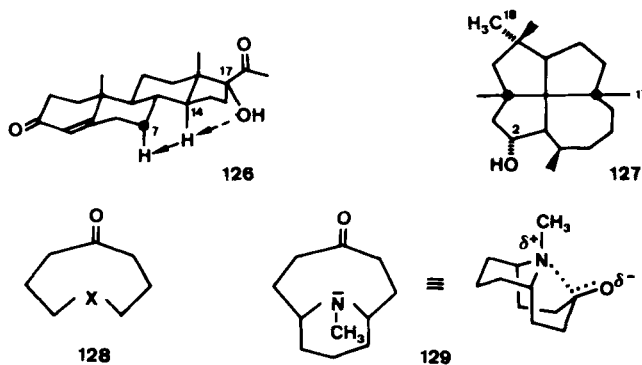
Even more pronounced downfield δ -SCSs on C(4) values of nearly $+6$ were detected in 7-*endo*-substituted tetracycloheptanes **123** ($\text{X} = \text{F}, \text{Cl}, \text{or Br}$) (205). On the other hand, in the corresponding *exo* isomers **124**, $\delta\text{-SCS}(\text{X})$ values on C(3) are drastically shielding (for $\text{X} = \text{F}$, -9.1 ; for $\text{X} = \text{Cl}$, -4.8 ; and for $\text{X} = \text{Br}$, -4.1) (205). This was ascribed to a less efficient electron delocalization from C(2)–C(3) and C(5)–C(3) bonds to the unoccupied Walsh orbital of the C(1)–C(6)–C(7) ring (cf. orbital representation of **124** in Scheme 39), because the latter is raised in energy due to an interaction with the n -orbital of X (205).

The δ -SCS of the exo oxygen in **125** (as compared with the corresponding thiirane) is even larger, -23.0 (204).

F. Long-Range Effects

In general, long-range SCSs are relatively small ($<|1|$), since through-bond influences even from highly electronegative substituents fade away when five or more atoms intervene. Thus, palpable substituent effects can be discerned only if either the introduction of a substituent is associated with a geometrical distortion of the molecular framework or the substituent is particularly effective in exerting long-range through-space effects. In addition, it may happen that a flexible molecule adopts a conformation in which the carbon atom observed, although many bonds away, is rather near the substituent in space and thus exposed to through-space influences.

Long-range SCSs are sometimes observed in extended polycyclic compounds, for example steroids; slight geometric changes may be propagated to a remote part of the molecular backbone (253). There seems to exist a tendency to high-field long-range SCSs (117), but deshielding may be observed as well. An example is progesterone (**126**). Introduction of a hydroxyl group in the 17α -position causes a -1.2 -ppm shift of the C(7) signal (ϵ -SCS), which has been explained by transmission of steric interference via the 14α -hydrogen atom (254). Another instance is a ζ -SCS(OH) of $+1.2$ on C(18) in 2α -hydroxy- $1\beta H$ -laurenane (**127**), a derivative of a naturally occurring fenestrane (255); significant ϵ -SCS(OH) values on C(17) ($+1.2$ to $+1.7$) were also noticed in these molecules (255). Through-space, that is, LEF, effects over long distances are expected if the target carbon atom is involved in a bond that is suitably oriented and, additionally, highly polarizable. The latter condition is not met in C-H and C-C single bonds, so electric fields do not induce noticeable signal shifts at remote unsubstituted sp^3 carbon atoms. Long-range SCSs on alkene carbon atoms, however, have been discussed in terms of LEF effects (78,80,84).



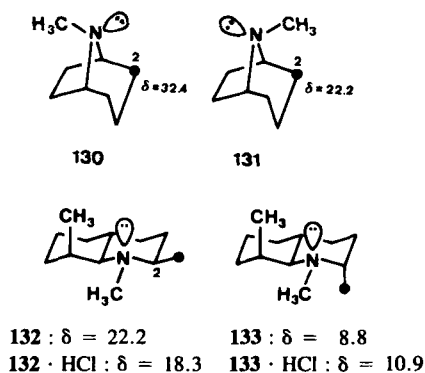
Scheme 40

In this context transannular interactions must be mentioned, although there are very few authenticated reports of such effects, and they involve solely sp^2 carbon atoms. Thus, Maciel and Nakashima (256) ascribed a shielding of the carbonyl atom in **129** of approximately 10 ppm relative to **128** ($\text{X} = \text{CH}_2, \text{O}, \text{S}$) to a transannular interaction associated with a partial charge separation (Scheme 40). Less clear-cut results were obtained from the spectra of 3- and 4-thiacyclohexanone (199,257). For the sake of completeness we note that aromatic carbon atoms experience considerable deshielding (6–9 ppm) in bi- and multi-layered [2.2]paracyclophanes (258,259). This was attributed to a decrease of the excitation-energy term in the σ_p expression (eq. [3], p. 222).

G. Lone-Electron-Pair Effects

It was pointed out in Section III-D that free electron pairs at heteroatoms may be involved in the transmission mechanism of γ_s -SCSSs. This participation can be probed effectively using conformationally rigid molecules with built-in heteroatoms in which the stereochemical orientation of the lone pair can be varied. Nitrogen is very suitable for this purpose, so most of the pertinent work has been done with piperidines and related bicyclic analogs.

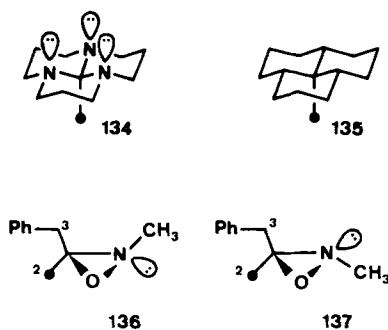
Hamlow and co-workers (260), and later several other authors, found that in piperidines nitrogen lone pairs can give rise to significant shieldings of antiperiplanar protons (261,262, and references cited therein). Analogous phenomena have been looked at for ^{13}C nuclei. The C(2) atom of **131** gives a signal approximately 10 ppm to higher field than that of **130** (263). Since the γ_g -effect of the *N*-methyl group in **131** is expected to contribute only -6 , the authors conclude that a considerable part of the 10-ppm shielding must be due to the antiperiplanar orientation of the free electron pair of nitrogen (263). Consequently, the upfield shift is reduced when methanol is used as solvent, because the lone pair is then involved in hydrogen bridging (263). Eliel, Vierhapper, and co-workers have



Scheme 41

investigated lone-pair effects on carbon shieldings in a great variety of decahydroquinolines (142,165,194,262,264,265), such as **132** and **133**. The chemical shifts of the methyl groups at C(2) are $\delta = 22.2$ in **132** and $\delta = 8.8$ in **133** (142,262,264), a difference too large to be explained merely by a γ -gauche effect of the *N*-methyl group. The chemical-shift difference of the corresponding hydrochlorides is reduced by nearly half (to 7.4), so it is concluded that a considerable portion of the C(2)-methyl shielding in **133** originates from the presence of an antiperiplanar lone pair. Surprisingly, however, the evidence of free-electron-pair effects is restricted to *N*-methylated compounds; there is no corresponding effect in NH derivatives (194,262). The reasons for this are not understood.

Corresponding lone-pair effects were reported in other piperidines (235,266,267), in some orthoamides, and in oxaziridines (**134** to **137**). The CH₃ signal in the orthoacetamide **134** appears at $\delta = -4.0$, compared with $\delta = +6.8$ in the carbon analog **135** (267). Even if enhanced steric compression in **134** due to shorter C–N bond distances is allowed for, the considerable net shielding effect must be explained by a triple hyperconjugative stabilizing overlap of nitrogen lone pairs and the antibonding σ^* -orbital of the antiparallel C–C bond (267). Differences in methyl signals for substituted oxaziridines **136** and **137** and related compounds were interpreted along analogous lines (268): The C(2) chemical shifts in **136** and **137** are $\delta = 23.1$ and 14.4, respectively, and a reciprocal CH₂Ph-signal-shift difference is observed (268). It is interesting that ¹⁵N nuclei are significantly shielded if hydrogen atoms antiperiplanar to the free electron pair are replaced by carbon atoms (269).

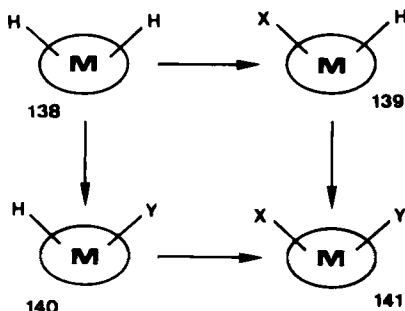


Scheme 42

The picture is less clear when free electron pairs on other heteroatoms (O, S, etc.) are involved. There is only one clear-cut case providing evidence concerning endocyclic sulfoxides: The unusually large shieldings of carbon atoms in gauche position relative to an axial oxygen atom in thiane oxides **79**, **80**, **82**, and **83** (p. 252) (200,201) have been partially ascribed to an upfield-shifting effect of the equatorial antiperiplanar lone pair (cf. Section III-C).

IV. INTRAMOLECULAR INTERACTION EFFECTS

In the preceding section substituent effects on aliphatic carbon atoms, mostly in monosubstituted molecules, were examined by comparing their ^{13}C chemical shifts with those of the respective unsubstituted parent compounds. If one proceeds to molecules **M** bearing two substituents (X, Y; Scheme 43) it often happens that $\text{SCS}(\text{X})$ (**140** \rightarrow **141**) or $\text{SCS}(\text{Y})$ (**139** \rightarrow **141**) differ considerably from the values expected for the monosubstituted prototypes (**138** \rightarrow **139** and **138** \rightarrow **140**, respectively).



Scheme 43

Two reasons for the discrepancy are conceivable: First, the conformational equilibria in the four derivatives, that is, the parent and the mono- and disubstituted derivatives, may be altered, for instance by unfavorable steric interference of one substituent with the other or with the backbone of the molecule. Thus, the individual $\text{SCS}(\text{X})$ and $\text{SCS}(\text{Y})$ are changed in magnitude or even produced by different transmission mechanisms (e.g., a γ_{g} -SCS may be turned into a γ_{a} -SCS). Even slight geometric distortions of a molecule in a "stable rigid" conformation, as, for example, frequently occur in highly substituted cyclohexanes, must be considered. Second, there may exist an electronic interaction, either through space or through bond, between the substituents. This means that the properties of a given substituent (e.g., its inductive or field effect) are changed, because its electronic environment is perturbed by the influence of another substituent.

Thus it is evident that a survey of effects on ^{13}C chemical shifts cannot avoid a detailed discussion of such substituent-induced changes of SCSs. Since the following is the first review of this subject, the restriction to aliphatic compounds imposed elsewhere in this chapter is somewhat relaxed; thus effects on unsaturated carbon atoms are occasionally included, without, however, abandoning the general target group of aliphatic molecules. Therefore typical aromatics, in which the substituent interaction is propagated through an extended π -electron system, are still excluded.

There is considerable need for exploration of interaction effects: If SCSs are to be used for signal assignments or structure determinations, it is essential to know about alterations of SCSs by interactions with other substituent(s) to avoid misinterpretations. Additionally, interaction effects provide valuable information about the σ -electron distribution and its dependence on structure, since it is well known that ^{13}C chemical shifts are highly sensitive to changes in the geometry and/or electronic state of the molecule. This research area is not easily accessible experimentally by other spectroscopic methods, at least for larger molecules, which are also beyond the reach of most theoretical calculations.

When interaction effects are to be estimated and interpreted, the first problem that arises is which parts of the molecule are to be considered as substituents and which as the molecular backbone that is held constant. The decision is clear if exocyclic substituents (e.g., CH_3 , C_6H_5 , or COOR) are involved; exoolefins, ketones, imines, or thiones can be treated in the same way by defining appropriate doubly bonded carbon, oxygen, nitrogen, and sulfur substituents, respectively. The situation, however, is more complicated if substituents are endocyclic, for example the double bond in a cyclohexene derivative or a cyclic ether oxygen atom, because in that case the reference compound without those groups or atoms is, of course, no longer cyclic. It is simple—at least in principle—to replace one of several exocyclic substituents by hydrogen, leaving the backbone untouched; taking away an endocyclic substituent generally means the destruction of the molecule. Even replacement by a saturated carbon fragment ($\text{>C=C<} \rightarrow \text{>CH-CH<}$ or $\text{-O-} \rightarrow \text{-CH}_2\text{-}$) is often not an appropriate compensation, since new atoms (here hydrogens) are added and bond angles and lengths changed.

Thus, in the endocyclic case, interaction effects can at best be estimated, whereas if exocyclic substituents are involved and the molecular framework is conformationally rigid, a reliable quantitative measure is obtainable.

The simplest approach is to compare experimental chemical shifts (δ_{exp}) in, say, a disubstituted compound with values calculated under the assumption of perfect additivity of the individual SCSs (δ_{calc}), where $\Delta\delta$ is defined as the difference between these. To denote the origin of these effects the designation ICS (intramolecular interaction chemical shift) $\equiv \Delta\delta$ is proposed in analogy to SCS (eq. [11], p. 230):

$$\Delta\delta = \delta_{\text{exp}} - \delta_{\text{calc}} = \text{ICS} \quad [18]$$

This approach is admissible because SCSs are well known to be additive unless (i) the conformational equilibrium of the molecule is altered by progressive substitution, and/or (ii) there is no intramolecular substituent interaction whatsoever. Thus, if application of eq. [18] to a rigid molecular system affords ICS values other than zero, such an interaction must exist. In earlier publications (216,221) the abbreviation NAE (nonadditivity effect)—a merely descriptive term—was employed.

Table 15
Calculation of ^{13}C Chemical Shifts of **142** Assuming Additivity of Individual SCSs,
and Comparison with Experimental Values

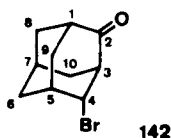
Carbon	Basic Value ^a	SCS(=O) ^b	SCS(Br) ^b	δ_{calc} ^c	δ_{exp}	ICS
1	28.5	18.4 (β)	-1.5 (δ_a)	45.4	45.0	-0.4
2	37.8	178.8 (α)	1.0 (γ_a)	217.6	210.4	-7.2
3	28.5	18.4 (β)	8.0 (β)	54.9	54.5	-0.4
4	37.8	1.4 (γ)	25.9 (α)	65.1	56.2	-8.9
5	28.5	-0.9 (δ)	8.0 (β)	35.6	34.7	-0.9
6	37.8	-1.5 (ϵ)	-6.1 (γ_a)	30.2	30.2	0.0
7	28.5	-0.9 (δ)	-0.8 (δ_a)	26.8	26.7	-0.1
8	37.8	1.4 (γ)	0.2 (ϵ)	39.4	39.2	-0.2
9	37.8	1.4 (γ)	1.0 (γ_a)	40.2	35.5	-4.7
10	37.8	1.4 (γ)	-6.1 (γ_a)	33.1	33.9	0.8

^aChemical shift of C(i) in the parent compound, here adamantane.

^bSCS derived from the respective monosubstituted adamantane; letters in parentheses denote the relative position of C(i) with respect to the substituent.

^c $\delta_{\text{calc}} = \text{basic value} + \text{SCS}(=\text{O}) + \text{SCS}(\text{Br})$.

Table 15 indicates how δ_{calc} values for 4^e-bromoadamantanone* (**142**) are determined, the two substituents being bromine and a doubly bonded oxygen atom.



Scheme 44

In compounds containing endocyclic substituents the individual SCSs will be referred to the corresponding saturated carbocyclic analog.

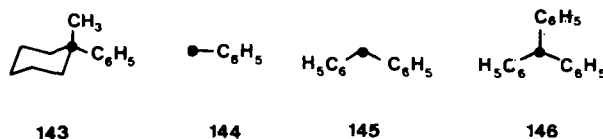
A. Geminal Substituents; Heavy-Atom Effects

Geminal substituents in multiply substituted compounds present the situation of closest mutual proximity. For that reason it is often difficult, if not impossible, to separate steric from electronic contributions to nonadditivity effects (NAEs, ICSs). A predominance of steric contributions to the ICS is expected when at

*The superscript "e" refers to the equatorial position of a substituent (here Br) in that ring of the adamantane which is disubstituted [here the cyclohexanone ring C(1,2,3,4,5,9)]. A superscript "a" denotes the corresponding axial position.

least one of a pair of interacting substituents is alkyl. The geminal dimethyl α -ICS in cyclohexane on the substituted carbon atom is -3.8 ± 0.3 (100). This means that the combined α -SCS(CH_3) is smaller than that calculated by adding the α -SCS of an equatorial and an axial CH_3 in methylcyclohexane. The neighboring (β -) atoms also experience a negative ICS (-1.3 ± 0.2), and the next further (γ -) atoms a positive ICS ($+2.0 \pm 0.2$) (100). Rather similar α -ICS(CH_3/CH_3) values were found in 1,3-dioxanes and -dithianes (270–272) as well as in cyclobutanes (273). Larger effects, are encountered in cyclopentane (174,273) and oxirane (274), whereas they are smaller in cyclopropane (275) and aziridine (276). In the latter compounds the decrease of α -ICS(CH_3/CH_3) compared with that in 1,1-dimethylcyclohexane is explained by lesser steric constraints, since the $\text{CH}_3\text{--C}^\alpha\text{--CH}_3$ bond angle is widened (276).

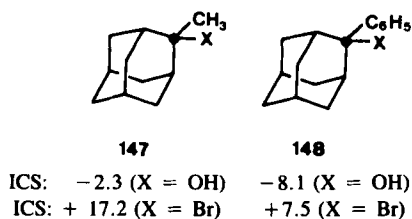
If one methyl group is replaced by phenyl, the α -ICSs seem to tend to stronger shieldings; in the cyclohexane conformer **143** a value of ca. -7 can be estimated (277); in the conformer in which the substituents are interchanged, the value is ca. -5 (277).



Scheme 45

Individual substituent effects of phenyl groups in substituted methanes and ethanes are not additive either (278), but decrease with progressive substitution: In methane derivatives the first α -SCS (**144**) is 23.5, the second (**144** \rightarrow **145**) 20.7, and the third (**145** \rightarrow **146**) 14.7 (278). Although these values differ markedly from those of corresponding methylated compounds (methyl instead of phenyl) (169), the tendencies are in good qualitative agreement in both cases.

In 1-methylcyclohexanol the α -ICS is -1.7 if the hydroxyl group is axial, but negligible if it is equatorial (234); the β -ICSs of these two combinations are -2.8 and $+0.1$, respectively (234). The γ -ICS of $+4.8$ in the epimer with equatorial OH is remarkable (234). Apparently, a great proportion of it originates from the fact that a γ_α -SCS(OH) in a tertiary substrate is more deshielding than that in a secondary one (cf. Section III-D). Large downfield α -ICSs were reported for geminally halogenated methylcyclohexanes (177): $+5.3$ (axial Cl), $+7.8$ (equatorial Cl), $+9.6$ (axial Br), and $+11.3$ (equatorial Br). Some related 2-substituted 2-methyladamantanes **147** (105) exhibit an analogous trend in their α -ICSs, whereas in the phenyl derivatives **148** the corresponding parameters are strongly shielding relative to those of **147** (105). This seems to indicate that in addition to an ICS contribution of steric origin (slightly shielding for CH_3/OH but significantly deshielding for CH_3/Cl and CH_3/Br), there is a shielding electronic interaction between the heterosubstituent X and a phenyl group (279).



Scheme 46

Upfield shifts of multiply heterosubstituted carbon atoms are well known in the ^{13}C NMR literature. Some representative examples are shown in Figure 9 and Table 16, where the actual ^{13}C chemical shifts and individual α -SCSs, respectively, for each newly introduced substituent in methane derivatives are compiled. The ICSs can be calculated by subtracting any α -SCS from its respective predecessor within a given row in Table 16. The general trend is toward a distinct decrease of α -SCS with progressive substitution; that is, all the ICSs are negative.

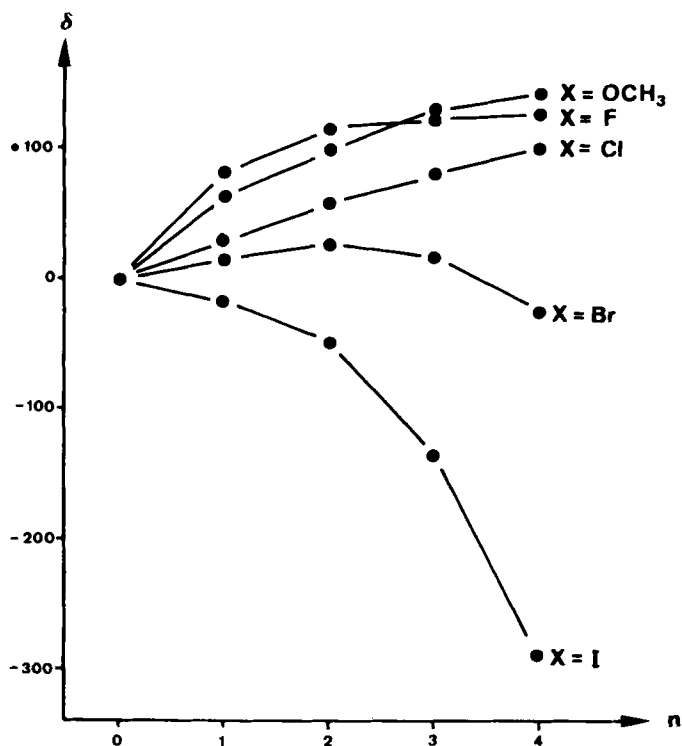
Figure 9. Chemical shifts δ in some substituted methanes $\text{CH}_{4-n}\text{X}_n$.

Table 16
Individual α -SCSs in Substituted Methanes^a

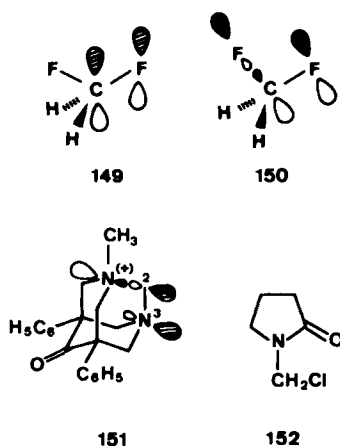
X	Substituted Methane				Ref.
	CH ₃ X	CH ₂ X ₂	CHX ₃	CX ₄	
OCH ₃	61.5	34.8	33.0	12.0	2
F	79.6	33.8	7.4	5.2	280
Cl	27.2	29.1	23.5	19.0	2
Br	12.3	11.4	-9.3	-40.8	2
I	-18.4	-33.3	-85.9	-152.6	2

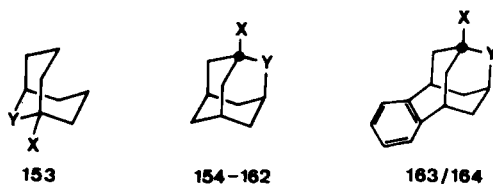
^aFor explanation, see text.

It is obvious that there is a basic difference between assemblies of second- and third-row substituents (OCH₃, F, Cl; Category I) and those of higher rows (Br, I; Category II). In the latter the signals are not shifted less downfield than expected (see below) by additional substitution, but rather upfield, culminating in a chemical shift of $\delta = -292.3$ in Cl₄ (281). This latter phenomenon has been designated the "heavy-atom effect" (57).

Category I Substituent Assemblies: The first rationalization of the observation that in acetal-type compounds the α -SCS of the second oxygen function is considerably smaller than that of the first (70,239) was the assumption that an adjacent oxygen atom reduces the polarizability of the α -carbon atom, so that it cannot be polarized as effectively by the second substituent (142).

In the difluoro case a significant C-F double-bond contribution ($n\pi^*$ interaction, 149) was shown, by *ab initio* calculations of carbon shieldings in fluorinated methanes (280) to occur if at least one pair of fluorine atoms is present





Scheme 47

(cf. also ref. 213). Thereby weakened α -SCS(F)s (negative ICSs) are operative. Double-bond character was invoked also by Block (282) and Zeroka (283), who found that the data points for fluoromethanes do not fit a correlation between carbon chemical shifts and carbon $1s$ -electron binding energies that holds for chloro- and bromomethanes. Raines (284), however, has pointed out that π -bonding is probably not the only explanation for such ICS effects. Another interaction mechanism is conceivable, namely $n\sigma^*$ (150), which is considered to be the electronic background of the "anomeric effect" (285,286). Wolfe and co-workers (287) found, by PMO calculations, that in CH_2F_2 the $n\sigma^*$ interaction must be larger than that of $n\pi^*$. However that may be, $n\sigma^*$ -type interactions seem to play a significant role in molecules containing $\text{X}-\text{C}-\text{Y}$ moieties ($\text{X}, \text{Y} = \text{O}, \text{N}, \text{S}, \text{F}, \text{Cl}$) and may be at least in part responsible for a α -ICS of such compounds. This is consistent with some other experimental evidence for $n\sigma^*$ interactions: Zefirov and co-workers (288) found an unusually short $\text{N}(3)-\text{C}(2)$ distance in **151**, and another Russian group (289) concluded that analogous effects are operating between N and the $\text{C}-\text{Cl}$ bond in *N*-chloromethylpyrrolidone (**152**).

Table 17
 α -SCS(X) and α -ICS(X/Y) Values in 1-Substituted Adamantanes and 2-Heteroadamantanes **154** to **162** (238) as well as benzohomoadamantenes **163** and **164** (156)

	X	Y	α -SCS (X)	α -ICS(X/Y)
154	OH	CH_2	39.4	—
155		O	25.8	-13.6
156		NH	32.1	-7.3
157	NH_2	CH_2	18.6	—
158		O	12.1	-6.5
159		NH	15.0	-3.6
160	Cl	CH_2	39.7	—
161		O	29.5	-10.2
162		NH	35.5	-6.2
163	Br	CH_2	39.3	—
164		O	28.5	-10.8

1-Substituted 9-heterobicyclo[3.3.1]nonanes **153** (233) and 2-heteroadamantanes **154** to **162** (238) offer a rare opportunity for systematic investigation of how ICSs are dependent on the nature of the substituents, since derivatives with a variety of heteroatoms attached to one carbon are quite stable. The following empirical equations can be derived from the data in Table 17:

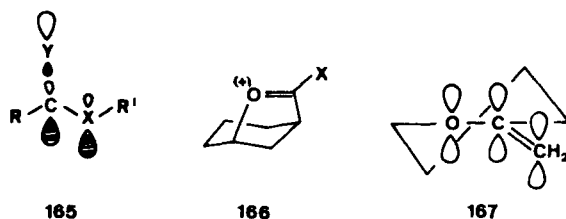
$$(a) \quad \text{ICS}(\text{X/O}) \approx 2 \cdot \text{ICS}(\text{X/NH}) \quad [19]$$

$$(b) \quad \text{ICS}(\text{OH/Y}) \approx 2 \cdot \text{ICS}(\text{NH}_2/\text{Y}) \quad [20]$$

That means oxygen is by far more capable of undergoing an interaction with the other heteroatom than nitrogen is. Halogen substituents produce ICSs nearly as large as those produced by hydroxy groups. The existence of $n\sigma^*$ interactions between X and Y in **154** to **164** is confirmed by the fact that the acceptor ability of a C–O σ^* -bond is better than that of a C–N bond (212,213). On the other hand, a lone pair on nitrogen is a better donor than one on oxygen. Since it is not obvious how one may evaluate the balance of these counteracting influences, the ultimate assignment of the ICS mechanism is still pending. It should be noted that in dithioacetals negative deviations from additivity of individual α -SCS(SR)s are observed as well (290).

Category II Substituent Assemblies: The observation of extraordinary shieldings of carbon atoms multiply substituted by bromine and iodine (2,57) is puzzling and still escapes convincing rationalizations. Early hypotheses based on intramolecular dispersion effects (87), effective electronegativities modified by interacting geminal substituents (291), or partially ionic C–I bond character (292) have not been followed up in recent years. Litchman and Grant (148) have suggested that these effects are due primarily to nonbonded steric interaction causing severe changes in the $\langle r^{-3} \rangle_{2p}$ factor of eq. [3] (p. 222) that can be accounted for by additional pair-interaction terms. This approach was refined by the introduction of trio-interaction terms (293,294) and applied to a great number of halogenated methanes, including some with different halogen atoms in the molecule. The most interesting explanation for the heavy-atom-effect was presented by Nomura (295), Morishima (296), and their co-workers, who proposed that spin-orbit interactions of the heavy halogens give rise to spin polarizations roughly analogous to contact shifts (57). Cheremisin and Schastnev (297) confirmed this approach by calculating spin-orbit contributions in their INDO approximation using third-order perturbation theory. Recently, a heavy-chalcogen effect in tellurium compounds was reported (298) that parallels the heavy-halogen-effect, but is smaller, at least compared with that of iodine.

We now turn to molecules containing double-bonded atoms, such as those with the substructure $\text{C}(=\text{Y})\text{--X}$. Carboxylic acid derivatives with $\text{X} = \text{OR}$, NR_2 , or Hal and $\text{Y} = \text{O}$, S , or NR belong to this category. The sp^2 carbon atoms in such compounds are significantly shielded (ca. 20–30 ppm) compared with those in corresponding ketone or aldehyde analogs. This has been ascribed



Scheme 48

(2) to the well-known electron release from the heteroatom X, leading to the C-X bond's having partial double-bond character ($n_{\text{X}}\pi^*_{\text{CY}}$ interaction). Thereby the overall electron density around the sp^2 carbon atom is increased, reducing the σ_{p} contribution in eq. [3] (p. 222) by enhanced average $2p$ -electron dimensions (2). In another context Kirby (286) suggested that at least in the Z conformation (165), a $n_{\text{X}}\sigma^*_{\text{CY}}$ interaction must be taken into account. The sp^2 carbon atoms in some cyclic oxonium salts like 166 were investigated by Bégue and Bonnet-Delpont (299). In accordance with the $n\pi^*$ -interaction model, they found a good correlation of the pertinent chemical shifts with calculated π -charge densities using π -bond-order terms. Finally, analogous interactions between $\text{C}=\text{C}$ double bonds and directly attached heteroatoms (N, O) deserve attention. Hickmott and co-workers (300) reported α -SCSs of morpholino substituents in various enamines that amount to only about 55% of those in the corresponding saturated derivatives; for pyrrolidino substituents the percentage is 52. These authors argue that the LUMO energy, and thereby the ΔE term of σ_{p} in eq. [3], is increased by an $n_{\text{N}}\pi^*_{\text{CC}}$ interaction; a reduction of the bond-order term, however, is not excluded. Similar effects of oxygen in enol ethers (301) and halogen in vinyl halides (302) have been reported.

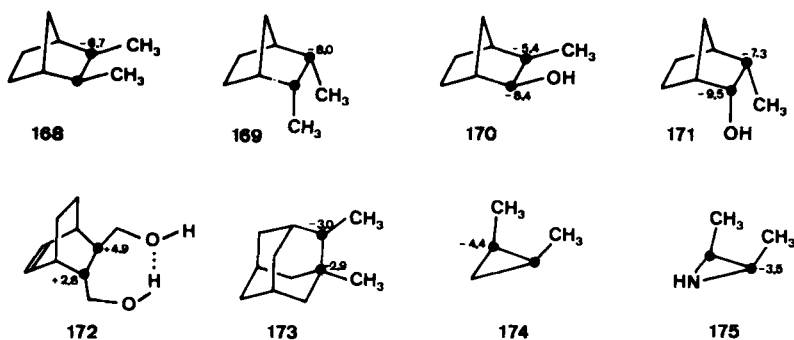
Enol ethers of various configurations, including acyclic vinyl and divinyl ethers and cyclic compounds with endocyclic oxygen atoms or double bonds, have been investigated intensively by Taskinen (303). Again a p - π conjugation leading to double-bond polarization is invoked (303). It is interesting that in compounds with exomethylene groups, like 2-methylenetetrahydropyran (167), the interaction is essentially weaker, since this molecule has to adopt the energetically disfavored half-chair conformation for optimal orbital orientation. The dependence of the efficiency of SCS transmission on conformational behavior in various alkyl vinyl ethers has also been studied (304).

B. Vicinal Substituents

Nonadditivities of individual effects of vicinal substituents were recognized early. Dalling and Grant (100,101) reported that upfield (i.e., negative) α -ICSs of 2.5 to 3.5 occur at signals of substituted carbon atoms in 1,2-dimethylcyclohexanes if the methyl groups are in gauche orientation to each

other (*cis*- or *trans*-diequatorial). This was attributed to steric interaction (7). Effects on unsubstituted carbon atoms are clearly smaller or even negligible (100,101), and this is true generally; therefore the following discussion is confined to ICSs at substituted α -carbon atoms.

The ICS values in a variety of *cis*-2-methylcyclohexanols (305) are quite similar. In 2,3-disubstituted bicyclo[2.2.1]heptanes and -[2.2.2]octanes bearing two methyl groups or one methyl and one hydroxyl, for example **168** to **171**, vicinal upfield shifts (negative ICSs) at the C(2) and C(3) signals can attain much larger magnitudes (92,93,306–308), probably because of the eclipsed orientation of these substituents; the methyl carbon atoms are affected to a similar extent. If, however, the substituents are *trans*-configured ($\tau = 120^\circ$ to 180°), there is nearly perfect additivity (7,306,308), indicating the absence of steric interaction; an exception is the glycol **172** (308), where positive ICSs occur. This can be explained by a change in conformational equilibrium of the hydroxymethylene groups due to stabilizing hydrogen bridging (308). Effects of a similar kind were reported for other methylated compounds, such as adamantanes **173** (309,310), cyclopropanes **174** (275), and aziridines **175** (276). Phenyl groups may interact with each other in *gauche* or *syn*-periplanar orientations. In aziridines (276), for example, the ICSs are similar or slightly smaller than in corresponding methyl derivatives. In the conformationally mobile 1,2-diphenylethane, vicinal effects are negligible (187,278). Only in tri-, tetra, and pentaphenylethanes, where steric crowding cannot be avoided, are negative ICSs encountered (187,278).



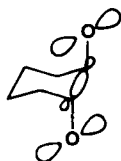
Scheme 49^a

The situation is different if electronic interaction between vicinal substituents is involved. Maciel and co-workers, for example, found large deviations from SCS additivity in 1,2-substituted ethanes if the substituents $-I$ or $-C\equiv CH$ are involved; the deviations could be accounted for by the high polarizability of the two groups (311,312). Steric, electronic, and hydrogen-bridging effects are

^aThe numerical values shown are ICSs.

observed when phenyl and carboxyl groups interfere in *cis*-2,3-disubstituted bicyclo[2.2.1]hept-5-enes (313).

Interaction effects in compounds with two vicinal heterosubstituents are well documented; thus, dihydroxy derivatives of steroids in various configurations have been investigated (314–318). Three different arrangements are conceivable (315): (i) In diequatorial (ee) cases the ICSs are about -4 , which corresponds nicely to the presence of a new γ -gauche interaction of each OH with the other (cf. The corresponding dependencies of α - and β -SCSs, Sections III-A and III-B); 1,2-dihydroxyadamantane (319) furnishes practically the same values. (ii) The ICSs in equatorial-axial (ea) isomers are negative as well, but larger (-5 to -7) (315,318). This was attributed (315) to greater steric interference as compared with the ee case, since the torsional angles between the C–O bonds are smaller. (iii) The diaxial (aa) glycols exhibit negative deviations (-3 to -4) as well, in contrast to corresponding alkyl-substituted compounds. This must be ascribed to electronic interaction. Djerassi and co-workers have formulated (315) a model of oxygen lone pairs mutually influencing one another via an intervening parallel C–C bond orbital (176) (Scheme 50). In principle, the same effects were

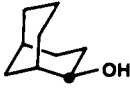

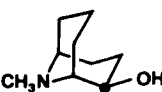







176

Scheme 50

determined by Schneider and colleagues (236,320) for substituents other than hydroxyl in *cis*- and *trans*-1,2-disubstituted cyclohexanes. There is a tendency toward larger absolute ICS values for more electronegative substituents; values of up to -10 for signals of fluorinated carbon atoms have been reported (320). These effects were suggested to be caused by attenuated α -SCSs for each substituent due to the influence of the electric fields of one C–X dipole on the other (236,320). It was pointed out that attractive and repulsive electronic interactions between vicinal heterosubstituents are large enough to govern the position of conformational equilibria (gauche effect) (286,321) and therefore may reasonably form the basis of the observed ICS.

In five-membered rings large negative deviations from additivity have been observed as well (315,322,323). In eclipsed *cis*-glycols the ICS values can be as large as -15 (315,322); they are somewhat smaller if vicinal bromo, azido, or acetamido substituents are involved. As a rule, upfield ICSs are palpably reduced in the *trans* isomers (322,323), especially for carbon atoms bearing less electronegative substituents, such as Br, SH, and N_3 .

				
	177	178	179	180
SCS;	39.2	39.3	42.7	37.7
				
	181	182	183	184
SCS:	42.6	39.4	36.9 (X = OH) 30.9 (X = Cl) 25.9 (X = Br)	34.5 (X = OH) 26.0 (X = Cl) 20.4 (X = Br)

Scheme 51

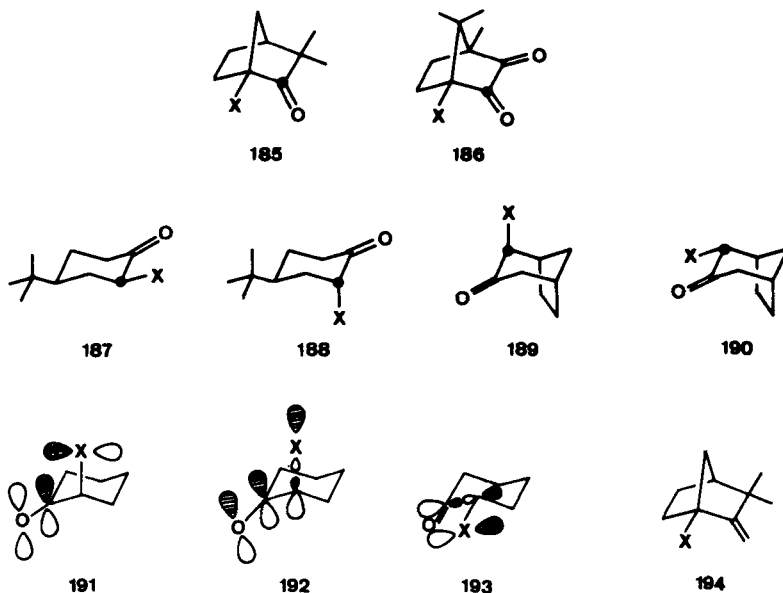
Vicinal effects in compounds with one endocyclic heterosubstituent can be estimated by comparison with corresponding carbocycles. In Scheme 51 α -SCS values in 9-heterobicyclo[3.3.1]nonanes **178** to **180** and **182** (197,324,325) and oxaadamantanes **184** (326) are thus compared with those in **177**, **181** (327), and **183**, respectively (232).

α -Heterosubstituted ketones represent another important class of molecules in which interactions between the heteroatoms and the neighboring carbonyl oxygen atom have been monitored by ICS determinations. Systematic studies by Morris and co-workers revealed large upfield β -effects of substituents on the carbonyl carbon atoms in camphenilones **185** (328) and bornadiones **186** (329) that can be explained only by postulating significantly shielding interaction effects (Table 18). Other authors have examined α -halocyclohexanones in fixed chair conformations. Jantzen and co-workers (330) observed α -SCS(X) values in compounds **187** and **188** (X = F, Cl, Br) to be 9–13 ppm smaller than those in corresponding halocyclohexanes (113); again a shielding mechanism is operating. Moreover, a comparison of α -SCS values for a given substituent in equatorial

Table 18
 β -SCS(X) Values for Carbonyl Signals in Camphenilones
185 (328) and Bornadiones **186** (329)

	X =			
	Cl	Br	COOH	NO ₂
185	-9.0	-9.2	-5.7	-14.1
186	-7.1	-7.5	-7.1	-13.6

vs. axial position shows a reversed tendency compared with that in halocyclohexanes. Thus, for example, the difference $\Delta = \alpha\text{-SCS}(\text{Br}^{\text{eq}}) - \alpha\text{-SCS}(\text{Br}^{\text{ax}})$ is $+4.6$ in **187** vs. **188** (330), but -2.9 in the bromocyclohexanes (113). The divergence of the $\alpha\text{-SCS}(\text{X})$ values in the two systems is plausibly rationalized in terms of a decrease of inductive effects caused by $n_{\text{X}}\pi^*_{\text{C=O}}$ interactions (331).

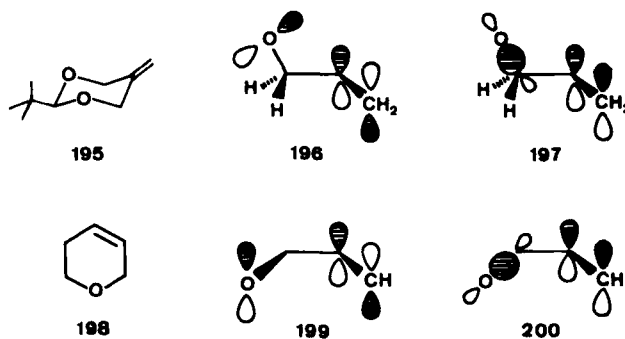


Scheme 52

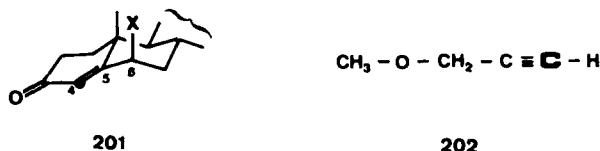
The ^{13}C NMR spectra of a great variety of bicyclic compounds containing α -halocyclohexanone substructures, for example **189** and **190**, have been discussed by another research group (332,333), who obtained similar findings. For axial bromo substituents in particular, the authors proposed a strong $n\pi^*$ interaction (333). This and alternative interaction mechanisms were investigated by Metzger and co-workers (334), who studied conformationally fixed α -substituted decalones and related bicyclic derivatives for a very wide range of substituents. They also observed reversed tendencies (relative to saturated analogs) when they compared $\alpha\text{-SCS}$ s in equatorially vs. axially substituted compounds, and found that the larger perturbation of the $\alpha\text{-SCS}$ of a given substituent occurs in the thermodynamically more stable epimer (334), since more effective electronic interaction enhances both stability and $\alpha\text{-SCS}$. Besides $n_{\text{X}}\pi^*_{\text{C=O}}$ (**191**) and $\pi_{\text{C=O}}\sigma^*_{\text{C-X}}$ (**192**) interactions for axially substituted ketones, the authors discuss a $n_{\text{X}}\sigma^*_{\text{C-C}}$ (**193**) interaction for equatorial orientation (334). Recently, negative ICSs were reported also for acyclic α -chlorinated carboxylic esters (335,336). Large shielding effects of endocyclic nitrogen substituents on C=O carbon atoms

were detected in an investigation of 3-aza-cyclohexanones (337) and attributed to a dipole-dipole interaction ($R-N \cdots C=O$), whereas a direct $n_N\pi^*_{C=O}$ orbital interaction was rejected. A $\sigma-\pi$ conjugation between $C-Hg$ σ - and $C=O$ π -bonds was identified in α -mercuricyclohexanones when the mercury substituent was in the axial position (195); in these epimers the carbonyl resonance is shifted upfield by 2.5 to 3 ppm.

Shieldings of olefinic sp^2 carbon atoms induced by α -substituents were also observed when Morris and Murray investigated a series of 1-substituted camphenes **194** (338). A Japanese group (339,340) has studied interactions in allyl alcohols and ethers. The authors detected a considerable polarization of the double bond, manifested in large upfield shifts of the β - and downfield shifts of the γ - sp^2 carbon signals, if the torsional angle τ between the $C-O$ and $C=C$ bonds is 90° to 150° (anticlinal, 195). This observation was rationalized (339,340) by assuming the operation of two interaction mechanisms: (i) through-space interaction of n_O and π^* (196), and (ii) homoconjugation between σ_{C-O} and π -orbitals (197). This interpretation is in accord with the finding that corresponding sp^2 carbon signal shifts do not appear in synperiplanar configurations ($\tau = 0^\circ$ to 30°), for example in dihydropyrans **198** (339,340). The orbitals concerned are too far removed from each other for effective through-space interaction (199), and homoconjugation is prohibited by their perpendicular orientation (200). It should be mentioned that the concept of a corresponding $n_O\pi^*$ stabilizing interaction in axial 2-methoxymethylenecyclohexanes (341) was rejected by Lessard and colleagues (342,343) on the basis of conformational studies.



Scheme 53



Scheme 54

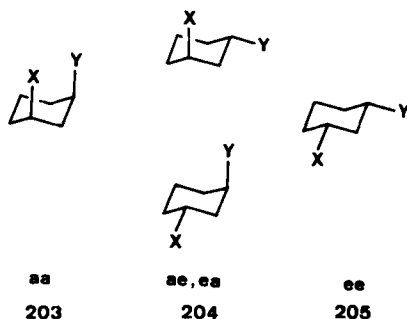
An interaction between a C(4)–C(5) double bond and the axial halogen atoms in the 6-position of steroidal enones **201** was reported (344) that leads to significant downfield shifts of the C(4) signals. This is reminiscent of what happens in the α -haloketone case (330).

Finally, compound **202** constitutes an interesting example of apparent interaction of oxygen and acetylenic carbon atoms (345); the oxygen atom exerts a 7.6-ppm deshielding effect on the terminal *sp* carbon atom.

Molecular moieties with two doubly bonded substituents, for instance butadienes and α,β -enones or -diketones, represent the typical case of conjugative interaction, which has been discussed extensively in reviews and textbooks (e.g., refs. 2, 3, and 8); they will not be discussed here.

C. Remote Substituents

Interactions of substituents separated by more than two carbon atoms (three bonds) can also give rise to considerable ICSs. In cyclohexane-type molecules, three different configurations of two monovalent substituents in 1,3-position are conceivable (Scheme 55).



Scheme 55

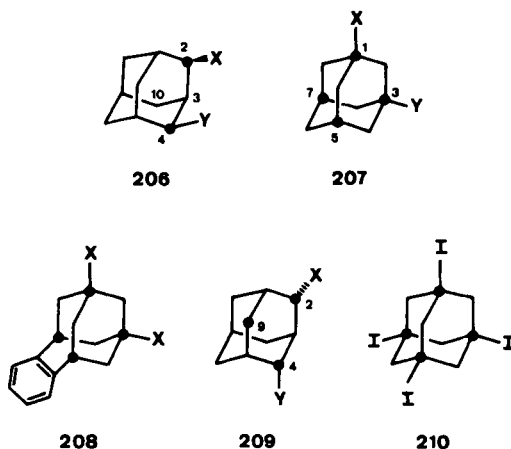
It is obvious that in the diaxial (aa) orientation (**203**) severe steric interactions are to be expected. Djerassi and co-workers (315) noticed positive ICSs for the signals of the hydroxylated carbon atoms in diaxial 1,3-diols and interpreted them as resulting from the lack of one γ -gauche hydrogen atom for each hydroxy group leading to a missing shielding effect. Later, this point was investigated systematically for a variety of substituents in 2,4-disubstituted adamantanes **206** (232,319,346). The data (Table 19) reveal that the missing γ_g -SCS alone cannot be the cause of C(2) and C(4) signal ICSs, since the latter become smaller and may even turn negative when the atomic weight of the substituents X and/or Y increases. Probably an electronic interaction—via intramolecular field effects and/or direct orbital interference—is operating. An indication of severe skeletal distortion is the significant deviation from SCS additivity at C(3) and C(10) when

Table 19
ICSs in Various Diaxially 2,4-Disubstituted Adamantanes **206** (232,346)

	X/Y								
	OH/OH	OH/Cl	OH/Br	OH/CH ₃	OH/ SiMe ₃	F/F	Cl/Cl	Br/Br	SiMe ₃ / SiMe ₃
C-2	+7.9	+7.7	+7.2	+8.0	+2.4	+5.6	+1.5	-1.7	— ^a
C-3	-2.2	-1.7	-1.7	0.0	+0.2	-0.2	-2.0	-2.9	-3.9
C-4	+7.9	+5.6	+3.0	+6.6	+3.6	+5.6	+1.5	-1.7	— ^a
C-10	-0.4	+0.8	+1.5	-0.2	+0.5	+1.7	+1.1	+1.8	+7.8

^aNot reported.

the substituents become more space demanding. The largest values were reported for bis(trimethylsilyl)adamantane (**346**).



Scheme 56

In the equatorial-axial (ea) configuration (**204**) direct steric contact between the substituents is excluded. Nevertheless, ICSs at the signals of substituted carbon atoms may be observed (232). Recently, some of these were rationalized in terms of γ_a -SCS modifications by molecular-structure variation and LEF effects (223; cf. Section III-D).

The third arrangement (ee, **205**) is of particular interest because considerable ICSs were reported (indicating intramolecular through-bond interactions) when the substituents had lone electron pairs available. Again adamantanes, such as **207** to **209**, served as model compounds in systematic studies (176,218,232). Whereas Lippmaa and co-workers (176) found noticeable ICSs in their derivatives of **207** (X, Y = OH, Br, aryl, COOH, CH₂COOH, CH₂Br) only for the

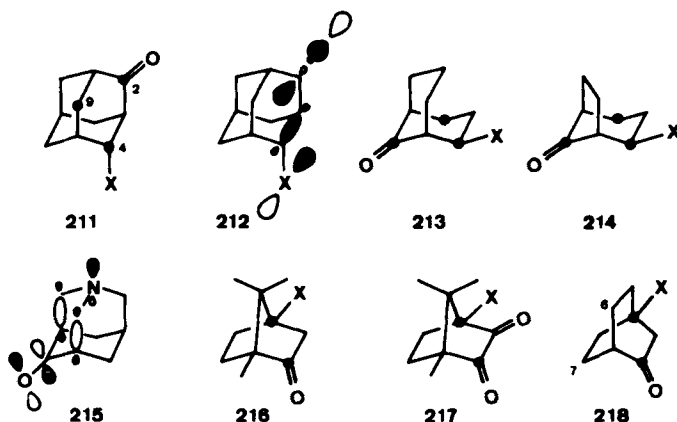
Table 20
ICS Values in Various Diequatorially 2,4-Disubstituted Adamantanes **209**
(232,346,347)

	X/Y										
	OH/ OH	OH/Cl	OH/Br	OH/I	F/F	Cl/Cl	Br/Br	I/I	OH/ CH ₃	Br/ SiMe ₃	SnMe ₃ / SnMe ₃
C-2	-0.1	-1.6	-1.9	-2.3	-2.1	-4.0	-6.7	-9.3	-0.8	+0.2	+0.9
C-4	-0.1	-2.3	-3.7	-5.1	-2.1	-4.0	-6.7	-9.3	-0.3	+0.9	+0.9
C-9	-2.2	-2.3	-2.2	-1.8	— ^a	-2.2	-1.8	-0.8	-0.9	+0.3	+0.3

^aNot reported.

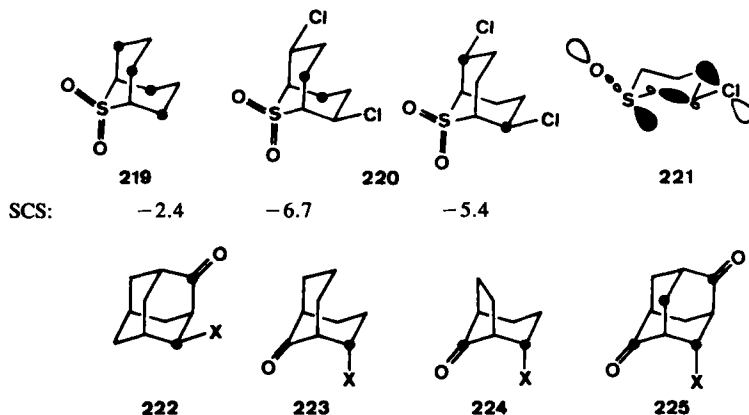
signals of brominated carbon atoms, Pincock and Perkins (218), investigating dihaloadamantanes **207**, reported ICSs for C(1) and C(3) of -2.0 (difluoro-), -4.7 (dichloro-), -8.5 (dibromo-), and -10.5 (diiodoadamantane). Moreover, slight negative deviations from SCS additivity occur at C(5) and C(7) which are antiperiplanar to both substituents (218). These findings correspond to those in respective dihalobenzohomoadamantenes **208** (156). Compounds of type **209** (221,232,346,347) show similar ICSs (Table 20). Increasing the atomic weight of substituents with lone pairs enhances the sensitivity of the attached carbon atoms to the intramolecular interaction. Simple electric-field effects cannot explain these effects, since, for instance, the smaller dipole C(2)-I clearly induces a larger effect on an iodine-bearing γ -anti C(4) than does a larger dipole, such as C(2)-OH. If at least one substituent does not possess lone electron pairs, the ICS falls off sharply to practically zero. The effects in Table 20 have been explained by a hyperconjugative interaction between the X substituents' lone pairs and C-Y σ^* -orbitals (216,232) whereby the γ_a -SCS of each substituent is affected. Thus, ICSs can also be monitored at the signals of C(9) which is antiperiplanar to both substituents (cf. also C(5) and C(7) in **207**). These investigations can be extended to compounds containing several mutually interacting pairs of substituents, for example 1,3,5-tri- and 1,3,5,7-tetrasubstituted adamantanes (218), and the effects culminate in an ICS of -33.4 for the iodo derivative **210**.

Very similar findings were reported for compounds containing equatorially β -substituted cyclohexanone moieties in chair conformations (244,327,348,349), namely **211** to **214**. Using data for a large series of different equatorial substituents X in **211** (216,346), Duddeck and co-workers observed negative ICSs throughout, and concluded that these originate from an $n_X\sigma^*_{\text{C=O}}$ interaction as depicted by **212**. If there is no lone electron pair at X [X = CH₃, COOCH₃, CN, C₆H₅, Si(CH₃)₃ etc.], there is still a field effect that weakly polarizes the carbonyl group. Alternative interaction mechanisms were suggested by Heumann and Kolshorn (327,349): back-lobe overlap (93) or through-bond interaction



Scheme 57

between the heteroatom lone pairs and the n_X - and carbonyl π -orbitals. An interaction of the latter type was established by ultraviolet and photoelectron spectroscopy of azaadamantanone (**215**) (350–353) and compounds with related configurations (354,355). These molecular systems, however, in general do not show sizable ICSs reflecting the $n\pi^*$ interactions; that is, this mechanism is probably of little significance when ICSs in **211** to **214** are to be rationalized. An explanation on the basis of through-space dipole interaction (325) does not seem to be adequate either. Corresponding effects were found for cyclohexanones fixed in boat conformations **216** to **218** (216,329,348,356). In **218**, however, interaction effects at unsubstituted C(6)/C(7) atoms antiperiplanar to the hetero-substituent X are negligible, in agreement with the hyperconjugative nature of that interaction and of the γ_s -SCS of X (216,348).



Scheme 58

A hitherto mysterious observation reported by Wiseman and co-workers (197) is now easily explainable. They found unusually large shielding γ -SCSs of the oxygen atoms in the sulfone **220** ($-\text{S}- \rightarrow -\text{SO}_2-$) containing endo chlorine substituents compared with those in the parent compound **219**. The difference can now be interpreted in terms of an $n_{\text{Cl}}\sigma^*_{\text{S}=\text{O}}$ interaction (as depicted in the "half-formula" **221**) in analogy to that in equatorially β -substituted cyclohexanones.

If the substituent X is in an axial position (cf. **222** to **224**) (244,327,348,349), ICSs are found at signals of substituted carbon atoms only and are of completely different magnitude from those of the molecules in Scheme 57, so the underlying interaction mechanism is assumed to be of a totally different kind. Generally, the effects are deshielding except for halogenated carbon atoms (216), and are probably due to through-space orbital interference and π -charge polarization in the carbonyl double bond (216,350). Interestingly, in molecules containing both types of configurations, for example **225**, the ^{13}C chemical shifts of all carbon signals can be predicted satisfactorily by considering the ICS for each pairwise interaction; that is, the nonadditivity effects are additive (357).

When the oxygen atoms in the ketones **211** and **222** are replaced by S, NOCH_3 , CH_2 , or $\text{C}(\text{CN})_2$ the ICSs are qualitatively comparable for a given X, although they differ in their magnitudes (216).

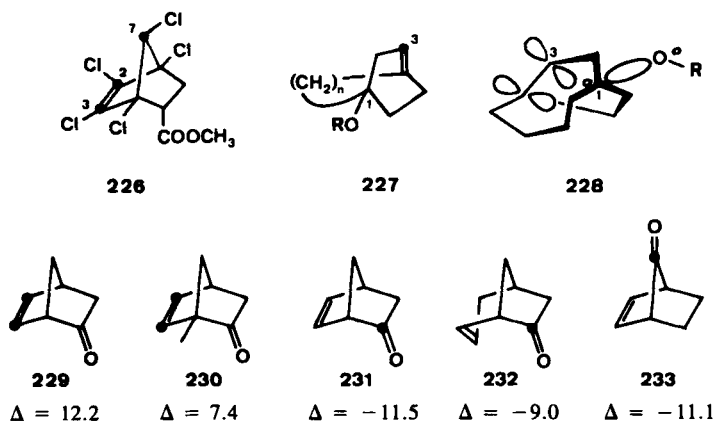
Interactions of C-Cl dipoles with π -electrons in highly chlorinated bicyclo[2.2.1]heptenes such as **226** were invoked to explain the chemical shifts of C(2), C(3), and C(7) (358). Similarly, remarkably large upfield γ_s -SCS(OR) values in **227** ($n = 2$ to 4) were attributed to a back-lobe interaction of the C(1)-O bond with the p -orbital of C(3) in the distorted double bond (cf. **228**) (359).

Two doubly bonded substituents in 1,3-position form a molecular arrangement where homoconjugation is expected. In fact, influences of carbonyl groups on β,γ -double bond resonances were recognized early (153,360) and are manifested in double-bond polarization effects, Δ , for example in **229** and **230**. The carbonyl signal is shifted as well. In a variety of bicyclic compounds, for example **231** and **232**, Stothers and co-workers (361) found upfield $\text{C}=\text{O}$ signal shifts of -2 to -11.5 , but they were not able to describe a quantitative correlation between the shift magnitudes and structural features like relative orientation of the two double bonds. Similar homoconjugation effects were determined in **233** (362). Vogel and co-workers (363) introduced the molecular system **234** with interacting carbonyl and *s-cis*-butadiene chromophores and reported homoconjugative polarization effects Δ of 16.5 for the β,γ - and 6.5 for the γ,δ -double bond. The ^{13}C chemical shifts of sp^2 carbon atoms in β,γ -dienes were studied by the same group (364). In compounds like **235** the authors rationalized a distinct change in the exocyclic olefin chemical shifts originating from introduction of the endocyclic double bond in terms of a hyperconjugative molecular orbital (MO) interaction between the HOMO- σ_π (A) of the puckered cyclopentene and the HOMO- π_2 (A) of the *s-cis*-butadiene (364). The exocyclic double bonds in **236** and **237** experience pronounced polarization effects due to homoconjugative interaction

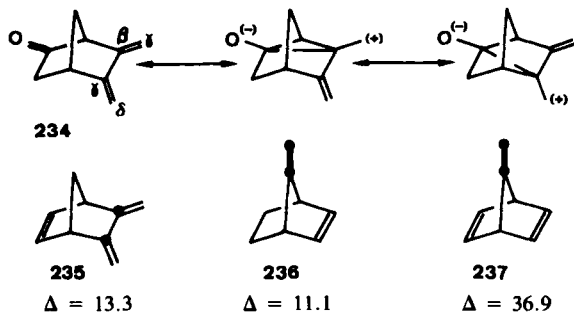
Table 21
ICS Values in Adamantane Derivatives 238 to 240

	238	239	240
C-2	-10.4	-5.5	-3.8
C-3	+3.0	-0.7	-0.1
C-4	-10.4	-7.3	-3.8
C-9	-10.6	-3.6	-1.8
C-10	+3.4	+0.9	0.0

with the endocyclic ethylene chromophores (365,366). Further examples of homoconjugative interaction are represented by the adamantane derivatives 238 to 240. Table 21 indicates that within a fixed geometry homoconjugative interaction effects on a C=O are much more pronounced than on a C=C bond. Furthermore, it shows that neighboring sp^3 carbon atoms can also be affected to a considerable extent.



Scheme 59

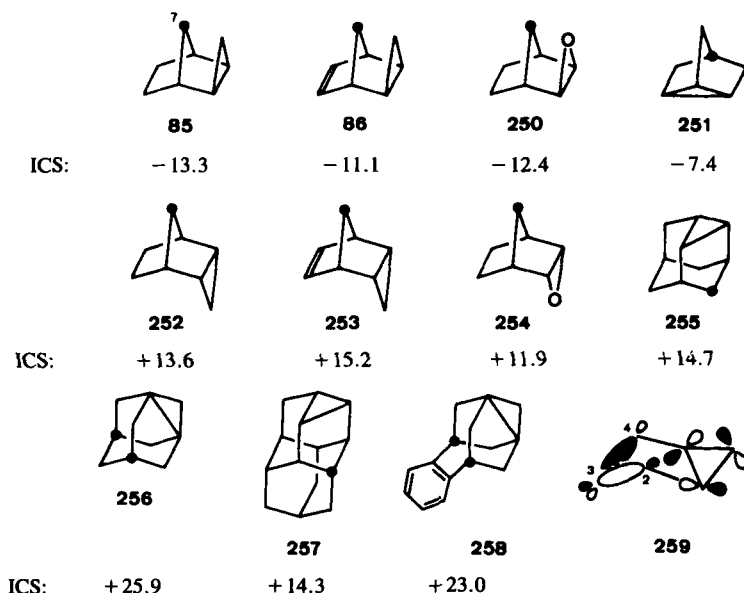


Scheme 60

D. Three-Membered Rings

Because of the unique electronic properties of cyclopropanes and related three-membered ring systems, this separate section is devoted to the ^{13}C NMR spectral characteristics of such compounds. First of all, it is well known that three-membered-ring carbon atoms themselves resonate at relatively high fields (69,70; cf. Section II-B-2). Beyond that three-membered ring systems have interesting influences on neighboring carbon atoms as well.

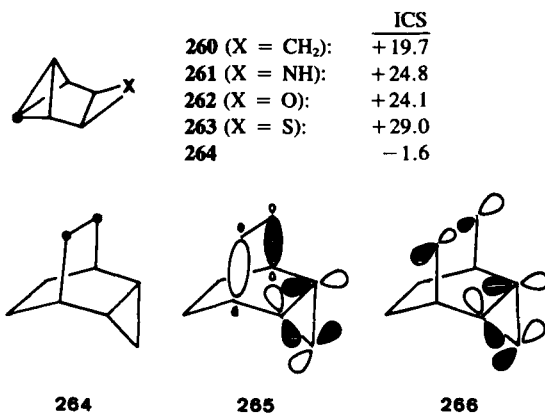
The unusually pronounced shielding effect on the C(7) methylene group of an annelated three-membered ring, as in **85** (202,203), **86** (371), and **250** (372), has already been mentioned (cf. Section III-C) and exists also, although to a somewhat lesser extent, in nortricyclene (**251**) (373).



Scheme 62

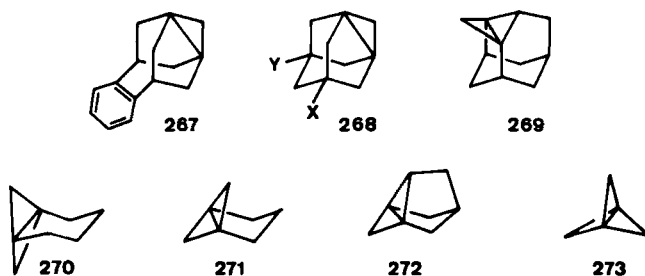
More intriguing, however, is the effect on γ -anti-positioned carbon atoms, which are shifted downfield considerably. The values given for **252** (202), **253** (371), **254** (372), **255** (374), **256** (374), **257** (375), and **258** (376) in Scheme 62 are calculated by comparison with the corresponding parent compounds (norbornane, norbornene, adamantane, diamantane, and benzohomoadamantene, respectively). A plausible explanation for this effect was given by Christl and co-workers (203,204,377), who invoked an interaction between an unoccupied Walsh orbital and the HOMOs of the C(2)–C(3) and C(3)–C(4) bonds (**259**).

This causes electron-density changes that could be reproduced by MINDO/2 and *ab initio* calculations (377). It cannot yet be decided, however, whether this deshielding effect originates from an electron back-donation from the filled σ -orbitals into the unoccupied Walsh orbital or from a decrease of the excitation term in the σ_p expression (eq. [3], p. 222) (204). Christl's interpretation is in accord with the increase of the effect in the tetracycloheptane **260** when the methylene group is replaced by NH (**261**), O (**262**), and S (**263**). Introduction of the heteroatom enhances the coefficient of the Walsh orbitals at the carbon center substantially, giving rise to a more effective orbital overlap (204). In the corresponding bicyclo[2.2.2]octane derivative **264**, strong downfield effects of cyclopropane annelation do not appear (378). This may be due to the reduced overlap of the orbitals concerned in this geometry (**265**) or to a back-donation as depicted in formula **266** such that both effects cancel each other (378).



Scheme 63

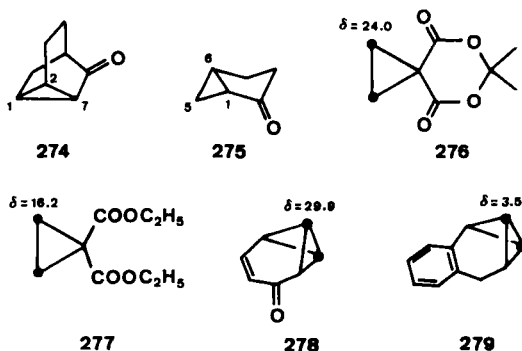
Very recently, a number of studies have appeared in the literature reporting chemical shifts of so-called inverted carbon atoms with all four valences reaching into one hemisphere (379). Such atoms occur in highly strained propellanes, such as **267** (376), **268** (374), **269** (380), **270** (381), **271** (204,382), **272** (383), and **273** (384). In the dehydroadamantane derivatives **267** and **268**, which represent [3.3.1]propellanes, the inverted carbon atoms exhibit unusually low-field shieldings that may be ascribed to a rehybridization (376,380). In the more strained [n.1.1]propellanes **269** to **272** ($n = 3$ and 4), however, they resonate at much higher fields (380), and in the smallest possible member of this series, [1.1.1]propellane (**273**), the chemical shift δ of the quaternary carbon atoms is only 1 (384). Surprisingly, the shifts of the methylene carbon atoms in the cyclopropane rings are quite large: 51.5 in **267**, 49.5 in **268** (X/Y = H/H), 40.9 in **269**, 53.3 or 42.5 in **271** (the assignment is not certain), and 74.2 in **273**.



Scheme 64

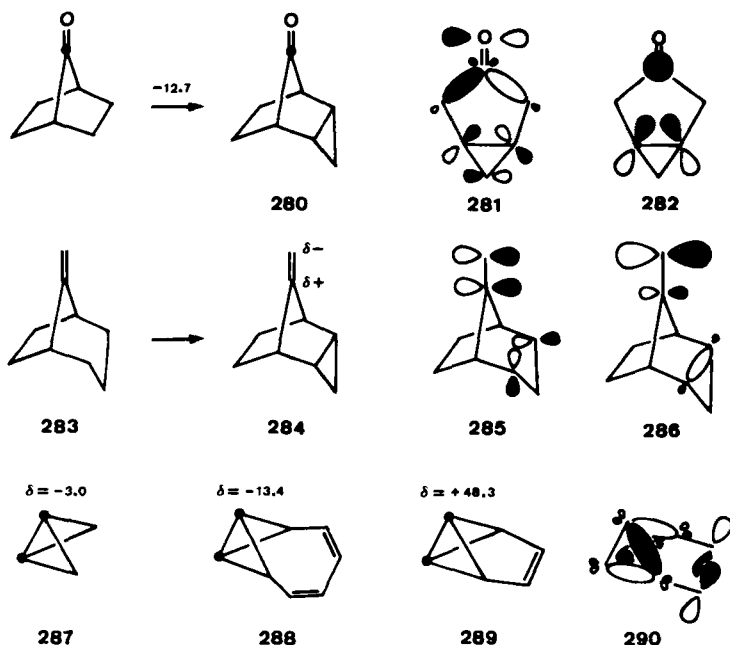
Clearly, understanding ^{13}C shieldings in these compounds is not a straightforward task and requires more experimental and theoretical investigation.

Interactions between electrons in three-membered rings and unsaturated groups in the same molecule have been detected via ^{13}C chemical-shift variations in a number of instances. Thus, introduction of the carbonyl function in tricyclo[3.2.1.0^{2,7}]decane (e.g., **274**) leads to significant downfield shifts of the signals of C(1) (+8.0), C(2) (+15.5), and C(7) (+7.7) (385), whereas corresponding effects in bicyclo[3.1.0]hexan-2-one (**275**) are smaller (385,386). A corresponding dependence was reported for **276** and **277** and related to more effective electron withdrawal in **276** (387). An even more pronounced deshielding effect was observed by Murata and co-workers (388,389) in the ketone **278** when they compared it with **279**.



Scheme 65

Strong shielding of the $\text{C}=\text{O}$ carbon atom in **280** by *endo*-cyclopropane annelation was reported by Kessler and co-workers (362) and rationalized in terms of an interaction between a Walsh orbital and the *n*-orbital of the carbonyl oxygen via the intervening C–C bonds (**281**); an alternative explanation—spatial interference with the $\pi^*_{\text{C}=\text{O}}$ orbital (**282**)—was mentioned as well (362). The double bond in **283** is polarized ($\Delta = 17.9$) when **283** is transformed into **284**



Scheme 66

(366), and these authors suggested that a charge-density shift occurs within the π -orbital so as to evade a destabilizing orbital interaction (**285** \rightarrow **286**).

Christl and Lang (390) noticed an upfield signal shift of about 10 ppm when they compared the methine carbon atoms in bicyclo[1.1.0]butane (**287**) (391) and octavallene (**288**). On the other hand, in benzvalene (**289**), the corresponding shielding is $+48.3$ (203), because in this molecule back-donation from the Walsh orbitals to the π^* -orbital of the olefinic group (**290**) is conceivable. Such an interaction is not possible in **288**, because the π^* -orbital of the diene chromophore is of different symmetry (390).

An example of subtle spiroconjugative interaction between a cyclopropane and cyclopentadiene systems was reported recently by Paquette and Charumilind (392).

V. SURVEY OF SUBSTITUENT EFFECTS

In the previous sections the main focus of the discussion of substituent effects was their dependence on structure (especially stereochemistry) and the underlying transmission mechanisms. Admittedly, it would still be very difficult to predict ^{13}C chemical shifts in more complicated and highly substituted aliphatic compounds with sufficient precision even if our knowledge about the physical back-

ground of substituent effects were more elaborate. Therefore, this section is designed to provide empirical data and prediction rules to those readers who need reference material for assigning ^{13}C signals to structures of their molecules without necessarily being interested in *how* such signal shifts come about. First, some empirical rules for ^{13}C chemical-shift calculations are reviewed; then SCS values in certain compounds are compiled.

A. ^{13}C Chemical-Shift Calculation Rules

One of the earliest empirical rules for predicting ^{13}C chemical shifts was that of Grant and Paul (169) for alkanes:

$$\delta_c(k) = B + \sum_l A_l n_{kl} + \sum S_{kl} \quad [21]$$

where $\delta_c(k)$ is the chemical shift of the carbon atom concerned, B a constant value of -2.3 (the chemical shift of methane), A_l an additive shift parameter of the l th carbon atom ($l = \alpha, \beta, \gamma$, etc.; Table 22) and n_{kl} is the number of such atoms in position l . Corrective terms S_{kl} are to be added for branched alkanes (Table 23). The first figure in the column heads in Table 23 indicates the branching at the observed carbon atom k (1° : methyl; 2° : methylene; 3° : methine; 4° : quaternary carbon atom) and that in parentheses the branching at the respective adjacent carbon atom.

The application of the Grant–Paul (GP) rule may be demonstrated by calculating the ^{13}C chemical shift of C(25) in 5 α -cholestane (291):

$$\delta[\text{C}(25)] = B + 3A_\alpha + A_\beta + A_\gamma + A_\delta + 2A_\epsilon + S[3^\circ(2^\circ)] = 28.7$$

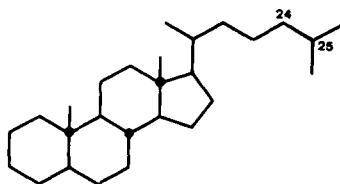
Table 22
Parameters A_l of Eq. [21] (169)

A_α	A_β	A_γ	A_δ	A_ϵ
9.1 (± 0.1)	9.4 (± 0.1)	-2.5 (± 0.1)	0.3 (± 0.1)	0.1 (± 0.1)

Table 23
Corrective Terms S_{kl} for Eq. [21] (169)

$1^\circ(3^\circ)$	$1^\circ(4^\circ)$	$2^\circ(3^\circ)$	$2^\circ(4^\circ)$	$3^\circ(2^\circ)$	$3^\circ(3^\circ)$	$4^\circ(1^\circ)$	$4^\circ(2^\circ)$
-1.1 (± 0.2)	-3.4 (± 0.4)	-2.5 (± 0.2)	-7.2 — ^a	-3.7 (± 0.2)	-9.5 — ^a	-1.5 (± 0.1)	-8.4 — ^a

^aOnly one observation.

**291***Scheme 67*

This compares with an experimental value of 28.0 (317). The corrective term must be added due to the presence of $\text{C}(24)\text{H}_2$.

Roberts and colleagues (102) extended this rule to alcohols by relating them to analogously constituted hydrocarbons in which the hydroxyl group is replaced by methyl. For carbon atoms in position l ($= \alpha, \beta, \gamma, \dots$) with respect to the hydroxyl groups the authors proposed the following equation:

$$\delta_c^{\text{ROH}} = A \delta_c^{\text{RCH}_3} + B \quad [22]$$

Table 24 shows the values of A and B for various positions l .

The GP rule (eq. [21]) suffers from the poor statistical analysis for parameters describing methine and quaternary carbon atoms in highly branched alkanes. This was improved by Lindeman and Adams (120), who introduced another equation based on data for 59 alkanes, C_5 through C_9 :

$$\delta_c(k) = B_S + \sum_{M=2}^4 D_M A_{SM} + \gamma_S N_{k3} + \delta_S N_{k4} \quad [23]$$

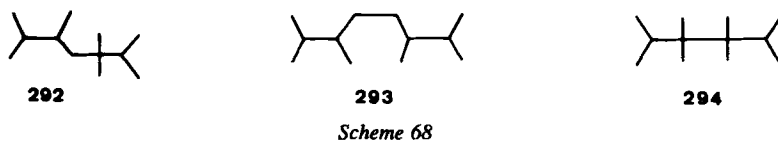
The B_S are constants indicating how many carbon atoms are attached to the observed C^k [$S = 1$: one adjacent C (i.e., C^k is CH_3); $S = 2$: C^k is CH_2 ; $S = 3$: C^k is CH ; $S = 4$: C^k is quaternary] and thereby contain α -parameters. For the remaining parameters there are independent sets for each S as well. A_{SM} denotes the steric configuration at the adjacent carbon atoms, where M is defined analogously to S ; for example, A_{23} signifies a contribution from the methine to the methylene atom under consideration. Consequently, the A_{SM} 's replace the β -

Table 24
Coefficients A and B in Eq. [22] (102)

	l			
	α	β	γ	δ (and further)
A	0.83	1	1	1
B	+10.5	+0.5	-1.7	0

parameters of eq. [21]. D_M is the number of α -carbon atoms with a given S - M combination. The parameters γ_s and δ_s are contributions from γ - (three bonds apart) and δ -positioned carbon atoms (four bonds apart), respectively; N_{k3} and N_{k4} denote the numbers of those γ - and δ -carbon atoms. It should be noted that A_{S1} values do not exist in this parameter set, since α -methyl groups are already taken into account by the choice of B_s .

The ability of the Lindeman-Adams (LA) rule to predict ^{13}C chemical shifts of even highly branched alkanes satisfactorily was proven impressively by calculations of the shieldings of the dodecanes **292** to **294** (393).



A comparative calculation of sterol side-chain chemical shifts using both GP and LA rules (394) showed that both are suitable, but the LA results are slightly preferable for signal assignments. It should be noted that revised LA coefficients have been suggested recently (395). The original LA coefficients are given in Table 25.

The LA rule was also extended to substituted derivatives. Eggert and Djerassi (396) presented an equation for aliphatic amines:

$$\delta_c = A\delta_c^{\text{LA}} + B \quad [24]$$

Table 25
Parameter Sets for Eq. [23] (120)^a

	B_s	A_{SM}	γ_s	δ_s
$S = 1$ ($\text{C}^k = \text{CH}_3$)	6.80	$A_{12} = 9.56$ $A_{13} = 17.83$ $A_{14} = 25.48$	-2.99	0.49
$S = 2$ ($\text{C}^k = \text{CH}_2$)	15.34	$A_{22} = 9.75$ $A_{23} = 16.70$ $A_{24} = 21.43$	-2.69	0.25
$S = 3$ ($\text{C}^k = \text{CH}$)	23.46	$A_{32} = 6.60$ $A_{33} = 11.14$ $A_{34} = 14.70$	-2.07	0
$S = 4$ ($\text{C}^k = \text{C}$)	27.77	$A_{42} = 2.26$ $A_{43} = 3.96$ $A_{44} = 7.35$	+0.68	0

^aStandard deviations are 0.1 to 0.8 ppm.

Table 26
 N_i Parameters for Eq. [25] (397)

N_α	N_β	N_γ	N_δ
22.58	2.02	0.20	1.63

where δ_c^{LA} is the LA chemical shift of the isostructural hydrocarbon ($\text{N} \rightarrow \text{CH}$). This rule requires 18 additional parameters A and B to transform the δ_c^{LA} 's to the amine shifts. A simpler parameter set was provided by Reilley and co-workers (397) for the same class of compounds:

$$\delta_c = H\delta_c^{\text{LA}} + N_i \quad [25]$$

where H is an attenuation factor equal to 0.932 and N_i ($i = \alpha, \beta, \gamma, \dots$) denotes an additional contribution from the nitrogen atom in position i relative to the carbon atom concerned (Table 26). Equation [25] can easily be modified for the calculation of shifts in compounds with n amine centers (397):

$$\delta_c = H^n \delta_c^{\text{LA}} + \sum_{j=1}^n (N_i)_j \quad [26]$$

The same research team (398) described how such calculations can be performed by computer.

Analogous modifications of the LA rule were introduced by Ejchart for predicting ^{13}C chemical shifts of acyclic alcohols (ROH compared with RCH_3) (121):

$$\delta_c = A_i \delta_c^{\text{LA}} + B_i \quad [27]$$

Table 27 lists parameters A_i and B_i for this equation. In addition, some correction terms for alcohols containing quaternary carbon atoms are presented, since the LA rule for the corresponding hydrocarbons is not very precise (121). For quite

Table 27
 Parameters A_i and B_i for Eq. [27] (121)

C^k	Alcohol					
	Primary		Secondary		Tertiary	
	A_i	B_i	A_i	B_i	A_i	B_i
C^α	0.709	46.45	0.786	45.65	0.755	48.37
C^β	0.963	1.81	0.958	2.07	1.029	-0.06
C^γ	0.963	-2.28	0.982	-0.48	1.137	-1.03
C^δ					0.995	0.07

a large variety of different substituents Echart published separate sets of coefficients (a_x and b_x) for primary (399,400) and secondary derivatives (401) to be used in the following equation:

$$\delta_c = a_x \delta_c^{LA} + b_x \quad [28]$$

These are given in Table 28. It is important to note that for δ_c^{LA} calculations each atom other than hydrogen has to be replaced by carbon and all remaining free

Table 28
Parameters a_x and b_x for Eq. [28] (399–402)^a

X	Primary			Secondary		
	C ^α	C ^β	C ^γ	C ^α	C ^β	C ^γ
OH	0.707	0.937	0.979	0.796	0.935	0.972
	46.88	2.70	-2.51	45.45	2.55	-0.39
OC ₂ H ₅	0.716	0.935	1.005			
	49.83	2.34	-2.96			
OCOCH ₃	0.620	0.941	1.016	0.683	0.946	0.983
	48.01	0.92	-3.44	50.01	0.85	-1.28
OCOCCl ₃	0.578	0.941	1.015	0.688	0.951	0.976
	53.66	0.51	-3.76	56.46	0.18	-1.46
COOH	0.945	0.975	0.998	1.134	0.956	0.986
	-2.65	-0.82	-0.47	-5.08	1.46	0.25
COOCH ₃	0.928	0.961	1.036	1.145	0.907	0.984
	0.32	-0.68	-1.13	-3.18	1.06	0.37
COCl	0.886	0.957	1.003	1.074	0.936	0.984
	12.55	0.01	-1.12	9.25	1.91	-0.16
COCH ₃	0.935	0.959	1.034			
	7.08	-1.54	-1.09			
C ₆ H ₅	0.982	0.997	1.027			
	2.91	4.10	-0.97			
Cl	0.761	0.898	0.944	1.026	0.882	0.963
	28.01	4.06	-0.65	29.66	5.72	0.74
Br	0.898	0.883	0.926	1.282	0.857	0.957
	13.67	4.39	0.82	15.19	7.30	1.91
I	1.143	0.864	0.939	1.761	0.808	0.948
	-18.93	5.69	2.62	-19.85	10.73	3.98
NO ₂	0.713	0.916	1.093	0.978		
	48.00	3.14	-5.03	44.35		
NH ₂	0.819			0.836	0.945	0.976
	24.24			22.69	2.93	0.09

^aThe upper value in each entry represents a_x ; the lower, b_x . Standard deviations σ are 0.09 to 0.97 ppm.

valences are satisfied by adding hydrogens. Thus, for instance, CH_3 stands for OH, Cl, Br, or I; isobutyl, for acetate; and so on.


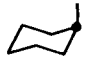




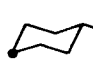

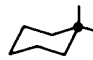



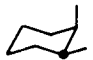



The preceding prediction rules are largely restricted to acyclic compounds. But there is also a considerable need for parameter sets enabling the spectroscopist to calculate ^{13}C chemical shifts of conformationally defined cyclic molecules, especially of the cyclohexane type. Methyl-group effects in methylcyclohexanes (100,101) that are to be added to the basic value for cyclohexane itself ($\delta = 27.3$) are listed in Table 29. Analogous methyl-group parameters in tetralins and tetrahydroanthracenes have been reported (403).

Hydroxyl group effects were determined by Djerassi and co-workers (110) (cf. Sect. III) by analysis of 31 monohydroxylated steroids. The following relationships were given:

$$\alpha\text{-C's: } \delta_c = 45.0 + 3.5 p - 3.5 n \quad [29]$$

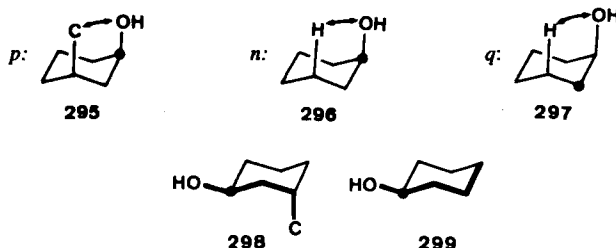
where p is the number of skew pentane syn-axial interactions (295) of the hydroxyl group with carbon atoms and n the number of carbon atoms in γ -gauche orientation to OH (296); and

Table 29
Methyl-Group Parameters in Methylcyclohexanes (100,101)

			
$\alpha_e = 6.0$	$\alpha_a = 1.4$	$\beta_e = 9.0$	$\beta_a = 5.4$
			
$\gamma_e = 0.0$	$\gamma_a = -6.4$	$\delta_e = -0.2$	$\delta_a = 0.0$
			
$G^a = -3.8$	$G^b = -1.3$	$G^c = 2.0$	
 $V_{ee}^a = -2.5$			
			
$V_{ea}^a = -2.9$	$V_{ea}^a = -3.4$	$V_{ea}^b = -0.8$	$V_{ea}^b = 1.6$

$$\beta\text{-C's: } \delta_c = 9.3 - 2.4 q \quad [30]$$

where q indicates the number of OH-C γ -gauche interactions (297). Parameters for γ - and δ -positioned carbon atoms with respect to the hydroxyl group are discussed in Sects. III-C to III-E.



Scheme 69

A more general treatment was introduced by Beierbeck, Saunders, and ApSimon (149), who derived semiempirical parameters for cyclohexane-type polycyclic hydrocarbons, secondary alcohols, endocyclic amines (piperidines), and corresponding ketones and olefins, so that their rules cover a broad range of naturally occurring compounds such as steroids, terpenes, and alkaloids. Their parameter set is divided into two sections: (i) basic values describing the substitution pattern of the carbon atom concerned, and (ii) additional increments denoting stereochemical and relative positions with respect to functional groups. This parametric treatment (149) is very helpful in assigning ^{13}C chemical shifts to natural products with six-membered rings. Moreover, it has been applied even to acyclic hydrocarbons, for which conformer populations can be derived (404,405).

For the $\alpha\text{-SCS(OH)}$ values in cyclohexanol derivatives Wray (406) has suggested that a further parameter is necessary to account for four-bond interactions, as indicated in 298 and 299. He remarked that significant deviations from the experimental chemical shifts indicate conformational distortion of the parent compound, and that such SCS values cannot be calculated for five-membered ring alcohols (406).

Further increment rules for the calculation of ^{13}C shieldings in various types of saturated and unsaturated compounds may be found elsewhere (11). In a totally mathematical approach, Wiberg and co-workers (407,408) analyzed data for 18 sets of aliphatic and alicyclic halides ($\text{X} = \text{F}, \text{Cl}, \text{Br}, \text{or I}$) by means of factor analysis. They found that three parameter terms suffice to correlate all the shielding data:

$$i\text{-SCS(X)} = a_{x1}b_{1i} + a_{x2}b_{2i} + a_{x3}b_{3i} \quad [31]$$

where X refers to the halogens (F to I) and i denotes the relative position (α to ϵ). The a values are "intrinsic" substituent effects characteristic for each halogen:

a_{X1} is essentially constant (≈ 1) for all X and can be related to the polar effect of X relative to hydrogen; a_{X2} refers to the "freeness" of valence electrons about the halogens and increases in the sequence $\text{F} < \text{Cl} < \text{Br} < \text{I}$, with approximate values of 1, 2, 3, and 4, respectively; and a_{X3} is much less important and may be assigned to conformational effects. It is interesting that a_{X2} can be related to non-NMR parameters although there is no *a priori* assumption about such a relation in the calculation procedure. Among those physical parameters are the reciprocals of the ionization potentials, the wavelengths of the first electronic transitions of methyl halides, longitudinal and transverse C-X bond polarizabilities, and atomic contributions to the molar diamagnetic susceptibility. The b values in eq. [31] are attenuation parameters reflecting the sensitivity of the position of the carbon atom concerned in the given parent compound with respect to the substituent X. Through their structure dependence they contain information about the three halogen effects represented by a_{X1} , a_{X2} , and a_{X3} . It should be mentioned that the same research group extended the factor analysis of halide substituent effects to unsaturated and aromatic derivatives (409).

Dubois and co-workers (119,410-415) characterized alkyl (R) substituent effects in simple and sterically congested alkanes, alkenes, carboxylic acid derivatives, ketones, amines, alcohols, and so on by the use of topological parameters λ_R :

$$\delta_c = \omega_c \lambda_R + \eta_c \quad [32]$$

In this equation ω_c stands for the sensitivity of the observed carbon atom within a given parent compound family, and η_c is a reference shift. The λ_R values are obtained by DARC/PELCO topological analysis (416).

B. Specific Substituents and Molecular Systems

Effects of various substituents on ^{13}C chemical shifts can be found in textbooks (2-5,11) or reviews concerned with applications of ^{13}C NMR spectroscopy to specific classes of chemical compounds (16-24,142). Therefore, this section is limited to recent information about effects of less common substituents and to reference data for various carbo- and heterocyclic molecules. It is not the author's intention to present a comprehensive survey; rather, a number of typical examples have been selected. The reader may use this section as an entry into the original papers and the references cited therein.

1. Special Substituents

Carboxyl and cyano substituent effects have been investigated in unsaturated and branched acyclic (79,417,418), cyclohexane (419), and certain piperidine (420) derivatives. A great variety of diesters and anhydrides have also been

discussed (421,422). A systematic study of phenyl-group effects in linear and branched alkyl benzenes has been reported by Hearmon (423).

SCS values of other Group IVa substituents $M(\text{CH}_3)_3$ ($M = \text{Si, Ge, Sn, or Pb}$) are mentioned in Section III (133,134,346,347).

Amino substituents in acyclic derivatives have been discussed by Eggert and Djerassi (396), who emphasize structural and conformational effects, whereas Batchelor has investigated SCS(NH_2) and nitrogen protonation shifts in methylated cyclohexylamines (424). The ^{13}C NMR spectra of amino acids have been compared with those of amines and carboxylic acids (425,426). The transmission mechanisms of amino, ammonium, trimethylammonium, acetamido, and diacetamido groups have been examined by Faure and co-workers (427), the SCSs of nitro groups by Ejchart (400), and those of azido functions in steroids by Lukacs and co-workers (428).

A great variety of tri- and tetravalent phosphorus compounds have been studied, by several research teams. Conformations of menthane and neomenthane derivatives containing diphenylphosphine and diphenylphosphine oxide substituents have been investigated (231), and Quin and colleagues have published a series of papers (127,128,429–431) in which many different phosphorus substituents (e.g., $-\text{PH}_2$, $-\text{PR}_2$, $-\text{PCl}_2$, $-\text{POR}_2$, $-\text{PSR}_2$, and charged species) were examined in alkane chains, cyclohexanes, and norbornanes. Phosphono substituent effects have been determined by Buchanan and co-workers (129,432).

The ^{13}C chemical shifts of methyl derivatives with sulfur substituents [e.g., $-\text{SH}$, $-\text{S}^-$, $-\text{SCH}_3$, $-\text{SSCH}_3$, $-\text{SSSCH}_3$, $-\text{S}(\text{O})\text{CH}_3$, $-\text{SO}_2\text{CH}_3$, $-\text{S}(\text{CH}_3)_2^+$, $-\text{SC}(\text{O})\text{CH}_3$, $-\text{SC}(\text{S})\text{CH}_3$, and $-\text{SC}(\text{S})\text{SCH}_3$] (130,131) and of vicinal and geminal bis-sulfides (290) have been reported. Freeman and co-workers have published similar studies on thiols, sulfides, disulfides, and sulfinic and sulfonic acid derivatives (131,132,433); and Tseng and Bowler (434), on thiocarbamates, their *S*-oxides and *S,S*-dioxides [$\text{R}-\text{X}-\text{C}(\text{O})-\text{NR}'_2$ with $\text{X} = \text{S, SO, SO}_2$].

An investigation of substituent effects of perfluoro groups $\text{C}_n\text{F}_{2n+1}$ ($n = 1$ to 4) has shown that their influence is essentially the same regardless of chain length n (435). The chemical shifts and SCSs in a large series of poly- and perchlorinated alkanes, alkenes, and their ketones have been reported (436). Chlorine substituent effects led to the establishment of the configurations of mono- and dichlorohexanes and -heptanes (122), and a Russian group presented detailed discussions of SCSs and ICSs in mixed polyhalogenated (chlorine and bromine) alkanes (437) and esters (438).

Lithiation shifts obtained by comparison of ^{13}C chemical shifts in lithium dialkylamides and the corresponding amines have been found to be quite substantial and decrease in the order $\alpha > \beta > \gamma > \delta$ (439).

Recently, deuterium isotope effects have attracted considerable attention. In most cases (440) carbon nuclei are shielded when hydrogen atoms in the molecules are replaced by deuterium. A torsional-angle dependence on deuterium

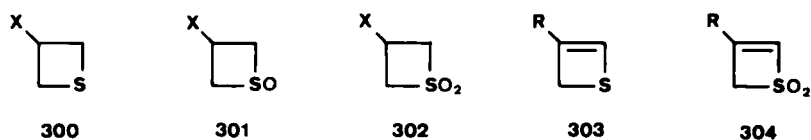
isotope effects over three bonds was detected (441). Deshielding effects are rare (442,443, and references cited therein).

2. Specific Molecular Systems

Much work has been done to determine sets of substituent effects in specific conformationally mobile or rigid frameworks, since a knowledge of such effects often furnishes valuable conformational information. For instance, it was concluded from γ_{e} - and δ -SCS values that substituents ($\text{X} = \text{OH}, \text{I}$) on the C(19) methyl group in some cholest-5-enes prefer an antiperiplanar orientation [$\text{X}-\text{C}(19)\text{H}_2-\text{C}(10)-\text{C}(1)$] with respect to C(1) (81). In the following, SCS information for various classes of cyclic systems is discussed, with particular emphasis on configurational and conformational analysis.

a. Three-Membered Rings. A survey of cyclopropane, oxirane, aziridine, and oxaziridine ^{13}C chemical shifts and alkyl substituent effects on these was presented by Eliel and Pietrusiewicz (142). Only a few systematic studies of three-membered ring systems have appeared subsequent to this review. Touillaux and co-workers have reported shifts for some mono- and geminally disubstituted cyclopropanes (444). In a much broader survey, Rol and Clague (445) discussed the spectra of 68 cyclopropane derivatives bearing up to five substituents of various types, and confirmed an earlier SCS additivity rule (275) for such compounds. For a discussion of orbital interactions in three-membered rings and the marked γ -effects in fused polycyclic systems containing cyclopropane moieties, the reader is referred to the discussion in Section IV-D, to a paper on epoxides derived from dicyclopentadienes (446), and to a paper on *para*-substituted C-aryloxaziridines (447).

b. Four-Membered Rings. Basic chemical shifts and methyl substituent effects in cyclobutanes, oxetanes, and aza, thia, and phospho analogs have been summarized by Eliel and co-workers (142). Further data on methylated cyclobutanes (273), including some with additional chloro and bromo substituents (448), have been reported elsewhere. In cyclobutanes, halogen substituents exhibit a greater preference for pseudo-equatorial positions than methyl groups do (448). A series of 3-substituted thiethanes (300), corresponding 1-oxides (301), 1,1-dioxides (302), and unsaturated derivatives (303 and 304) (449), as well as various β -lactams (450), have also been investigated.



Scheme 70

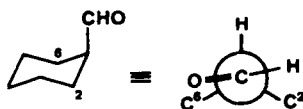
c. Five-Membered Rings. Eliel's review on nonaromatic heterocycles (142) incorporates many details of the ^{13}C NMR spectral properties of cyclopentanes and their oxa, thia, aza, and phospho analogs. Particular emphasis has been put on the determination of substituent effects of methyl and hydroxyl groups (142,174,451) in tetrahydrofurans and 1,3-dioxolanes; additional tetrahydrofuran data have been supplied by Huet and co-workers (452). Recently, a number of cis and trans isomers of 4,5-disubstituted 2,2-dimethyl-1,3-dioxolanes were investigated (453) in which the substituents were saturated and unsaturated carbon chains and various aryl groups. The authors established an increment rule by which the cis-trans isomerism can conveniently be assigned (453). Substituent effects in methylated 2-oxo-1,3-dioxolanes (454), *S*-methylthiolanium cations (142,455), and 1,3-dithiolanes (456,457) indicate that the five-membered rings in these compounds prefer half-chair conformations. Analogous conformations with maximum puckering at C(3) and C(4) were reported for methylated cyclopentanones (458). Conformations of oxathiazolidine derivatives have also been analyzed by ^{13}C NMR spectroscopy (459).

d. Six-Membered Rings. The vast majority of stereochemical analyses using substituent-effect information relate to cyclohexanes and their hetero analogs. Effects of methyl (100,101) and many other substituents in cyclohexanes are tabulated in previous sections of this chapter, textbooks (2-4), articles (7,9), and data collections (11).

Highly branched substituents, such as *tert*-butyl or trimethylammonium, rarely occupy axial positions in cyclohexane derivatives, because if they did steric repulsion within the molecule would be too severe. Instead, in such cases the six-membered ring systems usually prefer twist conformations (460,461), which can be detected by the absence of deshielding δ -effects (460); generally, carbon signals in twist forms are, on the average, at higher field than those in equatorially substituted epimers (460), although one has to be careful not to confuse twist and axially substituted chair conformers.

Conformational analysis in connection with determinations of free-energy differences (ΔG°) between axial and equatorial conformers is still attracting interest. Schneider and Hoppen (114) discussed *A* values ($-\Delta G^\circ$) and preferred orientations of axial substituents with lone pairs at heteroatoms directly attached to C^α (e.g., $-\text{OR}$, $-\text{NR}_2$, and $-\text{N}_3$), as well as of some other nonspherical substituents ($\text{X} = -\text{NC}$, $-\text{NCS}$, $-\text{CN}$, $-\text{C}\equiv\text{CH}$). Phenyl and vinyl groups were investigated by Eliel and Manoharan (277), who found *A* values of 2.87 ± 0.09 kcal/mol for phenyl and 1.68 ± 0.06 kcal/mol for vinyl. The latter value was essentially confirmed by Buchanan (196); the formyl group ($A = 0.84 \pm 0.08$ kcal/mol) in axial position adopts a predominant (93%) conformation (305) with the plane of the axial CHO group nearly perpendicular to the plane of symmetry of the cyclohexyl residue (Scheme 71) (196).

The conformational equilibria of various methylated cyclohexanols have been



305

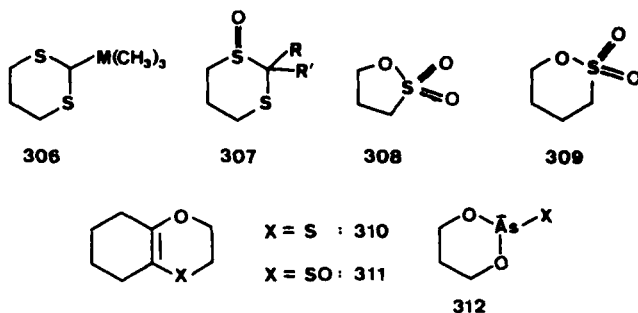
Scheme 71

determined (305,462), and the SCS values of equatorial and axial alkyl, methoxy, and phthalimido groups have been reported (463). The rotamer populations of methoxy substituents about the $\text{C}^\alpha\text{-OCH}_3$ bond can be derived from their effects on neighboring C(2) and C(6) atoms (464). Quin and Gordon (128) have studied the conformational effect of phosphorus groups in *cis*-4-*tert*-butylcyclohexyl derivatives. Whereas trivalent functions ($-\text{PH}_2$, $-\text{PX}_2$) readily occupy the normal axial position, tetravalent substituents [$-\text{PS}(\text{CH}_3)_2$, $-\text{P}(\text{CH}_3)_3^+$] cause significant ring distortions either through ring flattening or by forcing the ring into twist conformations (128).

Substituent effects of carboxyl and amino groups in α -amino acids on signals of γ -carbon atoms in the side chain allow conformational analysis of such compounds, and geminally disubstituted cyclohexanes were used as model compounds to derive quantitative equations (465). In systematic studies of large series of monosubstituted *p*-menthane and -isomenthane, derivatives were obtained that are useful for configurational and conformational assignments in this class of compounds (115,466,467). The effects and stereochemical positions of the isopropyl groups are particularly noteworthy (115). Even for highly substituted cyclohexanes, such as inositols and their *O*-methylated derivatives, quantitative correlations can be obtained (468).

The section on six-membered nonaromatic heterocycles in Eliel's review (142) contains so much information that only limited supplementary data are presented here to update that article. Eliel himself has expanded our knowledge of substituent effects in tetrahydropyrans (oxanes) (469) and the conformational behavior of such compounds (470) by obtaining ^{13}C NMR data on 68 derivatives carrying $-\text{CH}_3$, $-\text{C}_2\text{H}_5$, $-\text{CH}=\text{CH}_2$, $-\text{C}\equiv\text{CH}$, $-\text{COOCH}_3$, and $-\text{CH}_2\text{OH}$ groups. He derived a set of methyl substitution parameters (469) in analogy to that of Dalling and Grant (100,101), and as expected, the values are rather similar, with only a few exceptions; corresponding parameter sets are given for the other substituents also. In a study of the conformational equilibrium of 1-methoxytetrahydropyran, Booth and co-workers (471) analyzed the contributions of the three rotamers for both methoxyl-group positions, axial and equatorial. For 1,3-dioxanes (142,271,272) and morpholines (472), methyl parameter sets have been established as well. Pihlaja and co-workers (271,272) showed that their magnitudes clearly reflect the ring geometry and chair-twist equilibria. 2-Methoxy-1,3-dioxanes have also been studied (473).

The ^{13}C NMR spectra of alkylated thianes (474) have been published and

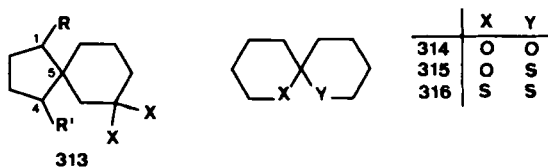


Scheme 72

supplement earlier data (142). Drew and Kitching (240) found that in some 2-(Group IVa)-substituted 1,3-dithianes **306** ($M = \text{Si, Ge, Sn, or Pb}$) the substituents have a much greater preference for an equatorial orientation over an axial one than in corresponding cyclohexanes. A "reversed" anomeric effect (286,475) was suggested to explain this observation. This is in accord with the behavior of the 1,3-dithiane-2-carbanion (476). In contrast to thiane oxide (161), 1,3-dithiane-1-oxide (142,477) and 1,3,5-trithiane-1-oxide (478) prefer the equatorial oxide conformer. In 2,2-disubstituted 1,3-dithiane-1-oxides **307** ($R/R' = \text{CH}_3/\text{CH}_3$ or $\text{CH}_3/\text{C}_6\text{H}_5$) the existence of considerable contributions of twist conformers was inferred from the ^{13}C chemical shifts of these compounds (477). Methyl substituent effects in thirty-five 1,3,2-dioxathiane-2-oxides (trimethylene sulfites) have been analyzed (479). The stereochemical orientation of the $\text{S}=\text{O}$ oxygen was found to be dependent on the substitution pattern, and in some compounds nonchair conformations were claimed (479). This situation is reminiscent of the findings in the 4-*tert*-butyl derivative of this six-membered cyclic sulfite (142). The ^{13}C chemical shifts of γ - and δ -sultones (**308** and **309**, respectively) and 20 derivatives thereof have been reported recently (480). Substituent effects and intramolecular electronic interactions in various 1,4-oxathiins and their mono- and dioxides have been discussed (481). In the bicyclic derivatives **310** and **311** the hetero rings may exist in slightly flattened boat conformations (481). The ^{13}C NMR data of a series of twenty-one 1,3,2-dioxarsenanes **312** have been discussed in terms of methyl SCSs (482). A comparison with corresponding 1,3-dioxanes revealed that the values are quite close in both systems, except that the SCSs of axial methyl groups differ considerably (482).

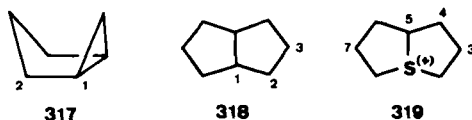
e. Polycyclic Systems. In a detailed ^{13}C NMR study of a large series of 1,4-dialkyl-spiro[4.5]decanes **313**, Kutschan and colleagues (483) made extensive use of γ - and δ -substituent effects in the differential recognition of 1,4-*cis*- and *trans*-configured spiranes. In addition, they determined the relative configuration of the spiro-chirality center C(5) (483). A group of Canadian authors has published a series of papers investigating the synthesis, stereochemistry, and

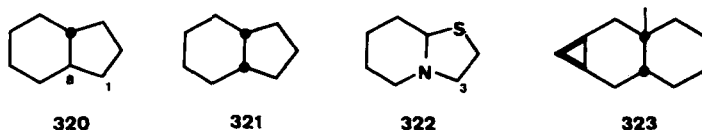
^{13}C NMR spectroscopy of 1,7-dioxa- (314), 1-oxa-7-thia- (315), and 1,7-dithiaspiro[5.5]undecane (316) and many of their derivatives, with special emphasis on stereoelectronic and steric effects governing the configurational and conformational properties of these compounds (484–486). This work showed that chemical-shift parameters developed for six-membered carbocyclic compounds in chair conformations (149) could be applied successfully only to sulfur and not to oxygen heterocycles (486).



Scheme 73

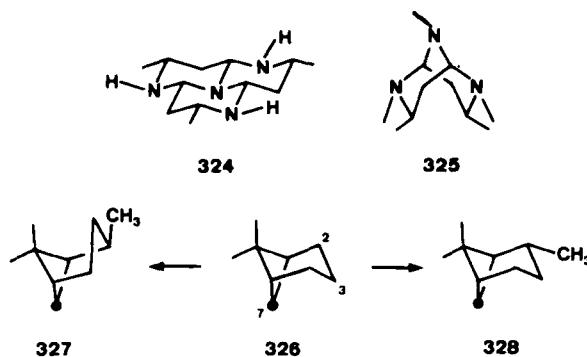
The preferred conformations in some fused polycyclic cyclopropane derivatives have been determined by estimating cyclopropane annelation shifts on γ -carbon atoms (377) (cf. Section IV-D). For instance, bicyclo[3.1.0]hexane (317) adopts the seemingly unfavorable boat conformation, apparently because in this form the hydrogen atoms at C(1) and C(2) are staggered, whereas they are eclipsed in the chair form (377). Whitesell and Matthews (487) have established substituent parameter sets for 2- and 3-substituted derivatives of bicyclo[3.3.0]octanes (318) as well as corresponding olefins. In addition to doing statistical assessments, these authors were able to predict the ^{13}C chemical shifts of polyfunctionalized derivatives, so that regio- and stereochemical assignments became possible (487). Based on these data and corresponding ones for monocyclic thiolanium cations (455), Fava and co-workers (488) investigated the ^{13}C NMR spectra of the *cis*-1-thioniabicyclo[3.3.0]octane salt (319) as well as some of its monosubstituted derivatives. They found that substituent effects enable conclusions to be drawn about the configurations and conformations of the molecules. For example, in 4-*endo*-substituted compounds the β -SCS values of OH, Cl, and Br on C(5) are essentially nil, in contrast to the situation in the corresponding carbocyclic analogs, whereas clear deshielding effects (+7.4, +9.1, and +9.5, respectively) are observed in the 4-*exo* series (488). The large (4-ppm) divergence between the ϵ -SCS(CH_3) values at C(7) in the two epimeric 3-methylated compounds is understandable only if one assumes different conformations of the bicyclic framework (488).





Scheme 74

The conformations of *trans*- and *cis*-fused bicyclo[4.3.0]nonanes (320 and 321, respectively) and some 1- and 8-monosubstituted ($X = \text{OH}, \text{Cl}, \text{Br}$) derivatives thereof have been analyzed (489). The authors found that effects of substituents at C(8) on six-membered-ring carbon atoms nicely agree with those in corresponding cyclohexanes (114). More information about the conformations of these and related bicyclo[4.*n*.0]alkanes ($n = 2,3,4$) as well as a variety of unsaturated and substituted derivatives was supplied shortly thereafter (490,491) in papers emphasizing particularly the assignment of ring junction configurations (491). The conformational equilibria of hexahydro[1,3]thiazolo[3,2-*a*]pyridine (322) and some 3-alkylated derivatives have been investigated and interpreted in terms of minimization of dipolar interaction of the heteroatoms (492). The decalin system has attracted particular interest, because it represents a substructure inherent in many natural compounds (e.g., steroids). In analogy to their study of cyclohexanes (100,101), Grant and co-workers have derived methyl parameter sets from data on mono- and dimethyldecalins (172). Conformational preferences of a series of diversely substituted *cis*-decalins have been determined by Stothers and co-workers (493), who also published ^{13}C NMR spectral characteristics of similar *trans*-decalins (249). Signal and configurational assignments in various dimethylamino-*trans*-decalins and -decalols were achieved by SCS evaluations (494). The conformational behavior of cyclopropanodecalins, for example 323, was investigated by Wenkert and co-workers (495). A review containing a wealth of SCS and ICS information along with reference data on more than 400 steroids (317) must mentioned in this context; the allylic and



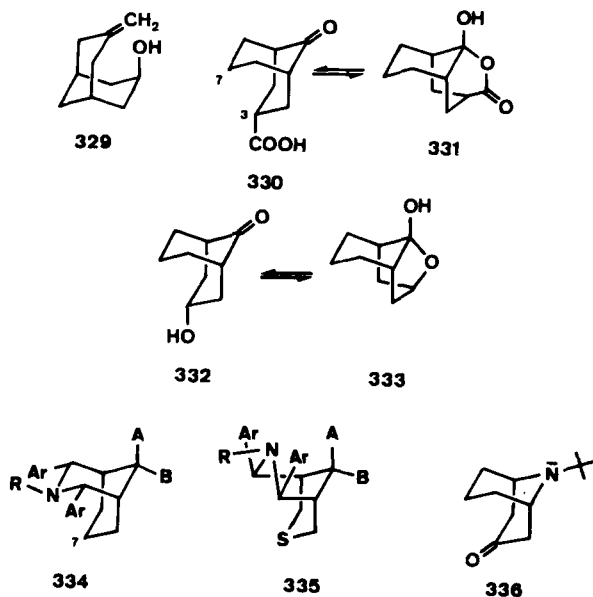
Scheme 75

homoallylic effects of endocyclic double bonds in that class of compounds have been analyzed in great detail (496).

Hetero analogs of decalin and related tri- and tetracyclic compounds have been amply discussed (142), so we shall mention the results of only one more publication: Katritzky and co-workers (497) studied the conformational equilibria of 1,3-diazacyclohexanes and similar bi- and tricyclic compounds, for instance **324** and **325** by variable-temperature ^{13}C NMR, and assigned the structures of the isomers based on γ -gauche-substituent-induced carbon shieldings. Katritzky's paper also deals with bridged molecules, many ^{13}C NMR data of which have been mentioned earlier in this chapter and in other reviews (3,24). Garratt and Rigueira (180,181,498) have reported on various substituted bicyclo[2.2.2]octanes and derived substituent effects of CH_3 , OH, COOH, and ketone oxygen atoms (180,181). In addition, they compared the ^{13}C chemical shifts of hydroxy acids and δ -lactones prepared from them. It emerged that lactonization affects the shieldings of nearby carbon atoms in two different ways (498): In addition to modifications in electron-charge distributions, the molecular backbone conformation is changed from flexible boat-twist to rigid twist.

An unusually large (+7.45 ppm) γ -SCS of a methyl group at C(7) was observed in *cis*-pinane (**327**) when compared with norpinane (**326**) (499). This difference does not originate only in the methyl effect transmitted through the bonds; also, the γ_g -effect from C(3) is missing due to the flip of the six-membered ring (499). In the *trans* isomer **328** the C(7) signal shows an upfield shift of 3.5 ppm, as expected (499).

Bicyclo[3.3.1]nonanes prefer to exist in slightly flattened double-chair (CC) conformations (142) unless at least one 3- or 7-endo substituent is present (142,219); then boat-chair (BC, CB) or even double-boat (BB) forms predominate. This general pattern apparently does not hold in the (CC) endo alcohol **329**; hydrogen bonding with the π -orbital is suggested to be the cause (370). Beside the steric transannular 3,7-interaction of endo substituents, another factor stabilizing CB conformations of bicyclo[3.3.1]nonanes was discovered by Speckamp and colleagues (500,501): In 9-oxo derivatives, reversible bridging occurs, forming hemiacylals or -acetals (e.g., **330** to **333**). Eliel and co-workers have reported very recently on the conformational equilibria of a large series of 2,4-diaryl-3-azabicyclo[3.3.1]nonanes and their 7-thia analogs, as well as 9-oxo and 9-hydroxy derivatives of these compounds (502,503); in contrast to the 7- CH_2 series, the 7-thia analogs exist mainly in a CB conformation, with the piperidine ring adopting a boat form (cf., for instance, **334** and **335**). Wiseman and co-workers (504) concluded from the relatively small γ_g -SCS value of the *tert*-butyl group in *N-tert*-butyl-9-azabicyclo[3.3.1]nonan-3-one (**336**) that this group must be tilted away to avoid steric interference with 1,3-diaxial hydrogen atoms, so that the nitrogen pyramid is flattened. Finally, we call attention to the ^{13}C NMR investigations of oxa- and azabicyclo[3.3.1]- and -[4.2.1]nonanes (324) and 8-phospha-bicyclo[3.2.1]octanes (505).



Scheme 76

VI. CONCLUSION AND PROSPECTS

From all the data presented in this chapter it is evident that interpretation of ^{13}C chemical-shift information is still dependent on the spectroscopist's imagination and experience. This situation will probably continue in the near future, although a number of helpful aids have become available in recent years:

1. First, various advanced multipulse techniques have been developed since the mid-1970s, and nowadays are routinely applicable on spectrometers of the latest generation. Particularly innovative and ingenious among these methods are two-dimensional NMR techniques (506–508) and double quantum transition measurements (INADEQUATE) (507–509), which allow one to determine connectivities between carbon atoms within a molecule.

2. Second, considerable effort has been expended to create ^{13}C NMR reference data systems that will enable spectroscopists to extract structural information from their experimental results by comparing them with documented spectra of related compounds; data banks stored in computers have been compiled and are accessible for substructure searches (510–519). The advent of these facilities means that SCS evaluations have been—at least in principle—outstripped in an important field of their application, namely in their use for establishing molecular constitution and assigning signals. In cases of doubt one should rely

on direct experimental techniques. It is, however, not obvious how stereochemical conclusions drawn from SCS information could be replaced as easily in the near future by applying similar experimental methods. Thus, the investigations described in this chapter will retain their importance.

3. The third area of interest in SCS determinations, namely the interpretation of experimental data in terms of changes in the electronic environment of the nuclei, is intrinsically not amenable to the above techniques. Although the field is still in its infancy, one may expect that someday ^{13}C NMR spectroscopy will rank among those methods that allow one to detect intramolecular electron interactions and proximity effects (520).

Carbon-13 NMR spectroscopy is currently being studied from different points of view. Some research workers try to investigate the NMR parameters of chemical shift, coupling constant, and relaxation time, as well as their dependence on structure, using an empirical approach. Others are interested in theoretical understanding and prediction of these parameters and establishing physical and mathematical models for their description. The present state of research may be compared with digging a tunnel through a mountain starting from opposite sides, the empirical and the theoretical. Though a good distance has been covered, the breakthrough still lies ahead and probably must come from the theoretical side. Then, a situation will be attained that was prophesied by Olah and Watkins (187) in their study of substituent effects in crowded phenylethanes: "It is hoped that ultimately a model will be devised in which a term as vague as a 'substituent effect' can be eliminated and replaced with one reflecting the change in the electronic properties induced in a molecule by the substituents and thus make it possible to have a model based on experimental observations as interpreted by theory to predict the electronic as well as steric properties of a molecule."

ACKNOWLEDGMENTS

The author is grateful to Professor G. Snatzke, Bochum, for many helpful discussions, and not only during the writing of this review. He is particularly indebted to Professor E. L. Eliel, Chapel Hill, for detailed discussions and to Dr. S. Wilen, New York, and Dr. G. Tóth, Budapest, for a careful reading of the chapter and helpful critical comments. A number of enthusiastic co-workers took part in the author's research, mainly by synthesizing model compounds in what often was a demanding task. Mrs. E. Sauerbier's invaluable assistance in the preparation of the manuscript and the drawings is also acknowledged. Financial support for the author's research was generously supplied by the Deutsche Forschungsgemeinschaft and Fonds der Chemischen Industrie.

REFERENCES

1. For a comprehensive compilation of books and review articles see the book series "Nuclear Magnetic Resonance, a Specialist Periodical Report"; Harris, R. K., Ed.; Royal Society of Chemistry: London, annual edition since 1972; refs. 2 to 24 give only a selection.
2. Stothers, J. B. "Carbon-13 NMR Spectroscopy"; Academic: New York, London, 1972.
3. Levy, G. C.; Lichter, R. L.; Nelson, G. L. "Carbon-13 Nuclear Magnetic Resonance Spectroscopy," 2nd ed.; Wiley: New York, 1980.
4. Wehrli, F. W.; Wirthlin, T. "Interpretation of Carbon-13 Nuclear Magnetic Resonance Spectra"; Heyden: London, 1976.
5. Breitmaier, E.; Voelter, W. "¹³C NMR Spectroscopy," 2nd ed.; Verlag Chemie: Weinheim, 1978.
6. Pregosin, P. S.; Randall, E. W. In "Determination of Organic Structures by Physical Methods," Vol. 4; Nachod, F. C.; Zuckerman, J. J., Eds.; Academic: New York, 1971, p. 263.
7. Wilson, N. K.; Stothers, J. B. *Top. Stereochem.* **1974**, *8*, 1.
8. Nelson, G. L.; Williams, E. A. *Progr. Phys. Org. Chem.* **1976**, *12*, 229.
9. Perkin, A. S. In "Isotopes in Organic Chemistry," Vol. 3; Buncl, E.; Lee, C. C., Eds.; Elsevier: Amsterdam, 1977, p. 171.
10. Johnson, L. F.; Jankowski, W. C. "Carbon-13 NMR Spectra"; Wiley: New York, 1972.
11. Clerc, J. T.; Pretsch, E.; Sternhell, S. "¹³C-Kernresonanzspektroskopie"; Akademische Verlagsgesellschaft: Frankfurt, 1973. Pretsch, E.; Clerc, T.; Seibl, J.; Simon, W. "Tabellen zur Strukturaufklärung organischer Verbindungen mit spektroskopischen Methoden"; Springer: Berlin, Heidelberg, 1976. Clerc, J. T.; Pretsch, E.; Seibl, J. "Structural Analysis of Organic Compounds by Combined Application of Spectroscopic Methods"; Elsevier: Amsterdam, and Akadémiai Kiadó: Budapest, 1981. Pretsch, E.; Clerc, T.; Seibl, J.; Simon, W. "Tables of Spectral Data for Structure Determination of Organic Compounds: ¹³C-NMR, ¹H-NMR, IR, MS, UV/VIS. Chemical Laboratory Practice"; Springer: Berlin, 1983.
12. Breitmaier, E.; Haas, G.; Voelter, W. "Atlas of Carbon-13 NMR Data"; Heyden: London, 1979.
13. Formacek, V.; Desnoyer, L.; Kellerhals, H. P.; Keller, T.; Clerc, J. T. "¹³C Data Bank"; Bruker Physik: Karlsruhe, 1976.
14. Bremser, W.; Ernst, L.; Franke, B.; Gerhards, R.; Hardt, A. "Carbon-13 NMR Spectral Data," 3rd ed.; Verlag Chemie: Weinheim, 1982 (comprises 30,000 spectra of 23,450 compounds). Bremser, W.; Franke, B.; Wagner, H. "Chemical Shift Ranges in Carbon-13 NMR Spectroscopy"; Verlag Chemie: Weinheim, 1982.
15. "Sadtler Standard Carbon-13 NMR Spectra"; Sadtler Research Laboratories: Philadelphia, 1977.
16. *General*: Wenkert, E.; Buckwalter, B. L.; Burfitt, I. R.; Gasić, M. J.; Gottlieb, H. E.; Haganman, E. W.; Schell, F. M.; Wovkulich, P. M. In "Topics in Carbon-13 NMR Spectroscopy," Vol. 2, Levy, G. C., Ed.; Wiley: New York, 1976, p. 81. Wehrli, F. W.; Nishida, T. *Progr. Chem. Org. Nat. Prod.* **1979**, *36*, 1.
17. *Biosynthetic studies*: Séquin, U.; Scott, A. I. *Science* **1974**, *186*, 101. McInnes, A. G.; Wright, J. L. C. *Acc. Chem. Res.* **1975**, *8*, 313. Simpson, T. J. *Chem. Soc. Rev.* **1975**, *4*, 497. McInnes, A. G.; Walters, J. A.; Wright, J. L. C.; Vining, L. C. In "Topics in Carbon-13 NMR Spectroscopy," Vol. 2; Levy, G. C., Ed.; Wiley: New York, 1976, p. 123. Kunesch, G.; Poupat, C. In "Isotopes in Organic Chemistry," Vol. 3; Buncl, E.; Lee, C. C., Eds.; Elsevier: Amsterdam, 1977, p. 105.
18. *Amino acids and peptides*: Deslauriers, R.; Smith, I. C. P. In "Topics in Carbon-13 NMR Spectroscopy," Vol. 2; Levy, G. C., Ed.; Wiley: New York, 1976, p. 1. Howarth, O. W.;

- Lilley, D. M. J. In "Progress in NMR Spectroscopy," Vol. 12; Emsley, J. M.; Feeney, J.; Sutcliffe, L. M.; Eds.; Pergamon: Oxford, 1978, p. 1.
19. *Steroids*: Blunt, J. W.; Stothers, J. B. *Org. Magn. Reson.* **1977**, *9*, 439. Smith, W. B. In "Annual Reports on NMR Spectroscopy," Vol. 8; Webb, G. A., Ed.; Academic: London, 1978, p. 199.
20. *Terpenes*: Bohlmann, F.; Zeisberg, R.; Klein, E. *Org. Magn. Reson.* **1975**, *7*, 426.
21. *Alkaloids*: Wenkert, E.; Bindra, J. S.; Chang, C.-J.; Cochran, D. W.; Schell, F. M. *Acc. Chem. Res.* **1974**, *7*, 46. Tourwé, D.; van Binst, G. *Heterocycles* **1978**, *9*, 507. Shamma, M.; Hindenlang, D. M. "Carbon-13 NMR Shift Assignments of Amines and Alkaloids"; Plenum: New York, London, 1979. Crabb, T. A. In "Annual Reports on NMR Spectroscopy," Vol. 8; Webb, G. A., Ed.; Academic Press: London, 1978, p. 1. Hughes, D. W.; McLean, D. B. In "The Alkaloids," Vol. 18; Manske, R. H. F., Ed.; Academic: New York, 1981, p. 217.
22. *Carbohydrates*: Kotowycz, G.; Lemieux, R. U. *Chem. Rev.* **1973**, *73*, 669.
23. *Coumarins*: Duddeck, H.; Kaiser, M. *Org. Magn. Reson.* **1982**, *20*, 55.
24. Marchand, A. P. "Stereochemical Applications of NMR Studies in Rigid Bicyclic Systems"; Verlag Chemie International: Deerfield Beach, Florida, 1982.
25. Martin, G. J.; Martin, M. L.; Odier, S. *Org. Magn. Reson.* **1975**, *7*, 2.
26. Ewing, D. F. *Org. Magn. Reson.* **1979**, *12*, 499.
27. Topsom, R. D. *Acc. Chem. Res.* **1983**, *16*, 292.
28. For a leading reference, see Adcock, W.; Khor, T.-C. *J. Am. Chem. Soc.* **1978**, *100*, 7799.
29. Ramsey, N. F. *Phys. Rev.* **1950**, *78*, 699; **1952**, *86*, 243.
30. Saika, A.; Slichter, C. P. *J. Chem. Phys.* **1954**, *22*, 26.
31. Lamb, W. E. Jr. *Phys. Rev.* **1941**, *60*, 817.
32. Karplus, M.; Pople, J. A. *J. Chem. Phys.* **1963**, *38*, 2803. Pople, J. A. *Mol. Phys.* **1964**, *9*, 301.
33. Cheney, B. V.; Grant, D. M. *J. Am. Chem. Soc.* **1967**, *89*, 5319.
34. Wolff, R.; Radeaglia, R. Z. *Phys. Chem. [Leipzig]* **1980**, *261*, 726.
35. Raynes, W. T. In "Nuclear Magnetic Resonance, A Specialist Periodical Report," Vol. 2; Harris, R. K., Ed.; The Chemical Society: London, 1973, p. 36.
36. McLachlan, A. D. *J. Chem. Phys.* **1960**, *32*, 1263.
37. Savitzky, G. B.; Namikawa, K.; Zweifel, G. *J. Phys. Chem.* **1965**, *69*, 3105.
38. Baird, N. C.; Teo, K. C. *J. Magn. Reson.* **1976**, *24*, 87.
39. Sadlej, A. J. *Org. Magn. Reson.* **1970**, *2*, 63. Solkan, V. N.; Mamayev, V. M.; Sergeyev, N. M.; Ustynyuk, Yu. A. *Org. Magn. Reson.* **1971**, *3*, 567.
40. Mason, J. J. *Chem. Soc. (A)* **1971**, 1038.
41. Mason, J. J. *Chem. Soc., Perkin II* **1976**, 1671.
42. Flygare, W. H.; Goodisman, J. J. *Chem. Phys.* **1968**, *49*, 3122. Gierke, T. D.; Flygare, W. H. *J. Am. Chem. Soc.* **1972**, *94*, 7277.
43. Malli, G.; Fraga, S. *Theor. Chim. Acta* **1966**, *5*, 275.
44. Mason, J. *Org. Magn. Reson.* **1977**, *10*, 188.
45. Shabab, Y. A. *Org. Magn. Reson.* **1977**, *9*, 580.
46. Ebraheem, K. A. K.; Webb, G. A.; Witanowski, M. *Org. Magn. Reson.* **1976**, *8*, 317.
47. Ditchfield, R.; Ellis, P. D. In "Topics in Carbon-13 NMR Spectroscopy," Vol. 1; Levy, G. C., Ed.; Wiley: New York, 1974, p. 1.
48. Lazzeretti, P.; Taddei, F. *Org. Magn. Reson.* **1971**, *3*, 113.
49. Miyajima, G.; Nishimoto, K. *Org. Magn. Reson.* **1974**, *6*, 313.
50. Maciel, G. E.; Dallas, J. L.; Elliot, R. L.; Dorn, H. C. *J. Am. Chem. Soc.* **1973**, *95*, 5857.
51. Ellis, P. D.; Maciel, G. E.; McIver, J. W. Jr. *J. Am. Chem. Soc.* **1972**, *94*, 4069.
52. Cheremisin, A. A.; Schastnev, P. V. *Zh. Strukt. Khim.* **1979**, *20*, 999.

53. Cyr, N.; Perlin, A. S.; Whitehead, M. A. *Can. J. Chem.* **1972**, *50*, 814.
54. Roberge, R.; Fliszár, S. *Can. J. Chem.* **1975**, *53*, 2400. Fliszár, S. *Can. J. Chem.* **1976**, *54*, 2839. Kean, G.; Gravel, D.; Fliszár, S. *J. Am. Chem. Soc.* **1976**, *98*, 4749. Henry, H.; Kean, G.; Fliszár, S. *J. Am. Chem. Soc.* **1977**, *99*, 5889.
55. Schindler, M.; Kutzelnigg, W. *J. Am. Chem. Soc.* **1983**, *105*, 1360; *J. Chem. Phys.* **1982**, *76*, 1919; *Mol. Phys.* **1983**, *48*, 781.
56. Raynes, W. T. *Mol. Phys.* **1971**, *20*, 321.
57. Maciel, G. E. In "Topics in Carbon-13 NMR Spectroscopy," Vol. 1; Levy, G. C., Ed.; Wiley: New York, 1974, p. 53.
58. Lauterbur, P. C. *Ann. N.Y. Acad. Sci.* **1958**, *70*, 841.
59. Spiess, H.; Schneider, W. G. *J. Chem. Phys.* **1961**, *35*, 722.
60. For example, Pehk, T.; Lippmaa, E. *Org. Magn. Reson.* **1971**, *3*, 679.
61. Pople, J. A.; Gordon, M. S. *J. Am. Chem. Soc.* **1967**, *89*, 4253.
62. Bucci, P. *J. Am. Chem. Soc.* **1968**, *90*, 252.
63. Pople, J. A. *Proc. Roy. Soc. London* **1957**, A239, 550.
64. McConnell, H. M. *J. Chem. Phys.* **1957**, *27*, 226.
65. Charrier, C.; Dorman, D. E.; Roberts, J. D. *J. Org. Chem.* **1973**, *38*, 2644.
66. Ellis, G. E.; Jones, R. G.; Papadopoulos, M. G. *J. Chem. Soc., Perkin II* **1974**, 1381.
67. Jones, A. J.; Alger, T. D.; Grant, D. M.; Litchman, W. M. *J. Am. Chem. Soc.* **1970**, *92*, 2386. Jones, A. J.; Gardner, P. D.; Grant, D. M.; Litchman, W. M.; Boekelheide, V. *J. Am. Chem. Soc.* **1970**, *92*, 2395.
68. Günther, H.; Schmickler, H.; Königshofen, H.; Recker, K.; Vogel, E. *Angew. Chem.* **1973**, *85*, 261; *Angew. Chem. Int. Ed. Engl.* **1973**, *12*, 243.
69. Burke, J. J.; Lauterbur, P. C. *J. Am. Chem. Soc.* **1964**, *86*, 1870.
70. Maciel, G. E.; Savitzky, G. B. *J. Phys. Chem.* **1965**, *69*, 3925.
71. Buckingham, A. D. *Can. J. Chem.* **1960**, *38*, 300.
72. Feeney, J.; Sutcliffe, L. H.; Walker, S. M. *Mol. Phys.* **1966**, *11*, 117, 129.
73. Yonemoto, T. *Can. J. Chem.* **1966**, *44*, 223.
74. Horsley, W. J.; Sternlicht, H. *J. Am. Chem. Soc.* **1968**, *90*, 3738.
75. Batchelor, J. G. *J. Am. Chem. Soc.* **1975**, *97*, 3410.
76. Schneider, H.-J.; Freitag, W. *J. Am. Chem. Soc.* **1977**, *99*, 8363.
77. Schneider, H.-J.; Freitag, W.; Gschwendtner, W.; Maldener, G. *J. Magn. Reson.* **1979**, *36*, 273.
78. Batchelor, J. G.; Prestegard, J. H.; Cushley, R. J.; Lipsky, S. R. *J. Am. Chem. Soc.* **1973**, *95*, 6358.
79. Batchelor, J. G.; Cushley, R. J.; Prestegard, J. H. *J. Org. Chem.* **1974**, *39*, 1698.
80. Schneider, H.-J.; Gschwendtner, W.; Buchheit, U. *J. Magn. Reson.* **1977**, *26*, 175.
81. Scott, K. N.; Mareci, T. H. *Can. J. Chem.* **1979**, *57*, 27.
82. Van Dommelen, M. E.; de Haan, J. W.; Buck, H. M. *Org. Magn. Reson.* **1980**, *13*, 447.
83. Van Dommelen, M. E.; de Haan, J. W.; Buck, H. M. *Org. Magn. Reson.* **1980**, *14*, 497.
84. Van Dommelen, M. E.; van de Ven, L. J. M.; Buck, H. M.; de Haan, J. W. *Recl. Trav. Chim. Pays-Bas* **1981**, *100*, 180.
85. Schneider, H.-J.; Gschwendtner, W. *J. Org. Chem.* **1982**, *47*, 4216. Schneider, H.-J.; Buchheit, U.; Gschwendtner, W.; Lonsdorfer, M. In "Molecular Structure And Biological Activity"; Griffin, J. F.; Duax, W. L., Eds.; Elsevier: Amsterdam, 1982, p. 165.
86. Seidman, K.; Maciel, G. E. *J. Am. Chem. Soc.* **1977**, *99*, 3254.
87. Schaefer, T.; Reynolds, W. F.; Yonemoto, T. *Can. J. Chem.* **1963**, *41*, 2969.
88. Grant, D. M.; Cheney, B. V. *J. Am. Chem. Soc.* **1967**, *89*, 5315.
89. Fritz, H.; Logemann, E.; Schill, G.; Winkler, T. *Chem. Ber.* **1976**, *109*, 1258.

90. Perlin, A. S.; Koch, H. J. *Can. J. Chem.* **1970**, *48*, 2639.
91. Dheu, M.-L.; Gagnière, D.; Duddeck, H.; Hollowood, F.; McKervey, M. A. *J. Chem. Soc., Perkin II* **1979**, 357.
92. Stothers, J. B.; Tan, C. T. *Can. J. Chem.* **1976**, *54*, 917.
93. Grutzner, J. B.; Jautelat, M.; Dence, J. B.; Smith, R. A.; Roberts, J. D. *J. Am. Chem. Soc.* **1970**, *92*, 7107.
94. Dubowchik, G. M.; Gottschall, D. W.; Grossman, M. J.; Norton, R. L.; Yoder, C. H. *J. Am. Chem. Soc.* **1982**, *104*, 4211.
95. Salman, S. R. *J. Iraqi Chem. Soc.* **1976**, *1*, 11; *Chem. Abstr.* **1977**, *86*, 170659q.
96. Van Dommelen, M. E.; Buck, H. M.; de Haan, J. W. *Chem. Phys. Lett.* **1978**, *57*, 80.
97. Inamoto, N.; Masuda, S. *Tetrahedron Lett.* **1977**, 3287.
98. Inamoto, N.; Masuda, S.; Tori, K.; Nishikawa, J. *Tetrahedron Lett.* **1983**, *24*, 5265.
99. Sasaki, Y.; Tsujimoto, T.; Takai, H.; Sugiura, M. *Chem. Pharm. Bull.* **1980**, *28*, 3106.
100. Sasaki, Y.; Takai, H.; Tsujimoto, T. *Chem. Pharm. Bull.* **1980**, *28*, 677.
101. Dalling, D. K.; Grant, D. M. *J. Am. Chem. Soc.* **1967**, *89*, 6612.
102. Dalling, D. K.; Grant, D. M. *J. Am. Chem. Soc.* **1972**, *94*, 5318.
103. Roberts, J. D.; Weigert, F. J.; Kroschwitz, J. I.; Reich, H. J. *J. Am. Chem. Soc.* **1970**, *92*, 1338.
104. Beierbeck, H.; Saunders, J. K. *Can. J. Chem.* **1975**, *53*, 1307.
105. Beierbeck, H.; Saunders, J. K. *Can. J. Chem.* **1976**, *54*, 632.
106. Duddeck, H.; Hollowood, F.; Karim, A.; McKervey, M. A. *J. Chem. Soc., Perkin II* **1979**, 360.
107. Altona, C.; Sundaralingam, M. *Tetrahedron* **1970**, *26*, 925, and references cited therein.
108. Sandris, C.; Ourisson, G. *Bull. Soc. Chim. France* **1958**, 1524; Waegell, B.; Pouzet, P.; Ourisson, G. *Bull. Soc. Chim. Fr.* **1963**, 1821. Biellmann, J.-F.; Hanna, R.; Ourisson, G.; Sandris, C.; Waegell, B. *Bull. Soc. Chim. Fr.* **1960**, 1429.
109. Bucourt, R. *Top. Stereochem.* **1974**, *8*, 159.
110. Daneels, D.; Anteunis, M. *Tetrahedron* **1975**, *31*, 1689.
111. Eggert, H.; VanAntwerp, C. L.; Bhacca, N. S.; Djerassi, C. *J. Org. Chem.* **1976**, *41*, 71.
112. Schwenzer, G. M. *J. Org. Chem.* **1978**, *43*, 1079.
113. Allinger, N. L.; Tribble, M. T.; Miller, M. A.; Wertz, D. H. *J. Am. Chem. Soc.* **1971**, *93*, 1637. Wertz, D. H.; Allinger, N. L. *Tetrahedron* **1974**, *30*, 1579.
114. Schneider, H.-J.; Hoppen, V. *Tetrahedron Lett.* **1974**, 579.
115. Schneider, H.-J.; Hoppen, V. *J. Org. Chem.* **1978**, *43*, 3866.
116. Firl, J.; Kresze, G.; Bosch, T.; Arndt, V. *Liebigs Ann. Chem.* **1978**, 87.
117. Bégué, J. P.; Bonnet-Delpon, D. *Org. Magn. Reson.* **1982**, *18*, 190.
118. Grover, S. H.; Stothers, J. B. *Can. J. Chem.* **1974**, *52*, 870.
119. Kleinpeter, E.; Borsdorf, R. *J. Prakt. Chem. [Leipzig]* **1977**, 319, 458.
120. Dubois, J.-E.; Doucet, J.-P.; Panaye, A. *Tetrahedron Lett.* **1980**, *21*, 2905.
121. Lindeman, L. P.; Adams, J. Q. *Anal. Chem.* **1971**, *43*, 1245.
122. Ejchart, A. *Org. Magn. Reson.* **1977**, *9*, 351.
123. Nougier, R.; Surzur, J.-M.; Virgilli, A. *Org. Magn. Reson.* **1981**, *15*, 155.
124. Marker, A.; Doddrell, D.; Riggs, N. V. *J. Chem. Soc., Chem. Comm.* **1972**, 724.
125. Maciel, G. E.; Dorn, H. C.; Greene, R. L.; Kleschick, W. A.; Peterson, M. R., Jr.; Wahl, G. H., Jr. *Org. Magn. Reson.* **1974**, *6*, 178.
126. Poindexter, G. S.; Kropp, P. J. *J. Org. Chem.* **1976**, *41*, 1215.
127. Della, E. W.; Cotsaris, E.; Hine, P. T. *J. Am. Chem. Soc.* **1981**, *103*, 4131.
128. Quin, L. D.; Gordon, M. D.; Ok Lee, S. *Org. Magn. Reson.* **1974**, *6*, 503.
129. Gordon, M. D.; Quin, L. D. *J. Org. Chem.* **1976**, *41*, 1690.
130. Buchanan, G. W.; Bowen, J. H. *Can. J. Chem.* **1977**, *55*, 604.

130. Barbarella, G.; Dembech, P.; Garbesi, A.; Fava, A. *Org. Magn. Reson.* **1976**, *8*, 108.
- Dauphin, G.; Cuer, A. *Org. Magn. Reson.* **1979**, *12*, 557.
131. Freeman, F.; Angeletakis, C. N.; Maricich, T. J. *Org. Magn. Reson.* **1981**, *17*, 53.
132. Freeman, F.; Angeletakis, C. N. *Org. Magn. Reson.* **1983**, *21*, 86.
133. Doddrell, D.; Burfitt, I.; Kitching, W.; Bulpitt, M.; Lee, C.-H.; Mynott, R. J.; Considine, J. L.; Kuivila, H. G.; Sarma, R. H. *J. Am. Chem. Soc.* **1974**, *96*, 1640. Kitching, W.; Marriott, M.; Adcock, W.; Doddrell, D. *J. Org. Chem.* **1976**, *41*, 1671.
134. Kitching, W.; Doddrell, D.; Grutzner, J. B. *J. Organometal. Chem.* **1976**, *107*, C 5.
135. Mitchell, T. N. *Org. Magn. Reson.* **1976**, *8*, 34.
136. Kuivila, H. G.; Considine, J. L.; Sarma, R. H.; Mynott, R. J. *J. Organometal. Chem.* **1976**, *111*, 179.
137. Della, E. W.; Patney, H. K. *Aust. J. Chem.* **1979**, *32*, 2243.
138. Leibfritz, D.; Wagner, B. O.; Roberts, J. D. *Liebigs Ann. Chem.* **1972**, *763*, 173.
139. Kress, W.; Breitingner, D. K.; Sendelbeck, R. *J. Organometal. Chem.* **1983**, *246*, 1.
140. Anet, F. A. L.; Krane, J.; Kitching, W.; Doddrell, D.; Praeger, D. *Tetrahedron Lett.* **1974**, 3255.
141. Barron, P. F.; Doddrell, D.; Kitching, W. *J. Organometal. Chem.* **1977**, *132*, 351.
142. Eliel, E. L.; Pietrusiewicz, K. M. In "Topics in Carbon-13 NMR Spectroscopy," Vol. 3; Levy, G. C., Ed.; Wiley: New York, 1979, p. 171.
143. Lambert, J. B.; Netzel, D. A.; Sun, H.-N.; Lilianstrom, K. K. *J. Am. Chem. Soc.* **1976**, *98*, 3778.
144. Lauterbur, P. C. *Ann. N.Y. Acad. Sci.* **1958**, *70*, 841; *J. Am. Chem. Soc.* **1961**, *83*, 1846.
145. Savitzky, G. B.; Namikawa, K. *J. Phys. Chem.* **1963**, *67*, 2430; **1964**, *68*, 1956.
146. Beierbeck, H.; Saunders, J. K. *Can. J. Chem.* **1976**, *54*, 2985.
147. Wertz, D. H.; Allinger, N. L. *Tetrahedron* **1974**, *30*, 1579.
148. Litchman, W. M.; Grant, D. M. *J. Am. Chem. Soc.* **1968**, *90*, 1400.
149. Beierbeck, H.; Saunders, J. K.; ApSimon, J. W. *Can. J. Chem.* **1977**, *55*, 2813.
150. Schneider, H.-J.; Freitag, W. *Chem. Ber.* **1979**, *112*, 16.
151. Freitag, W.; Schneider, H.-J. *Isr. J. Chem.* **1980**, *20*, 153.
152. Stothers, J. B.; Tan, C. T.; Teo, K. C. *Can. J. Chem.* **1973**, *51*, 2893.
153. Lippmaa, E.; Pehk, T.; Paasivirta, J.; Belikova, N.; Platé, A. *Org. Magn. Reson.* **1970**, *2*, 581.
154. Morris, D. G.; Murray, A. M. *J. Chem. Soc., Perkin II* **1975**, 734.
155. Beierbeck, H.; Saunders, J. K. *Can. J. Chem.* **1977**, *55*, 3161.
156. Duddeck, H.; Klein, H. *Tetrahedron* **1977**, *33*, 1971.
157. Batchelor, J. G.; Feeney, J.; Roberts, G. C. K. *J. Magn. Reson.* **1975**, *20*, 19.
158. Periasamy, M. *Heterocycles* **1982**, *18*, 127.
159. Schneider, H.-J.; Weigand, E. F. *J. Am. Chem. Soc.* **1977**, *99*, 8362.
160. Schneider, H.-J.; Ansorge, W. *Tetrahedron* **1977**, *33*, 265.
161. Buchanan, G. W.; Durst, T. *Tetrahedron Lett.* **1975**, 1683.
162. Willer, R. L.; Eliel, E. L. *Org. Magn. Reson.* **1977**, *9*, 285.
163. Barbarella, G.; Dembech, P.; Garbesi, A.; Fava, A. *Org. Magn. Reson.* **1976**, *8*, 469.
164. Lambert, J. B.; Vagenas, A. R. *Org. Magn. Reson.* **1981**, *17*, 270.
165. Eliel, E. L.; Rao, V. S.; Vierhapper, F. W.; Zúñiga Juaristi, G. *Tetrahedron Lett.* **1975**, 4339.
166. Willer, R. L.; Eliel, E. L. *J. Am. Chem. Soc.* **1977**, *99*, 1925.
167. Eliel, E. L.; Rao, V. S.; Riddell, F. G. *J. Am. Chem. Soc.* **1976**, *98*, 3583.
168. Pihlaja, K.; Björkqvist, B. *Org. Magn. Reson.* **1977**, *9*, 533.
169. Grant, D. M.; Paul, E. G. *J. Am. Chem. Soc.* **1964**, *86*, 2984.
170. Woolfenden, W. R.; Grant, D. M. *J. Am. Chem. Soc.* **1966**, *88*, 1496.

171. Alger, T. D.; Grant, D. M.; Paul, E. G. *J. Am. Chem. Soc.* **1966**, *88*, 5397.
172. Dalling, D. K.; Grant, D. M.; Paul, E. G. *J. Am. Chem. Soc.* **1973**, *95*, 3718.
173. Buckwalter, B. L.; Burfitt, I. R.; Nagel, A. A.; Wenkert, E.; Näf, F. *Helv. Chim. Acta* **1975**, *58*, 1567.
174. Christl, M.; Reich, H. J.; Roberts, J. D. *J. Am. Chem. Soc.* **1971**, *93*, 3463; Schneider, H.-J.; Nguyen-Ba, N.; Thomas, F. *Tetrahedron* **1982**, *38*, 2327.
175. Pfenninger, J.; Graf, W. *Helv. Chim. Acta* **1980**, *63*, 2338.
176. Pehk, T.; Lippmaa, E.; Sevostjanova, V. V.; Krayuschkin, M. M.; Tarasova, A. I. *Org. Magn. Reson.* **1971**, *3*, 783.
177. Subbotin, O. A.; Sergeev, N. M. *Zh. Org. Khim.* **1978**, *14*, 1486.
178. Giannini, D. D.; Kollman, P. A.; Bhacca, N. S.; Wolff, M. E. *J. Am. Chem. Soc.* **1974**, *96*, 5462.
179. Ernst, L. *J. Magn. Reson.* **1975**, *20*, 544.
180. Garratt, P. J.; Riguera, R. *J. Org. Chem.* **1976**, *41*, 465.
181. Riguera, R.; Garratt, P. J. *An. Quím.* **1978**, *74*, 216.
182. Kleinpeter, E.; Kühn, H.; Mühlstädt, M.; Jancke, H.; Zeigan, D. *J. Prakt. Chem. [Leipzig]* **1982**, *324*, 609.
183. Duddeck, H. Unpublished results.
184. Grover, S. H.; Guthrie, J. P.; Stothers, J. B.; Tan, C. T. *J. Magn. Reson.* **1973**, *10*, 227.
185. Seidman, K.; Maciel, G. E. *J. Am. Chem. Soc.* **1977**, *99*, 659.
186. Warshel, A.; Lifson, S. *J. Chem. Phys.* **1970**, *53*, 582. Ermer, O.; Lifson, S. *J. Am. Chem. Soc.* **1973**, *95*, 4121.
187. Watkins, M. I.; Olah, G. A. *J. Am. Chem. Soc.* **1981**, *103*, 6566.
188. De Hoog, A. *J. Org. Magn. Reson.* **1974**, *6*, 233.
189. Wiberg, K. B.; Pratt, W. E.; Bailey, W. F. *Tetrahedron Lett.* **1978**, 4865.
190. De Haan, J. W.; van Dommelen, M. E.; van de Veen, L. J. M.; Corvers, A. *Org. Magn. Reson.* **1978**, *11*, 316.
191. Gorenstein, D. G. *J. Am. Chem. Soc.* **1977**, *99*, 2254, and references cited therein.
192. Olah, G. A.; Donovan, D. J. *J. Org. Chem.* **1978**, *43*, 1743.
193. Batchelor, J. G. *J. Magn. Reson.* **1975**, *18*, 212.
194. Vierhapper, F. W.; Eliel, E. L. *J. Org. Chem.* **1979**, *44*, 1081.
195. Kitching, W.; Drew, G. M. *J. Org. Chem.* **1981**, *46*, 2695.
196. Buchanan, G. W. *Can. J. Chem.* **1982**, *60*, 2908.
197. Wiseman, J. R.; Krabbenhoft, H. O.; Anderson, B. R. *J. Org. Chem.* **1976**, *41*, 1518.
198. Buchanan, G. W.; Cousineau, C. M. E.; Mundell, T. C. *Can. J. Chem.* **1978**, *56*, 2019.
199. Hirsch, J. A.; Havinga, E. *J. Org. Chem.* **1976**, *41*, 455.
200. Rooney, R. P.; Evans, S. A., Jr. *J. Org. Chem.* **1980**, *45*, 180.
201. Bass, S. W.; Evans, S. A., Jr. *J. Org. Chem.* **1980**, *45*, 710.
202. Bicker, R.; Kessler, H.; Zimmermann, G. *Chem. Ber.* **1978**, *111*, 3200.
203. Christl, M.; Herbert, R. *Org. Magn. Reson.* **1979**, *12*, 150.
204. Christl, M.; Leininger, H.; Brunn, E. *J. Org. Chem.* **1982**, *47*, 661.
205. Christl, M.; Buchner, W. *Org. Magn. Reson.* **1978**, *11*, 461.
206. Duthaler, R. O.; Williamson, K. L.; Giannini, D. D.; Bearden, W. H.; Roberts, J. D. *J. Am. Chem. Soc.* **1977**, *99*, 8406. Levy, G. C.; Lichter, R. L. "Nitrogen-15 Nuclear Magnetic Resonance Spectroscopy"; Wiley: New York, 1979.
207. Delseeth, C.; Kintzinger, J.-P. *Helv. Chim. Acta* **1978**, *61*, 1327. Eliel, E. L.; Liu, K.-T.; Chandrasekaran, S. *Org. Magn. Reson.* **1983**, *21*, 179.
208. Ayer, W. A.; Browne, L. M.; Fung, S.; Stothers, J. B. *Can. J. Chem.* **1976**, *54*, 3272.
209. Stothers, J. B.; Tan, C. T. *Can. J. Chem.* **1977**, *55*, 841.
210. Hoffmann, R. *Acc. Chem. Res.* **1971**, *4*, 1.

211. Gleiter, R. *Angew. Chem.* **1974**, *86*, 770; *Angew. Chem. Int. Ed. Engl.* **1974**, *13*, 696.
212. Jorgensen, W. L.; Salem, L. "The Organic Chemist's Book of Orbitals"; Academic: New York, 1973.
213. Epiotis, N. D.; Cherry, W. R.; Shaik, S.; Yates, R. L.; Bernardi, F. *Top. Curr. Chem.* **1977**, *70*.
214. Pople, J. A.; Santry, D. P. *Mol. Phys.* **1963**, *7*, 269.
215. Forrest, T. P.; Webb, J. G. K. *Org. Magn. Reson.* **1979**, *12*, 371.
216. Duddeck, H.; Feuerhelm, H.-T. *Tetrahedron* **1980**, *36*, 3009.
217. Phillips, L.; Wray, V. J. *Chem. Soc., Perkin II* **1972**, 223.
218. Perkins, R. R.; Pincock, R. E. *Org. Magn. Reson.* **1976**, *8*, 165.
219. Schneider, H.-J.; Ansorge, W. *Tetrahedron* **1977**, *33*, 265.
220. Eliel, E. L.; Bailey, W. F.; Kopp, L. D.; Willer, R. L.; Grant, D. M.; Bertrand, R.; Christensen, K. A.; Dalling, D. K.; Duch, M. W.; Wenkert, E.; Schell, F. M.; Cochran, D. W. *J. Am. Chem. Soc.* **1975**, *97*, 322.
221. Duddeck, H.; Islam, M. R. *Tetrahedron* **1981**, *37*, 1193.
222. Duddeck, H.; Islam, M. R. *Org. Magn. Reson.* **1981**, *16*, 32.
223. Duddeck, H.; Islam, M. R. *Org. Magn. Reson.* **1983**, *21*, 727.
224. Le Fèvre, R. J. W. *Adv. Phys. Org. Chem.* **1965**, *3*, 1.
225. Ishihara, T.; Ando, T.; Muranaka, T.; Saito, K. *J. Org. Chem.* **1977**, *42*, 666.
226. Morishima, I.; Okada, K.; Yonezawa, T.; Goto, K. *J. Am. Chem. Soc.* **1971**, *93*, 3922.
227. Morishima, I.; Yoshikawa, K.; Okada, K. *J. Am. Chem. Soc.* **1976**, *98*, 3787.
228. Barfield, M.; Conn, S. A.; Marshall, J. L.; Miller, D. E. *J. Am. Chem. Soc.* **1976**, *98*, 6253. Barfield, M. *J. Am. Chem. Soc.* **1980**, *102*, 1. Barfield, M.; Marshall, J. L.; Canada, E. D., Jr. *J. Am. Chem. Soc.* **1980**, *102*, 7. Barfield, M.; Brown, S. E.; Canada, E. D., Jr.; Ledford, N. D.; Marshall, J. L.; Walter, S. R.; Yakali, E. *J. Am. Chem. Soc.* **1980**, *102*, 3355. Barfield, M.; Della, E. W.; Pigou, P. E.; Walter, S. R. *J. Am. Chem. Soc.* **1982**, *104*, 3549.
229. Berger, S. J. *Org. Chem.* **1978**, *43*, 209.
230. Wray, V. J. *Am. Chem. Soc.* **1978**, *100*, 768.
231. Aguiar, A. M.; Morrow, C. J.; Morrison, J. D.; Burnett, R. E.; Masler, W. F.; Bhacca, N. S. *J. Org. Chem.* **1976**, *41*, 1545.
232. Duddeck, H. *Tetrahedron* **1978**, *34*, 247.
233. Wiseman, J. R.; Krabbenhoft, H. O. *J. Org. Chem.* **1977**, *42*, 2240.
234. Senda, Y.; Ishiyama, J.; Imaizumi, S. *Tetrahedron* **1975**, *31*, 1601.
235. Casy, A. F.; Iorio, M. A.; Podo, F. *Org. Magn. Reson.* **1981**, *15*, 275.
236. Schneider, H.-J.; Freitag, W.; Weigand, E. *Chem. Ber.* **1978**, *111*, 2656.
237. Wiberg, K. B.; Barth, D. E.; Pratt, W. E. *J. Am. Chem. Soc.* **1977**, *99*, 4286.
238. Duddeck, H.; Wolff, P. *Org. Magn. Reson.* **1976**, *8*, 593.
239. De Hoog, A. J. *Org. Magn. Reson.* **1974**, *6*, 233.
240. Drew, G. M.; Kitching, W. J. *Org. Chem.* **1981**, *46*, 558.
241. Vierhapper, F. W.; Willer, R. L. *Org. Magn. Reson.* **1977**, *9*, 13.
242. Zefirov, N. S. *Tetrahedron Lett.* **1975**, 1087.
243. Hoffmann, R.; Mollère, P. D.; Heilbronner, E. *J. Am. Chem. Soc.* **1973**, *95*, 4860.
244. Duddeck, H. *Org. Magn. Reson.* **1975**, *7*, 151.
245. Duddeck, H.; Dietrich, W. *Tetrahedron Lett.* **1975**, 2925.
246. Gerhards, R.; Dietrich, W.; Bergmann, G.; Duddeck, H. *J. Magn. Reson.* **1979**, *36*, 189.
247. Duddeck, H.; Islam, M. R. *Org. Magn. Reson.* **1983**, *21*, 140.
248. Kitching, W.; Adcock, W.; Khor, T. C.; Doddrell, D. *J. Org. Chem.* **1976**, *41*, 2055.
249. Ayer, W. A.; Browne, L. M.; Fung, S.; Stothers, J. B. *Org. Magn. Reson.* **1978**, *11*, 73.
250. Pearson, H. *J. Chem. Soc., Chem. Comm.* **1975**, 912.
251. Anderson, J. E.; Franck, R. W. *Nouv. J. Chim.* **1983**, *7*, 169.

252. Engelhardt, G.; Jancke, H.; Zeigan, D. *Org. Magn. Reson.* **1976**, *8*, 655.
253. Barton, D. H. R.; Head, A. J.; May, P. J. *J. Chem. Soc.* **1957**, 935. Cf. Eliel, E. L.; Allinger, N. L.; Angyal, S. J.; Morrison, G. A. "Conformational Analysis"; Wiley: New York, 1965, p. 345 ff.
254. Bhacca, N. S.; Giannini, D. D.; Jankowski, W. S.; Wolff, M. E. *J. Am. Chem. Soc.* **1973**, *95*, 8421.
255. Eaton, P. J.; Lauren, D. R.; O'Connor, A. W.; Weavers, R. T. *Aust. J. Chem.* **1981**, *34*, 1303.
256. Nakashima, T. T.; Maciel, G. E. *Org. Magn. Reson.* **1972**, *4*, 321.
257. Hirsch, J. A.; Jarmas, A. A. *J. Org. Chem.* **1978**, *43*, 4106.
258. Tokita, K.; Takemura, T.; Kondo, S.; Mori, N. *Bull. Chem. Soc. Japan* **1980**, *53*, 450.
259. Kaneda, T.; Otsubo, T.; Horita, H.; Misumi, S. *Bull. Chem. Soc. Japan* **1980**, *53*, 1015.
260. Hamlow, H. P.; Okuda, S.; Nakagawa, N. *Tetrahedron Lett.* **1964**, 2553.
261. Lambert, J. B.; Oliver, W. L., Jr.; Jackson, G. F., III. *Tetrahedron Lett.* **1969**, 2027. Lambert, J. B.; Featherman, S. I. *Chem. Rev.* **1975**, *75*, 611.
262. Vierhapper, F. W.; Eliel, E. L.; Zúñiga, G. J. *Org. Chem.* **1980**, *45*, 4844.
263. Schneider, H.-J.; Sturm, L. *Angew. Chem.* **1976**, *88*, 574; *Angew. Chem. Int. Ed. Engl.* **1976**, *15*, 545.
264. Eliel, E. L.; Vierhapper, F. W. *J. Org. Chem.* **1976**, *41*, 199.
265. Vierhapper, F. W.; Eliel, E. L. *J. Org. Chem.* **1977**, *42*, 51.
266. Nelsen, S. F.; Weisman, G. R.; Clennan, E. L.; Peacock, V. E. *J. Am. Chem. Soc.* **1976**, *98*, 6893.
267. Weisman, G. R.; Johnson, V. B.; Coolidge, M. B. *Tetrahedron Lett.* **1981**, *22*, 4365.
268. Jordan, G. J.; Christ, D. R. *Org. Magn. Reson.* **1977**, *9*, 322.
269. Vierhapper, F. W.; Furst, G. T.; Lichter, R. L.; Fanso-Free, S. N. Y.; Eliel, E. L. *J. Am. Chem. Soc.* **1981**, *103*, 5629.
270. Pihlaja, K.; Björkqvist, B. *Org. Magn. Reson.* **1977**, *9*, 533.
271. Pihlaja, K.; Nurmi, T. *Isr. J. Chem.* **1980**, *20*, 160.
272. Pihlaja, K.; Kivimäki, M.; Myllyniemi, A.-M.; Nurmi, T. *J. Org. Chem.* **1982**, *47*, 4688.
273. Eliel, E. L.; Pietrusiewicz, K. M. *Org. Magn. Reson.* **1980**, *13*, 193.
274. Davies, S. G.; Witham, G. H. *J. Chem. Soc., Perkin II* **1975**, 861.
275. Monti, J. P.; Faure, R.; Vincent, E.-J. *Org. Magn. Reson.* **1976**, *8*, 611.
276. Mison, P.; Chaabouni, R.; Diab, Y.; Martino, R.; Lopez, A.; Lattes, A.; Wehrli, F. W.; Wirthlin, T. *Org. Magn. Reson.* **1976**, *8*, 79.
277. Eliel, E. L.; Manoharan, M. *J. Org. Chem.* **1981**, *46*, 1959.
278. Proulx, T. W.; Smith, W. B. *J. Magn. Reson.* **1976**, *23*, 477.
279. Fong, C. W. *Aust. J. Chem.* **1980**, *33*, 1291.
280. Ditchfield, R.; Hehre, W. J.; Pople, J. A. *Chem. Phys.* **1971**, *54*, 724.
281. Howarth, O. W.; Lynch, R. J. *Mol. Phys.* **1968**, *15*, 431.
282. Block, R. E. *J. Magn. Reson.* **1971**, *5*, 155.
283. Zeroka, D. *Chem. Phys. Lett.* **1972**, *14*, 471.
284. Raynes, W. T. In "Nuclear Magnetic Resonance, A Specialist Periodical Report," Vol. 3; Harris, R. K., Ed.; The Chemical Society: London, 1974, p. 7.
285. Szarek, W. A.; Horton, D.; Eds. "Anomeric Effect—Origin and Consequences," ACS Symposium Series, Vol. 87; American Chemical Society: Washington, D.C., 1979.
286. Kirby, A. J. "The Anomeric Effect and Related Stereoelectronic Effects at Oxygen"; Springer: Berlin, Heidelberg, 1983.
287. Wolfe, S.; Whangbo, M.-H.; Mitchell, D. J. *Carbohydr. Res.* **1979**, *69*, 1.
288. Kurkutova, E. N.; Goncharov, A. V.; Zefirov, N. S.; Palyulin, V. A. *Zh. Strukt. Khim.* **1976**, *17*, 687.
289. Nasyrov, D. M.; Vereshchagin, A. N. *Izv. Akad. Nauk SSR, Ser. Khim.* **1981**, 580.

290. Petrova, R. G.; Kandror, I. I.; Dostovalova, V. I.; Churkina, T. D.; Freidlina, R. Kh. *Org. Magn. Reson.* **1978**, *11*, 406.
291. Phillips, L.; Wray, V. *J. Chem. Soc., Perkin II* **1972**, 214.
292. Marker, A.; Doddrell, D.; Riggs, N. V. *J. Chem. Soc., Chem. Comm.* **1972**, 724.
293. Somayajulu, G. R.; Zwolinski, B. J. *J. Magn. Reson.* **1978**, *30*, 51.
294. Somayajulu, G. R.; Kennedy, J. R.; Vickrey, T. M.; Zwolinski, B. J. *J. Magn. Reson.* **1979**, *33*, 559.
295. Nomura, Y.; Takeuchi, Y.; Nakagawa, N. *Tetrahedron Lett.* **1969**, 639.
296. Morishima, I.; Endo, K.; Yonezawa, T. *J. Chem. Phys.* **1973**, *59*, 3356.
297. Cheremisin, A. A.; Schastnev, P. V. *J. Magn. Reson.* **1980**, *40*, 459.
298. Laitem, L.; Christiaens, L.; Renson, M. *Org. Magn. Reson.* **1980**, *13*, 319.
299. Bégué, J. P.; Bonnet-Delpon, D. *Org. Magn. Reson.* **1980**, *14*, 349.
300. Ahmed, M. G.; Hickmott, P. W.; Soelistyowati, R. D. *J. Chem. Soc., Perkin II* **1978**, 372.
301. Hatada, K.; Nagata, K.; Yuki, H. *Bull. Chem. Soc. Japan* **1970**, *43*, 3195.
302. Maciel, G. E. *J. Phys. Chem.* **1965**, *59*, 1947.
303. Taskinen, E. *J. Org. Chem.* **1978**, *43*, 2773, 2776; *Tetrahedron* **1978**, *34*, 433; *Acta Chem. Scand.* **1980**, *B34*, 203, and references cited therein.
304. Webb, J. G. K.; Yung, D. K. *Can. J. Chem.* **1983**, *61*, 488.
305. Subbotin, O. A.; Sergeev, N. M.; Chlopkov, V. N.; Nikishova, N. G.; Bundel', Yu. G. *Org. Magn. Reson.* **1980**, *13*, 259.
306. Stothers, J. B.; Tan, C. T.; Teo, K. C. *J. Magn. Reson.* **1975**, *20*, 570.
307. Stothers, J. B.; Tan, C. T.; Teo, K. C. *Can. J. Chem.* **1976**, *54*, 1211.
308. Brouwer, H.; Stothers, J. B.; Tan, C. T. *Org. Magn. Reson.* **1977**, *9*, 360.
309. Murakhovskaya, A. S.; Stepanyants, A. U.; Bagrii, E. I.; Dolgopola, T. N.; Frid, T. Yu.; Zimina, K. I.; Sanin, P. I. *Izv. Akad. Nauk SSR, Ser. Khim.* **1975**, 1304.
310. Murakhovskaya, A. S.; Stepanyants, A. U.; Zimina, K. I. *Izv. Akad. Nauk SSR, Ser. Khim.* **1977**, 1072.
311. Maciel, G. E.; Simeral, L.; Elliott, R. L.; Kaufman, B.; Cribley, K. *J. Phys. Chem.* **1972**, *76*, 1466.
312. Simeral, L.; Maciel, G. E. *J. Phys. Chem.* **1973**, *77*, 1590.
313. Nicolas, L.; Beugelmans-Verrier, M.; Guilhem, J. *Tetrahedron* **1981**, *37*, 3847.
314. Konno, C.; Hikino, H. *Tetrahedron* **1976**, *32*, 325.
315. VanAntwerp, C. L.; Eggert, H.; Meakins, G. D.; Miners, J. O.; Djerassi, C. *J. Org. Chem.* **1977**, *42*, 789.
316. Bull, J. R.; Chalmers, A. A. *S. Afr. Chem.* **1977**, *30*, 105.
317. Blunt, J. W.; Stothers, J. B. *Org. Magn. Reson.* **1977**, *9*, 439.
318. Engelhardt, G.; Zeigan, D.; Schönecker, B. *J. Prakt. Chem. [Leipzig]* **1978**, *320*, 377.
319. Schraml, J.; Jancke, H.; Engelhardt, G.; Vodička, L.; Hlavatý, J. *Coll. Czech. Chem. Comm.* **1979**, *44*, 2230.
320. Schneider, H.-J.; Becker, G.; Freitag, W.; Hoppen, V. *J. Chem. Res. (S)* **1979**, *14*; *J. Chem. Res. (M)* **1979**, 0421.
321. Zefirov, N. S.; Gurvich, L. G.; Shashkov, A. S.; Krimer, M. Z.; Vorob'eva, E. A. *Tetrahedron*, **1976**, *32*, 1211. Zefirov, N. S.; Samoshin, V. V.; Subbotin, O. A.; Baranenkova, V. I.; Wolfe, S. *Tetrahedron* **1978**, *34*, 2953. Zefirov, N. S.; Samoshin, V. V.; Subbotin, O. A.; Sergeev, N. M. *Zh. Org. Khim.* **1981**, *17*, 1462.
322. Engelhardt, G.; Zeigan, D.; Schönecker, B. *Org. Magn. Reson.* **1979**, *12*, 628.
323. Kleinpeter, E.; Haufe, G.; Borsdorf, R. *J. Prakt. Chem. [Leipzig]* **1980**, *322*, 125. Kleinpeter, E.; Hodeck, W.; Haufe, G.; Borsdorf, R. *J. Prakt. Chem. [Leipzig]* **1982**, *324*, 687.
324. Barelle, M.; Apparau, M.; Gey, C. *Can. J. Chem.* **1978**, *56*, 85.
325. De Haan, J. W.; van de Ven, L. J. M.; Vlems, H.; Scheffers-Sap, M. M. E.; Gillisen, H.; Buck, H. M. *Tetrahedron* **1980**, *36*, 799.

326. Duddeck, H.; Wiskamp, V. *Org. Magn. Reson.* **1981**, *15*, 361.
327. Heumann, A.; Kolshorn, H. *Tetrahedron* **1975**, *31*, 1571.
328. Brown, F. C.; Morris, D. G. *J. Chem. Soc., Perkin II* **1977**, 125.
329. Brown, F. C.; Morris, D. G.; Murray, A. M. *Tetrahedron* **1978**, *34*, 1845.
330. Jantzen, R.; Tordeux, M.; de Villardi, G.; Chachaty, C. *Org. Magn. Reson.* **1976**, *8*, 183.
331. Eisenstein, O.; Trong Anh, N.; Jean, Y.; Devaquet, A.; Cantacuzène, J.; Salem, L. *Tetrahedron* **1974**, *30*, 1717.
332. Zahra, J. P.; Waegell, B.; Reisse, J.; Pouzard, G.; Fournier, J. *Bull. Soc. Chim. France* **1976**, 1896.
333. Reisse, J.; Piccini-Leopardi, C.; Zahra, J. P.; Waegell, B.; Fournier, J. *Org. Magn. Reson.* **1977**, *9*, 512.
334. Metzger, P.; Casadevall, E.; Casadevall, A.; Pouet, M.-J. *Can. J. Chem.* **1980**, *58*, 1503.
335. Pitkänen, M. T.; Korhonen, I. O. O.; Korvola, J. N. J. *Tetrahedron* **1981**, *37*, 529.
336. Pitkänen, M. *Org. Magn. Reson.* **1982**, *18*, 165.
337. Langford, G. E.; Auksi, H.; Gosbee, J. A.; McLachlan, F. N.; Yates, P. *Tetrahedron* **1981**, *37*, 1091.
338. Morris, D. G.; Murray, A. M. *J. Chem. Soc., Perkin II* **1975**, 539.
339. Senda, Y.; Ishiyama, J.-I.; Imaizumi, S. *Tetrahedron Lett.* **1978**, 1805.
340. Ishiyama, J.-I.; Senda, Y.; Imaizumi, S. *J. Chem. Soc., Perkin II* **1982**, 71.
341. Zefirov, N. S.; Baranenkova, I. V.; Mursakulov, I. G. *Zh. Org. Khim.* **1979**, *15*, 2212.
342. Lessard, J.; Phan Viet, M. T.; Martino, R.; Saunders, J. K. *Can. J. Chem.* **1977**, *55*, 1015.
343. Lessard, J.; Saunders, J. K.; Phan Viet, M. T. *Tetrahedron Lett.* **1982**, *23*, 2059.
344. Holland, H. L.; Thomas, E. M. *Can. J. Chem.* **1979**, *57*, 3069.
345. Al-Rawi, J. M. A.; Behnam, G. Q.; Salman, S. R.; Muhi-Eldeen, Z.; Al-Jawad, F. H. *Org. Magn. Reson.* **1982**, *19*, 91.
346. Duddeck, H.; Islam, M. R. *Chem. Ber.* **1984**, *117*, 554.
347. Duddeck, H.; Islam, M. R. *Chem. Ber.* **1984**, *117*, 565.
348. Duddeck, H.; Wolff, P. *Org. Magn. Reson.* **1977**, *9*, 528.
349. Heumann, A.; Kolshorn, H. *J. Org. Chem.* **1979**, *44*, 1575.
350. Sasaki, T.; Eguchi, S.; Kiriya, T.; Sakito, Y.; Kato, H. *J. Chem. Soc., Chem. Comm.* **1974**, 725.
351. Dekkers, A. W. J. D.; Verhoeven, J. W.; Speckamp, W. N. *Tetrahedron* **1973**, *29*, 1691.
352. Worrell, C.; Verhoeven, J. W.; Speckamp, W. N. *Tetrahedron* **1974**, *30*, 3525.
353. Pasman, P.; Verhoeven, J. W.; de Boer, Th. J. *Tetrahedron* **1976**, *32*, 2877.
354. Pasman, P.; Verhoeven, J. W.; de Boer, Th. J. *Tetrahedron Lett.* **1977**, 207.
355. Sarneel, R.; Worrell, C. W.; Pasman, P.; Verhoeven, J. W.; Mes, G. F. *Tetrahedron* **1980**, *36*, 3241.
356. Morris, D. G.; Murray, A. M. *J. Chem. Soc., Perkin II* **1976**, 1579.
357. Duddeck, H. *Tetrahedron* **1983**, *39*, 1365.
358. Sera, A.; Takagi, K.; Nakamura, M.; Seguchi, K. *Bull. Chem. Soc. Japan* **1981**, *54*, 1271.
359. Sakai, Y.; Toyotani, S.; Ohtani, M.; Matsumoto, M.; Tobe, Y.; Odaira, Y. *Bull. Chem. Soc. Japan* **1981**, *54*, 1474.
360. Gurudata; Stothers, J. B. *Can. J. Chem.* **1969**, *47*, 3601.
361. Stothers, J. B.; Swenson, J. R.; Tan, C. T. *Can. J. Chem.* **1975**, *53*, 581.
362. Bicker, R.; Kessler, H.; Steigel, A.; Zimmermann, G. *Chem. Ber.* **1978**, *111*, 3215.
363. Quarroz, D.; Sonney, J.-M.; Chollet, A.; Florey, A.; Vogel, P. *Org. Magn. Reson.* **1977**, *9*, 611.
364. Hardy, M.; Carrupt, P.-A.; Vogel, P. *Helv. Chim. Acta* **1976**, *59*, 1685.
365. Knothe, L.; Wep, J.; Babsch, H.; Prinzbach, H.; Fritz, H. *Liebigs Ann. Chem.* **1977**, 709.
366. Hoffmann, R. W.; Kurz, H. R.; Becherer, J.; Martin, H.-D. *Chem. Ber.* **1978**, *111*, 1275.
367. Werstiuk, N. H.; Taillefer, R.; Bell, R. A.; Sayer, B. G. *Can. J. Chem.* **1972**, *50*, 2146.

368. Majerski, Z.; Vinković, V.; Meić, Z. *Org. Magn. Reson.* **1981**, *17*, 169.
369. Kasturi, T. R.; Reddy, S. M.; Murthy, P. S. *Org. Magn. Reson.* **1982**, *20*, 42.
370. Senda, Y.; Ishiyama, J.-I.; Imaizumi, S. *J. Chem. Soc., Perkin II* **1981**, 90.
371. Tori, K.; Ueyama, M.; Tsuji, T.; Matsumura, H.; Tanida, H.; Iwamura, H.; Kushida, K.; Nishida, T.; Satoh, S. *Tetrahedron Lett.* **1974**, 327.
372. Zefirov, N. S.; Kasyan, L. I.; Gnedenkov, L. Yu.; Shashkov, A. S.; Cherepanova, E. G. *Tetrahedron Lett.* **1979**, 949.
373. Lippmaa, E.; Pehk, T.; Paasivirta, J. *Org. Magn. Reson.* **1973**, *5*, 277.
374. Pincok, R. E.; Fung, F.-N. *Tetrahedron Lett.* **1980**, 19.
375. Hájek, M.; Triška, J.; Isajev, S. D.; Vodička, L. *Org. Magn. Reson.* **1982**, *20*, 1.
376. Duddeck, H.; Klein, H. *Tetrahedron Lett.* **1976**, 1917.
377. Christl, M. *Chem. Ber.* **1975**, *108*, 2781.
378. Günther, H.; Herrig, W.; Seel, H.; Tobias, S.; de Meijere, A.; Schrader, B. *J. Org. Chem.* **1980**, *45*, 4329.
379. Ginsburg, D. *Acc. Chem. Res.* **1972**, *5*, 249. Wiberg, K. B.; Ellison, G. B. *Tetrahedron* **1974**, *30*, 1573. Ginsburg, D. "Propellanes: Structure and Reactions"; Verlag Chemie: Weinheim, 1975. Gleiter, R.; Ginsburg, D. *Pure Appl. Chem.* **1979**, *51*, 1301.
380. Majerski, Z.; Mlinarić-Majerski, K.; Meić, Z. *Tetrahedron Lett.* **1980**, *21*, 4117. Mlinarić-Majerski, K.; Majerski, Z. *J. Am. Chem. Soc.* **1980**, *102*, 1418.
381. Hamon, D. P. G.; Trenerry, V. C. *J. Am. Chem. Soc.* **1981**, *103*, 4962.
382. Gassman, P. G.; Proehl, G. S. *J. Am. Chem. Soc.* **1980**, *102*, 6862.
383. Vinković, V.; Majerski, Z. *J. Am. Chem. Soc.* **1982**, *104*, 4027.
384. Wiberg, K. B.; Walker, F. H. *J. Am. Chem. Soc.* **1982**, *104*, 5239.
385. Cory, R. M.; Stothers, J. B. *Org. Magn. Reson.* **1978**, *11*, 252.
386. Grover, S. H.; Marr, D. H.; Stothers, J. B.; Tan, C. T. *Can. J. Chem.* **1975**, *53*, 1351.
387. Helferty, P. H.; Yates, P. *Org. Magn. Reson.* **1983**, *21*, 352.
388. Uyegaki, M.; Ito, S.; Sugihara, Y.; Murata, I. *Tetrahedron Lett.* **1976**, 4473.
389. Sugihara, Y.; Morokoshi, N.; Murata, I. *Tetrahedron Lett.* **1977**, 3887.
390. Christl, M.; Lang, R. *J. Am. Chem. Soc.* **1982**, *104*, 4494.
391. Wüthrich, K.; Meiboom, S.; Snyder, L. C. *J. Chem. Phys.* **1970**, *52*, 230.
392. Paquette, L. A.; Charumilind, P. *J. Am. Chem. Soc.* **1982**, *104*, 3749.
393. Gouverneur, P. J. L. *J. Org. Chem.* **1977**, *42*, 3051.
394. Kelecom, A. *Bull. Soc. Chim. Belg.* **1980**, *89*, 343.
395. Frêche, P.; Grenier-Loustalot, M.-F.; Metras, F. *Makromol. Chem.* **1983**, *184*, 569.
396. Eggert, H.; Djerassi, C. *J. Am. Chem. Soc.* **1973**, *95*, 3710.
397. Sarneski, J. E.; Surprenant, H. L.; Molen, F. K.; Reilley, C. N. *Anal. Chem.* **1975**, *47*, 2116.
398. Surprenant, H. L.; Reilley, C. N. *Anal. Chem.* **1977**, *49*, 1134.
399. Ejchart, A. *Org. Magn. Reson.* **1980**, *13*, 368.
400. Ejchart, A. *Org. Magn. Reson.* **1977**, *10*, 263.
401. Ejchart, A. *Org. Magn. Reson.* **1981**, *15*, 22.
402. Ejchart, A. *Pol. J. Chem.* **1981**, *55*, 1169.
403. Morin, F. G.; Horton, W. J.; Grant, D. M.; Dalling, D. K.; Pugmire, R. J. *J. Am. Chem. Soc.* **1983**, *105*, 3992.
404. Beierbeck, H.; Saunders, J. K. *Can. J. Chem.* **1977**, *55*, 771.
405. Beierbeck, H.; Saunders, J. K. *Can. J. Chem.* **1980**, *58*, 1258.
406. Wray, V. *Tetrahedron* **1981**, *37*, 777.
407. Wiberg, K. B.; Pratt, W. E.; Bailey, W. F. *Tetrahedron Lett.* **1978**, 4861.
408. Wiberg, K. B.; Pratt, W. E.; Bailey, W. F. *J. Org. Chem.* **1980**, *45*, 4936.
409. Bailey, W. F.; Cioffi, E.-A.; Wiberg, K. B. *J. Org. Chem.* **1981**, *46*, 4219.
410. Dubois, J.-E.; Doucet, J.-P.; Tiffon, B. *J. Chim. Phys.* **1973**, *70*, 805.
411. Dubois, J.-E.; Carabedian, M. *Org. Magn. Reson.* **1980**, *14*, 264.

412. Panaye, A.; Doucet, J.-P.; Dubois, J.-E. *Tetrahedron Lett.* **1980**, 21, 1235.
413. Doucet, J.-P.; Panaye, A.; Dubois, J.-E. *Tetrahedron Lett.* **1981**, 22, 3517.
414. Dubois, J.-E.; Doucet, J.-P.; Panaye, A. *Tetrahedron Lett.* **1981**, 22, 3521.
415. Doucet, J.-P.; Yuan, S. G.; Billon, P.; Dubois, J.-E. *Tetrahedron Lett.* **1982**, 23, 4241.
416. Dubois, J.-E.; Laurent, D.; Aranda, A. *J. Chim. Phys.* **1973**, 70, 1608, 1616.
417. Schwarz, R. M.; Rabjohn, N. *Org. Magn. Reson.* **1980**, 13, 9.
418. Marr, D. H. *Org. Magn. Reson.* **1980**, 13, 28.
419. Senda, Y.; Ishiyama, J.-I.; Imaizumi, S. *Bull. Chem. Soc. Japan* **1976**, 49, 1359.
420. Koskinen, A.; Lounasmaa, M. *Heterocycles* **1983**, 20, 563.
421. James, D. E.; Stille, J. K. *J. Org. Chem.* **1976**, 41, 1504.
422. Williamson, K. L.; Hasan, M. U.; Clutter, D. R. *J. Magn. Reson.* **1978**, 30, 367.
423. Hearmon, R. A. *Org. Magn. Reson.* **1982**, 19, 54.
424. Batchelor, J. B. *J. Chem. Soc., Perkin II* **1976**, 1585.
425. Rabenstein, D. L.; Sayer, T. L. *J. Magn. Reson.* **1976**, 24, 27.
426. Batchelor, J. G. *J. Magn. Reson.* **1977**, 28, 123.
427. Llinarés, J.; Elguero, J.; Faure, R.; Vincent, E.-J. *Org. Magn. Reson.* **1980**, 14, 20.
428. Pancrazi, A.; Kaboré, I.; Delpech, B.; Astier, A.; Khuong-Huu, Q.; Lukacs, G. *Can. J. Chem.* **1977**, 55, 2829.
429. Quin, L. D.; Breen, J. J. *Org. Magn. Reson.* **1973**, 5, 17.
430. Littlefield, L. B.; Quin, L. D. *Org. Magn. Reson.* **1979**, 12, 199.
431. Quin, L. D. "The Heterocyclic Chemistry of Phosphorus"; Wiley: New York, 1981.
432. Buchanan, G. W.; Morin, F. G. *Can. J. Chem.* **1977**, 55, 2885.
433. Freeman, F.; Angeletakis, Ch. N. *J. Am. Chem. Soc.* **1983**, 105, 4039.
434. Tseng, C. K.; Bowler, D. J. *Org. Magn. Reson.* **1981**, 17, 131.
435. Tordeux, M.; Leroy, J.; Wakselman, C. *Org. Magn. Reson.* **1980**, 14, 407.
436. Hawkes, G. E.; Smith, R. A.; Roberts, J. D. *J. Org. Chem.* **1974**, 39, 1276.
437. Dostovalova, V. I.; Velichko, F. K.; Vasil'eva, T. T.; Kruglova, N. V.; Freidlina, R. Kh. *Org. Magn. Reson.* **1981**, 16, 251.
438. Velichko, F. K.; Dostovalova, V. I.; Vinogradova, L. V.; Freidlina, R. Kh. *Org. Magn. Reson.* **1980**, 13, 442.
439. Fraser, R. R.; Baignée, A.; Bresse, M.; Hata, K. *Tetrahedron Lett.* **1982**, 23, 4195.
440. Hansen, P. E.; Led, J. J. *Org. Magn. Reson.* **1981**, 15, 288.
441. Jurlina, J. L.; Stothers, J. B. *J. Am. Chem. Soc.* **1982**, 104, 4677.
442. Aydin, R.; Günther, H. *J. Am. Chem. Soc.* **1981**, 103, 1301.
443. Ernst, L.; Eltamany, S.; Hopf, H. *J. Am. Chem. Soc.* **1982**, 104, 299.
444. Touillaux, R.; Van Meerssche, M.; Dereppe, J. M.; Leroy, G.; Weiler, J.; Wilante, C. *Org. Magn. Reson.* **1981**, 16, 71.
445. Rol, N. C.; Clague, A. D. H. *Org. Magn. Reson.* **1981**, 16, 187.
446. Matoba, Y.; Kagayama, T.; Ishii, Y.; Ogawa, M. *Org. Magn. Reson.* **1981**, 17, 144.
447. Jennings, W. B.; Wilson, V. E.; Boyd, D. R.; Coulter, P. B. *Org. Magn. Reson.* **1983**, 21, 279.
448. Hittich, R. *Org. Magn. Reson.* **1982**, 18, 214.
449. Dittmer, D. C.; Patwardhan, B. H.; Bartholomew, J. T. *Org. Magn. Reson.* **1982**, 18, 82.
450. Bose, A. K.; Srinivasan, P. R. *Org. Magn. Reson.* **1979**, 12, 34.
451. Eliel, E. L.; Rao, V. S.; Pietrusiewicz, K. M. *Org. Magn. Reson.* **1979**, 12, 461.
452. Accary, A.; Huet, J.; Infarnet, Y.; Duplan, J. C. *Org. Magn. Reson.* **1978**, 11, 287.
453. Dana, G.; Danechpajouh, H. *Bull. Soc. Chim. France* **1980**, II-395.
454. Pihlaja, K.; Rossi, K. *Acta Chem. Scand.* **1977**, B31, 899.
455. Barbarella, G.; Dembech, P. *Org. Magn. Reson.* **1981**, 15, 72.
456. Pihlaja, K.; Eskonmaa, M.; Keskinen, R.; Nikkilä, A.; Nurmi, T. *Org. Magn. Reson.* **1981**, 17, 246.
457. Pihlaja, K.; Keskinen, R.; Eskonmaa, M.; Nurmi, T. *Org. Magn. Reson.* **1983**, 21, 151.

458. Stothers, J. B.; Tan, C. T. *Can. J. Chem.* **1974**, *52*, 308.
459. Yamada, F.; Nishiyama, T.; Samukawa, H. *Bull. Chem. Soc. Japan* **1975**, *48*, 1878. Nishiyama, T.; Mizuno, T.; Yamada, F. *Bull. Chem. Soc. Japan* **1978**, *51*, 323.
460. Loomes, D. J.; Robinson, M. J. T. *Tetrahedron* **1977**, *33*, 1149.
461. Jancke, H.; Werner, H. *J. Prakt. Chem. [Leipzig]*, **1980**, 322, 247.
462. Pehk, T.; Kooskova, H.; Lippmaa, E. *Org. Magn. Reson.* **1976**, *8*, 5.
463. Booth, H.; Everett, J. R.; Fleming, R. A. *Org. Magn. Reson.* **1979**, *12*, 63.
464. Haines, A. H.; Shandiz, M. S. *J. Chem. Soc., Perkin II* **1981**, 1671.
465. Hansen, P. E.; Batchelor, J. G.; Feeney, J. J. *J. Chem. Soc., Perkin II* **1977**, 50.
466. Senda, Y.; Imaizumi, S. *Tetrahedron* **1975**, *31*, 2905.
467. Däuzonne, D.; Goasdoue, N.; Platzer, N. *Org. Magn. Reson.* **1981**, *17*, 18.
468. Dorman, D. E.; Angyal, S. J.; Roberts, J. D. *J. Am. Chem. Soc.* **1970**, *92*, 1351.
469. Eliel, E. L.; Manoharan, M.; Pietrusiewicz, K. M.; Hargrave, K. D. *Org. Magn. Reson.* **1983**, *21*, 94.
470. Eliel, E. L.; Hargrave, K. D.; Pietrusiewicz, K. M.; Manoharan, M. *J. Am. Chem. Soc.* **1982**, *104*, 3635.
471. Booth, H.; Grindley, T. B.; Khedhair, K. A. *J. Chem. Soc., Chem. Comm.* **1982**, 1047.
472. Nilsson, B.; Hermestam, S. *Org. Magn. Reson.* **1978**, *11*, 116.
473. Rao, V. S. *Can. J. Chem.* **1982**, *60*, 1067.
474. Krapivin, A. M.; Perepelitchenko, L. I. *Izv. Akad. Nauk SSR, Ser. Khim.* **1982**, 452.
475. Lemieux, R. U.; Morgan, A. R. *Can. J. Chem.* **1965**, *43*, 2205.
476. Lehn, J.-M.; Wipff, G. *J. Am. Chem. Soc.* **1976**, *98*, 7498.
477. Carey, F. A.; Dailey, O. D., Jr.; Hutton, W. C. *J. Org. Chem.* **1978**, *43*, 96, and references cited therein.
478. Khan, S. A.; Lambert, J. B.; Hernandez, O.; Carey, F. A. *J. Am. Chem. Soc.* **1975**, *97*, 1468.
479. Hellier, D. G.; Phillips, A. M. *Org. Magn. Reson.* **1982**, *18*, 178.
480. Smith, M. B.; Wolinsky, J. *Org. Magn. Reson.* **1982**, *19*, 129.
481. Rooney, R. P.; Dyer, J. C.; Evans, S. A., Jr.; *Org. Magn. Reson.* **1981**, *16*, 266.
482. Aksnes, D. W.; Strømme, O. *Acta Chem. Scand.* **1979**, *A33*, 753.
483. Kutschan, R.; Ernst, L.; Wolf, H. *Tetrahedron* **1977**, *33*, 1833.
484. Deslongchamps, P.; Rowan, D. D.; Pothier, N.; Sauvé, T.; Saunders, J. K. *Can. J. Chem.* **1981**, *59*, 1105.
485. Deslongchamps, P.; Rowan, D. D.; Pothier, N.; Saunders, J. K. *Can. J. Chem.* **1981**, *59*, 1122.
486. Pothier, N.; Rowan, D. D.; Deslongchamps, P.; Saunders, J. K. *Can. J. Chem.* **1981**, *59*, 1132.
487. Whitesell, J. K.; Matthews, R. S. *J. Org. Chem.* **1977**, *42*, 3878.
488. Calderoni, C.; Ceré, V.; Pollicino, S.; Sandri, E.; Fava, A.; Guerra, M. *Org. Magn. Reson.* **1980**, *45*, 2641.
489. Schneider, H.-J.; Nguyen-Ba, N. *Org. Magn. Reson.* **1982**, *18*, 38.
490. Metzger, P.; Cabestaing, C.; Casadevall, E.; Casadevall, A. *Org. Magn. Reson.* **1982**, *19*, 144.
491. Metzger, P.; Casadevall, E.; Pouet, M. *J. Org. Magn. Reson.* **1982**, *19*, 229.
492. Barbry, D.; Ricart, G.; Couturier, D. *Org. Magn. Reson.* **1981**, *17*, 103.
493. Browne, L. M.; Klinck, R. E.; Stothers, J. B. *Org. Magn. Reson.* **1979**, *12*, 561.
494. Laffite, C.; Wylde, R.; Mavel, G. *Org. Magn. Reson.* **1979**, *12*, 77.
495. Fringuelli, F.; Hagaman, E. W.; Moreno, L. N.; Taticchi, A.; Wenkert, E. *J. Org. Chem.* **1977**, *42*, 3168.
496. Tsuda, M.; Schroepfer, G. J., Jr. *Chem. Phys. Lipids* **1979**, *25*, 49.
497. Katritzky, A. R.; Baker, V. J.; Ferguson, I. J.; Patel, R. C. *J. Chem. Soc., Perkin II* **1979**, 143.

498. Riguera, R. *Tetrahedron* **1978**, *34*, 2039.
499. Weigand, E. F.; Schneider, H.-J. *Org. Magn. Reson.* **1979**, *12*, 637.
500. Van Oosterhout, H.; Kruk, C.; Speckamp, W. N. *Tetrahedron Lett.* **1978**, 653.
501. Reints Bok, Th.; Kruk, C.; Speckamp, W. N. *Tetrahedron Lett.* **1978**, 657.
502. Jeyaraman, R.; Jawaharsingh, C. B.; Avila, S.; Eliel, E. L.; Manoharan, M.; Morris-Natschke, S. *J. Heterocyclic Chem.* **1982**, *19*, 449.
503. Eliel, E. L.; Manoharan, M.; Hodgson, D. J.; Eggleston, D. S.; Jeyaraman, R. *J. Org. Chem.* **1982**, *47*, 4353.
504. Wiseman, J. R.; Krabbenhoft, H. O.; Lee, R. E. *J. Org. Chem.* **1977**, *42*, 629.
505. Rudi, A.; Kashman, Y. *Org. Magn. Reson.* **1977**, *10*, 245.
506. Freeman, R.; Morris, G. A. *Bull. Magn. Reson.* **1979**, *1*, 5.
507. Bax, A. "Two-Dimensional Nuclear Magnetic Resonance in Liquids"; Reidel: Dordrecht, 1982.
508. Benn, R.; Günther, H. *Angew. Chem.* **1983**, *95*, 381; *Angew. Chem. Int. Ed. Engl.* **1983**, *22*, 390.
509. Bax, A.; Freeman, R.; Kempell, S. P. *J. Magn. Reson.* **1980**, *41*, 349; *J. Am. Chem. Soc.* **1980**, *102*, 4849.
510. Bremser, W. *Fresenius Z. Anal. Chem.* **1977**, *286*, 1; *Anal. Chim. Acta* **1978**, *103*, 355.
511. Schwarzenbach, R.; Meili, J.; Kónitzer, H.; Clerc, J. T. *Org. Magn. Reson.* **1976**, *8*, 11. Clerc, J. T.; Sommerauer, H. *Anal. Chim. Acta* **1977**, *95*, 33.
512. Schwenzer, G. M.; Mitchell, T. M. In "Computer-Assisted Structure Elucidation," ACS Symposium Series, Vol. 54; American Chemical Society: Washington, D.C., 1977, pp. 58-76; *Chem. Abstr.* **1977**, *87*: 166996a. Mitchell, T. M.; Schwenzer, G. M. *Org. Magn. Reson.* **1978**, *11*, 378.
513. Smith, D. H.; Jurs, P. C. *J. Am. Chem. Soc.* **1978**, *100*, 3316.
514. Dalrymple, D. L.; Wilkins, C. L.; Milne, G. W. A.; Heller, S. R. *Org. Magn. Reson.* **1978**, *11*, 535. Milne, G. W. A.; Zupan, J.; Heller, S. R.; Miller, J. A. *Org. Magn. Reson.* **1979**, *12*, 289. Zupan, J.; Heller, S. R.; Milne, G. W. A.; Miller, J. A. *Anal. Chim. Acta* **1978**, *103*, 141.
515. Woodruff, H. B.; Snelling, C. R., Jr.; Shelley, C. A.; Munk, M. E. *Anal. Chem.* **1977**, *49*, 2075. Shelley, C. A.; Munk, M. E. *Anal. Chem.* **1982**, *54*, 516.
516. Mlynárik, V.; Vida, M.; Kellö, V. *Anal. Chim. Acta* **1980**, *122*, 47.
517. Gray, N. A. B.; Crandell, C. W.; Nourse, J. G.; Smith, D. M.; Dageforde, M. L.; Djerassi, C. *J. Org. Chem.* **1981**, *46*, 703. Gray, N. A. B.; Nourse, J. G.; Crandell, C. W.; Smith, D. H.; Djerassi, C. *Org. Magn. Reson.* **1981**, *15*, 375. Lindley, M. R.; Gray, N. A. B.; Smith, D. H.; Djerassi, C. *J. Org. Chem.* **1982**, *47*, 1027.
518. Sasaki, S.; Fujiwara, I.; Abe, H.; Yamasaki, T. *Anal. Chim. Acta* **1980**, *122*, 87. Fujiwara, I.; Okuyama, T.; Yamasaki, T.; Abe, H.; Sasaki, S. *Anal. Chim. Acta* **1981**, *133*, 527. Sasaki, S.; Abe, H.; Fujiwara, I. *Stud. Phys. Theor. Chem.* **1981**, 186; *Chem. Abstr.* **1982**, *97*: 5707y. Sasaki, S.; Abe, H.; Fujiwara, I.; Yamasaki, T.; Hippe, Z.; Debska, B.; Duliban, J.; Guzowska-Swider, B. *Chem. Anal. (Warsaw)* **1982**, *27*, 171; *Chem. Abstr.* **1983**, *99*: 104412w.
519. Sjöström, M.; Edlund, U. *J. Magn. Reson.* **1977**, *25*, 285. Edlund, U.; Wold, S. *J. Magn. Reson.* **1980**, *37*, 183. Albano, C.; Blomquist, G.; Dunn, W., III; Edlund, U.; Eliasson, B.; Johansson, E.; Nordén, B.; Sjöström, M.; Söderström, B.; Wold, S. *Int. Congr. Pure Appl. Chem., [Proc.]* **1980**, *27th*, 377; *Chem. Abstr.* **1980**, *93*: 145791p.
520. Martin, H.-D.; Mayer, B. *Angew. Chem.* **1983**, *95*, 281; *Angew. Chem. Int. Ed. Engl.* **1983**, *22*, 283.

SUBJECT INDEX

- ab initio* calculations, 224, 273
- Absolute configuration, 3–6, 9–11, 24, 28, 30, 33, 35, 38, 39, 41, 44, 46, 48, 49, 54, 56, 60, 61, 63, 66, 70, 73, 74, 77–80, 100, 200
 - assignment, using centrosymmetric crystals, 38
 - from chemical reactivity in polar and enantiopolar crystals, 61
 - of chiral crystal, 79
 - direct assignment of, 35, 41
 - by electron microscopy, 74
 - by lattice imaging, 77
 - relative assignment of, 24
- Absolute polarity, 10, 63
- 4-Acetoxypyridine, 153
- Acetyl benzoyl peroxide, photolysis of, 205
- Achiral crystals, noncentrosymmetric, 42, 55
- Acridine, 9-*p*-hydroxyphenyl, 160
- Active site, 95
- Adamantane derivatives, 224, 232, 236, 242, 246, 247, 254, 255, 258, 262, 277, 282, 283, 287
- Additive molecules, selective adsorption of, 33
- Additive, tailor made, 4, 25, 28, 58
- Adsorption, selective, 42
- Alanine, 56–58
- Alkaloid conformation, 93
- Alkaloids, 299
- Alkane derivatives, 224, 238
- Alkyl vinyl ethers, 276
- Alkynes, 227
- Allyl alcohols, 281
- Allyl ethers, 281
- α effects, 233
- Alpha-helix, 74
- Amides, unsaturated, photodimerization of, 171
- Amine addition, to carbonyl, 156
- Amino acids, 301, 304
- Aminobenzoquinones, 151
- 2-Amino-3-hydroxy-6-phenylazopyridine, 164
- Aminoketones, ring closure of, 151
- Amino substituents, 301
- Ammonia/*p*-bromobenzoic anhydride, 62, 73
- Ammonium salts, chiral, 114
- Androstanols, 234, 242
- Anisotropic distribution, of occluded additive, 31, 33
- Anisotropy effect:
 - magnetic, 244
 - neighbor, 225, 227
- Anomalous dispersion, 63
- Anomalous X-ray scattering, 9, 10, 79
- Anomeric effect, 274
 - reversed, 305
- Anthracene derivatives, 174, 175
- Anthranilic acid, 161
- 1-Arylethanol anthroates, 208
- Asparagine, 22, 23, 26, 27, 61
 - aspartic acid system, 61
 - monohydrate, 19, 22, 23, 25, 26, 60
- Aspartic acid, 25
- Asymmetric habit, macroscopic, 66
- Asymmetric induction, 179, 201
- Asymmetric synthesis, 95, 179, 198
 - in chiral crystals, 207
 - in racemic crystals, 207
- Attachment energy, 67, 68
- A values, 303
- Azaadamantanone, 285
- Azabicyclo[3.3.1]nonane derivatives, 308
- Azabicyclo[4.2.1]nonane derivatives, 308
- 3-Azacyclohexanone derivatives, 281
- Azido substituents, 301
- Aziridines, 228, 271, 277, 302
- Azoalkanes, solid-state chemistry of, 203
- Azobisisobutyronitrile, 203
- Azobis-3-phenyl-3-pentane, 204
- Azonaphthols, 162
- Azophenols, 162
- Back-donation, 292
- Benzaldehyde, 92, 122
- Benzamide, 12, 15, 17, 22, 59, 68

- Benzamide (*Continued*)
 crystal of, 17
Benzo[ghi]fluoranthene, 227
Benzohomoadamantenes, 284
Benzoic acid, substituted, 161
Benzophenone imines, 148
Benzoquinone derivatives, 251
Benzoquinone oxime–nitrosophenol system,
 140, 158
Benzoyl group migration, 153
6-Benzoyloxyphenanthridine, 153
6-Benzoyl-6(5H)-phenanthridone, 153
Benzvalene, 292
2-Benzyl-5-*p*-bromobenzylidenecyclopentanone,
 186
Benzylideneanilines, 145
Benzylidenebutyrolactone, photodimers of,
 169
Benzylquininium chloride, 98, 114, 116–118,
 120, 121
 β effects, 241
Bicyclo[4.n.0]alkane derivatives, 307
Bicyclo[1.1.0]butane, 292
Bicyclo[2.2.1]heptane derivatives, 257, 277
Bicyclo[2.2.1]heptene derivatives, 257
Bicyclo[2.2.1]hept-5-enes, *cis*-2,3-
 disubstituted, 278
Bicyclo[3.1.0]hexane, 306
Bicyclo[3.1.0]hexan-2-one, 291
Bicyclo[4.3.0]nonane, 307
Bicyclo[3.3.1]nonane derivatives, 308
Bicyclo[2.2.2]octane, 290
Bicyclo[2.2.2]octane derivatives, 224, 237,
 247, 263, 277, 308
Bicyclo[3.3.0]octane derivatives, 306
Bicyclo[3.2.0]-6-one derivatives, 152
Bifunctional catalysis, 94
Bijvoet method, 3, 7–10, 73, 80
Biphenyls, 142
Biradical intermediates, 180, 181
Bisfluoronylidenes, 149
Bis(N-methylphenethylammonium)
 tetrachlorocuprate, 158
Boat-chair conformation, 308
Boat conformation, 306
Bond angle, 231, 232, 243, 250, 260, 264,
 269, 271
Bond length, 231, 269
Bond order, 223
 π , 276
Bond polarization, 245, 249, 255
Bornadione derivatives, 279
Bornane derivatives, 232, 243
Branching effect, 236
4^c-Bromoadamantanone, 270
p-Bromobenzoic anhydride, 62, 63, 73
2-Bromo-1,1-di-*p*-tolylethylene, 144
Bromo substituents, 302
Brucine, 124
cis-Butene derivatives, 263
t-Butoxycarbonylphenylalanine, 141
sec-Butyl group, conformation of, 146
t-Butylhydroperoxide, 119, 120
t-Butyl substituent, 251, 303
3-(*p*-*t*-Butylphenylthio)cyclohexanone, 105
3-(*p*-*t*-Butylphenylthio)-5-
 methylcyclohexanone, 104
sec-Butylphthalamide, 147
p-*t*-Butylthiophenol, 108
Cadmium complexes, five coordinated, 155
Cage effect, 203, 205
Camphene derivatives, 281
Camphenilone derivatives, 279
Captopril®, 107
2-Carbethoxycyclohexanone, 98
Carbon atoms, inverted, 290
Carbon–fluorine coupling constants, 238
Carbonic anhydrase, 90
Carbon–metal σ bond, 240
Carboxylic acids, 301
 derivatives, 275
Carboxyl substituent, 300
Carboxylic esters:
 α -chlorinated, 280
 bifunctional, 94
Catalysts:
 non-enzymic, 90
 polymeric, chiral, 97
Centrosymmetric crystal, 38, 41, 42, 44, 61,
 63, 73, 81
 racemic, 41
Centrosymmetric structure, 5, 39, 59
Chain reactions, in crystal, 154
Chair-boat conformation, 308
Chalcones, 98, 114, 119, 120
 epoxidation of, 116, 119
Charge density, 229
 local, 223
 π , 276
 σ -electron, 224
Charge polarization, 223

- Charge transfer, 95, 172
Charge transfer complex, 157, 164, 194
Chemical shift, substituent induced, *see*
 Substituent-induced chemical shift
 (SCS)
Chiral crystals, 38, 135, 144, 179, 207
Chiral discrimination:
 in crystals, 146
 of *sec*-butyl group, 146
 in tri-*o*-thymotide, 147, 148
Chloral, 92, 122
Chlorine atoms, interaction between, 145
Chlorine substituents, 301, 302
p-Chlorocinnamide, 13
Choleic acids, 199
5 α -Cholestane, 293
Cholestane derivatives, 229, 247
Cholestanols, 234
Cholest-5-ene derivatives, 302
Chromoisomerism, 157
Cinchona alkaloids, 88, 91, 125
Cinchonidine, 91, 92, 101, 105, 106, 108,
 110, 111, 119
Cinchonine, 91, 107
Cinnamic acid, 14, 15, 65
 photodimerization of, 167, 186
Cinnamide, 12-16, 22, 25, 59, 65, 68
 packing arrangement of, 14
Cinnamide/cinnamic acid, 65
Cinnamoylalanine, 29, 30
Circular dichroism (CD), 104
Citramalic acid, 89
Claisen rearrangement, of cinnamyl phenyl
 ether, 197
Clathrates, 193
 acetic acid in, 196
 of deoxycholic acid, 198
 Dianin-type, 195
 gas-solid reactions of, 198
 host-guest reactions in, 199
 inhibition of thermal reaction in, 197
 kinetic stabilization in, 196
 photochemical reactions in, 197
 photocyclization of ketones in, 197
 stabilization of conformations in, 196
13-C *nmr* reference data system, 309
Complex:
 between carboxylic acids and amides, 194
 charge transfer, 157, 164, 194
 crystalline, with crown-type host
 compounds, 194
 solid-state, 193
Complexes and salts, from acids and bases,
 193
Compression, steric, 271
Configuration, 9
 absolute, *see* Absolute configuration
Conformation, 232
 of *sec*-butyl group, 146
 of α -diketones, 137
 endo, 36, 37
 of ethanes and related molecules, 137
 of α -haloacetyl derivatives, 137
 of paraffin chains, 138
 of symmetry-independent molecules, 136,
 138, 139, 141
 of vitamin D, 139
Conformational analysis, 302
Conformational disorder, 144
Conformational equilibrium, 268, 269, 277
Conformational flip, 140, 181
Conglomerate, 18, 19, 24
Conjugation, p - π , 276
Conjugative interaction, 225, 282
Connectivity, 309
Constitution, of symmetry-independent
 molecules, 152
Contact shift, 275
Cope rearrangement, 177
Copolymer single crystals, 193
Cortisol derivatives, 247
Coulomb interactions, 16
Coulomb potential, 68
Coumarins, 175
Coupling constant, three-bond, 257, 260
Crotonic acid, 3-alkylamine esters of, 149
Crown ether, chiral, 99
Crystal(s):
 absolute polarity of, 67
 centrosymmetric, *see* Centrosymmetric
 crystal
 defects, 161, 167, 173, 190
 disorder in, 146, 150, 151
 dissolution, in presence of additives, 24
 enantiomorphous, 38, 42
 engineering, 134, 145, 171, 179, 193
 by charge transfer complex, 172
 by complexation, 172
 by halogen . . . halogen interactions,
 171
 by primary amide interactions, 171
 faces, hemihedral, 11

Crystal(s) (*Continued*)

- growth, 67, 209
- inhibitors, 79
- habit, 67
 - change in, 60
- interactions, influence on molecular geometry, 136
- morphology, 4, 12, 15, 16, 46, 67, 209
- optical activity in, 72
- polar, 60, 61, 68
- reactivity, 62
- structure:
 - centrosymmetric, *see* Centrosymmetric crystal
 - constraint, on reaction pathway, 184
 - effect on biradical intermediate, 181
 - of triglycine sulfate, 73
 - symmetry, 134
- Cyanohydrin synthesis, 95
- Cyano substituent, 300
- Cyclo(L-Phe-L-His), 95
- Cyclobutane, ring opening of, 152
- Cyclobutane derivatives, 271, 302
- Cyclobutene, ring opening of, 176
- Cyclodextrin complexes, 198
- Cyclodextrins, 195
 - halogen addition to guests in, 198
- Cyclohexane, 234
- Cyclohexane derivatives, 138, 229, 232, 234, 236, 238, 242, 257, 261, 263, 271, 300, 303
- Cyclohexane-1,4-diones, 181
- Cyclohexanes, 1,2-disubstituted, 278
- Cyclohexanols, 224, 242, 299
- Cyclohexanone, 3-thiosubstituted, 100
- Cyclohexanones, β -substituted, 284
- 2-Cyclohexen-1-ol, 116
- Cyclohexenone, 99, 114
 - epoxidation of, 119, 120
- Cyclohexenone epoxide, 119
- Cyclohexylamine derivatives, 301
- Cyclohexylmercuric acetate, 240
- Cyclopentane derivatives, 271, 303
- Cyclopentanone derivatives, 303
- Cyclopropane, 228, 253, 264, 302, 306
 - derivatives, 271, 277, 289
- Dark field image, 76
- Decahydroquinoline derivatives, 267
- Decalin derivatives, 234, 307
- Decalols, 246
- Decalone derivatives, 280
- Dehydroadamantane, 290
- 3-Dehydrogibberelin, 170
- δ -effects, 261
- Deoxycholic acid:
 - acetophenone complex with, 201
 - as crystalline host, 196, 199
 - oxidation of guests in, 198
 - photoaddition of guest ketone to, 200
- Deuterium isotope shift, 262, 263, 301, 302
- o*-Diacetylene-bis(phenylglutarate), 189
- Diacetylenes:
 - copolymerization of, 192
 - cyclic, 191
 - solid-state polymerization of, 187, 206
- Diacyl peroxides, solid state chemistry of, 203
- Dialkyl-naphthalene derivatives, 263
- Diamagnetic shielding contribution, 234, 251
- Diamagnetic susceptibility, 300
- Diamagnetic term, 223, 224
 - of nuclear shielding, 222
- Diamondoid compounds, 234, 243, 260
- 2,4-Diaryl-3-azabicyclo[3.3.1]nonane derivatives, 308
- 2,4-Diaryl-3-azabicyclo[3.3.1]-7-thianonane derivatives, 308
- 1,3-Diazacyclohexane derivatives, 308
- Dibenzoylmethane, 140, 158
- 3,3'-Di-*t*-butyl-5,5'-diphenyl-4,4'-diphenylquinone, 149
- Di-*t*-butyl phosphite, 122
- Di-*t*-butyl diperoxycarbonate, 199
- cis*-1,2-Dicarboxylic acids, 176
- Dichloroaromatics, 145
- 1,6-Di(*o*-chlorophenyl)-1,6-diphenylhexa-2,4-diyne-1,6-diol, 119
- Dichlorostyrenes, photodimerization of, 171
- Dicyclopentadiene derivatives, 247, 302
- 1,4-Diene-3-ones, 1,5-disubstituted, photodimerization of, 133
- Diethylzinc, 124
- Dihydropyran derivatives, 281
- 1,2-Dihydroxyadamantane, 278
- Dimethyl dibromoadipate, 132
- Dimethyl 3,6-dichloro-2,5-dihydroxyterephthalate, 140
- Dimethyl ether, 235
- Dimethyl *cis,trans*-muconate, 176
- Dimethyl phosphite, 92
- 8-Dimethylamino-1-naphthoic acid, 156
- 1,1-Dimethylcyclohexane, 271

- 1,2-Dimethylcyclohexanes, 276, 277
4,4-Dimethyl-2-cyclohexenol, 110
5,5-Dimethylcyclohexenone, 92, 109
4,4-Dimethyl-3-(*p*-methylphenylseleno)-
cyclohexanone, 110, 111
1,3-Dioxane derivatives, 271, 304
1,7-Dioxo[5.5]undecane, 306
1,4-Dioxanes, 139
1,3,2-Dioxarsenane derivatives, 305
1,3,2-Dioxathiane 2-oxide derivatives, 305
1,3-Dioxolane derivatives, 303
Dipeptides cyclic, 95
3,7-Diphenyl-1,2-diaza-1-cyclopentene, 202
1,3-Diphenyl-2-indanone, 202
1,5-Diphenyl-1,4-pentadien-3-one, 133
Dipole-dipole interaction, 281, 288, 307
 through-space, 285
Disorder, in crystals, 146, 150, 151, 173
Disordered structures, 144
Dispersion, anomalous, 9
Dispersion effect, intramolecular, 229, 275
Dissolution, of crystals, 4, 25
Distortion, molecular, 265
Distyrylpyrazine:
 derivatives, 177
 polymerization of, 177
Disulfides, 301
1,3-Dithiane 2-carbanion, 305
1,3-Dithiane derivatives, 271, 305
1,3-Dithiane 1-oxide, 305
Dithianes, 245
1,3-Dithianes, 2-substituted, 261
1,7-Dithiaspiro[5.5]undecane, 306
Dithioacetals, 275
1,3-Dithiolane derivatives, 303
cis-1,2-Divinylcyclobutanes, 176
Divinyl ethers, 276
DNA, 75, 77
Dodecane derivatives, 295
Dodecanethiol, 99
Double-boat conformation, 308
Double bond character, 273
Double bonds:
 crystal effects on, 148
 endocyclic, 308
 partial, 276
Electric field effect, 225, 227–229, 243, 249,
 254, 278, 282
 linear, 228, 243
 square, 229
Electron binding energy, 274
Electron charge polarization, 243
Electron delocalization, 264
Electron diffraction, 78
Electronic interaction, 271, 277, 282
 intramolecular, 310
Electron imaging, 74
Electron microscopy, 74–78
Electronegativity, 226, 233, 236, 239, 241,
 244, 250, 254, 259, 262, 265
 effective, 275
Enantiomeric additive, 42
Enantiomeric segregation, 44
Enantiomers, resolution of, by crystallization,
 209
Enantiomorphic crystals, 2, 3, 38, 42, 61
Enantiomorphism, 2
Enantiomorphous, *see* Enantiomorphic crystals
Enantiopolar axis, 44, 46
Enantiopolar crystal, 42, 61
Enantiopolar set, 48, 54, 55
Enantioselective segregation, 45
 total, 49
Enantiotopic faces, 41, 42, 44, 45, 49
Endocyclic substituent, 244
Entropy term, 234
Enzymes, 88, 90
 artificial, 88
 stereospecificity of, 90
Ephedrine, 119
Epimers, in solids, 150
Epiquinine, 109
Epoxidation, 89
 asymmetric, 114
Epoxy alcohols, 152
Epoxychalcone, 114, 115
Epoxycyclohexanone, 116
Etchants, surface, 79
Etch figure, 58
Etch pits, 4, 25, 45, 49
Ethane derivatives, 226, 234, 271
Ethanes, 1,2-disubstituted, 277
Excitation energy, 223, 266, 276,
 290
 diffusion of, 167
 effective, 223
Excited states, 223
Faces, hemihedral:
 polar, 66, 68
 see also Hemihedral faces

- Factor analysis, 299
Fenestrane, 265
Ferroelectric crystals, 72, 73
Ferroelectricity, 159
Ferroelectric medium, 72
Field effects, electric, *see* Electric field effect
Fluorescence, 160, 208
Fluoride, 98
Fluorine coupling constant, 260
Fluorine substituent effects, 224
Fluorocyclobutane, 260
Force field calculation, 234, 242, 249, 264
Formylcyclohexane, 252
Free energy difference, conformational, 303
Friedel's law, 5, 7, 8
Frontier orbital, 262
Fumarate hydratase, 89
Furopyridone, 158
- γ antiperiplanar substituent effect, 231, 254
 γ gauche substituent effect, 231, 245, 278
Gas-solid reactions:
 of clathrates, 198
 in polar crystals, 62
Geminal substituent, 270
Geometric distortion, 268
Geometric isomerization, 136
D-Glucose, 224
Glutamic acid, 51
Glutamic acid hydrochloride, 18–20
 crystal structure of, 18
 morphology of, 18
Glycine, 42, 48–51, 54, 58, 59, 67, 73
 crystal of, 48
 α -form of, 49
Glycylglycine, 42, 51–54
Glycylleucine, 52
Grant–Cheney approach, 245, 263
Grant–Paul rule, 293
- Habit:
 asymmetric, macroscopic, 66
 crystal, 68
 of crystals of cinnamide, 14
 modification, 16
Haemanthidine, 150
Half-chair conformation, 303
Halobicyclo[2.2.1]heptane derivatives, 250
Halocyclohexanes, 279
 α -Halocyclohexanones, 279
- Halogen substituents, 302
Hammett-type reactivity constants, 230, 234
Heavy atom effect, 270, 273
Heavy-chalcogen effect, 275
Heilbron complexes, 138
Helical DNA, 77
Helix, 74, 75, 77
 dextro and levorotatory, 74
Hemiacetals, 308
Hemiacylals, 308
Hemihedral faces, 18, 66–68
Heteroadamantane derivatives, 275
9-Heterobicyclo[3.3.1]nonane derivatives, 275, 279
Heterocyclohexanes, 244
Heterogeneous reaction, 61
2,4-Hexadiyne-1,6-diol bis(*p*-toluenesulfonate), 190
Hexa host, 195, 196
Hexahydro[1,3]thiazole[3,2-*a*]pyridine, 307
Homoconjugation $\sigma\pi$, 281, 286
Homotopic{100}faces, 44, 45
Host-guest reactions, in clathrates, 199
Hybridization state, 232
Hydrogen abstraction, intramolecular, 184
Hydrogenation catalyst, 96
Hydrogen bonding, 158, 266, 277, 308
 effect, intramolecular, 230
Hydrogen cyanide, 92
 β -Hydroxyamine, 93
7-Hydroxybicyclo[2.2.1]heptane, 253
Hydroxycarboxylic acids, chiral, 123
6-Hydroxyaminamine, 150
Hydroxydiazines, 162
9-(2-Hydroxyethoxymethyl)guanine, 142
2 α -Hydroxy-1 β H-laurenane, 265
2-(Hydroxymethyl)quinuclidine, 97
3-Hydroxy-9-phenylacridine, 163
Hyperconjugation, 267
Hyperconjugative effect, 225
Hyperconjugative interaction, 252, 284
Hyperconjugative mechanism, 257, 260
Hyperconjugative orbital interaction, 230
- ICS (intramolecular interaction chemical shift), 220, 269
Image, 75
Imaging, of crystal, 78
Imidazole, 161
Iminodiacetic acid, 138

- INADEQUATE METHOD, 309
Inclusion complexes, 138, 184, 193
 polymerization in, 196
 in thiourea, 139
Indanone, 198
Indene, 198
Inductive σ^* constants, 254
Inductive effect, 225–227, 233, 236, 241, 254, 280
Inductive parameter, 234
Inhibitor, "tailor-made," 18
Inositols, 304
Interaction:
 back-lobe, 286
 hyperconjugative, 286
 steric, 270, 275
 through-bond, 254, 268, 283, 284
 through-space, 254, 268
Interaction effect, intramolecular, 268
Interference, through-space, 288
Intermolecular effects, 225
Intramolecular interaction chemical shift, *see* ICS
Intramolecular interaction effects, 230, 305
Intramolecular substituent interaction, 269
Ionization potential, 229, 300
Isochromane, 198
Isocytosine, 161
Isoleucine, 146
 hydrobromide, 9
Isomenthane derivatives, 304
Isomerization:
 configurational, 141
 geometric, 136, 148
 keto acid–lactone alcohol, 156
 torsional, 141
Isometric structure, 38
Isopropenyl methyl ketone, 99
Isopropyl substituents, 304
Isoxazoline, 144

Ketene, 92
Keto–enol tautomerism, 140, 158, 162, 163
Kinetic resolution, 17, 24, 104

 β -Lactams, 302
 β -Lactones, 122
 α -Lactose, 33, 34
 β -Lactose, 33, 34
Lanthanide shift reagents, 262

Layer energy, 67
LEF (linear electric field), 220, 255, 262, 265
Lindeman-Adams rule, 294, 295
Linear electric field, *see* LEF (linear electric field)
Liquid-solid reactions, in centrosymmetric crystals, 63
Lithium dialkylamides, 301
Lone electron pair, 226, 234, 250, 252, 254, 257, 258, 266, 283
Longitudinal relaxation time, 262
Long-range effects, 265
Lysine, 20, 33
Lysine hydrochloride, 29, 31–33
 anisotropic distribution of occluded additive in, 31

Macromolecules:
 biological, 75
 helicity of, 74, 76
 imaging of, 74, 76
Macroscopic asymmetric habit, 66
Macroscopic phenomena, 79, 80
Magnetic anisotropy effect, 233
Magnetic susceptibility, 227
Malic acid, 89, 123
Mandelic acid, 55
Menthane derivatives, 301, 304
 α -Mercurycyclohexanone derivatives, 281
Mercurimethanes, 240
Mercury-bis(diacetylene), 192
Mercury substituent, 251, 281
Mesaconase, 89
Mesaconic acid, 89
Meso carbon, 108
Mesomeric effect, 230
Methane derivatives, 223, 224, 226, 233, 234, 271, 272
Methanes, fluorinated, 273
Methanol, 235
o-Methoxy-*cis*-cinnamic acid, 186
7-Methoxycoumarin, 175
2-Methoxymethylenecyclohexane derivatives, 281
Methoxy substituents, 304
2-Methyladamantanes, 2-substituted, 271
1-Methylbicyclo[2.2.1]heptane, 237
2-Methylbicyclo[2.2.2]heptane, 232
Methylbicyclo[2.2.1]heptane derivatives, 249

- 1-Methylbicyclo[2.2.2]octane, 232
Methylcyclohexane, 249, 271
 derivatives, 289
Methylcyclohexanes, geminally halogenated, 271
1-Methylcyclohexanol, 271
cis-2-Methylcyclohexanol derivatives, 277
5-Methyl-2-cyclohexen-1-one, 104
Methylcyclopentane, 246
Methyldecalol, 235
Methyl *p*-dimethylaminobenzenesulfonate, 153
2-Methylenetetrahydropyran, 276
Methyl methacrylate, 107
3-Methyl-3-phenylbutanoyl peroxide:
 decomposition of, 206
 photolysis of, 206
4-Methyl-4-phenylcyclohexa-2,5-dienone, 108
3-(*p*-Methylphenylseleno)cyclohexanone, 110, 111, 113
Methyl vinyl ketone, as Michael acceptor, 91
Michael reaction, 96
 chiral amine catalyzed, 99
 intramolecular, 98
Molar activity, of enzymes, 90
Molecular compound, 156
Molecular constitution, crystal effects on, 150
Monomers, bifunctional, 177
Morpholine derivatives, 304
Morphological change, 11, 12, 18, 28, 30, 33, 41–43, 49
Morphology, theoretical, 68
Multipulse techniques, 309

N-acetyl-4-pyridone, 153
N-acetylvaline, 42, 46–58, 54
NAE (non-additivity effect), 220, 269, 270, 276
Naphthalene derivatives, 247
Naphthazarine, 165
Naphthoquinone monooximes, 158
N-*t*-butyl-9-azabicyclo[3.3.1]nonan-3-one, 308
N-chloromethylpyrrolidone, 275
Neighbor anisotropy effect, 225. *See also*
 Anisotropy effect
Neighbor atom effects (on nuclear shielding), 223
Neomenthane derivatives, 301
Neutron diffraction, 9, 59
Neutrons:
 anomalous dispersion of, 9
 anomalous scattering of, 6
 scattering of, 9
Nitric acid hydrate, 158
o-Nitrobenzaldehyde, 92
Nitrogen substituents, endocyclic, 280
Nitromethane, 98
Nitrosobenzenes, 149
Nitro substituents, 301
N-methylcinnamide, 13, 15
nmr:
 solid-state, 161, 165
 two-dimensional, 309
N-nitrosopiperazines, 227, 243
N-nitrosopiperidines, 227, 243
Non-additivity effects, *see* NAE
Noncentrosymmetric achiral space group, 42, 55
Noncentrosymmetric symmetry, 42
Non-isometric arrangements, 38, 39
Norbornane, 253
 derivatives, 301
Norcaranes, 257
Norpinane, 308
Nortricyclene, 289
 $n\sigma^*$ interaction, 274
Nuclear charge, effective, 234
Nuclear shielding, 222

Occluded additive, distribution in crystal, 4
Occlusion of additives, selective, 79
Octant rule, 103
Octavalene, 292
Olefins, electron-poor, epoxidation, 113
Optical activity, 71
 abiotic generation of, 207
 in crystals, 72, 79
Optical purity, enhancement of, 208
Orbital interaction, 254, 302
 $n\pi^*$, 273, 276, 280, 281, 285
 $n\sigma^*$, 275, 276, 280, 284, 286
 $\pi\sigma^*$, 280, 288
Orbital interference, through-space, 286
Organostannanes, 239
Orthoacetamide, 267
Orthorhombic crystals, centrosymmetric, 54
Osmium tetroxide/tiglic acid, 63
Overlap, back-lobe, 257, 284
Oxaadamantane derivatives, 279
Oxabicyclo[3.3.1]nonane derivatives, 308
Oxabicyclo[4.2.1]nonane derivatives, 308
Oxane derivatives, 304
1-Oxa-7-thia[5.5]undecane, 306

- Oxathiazolidine derivative, 303
1,4-Oxathiin, 305
1,4-Oxathiin dioxide, 305
1,4-Oxathiin oxide, 305
Oxaziridines, 267, 302
Oxetane derivatives, 302
Oxirane, 228, 302
 derivatives, 271
2-Oxo-1,3-dioxolane derivatives, 303
Oxonium salt, 276
D-Oxynitrilase, 95
- Pair-interaction terms, 275
Paramagnetic shielding contribution, 234, 246
Paramagnetic term (of nuclear shielding), 222
Partial double bond character, 276
Pasteur-type resolution, 3, 17, 25
1,3-Pentadiene, asymmetric polymerization of, 196
Pentamethylene heterocycles, 240, 241
Pentane derivatives, 261
Perfluoro substituents, 301
Perhydrotriphenylene, as crystalline host, 196
Phase change, 139
Phase transfer alkylation, 119
Phase transfer catalyst, chiral, 98, 113
Phase transformation, 72
Phenylazophenylpalladium
 hexafluoroacetylacetone, 157
5-Phenylbutadienoic acids, 167
Phenylethane derivatives, 249
Phenylethylcarbinol, 124
Phenylethylmalonic acid, decarboxylation of, 198
 β -Phenylglutaric anhydride, 108
Phenyllactic acid, 114
Phenyl substituent, 301
4-Phenylsulfonfylazetidin-2-one, 106
4-Phenylthioacetidin-2-one, 106
3-Phenylthiocyclohexanone, 100
8-Phosphabicyclo[3.2.1]octane derivatives, 308
Phosphite esters, 122
Phosphorus substituent, 257, 301, 304
Photochemical reaction, in solid, 166
Photochromism, 160
Photocycloaddition, 183
Photodimerization:
 of anthracene derivatives, 174
 of benzylidene ketones, 185
 of chiral anthroates, 208
 of cinnamic acids, 167, 186
 crystal engineering for, 170
 at defects, 174
 of 3-dehydrogibberilin- α 3 methyl ester, 175
 of dichlorophenyldienes, 173
 of dichlorostyryl derivatives, 171
 and energy transfer, 174
 geometric requirements for, 168
 in mixed crystals, 201
 multiple products from, 173
 in non-crystalline phases, 179
 non-topochemical, 173, 174
 of quinones, 170
 selectivity in, 168
 solid-state, 167
 of sorbic acid, 173
 substrates for, 168
 of tetrahydroquinones, 181
 of α,β -unsaturated primary amides, 171
Photodimers:
 of benzylidenebutyrolactone, 169
 in Cope rearrangement, 177
 ring-opening reactions of, 176
Photoelimination, in solid-state, 202
Photooligomerization, 177
Photopolymerization, 177
Photorearrangements, in solids, 180
Phthalimido substituents, 304
Piezoelectricity, 3, 7, 59, 71, 72
Pinane, 308
Piperidine derivatives, 266, 300
Point dipole, 228
Polar axis, 6, 28, 33, 34, 56, 58, 60, 61
 absolute, direction of, 27
Polar crystal, 44, 60, 61, 66, 68
Polar effect, 300
Polar faces, 66, 68
Polarity, absolute, 6, 80
Polarizability, 229, 235, 243, 273, 277, 300
Polarization, 286
 of double bond, 276, 281, 286
 π -charge, 286
Polyatomic substituents, 235
Poly(5-benzyl-L-glutamate), 100
Polydiacetylenes, 188
 crystal defect in, 190
Polymer, stereoregular, 177
Polymer catalysts, chiral, 97
 single-crystal, 188, 190
Polymerization:
 asymmetric, 179, 191, 196
 in solid, homogenous, 187, 191

- Polymerization (*Continued*)
 solid-state, 177
 homogeneous, 187, 191
Polymolecular aggregates, 141
Polymorphism, 135, 136, 140, 145, 148, 149,
 157, 164, 165, 177, 187, 203
 and proton transfer, 163
Polypeptides, chiral, 122
Polyphenyls, 142
Polystyrenes, crosslinked, chloromethylated, 97
Potential energy surface, 154
Pressure-induced solid-solid transformation,
 137
Principal quantum number, effective, 234
Progesterone, 265
Propane derivatives, 231
 [1.1.1]Propellane, 290
 [3.3.1]Propellane derivatives, 290
 [n.1.1]Propellane derivatives, 290
Propellanes, strained, 290
Prothrombin biosynthesis, 116
Proton conduction, 159
Proton delocalization, 159, 161
Proton exchange, 165
Proton transfer, 158
 electric field induced, 159
 photo-induced, 160
 and polymorphism, 162
Proximity effects, 249, 310
Pyranopyridone, 158
Pyridines, substituted, 161
Pyroelectric crystal, 72
Pyroelectricity, 3, 7, 59, 71–73, 79

Quasi-racemates, 24
Quibec, *see* Benzylquininium chloride
Quinidine, 91, 93, 123
Quinine, 88, 91, 93, 95, 111, 119, 122, 124,
 125
Quinine methohydroxide, 98
Quinones, 114
 photodimerization to oxetanes, 170

Radical pair reactions, 202
Radical pairs, disproportionation of, 203
Reaction cavity, 184, 186
Reaction path degeneracy, reduction in crystal,
 205
Reactions:
 ligand exchange, 155
 in mono- and multi-layers, 188
 photochemical in solid, 166
 S_N2 , 155
 S_N1 , 156
Rearrangement reaction, in solid, 153
Relaxation time, longitudinal, 262
Repulsive forces, 246
Resolution of enantiomers, by crystallization,
 209
Resorcinol, 58, 68, 69, 71
 polar crystals of, 68, 70
Reverse electric field, 72
Rhodium complexes, chiral, 96
Rhodium phosphine catalysts, chiral, 89
Ring closure, transannular, 152
Ring current effect, 223, 225, 227, 228
Ring flattening, 304
Ring inversion, 139

Salicylideneanilines, 145, 159
 thermo- and photochromic behavior, 160
Salt formation, between benzoic acid and
 pyridines, 161
Scattering, anomalous, 8–10, 79
 s character, 238
Schiff bases of aminoalcohols, 151
SEF (square electric field), 220
Selenophenol addition, 110, 111
Semiempirical calculations, 224
Serine, 42–45, 54, 58, 68
 electron microscope picture of, 47
Serine-allothreonine system, 45
Serine-threonine system, 45, 60
 σ^* constants, inductive, 261
 σ -electron delocalization, 254
 σ -electron distribution, 269
Single crystal to single crystal transformation,
 184, 186, 188
Skeletal distortion, 246, 282
S-methylthanium salts, 244
S-methylthiolanium cations, 303
Sodium ammonium tartrate, 2, 18
Solids, two-component, 193
Solid-solid transformation, pressure induced,
 137
Solid solutions, 135, 147, 187, 190, 193
 conditions for formation of, 145, 201
 engineering of, 201
 halogen . . . halogen interactions and, 201
 hydrogen bonding in, 201

- photodimerization in, 201
- and reduction in crystal symmetry, 58
- Solid-state chemistry, of azoalkanes, 203
 - of diacylperoxides, 203
- Solid-state phase transformation, 185
- Solid-state photoelimination, 202
- Solid-state polymerization, of diacetylenes, 206
- Solid-state reactions:
 - analogy to phase changes, 135
 - conformational effects in, 134, 136
 - geometric factors in, 134
 - homogeneous, 184
 - one- and two-step, 136
 - strain and stress in, 189, 205, 206
 - symmetry aspects of, 134
 - thermal, 135
- Solvent effect, 66–68, 79, 118
 - in asymmetric catalysis, 100
- Solvent-surface interactions, 11, 67, 68, 70, 79
- Sorbamide, 177
- Sorbic acid, 177
 - photodimerization of, 173
- Spin-orbit interaction, 275
- Spin polarization, 275
- Spiro-chirality center, 305
- Spiroconjugation, 292
- Spiro[4.5]decane derivatives, 305
- Spontaneous resolution, 135, 146
- Stereoelectronic effect, 306
- Steric compression effect, 230, 263, 264, 267
- Steric compression shift, 251
- Steric contact, 254
- Steric crowding, 247, 277
- Steric effect, 225, 306
- Steric interaction, 234, 253, 277, 282, 308
- Steric interference, 265, 268
- Steric origin, of ICS contribution, 271
- Steric repulsion, 249, 303
- Steroids, 234, 242, 246, 248, 264, 265, 278, 282, 295, 299, 301, 307
 - monohydroxylated, 298
- Strain, 237
 - and stress, in solid-state reactions, 189, 205, 206
- Structural mimicry, 145
- Substituent effect, 230
 - γ -antiperiplanar, 231
 - of fluorine, 224
 - γ -gauche, 231
 - δ -gauche, 231
- Substituent induced chemical shift (SCS):
 - additivity, 269
 - definition of, 220, 230
- Substituent interaction, intramolecular, 269
- Substituents:
 - amino, 301
 - azido, 301
 - bromo, 302
 - t*-butyl, 251
 - carboxyl, 301
 - chloro, 301, 302
 - cyano, 301
 - endocyclic, 240, 244, 269, 270, 279
 - $\text{Ge}(\text{CH}_3)_3$, 257, 261, 301
 - group IVa, 238, 301
 - halogen, 302
 - isopropyl, 303
 - mercury, 251
 - methoxy, 303
 - nitro, 301
 - $\text{Pb}(\text{CH}_3)_3$, 251, 257, 261, 301
 - perfluoro, 301
 - phosphorus, 251, 301, 303
 - phthalimido, 303
 - $\text{Si}(\text{CH}_3)_3$, 251, 257, 261, 301
 - $\text{Sn}(\text{CH}_3)_3$, 251, 257, 261, 301
 - sulfur, 238, 301
 - thallium, 240, 251
 - tin, 238
 - trimethylammonium, 251
- Substructure search, 309
- Succinodinitrile, 137
- Sucrose, 29, 30, 35–37
- Sulfides, 301
 - oxidation, asymmetric, 96
- Sulfinic acid derivatives, 301
- Sulfones, 252
- Sulfonic acid derivatives, 301
- Sulfoxides, 252, 267
 - chiral, 96
- Sulfur substituents, 238, 301
- Sultones, 305
- Surface etchants, 79
- Symmetry, reduced, 59–61
- Tartaric acid, 9, 11, 66
- Tautomerism, 158, 165
 - in picric acid-amine system, 164
 - ring chain, 151, 152, 157
- Tellurium derivatives, 275

- Terpenes, 299
Tetracycloheptane, 290
Tetracycloheptene derivatives, 264
Tetradylene, cyclic, 191
Tetrahydroanthracene derivatives, 298
Tetrahydrofuran derivatives, 303
Tetrahydro-1-naphthoquinone-4-ols:
 hydrogen abstraction in, 183
 intramolecular cycloaddition of, 183
 photochemistry of, 183
Tetrahydropyran derivatives, 304
Tetrahydroquinones:
 electronic states of, 181
 hydrogen abstraction in, 180
 photochemistry of, 181
 photodimerization of, 181
 photorearrangement of, 180
Tetraline derivatives, 298
TGS, *see* Triglycine sulfate
Thallium substituents, 240, 251
Thermochromism, 159
Thiacyclohexanone, 266
Thiane oxides, 244, 252, 267, 305
Thianes, 245, 250, 252, 304
Thiathiophthenes, 155
Thienamycin, 106
Thietane derivatives, 302
Thietane 1,1-dioxides, 302
Thietane 1-oxides, 302
Thiirane, 228
Thioacetal function, 103
Thiocarbamate S-oxide, 301
Thiocarbamate S,S-dioxides, 301
Thiocarbamates, 301
Thiol 1,4-addition reaction, mechanism of, 108
Thiolacetic acid, 107
Thiolanium cations, 306
Thiols, 301
 cis-1-Thioniabicyclo[3.3.0]octane salt, 306
Thiophenol, 92, 99, 104, 106, 109
Threonine, 18, 21, 42, 43, 57, 58
Through-space effects, 265
Tiglic acid, 63, 64
 asymmetric hydroxylation of, 207
Tin substituents, 238
Titanium isopropoxide - tartrate complex, 89
Toluene derivatives, 263
Topochemical control, 200
Topochemical reactions, in enantiopolar
 crystals, 65
Topological analysis, 300
Torsional distortions, 136
Torsion angle, 231, 234, 243, 247, 250, 260,
 278, 281, 301
Transannular interactions, 152, 266, 308
Transition, double quantum, 309
Triacetylenes, 191
Triamantane, 232
Tricyclene derivatives, 264
Tricyclo[3.2.1.0]^{2,7}decane, 290
Triglycine sulfate, 72, 73
Triiodide ion, 155
Trimethylammonium substituent, 251, 303
1,2,3-Trimethyl-2-
 butenyldienebenzenesulfonamide, 148
Trimethylene sulfite derivatives, 305
Trio-interaction terms, 275
2,2,2-Triphenylethyl radical, rearrangement of,
 206
Triterpenes, 234
1,3,5-Trithiane 1-oxide, 305
Trio-*o*-thymotide, inclusion complexes of, 148
 photoisomerization of stilbene in, 198
Turnover number, 90
Turnover rate, 90
Twistane derivatives, 243
Twist conformation, 303-305

Valence electrons, 300
van-der-Waals compression, 225, 230, 254
van-der-Waals interactions, 230, 249
Vicinal substituents, 276
Vinylogous amide, 141
Vitamin D-3, 139
Vitamin K epoxide, 116

Walsh orbital, 264, 289, 291

X-ray analysis, 38
X-ray diffraction, 9, 10, 38, 59
 conventional, 28, 61
X-ray dispersion, anomalous, 5
X-rays, scattering of, by electrons, 9
X-ray scatterer, anomalous, 9, 10
X-ray scattering, anomalous, 36
9- β -D-Xylofuranosyladenine, 142

Zinc-blende, absolute polarity of, 10
Zinc sulfide, 8

CUMULATIVE INDEX, VOLUMES 1-16

	VOL.	PAGE
Absolute Configuration of Planar and Axially Dissymmetric Molecules (<i>Krow</i>).....	5	31
Absolute Stereochemistry of Chelate Complexes (<i>Saito</i>).....	10	95
Acetylenes, Stereochemistry of Electrophilic Additions (<i>Fahey</i>).....	3	237
Aldol Condensations, Stereoselective (<i>Evans, Nelson and Taber</i>).....	13	1
Alkaloids, Asymmetric Catalysis by (<i>Wynberg</i>).....	16	87
Aluminum Hydrides and Tricoordinate Aluminum Reagents, Asymmetric Reductions with Chiral Complex (<i>Haubenstock</i>).....	14	231
Analogy Model, Stereochemical (<i>Ugi and Ruch</i>).....	4	99
Asymmetric Reductions with Chiral Complex Aluminum Hydrides and Tricoordinate Aluminum Reagents (<i>Haubenstock</i>).....	14	231
Asymmetric Synthesis, New Approaches in (<i>Kagan and Fiaud</i>).....	10	175
Asymmetric Synthesis Mediated by Transition Metal Complexes (<i>Bosnich and Fryzuk</i>).....	12	119
Atomic Inversion, Pyramidal (<i>Lambert</i>).....	6	19
Atropisomerism, Recent Advances in (<i>Oki</i>).....	14	1
Axially and Planar Dissymmetric Molecules, Absolute Configuration of (<i>Krow</i>).....	5	31
Barriers, Conformational, and Interconversion Pathways in Some Small Ring Molecules (<i>Malloy, Bauman, and Carriera</i>).....	11	97
Barton, D. H. R., and Hassel, O.-Fundamental Contributions to Conformational Analysis (<i>Barton, Hassel</i>).....	6	1
Bicyclic Compounds, Walk Rearrangements in [n.1.0] (<i>Klarner</i>).....	15	1
Carbene Additions to Olefins, Stereochemistry of (<i>Closs</i>).....	3	193
Carbenes, Structure of (<i>Closs</i>).....	3	193
sp ² -sp ³ Carbon-Carbon Single Bonds, Rotational Isomerism about (<i>Karabatsos and Fenoglio</i>).....	5	167
Carbonium Ions, Simple, the Electronic Structure and Stereochemistry of (<i>Buss, Schleyer and Allen</i>).....	7	253
Chelate Complexes, Absolute Stereochemistry of (<i>Saito</i>).....	10	95
¹³ C Chemical Shifts in Aliphatic Molecular Systems, Substituent Effects on. Dependence on Constitution and Stereochemistry (<i>Duddeck</i>).....	16	219
Chirality, On Factoring Stereoisomerism and (<i>Hirschmann and Hanson</i>)....	14	183
Chirality Due to the Presence of Hydrogen Isotopes at Noncyclic Positions (<i>Arigoni and Eliel</i>).....	4	127
Chiral Lanthanide Shift Reagents (<i>Sullivan</i>).....	10	287
Chiral Monolayers at the Air-Water Interface (<i>Stewart and Arnett</i>).....	13	195

	VOL.	PAGE
Chiral Organic Molecules with High Symmetry, The Synthesis and Stereochemistry of (<i>Nakazaki</i>)	15	199
Chiral Organosulfur Compounds (<i>Mikolajczyk and Drabowicz</i>)	13	333
Chiral Solvating Agents, in NMR (<i>Pirkle and Hoover</i>)	13	263
Classical Stereochemistry, The Foundations of (<i>Mason</i>)	9	1
Conformational Analysis, Applications of the Lanthanide-induced Shift Technique in (<i>Hofer</i>)	9	111
Conformational Analysis, The Fundamental Contributions of D. H. R. Barton and O. Hassel (<i>Barton, Hassel</i>)	6	1
Conformational Analysis of Intramolecular Hydrogen-Bonded Compounds in Dilute Solution by Infrared Spectroscopy (<i>Aaron</i>)	11	1
Conformational Analysis of Six-membered Rings (<i>Kellie and Riddell</i>)	8	225
Conformational Analysis and Steric Effects in Metal Chelates (<i>Buckingham and Sargeson</i>)	6	219
Conformational Analysis and Torsion Angles (<i>Bucourt</i>)	8	159
Conformational Barriers and Interconversion Pathways in Some Small Ring Molecules (<i>Malloy, Bauman and Carreira</i>)	11	97
Conformational Changes, Determination of Associated Energy by Ultrasonic Absorption and Vibrational Spectroscopy (<i>Wyn-Jones and Pethrick</i>)	5	205
Conformational Changes by Rotation about sp^2 - sp^3 Carbon-Carbon Single Bonds (<i>Karabatsos and Fenoglio</i>)	5	167
Conformational Energies, Table of (<i>Hirsch</i>)	1	199
Conformational Interconversion Mechanisms, Multi-step (<i>Dale</i>)	9	199
Conformations of 5-Membered Rings (<i>Fuchs</i>)	10	1
Conjugated Cyclohexenones, Kinetic 1,2 Addition of Anions to, Steric Course of (<i>Toromanoff</i>)	2	157
Crystals as Probes for the Direct Assignment of Absolute Configuration of Chiral Molecules, A Link Between Macroscopic Phenomena and Molecular Chirality (<i>Addadi, Berkovitch-Yellin, Weissbuch, Lahav, and Leiserowitz</i>)	16	1
Crystal Structures of Steroids (<i>Duax, Weeks and Rohrer</i>)	9	271
Cyclobutane and Heterocyclic Analogs, Stereochemistry of (<i>Moriarty</i>)	8	271
Cyclohexyl Radicals, and Vinylic, The Stereochemistry of (<i>Simamura</i>)	4	1
Double Bonds, Fast Isomerization about (<i>Kalinowski and Kessler</i>)	7	295
Electronic Structure and Stereochemistry of Simple Carbonium Ions, (<i>Buss, Schleyer and Allen</i>)	7	253
Electrophilic Additions to Olefins and Acetylenes, Stereochemistry of (<i>Fahey</i>)	3	237
Enzymatic Reactions, Stereochemistry of, by Use of Hydrogen Isotopes (<i>Argoni and Eliel</i>)	4	127
1,2-Epoxides, Stereochemistry Aspects of the Synthesis of (<i>Berti</i>)	7	93
EPR, in Stereochemistry of Nitroxides (<i>Janzen</i>)	6	177
Ethylenes, Static and Dynamic Stereochemistry of Push-Pull and Strained (<i>Sandström</i>)	14	83
Five-Membered Rings, Conformations of (<i>Fuchs</i>)	10	1
Foundations of Classical Stereochemistry (<i>Mason</i>)	9	1

	VOL.	PAGE
Geometry and Conformational Properties of Some Five- and Six-Membered Heterocyclic Compounds Containing Oxygen or Sulfur (<i>Romers, Altona, Buys and Havinga</i>).....	4	39
Hassel, O. and Barton, D. H. R.-Fundamental Contributions to Conformational Analysis (<i>Hassel, Barton</i>)	6	1
Helix Models, of Optical Activity (<i>Brewster</i>)	2	1
Heterocyclic Compounds, Five- and Six-Membered, Containing Oxygen or Sulfur, Geometry and Conformational Properties of (<i>Romers, Altona, Buys and Havinga</i>)	4	39
Heterocyclic Four-Membered Rings, Stereochemistry of (<i>Moriarty</i>)	8	271
Heterotopism (<i>Mislow and Raban</i>)	1	1
Hydrogen-Bonded Compounds, Intramolecular, in Dilute Solution, Conformational Analysis of, by Infrared Spectroscopy (<i>Aaron</i>)	11	1
Hydrogen Isotopes at Noncyclic Positions, Chirality Due to the Presence of (<i>Arigoni and Eliel</i>)	4	127
Infrared Spectroscopy, Conformational Analysis of Intramolecular Hydrogen-Bonded Compounds in Dilute Solution by (<i>Aaron</i>).....	11	1
Intramolecular Hydrogen-Bonded Compounds, in Dilute Solution, Conformational Analysis of, by Infrared Spectroscopy (<i>Aaron</i>)	11	1
Intramolecular Rate Processes (<i>Binsch</i>)	3	97
Inversion, Atomic, Pyramidal (<i>Lambert</i>)	6	19
Isomerization, Fast, About Double Bonds (<i>Kalinowski and Kessler</i>).....	7	295
Ketones, Cyclic and Bicyclic, Reduction of, by Complex Metal Hydrides (<i>Boone and Ashby</i>).....	11	53
Lanthanide-induced Shift Technique—Applications in Conformational Analysis (<i>Hofer</i>).....	9	111
Lanthanide Shift Reagents, Chiral (<i>Sullivan</i>)	10	287
Mass Spectrometry and the Stereochemistry of Organic Molecules (<i>Green</i>) ..	9	35
Metal Chelates, Conformational Analysis and Steric Effects in (<i>Buckingham and Sargeson</i>)	6	219
Metal Hydrides, Complex, Reduction of Cyclic and Bicyclic Ketones by (<i>Boone and Ashby</i>)	11	53
Metallocenes, Stereochemistry of (<i>Schlogl</i>)	1	39
Metal Nitrosyls, Structures of (<i>Feltham and Enemark</i>).....	12	155
Molecular Mechanics Calculations—Application to Organic Chemistry (<i>Osawa and Musso</i>)	13	117
Monolayers, Chiral, at the Air-Water Interface (<i>Stewart and Arnett</i>).....	13	195
Multi-step Conformational Interconversion Mechanisms (<i>Dale</i>).....	9	199
Nitroxides, Stereochemistry of (<i>Janzen</i>).....	6	177
Non-Chair Conformations of Six Membered Rings (<i>Kellie and Riddell</i>)	8	225
Nuclear Magnetic Resonance, ¹³ C, Stereochemical Aspects of (<i>Wilson and Stothers</i>)	8	1

	VOL.	PAGE
Nuclear Magnetic Resonance, Chiral Solvating Agents in (<i>Pirkle and Hoover</i>)	13	263
Nuclear Magnetic Resonance, for Study of Intra-Molecular Rate Processes (<i>Binsch</i>)	3	97
Nuclear Overhauser Effect, Some Chemical Applications of (<i>Bell and Saunders</i>)	7	1
Olefins, Stereochemistry of Carbene Additions to (<i>Closs</i>)	3	193
Olefins, Stereochemistry of Electrophilic Additions to (<i>Fahey</i>)	3	237
Optical Activity, Helix Models of (<i>Brewster</i>)	2	1
Optical Circular Dichroism, Recent Applications in Organic Chemistry (<i>Crabbe</i>)	1	93
Optical Purity, Modern Methods for the Determination of (<i>Raban and Mislow</i>)	2	199
Optical Rotatory Dispersion, Recent Applications in Organic Chemistry (<i>Crabbe</i>)	1	93
Organic Solid-State, Stereochemistry and Reactions (<i>Green, Arad-Yellin, and Cohen</i>)	16	131
Organosulfur Compounds, Chiral (<i>Mikolajczyk and Drabowicz</i>)	13	333
Overhauser Effect, Nuclear, Some Chemical Applications of (<i>Bell and Saunders</i>)	7	1
Phosphorus Chemistry, Stereochemical Aspects of (<i>Gallagher and Jenkins</i>)	3	1
Phosphorus-containing Cyclohexanes, Stereochemical Aspects of (<i>Maryanoff, Hutchins and Maryanoff</i>)	11	186
Piperidines, Quaternization Stereochemistry of (<i>McKenna</i>)	5	275
Planar and Axially Dissymmetric Molecules, Absolute Configuration of (<i>Krow</i>)	5	31
Polymer Stereochemistry, Concepts of (<i>Goodman</i>)	2	73
Polypeptide Stereochemistry (<i>Goodman, Verdini, Choi and Masuda</i>)	5	69
Pyramidal Atomic Inversion (<i>Lambert</i>)	6	19
Quaternization of Piperidines, Stereochemistry of (<i>McKenna</i>)	5	75
Radicals, Cyclohexyl and Vinylic, The Stereochemistry of (<i>Simamura</i>)	4	1
Reduction, of Cyclic and Bicyclic Ketones by Complex Metal Hydrides (<i>Boone and Ashby</i>)	11	53
Resolving-Agents and Resolutions in Organic Chemistry (<i>Wilen</i>)	6	107
Rotational Isomerism about sp^2 - sp^3 Carbon-Carbon Single Bonds (<i>Karabatsos and Fenoglio</i>)	5	167
Small Ring Molecules, Conformational Barriers and Interconversion Pathways in Some (<i>Malloy, Bauman and Carreira</i>)	11	97
Stereochemical Aspects of ^{13}C Nmr Spectroscopy (<i>Wilson and Stothers</i>)	8	1
Stereochemical Aspects of Phosphorus-containing Cyclohexanes (<i>Maryanoff, Hutchins and Maryanoff</i>)	11	186
Stereochemical Nomenclature and Notation in Inorganic Chemistry (<i>Sloan</i>)	12	1
Stereochemistry, Classical, The Foundations of (<i>Mason</i>)	9	1

	VOL.	PAGE
Stereochemistry, Dynamic, A Mathematical Theory of (<i>Ugi and Ruch</i>)	4	99
Stereochemistry of Biological Reactions at Propochiral Centers (<i>Floss, Tsai, and Woodard</i>)	15	253
Stereochemistry of Chelate Complexes (<i>Saito</i>)	10	95
Stereochemistry of Cyclobutane and Heterocyclic Analogs (<i>Moriarty</i>)	8	271
Stereochemistry of Germanium and Tin Compounds (<i>Gielen</i>)	12	217
Stereochemistry of Nitroxides (<i>Janzen</i>)	6	177
Stereochemistry of Organic Molecules, and Mass Spectrometry (<i>Green</i>)	9	35
Stereochemistry of Push-Pull and Strained Ethylenes, Static and Dynamic (<i>Sandström</i>)	14	83
Stereochemistry of Reactions of Transition Metal-Carbon Sigma Bonds (<i>Flood</i>)	12	37
Stereochemistry at Silicon (<i>Corriu, Guérin, and Moreau</i>)	15	43
Stereochemistry of Transition Metal Carbonyl Clusters (<i>Johnson and Benfield</i>)	12	253
Stereoisomeric Relationships, of Groups in Molecules (<i>Mislow and Raban</i>)..	1	1
Stereoisomerism, On Factoring Chirality and (<i>Hirschmann and Hanson</i>)	14	183
Stereoselective Aldol Condensations (<i>Evans, Nelson and Taber</i>)	13	1
Steroids, Crystal Structures of (<i>Duax, Weeks and Rohrer</i>)	9	271
Structures, Crystal, of Steroids (<i>Duax, Weeks and Rohrer</i>)	9	271
Torsion Angle Concept in Conformational Analysis (<i>Bucourt</i>)	8	159
Ultrasonic Absorption and Vibrational Spectroscopy, Use of, to Determine the Energies Associated with Conformational Changes (<i>Wyn-Jones and Pethrick</i>)	5	205
Vibrational Spectroscopy and Ultrasonic Absorption, Use of, to Determine the Energies Associated with Conformational Changes (<i>Wyn-Jones and Pethrick</i>)	5	205
Vinylic Radicals, and Cyclohexyl, The Stereochemistry of (<i>Simamura</i>)	4	1
Wittig Reaction, Stereochemistry of (<i>Schlosser</i>)	5	1

